ABSTRACTS FOR THE

54th Annual Meeting of the Meteoritical Society

July 21 - 26, 1991
Monterey, California

ABSTRACTS FOR THE

54th Annual Meeting of the Meteoritical Society

Sponsored by

San Jose State University
Lunar and Planetary Institute
California Institute of Technology
University of California at Berkeley
Lawrence Livermore National Laboratory
NASA Exobiology Program
Division of Planetary Sciences, AAS
Commission on Comparative Planetology, IUGS
Barringer Crater Company
Charles Evans & Associates
CAMECA Instruments
Fisons Instruments

Additional Support by

California State University, Fullerton
Perkin Elmer
Fenestra Winery

July 21-26, 1991
Monterey, California

LPI Contribution No. 766

Compiled in 1991 by the

Lunar and Planetary Institute
3303 NASA Road 1
Houston TX 77058-4399

The Lunar and Planetary Institute is operated by the Universities Space Research Association under Contract No. NASW-4574 with the National Aeronautics and Space Administration.

Preface

This volume contains abstracts that have been accepted by the Program Committee for presentation at the 54th Annual Meeting of the Meteoritical Society.

Members of the Organizing Committee were Edward Anders (Ex Officio; University of Chicago), T. E. Bunch (NASA Ames Research Center), Donald Burnett (California Institute of Technology), Mark Caffee (Lawrence Livermore National Laboratory), Patrick Cassen (NASA Ames Research Center), Sherwood Chang (NASA Ames Research Center), Peter Englert (Chair; San Jose State University), Sidney Niemeyer (Lawrence Livermore National Laboratory), Filippo Radicati di Brozolo (Charles Evans & Associates), John Reynolds (University of California at Berkeley), Gerald Wasserburg (California Institute of Technology), and Dorothy Woolum (California State University, Fullerton).

Members of the Program Committee were Daniel Britt (University of Arizona), Donald Burnett (Chair; California Institute of Technology), Mark Caffee (Lawrence Livermore National Laboratory), Patrick Cassen (NASA Ames Research Center), Sherwood Chang (NASA Ames Research Center), Peter Englert (San Jose State University), Julie Paque (Stanford University), John Reynolds (University of California at Berkeley), Ann Vickery (University of Arizona), and Dorothy Woolum (California State University, Fullerton).

Members of the Student Award Committee were Peter Englert (San Jose State University), John Reynolds (University of California at Berkeley), and Dorothy Woolum (California State University, Fullerton).

Logistics and administrative support for the meeting were provided by the staff of the Program Services Department at the Lunar and Planetary Institute. This abstract volume was prepared by the Publications Services Department staff at the Lunar and Planetary Institute.

PROGRAM
for the
54th Annual Meteoritical Society Meeting

Monday, July 22, 1991
ANTARCTIC METEORITES
8:30 a.m. Room A

Chairmen: **T. Bunch**
R. C. Reedy

8:30-8:45 Nishiizumi K.* Sharma P. Kubik P. W. Arnold J. R.
^{36}Cl Terrestrial Ages of Antarctic Meteorites

8:45-9:00 Wacker J. F.*
Cosmogenic ^{26}Al Activities in Antarctic and Non-Antarctic Meteorites

9:00-9:15 Benoit P. H.* Sears H. Sears D. W. G.
Thermoluminescence of Meteorites from the Lewis Cliff: Ice Movements, Pairing, Orbit, and Antarctic/Non-Antarctic Comparisons

9:15-9:30 Bishop J. L.* Pieters C. M.
Mid-IR Spectroscopy of Antarctic Consortium Meteorites: B-7904, Y-82162 and Y-86720

9:30-9:45 Bremer K.* Herpers U. Delisle G. Höfle H. C.
van de Wateren D. W. Hofmann H. J. Wölfli W.
^{10}Be Content of Quartz Grains Collected in North Victoria Land and the Glacial History of the Frontier Mountain Range in Antarctica

9:45-10:00 Delisle G.*
Global Change, the East Antarctic Ice Budget and the Evolution of the Frontier Mountains Meteorite Trap, North Victoria Land, Antarctica

10:00-10:15 Wolf S. F. * Lipschutz M. E.
Labile Trace Element Comparisons in H Chondrites from Victoria Land and Queen Maud Land: A Progress Report

POSTER PRESENTATIONS
TO BE FEATURED MONDAY IN POSTER SESSION I
4:00-6:00 p.m. Room C

Harvey R. P. Score R.
Direct Evidence of In-Ice or Pre-Ice Weathering of Antarctic Meteorites

Benoit P. H. Sears H. Sears D. W. G.
Ice Movement, Pairing and Meteorite Showers of Ordinary Chondrites from the Allan Hills

Pieters C. M. Britt D. Bishop J.
VIS/Near IR Reflectance Spectra of CI/CM Antarctic Consortium Meteorites: B7904, Y82162, Y86720

10:15-10:30 **COFFEE BREAK**

Monday, July 22, 1991
NEBULA AND PARENT BODY PROCESSING I
10:30 a.m. Room A

Chairman: **D. Woolum**

10:30-11:00 Sargent A.* Beckwith S.
Observational Evidence for Proto-planetary Disks

11:00-11:30 Cassen P.*
A Guide to the Use of Theoretical Models of the Solar Nebula for the Interpretation of the Meteoritic Record

Monday, July 22, 1991
PRIMARY AND SECONDARY SNC PARENT PLANET PROCESSES
8:30 a.m. Room B

Chairmen: **G. McKay**
H. Y. McSween, Jr.

8:30-8:45 McKay G.* Le L. Wagstaff J.
Olivines in Angrite LEW87051: Phenos or Xenos?

8:45-9:00 Kring D. A.* Boynton W. V. Hill D. H. Haag R. A.
Petrologic Description of Eagles Nest: A New Olivine Achondrite

9:00-9:15 Harvey R. P.* McSween H. Y. Jr.
Parental Magmas of the Nakhlites: Clues from the Mineralogy of Magmatic Inclusions

9:15-9:30 Jones J. H. Jurewicz A. J. G.* Le L.
A Liquidus Phase Diagram for a Primitive Shergottite

9:30-9:45 Nyquist L. E.* Harper C. L. Wiesmann H. Bansal B. Shih C.-Y.
$^{142}Nd/^{144}Nd$ in SNCs and Early Differentiation of a Heterogeneous Martian (?) Mantle

9:45-10:00 Wadhwa M.* McSween H. Y. Jr. Crozaz G.
Trace Element Distributions in Minerals of EETA79001: Clues to the Petrogenesis of a Unique Shergottite

10:00-10:15 Michel R.* Audouze J. Begemann F. Cloth P. Dittrich B. Dragovitsch P. Filges D. Herpers U. Hofmann H. J. Lavielle B. Lüpke M. Richardt S. Rösel R. Rüter E. Schnatz-Büttgen M. Signer P. Simonoff G. N. Weber H. Wieler R. Wölfli W. Zanda B.
Simulation of the Interaction of Galactic Protons with Meteoroids: Isotropic Irradiation of an Artificial Meteoroid with 1.6 GeV Protons

10:15-10:30 Treiman A. H.* Gooding J. L.
Iddingsite in the Nakhla Meteorite: TEM Study of Mineralogy and Texture of Pre-Terrestrial (Martian?) Alterations

10:30-10:45 Karlsson H. R.* Clayton R. N. Gibson E. K. Mayeda T. K. Socki R. A.
Extraterrestrial Water of Possible Martian Origin in SNC Meteorites: Constraints from Oxygen Isotopes

10:45-11:00 Hartmetz C. P.* Wright I. P. Pillinger C. T.
Attempts to Constrain the Carbon Isotopic Composition of Dispersed Carbonate in EETA 79001

11:00-11:15 Wentworth S. J. Gooding J. L.*
Carbonate and Sulfate Minerals in the Chassigny Meteorite

11:15-11:30 Lindstrom D. J.*
Microprobe Studies of Microtomed Particles of "White Druse" Salts in Shergottite EETA 79001

POSTER PRESENTATION
TO BE FEATURED MONDAY IN POSTER SESSION I
4:00-6:00 p.m. Room C

Herpers U. Rösel R. Michel R. Lüpke M. Filges D. Dragovitsch P. Wölfli W. Dittrich B. Hofmann H. J.
Simulation of the Interaction of Galactic Protons with Meteoroids: On the Production of ^{7}Be, ^{10}Be and ^{22}Na in an Artificial Meteoroid Irradiated Isotropically with 1.6 GeV Protons

Monday, July 22, 1991
NEBULA AND PARENT BODY PROCESSING I (CONTINUED)
1:15 p.m. Room A

Chairmen: **C. L. Harper**
A. Sargent

1:15-1:30 Harper C. L.* Wiesmann H. Nyquist L. E.
^{135}Cs-^{135}Ba: A New Cosmochronometric Constraint on the Origin of the Earth and the Astrophysical Site of the Origin of the Solar System

1:30-1:45 Cuzzi J. N.* Champney J. M. Dobrovolskis A. R.
Particle-Gas Dynamics in the Protoplanetary Nebula

1:45-2:00 Kurat G. Brändstatter F. Palme H.* Spettel B. Prinz M.
Maralinga (CK4): Record of Highly Oxidizing Nebular Conditions

2:00-2:15 Nagahara H.* Kushiro I. Mysen B. O.
Gas--Solid Phase Diagram of Olivine and Its Application to Chondrites

2:15-2:30 Palme H.* Weinbruch S. El Goresy A.
Reheating of Allende Components Before Accretion

2:30-2:45 Hua X.* Buseck P. R. El Goresy A.
Fayalitic Halos Around FeNi Inclusions in Forsterite in the Kaba Carbonaceous Chondrite

2:45-3:00 Metzler K.* Bischoff A. Morfill G.
Accretionary Dust Mantles in CM Chondrites: Chemical Variations and Calculated Time Scales of Formation

3:00-3:15 Brearley A. J.* Geiger T.
Mineralogical and Chemical Studies Bearing on the Origin of Accretionary Rims in the Murchison CM2 Carbonaceous Chondrite

3:15-3:30 Alexander C. M. O'D.*
The Origin of Matrix and Rims in Bishunpur (L/LL3); An Ion Probe Study

3:30-3:45 Bourcier W. L.* Zolensky M. E.
Aqueous Alteration on the Parent Bodies of Carbonaceous Chondrites: Computer Simulations of Late-Stage Oxidation

3:45-4:00 Hyman M.* Zinner E. K. Rowe M. W.
Oxygen Isotopic Compositions of Individual Meteoritic Magnetite Grains from Carbonaceous Chondrites

POSTER PRESENTATION
TO BE FEATURED MONDAY IN POSTER SESSION I
4:00-6:00 p.m. Room C

Stepinski T.
Magnetization of Meteorites by Dynamo-generated Magnetic Fields in the Solar Nebula

Weinbruch S. Palme H. El Goresy A.
Metal-Forsterite Equilibration in Allende

Monday, July 22, 1991
ENSTATITE CHONDRITES AND AUBRITES
1:15 p.m. Room B

Chairmen: **C. Caillet**
G. Crozaz

1:15-1:30 Blander M.* Unger L. Pelton A. Ericksson G.
A Possible Origin of EII Chondrites from a High-Temperature--High Pressure Solar Gas

1:30-1:45 Lofgren G. E.* DeHart J. M. Lanier A. B.
Dynamic Crystallization Characteristics of Enstatite Chondrite Chondrules

1:45-2:00 Zinner E. Crozaz G.* Lundberg L. El Goresy A. Nagel H.-J.
Evidence for ^{53}Cr Excess in the EL3 Chondrite MAC 88136

2:00-2:15 Hutson M. L.*
Na-Cr Sulfide Phases in the Indarch (EH4) Chondrite

2:15-2:30 Muenow D. M. Keil K.* Wilson L.
High-Temperature Mass Spectrometric Degassing of Enstatite Chondrites: Implications for Pyroclastic Volcanism on the Aubrite Parent Body

2:30-2:45 Grady M. M.* Ash R. D. Morse A. D. Pillinger C. T.
Acfer 182: An Unusual Chondrite with Affinities to ALH 85085

2:45-3:00 Wasson J.* Kallemeyn G. W. Zhou L. Rubin A. E.
Qingzhen Chunks: Nebular Components at the Formation Location of the EH Chondrites

3:00-3:15 Hutcheon I. D.* Bar-Matthews M. Carpenter P. K.
Cr Isotopic Composition of Sulfides in the Qingzhen Enstatite Chondrite

3:15-3:30 Chen Y.* Pernicka E. Wang D.
The Trace Element Chemistry and Composition of Niningerite in Enstatite Meteorites

3:30-3:45 Floss C.* Crozaz G.
REE Variations in Oldhamite from Aubrites and EL6 Chondrites

3:45-4:00 Prinz M.* Weisberg M. K. Chatterjee N.
LEW88055: Aubritic Inclusions in a Si-Free Iron Meteorite

4:00-4:15 Murty S. V. S.* Sheel V.
Production Rate of Cosmogenic Nitrogen from Norton County Aubrite

POSTER PRESENTATIONS
TO BE FEATURED MONDAY IN POSTER SESSION I
4:00-6:00 p.m. Room C

Chen Y. Lin Y. Pernicka E. Wang D.
The Positive Eu Anomaly and Sc Enrichment of Minerals A and B in Enstatite Meteorites

Russell S. Pillinger C. T. Arden J. W.
A New Kind of Meteoritic Diamond in Abee

Tuesday, July 23, 1991
NEBULA AND PARENT BODY PROCESSING II
8:30 a.m. Room A

Chairmen: C. Göpel
A. E. Rubin

8:30-9:00 Basri G.
Violent Variability in the Young Solar Nebula: Case Studies from the T Tauri Stars

9:00-9:30 Backman D. E.* Paresce F.
Nearby Main Sequence Stars with Cool Circumstellar Material

9:30-9:45 Göpel C.* Manhes G. Allegre C. J.
Constraints on the Time of Accretion and Thermal Evolution of Chondrite Parent Bodies by Precise U-Pb Dating of Phosphates

9:45-10:00 Wetherill G. W.*
A New Model for the Formation of the Asteroids--The Parent Bodies of the Meteorites

10:00-10:15 Nakamura T.* Tomeoka K. Takeda H.
Shock-induced Deformation Recorded in the Leoville CV Carbonaceous Chondrite

10:15-10:30 Stöffler D.* Keil K. Scott E. R. D.
Proposal for a Revised Petrographic Shock Classification of Chondrites

10:30-10:45 Scott E. R. D.* Keil K. Stöffler D.
Impact Heating of Shocked Chondrites

10:45-11:00 Rubin A. E.*
Silicate Darkening and Heterogeneous Plagioclase in CK and Ordinary Chondrites

11:00-11:15 Lodders K.* Palme H.
The Role of Sulfur in Planetary Core Formation

11:15-11:30 Zahnle K.*
Fractionation of Terrestrial Neon by Hydrodynamic Hydrogen Escape from Ancient Steam Atmospheres

POSTER PRESENTATION
TO BE FEATURED MONDAY IN POSTER SESSION I
4:00-6:00 p.m. Room C

Stöffler D. Keil K. Scott E. R. D.
New Shock Classification of Chondrites: Implications for Parent Body Impact Histories

Tuesday, July 23, 1991
ACHONDRITE STEW
8:30 a.m. Room B

Chairmen: **D. D. Bogard**
J. S. Delaney

8:30-8:45 Kagi H.* Takahashi K. Masuda A.
Raman Scattering and Laser-Induced Luminescence from Micro Diamonds in Ureilites

8:45-9:00 Miyamoto M. Takeda H.*
Cooling Histories of Primitive Achondrites Yamato 74357 and MAC88177

9:00-9:15 Yanai K.*
Unbrecciated and Porphyritic Eucrite Asuka-15 Composed of Silica Mineral-Plagioclase-Pyroxenes

9:15-9:30 Delaney J. S.*
Fe/Mn Ratios in Basaltic Achondrites and Primitive Meteorites

9:30-9:45 Lugmair G. W.* Galer S. J. G. Carlson R. W.
Isotope Systematics of Cumulate Eucrite EET-87520

9:45-10:00 Bogard D. D.* Garrison D. H.
^{39}Ar-^{40}Ar Ages of Achondrites: Evidence for a Lunar-Like Cataclysm?

10:00-10:15 Yamaguchi A.* Takeda H.
Textural Variations and the Impact History of the Millbillillie Eucrite

10:15-10:30 Ruzicka A.* Boynton W. V.
Zone Sequences, Widths and Compositions of Olivine Coronas in Mesosiderites

10:30-10:45 Kennedy A. K.* Stewart B. W. Hutcheon I. D. Wasserburg G. J.
Trace Element Partitioning Within Mesosiderite Clasts

10:45-11:00 Mittlefehldt D. W.* Myers B.
Petrology and Geochemistry of the EETA79002 Diogenite

11:00-11:15 Welten K. C.* Lindner L. Alderliesten C. de Jong A. F. M. Oosterbaan W. A. van der Borg K. Schultz L. Weber H. W.
Cosmic-Ray Exposure Ages of Diogenites and Prospects for ^{10}Be as Shielding Parameter in HED-Achondrites

11:15-11:30 Swindle T. D.* Burkland M. K.
Noble Gases in the Monticello Howardite

11:30-11:45 Bukovanska M.* Ireland T. R. El Goresy A.
Zircons in Padvarninkai Brecciated Eucrite

POSTER PRESENTATION
TO BE FEATURED MONDAY IN POSTER SESSION I
4:00-6:00 p.m. Room C

Takeda H. Yamaguchi A.
Recrystallization and Shock Textures of Old and New Samples of Juvinas in Relation to its Thermal History

PRESENTED BY TITLE ONLY

Britt D. T. Pieters C. M. Petaev M. I. Zaslavskaya N. I.
Bidirectional Reflectance Spectra of the Divnoe Anomalous Achondrite

Tuesday, July 23, 1991
REFRACTORY INCLUSIONS
1:15 p.m. Room A

Chairmen: **I. D. Hutcheon**
J. Pague

1:15-1:30 Greenwood R. C.* Hutchison R. Cressey G.
Spinel-bearing Refractory Inclusions in Cold Bokkeveld (CM2)

1:30-1:45 Lee M. R.* Barber D. J.
Formation and Alteration of Refractory Inclusions Within the CM Chondrites Cold Bokkeveld, Murchison and Murray

1:45-2:00 Lin Y. T.* El Goresy A. Fang H.
Ca-Al-rich Inclusions in Ningqian (CV3) Chondrite: Evidence for Primordial High Enrichment in Re in Pt-Group Element Nuggets

2:00-2:15 Davis A. M.*
Ultrarefractory Inclusions and the Nature of the Group II REE Fractionation

2:15-2:30 Jochum K. P.* Palme H. Spettel B.
Large Nb-Ta Fractionations in Allende Ca, Al-rich Inclusions

2:30-2:45 Simon S. B. Grossman L.*
Profiles of Ti^{3+}/Ti^{tot} Ratios in Zoned Fassaite in Allende Refractory Inclusions

2:45-3:00 Caillet C.* MacPherson G. J. Zinner E. K.
Al-Mg Isotopic Record of Recrystallization of a Refractory Inclusion During Accretion into the Leoville Parent Body

3:00-3:15 Sheng Y. J.* Hutcheon I. D. Wasserburg G. J.
An Experimental Study of Mg Self-Diffusion in Spinel

3:15-3:30 Podosek F. A.* Prombo C. A. Grossman L. Zinner E. K.
Chromium Isotopic Compositions of Individual Spinel Crystals from the Murchison Meteorite

3:30-3:45 Hashimoto A.*
Evaporation of Melilite

3:45-4:00 Eisenhour D. D.* Buseck P. R.
Nanophase Metals in Fremdlinge from Allende: "Smokes" from the Early Solar System?

4:00-4:15 Goswami J. N.* Srinivasan G. Ulyanov A. A.
Titanium, Calcium and Magnesium Isotopic Compositions in a Hibonite-rich Inclusion from Efremovka

POSTER PRESENTATIONS
TO BE FEATURED MONDAY IN POSTER SESSION I
4:00-6:00 p.m. Room C

Benstock E. J. Buseck P. R.
TEM Cathodoluminescence Spectra of Meteoritic Minerals

Nagahara H. Mysen B. O.
Evaporation of Perovskite

Ruzicka A. Boynton W. V.
A Survey of CAIs in Leoville and Vigarano: Rim Layers, Brecciation, Metamorphism, and Alteration

Weisberg M. K. Prinz M. Kennedy A. Hutcheon I. D.
Trace Elements in Refractory-rich Inclusions in CR2 Chondrites

Srinivasan G. Ulyanov A. A. Goswami J. N.
Magnesium Isotopic Fractionation in Refractory Inclusions: Indications for a Mineralogic Control

Stephan T.
TOF-SIMS, Applications in Meteorite Research, First Results

Tuesday, July 23, 1991
METEORITE EXPOSURE AGES AND SIZES
1:15 p.m. Room B

Chairmen: **P. A. J. Englert**
G. F. Herzog

1:15-1:30 Nishiizumi K. Caffee M. W.* Finkel R. C. Arnold J. R.
^{10}Be and ^{53}Mn in Non-Antarctic Iron Meteorites

1:30-1:45 Garrison D. H.* Bogard D. D. Herzog G. F.
Cosmogenic ^{36}Ar from Neutron Capture by ^{35}Cl in the Chico L6 Chondrite: Additional Evidence for Large Shielding

1:45-2:00 Klein J.* Fink D. Middleton R. Vogt S. Herzog G. F.
^{41}Ca in the Jilin (H5) Chondrite: A Matter of Size

2:00-2:15 Honda M.* Nagai H. Imamura M. Kobayashi K.
Size and Composition Effects to Cosmogenic Nuclides in Meteorites

2:15-2:30 Bhandari N.* Mathew K. J. Rao M. N. Herpers U. Bremer K. Vogt S. Wölfli W. Hofmann H. J. Michel R. Bodemann R.
Depth and Size Dependence of Cosmogenic Nuclide Production Rates in Meteoroids

2:30-2:45 Reedy R. C.*
Cosmogenic-Nuclide Production in Very Large Meteorites

2:45-3:00 Vogt S. Albrecht A. Herzog G. F.* Klein J. Fink D. Middleton R. Weber H. Schultz L.
Cosmogenic Nuclides in Short-lived Meteorites

3:00-3:15 Graf Th.* Marti K.
Exposure Ages of LL- and L/LL-Chondrites and Implications for Parent Body Histories

3:15-3:30 Michel Th. Eugster O.* Niedermann S.
Determination of the ^{81}Kr Saturation Activity and Kr Production Rates for Various Meteorite Classes; Application to Exposure Ages and Terrestrial Ages

3:30-3:45 Gilabert E. Lavielle B.*
A Noble Gas Study in St. Severin Core AIII and Knyahinya Samples

3:45-4:00 Benoit P. H. Lu J. Jull A. J. T. Sears D. W. G.*
Thermoluminescence and C-14 of Non-Antarctic Meteorites: Terrestrial Ages of Prairie State Finds

4:00-4:15 Sisterson J. M.* Jull A. J. T. Donahue D. J. Koehler A. M. Reedy R. C. Englert P. A. J.
Cross Sections for Production of Carbon-14 from Oxygen and Silicon: Implications for Cosmogenic Production Rates

POSTER PRESENTATIONS
TO BE FEATURED MONDAY IN POSTER SESSION I
4:00-6:00 p.m. Room C

Nishiizumi K. Arnold J. R. Fink D. Klein J. Middleton R.
^{41}Ca Production Profile in the Allende Meteorite

Vogt S. Fink D. Klein J. Korschinek G. Middleton R. Herzog G. F.
^{41}Ca and ^{36}Cl Depth Profiles in the Iron Meteorite Grant

Tuesday, July 23, 1991
STEINBECK LECTURE
8:00 p.m. Room B

Susan Shillinglaw
The Valley, the Mountains, the Sea: John Steinbeck's California

Wednesday, July 24, 1991
INTERSTELLAR/METEORITE CONNECTIONS
I. ORGANICS AND ICES
8:30 a.m. Room A

Chairmen: **S. Sandford**
E. Zinner

8:30-9:00 Allamandola L. J.*
Interstellar Organics and Possible Connections with the Carbonaceous Components of Meteorites and IDPs

9:00-9:15 Allamandola L. J. Sandford S. A.* Tielens A. G. G. M. Herbst T.
Methanol in the Sky with Diamonds

9:15-9:30 Blake D. F.* Allamandola L. J. Sandford S. Freund F.
Clathrate Type II Hydrate Formation In Vacuo Under Astrophysical Conditions

9:30-9:45 Kerridge J. F.*
Interstellar Precursors in Synthesis of Meteoritic Organic Matter

9:45-10:00 Lerner N. R.* Peterson E. Chang S.
Evaluation of the Strecker Synthesis as a Source of Amino Acids on Carbonaceous Chondrites

10:00-10:15 Morgan W. A. Jr.* Feigelson E. D. Wang H. Frenklach M.
A New Mechanism for the Formation of Meteoritic Kerogen-like Material

10:15-10:30 Gilmour I.* Franchi I. A. Pillinger C. T. Eakin P. Fallick A.
Compound Specific Isotope Analysis of Polycyclic Aromatic Hydrocarbons in Carbonaceous Chondrites

10:30-10:45 Peterson E.* Hörz F. Haynes G. See T.
Modification of Amino Acids at Shock Pressures of 3 to 30 GPa: Initial Results

INTERSTELLAR/METEORITE CONNECTIONS
II. DIAMONDS, SiC AND RELATED ANOMALIES

10:45-11:00 Hartmann D. H.* Howard W. M. Meyer B. S.
Nucleosynthesis in Neutron-rich Supernova Ejecta

11:00-11:15 Obradovic M.* Brown L. E. Guha S. Clayton D. D.
Silicon, Carbon and Titanium Isotopes in SiC from AGB Stars

11:15-11:30 Howard W. M.* Clayton D. D. Meyer B. S.
Xe-H and Ba-H from Weak Neutron Burst

11:30-11:45 Fegley B. Jr.*
Condensation of Graphite and Refractory Carbides in Stellar Atmospheres

POSTER PRESENTATIONS
TO BE FEATURED MONDAY IN POSTER SESSION I
4:00-6:00 p.m. Room C

Sugiura N. Hashizume K.
Nitrogen Isotope in a Eucrite Yamato-792510

Wang S. Cheng P. Buseck P. R.
Imaging C_{60} Bucky Balls--Are They Really Round, Firm, and Closely Packed?

Clemett S. J. Kovalenko L. J. Maechling C. R. Zare R. N.
Two-Step Laser Mass Spectrometry: Analysis at High Spatial Resolution of Cosmochemical Samples

Adriaens M. Hyman M. Brownlee D. E. Adams F. Rowe M. W.
Magnesium Isotopes in Particles Separated from Carbonaceous Chondrites

Goswami J. N.
Meteoritic Evidence for an Active Early Sun

Wednesday, July 24, 1991
LUNAR ORIGINS, PROCESSES AND METEORITES
8:30 a.m. Room B

Chairmen: **O. Eugster**
R. L. Korotev

8:30-8:45 Symes S.* Benoit P. H. Sears H. Sears D. W. G.
Natural Thermoluminescence and Anomalous Fading: Terrestrial Age, Transmit Times and Perihelia of Lunar Meteorites

8:45-9:00 Gault D. E.* Schultz P. H.
Ejecta from Lunar Impacts: Where is it on Earth?

9:00-9:15 Hill D. H.* Boynton W. V. Haag R. A.
Calcalong Creek: A KREEPy Lunar Meteorite

9:15-9:30 Lindstrom M. M.*
Relationships Among Basaltic Lunar Meteorites

9:30-9:45 James O. B. McGee J. J.*
FeO and MgO Trends in the Plagioclases of Two Apollo 15 Mare Basalts

9:45-10:00 Ryder G.*
Plagioclase, Ilmenite, Lunar Magma Oceans, and Mare Basalt Sources

10:00-10:15 Korotev R. L.*
There Are Too Many Kinds of Mafic Impact Melt Breccias at Apollo 16 for Them All to be Basin Products

10:15-10:30 Jakes P.* Sen S. Matsuishi K.
Silicate Melt Structures, Physical Properties, and Planetary Accretion

10:30-10:45 Warren P. H.*
Possible Inheritance of Silicate Differentiation During Lunar Origin by Giant Impact

10:45-11:00 Takahashi K.* Masuda A.
Remnant of Water-Rock Interaction on the Lunar Surface

11:00-11:15 Keller L. P. McKay D. S.*
The Origin of Amorphous Rims on Lunar Plagioclase Grains: Solar Wind Damage or Vapor Condensates?

11:15-11:30 Niedermann S.* Eugster O.
Terrestrial Kr and Xe in Extraterrestrial Rocks: Chemical Adsorption of Noble Gases?

Wednesday, July 24, 1991
INTERSTELLAR/METEORITE CONNECTIONS
II. DIAMONDS, SiC AND RELATED ANOMALIES (CONTINUED)
1:30 p.m. Room A

Chairmen: **F. A. Podosek**
U. Ott

1:30-1:45 Ozima M.* Zashu S.
Radiation-induced Diamond (Carbonado): A Possible Mechanism for the Origin of Diamond in Some Meteorites

1:45-2:00 Lewis R. S.* Huss G. R. Anders E. Liu Y.-G. Schmitt R. A.
Elemental Abundance Patterns in Presolar Diamonds

2:00-2:15 Verchovsky A.* Ott U.
A New Xe Component in Diamond-rich Acid Residues from Efremovka CV3 Carbonaceous Chondrite

2:15-2:30 Ott U.* Löhr H. P. Begemann F.
Ne-E(H) and Kr-, Xe-S in Indarch and Krymka: Are They a Measure of the SiC Abundance?

2:30-2:45 Nichols R. H. Jr.* Hohenberg C. M. Amari S. Lewis R. S.
^{22}Ne-E(H) and ^{4}He Measured in Individual SiC Grains Using Laser Gas Extraction

2:45-3:00 Russell S. S.* Ash R. D. Pillinger C. T. Arden J. W.
Meteoritic Silicon Carbide--Separate Grain Populations and Multiple Components Revealed by Stepped Combustion

3:00-3:15 Hoppe P.* Geiss J. Bühler F. Neuenschwander J. Amari S. Lewis R. S.
Carbon, Nitrogen and Silicon Isotopes in Small Interstellar SiC Grains from the Murchison C2 Chondrite

3:15-3:30 Amari S.* Zinner E. Lewis R.
Ca, Ti and Sm Isotopic Compositions of Fine-grained Interstellar SiC

3:30-3:45 Ireland T. R.* Zinner E. K. Amari S. Anders E.
More Ti Isotopic Compositions of Presolar SiC from the Murchison Meteorite

3:45-4:00 Prombo C. A.* Podosek F. A. Amari S. Anders E. Lewis R. S.
S-Process Ba in SiC from Murchison Series KJ

4:00-4:15 Zinner E.* Amari S. Lewis R.
Silicon Carbide from a Supernova?

4:15-4:30 Huss G. R.* Lewis R. S.
Two Distinct 'Normal Planetary' Noble Gas Carriers in Chondrites

4:30-4:45 Hashizume K.* Sugiura N.
The Correlation Between the Primordial Argon and Nitrogen in UOCs

Wednesday, July 24, 1991
CRATERS, CRATERING AND TEKTITES
1:30 p.m. Room B

Chairmen: **C. Koeberl**
H. J. Melosh

1:30-1:45 Schultz P. H.* Gault D. E.
Are Twin Craters Caused by Double Impactors?

1:45-2:00 Melosh H. J.* Stansberry J.
Doublet Craters and the Tidal Disruption of Binary Asteroids

2:00-2:15 Langenhorst F.* Deutsch A.
Hot Shock Experiments: Simulation of an Important Process in the Early Solar System and in Multi-Ring Cratering

2:15-2:30 Miura Y. Kato T.
Anomalous Shocked Quartz in Australian Impact Craters

2:30-2:45 Zhou Y. Q.* Chai C. F.
The Discovery of Shocked Quartz and Stishovite in the Permian/Triassic Boundary Clay of Huangshi, China

2:45-3:00 Schmidt G.* Pernicka E.
The Determination of Platinum Group Elements (PGE) in Target Rocks and Fall-Back Material of the Nördlinger Ries Impact Crater (Germany)

3:00-3:15 Koeberl C.* Fiske P. S.
Beaverhead Impact Structure, Montana: Geochemistry of Impactites and Country Rock Samples

3:15-3:30 Hörz F.* Mittlefehldt D. W. See T. H.
Dissemination and Fractionation of Projectile Material in Impact Melts from the Wabar Crater, Saudi Arabia

3:30-3:45 Melnik W. L.*
Ablation of Australian Tektites Supportive of a Terrestrial Origin

3:45-4:00 Vickery A. M.* Browning L.
Water Depletion in Tektites

4:00-4:15 King E. A.* Koeberl C.
Muong Nong-type and Splashform-type Tektites from Hainan, China

4:15-4:30 Dietz R. S.* McHone J. F.
Astroblemes Recently Confirmed with Shatter Cones

4:30-4:45 Hartung J.* Kunk M. Reimold W. Miller R. Grieve R.
Roter Kamm Crater Age: 3.5 to 4.0 Ma

POSTER PRESENTATIONS
TO BE FEATURED TUESDAY IN POSTER SESSION II
4:00-6:00 p.m. Room C

Barlow N. G.
Degradation Studies of Martian Impact Craters

Bouska V. Maslowska H.
Discriminant Analysis of the Tektite Chemical Data

Read W. F.
Two Relatively Young Impact Craters Near Waupun, Wisconsin

Ouyang Z. Guan Y. Cheng H. Zhang Y.
Paleoclimate Cycles Due to Impacts by Extraterrestrial Bodies--A Study on the Possibility

Deutsch A.* Langenhorst F.
Hot Shocked Bushveld Gabbro (60 GPa-630^{o} C): Mineralogy and Rb - Sr Systematics

Miura Y. Kato T. Okamoto M.
Anomalous Quartz from Possible Impact Craters in Japan

Wu S. Zhang J. Liu G.
Two New Impact Craters: Zhuola and Hong Kong

PRESENTED BY TITLE ONLY

Mardon E. G. Mardon A.
The 1095 AD Meteor Event as Described in the Anglo Saxon Chronicle

Wednesday, July 24, 1991
CRETACEOUS-TERTIARY IMPACT(S)
8:00 p.m. Room A

Chairman: **A. Vickery**

8:00-8:30 Alvarez W.
Impact and Mass Extinction at the Cretaceous-Tertiary Boundary: The Search for the Crater(s)

8:30-8:45 Hildebrand A. R.* Boynton W. V.
Proximal Ejecta of the Chicxulub Crater, Yucatán Peninsula, Mexico

8:45-9:00 Bohor B. F.* Betterton W. J.
Maximum Shocked Grain Dimensions from K/T Ejecta, Western Interior

9:00-9:15 Bohor B. F.* Betterton W. J.
K/T Spherules Are Altered Microtektites

9:15-9:30 Kyte F. T.* Zhou L. Bohor B. F.
Magnesiowüstite--A New High-Temperature Mineral in K/T Boundary Sediments

Thursday, July 25, 1991
IDPs: LDEF, STRATOSPHERE, GREENLAND AND ANTARCTICA
8:30 a.m. Room A

Chairmen: **G. J. Flynn**
E. K. Jessberger

8:30-8:45 Borg J.* Vassent B. Bibring J.-P. Mandeville J.-Cl. Laval R.
Detection of Cosmic Dust Particles: Data from COMET Experiment and FRECOPA Payload

8:45-9:00 Brownlee D. E.* Hörz F. Laurance M. Bernhard R. P. Warren J. Bradley J. P.
The Composition of Meteoroids Impacting LDEF

9:00-9:15 Lyon I. C.* Gilmour J. D. Saxton J. M. Turner G.
Oxygen Isotopes Implanted in the LDEF Spacecraft

9:15-9:30 Amari S. Foote J. Jessberger E. K. Simon C. Stadermann F.* Swan P. Walker R. M. Zinner E.
SIMS Analysis of Micrometeoroid Impacts on LDEF

9:30-9:45 Yiou F.* Raisbeck G. M. Jéhanno C.
The Micrometeorite Flux to the Earth During the Last ~200,000 Years as Deduced from Cosmic Spherule Concentration in Antarctic Ice Cores

9:45-10:00 Nolan M.* Greenberg R.
Delivery of Meteorites from the Asteroid Belt

10:00-10:15 Jessberger E. K.* Bohsung J. Chakaveh S. Traxel K.
New PIXE Analyses of Interplanetary Dust Particles

10:15-10:30 Bradley J. P.*
Electron Energy Loss Spectroscopy of the Fine Grained Matrices of Interplanetary Dust Particles

10:30-10:45 Flynn G. J.* Sutton S. R.
Average Minor and Trace Element Contents in Seventeen "Chondritic" IDPs Suggest a Volatile Enrichment

10:45-11:00 Keller L. P.* Thomas K. L. McKay D. S.
Transmission Electron Microscopy of an Interplanetary Dust Particle With Links to CI Chondrites

11:00-11:15 Albrecht A.* Hall G. S. Herzog G. F. Brownlee D. E.
Determination of Trace Elements in Extraterrestrial Materials by ICP/MS

11:30-11:45 Nier A. O.* Schlutter D. J.
Extraction of ^{4}He from IDPs by Step-Heating

POSTER PRESENTATIONS
TO BE FEATURED TUESDAY IN POSTER SESSION II
4:00-6:00 p.m. Room C

Flynn G. J. Sutton S. R. Klock W.
Volatile Trace Elements in Large Micrometeorites from Greenland

Yates P. D. Wright I. P. Pillinger C. T. Hutchison R.
A Possible Link Between Melted Micrometeorites from Greenland and Antarctica with an Asteroidal Origin: Evidence from Carbon Stable Isotopes

Radicati di Brozolo F. Harris D. W. Chakel J. A. Fleming R. H. Bunch T. E.
Imaging Analysis of LDEF Craters

PRESENTED BY TITLE ONLY

Rietmeijer F. J. M.
Dynamic Pyrometamorphism of Interplanetary Dust Particles Compared to Atmospheric Entry Model Temperatures

Thursday, July 25, 1991
CHONDRULES
8:30 a.m. Room B

Chairmen: **J. N. Grossman**
J. A. Wood

8:30-8:45 Skinner W. R.* Leenhouts J. M.
Implications of Chondrule Sorting and Low Matrix Contents of Type 3 Ordinary Chondrites

8:45-9:00 Presper T.* Palme H.
Are Chondrules Precursors of Some Cosmic Spherules?

9:00-9:15 Bunch T.* Cassen P. Reynolds R. Chang S. Podolak M. Schultz P.
Could Chondrule Rims Be Formed or Modified by Parent Body Accretion Events?

9:15-9:30 Grossman J. N.*
Co-Evolution of Chondrules and Matrix in Ordinary Chondrites

9:30-9:45 Nehru C. E.* Prinz M. Weisberg M. K. Clayton R. N. Mayeda T. K.
Matrix Lumps in Dhajala and Mezö-Madaras: Implications for Chondrule-Matrix Relationships in Ordinary Chondrites

9:45-10:00 Lee M. S.* Rubin A. E. Wasson J. T.
Compound Chondrules in Ordinary Chondrites

10:00-10:15 Connolly H. C. Jr.* Jones B. D. Hewins R. H.
The Effect of Precursor Grain Size on Chondrule Textures

10:15-10:30 McCoy T. J.* Pun A. Keil K.
Spinel-bearing, Al-rich Chondrules: Modified by Metamorphism or Unchanged Since Crystallization?

10:30-10:45 Nakamura N.* Inoue M.
Highly Fractionated REE in Chondrules and Mineral Fragments from Murchison (CM2): Alteration or Igneous?

10:45-11:00 Wood J. A.*
Alkali Fractionation Among Chondrules of the Mezo-Madaras Chondrite

11:00-11:15 Lu J.* Sears D. W. G. Benoit P. H. Prinz M. Weisberg M. K.
Related Compositional and Cathodoluminescence Trends in Chondrules from Semarkona

11:15-11:30 DeHart J. M.* Lofgren G. E.
Low Temperature Annealing and Cathodoluminescence Studies of Type I Chondrule Compositions

11:30-11:45 Fredriksson K.* Wlotzka F. Spettel B.
To Make, Perhaps, or Not to Make Chondrules

POSTER PRESENTATIONS
TO BE FEATURED TUESDAY IN POSTER SESSION II
4:00-6:00 p.m. Room C

Leenhouts J. M. Skinner W. R.
Shape-Differentiated Size Distributions of Chondrules in Type 3 Ordinary Chondrites

Sears D. W. G. Lu J. Benoit P. H.
Volatile Loss During Chondrule Formation

Thursday, July 25, 1991
PLENARY SESSION: MEDAL WINNERS' PRESENTATIONS
1:30 p.m. Room A

Chairman:	**E. Anders**
1:30-2:00	Clayton D. D., 1991 Leonard Medal Recipient *Meteoritics and the Origins of Atomic Nuclei*
2:00-2:30	Masaitis V. L., 1991 Barringer Medal Recipient *Impact Craters: Are they Useful?*
2:30-2:45	**COFFEE BREAK**

Thursday, July 25, 1991
ORDINARY CHONDRITES
2:45 p.m. Room A

Chairmen: **R. Hutchison**
G. J. MacPherson

2:45-3:00 Marti K.* Kim J. S. Kim Y. Lavielle B. Prinz M.
Progress in the Acapulco Consortium

3:00-3:15 Hutchison R.* Reed S. J. B. Ash R. D. Pillinger C. T.
Adrar 003: A New Extraordinary Unequilibrated Ordinary Chondrite

3:15-3:30 Ebihara M.*
REE Abundance in Acid Residues of UOC's--A Possible Index for Subclassification

3:30-3:45 Brearley A. J.* Casanova I. Miller M. L. Keil K.
Mineralogy of an Unusual Cr-rich Inclusion in the Los Martinez (L6) Chondritic Breccia

3:45-4:00 Kim J. S.* Marti K. Perron C. Pellas P.
Xenon in Chondritic Metals

4:00-4:15 Socki R. A. Gibson E. K.* Jull A. J. T. Karlsson H. R.
Carbon and Oxygen Isotope Composition of Carbonates from an L6 Chondrite: Evidence for Terrestrial Weathering from the Holbrook Meteorite

4:15-4:30 Pedroni A.* Weber H. W.
Exceptionally Unfractionated Solar Noble Gases in the H3-H6 Chondrite Acfer 111

4:30-4:45 Thakur A. N.*
Thermal Release Pattern of Hg Isotopes in Chondrites

POSTER PRESENTATIONS
TO BE FEATURED TUESDAY IN POSTER SESSION II
4:00-6:00 p.m. Room C

Hutchison R. Barton J. C. Pillinger C. T.
The L6 Chondrite Fall at Glatton, England, 1991 May 5

Xie X. Li Z. Wang D. Liu J. Hu R. Chen M.
The New Meteorite Fall of Yanzhuang, A Severely Shocked H6 Chondrite with Black Molten Materials

Li Z. Xie X. Zhang D.
The Discovery of Four Concentric Ring Growth Pattern of Fe-Ni Metal Nucleation and Crystallization in Space

Thursday, July 25, 1991
IRON METEORITES
2:45 p.m. Room B

Chairmen: **J. G. Goldstein**
S. Niemeyer

2:45-3:00 Casanova I.*
Distribution of Silicon Between Kamacite and Taenite

3:00-3:15 Bajt S.* Rasmussen K. L.
PIXE Measurements on the Iron Meteorite Mundrabilla

3:15-3:30 Goldstein J. I.* Williams D. B. Zhang J.
The Plessite Structure in Iron Meteorites

3:30-3:45 Kracher A.*
Microdistribution of Chromium in Metal and Sulfide of IAB Silicate Inclusions and Winonaites

3:45-4:00 Niemeyer S.* Esser B. K.
Re-Os Chronology of IAB, IIE, and IIIAB Iron Meteorites

4:00-4:15 Esat T.* Bennett V.
Negative Thermal Ionization and Isotope Dilution Applied to the Determination of Re and Os Concentrations and Os Isotopic Compositions in Iron Meteorites

4:15-4:30 Birck J. L.* Roy-Barman M. Allegre C. J.
The Rhenium Osmium Chronometer: The Iron Meteorites Revisited

4:30-4:45 Lu Q.* Masuda A.
Abundance Ratios of Molybdenum Isotopes in Some Iron Meteorites

POSTER PRESENTATIONS
TO BE FEATURED TUESDAY IN POSTER SESSION II
4:00-6:00 p.m. Room C

Smith S. P. Huneke J. C.
High Sensitivity Survey Chemical Analysis of Metal-rich Meteorites by Secondary Ion Mass Spectrometry and Glow Discharge Mass Spectrometry

Lipschutz M. E. Vogt S. Elmore D. Rickey F. A. Simms P. C.
PRIME Lab: A Dedicated AMS Facility for Earth and Planetary Science Research

Haack H.
Evidence for Crystallization of the IIIAB Core by Inwards Dendritic Growth

Friday, July 26, 1991
S ASTEROIDS ARE NOT ORDINARY CHONDRITES?
8:30 a.m. Room A

Chairmen:	**D. T. Britt** **J. F. Bell**
8:30-8:55	Bell J. F.* *The S-Class Asteroid Debate: Historical Outline*
8:55-9:15	Lipschutz M. E.* *Ordinary Chondrite Classification and Meteoritic Evidence Regarding Parent Bodies*
9:15-9:40	Gaffey M. J.* *The Mineralogy of S-type Asteroids: Why Doesn't Spectroscopy Find Ordinary Chondrites in the Asteroid Belt?*
9:40-10:00	Pellas P.* *Exotic Clasts in Meteoritic Breccias*
10:00-10:20	Wetherill G. W.* *S Asteroids: Evidence from Astronomy and Orbital Mechanics*
10:20-10:40	Ostro S. J.* *Radar Constraints on Asteroid Metal Abundances and Meteorite Associations*
10:40-11:00	Chapman C. R.* *S-type Asteroids and the Gaspra Fly-By*
11:00-11:20	Britt D. T.* *"Space Weathering": Are Regolith Processes an Important Factor in the S-type Controversy?*
11:20-11:35	McSween H. Y. Jr.* *Oxidation During Metamorphism: Another Argument Against S-Asteroids Having Chondritic Compositions*
11:35-11:50	Lebofsky L. A.* Howell E. S. Britt D. T. *Characterization of Low Albedo Asteroids*

POSTER PRESENTATIONS
TO BE FEATURED TUESDAY IN POSTER SESSION II
4:00-6:00 p.m. Room C

Bell J. F.
Size-dependent Composition in the Meteoroid/Asteroid Population: Probable Causes and Possible Implications

Howell E. S. Merényi E. Lebofsky L. A.
Using Neural Networks to Classify Asteroid Spectra

Saito J. Takeda H.
Mineralogical Study of Metals in MAC88177 with Reference to S-type Asteroids

Friday, July 26, 1991
CARBONACEOUS CHONDRITES
8:30 a.m. Room B

Chairmen: **A. El Gorsey**
M. E. Zolensky

8:30-8:45 Geiger T.* Bischoff A.
The CK Chondrites--Conditions of Parent Body Metamorphism

8:45-9:00 Zolensky M. E.*
Mineralogy and Matrix Composition of "CR" Chondrites Renazzo and EET 87770, and Ungrouped Chondrites Essebi and MAC 87300

9:00-9:15 Kallemeyn G. W.*
Compositional Studies of Antarctic Carbonaceous Chondrites Possibly Related to Al Rais and Renazzo

9:15-9:30 Weisberg M. K.* Prinz M. Chatterjee N. Clayton R. N. Mayeda T. K.
Dark Inclusions in CR2 Chondrites

9:30-9:45 Ash R. D.* Grady M. M. Morse A. D. Pillinger C. T.
Renazzo-like Chondrites; A Light Element Stable Isotope Study

9:45-10:00 Jones R. H.*
Effect of Metamorphism on Isolated Olivine Grains in CO3 Chondrites

10:00-10:15 Xiao X. Lipschutz M. E.*
Volatile Trace Elements in Antarctic Carbonaceous Chondrites: Sturm und Schlang

10:15-10:30 Weber H. W. Schultz L.*
Noble Gases in Eight Unusual Carbonaceous Chondrites

10:30-10:45 Takaoka N.* Nagao K. Miura Y.
Noble Gases in Y-74063 (Unique)

10:45-11:00 Rotaru M.* Birck J. L. Allegre C. J.
Chromium Isotopic Composition in the Enstatite Chondrite Qingzhen and in Magnetitite of Orgueil

11:00-11:15 Thiel K.* Kölzer G.
Dust Investigation of Insolated Comet Nucleus Analogues

11:15-11:30 Schmitt B. Espinasse S. Klinger J.*
A Possible Mechanism for Outbursts of Comet P/Halley at Large Heliocentric Distances

POSTER PRESENTATIONS
TO BE FEATURED TUESDAY IN POSTER SESSION II
4:00-6:00 p.m. Room C

Weisberg M. K. Prinz M.
El Djouf 89001: A New CR2 Chondrite

Bischoff A. Palme H. Clayton R. N. Mayeda T. K. Grund T. Spettel B. Geiger T. Endress M. Beckerling W. Metzler K.
New Carbonaceous and Type 3 Ordinary Chondrites from the Sahara Desert

Albrecht A. Vogt S. Herzog G. F. Klein J. Fink D. Middleton R.
^{26}Al and ^{10}Be Contents of the Murchison (C2) Chondrite

Palma R. L. Chaffee S. Hyman M. Rowe M. W.
Plasma Chemical Inert Gas Release from the Allende Meteorite

Contents

Magnesium Isotopes in Particles Separated from Carbonaceous Chondrites. M. Adriaens,[1] M. Hyman,[2] D. E. Brownlee,[3] F. Adams[1] and M. W. Rowe[2]. [1]Department of Chemistry, University of Antwerp, Wilrijk, Belgium, [2]Department of Chemistry, Texas A&M University, College Station, TX 77843, USA, [3]Department of Astronomy, University of Washington, Seattle, WA 98195, USA.

Carbonaceous chondrites contain slightly magnetic, regularly shaped subrounded particles ~ 20 to 100 μm in size; an SEM photomicrograph of a typical example is shown in Fig. 1. Although when whole these particles appear nearly opaque, they seem brown when crushed, as viewed by transmitted light with an optical microscope. In magnetic-density separations, they concentrate in the fraction which floats in bromoform, $\rho < 2.85$ g/cm^3. We analyzed them semi-quantitatively with a JEOL 735 SEM with EDS. The results are typified by the following ranges observed in elemental ratios from seven Alais particles: Mg/Si = 0.6 to 0.9; Al/Si = 0.09 to 0.10; S/Si = 0.03 to 0.05; Ca/Si = 0.01 to 0.02; Cr/Si = 0.01 to 0.08; Fe/Si = 0.5 to 1.1; and Ni/Si = 0.03 to 0.06.

Examples of these particles from Alais, Ivuna, Orgueil and Revelstoke CI1s, and Bells, Essebi and Haripura CM2s, and Renazzo CR2 were embedded in epoxy, polished and coated with gold in preparation for isotopic analysis of the magnesium isotopes. We present here a progress report of the isotopic composition of magnesium in particles from these eight meteorites using a Cameca IMS 4f secondary ion mass spectrometer. For each meteorite, five to fifteen particles of about 30 - 50 μm in diameter were analyzed; about four analyses were performed per particle. Additionally, terrestrial olivine particles were measured under the same analytical conditions. The isotopic ratios of $^{25}Mg/^{24}Mg$ and $^{26}Mg/^{24}Mg$ were calculated from the measured intensities. Their corresponding δ values, deviations of the ratios from their references values (1), were plotted in a three isotope plot of magnesium. A linear relationship was calculated between both δ values, taking into account the error of both variables (2).

The data of the terrestrial olivine samples and most data of the meteorite samples plotted near the normal mass fractionation line with slope of 1/2. The Ivuna data were an exception to this and tended to fall on a line with a slope close to unity, indicating a probable excess in ^{24}Mg. The 95% confidence interval of the slope of the calculated regression line did not include the normal mass fractionation line. Nishimura *et al.* (3) earlier reported ^{24}Mg excesses in the chondrites, ALH-77278, Y-74640 and Y-74191. References: (1) Catanzaro E. J. *et al.* (1966) *J. Res. Nat. Bur. Stand.* **70a,** 453-458. (2) Davis O. L. and Goldsmith P. L. (eds). (1972), *Statistical Methods in Research and Production*, Imperial Chemical Industries Limited, Edinburgh. (3) H. Nishimura and J. Okano (1981) *Mem. Natl. Inst. Polar Res., Spec.* Issue **20**, 229-236 and (1983) *Secondary Ion Mass Spectrometry SIMS IV*, A. Benninghoven *et al.* (eds.) Springer-Verlag, Berlin, 475-477.

DETERMINATION OF TRACE ELEMENTS IN EXTRATERRESTRIAL MATERIALS BY ICP/MS. Albrecht A., Hall G.S., Herzog G.F.[1] and D.E. Brownlee[2]; 1) Dept. Chemistry, Rutgers Univ., New Brunswick, NJ 08903. 2) Dept. Astronomy, Univ. Washington, Seattle, WA 98195.

By coupling the high ionization efficiency of an inductively coupled plasma (ICP) with the sensitivity of a mass spectrometer one can achieve detection limits from 1 to 10 ppt in solution [1]. We report our first results obtained using a VG ICP-MS instrument (PQ2+turbo) to analyze the U.S.G.S. standard AGV-1, samples of the Murchison (C2) and Chico (L6) chondrites, and some deep-sea spheres (Table 1).

Samples were dissolved by 12 hours of digestion with HF, HNO_3, and $HClO_4$ in a Parr bomb heated to 140°C. After three evaporations with $HClO_4$ and HNO_3, the residue was taken up in 20% HNO_3 and diluted in enough 2% HNO_3 to reduce concentrations of interest below 200 ppb. A calibration line for each element was obtained from the analysis of three solutions prepared with the U.S.G.S. standard BCR-1 (507, 50.7, and 5.07 µg rock/mL). We used ^{115}In as an internal standard to correct for machine drift. Factors influencing drift include temperature variations, the purity of the Ar plasma, and the total concentration of solutes. A new procedure based on repeated runs of standards will help lower errors and increase the number of elements measured reliably. Although the deep-sea spheres were analyzed only once, by analyzing all other samples (and standards) three or more times we attained precision and accuracy better than 5-8% in most instances. At this level of precision, we did not see any influence of major element concentrations on trace element concentrations.

Table 1. Elemental concentrations (ppb or *ppm) in Murchison, Chico, and deep sea spheres.

	AGV-1		Murchison		Chico		Spheres	
	[2]		[3]		Melt	Chon.	KK1/a	KK1/b
La*	38	34.5	0.32	0.39	0.41	0.40	1.1	1.6
Ce*	67	67.4	0.88	0.84	1.0	1.13	1.8	7.2
Pr	7.6*	7.9*	130	140	157	152	290	403
Eu	1.64*	1.77*	79	78	123	75	230	179
Gd	5.0*	4.3*	290	240	284	268	626	921
Tb	700	600	56	55	50	66	47	83
Dy	3.6*	3.2*	330	368	377	475	361	801
Ho	670	610	84	88	93	87	89	166
Er	1.7*	1.68*	230	253	291	374	188	498
Tm	340	240	39	30	65	68		152
Ba*	1226	1241	3.1	2.5	6.5	3.2	8.8	51
Co*	15.3	13.5	600	594	291	563	354	287
Sr*	662	593	10.5	9.2	9.1	9.1	6.3	8.8
Th	6.5*	7.1*		68				
U	1.9*	2.4*	15	18				
Y*	20	16	1.9	2.0	2.3	3.1	1.6	3.5
Zr*	227	211	4.6	4.7	5.5	4.9	7.1	11.3

Results for melt and chondritic portions of Chico are relatively similar for Zr, Sr, Y, and the REE with the exception of a positive Eu anomaly in the melt portion. Ba is enriched and Co depleted by a factor of 2 in the melt phase. With respect to REE's, Chico is similar to Leedey [4].

Sample KK1/a consisted of ~90 deep sea spheres, average mass 16~µg; KK1/b consisted of 4 spheres, total mass 1.74 mg. The C2-normalized REE patterns show significant positive fractionation for Ce and Eu and some enrichment in La, Pr, and Gd. KK1/b is enriched by a factor of ~1.5 relative to KK1/a except for Ce and Ba, which are enriched by factors >4. Tb, Dy, Ho, and Er abundances in the small spheres and C2's are comparable; Sr is depleted in both samples. We attribute elemental fractionation and enrichment to weathering and seawater exchange [5]. Our results demonstrate the potential of ICP-MS in the study of extraterrestrial material and point toward some ways to improve data quality.

References: 1) Hall G.S. et al. (1990) *J. Radioanal. Chem. 146*, 255-265; Houk R.S. and Thompson J.J. (1988) *Mass Spectrom. Rev. 7*, 425-461. 2) Govindaraju K. (1989) *Geostand. Newslett. 13*, 1-113. 3) Showalter D.L. et al. (1972) Meteoritics, 7,#3, 295-301. 4) Masuda M. et al. (1973) *Geochim. Cosmochim. Acta 37*, 239-248. 5) Mittlefehldt D.W. and Lindstrom M.M. (1991) *Geochim. Cosmochim. Acta 55*, 77-87; Humphris S.E. and Thompson, G. (1978) *Geochim. Cosmochim. Acta 42*, 107-125.

^{26}Al AND ^{10}Be CONTENTS OF THE MURCHISON (C2) CHONDRITE. Albrecht A., Vogt S., Herzog G.F.[1], Klein J., Fink D. and Middleton R.[2] 1) Dept. Chemistry, Rutgers Univ., New Brunswick, NJ 08903. 2) Dept. Physics., Univ. Penn., Philadelphia, PA 19104

Many C2 meteorites have short exposure ages [1]. The exposure age of Murchison in particular has figured indirectly in estimates of the magnitude of an early irradiation [2]. However, the presence of trapped gas in bulk samples affects the measured ^{22}Ne/^{21}Ne ratios and hence may interfere with the determination of a shielding-corrected exposure age. Published activities of cosmogenic radionuclides in this stone generally pertain to different specimens so their interpretation is ambiguous. Coordinated measurements of ^{26}Al and ^{10}Be in short-lived objects can provide exposure ages that are virtually shielding independent although subject to uncertainties from other sources. ^{26}Al and ^{10}Be contents also supply information about the relative depths of samples, information that can be used later to investigate the behavior of neutron-produced nuclides such as ^{41}Ca.

We have measured by accelerator mass spectrometry [3] the ^{26}Al and ^{10}Be activities in 15 samples of Murchison (Table 1; U= U.S. Natl. Museum, Washington, D.C.; M=Field Museum of Natural History, Chicago, IL). The 1-σ error of each measurement is ±6-8%. The calculation of ^{26}Al activities is based on an assumed native ^{27}Al concentration of 1.14% [4]. ICP-MS analyses of the elemental Al concentrations in our samples gave preliminary values ranging from 1.22 to 1.28 %; use of these results would change the reported ^{26}Al contents by less than 3%.

Table 1. ^{26}Al and ^{10}Be in Murchison.

Sample	^{10}Be	^{26}Al
	dpm/kg	
U5452	8.7	29.3
M2641/2	8.8	28.3
U5450[1]	9.1	33.8
U5443	9.3	29.7
U2682/7	9.4	30.9
M2644/1[1]	9.9	37.9
M2752/8	10.1	33.0
M2640/3	10.3	37.4
M2684/5[2]	11.0	36.8
U5461	11.1	34.4
U5387	11.1	34.6
M2684/4[2]	11.1	34.9
U5469[1]	11.2	32.0
M2682/6	11.3	37.4
U5481[1]	11.8	31.8

1) Outlier from average. 2) Same name but different specimens.

The exposure age of Murchison is given implicitly by the relation $^{10}Be/^{26}Al = P_{10}/P_{26} * (1 - e^{-\lambda 10 t}) / (1 - e^{-\lambda 26 t})$. We will assume that the production rate ratio P_{10}/P_{26} is constant in the samples studied. In H-chondrites it has the value 0.345 [5]. We have converted this ratio to the one expected in Murchison, 0.46, with the aid of published equations (see [6]). The average observed ratio of ^{10}Be/^{26}Al for all 15 samples is 0.310±0.027 and 0.310±0.009 if we exclude the four worst outliers. The latter value gives an age of 1.75±0.20 Ma in good agreement with one given in [2]. This error is sensitive to the uncertainty in P_{10}/P_{26}, which we have not included. The ^{10}Be activities (8.7 - ~11.5 dpm/kg) can be converted to production rates and corrected to L-chondrite composition (P_{10}[L])/P_{10}[Murch.]=0.94). The resulting values go from about 14 to 19 dpm/kg. According to the model of [7], these values place upper and lower bounds on the radius of 100 cm and 40 cm, respectively. The lower bound is consistent with an estimate of >26.4 cm based on the recovered mass [8].

References. **1)** Mazor E. et al. (1970) *Geochim. Cosmochim. Acta 34*, 781-824. **2)** Hohenberg C.M. et al. (1990) *Geochim. Cosmochim. Acta 54*, 2133-2140. **3)** Middleton R. and Klein J. (1986) *Proc. Workshop Tech. Accel. Mass Spectrom.*, Oxford, England, 76-81; Middleton R. et al. (1983) *Nucl. Instrum. Meth. 218*, 430-436. **4)** Jarosewich E. (1971) *Meteoritics 6*, 49-52. **5)** Vogt S. et al. (1990) *Rev. Geophys. 28*, 253-275. **6)** Herzog G.F. (1990) *Workshop on Cosmogenic Nuclide Production Rates, LPI Tech. Rep. 90-05*, Lunar & Planet. Inst., Houston, TX, 51-52. **7)** Graf Th. et al. (1990) *Geochim. Cosmochim. Acta 54*, 2521-2534. **8)** Lovering J.F. et al. (1971) *Nature 230*, 18-20.

THE ORIGIN OF MATRIX AND RIMS IN BISHUNPUR (L/LL3); AN ION PROBE STUDY. C. M. O'D. Alexander. McDonnell Center for the Space Sciences, Washington University, St Louis, MO 63130.

Two competing, although not mutually exclusive, models for the origin of matrices in ordinary chondrites (OCs) suggest that they are dominated either by the products of chondrule fragmentation (1) or by nebula condensates (e.g. 2). There is now a general consensus that most matrix grains larger than 5μm are chondrule fragments (1,2). It is the origin of the <5μm fraction, particularly the predominant non-clastic component, that remains contentious. The clastic component in the <5μm fraction was probably also derived from chondrules (1,2).

Alexander *et al.* (1) suggest that most of the non-clastic material formed from chondrule glass which is underrepresented in the >5μm fraction. This would also explain the Na, K and Al enrichment, relative to the bulk meteorite, of the <5μm fraction in many or most OCs. On the other hand, Brearly *et al.* (2) prefer an amorphous condensate origin. Their conclusion is based in large part on the relatively unfractionated composition and the low abundance of >5μm clastic fragments (20-30 vol. %) in a 'matrix lump'.

In principle, trace element studies of the <5μm fraction should be able to differentiate between the two models. A major drawback of all previous trace element studies (e.g. 2,3) is their relatively low spatial resolution. Consequently, their results will reflect the bulk compositions of the matrix or rim samples which both models predict will be close to that of the bulk meteorite. 4 fine grained matrix areas, 2 rims and 4 chondrule glasses have been analysed in the ion probe, which has a resolution of 10-20μm, and the results for elements that are incompatible in olivine and low-Ca pyroxene, normalised to Al, are shown below.

In the matrix and rims the refractory incompatibles are, with the exception of Eu, uniformly depleted relative to Al and the volatile elements Na and Rb (and K) are enriched. The fractionation of Al from other refractory elements argues against a condensation origin. The similarity in trace element abundances between matrix and rims strongly argues for a genetic relationship. 3 of the 4 chondrule glasses have essentially chondritic abundances of refractory elements, relative to Al, but the glass in C17 closely mimics the refractory rim and matrix patterns, including a positive Eu anomaly, while the volatile elements are highly depleted. Clearly, if the 3 unfractionated glasses are representative of the chondrules from which the matrix could have formed, a chondrule origin would have to be ruled out. However, if C17 is more representative, a chondrule origin would seem likely.

(1) Alexander *et al.* (1989) *E.P.S.L.* 95, 187; (2) Brearly *et al.* (1989) *G.C.A.* 53, 2081; (3) Grossman and Wasson (1987) *G.C.A.* 51, 3003.

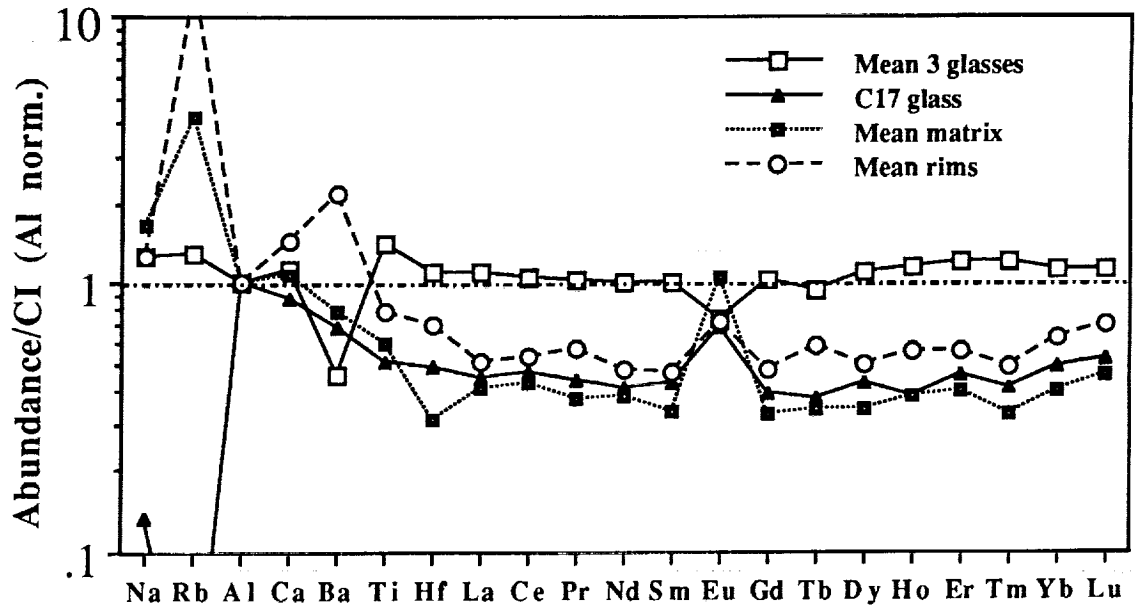

INTERSTELLAR ORGANICS AND POSSIBLE CONNECTIONS WITH THE CARBONACEOUS COMPONENTS OF METEORITES AND IDPs; L. J. Allamandola, NASA Ames Research Center, MS:245-6, Moffett Field, CA 94035-1000

Studying the chemical and isotopic composition of interstellar ice and dust provides insight into the composition and chemical history of the solid bodies in the solar nebula and the nature of the material subsequently brought into the inner part of the solar system by comets and meteorites. It is now possible to probe the composition of these microscopic interstellar particles (some hundreds of light years away), thanks to substantial progress in two areas: astronomical spectroscopic techniques in the middle-infrared, the spectral region most diagnostic of composition; and laboratory simulations which realistically reproduce the critical conditions in various interstellar environments.[1] High quality infrared spectra of many different astronomical sources, some associated with dark molecular clouds, and others in the diffuse interstellar medium (DISM) are now available. What comparisons of these spectra with laboratory spectra tell us about the complex organic components of these materials is the subject of this talk.

Most interstellar material is concentrated in large molecular clouds where simple molecules are formed by gas phase and dust grain surface reactions. Gaseous species (except H_2) striking the cold (10K) dust will stick, forming an icy grain mantle. This accretion, coupled with energetic particle bombardment and UV photolysis, will produce a complex chemical mixture containing volatile, non-volatile, and isotopically fractionated species. One can compare spectra of the diffuse and dense interstellar medium with the spectra of analogs produced in the laboratory under conditions which mimic those in these different environments. In this way one can determine the composition and abundances of the major constituents present and place general constraints on the types and relative abundances of organics coating the grains. Ices in dense clouds contain H_2O, CH_3OH, CO, perhaps some NH_3 and H_2CO, as well as nitriles and ketones or esters. There is some evidence that the later, more complex species, are also present on the grains in the DISM. The evidence for these materials, in addition to carbon rich materials such as amorphous carbon, microdiamonds, and polycyclic aromatic hydrocarbons will be reviewed and the possible connection with meteoritic organics will be discussed.

[1] Allamandola, L.J., and Tielens, A.G.G.M., (1989) eds., Interstellar Dust (Kluwer, Dordrecht).

METHANOL IN THE SKY WITH DIAMONDS; L.J. Allamandola, S.A. Sandford, A.G.G.M. Tielens, NASA/Ames Research Center, MS 245-6, Moffett Field, CA 94035, and T. Herbst, Univ. of Hawaii, Institute for Astronomy, 2680 Woodlawn Dr., Honolulu, HI 96822

The presence of gas phase methanol (CH_3OH) in dense interstellar molecular clouds was established by the radio detection of its rotational emission lines (1). The presence of solid state methanol in these clouds had not been as rigorously demonstrated (2). However, the position, width, and profile of an absorption band near 1470 cm^{-1} (6.8 μm) in the infrared spectra of many dense molecular clouds strongly suggests that solid methanol is an important component of interstellar ices. This identification of the 1470 cm^{-1} (6.8 μm) band is not unique, however, and other identifications of the feature have been suggested (3). In an attempt to better constrain the identification of the 1470 cm^{-1} (6.8 μm) feature we began a program to search for other characteristic absorption bands of solid state methanol in the spectra of objects known to produce the 1470 cm^{-1} (6.8 μm) band. One such feature has now been unambiguously identified in the spectra of several dense molecular clouds and its position, width, and profile fit well with those of laboratory H_2O:CH_3OH ices. Thus, the presence of methanol-bearing ices in space is confirmed.

In all the spectra in which the new methanol band was detected, and in several spectra in which the feature was not detected, a second, unexpected band was discovered. After consideration of the position, width, and profile of the new band we tentatively identify micro-diamonds to be the source material causing the new absorption feature. The identification of the absorption feature with micro-diamonds is supported by comparisons with spectra from vapor-condensed micro-diamonds studied in the laboratory. There are indications that this material is ubiquitous in space and it is therefore likely to be related to the meteoritic diamonds that carry interstellar signatures (4).

The abundances of these two important C-bearing materials, the implications of their detection in space, and the relationship of these diamonds to those identified in meteorites will be discussed in further detail in the talk.

References:

(1) cf. Irvine, W.M., Goldsmith, D.F., and Hjalmarson, A. (1987), in Interstellar Processes, eds. D. Hollenbach and H. Thronson, D. Reidel, 561-609.

(2) Allamandola, L.J. (1984), in Galactic and Extragalactic Infrared Spectroscopy, eds. M.F. Kessler and J.P. Phillips, Reidel, 5-35.

(3) Tielens, A.G.G.M. and Allamandola, L.J. (1987), in Physical Processes in Interstellar Clouds, eds. G. Morfil and M. Scholer, Reidel, 333-376.

(4) Lewis, R.S., Tang, M., Wacker, J.F., Anders, E., and Steel, E. (1987), Nature 326, 160-162.

SIMS ANALYSIS OF MICROMETEOROID IMPACTS ON LDEF;

S. Amari[1], J. Foote[1], E. K. Jessberger[2], C. Simon[1], F. Stadermann[2], P. Swan[1], R. M. Walker[1] and E. Zinner[1], [1]McDonnell Center for the Space Sciences and Physics Dept., Washington University, One Brookings Drive, St. Louis, MO 63132, [2]Max-Planck-Institut für Kernphysik, Postfach 103980, D6900, Heidelberg, Germany.

LDEF experiment AO187-2 consisted of 237 capture cells, 120 on the leading edge, the rest on the trailing edge. In each cell a 2 μm plastic foil, metallized on both sides, covered polished Ge targets. Although all plastic covers except for 12 cells on the trailing edge failed during flight, the Ge plates contain many extended impact features that were apparently produced by projectile material that had penetrated the plastic foils while they were still intact. We optically scanned all cells without plastic foil from the trailing edge and found extended impact features from 200 to 4000 μm in diameter with 4 characteristic morphologies: a. craters surrounded by deposits, b. ring-shaped features, c. sprays, and d. "spider webs." 53 impacts were selected as high priority candidates for ion probe analysis. After detailed documentation in the SEM impacts were analyzed in the ion microprobe for the chemical composition of the remaining projectile material. Prior simulation studies [1] had shown that extended impact on the Ge plates contained sufficient projectile material for chemical and isotopic analysis by SIMS. We made multi-element point analyses in lateral scans across the impact features. Each point analysis consisted of depth profiles of a number of elements. In all of 12 impacts so far studied we found evidence for the presence of projectile material in the form of elemental enhancements in the impact region, in 5 cases significant amounts of projectile material were detected. One such analysis is shown in Figs. 1 and 2. Fig. 1 shows ion signals of different isotopes normalized to the ^{76}Ge signal for a scan across a "spider web" impact. In Fig. 2 the selected signals of ^{27}Al, ^{28}Si, ^{40}Ca, ^{48}Ti and ^{56}Fe were normalized with relative sensitivity factors determined from laboratory studies [1] to obtain elemental abundance ratios relative to Mg. Their abundances indicate an extraterrestrial origin except for Si, which is anomalously high and is probably dominated by contamination from RTV glue used to bond the Ge plates to the Al substrate. Enough material is present to allow isotopic measurements, which will be reported at the meeting.

[1] Lange G. *et al*. (1986) *Lunar Planet. Sci.* **XVII**, 456.

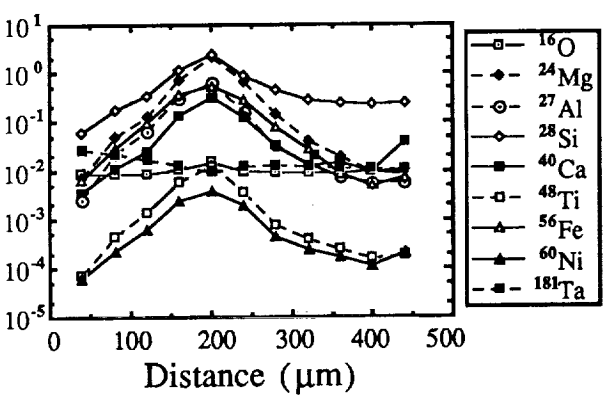

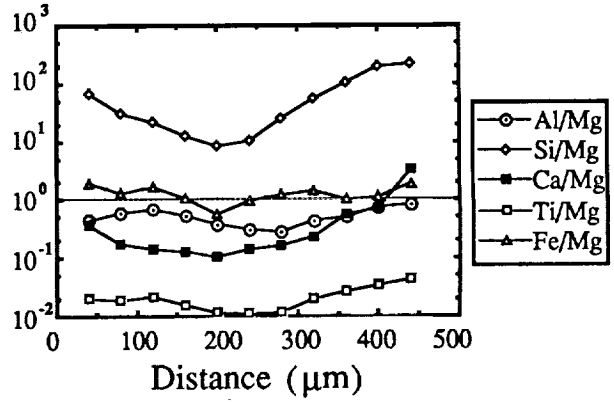

Ca, Ti AND Sm ISOTOPIC COMPOSITIONS OF FINE-GRAINED INTERSTELLAR SiC;

S. Amari[1,2], E. Zinner[1] and R. Lewis[2], [1]McDonnell Center for the Space Sciences and the Physics Dept., Washington University, One Brookings Drive, Saint Louis, MO 63130-4899 USA, [2] Enrico Fermi Institute, University of Chicago, 5630 S. Ellis Ave., Chicago, IL 60637-1433 USA.

We have extended ion probe isotopic measurements in fine-grained aggregates (≡ "bulk") of SiC from C, N, Si, Mg, Ba and Nd [1, 2] to Ca, Ti, Cr, Fe and Sm. Measurements were made on grain size fraction KJB (nominal size 0.1-0.2 μm) from the Murchison carbonaceous chondrite [3] . We used high mass resolving power for all elements except Sm which was analyzed (together with Ba and Nd) under energy filtering conditions. The results for Ca and Ti shown in Figs. 1 and 2 are averages of 16 measurements on different aggregates. The Ti pattern agrees better with the predictions for the He-burning shell of AGB stars [4] than the patterns obtained for large single grains [5] . The AGB model predicts a proportionately (relative to ^{42}Ca and ^{43}Ca) much smaller ^{44}Ca excess than what is actually observed (Fig. 2). This excess is probably due to the presence of rare exotic (≡X) SiC grains carrying large ^{44}Ca excesses [6] due to the decay of ^{44}Ti ($t_{1/2}$ = 47 years). This is indicated by large variations (from 20 ‰ to 160 ‰) of the ^{44}Ca excesses for different measurements, similar to the large variations of $^{26}Al/^{27}Al$ (grains X have a ratio of ~ 0.2 [6]) previously seen in "bulk" measurements of different grain size fractions [1] . The $^{53}Cr/^{52}Cr$ and $^{54}Fe/^{56}Fe$ ratios are normal within measurement errors. However, the concentrations of Ca and Fe are surprisingly high and it is likely that these two elements reside not in SiC but in other phases such as chromium spinels.

The isotopic measurements of Sm are complicated by the presence of isobaric interferences from Nd and Gd. We have measured masses 147, 148 and 149 and corrected for ^{148}Nd (a pure r-process nuclide). This cannot be done exactly since we do not know the composition of pure s-process Nd. An estimate was made by measuring the $^{135}Ba/^{136}Ba$ ratio and assuming the same s-process to normal mixing ratio for Ba and Nd. The Sm ratios are plotted in Fig. 3 with errors for $^{148}Sm/^{147}Sm$ that reflect the extremes of the estimated s-process Nd composition. They display an s-process signature, similar to Ba and Nd, which agrees reasonably well with theoretical predictions [7].

References: [1] Amari *et al.* (1991) *Lunar Planet. Sci.* **XXII**, 19; [2] Zinner *et al.* (1991) *Lunar Planet. Sci.* **XXII**, 1553; [3] Lewis *et al.* (1990) *Nature* **348**, 293; [4] Gallino *et al.*(1991) personal communication; [5] Ireland *et al.* (1991) *Ap. J. (Lett)* , in press; [6] Zinner *et al.* (1991) this volume; [7] Käppeler *et al.* (1989) *Rep. Prog. Phys.* **52**, 945.

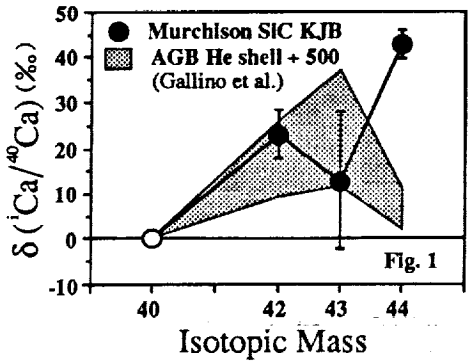

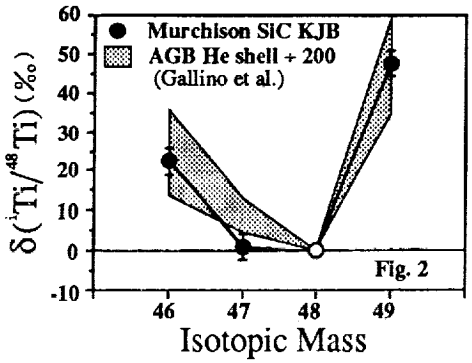

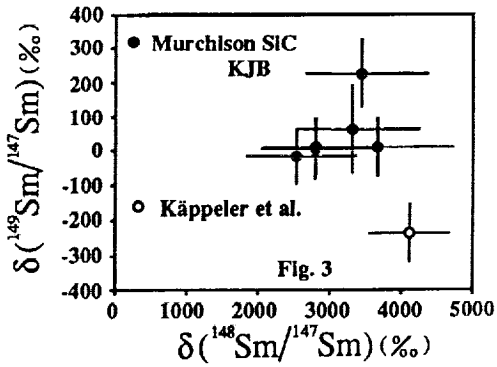

RENAZZO-LIKE CHONDRITES; A LIGHT ELEMENT STABLE ISOTOPE STUDY; R.D. Ash, M.M. Grady, A.D. Morse and C.T. Pillinger, Planetary Science Unit, Dept. of Earth Sciences, The Open University, Walton Hall, Milton Keynes, MK7 6AA, England.

Several meteorites from the Western Saharan desert have been likened, upon petrologic grounds, to the carbonaceous chondrite Renazzo. Renazzo has distinctive light element stable isotope signatures, with enrichments in deuterium and heavy nitrogen (1,2). Stepped combustion of the meteorite shows that the release profile of the carbon and the composition of its component parts are also quite unusual, although the bulk carbon isotopic signature is quite typical for carbonaceous chondrites. EET 87770, another CR, has similar isotopic properties, deuterium and ^{15}N enrichment (3).

The examined Saharan meteorites, a single find - El Djouf - and three specimens, found 500km to the north east, in close proximity to each other (Acfer 59, Acfer 139 and Acfer 186) were analysed to determine their carbon, nitrogen and hydrogen contents and isotopic compositions, along with Renazzo and EET 87770 for comparison.

The nitrogen stepped combustion analysis of El Djouf is very similar to that of EET 87770, with two yield maxima, between 400° and 600°C and between 650° and 900°C with a $\delta^{15}N$ between +120 and +180‰. Above 1000°C the $\delta^{15}N$ drops sharply, reaching minima of +22‰ in EET 87770 and -213‰ in El Djouf. This component, absent from Renazzo, may be due to presolar SiC which is ^{14}N enriched (4). Such a light $\delta^{15}N$ in a whole rock sample implies that it is present in unprecedented concentrations. The three Acfer 'CRs', analysed by single step combustion, showed lower $\delta^{15}N$ values than the other CRs, lying between +65‰ and +103‰ compared with El Djouf (+119‰) and Renazzo and EET 87770 (+163 and +158‰ respectively).

The carbon isotopic compositions of the meteorites lie within the field of all carbonaceous chondrites, with $\delta^{13}C$ values between -5.0 and -12‰. Stepped combustion analysis may give more unequivocal results, with Renazzo showing three distinct isotopic peaks, including a heavy carbon component (+40‰) combusting at high temperature.

The D/H signatures of the Saharan meteorites were unlike those of either Renazzo (+547 to +1054‰) or EET 87770 (+1309‰), with El Djouf showing a light isotopic composition (-71 to -159‰) and the Acfer samples a maximum enrichment in deuterium of up to +172‰.

Thus there are several isotopic similarities between the CRs and these desert meteorites, but the D/H ratios differ, whether due primary differences or to isotopic exchange during terrestrial weathering is unclear.

(1) Kolodny *et al.*, (1980) *E.P.S.L.* **46**, 149-158. (2) Kung & Clayton (1978) *E.P.S.L.* **38**, 421-435. (3) Grady *et al.*, (1991) *L.P.S.C.* **XXII**, 471-472 (4) Ash *et al.*, (1989) *Meteoritics* **22**, 248-249.

NEARBY MAIN SEQUENCE STARS WITH COOL CIRCUMSTELLAR MATERIAL:

Dana E. Backman, NASA/Ames Research Center, MS:245-6, Moffett Field, CA 94035, and Francesco Paresce, Space Telescope Science Institute, 3700 San Martin Drive, Baltimore, MD 21218

The discovery of the so-called "Vega phenomenon" was one of the most important and unexpected results of the IRAS mission. Several nearby main sequence stars were found to possess clouds of solid grains emitting strongly in the far-IR. Three of these objects (alpha Lyr = Vega, alpha Piscis Austrinis = Formalhaut, and beta Pic) were marginally resolved by IRAS. Beta Pic has since been resolved by ground-based infrared photometry and visual and near-infrared coronagraph imaging. Formalhaut has been resolved at sub-millimeter wavelengths.

The grains have typical temperatures of 50-150K and fractional bolometric luminosities (L_{grains}/L_{star}) in the range 10^{-5} to 10^{-3}. The comparable figures for the zodiacal dust in our solar system are 225 K and 10^{-7}. The spatial information available indicates that: (1) the grains are larger than interstellar grains, (2) the material may lie in disks in the stellar equatorial planes, (3) the material extends to distances of order 100-1000 AU from the stars, and (4) a zone with radius smaller than 50 AU around the central stars is relatively depleted of material. The total mass included in the small grains detected by IRAS is of order 10^{-2} to 10^{-1} earth masses, although much more mass could reside in larger, undetectable bodies.

Subsequent detailed surveys of IRAS data reveal more than 100 additional cases of main sequence stars of classes A-K having far-IR excesses with similar temperature and fractional luminosity to the three prototypes. To the extent that a determination can be made with the present small-number statistics, the amount of circumstellar material does not appear to be a function of stellar type. The 3 prototypes are all younger than 5×10^8 years, but some of the F, G, and K stars discovered in later surveys have ages estimated by various means to be $1\text{-}5 \times 10^9$ years. Thus, this phenomenon appears to be widespread and not limited to proto-planetary epochs.

Possible connection of this phenomenon to the existence of planets is tantalizing. The sizes of these clouds/disks correspond most closely to the hypothetical "Kuiper disk" component of our solar system, which is supposed to lie in the ecliptic plane outside the planetary region but well within the larger Oort cloud, providing a source for short period comets.

PIXE Measurements on the Iron Meteorite Mundrabilla S. Bajt[1] and K.L. Rasmussen[2]. [1]Max Planck Institut für Kernphysik, Postfach 103980, W-6900 Heidelberg, Germany. [2]Institute of Physics, Odense University, DK-5320 Odense, Denmark.

With the Heidelberg proton microprobe (PIXE) we have measured concentration profiles of Fe, Co, Ni, Cu, Ga, and Ge on the ungrouped iron meteorite Mundrabilla (Bajt et al. 1990). Absolute calibration of the Ni PIXE measurements were performed by analytical electron microscopy on known Fe-Ni standards.

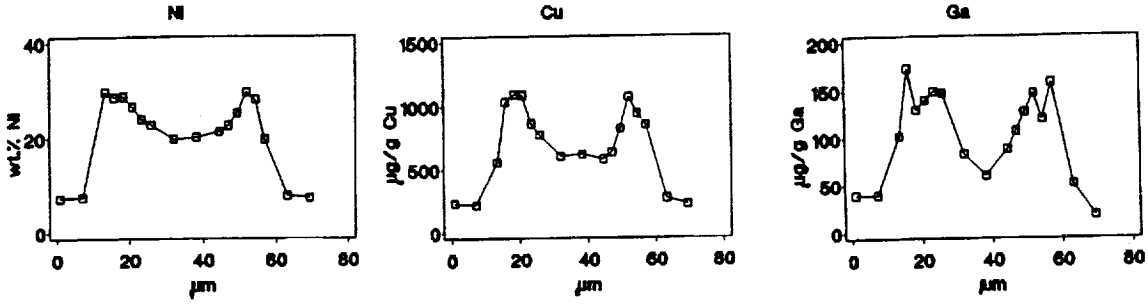

Classical cooling rate calculations of the Ni-profile were conducted (Rasmussen, 1989). Local bulk Ni and P values were not measured, but were assumed to be equal to the bulk meteorite values, 7.7 wt% Ni and 0.26 wt% P (Buchwald, 1975). A cooling rate of 400 K/My were found for Mundrabilla based on measurements of 2 taenite lamellae. This cooling rate is uncertain ca. by a factor of 2. In order to evaluate the future potential of the trace elements Co, Cu, Ga, and Ge as cooling rate indicators we calculated from our measurements two parameters for each element. The first parameter, DF, which we term the "driving force" was:

$$DF = [E_{max}(\gamma)-E(\alpha)]/E(\alpha)$$

where $E_{max}(\gamma)$ is the maximum elemental abundance in the taenite, i.e. the concentration at the rim, and $E(\alpha)$ is the average concentration in the kamacite. A higher driving force indicates a higher potential for this element to yield information about the cooling history of the meteorite. The second parameter, DS, reflects the "diffusion speed" of the each particular element:

$$DS = E_{MPC}(\gamma)/E(\alpha)$$

where $E_{MPC}(\gamma)$ is the Mid Profile Concentration, i.e. the elemental abundance in the middle of the taenite lamella. This parameter allows us to empirically compare the diffusion speed of the elements without knowing the actual diffusion coefficients. A DS value close to unity signifies relatively slow diffusion speed allowing the system to reach equilibrium, whereas a DS-value greater than one signifies faster diffusion speed and disequilibrium.

	Co	Ni	Cu	Ga	Ge
$E_{MPC}(\gamma)$	1054 µg/g	19.89 wt%	602 µg/g	83 µg/g	141 µg/g
$E(\alpha)$	2479 µg/g	7.50 wt%	236 µg/g	37 µg/g	188 µg/g
$E_{max}(\gamma)$	544 µg/g	29.79 wt%	1085 µg/g	166 µg/g	265 µg/g
DF	0.78	2.97	3,61	3,44	0,41
DS	2,35	2,65	2,56	2,23	0,75

Our measurements and calculations on Mundrabilla show that the "driving force" is highest for Cu and progressively less for Ga, Ni, Co and Ge. Our results also show that the relative diffusion speed is largest for Ni and progressively slower for Cu, Co, Ga and Ge.

References: Bajt, S., Pernicka, E. and Traxel, K. (1990) *Beih. z. Eur. J. Mineral.* **2**, 9. Buchwald, V.F. (1975) *Handbook of Iron Meteorites*. Rasmussen, K.L. (1989) *Icarus* **80**, 315-325.

DEGRADATION STUDIES OF MARTIAN IMPACT CRATERS. N. G. Barlow, SN21, NASA/Johnson Space Center, Houston, TX 77058.

Martian impact craters display a variety of preservational characteristics, ranging from very fresh to extremely degraded (1). This range in degradation states has led to numerous theories describing spatial and temporal variations in the martian obliterative history (2, 3, 4). These previous obliteration studies have relied on qualitative descriptions of martian impact crater degradation. The present study is quantifying the amount of obliteration suffered by martian impact craters by comparing measurable attributes of the current crater shape to those values expected for a fresh crater of identical size.

Crater diameters are measured from profiles obtained using photoclinometry across the structure. The relationship between the diameter of a fresh crater and the crater depth, floor width, rim height, central peak height, etc., have been determined by empirical studies performed on fresh martian impact craters (5). The corresponding values for the actual craters are measured using photoclinometric techniques (6). Errors are on the order of 5% for the photoclinometric analysis and 15% for the pristine crater estimated values. A comparison of present value to pristine value gives an estimate of the percentage change which the attribute has undergone.

In this study, we have utilized the changes in crater depth and rim height to judge the degree of obliteration suffered by martian impact craters. Initial analysis is concentrating on the proposed landing sites for future Mars surface missions (7) located within ±40° of the equator. Five sites have been analyzed to date using Viking Orbiter images of approximately 40 m/px resolution: one in the heavily cratered Arabia region and four located in various regions of the outflow channel Maja Valles. The analysis finds that crater depth values vary in a more systematic way than do rim height variations. Regional mapping of crater depth variations suggests that we can discern finer distinctions between areas of degradation than have been noted previously. Three of the five sites studied are in areas where the surrounding craters are highly degraded, suggesting that materials are likely to be very weathered in these regions. Two of the sites in Maja Valles are located in areas where crater depths are within 30-40% of their pristine values, indicating moderate amounts of obliteration. In terms of the martian relative chronology, the Arabia region dates from the period of heavy bombardment and the Maja sites formed during the post heavy bombardment period (8), indicating that a constant obliteration rate cannot explain the observed results. Slight variations in measured values among different sites are being studied for possible clues to variations in target characteristics and/or obliterative processes. This study will not only provide better information on the expected conditions at the proposed Martian landing sites, but also allow a more detailed analysis of the obliteration history of the planet.

REFERENCES: (1) McGill G.E. and Wise D.U. (1972) *J. Geophys. Res.*, pp. 2433-2441. (2) Hartmann W.K. (1973) *J. Geophys. Res.*, pp. 4096-4116. (3) Soderblom L.A. et al. (1974) *Icarus*, pp. 239-263. (4) Chapman C.R. and Jones K.L. (1977) *Ann. Rev. Earth Planet. Sci.*, pp. 515-540. (5) Pike R.J. and Davis P.A. (1984) *Lunar Planet. Sci. XV*, pp. 645-646. (6) Davis P.A. and Soderblom L.A. (1984) *J. Geophys. Res.*, pp. 9449-9457. (7) Greeley R. (1990) *NASA Ref. Publ. 1238*. (8) Barlow N.G. (1988) *Icarus*, pp. 285-305.

THE S-CLASS ASTEROID DEBATE: HISTORICAL OUTLINE

Jeffrey F. Bell (Dept. of Geology and Geophysics, SOEST, Univ. of Hawaii, Honolulu HI 96822)

The longest running argument in asteroid science concerns the mineral composition and meteoritical association of the asteroids assigned to taxonomic type S. Over the past 20 years this controversy has occupied an immense number of abstracts, funding proposals, telescope time requests, progress reports, workshop preceedings, Arizona "Blue Book" chapters, NASA SPs, CPs, TMs, JPL internal documents, and occasionally even refereed journal articles. Below are summarized the various proposed S asteroid surface compositions in roughly the order in which they appeared.

A) ORDINARY CHONDRITES: It was known long before asteroid spectroscopy began that ordinary chondrites (OCs) make up more than 75% of observed meteorite falls. Some meteoriticists of the 1960s came to believe that these fall statistics must reflect the proportions of meteorite parent bodies in the asteroid belt. Discovery of implanted solar-wind gases in OCs established that they had an extensive regolithic history at roughly the belt's solar distance (1), and that OC clasts were the second most common type of exotic material in meteorites (2). Thus when the first asteroid colors and albedos were obtained in the early 1970s there was a strong expectation that many asteroids would resemble OCs. Inevitably, when the early observations revealed an abundant class of asteroids with silicate absorption bands and OC-like albedos, many meteroriticists assumed that these were the OC parent bodies. Indeed, the spectral class "S" originally was intended to stand for "silicaceous" as "M=metal" and "C=carbonaceous" (3). Thus the original Big Three asteroid types neatly accounted for ordinary chondrites, irons, and carbonaceous chondrites. This view never gained universal support among spectroscopists since at the time there were few high-resolution spectra of asteroids and essentially none of meteorites. Indeed, 20 years later the meteroritical basis of this theory has been challenged by the discovery that OCs are virtually absent from the micrometeorites recently recovered in Antarctic and Greenland ice (4).

B) STONY-IRONS: Later, when spectra of ordinary chondrites were measured in the lab (5) it became apparent that they actually had little similarity to S asteroids other than having olivine and pyroxene absorption bands. The asteroid spectra slope steeply upward toward the red while OC spectra are flat, and the details of the silicate bands vary wildly, implying mineralogies usually far outside the OC range (6). To explain these facts it was suggested that most S-type surfaces are differentiated assemblages of metal, orthopyroxene, and olivine, similar to stony-iron meteorites such as pallasites and lodranites (7). This material would be the product of melting in the deep interiors of the asteroid parent bodies, subsequently exposed by the collisional disruption. Advocates of this hypothesis have proposed various alternate source bodies for OCs. Probably the least objectionable of these is the Q-class asteroids (8), which conveniently are all tiny Earth-crossing asteroids with low-quality spectra. But current collisional models of the asteroids require that this population be constantly replenished from a reservoir in the main belt, where no Q-types have been found.

C) WEATHERED ORDINARY CHONDRITES: Upon discovery of the continnuum slope problem, advocates of interpretation A) proposed that the red continuum of S asteroids is created by some "space weathering" process which alters the spectrum of the uppermost regolith. Usually they propose that this is associated with the metal component of chondrites, because it is obvious that pure-silicate asteroids of classes V, R, A, and E do not have any reddening. This proposal has inspired investigations of both synthetic metal-rich regoliths derived from OCs (9) and natural OC parent body regolith material preserved in some meteorite breccias (10). All these studies demonstrate that "weathered" OC material does not redden, but rather becomes spectrally flatter and in extreme cases approximates a C-type spectrum, never an S-type. In fact this similarity leads some to propose that the OCs actually come from C-type asteroids (11).

D) CARBONLESS CARBONACEOUS CHONDRITES: When the first near-IR spectra of S asteroids revealed that most had higher ol/pyx abundance ratios than any OC, it was proposed (12) that they represented unknown types of chondrites, specifically material with the silicate composition of carbonaceous chondrites but no carbon. But since no such meteorites have ever fallen on Earth, this hypothesis requires its advocates to abandon the very fall-statistics argument that had originally inspired the chondritic interpretation of S-types in the first place. Furthermore, the asteroid Flora which was cited in (12) as the most OC-like of the S-types in terms of ol/pyx abundance ratio was later shown to have large variations in silicate mineralogy between different regions of its surface, unlike the trends found in chondrite classes (13). As a

result, this hypothesis is almost forgotten, except by die-hard supporters of interpretation A) above who mistakenly cite (12) as supporting them.

An alternate explanation of the excess of olivine observed in most S-astreroids is that differential comminution of olivine and pyroxene grains during regolith gardening causes the two minerals to assume different particle sizes. Synthetic regoliths created by laboratory impacts (14) show that such an effect is small, and would act in the wrong direction to account for the S-asteroid/ OC discrepancy.

E) EVERYTHING: The mounting spectral evidence for wild variations in composition between different S asteroids and even across the surface of individual ones (15) leads some workers to wonder if both schools might be right. It is impossible to rule out some chondritic areas on the surfaces of S asteroids with the current data, if one allows some other areas to be made of extreme differentiated mineralogies (e.g. pure metal or pure olivine). Since we observe an entire "hemisphere" at once with Earth-based telescopes the chondritic areas could not be separated from the differentiated areas. Current ideas about asteroid differentiation lean toward such a complex pattern of heating. The fatal objection to this theory is that the actual OC breccias do not contain differentiated clasts, which would be sure to exist in the regolith of a "patchwork asteroid".

F) NOTHING: Alternatively one may take the wide variety of S spectra to indicate that there is really no such thing as a unified "S-type asteroid", but a variety of different objects with different origins and histories which we have not yet properly distinguished. For instance, the Eos asteroid family contains objects formally classified S in most systems, but with IR spectra that closely match those of CO or CV chondrites. A new class "K" was recently created to contain these objects (16). But this probably does not herald the beginning of the end for Class S. There does seem to be a hard core of well observed objects with classical S properties that will always remain even if some of the fainter objects which have only incomplete spectral data later turn out to be something else.

THE CURRENT POSITION: At present almost all scientists actively involved in research on asteroid composition appear to hold some version of interpretation B. In fact, no full journal article defending any other view has appeared for at least 10 years (the closest approximation being (17)). Yet some of them (especially C) continue to be defended vigorously in less formal situations. None can be rigourously excluded on the basis of current data, and very little new data is being collected due to funding and personnel shortages.

REFERENCES: (1) E. Anders, *Icarus* **24,** 363-371. (2) E. Anders, *NASA CP-2053*, p. 57-75; P. Pellas, *Meteoritics* **23,** 296. (3) C. R. Chapman, D. Morrison, and B. Zellner, *Icarus* **25,** 104-130. (4) D. E. Brownlee, *LPS XXII*, 147-148; W. Klock and W. Beckerling, *LPS XXII*, 725-726; I. M. Steele, *LPS XXII*, 1321-1322; J. F. Bell, this volume. (5) C. R. Chapman and J. W. Salisbury, *Icarus* **19,** 507-522; M. J. Gaffey, *J. Geophys. Res.*, **81,** 905-920. (6) M. J. Gaffey et al., *LPS XXI*, 399-400. (7) M. J. Gaffey and T. B. McCord, *Space Sci. Rev.* **21,** 555-628. (8) J. F. Bell et al., in *Asteroids II*, (Univ. Arizona Press), p. 921-945. (9) M. J. Gaffey, *Icarus* **66,** 468-486. (10) J. F. Bell and K. Keil, *Proc. LPSC 18th*, 573-580. (11) D. Britt et al., LPS XX, p.111-112. (12) M. Feierberg et al., *Astrophys J.* **257,** 361-372. (13) M. J. Gaffey, *Icarus* **60,** 83-114; H. Y. McSween et al, *Icarus* **90,** 107-116. (14) F. Horz et al., *LPS XVI*, 362-363. (15) M. J. Gaffey and S. J. Ostro, *LPS XVIII*, 310-311. (16) J. F. Bell, *Meteoritics* **23,** 256-257; E. F. Tedesco et al., *Astron. J.* **97,** 580-606. (17) G. W. Wetherill and C. R. Chapman, in *Meteorites and the Early Solar System*, (Univ. of Arizona Press), p.35-67.

SIZE-DEPENDENT COMPOSITION IN THE METEOROID/ASTEROID POPULATION: PROBABLE CAUSES AND POSSIBLE IMPLICATIONS. **Jeffrey F. Bell** (Planetary Geosciences Division, Dept. of Geology and Geophysics, Univ. of Hawaii at Manoa, Honolulu HI 96822)

Much evidence suggests that the meteorite/asteroid population exhibits a marked change in mineralogical composition with size, and that this variation is correlated with mechanical properties of the material. Consider the following four size ranges of projectiles striking the earth within the last million years:

1) Crater-forming projectiles (≥5000kg): All meteorite fragments found in association with recent observed craters are irons (~10) or stony-irons (~3) (1).

2) Non-Antarctic meteorite falls (~5kg): As is well known, this population contains only 15.6% irons and stony-irons, while there are 72% ordinary chondrites, 9.4% achondrites, and 3.1% carbonaceous chondrites by weight (2).

3) Antarctic meteorite finds (~10gm): The average size of this population is smaller that the traditional meteorite population, due to the careful search methodology employed and the ease of recognising small meteorites against the blue ice background. This population is 5.8% irons, 88.6% ordinary chondrites, 3.1% achondrites, and 2.5% carbonaceous chondrites by weight (2).

4) "Cosmic spherules" (~0.001gm): This population of 0.1-1mm particles found in Antarctic and Greenland ice has attracted considerable attention because studies of atmospheric entry heating show that particles in this size range cannot survive entry on typical cometary orbits. Therefore they should be of purely asteroidal origin, unlike the smaller (<10μm) stratospheric dust particles whose origins continue to be controversial (3). Furthermore, objects of this size range can be brought in from anywhere in the asteroid belt by Poynting-Robertson drag, while conventional meteorites are thought to come from narrow regions of resonant or chaotic orbital behavior. These arguments recently led to detailed studies of large numbers of these patrticles in the hope of seeing an unbiased sample of asteroid composition. Contrary to all expectations, this population was found to be predominantly CM chondrites (4).

The trend is clearly for increasingly smaller size fractions to be more dominated by mechanically weaker materials, suggesting that differential fragmentation is the cause. But is this fragmentation in space due to collisions with other particles, or fragmentation in the Earth's atmosphere? Several lines of evidence suggest that at least a significant portion of the effect must be due to collisions in space. Virtually the first result of lunar regolith studies was the discovery of a ubiquitous component of CI or CM material in the intercrater lunar regolith, attributed to gardening by carbonaceous chondrite dust (5). However, later studies of regolith or breccias derived from specific macroscopic impacts on the moon usually identified OC or iron meteorites as the projectiles. In addition, the much greater cosmic-ray exposure ages of irons versus chondrites has traditionally been attributed to increased resistance to collisions in space.

This concept has some interesting implications. First, the obsessive search by asteroid spectroscopists for an abundant class of ordinary chondrite asteroids is based on the historical accident that "classical" hand-sized meteorites were the first asteroidal samples to be studied in detail, which created the false impression that space was filled with OC material at all sizes. Second, since this idea "contradicts 20 years of work on asteroid colllisional models" (C. Chapman, personal communication) the fundamental assumptions of these models must be reevaluated. For instance, the mechanical strengths assumed in these models are usually uniform for all projectiles and targets, and the values selected are often based on studies of basalt or dunite, both very rare in the modern asteroid belt. There is a need for collisional models which incorporate realistic mechanical properties for both different orbital zones and different layers in differentiated asteroids.

References: (1) H. Palme et al. (1978) GCA 42, 313-323. (2) W. A. Cassidy and R. P. Harvey (1991) GCA 55, 99-104; G. R. Huss (1991) GCA 55, 105-111. (3) G. J. Flynn (1991) LPS XXII, 393-394. (4) D. E. Brownlee (1991) LPS XXII, 147-148; W. Klock and W. Beckerling (1991) LPS XXII, 725-726; I. M. Steele (1991) LPS XXII, 1321-1322. (5) Keays et al. (1970) SCIENCE 167, 490-493; J. T. Wasson et al. (1975) THE MOON 13, 121-141.

THERMOLUMINESCENCE AND C-14 OF NON-ANTARCTIC METEORITES: TERRESTRIAL AGES OF PRAIRIE STATE FINDS. P.H. **Benoit**[1], **Lu Jie**[1], A.J.T. **Jull**[2], and D.W.G. **Sears**[1]. [1]Cosmochemistry Group, Dept. of Chemistry and Biochemistry, University of Arkansas, Fayetteville, AR, 72701 USA. [2]NSF Accelerator Facility for Radioisotope Analysis, University of Arizona, Tucson, Arizona 85721, USA.

Radiocarbon analysis has proved of great value for terrestrial age determinations for most non-Antarctic finds (<~40,000 years) as demonstrated, for instance, by recent work on Roosevelt Country meteorites (1-2). In theory, the decay of natural thermoluminescence (TL) should also be useful for terrestrial age determinations, although the decay rate is a function of storage temperature (3). Comparisons of C-14 terrestrial ages and natural TL levels for Prairie State meteorites made a decade ago showed a suggestive but rather poor correlation (4-5). Recently, new radiocarbon measurements were made using accelerator mass spectrometry, and we have also obtained new TL data for about half of these samples (6).

Our new TL data confirm the earlier data (4) within instrumental uncertainties (< size of the symbols in Fig. 1), but many of the earlier radiocarbon dates appear to have been in error. Fig. 1 shows the TL data plotted against the new AMS C-14 data. Also shown in Fig. 1 are the theoretical 2nd-order TL decay curves for 0 and 20 °C using the TL parameters for Lost City (3). The correlation between natural TL and ^{14}C terrestrial age is now much improved over the earlier work. The experimental data seem to follow the curve expected for an effective theoretical storage temperature slightly less than 20 °C. Only Brownfield deviates markedly from this trend. It has apparently experienced a higher average storage temperature than the other meteorites, or has had an otherwise unusual thermal terrestrial history.

We also report data on a possible new Prairie State meteorite which was recently brought to our laboratory. We are presently undertaking its characterization and conducting a search for historical documentation, but it was apparently found by paleontologist H.T. Martin in the Kansas region at about the turn of the century. Initial work seems to indicate that it is L or LL of type 5-6. The stone, although fairly rusty, possesses an extensive scalloped fusion crust surface. Its natural TL level is 7.6+-0.1 krad, approximately equal to Keyes, which, in consideration of Fig. 1, indicates a terrestrial age of >10,000 years.

1) Jull et al. (1991) LPSC XXII, 667. 2) Jull et al. (1989) GCA 53, 2095. 3) McKeever (1982) EPSL 58, 419. 4) Sears and Durrani (1980) EPSL 46, 159. 5) Boeckl (1972) Nature 232, 25. 6) Jull, Wlotzka, and Donahue (unpub. data).

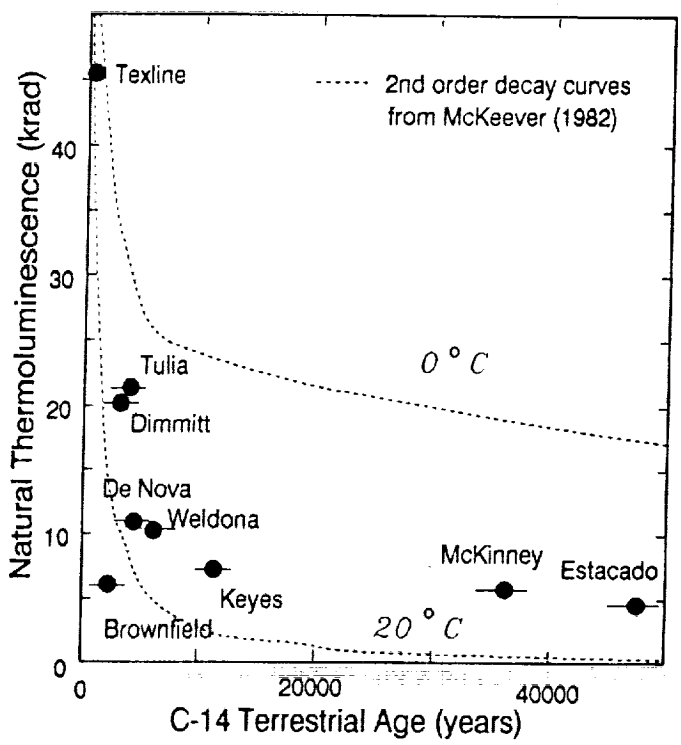

Fig. 1. Natural TL compared with terrestrial ages determined by AMS measurements for ^{14}C.

ICE MOVEMENT, PAIRING AND METEORITE SHOWERS OF ORDINARY CHONDRITES FROM THE ALLAN HILLS. P.H. **Benoit**, H. **Sears**, and D.W.G. **Sears**, Cosmochemistry Group, Dept. of Chemistry and Biochemistry, University of Arkansas, Fayetteville, AR 72701.

Almost two thousand meteorites have been returned from the Allan Hills region of Antarctica in the last decade or so (1). Since 1987, as part of the initial characterization of these meteorites, we have conducted a routine thermoluminescence (TL) survey of all returned samples large enough (>20g) for the technique (2-3) and we have also recently measured 50 EUROMET samples. We report here conclusions based on TL data for 161 meteorites from the Main, Far Western (FW) and Near Western (NW) ice fields at the Allan Hills.

We have investigated the degree of pairing in this dataset using fairly conservative criteria based on petrographic descriptions, find location, and natural and induced TL. We have identified 33 pairing groups (with 2-5 members), suggesting that our dataset contains a maximum of 123 individual meteorites.

The natural TL of meteorites from the Main field is generally low (5-30 krad), in agreement with the high terrestrial age for this field (4). The natural TL of meteorites from the NW and FW are, however, generally high (30-80 krad) in agreement with Huss' suggestion, based on meteorite concentrations, that these fields are much younger than the Main field (5). At all three fields there is a tendency for meteorites with low natural TL to be found down ice, suggesting that the Whillans-Cassidy mechanism for meteorite concentration is applicable to individual icefields as well as on a regional scale.

The induced TL sensitivity of the Allan Hills meteorites are generally lower than those of non-Antarctic falls which is either largely or wholly the effect of weathering (6). The induced TL peak temperature-width data of H-chondrites, which are not affected by weathering, show a broad range in temperature which differs significantly from the non-Antarctic falls and portions of the Lewis Cliff field (7). This suggests that at least a portion of the older Antarctic meteorites have experienced different thermal histories than younger Antarctic meteorites and modern falls as was noted earlier (8).

The 1988/89 German-American expedition (9) discovered a number of meteorites in a previously barren area along the escarpment west of the major meteorite concentration at the Main field. Ten of these are H5-6 chondrites ([ALH88026, 88030, 88033, 88035], [88029, 88042], [88018,88042], 88016, 88017) with atypically high (>100 krad) natural TL. Although our conservative pairing criteria separate these meteorites into three pairing groups and two unpaired samples, we think it likely that all ten are actually paired. This group is noteworthy for its extremely high natural TL, higher than most non-Antarctic falls. The fairly high degree of weathering indicates that the group is not a modern fall but its high natural TL and the number of fragments indicates that it is certainly younger than most Antarctic meteorites. The shower mmust have experienced an unusual radiation history to have orginally acquired such high natural TL levels. .

1) Schutt (1990) LPI Tech. Rep. 90-03. 2) Score and Lindstrom (1990) Ant. Met. Newsletter 13(1). 3) Benoit et al. (1990) Ant. Met. Newsletter 13(3), 20. 4) Nishiizumi et al. (1989) EPSL 93, 299. 5) Huss (1990) Meteoritics 25, 41. 6) Benoit et al., (in press) Meteoritics. 7) Benoit et al. (this meeting). 8) Haq et al. (1988) GCA 52, 1679. 9) EUROMET, LPSC XXII, 359.

Supported by NASA grant 9-81 and NSF grant DPP8817569.

THERMOLUMINESCENCE OF METEORITES FROM THE LEWIS CLIFF: ICE MOVEMENTS, PAIRING, ORBIT, AND ANTARCTIC/NON-ANTARCTIC COMPARISONS. P.H. **Benoit**, H. **Sears**, and D.W.G. **Sears**. Cosmochemistry Group, Dept.of Chemistry and Biochemistry, University of Arkansas, Fayetteville AR 72701.

The Lewis Cliff region has been a prolific source of meteorites. To date, with sampling basically completed, approximately 2000 meteorite fragments have been returned from this area (1). We have been engaged in a routine thermoluminescence (TL) survey of these meteorites as part of their initial characterization (2-3). We had noted several interesting features in the data (4) but only recently have we been able to examine the data in detail in the light of field and petrographic observations. We present here data for over 300 meteorites, this subset consisting of larger (>20g) samples which are suitable for this analysis.

The Lewis Cliff site consists of two major geographic divisions, the Lower and Upper ice tongues (LIT and UIT, respectively), and several adjoining sites (Meteorite Moraine and South Lewis Cliff). The Lewis Cliff site is younger than most of the Allan Hills sites and this is reflected in the generally higher natural TL values in the Lewis Cliff samples. Within the Lewis Cliff sites, however, there is evidence that the UIT has meteorites with lower natural TL than the LIT and Meteorite Moraine. This suggests that the UIT consists of older ice relative to the other sites. This difference between the adjoining LIT and UIT is accentuated by the differences in shape and orientation of 27 pairing groups; those of the UIT are strongly oriented N-S while those of the LIT are randomly oriented and are often non-linear. All the icefields have a similar percentage (~15%), after accounting for pairing, of very low natural TL meteorites (<5 krad), which reflects the proportion of meteorites with low perihelion orbits (5).

The induced TL sensitivity of most of the Lewis Cliff samples is significantly lower than those of non-Antarctic falls, a difference which can be attributed largely or wholly to weathering (6). There are, however, differences in induced TL peak temperature-width between sites (Fig. 1) which cannot be explained by weathering. UIT meteorites have a broad range of peak temperatures similar to Allan Hills meteorites (7-8). Meteorites from the LIT and Meteorite Moraine, however, tend to approach the non-Antarctic line.

We suggest that these data show that the ice at the UIT and the LIT is "uncoupled", with the older UIT overriding the LIT and Meteorite Moraine. The older meteorites (from UIT) are similar to those from the Allan Hills while the younger meteorites (LIT and Meteorite Moraine) are more similar to modern non-Antarctic meteorites. This suggests that there are at least two populations of meteorites in the Antarctic: an older group with more varied thermal (non-terrestrial) histories and a younger group with much more homogeneous histories.

1) Cassidy (1990) LPI Tech. Rep. 90-03. 2) Score and Lindstrom ed.s (1990) Ant. Met. Newsletter, 13. 3) Hasan et al. (in press) Smithson. Contrib. Earth Sci. 4) Hasan et al. (1988) 51st Met. Soc., F-2. 5) Benoit et al. (1991) LPSC XXII, 87. 6) Benoit et al. (in press) Meteoritics. 7) Sears and Benoit (1991) LPSC XXII, 1209. 8) Sears et al. (1991) GCA 55, 1193.
Supported by NASA grant 9-81 and NSF grant DPP 8817569.

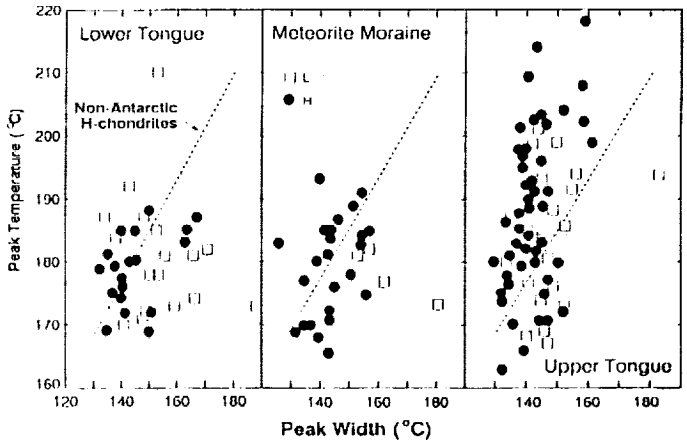

TEM CATHODOLUMINESCENCE SPECTRA OF METEORITIC MINERALS.

E.J. Benstock[1] and Peter R. Buseck[1,2]. Departments of Geology[1] and Chemistry[2], Arizona State University, Tempe, AZ., 85287-1404.

Most cathodoluminescence (CL) studies of minerals have been done using SEMs, electron microprobes, and petrographic microscopes (Luminoscopes). TEM CL measurements have been made on synthetic materials such as semiconductors. This is one of the first studies of CL of minerals using the TEM. We have been studying selected minerals in the Allende CV3 carbonaceous chondrite, following and extending the research of Steele (6, 7, 8).

We have determined that high-quality TEM CL spectra can be obtained from natural samples. TEM CL spectra are comparable in wavelengths of peaks and relative peak intensities to CL spectra from microprobes and Luminoscopes. Spectra taken at liquid nitrogen temperatures provided new spectral information. In such spectra of Allende forsterite, we found sharp peaks resembling those caused by Cr^{+3} in spinel (see Figure). Measurements of synthetic forsterites (Mg_2SiO_4 and Mg_2SiO_4:Cr^{+3}) support the conclusion that these peaks are caused by Cr^{+3}; however, the relationship between the sharp peaks from the two different minerals is not yet understood. In addition, the question remains as to the cause of the remaining broad band at 800 nm. It may be caused by Cr^{+3}, by another activator ion, or even by structural defects.

Anorthite from Allende CAIs gives a strong broad peak at 420 nm. The blue CL in lunar and terrestrial plagioclase has been related to the blue CL in forsterite and other silicate minerals (1). Blue luminescent intensity in quartz increases 1300 times when cooled to -100°C (3). Preliminary studies show that the blue luminescence in Allende forsterite increases when cooled to liquid nitrogen temperature, whereas the luminescence of anorthite is greatly decreased. This behavior suggests that the activator for blue luminescence in these minerals may not be the same. In fact, synthetic anorthites (2, 4) and synthetic forsterites from our study show no blue CL, while synthetic quartz does (3). This difference makes it questionable to attribute the blue CL to its cause in quartz (1).

References: (1) Geake et. al. (1971) *Proc. 2nd LSC* 2265-2275. (2) Geake et. al. (1974) *Proc. 4th LSC* 3181-3189. (3) Hanusiak, W.M., and White, E.W. (1975) *SEM* 126-132. (4) Marshall, D.J. (1988) Cathodoluminescence of Geological Materials 57-66. (5) Steele, I.M. (1986a) *Geochim. Cosmochim. Acta*, **50**, 1379-1395. (6) Steele, I.M. (1986b) *Am. Min.* **71**, 966-970. (7) Steele, I.M. (1988) *in* Spectroscopic Characterization of Minerals and Their Surfaces. Coyne, McKeever & Blake, *eds.* 150-164.

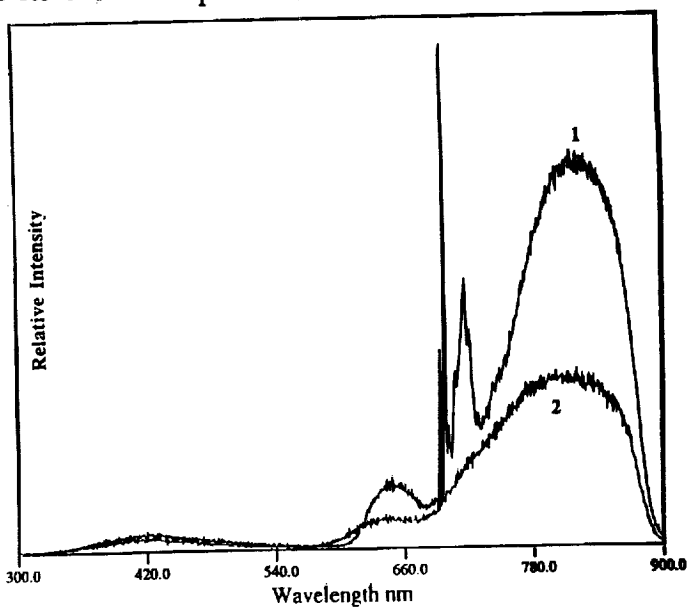

Caption: CL spectra of Allende forsterite at (1) liquid nitrogen temperature (~-170°C) and (2) room temperature. (Spectra are uncorrected for instrumental response.)

DEPTH AND SIZE DEPENDENCE OF COSMOGENIC NUCLIDE PRODUCTION RATES IN METEOROIDS. N. Bhandari[1], K. J. Mathew[1], M. N. Rao[1], U. Herpers[2], K. Bremer[2], S. Vogt[2], W. Wölfli[3], H. J. Hofmann[3], R. Michel[4] and R. Bodemann[4]

1 Physical Research Laboratory, Navrangpura. Ahmedabad, India.
2 Abteilung Nuklearchemie, Universität zu Köln, Köln, F.R.G.
3 Institut für Mittelenergiephysik, ETH Zürich, Switzerland.
4 Zentraleinrichtung für Strahlenschutz, Hannover, F.R.G.

Depth profiles of the cosmogenic isotopes ^{3}He, ^{21}Ne, ^{22}Ne, ^{10}Be and ^{26}Al have been measured in three chondrites: Madhipura, Udaipur and Bansur. Samples from known depths from the meteorite cores were chemically processed for Al and Be for measurement of ^{10}Be and ^{26}Al by accelerator mass spectrometry at Zürich [1].Track density and rare gas measurements were made at PRL. ^{53}Mn was measured in several fragments of Dhajala. ^{21}Ne exposure ages were calculated following Eugster [2]. Shielding depths of the samples and meteoroid sizes were derived from track density and the ^{21}Ne exposure ages.

The above data, together with ^{53}Mn profiles in these meteorites and depth profiles of several cosmogenic radionuclides, rare gas isotopes and tracks in ALHA 78084, Keyes, St. Severin, Knyahinya and Jilin, available in literature, provide an experimental data base describing the depth and size dependence of cosmogenic nuclides in chondrites for preatmospheric radii in the range of 8 to ~100 cm.

Production rates are found to change only slightly with depth in small meteoroids ($R \leq 15$ cm). For larger bodies ($15 < R < 30$ cm) the profiles show significant depth dependence increasing from surface to center by about 30%. The center production rates increase with meteoroid size and show a broad maxima for radii between 25 and 45 cm. The location of the maxima depend on whether the nuclides are predominantly produced from their target elements by high or low energy particles. For radii above ~ 70 cm a significant decrease of center production rates is seen for ^{10}Be, ^{26}Al and ^{21}Ne.

The observed depth profiles and the dependence of the center production rates on meteoroid size are well reproduced by model calculations based on Monte Carlo techniques using the HERMES code system [3,4,5]. The model calculations thus provide a basis for identification of meteorites having anomalous level of radioisotopes and give information about the irradiation history of meteorites and changes in the cosmic ray intensity with time or in orbital space of the meteoroid.

This work was supported by ISRO, DLR, Deutsche Forschungsgemeinschaft and the Swiss National Science Foundation.

REFERENCES [1] Herpers, U. *et al.*(1990), Nucl. Instr. Meth. Phys. Res. B52, 612. [2] Eugster, O. (1988), Geochim. Cosmochim. Acta 52, 1649. [3] Michel, R. *et al.*(1989), Lun. Planet. Sci. XX, 693. [4] Michel, R. *et al* (1990) LPI Technical Report 90-05, 86. [5] Cloth, P. *et al.* (1988), JUEL - 2203.

THE RHENIUM OSMIUM CHRONOMETER : THE IRON METEORITES REVISITED.

J.L. BIRCK, M. ROY-BARMAN and C.J. ALLEGRE (Lab. Géochimie & Cosmochimie, IPGP, 4 Place Jussieu 75252 Paris Cedex 05)

The ^{187}Re - ^{187}Os decay scheme has potentially a wide spread application in the field of geochronology. Its principal interest over the other common chronometers stands in the siderophilic nature of both elements. Its use has been limited by a number of setbacks : the level of Re and Os in natural samples is very low : generally in the sub ppb range ; due to its high ionization potential and to its refractory nature, Os has been very difficult to ionize in mass spectrometers.

The recent development of negative thermal ionization of volatile oxides (3,6) circumvents the ionization problem providing both very high sensitivy and the precision of thermal ionization mass spectrometers.

We present here some new-data making use of this technique. The Re-Os chronometer is particularly well suited for meteorites and is so far the only tool for dating directly the metal phase of iron meteorites. Among the iron meteorites, some have inclusions which have been already investigated with more traditional chronometers : K - Ar, Rb-Sr, U-Th-Pb. The inclusions of Kodaikanal have been reset for both Rb-Sr and U-Pb at 3,7 By. The purpose of this work is to investigate the metal phase itself in the hope to constrain more precisely the resetting event.

Our Re-Os experimental technique is close to those already published for the mass spectrometry (3,6). A new chemical separation method has been developed to better fit typical clean lab procedures.

Results : Os sample sizes of 5 to 10 ng provided typical precisions of 5 ε unit (10^{-4} in relative deviation) on the $^{187}Os/^{186}Os$ ratio. Ionization yields are comparable to other labs with the same method (3).

For this study, aliquots of 2 à 5 mg of iron meteorite have been used. Our measurement on Canyon Diablo is within analytical errors of previous ion probe data Kodaikanal shows a $^{187}Os/^{186}Os$ in the low end of iron meteorites close the IIIAs and the mesosiderite Estherville. Mineral separates and Re-Os concentrations are under investigation.

Sample	187Os/186Os	Error
Lab Standard	1.4455	0.0006
Canyon Diablo	1.1262	0.0009
Kodaikanal	1.0679	0.0007

References : **1)** Herr et al, Z. Natureforsch 16a, 1053 (1961) **2)** Luck J.M., Ph Thesis Paris (1982) **3)** Greaser et al G.C.A. 55, 397 (1991) **4)** Göpel et al, Nature 317, 341 (1985) **5)** Burnett et al EPSL 2,137 (1967) **6)** Völkening et al, preprint.

NEW CARBONACEOUS AND TYPE 3 ORDINARY CHONDRITES FROM THE SAHARA DESERT. A. Bischoff[1], H. Palme[2], R.N. Clayton[3], T.K. Mayeda[3], T. Grund[1], B. Spettel[2], T. Geiger[1], M. Endreß[1], W. Beckerling[1], and K. Metzler[1]. [1]Institut für Planetologie, Wilhelm-Klemm-Str. 10, 4400 Münster, Germany; [2]Max-Planck-Institut für Chemie, Saarstr. 23, 6500 Mainz, Germany; [3]Enrico Fermi Institute, University of Chicago, Chicago, IL 60637, USA.

From a total of about 300 new meteorite samples recovered from different locations in the Sahara desert in 1989, 1990, and 1991 (compare Meteoritical Bulletin No. 71, 1991), about 100 meteorites have been classified so far. Among these samples 12 type 3 ordinary chondrites (9 H3, 2 L3, 1 LL3) exist probably from 9 different falls. Three of the H3-chondrites are interesting chondritic breccias containing abundant H4-6 clasts. The LL3-chondrite Adrar-003 appears to be one of the most unequilibrated ordinary chondrites ever found. Among the other ordinary chondrites several spectacular chondritic breccias exist containing for example the rare phases ringwoodite and maskelynite (Acfer-040,-072, Hamada El Hamra-007). Besides two mesosiderites and one type IIIAB iron meteorite (Plateau du Tademait-002; Ni: 10.30 wt.%, Ga: 18 ppm, Ge: 33 ppm) a very interesting enstatite-rich meteorite exists that could be characterized as a metal-rich achondrite (Ilafegh-009).

The collection of Sahara meteorites contains a high proportion of carbonaceous chondrites. So far, 14 carbonaceous chondrites were identified resulting from at least five distinct falls (Table 1). Eight samples - CR-like chondrites (Acfer-059,-087,-097,-114,-139,-186,-187,-209) - were found within an area of approximately 45 x 12 km. A ninth CR-like sample (El Djouf-001) mineralogically very similar to and probably paired with the other eight meteorites (1) was found >500 km SW of the Acfer region. Acfer-097 has similar contents of Zn (60 ppm) and Se (4.68 ppm) to Renazzo; the refractory elements are enriched relative to CI by a factor of ≈1.4. Two CV-chondrites (Acfer-082, Acfer-086) were identified. Their refractory elements Sc, REE, Hf etc. are enriched relative to CI by a factor of ≈1.6. The sample Acfer-086 is contaminated by terrestrial products resulting in high Ca- and Sr-contents and the presence of abundant calcite. CAIs within Acfer-086 have a greenish appearance in thin section. Acfer-094 has trace element characteristics of CM-chondrites (Fe/Mn: 123; Se: 14.9 ppm; Zn: 205 ppm), but cannot be a CM-chondrite based on the oxygen isotopic composition (Table 1). Mineralogically, it appears to be a CO-chondrite. The samples Acfer-182 and -207 belong to a "unique" chondrite that clearly can be distinguished from the major chondritic groups by the peculiar mineralogical and chemical properties. They are similar to the anomalous chondritic breccia ALH85085 (2), but not identical. The Fe-content of 34.56 wt% is high like that of ALH 85085 (39.8 wt.%; (2)), and higher than in other carbonaceous chondrites. Like in ALH85085 the moderately volatile elements Na, K, Mn, Se, and Zn are depleted relative to CI by factors between 0.098 and 0.5. The refractory siderophile elements W, Re, Os, Ir, and Pt are enriched by a factor of ≈2 relative to CI.

Table 1: Oxygen isotopes

Sample	$\delta^{18}O$	$\delta^{17}O$	Class
Acfer-082	1.53	-2.93	CV3
Acfer-086	3.71	-1.48	CV3
Acfer-094	1.11	-3.91	CO/CM
Acfer-097	2.10	-1.53	CR
Acfer-182			unique
Ilafegh-013	3.68	2.66	H3

(1) Weber H.W. and Schultz L. (1991), this volume. (2) Bischoff A. et al. (1989), LPS XX, 80-81.

MID-IR SPECTROSCOPY OF ANTARCTIC CONSORTIUM METEORITES: B-7904, Y-82162 and Y-86720

Janice L. Bishop and Carlé M. Pieters. *Brown University, Box 1846, Providence, RI 02912.*

Diffuse reflectance of the Antarctic Consortium meteorites Yamato (Y)-86720, Yamato (Y)-82162 and Belgica (B)-7904 has been measured from 1-25 μm. Visible and near-infared reflectance spectra of these meteorites and the implications of their physical and spectral properties are discussed in a companion abstract (1). Descriptions of the petrology and chemistry of these samples are provided by (2,3). Spectra were measured using a Nicolet 740 FTIR in a purged (water and CO_2 free) environment. B-7904 and Y-86720 were examined both as chips and as powders with particle size <125 μm. Y-82162 was examined in the chip form only due to a surface coating. Independent measurements were made with KBr and gold as standards.

Mid-IR spectra of B-7904, Y-82162 and Y-86720 against KBr from 2 - 24 μm are shown below (variable wavelength scale). Each of the meteorite samples examined shows water absorptions at 3 μm (3450 cm^{-1}) and 6 μm (1640 cm^{-1}). The weak, sharp band at 4.3 μm (2350 cm^{-1}) is due to minor variations in the CO_2 level in the sample chamber. B-7904 and Y-86720 powders exhibit mineral and hydrous features comparable to those reported by (4, 5, 6). The strength of the reststrahlen bands near 11 μm is greatly enhanced in the spectra of the chip samples relative to the spectra of the particulate samples. The Y-82162 chip exhibits significantly stronger water absorptions at 3 μm (3450 cm^{-1}) and 6 μm (1640 cm^{-1}) than the others. The 6 μm feature appears to be anomalously strong, suggesting that more that one species may be contributing to the absorption. The spectrum of Y-82162 also shows a strong feature at 6.8 μm (1470 cm^{-1}) which has been attributed to carbonates by (7, 6, 5) and CO_3^{2-} by (8). Both the particulate and chip spectra of B-7904 and Y-86720 include weak absorption features at 7.4 μm (1350 cm^{-1}). This feature has been observed in all Antarctic meteorites measured in the Mid-IR and has been assigned to hydrous carbonates formed by terrestrial weathering (9 & ref. therein).

REFERENCES: [1]C. Pieters, D. Britt and J. Bishop (1991) *Met. Soc. Mtg*, submitted. [2]R. L. Paul and M. E. Lipschutz (1990) *Proc. NIPR Symp. Antarct. Meteorites* **3**: 80-95. [3]Y. Ikeda (1989) *Fourth (Antarctic Carbonaceous Chondrite) Consortium Circular.* [4]S. A. Sanford (1984) *Icarus* **60**: 115-126. [5]J. W. Salisbury, D. M. D'Aria and E. Jarosewich (1991) *Icarus*, submitted. [6]M. Miyamoto (1987) *Icarus***70**:146-152. [7]S. A. Sanford (1986) *Science* **231**:1540-1541. [8]K.Nakamoto (1986) *Infrared and Raman Spectra of Inorganic and Coordination Compounds* (John Wiley and Sons: New York) p. 476. [9]M. Miyamoto (1991) *Geochimica et Cosmochimica Acta* **55**: 89-98.

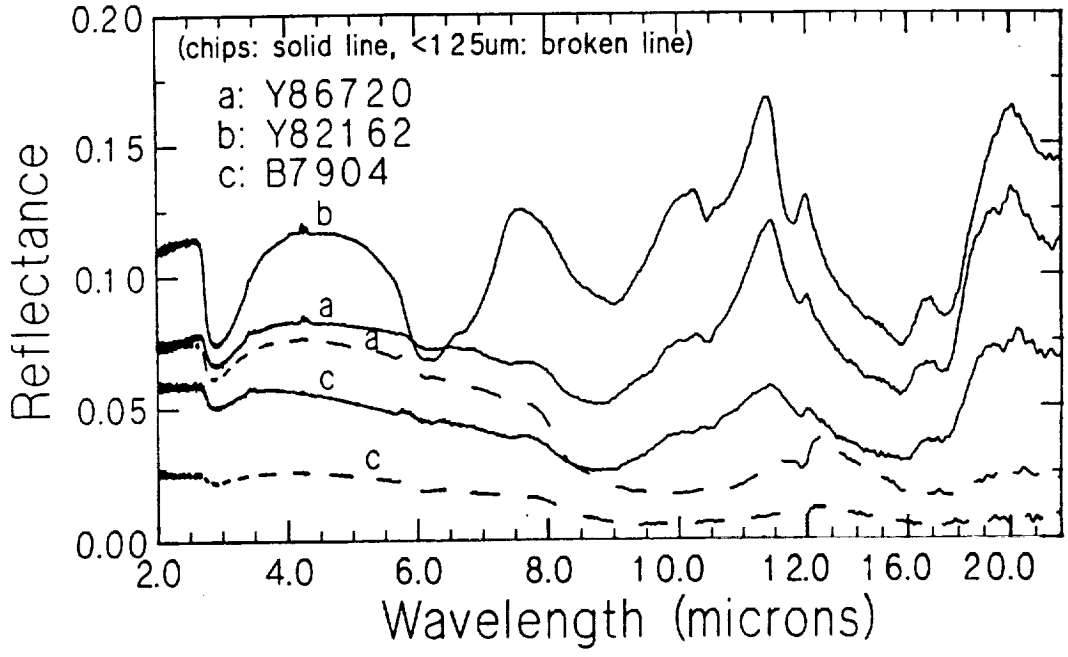

Clathrate Type II Hydrate Formation *in vacuo* under Astrophysical Conditions

Blake, D.F.,[1] Allamandola, L.J.,[2] Sandford, S.,[2] and Freund, F.[3]

[1]Planetary Biology Branch, MS 239-4 and
[2]Astrophysics Branch, MS 245-6
NASA/Ames Research Center
Moffett Field, CA 94035

[3]Department of Physics
San Jose State University
San Jose, CA 95192

Numerous authors have called on the properties of clathrate hydrates to explain the complex and poorly understood physical processes taking place within cometary nuclei and other icy solar system bodies.[1-3] However, suitable mechanisms for clathrate hydrate formation in the outer solar nebula, on the surfaces of planetesimals or in other low-pressure environments have not been identified. Recently the formation of clathrate type II hydrates was reported from vapor-deposited amorphous mixed molecular ices which were warmed in the high vacuum of an electron microscope.[4,5] There may be a variety of reasons why earlier published experiments apparently did not yield clathrate hydrates. Most importantly, most or all of the experiments previously conducted used starting compositions which would yield clathrate type I hydrates. The main criterion for type I vs. type II clathrate hydrate formation is the size of the guest molecule, which for clathrate type I is < 5.8 Å (dynamical diameter), and for type II, >5.8 Å.[3] The stoichiometry of the two structure types is quite different. A fully occupied clathrate contains ~6 mole % guest molecules for type II and ~17 mole % guest molecules for type I. In addition, the larger molecules which would form type II clathrate hydrates typically have lower vapor pressures. The result of these considerations is that at the temperatures where we have identified clathrate formation (120-130 K), it is more likely that type II clathrate hydrates will form.

We have also formed clathrate II hydrates of methanol by direct vapor deposition in the temperature range 125-135 K. This surprising result suggests that there may be other conditions, quite common in the Solar System, under which type II clathrates form. For example, if ices are vaporized by an impact, their recondensation may result in clathrates if the temperature regime is appropriate. Lastly, although clathrate type II hydrates can be formed only by relatively large molecules, there are two sites in the type II structure which may be filled by small molecules for each large site. Thus, small molecules can be passively incorporated into the smaller unoccupied cages of the type II structure either as it forms or at a later time.

1. A.H. Delsemme and P. Swings, (1952) *Ann. d'Ap.*,**15**, 1.
2. S.L. Miller, in *Physics and Chemistry of Ice*, E. Whalley,et al., eds. (Ottawa: Royal Society of Canada, 1973), pp. 42-50.
3. J.I. Lunine and D.J. Stevenson, (1985) *Astrophys. J. Supp Ser.* **58**, 493.
4. D.F. Blake, et al., (1991) *LPSC* **XXII** .
5. D.F. Blake, et al., *Science*, in submission.

A POSSIBLE ORIGIN OF EII CHONDRITES FROM A HIGH TEMPERATURE-HIGH PRESSURE SOLAR GAS

Milton Blander[1], Laura Unger[2], Arthur Pelton[3] and Gunnar Ericksson[3]
[1]Argonne National Laboratory, Argonne, IL 60439-4837
[2]Purdue University-North Central, Westville, IN 46391
[3]Ecole Polytechnique, Montreal, Quebec, Canada H3C 3A7

Calculations of condensates from a gas of "solar" composition were made to investigate the origins of EII chondrites using a unique free energy minimization computer program with a data base for the thermodynamic properties of multicomponent molten silicates as well as for solids, solid solutions and gaseous species. Because of the relatively high volatility of silicon and silica, the high silicon content of metal (2.6 mole percent) can only be produced at pressures greater than 10^{-2} atm at temperatures greater than 1475 K. At very high pressures (100-500 atm), a liquid silicate phase crystallizes at a temperature where the silicon content of the metal, the ferrosilite content of the enstatite and the albite concentration in the plagioclase are close to measured values. Thus, one attractive mode for freezing in the compositions of these three phases is the disappearance of the fluxing liquid. If the plagioclase can continue to react with the nebula without a liquid phase, then lower pressures of e.g. 10^{-1} to 1 atm might be possible. We are exploring the possibility that these assemblages might have condensed at lower pressures from gases of non-solar compositions.

^{39}Ar-^{40}Ar AGES OF ACHONDRITES: EVIDENCE FOR A LUNAR-LIKE CATACLYSM?.

D.D. Bogard and D.H. Garrison*, NASA Johnson Space Center, Houston TX 77058 (*also Lockheed-ESC)

The observation that the K-Ar, Pb-Pb, and Rb-Sr ages of a significant number of lunar highland rocks were reset in the interval of 4.1-3.8 Ga ago led to the concept of a cataclysmic bombardment of the moon during this period (e.g. 1,2). Histograms of ^{39}Ar-^{40}Ar ages of highland rocks (2,3) are strongly peaked at 3.8-3.95 Ga, 3.85-4.1 Ga, and 3.9-4.0 Ga for samples from Apollos 14, 16, and 17, respectively. Some disagreement exists as to whether these age clusters represent the termination of an ~0.6 Ga-long period of lunar bombardment or are primarily the result of resetting by a few large basin-forming events. Several lunar plutonic rocks indicate radiometric ages of 4.0-4.6 Ga (3), and some crustal rocks (e.g. anorthosites) show partial evidence of remnant ages older than 4.0 Ga, implying that some rocks either escaped the cataclysm or were incompletely reset by it. Crater densities demonstrate that during the time of formation of large mare ~3.2-3.8 Ga ago the lunar bombardment rate had dramatically decreased.

An important consideration for understanding the early bombardment history of the solar system, including the moon, is whether evidence also exists in meteorites for resetting of radiometric ages by cataclysmic bombardment of their parent bodies. The HED achondrites probably formed on a relatively large, common parent body that is known to have experienced extensive melting and differentiation about 4.5 Ga ago. Although a few HED meteorites show precise Sm-Nd or Rb-Sr isochrons of 4.46-4.56, others show considerable disturbance of radiometric systems, particularly K-Ar, probably caused by early impact metamorphism and brecciation on the parent body. A comparison of ^{39}Ar-^{40}Ar ages of achondritic meteorites with ages of lunar highland rocks should help elucidate the nature of the early bombardment of the solar system.

We are participating in various consortia studies of primarily Antarctic eucrites and howardites for which we have measured ^{39}Ar-^{40}Ar ages of various clasts and matrix samples. Some of these analyses have not been previously reported. Included in these data are ages of 3.9-4.0 Ga for two different clasts from howardite EET 87509 and a clast from polymict eucrite Yamato 790020, and ages of 3.4-3.5 Ga for clasts from polymict eucrite Yamato 791186 and monomict eucrite Yamato 792510. We have classified our data and literature data for ^{39}Ar-^{40}Ar analyses of HED meteorites into three groups: 1) most of the Ar release indicates a single age; 2) a significant fraction of the Ar release gives a common age, but some phases may have lost additional Ar or some phases may not have been completely degassed of Ar; and 3) a specific age is not suggested by the release. A histogram of ^{39}Ar-^{40}Ar ages of eucrites and howardites for the first two groups spreads between 3.4 and 4.4 Ga, but apparent age clusters occur at ~3.5 Ga and ~4.0 Ga. Ages from data group 1 fall in both age clusters. ^{39}Ar-^{40}Ar ages of 14 mesosiderites, another class of differentiated meteorite probably from a different parent body, are strongly clustered at ~3.8-4.1 Ga. Although the data base for impact metamorphic ages of HED meteorites is much smaller than that for the moon, these data suggest that at least two large meteorite parent bodies experienced significant impact metamorphism ~3.8-4.1 Ga ago, the same time period that the moon apparently experienced intense bombardment. Significant, early impact bombardment on meteorite parent bodies coincident with its occurrence on the moon would require that the process was spread across much of the solar system and would strongly imply that many craters observed on the Martian cratered terrain and on Jovian satellites also formed at the same time. The smaller cluster of HED ages at ~3.5 Ga does not have a known lunar counterpart.

It appears from the limited number of Sm-Nd and Rb-Sr isochron data that the ages may not be as completely affected for HED meteorites as for lunar highland rocks, an observation that might be due to the larger size of the moon. Given the same source of impacting objects, the fraction of material heated for a sufficient time/temperature to cause age resetting may be larger on the moon than on asteroids for more than one reason. Recent studies suggest that larger impactors may generate a greater fraction of strongly heated material (4), and larger craters are possible on the moon compared to asteroids before the parent would be disrupted. In addition, strongly heated ejecta may be spread further from the crater on asteroids compared to the moon (5), and this thinner ejecta on asteroids can be expected to cool faster and thus be less likely to experience age resetting.

(1) F.Tera et al, EPSL **22**, 1974; (2) B.V. Project, Ch.7.3, 1981; (3) L.Nyquist & C.Shih, GCA **55**, 1991; (4) M.Cintala & R.Grieve, LPS XXII, 1991; (5) M.Cintali et al, Proc.LPSC 9th, 1978.

K/T SPHERULES ARE ALTERED MICROTEKTITES; Bruce F. Bohor and William J. Betterton, U.S. Geological Survey, Box 25046, MS 972, Denver, CO 80225

Several years ago we proposed that the hollow spherules found in K/T claystones at both nonmarine sites in the Western Interior of North America and at marine sites worldwide were altered microtektites (1). The objects in question are type 1 spherules as defined by Bohor and Betterton (2). Type 1 spherules are characterized by completely spherical or other splash-form morphologies, usually hollow or secondarily filled, with thin outer walls replaced by secondary minerals and containing no magnesioferrite (spinel group) minerals. Although all of the hollow spherules that we studied are altered and none of the original material remains, several factors indicate that these bodies originally were solid droplets of impact glass thrown out from the crater during the melt ejection phase (1). The outer rims of these glass droplets were rapidly replaced by secondary minerals soon after deposition. The glassy cores, however, were slowly dissolved away, and some of the resulting hollow spherules were later filled by precipitates of secondary minerals.

Recently, the discovery of type 1 spherules preserved with original glassy cores intact at K/T boundary sites in Haiti (3) has reinforced our hypothesis. The Haitian spherules are either perfectly spherical or have splash-form shapes similar to tektites or microtektites. Their thin, smooth, outer shells are composed of smectite, with cores of pitted and scalloped black glass. Where solution of the glass cores is complete, the spherules are either hollow or filled with secondary smectite or barite. Thus, except for expected differences in maximum size and replacement minerals, the Haitian K/T spherules are nearly identical to spherules in the melt ejecta (kaolinitic) layer of the Western Interior sites (4).

The significance of the glass-cored Haitian K/T spherules is two-fold. Firstly, their close similarity to the type 1 hollow spherules in the kaolinitic layer of the Western Interior strongly supports the interpretation that the latter also originated as impact-generated glass droplets, and that the kaolinitic claystone containing them is an altered impact ejecta layer. Both of these concepts have been questioned by others (5). In support of this association of spherules and impact ejecta, instances of tektites and microtektites coexisting with shocked minerals and other ejecta have been documented recently from two younger impact horizons (6,7). Secondly, chemical analysis of the glass cores shows that the target rocks were predominately siliceous (3), indicating that the bolide struck continental crustal rocks. We have maintained this same conclusion for many years based on ejecta mineralogy, in opposition to those who argued that the target was oceanic crust, an interpretation based on geochemical data. Thus, the discovery of spherules with preserved glass cores strongly supports our two-stage model of a single impact into continental crust, as well as the interpretation of type 1 spherules as altered microtektites.

REFERENCES: (1) Bohor, F.B. and Betterton, W.J. (1988) Meteoritics **23**, 259; (2) Bohor, B.F. and Betterton, W.J. (1990) LPSC **XXI**, 107-108; (3) Sigurdsson, H., D'Hondt, S., Arthur, M.A., et al. (1991) Nature **349**, 482-487; (4) Bohor, B.F., et al. (1987) Geology **15**, 896-899; (5) Izett, G.A. (1990) GSA Spec. Pap. **249**, 100 pp.; (6) Bohor, B.F., Betterton, W.J. and Foord, E.E. (1988) LPSC **XIX**, 114-115; (7) Glass, B. (1991) EOS **72**, 181.

Acknowledgements: We thank D. Larue, Univ. of Puerto Rico, for samples of the Haitian K/T layer. Work partially supported by NASA Grant T-5715.

MAXIMUM SHOCKED GRAIN DIMENSIONS FROM K/T EJECTA, WESTERN INTERIOR; Bruce F. Bohor and William J. Betterton, U.S. Geological Survey, Box 25046, MS 972, Denver, CO 80225

We analyzed samples from several K/T boundary locations in the Western Interior of North America to determine if a lateral size gradation exists in shocked mineral grains from this ejecta. Previous analyses (1,2) showed no discernable progressive variation in grain size between these locations. Sampling locations ranged from the southernmost sites, located in the Raton Basin, Colo. (Starkville South and Berwind Canyon), northward through sites at Dogie Creek, Wyo.; Brownie Butte, Mont.; Morgan Creek and Frenchman Valley, Saskatchewan; to Scollard Canyon in the Red Deer Valley, central Alberta, Canada.

Sampling was controlled to eliminate contamination, utilizing blocks of the boundary claystone cut and preserved in the field whenever possible. The entire thickness of the upper fireball layer and the top portion of the underlying melt ejecta (kaolinitic) layers were sampled at each site. The upper part of the kaolinitic layer was included in the sampling because it was observed that some of the largest shocked grains occurred in this position. Presumably, these large, heavy grains settled out of the fireball plume early in its depositional history and became incorporated into the top of the still-soft melt ejecta layer. Original whole sample weights ranged between 40-125 gm. Only mild dispersal treatments were used to remove clay minerals and no acid-etch treatments were applied. Clay-free residues were sieved to isolate the largest grain sizes for microscopic examination. Maximum grain dimensions were measured microscopically using a calibrated reticle; grains also were checked for the presence of shock lamellae.

Detailed examination of the Scollard Canyon site in Red Deer Valley, Alberta, Canada, revealed evidence of severe contamination. The basal melt-ejecta layer was deposited directly on a muddy sand, resulting in detrital grains being incorporated into the ejecta. The upper fireball layer was also contaminated in this way, as well as by rooting and soft-sediment injection of the sand and basal ejecta material along vertical fractures. Detrital grains of the underlying sandstone were observed in the residues of both ejecta layers at this site. Therefore, previously reported geochemical and mineralogical data (3,4) on this site are severely compromised by this contamination, accounting for the anomalous results and interpretations. Our size analysis was not affected greatly by this contamination because we restricted our measurements to the shocked grains.

Results: Averaging the two Raton Basin samples together, the maximum shocked grain dimension for this location equalled 0.764 mm; Dogie Creek = 0.604 mm; Brownie Butte = 0.572 mm; Morgan Creek and Frenchman Valley = 0.483 mm; and Scollard Canyon = 0.467 mm. Thus, these results show a progressive decrease of maximum shocked grain size from south to north for these sites and indicate a probable locus for the putative K/T crater somewhere south of the North American continent. No evidence for the influence of the Manson impact crater, 800 km to the east of the Dogie Creek site, is indicated by these analyses.

References: (1) Bohor, B.F. and Izett, G.A. (1986) LPSC **XVII**, 68-69; (2) Izett, G.A. (1990) GSA Spec. Pap. **249**, 100 pp.; (3) Grieve, R.A.F. and Alexopoulos, J. (1988) Can. Jour. Earth Sci. **25**, 1530-1534; (4) Sharpton, V.L., Schuraytz, B.C., et al. (1990) GSA Spec. Pap. **247**, 349-357. Work supported by NASA Grant T-5715.

Detection of cosmic dust particles : data from COMET experiment and FRECOPA payload

J. Borg[1], B.Vassent[2], J-P.Bibring[1], J-Cl. Mandeville[3] and R.Laval[4]
1: IAS Bat 120 - 91406 Orsay; 2: CSNSM Bat 108 - 91406 Orsay; 3: ONERA-CERT 31000 Toulouse; 4: LEF Bat 221, 91406 Orsay.

Collectors of interplanetary matter have been exposed to space on board Saliout 7 in October 1985 (COMET experiment) and LDEF from 1984 to 1990 (FRECOPA payload). We compare here the results concerning hypervelocity impact features for grains with diameter ≤ 10 µm on the two types of experiments.

The instruments. - On COMET experiment, collectors consisted of high purity Au or Ni modules, of 2 cm^2 area, covered by an ultrathin (100 nm) Au film, having 2 main functions : i) protection against contamination, ii) identification of impact positions. 576 modules were allocated in 4 boxes opened and closed by the cosmonauts (1).

The FRECOPA tray was opposed to the velocity vector on LDEF. Thus, more than 95% of the particles impacting should be interplanetary dust particles (2). We analyzed thick Al targets of a few cm^2.

In both experiments, we could estimate size distribution of the impact features, allowing the evaluation of the incident microparticle flux in the near Earth environment. We could also determine the chemical composition of the impacting particles, generally physically destroyed and mixed with target material in the process of crater formation. We used a JEOL 840 SEM, equiped with an EDAX analysis TRACOR system. The Xray detector is protected by a thin carbon window, allowing analysis of elements down to C (but excluding N).

The results. - We found respectively for the density of impact features a cumulative flux $\sim 10^{-1}$ m^{-2} s^{-1} on COMET experiment and $\sim 2.10^{-4}$ $m^{-2}.s^{-1}$ on FRECOPA payload, for particles responsible of impact features ≤ 10 µm. The last value allows to extend the flux mass distribution found for larger craters (2) to such small sizes with a very good agreement. The flux measured on COMET experiment is mainly due to orbital debris, as confirmed by the chemical analysis : more than 90% of the analyzed impacts show composition with various proportions of Ti, Zn, K and Si (paint), Al (Al_2O_3 particles) or K rich particles (terrestrial origin).

In both experiments, extraterrestrial particles show various proportions of chondritic elements : Na, Al, Mg, Si, S, Ca and Fe, associated in most cases with various proportions of C and O. For some extraterrestrial particles, C and O are found alone.

Conclusions. - The systematic presence of low Z elements, either exclusively or associated with other elements whose abundances reflect a chondritic type composition can be compared to results obtained by the PUMA and PIA experiments which analyzed the grains in the close environnment of Halley nucleus (3) and demonstrated that at least 50% of the grains within the nucleus contain a phase made of C,H,O and N atoms. We have already proposed, on the basis of simulation experiments in our lab, that it may originate from an early irradiation of the ices, during the accretion of the nucleus, by the intense wind of the pre main-sequence sun (4). The existence of grains with similar compositions, close to the nucleus and in terrestrial orbit means that they are stable and refractory enough to survive up to thousands of years in the intense solar UV field. Such refracory phases might be accounted for by an irradiation origin. It seems that grains with this CHON phase survive more easily, as if this material acted like a coating protecting the grain against destruction.

References

(1) - B.Rosenbaum, Y.Langevin, F.Baron, J.Borg, B.Vassent, J-P.Bibring and P.Salvetat Rev. Sci. Instrum.(1989) 60 (6) 1089-1091
(2) - J.C.Mandeville (1990) To be published in 28th COSPAR book
(3) - Y. Langevin et al (1987) Astron. Astrophys. 187, 7919 - 741
(4) - J. Benit et J-P. Bibring (1990) XXI LPSC, LPI, 95

AQUEOUS ALTERATION ON THE PARENT BODIES OF CARBONACEOUS CHONDRITES: COMPUTER SIMULATIONS OF LATE-STAGE OXIDATION: W.L. Bourcier[1] and M.E. Zolensky[2], [1]Lawrence Livermore National Laboratory, L-219, Livermore, CA 94550, [2]Planetary Science Branch, SN2, NASA Johnson Space Center, Houston, TX 77058.

CI carbonaceous chondrites may be the products of hydrous alteration of CV- or anhydrous CM-type materials. The CIs typically contain veins filled with carbonates and sulfates, probably indicating a period of late stage aqueous alteration under oxidizing conditions. To test this idea, computer simulations of aqueous alteration of CV- and CM-type carbonaceous were performed. For this study, simulations were restricted to the oxidation of hydrous mineral assemblages produced in simulations reported previously [1] in order to determine whether further reaction and oxidation results in the phyllosilicate, carbonate, sulfate and oxide vein assemblages typical of CI carbonaceous chondrites. Our simulations were performed at 1, 25, 100 and 150°C (the appropriate temperature range) for the CV and CM mineral assemblages reported in [1] and using the computer code EQ3/6 [2].

For both the CV- and CM-type reactants, an oxidizing assemblage of phyllosilicates, sulfates, carbonates and oxide minerals is predicted to form from pre-oxidation hydrous mineral assemblages. The sulfide/sulfate fO_2 boundary is temperature dependent, located at 10^{-55} to 10^{-70} bars, at the temperatures of interest. Predicted phyllosilicates include chrysotile, greenalite, cronstedtite, saponitic smectite and chlorite-all minerals found in CI chondrites [3]. Calcium sulfates (gypsum and anhydrite) were predicted to form only in the CV-type reactant simulation, presumably because of the higher calcium concentrations in the CV source material [1]. The small amounts of calcium in the anhydrous CM-type reactants were preferentially incorporated into calcium silicate phases in the course of our simulations. The presence of primary gypsum rather than anhydrite indicates temperatures lower than 42°C during the oxidizing event, or at least the presence of liquid water below 42°C during the late stages of oxidation.

In order to get Mg-sulfate precipitates in the simulations it was necessary to inhibit the precipitation of several stable Mg-silicate phases. This may indicate that the oxidation event was rapid relative to the overall duration of the hydrous alteration and that the Mg-silicate phases were kinetically inhibited from precipitating. It could also indicate that the oxidizing fluid was enriched in sulfate, in which case Mg-sulfates would preferentially form. The simulations predict precipitation of several carbonate phases including dolomite, calcite and various carbonate solid-solution compositions that evolved from an early-formed Ca-rich to a later Mg-rich composition. No Fe-rich carbonates were predicted to form (although they are reported from CI chondrites).

Finally, magnetite and hematite were predicted to form at all temperatures in the CV and CM simulations except for the CM reactant at 1°C, where neither phase occurred. Only magnetite is reported in CI chondrites. However, even if the oxidation event was very rapid it is likely that the ferrihydrite observed in CI chondrites resulted from terrestrial oxidation. Observations of ferrihydrite on Earth indicate that it ages rapidly to more crystalline phases such as goethite.

We conclude that CI mineralogy is consistent with hydration and later relatively rapid oxidation of CV- or anhydrous CM-type mineralogies. More simulations using an improved thermodynamic data base will more narrowly define the conditions and sources of carbonaceous chondrites.

REFERENCES: [1] Zolensky, Bourcier and Gooding (1989) *Icarus 78*, 411-425; [2] Wolery (1979) Calculation of chemical equilibrium between aqueous solutions and minerals: the EQ3/6 software package. Lawrence Livermore Nat. Lab. *Report UCRL-52658*; [3] Zolensky and McSween (1988) in *Meteorites and the Early Solar System*, pp. 114-143..

DISCRIMINANT ANALYSIS OF THE TEKTITE CHEMICAL DATA.

V.Bouška and H.Maslowská, Faculty of Science, Charles University, Albertov 6, Praha 2, 128 43 Czechoslovakia

Im the paper /1/ there was demonstrated that discriminant analysis can be used to divide the moldavites on the basis of their chemical composition into three groups, partial strewn fields which expressed their inhomogeneous fall in the Badenian. The correctness of the assignment of moldavites by discriminant analysis was as high as 97.3 %, depending on the number of required and selected quantities and a priori probabilities. Newly the compiled data of chemical composition of tektites / bediasites(n = 27), georgianites(n = 6), urengoites(n = 4), moldavites(n = 158), tektites from the Ivory Coast (n = 11), microivorites(n = 41),irghizites(n = 32), australites(n = 48), indochinites(n= 29), javanites(n = 14), philippinites(n = 34)/ having used the main elements only were presented as multivariate data in the form of star symbols (polygons). The differences and similarities among the tektite groups were apparent. The same data were tested by the mean of discriminant analysis /2/. The jackknifed classification of tektite groups was found to be correct in 78.4 %.

The method enables to use the data of main chemical composition of tektites to classify the samples and to assign newly analyzed samples to the groups. From this point of view, e.g. the moldavites from Austria are much more similar to the southern Bohemia moldavites (Radomilice subfield, České Budějovice - Třeboň subfield) than to Moravian ones, the moldavites from Dresden area (FRG) better correspond to Moravian moldavites even if the limited number of analyses was at disposal. Also the Na-rich australites from South Australia can be distinguished as a partial group in the strewn field of the Australasian tektites.

References : /1/ Bouška V., Delano J.W., Maslowská H., Řanda Z. (1991) : Acta Univ. Carol., Geologica, in press, Prague. /2/ Dixon W.J. (1989): BMDP Statistical software. - Univ. Calif. Press, Berkeley.

ELECTRON ENERGY LOSS SPECTROSCOPY OF THE FINE GRAINED MATRICES OF INTERPLANETARY DUST PARTICLES

J. P. Bradley, McCrone Associates, Wesstmont, IL 60559-1275

The fine-grained matrices of some anhydrous IDPs are dominated by 1-20 nm diameter mineral grains. Such small grains have hindered mineralogical and petrographic studies, which are critical for understanding the origins and growth/aggregation modes of IDPs. Matrix compositions have been measured using x-ray spectroscopy with spatial resolution ≈50 nm, but compositional analyses at the individual 1-20 nm mineral grains within these matrices is not possible [1]. In the absence of the necessary (x-ray) spatial resolution, electron energy loss spectroscopy (EELS) offers an alternative means of probing the compositional, crystallographic, and electronic environment of elements on an atomic scale [2]. EELS in the electron microscope is particularly suitable for fine grained materials analysis, because it is inherently more sensitive than x-ray spectroscopy, and therefore lower beam currents and smaller electron probes can be used for data acquisition.

Figure 1 shows EELS edges for iron and oxygen obtained from minerals in thin sections of IDPs. Fe and O were selected because they are major components of chondritic materials, they reside in several phases, and their core scattering edges are relatively well understood [2,3]. In IDPs, Fe is present in alloys, silicates, sulfides, and oxides, while O is present in silicates and oxides. Comparison of the core scattering edges in Figures 1a and 1b demonstrates that reduced iron (Fe^{O}) can be distinguished from oxidized iron (Fe^{2+} or Fe^{3+}). In principle, it is also possible to distinguish between Fe^{2+} and Fe^{3+} by measuring a chemical shift (≈2 eV) of the edge position [4], and possibly determine the ratio of total oxidized to total reduced iron ($Fe^{2+} + Fe^{3+}/Fe^{O}$) in an IDP thin section. Figures 1c and 1d suggest that it is possible to distinguish oxygen in a silicate network from oxygen in oxides. Core scattering edges from other important chondritic elements (e.g. C, Mg, Si, S, Mg, Ni) may also be exploited to probe their local solid state environments in the matrices of IDPs.

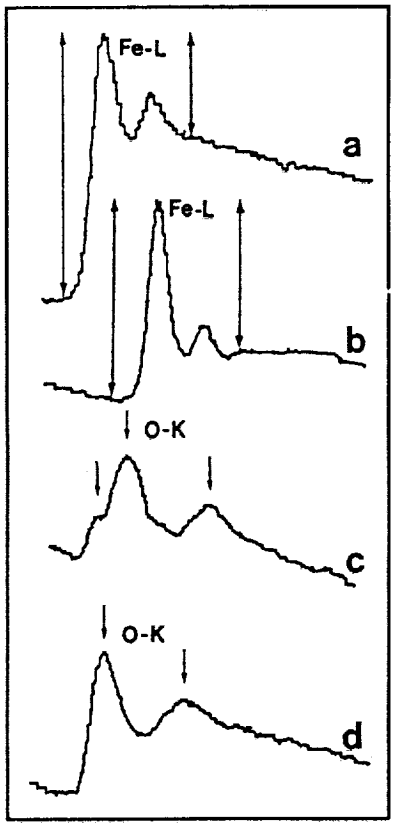

REFERENCES [1] M.S. Germani, J.P. Bradley, D.E. Brownlee, Earth Planet. Sci. Lett., 101, 162-179, 1990. [2] R.F. Egerton, Electron Energy Loss Spectroscopy in the Electron Microscope, Plenum, New York, 1986, 410 pp. [3] J. Tafto and J. Zhu, Ultramicroscopy, 9, 349-354, 1982. [4] J. Tafto and O.L. Krivanek, Phys. Rev. Lett., 48, 560-563, 1982.

FIGURE 1 Electron energy loss core scattering edges. (a) Fe-$L_{2,3}$ (≈708 eV) for Fe^{O} in kamacite [FeNi], (b) Fe-$L_{2,3}$ edge (≈708 eV) for Fe^{n+} in magnetite $[(Fe^{2+}Fe^{3+})_3O_4]$, (c) O-K edge (≈532 eV) for oxygen in magnetite, (d) O-K edge (≈532 eV) for oxygen in enstatite ($MgSiO_3$).

MINERALOGICAL AND CHEMICAL STUDIES BEARING ON THE ORIGIN OF ACCRETIONARY RIMS IN THE MURCHISON CM2 CARBONACEOUS CHONDRITE.
Adrian J. Brearley[1] and Thomas Geiger[2]. [1]Institute of Meteoritics and Department of Geology, University of New Mexico, Albuquerque, New Mexico 87131-1126 [2]Institut fur Planetologie, Wilhelm-Klemm-Str. 10, D4400, Munster, Germany.

Chondrules in CM2 carbonaceous chondrites are often mantled by up to 3 distinct rims of fine-grained material, which can be distinguished on compositional and textural grounds [1]. The diversity in the rims may represent successive generations of nebula dust that were sampled by chondrules prior to parent body accretion. This suggests that the physical and mineralogical characteristics of primitive dust must have varied either temporally and/or spatially within the nebular. We are investigating in detail the composition and mineralogy of rims in Murchison to better understand these variations as well as the aqueous alteration of rim materials. The phyllosilicate minerals in CM2 chondrite matrices are widely believed to have formed by parent body aqueous alteration [2,3], although a nebular setting has also been suggested [4]. These alternative hypotheses can be tested by examining in detail the mineralogy of rims in CM2 chondrites. Each rim represents a well-defined local bulk rock composition. During alteration on a parent body, rims with the same chemistry should produce the same mineral assemblage. In this case mineralogical studies can also determine how the local bulk composition controls the mineral assemblage which forms. Alternatively, if rims in the same meteorite with identical bulk compositions contain significantly different mineral assemblages, the implication is that the minerals formed prior to accretion, possibly in the nebula.

We have carried out detailed SEM, microprobe and TEM studies of a number of chondrule rim sequences in Murchison. Our results show that complex textural and mineralogical variations exist, both from rim to rim on the same chondrule and between rims on different chondrules. We have found, as reported previously, that inner rims are typically more Mg-rich [1]. TEM studies have revealed that within any given rim the textures and mineral compositions observed are relatively uniform and that the mineralogy and grain size observed are a strong function of the bulk Fe/(Fe+Mg) ratio of that rim. The most Mg-rich inner rims consist of pentlandites (20-40nm) set in a matrix of amorphous material and microcrystalline Mg-serpentine (1-4nm in thickness). With increasing Fe/(Fe+Mg) ratio coarse cronstedtites coexisting with pentlandite become increasingly abundant within the microcrystalline serpentine matrix. However, in the most Fe-rich rim compositions (usually outer rims), coarse tochilinite is present typically without cronstedtite and there is no evidence of rims which contain both abundant cronstedtite and tochilinite. We have also found that the abundance of anhydrous silicate phases such as forsteritic olivine varies significantly from rim to rim and is generally high in Fe-rich rims.

This study shows that there are consistent relationships between the bulk composition of any individual rim and its mineralogy. For example we have not observed any Mg-rich rims which contain tochilinite. This evidence strongly supports the idea that aqueous alteration occurred *in situ* and that the mineral assemblage which forms is controlled by the bulk chemistry of the rim. If aqueous alteration had occurred in the nebula, mixing of different phyllosilicate components would be expected, as is observed in the anhydrous rim materials in the CO3 chondrites, ALH A77307 and Adelaide [5,6]. The variation in grain size of the reaction products is probably strongly controlled by the physical properties of the precursor materials (e.g. grain size, crystalline or amorphous). For example, perhaps the inner Mg-rich rims originally consisted of amorphous material, such as that found in rim material in ALH A77307 [5]. If this is the case then individual rims must have sampled reservoirs of nebular dust with very diverse physical and, possibly chemical, characteristics. **References.** [1] Metzler, K. and Bischoff, A. (1987) *Meteoritics* **22**, 458. [2] Bunch, T.E. and Chang, S. (1980) *GCA* **44**, 1543-1577. [3] McSween, H.Y. (1987) *GCA* **51**, 2469-2477. [4] Metzler, K. and Bischoff, A. (1991) *LPS XXII*, **893**. [5] Brearley, A.J. (1990) *LPS* **XXI**, 125. [6] Brearley, A.J. (1991) *LPS* **XXII**, 133.

N92-12909

MINERALOGY OF AN UNUSUAL Cr-RICH INCLUSION IN THE LOS MARTINEZ (L6) CHONDRITIC BRECCIA. Adrian J. Brearley[1], I. Casanova[2], M.L. Miller[1] and Klaus Keil[3]. [1]Institute of Meteoritics and Department of Geology, University of New Mexico, Albuquerque, New Mexico 87131-1126. [2]SN2/Planetary Science Branch, NASA/Johnson Space Center, Houston, TX 77058. [3]Planetary Geosciences Division, School of Ocean and Earth Science and Technology, University of Hawaii, Honolulu, HI 96822.

During a petrological study of the L6 chondritic breccia, Los Martinez, we discovered a large, highly unusual Cr-rich inclusion whose mineralogy appears to be unique in both terrestrial and extraterrestrial occurrences. We have carried out electron microprobe, SEM and TEM investigations of this inclusion in order to determine its composition and mineralogy in detail and to establish its origin and possible relationship to other Cr-rich objects in chondritic meteorites. Optical studies of the inclusion (3x3 mm in size) show that it consists of a cloudy core grading into an opaque rim on the outer 200 μm of the inclusion. Backscattered electron imaging shows that this clouding is due to the presence of myriad opaque particles which are present in the core of the inclusion and increase dramatically in abundance toward the rim. Broad beam electron microprobe traverses across the inclusion show that it is compositionally highly zoned with a Si, Ca and Al-rich core. The core composition superficially resembles an anorthitic plagioclase, but in detail is significantly depleted in Si and enriched in Al relative to stoichiometric plagioclase. As the rim is approached there is a dramatic increase in the concentrations of Cr_2O_3 (24 wt%), FeO (12 wt%) and Na_2O (5 wt%), whilst CaO, SiO_2 and Al_2O_3 show concomitant decreases. TEM studies of the inclusion show that the second phase particles observed by BSE imaging are Cr-rich spinels with a grain size of 0.3-3 μm, which are set in a plagioclase host. In the very outer rim the spinel constitutes ~50 vol% of the inclusion. The spinel crystals throughout the inclusion are always oriented with respect to the plagioclase and have the crystallographic orientation relationship $[110]_{sp}//[221]_{pl}$ and $(110)_{sp}//(110)_{pl}$. Such a relationship is consistent with exsolution of the spinel at some stage during the inclusion's thermal history. Analytical electron microscope studies reveal that the composition of the spinel and the coexisting plagioclase vary dramatically along the zoning profile found by electron microprobe studies. At the rim the spinels are essentially chromite and coexist with an albitic plagioclase (Ab_{84}), but in the core spinels become more aluminous and Mg-rich and coexist with calcic plagioclase (An_{85}).

The origin and thermal history of the inclusion appears to be complex and unusual. Mineralogically and compositionally the inclusion may be most closely related to the chromite-plagioclase chondrules found in ordinary chondrites [1], although it differs considerably in texture. The zoning in the inclusion appears to be consistent with fractional crystallization from a small volume of melt, as indicated by the rapid increase in incompatible element concentrations in the rim. The origin of this melt is problematical, but it may have been a liquid condensate of some kind, because its composition (ignoring Cr) plots on the theoretical trajectories for liquid condensates in the system $(CaO+Al_2O_3)$-SiO_2-MgO [2,3]. One of the most enigmatic features of the inclusion is the problem of exactly what phase crystallized from this liquid. We believe that the spinel is the product of an exsolution reaction from a host phase, which had the local bulk chemistry of the inclusion. However, the composition of the inclusion is not consistent with any known phase and appears to be intermediate in composition between a plagioclase and a Ca-Tschermak-rich pyroxene. This phase may have been a metastable crystallization product. We suggest that exsolution and decomposition of this phase to the observed plagioclase and chromite intergrowth occurred at high temperature, probably during parent body metamorphism.

References. [1] Ramdohr, P. (1967) *GCA*, **31**: 1961-1967. [2] Wagner, R.D. and Larimer, J.W. (1978) *Meteoritics* **12**, 651. [3] Wark, D.A. (1987) *GCA* **51**, 221-242.

^{10}Be Content of Quartz Grains collected in North Victoria Land and the Glacial History of the Frontier Mountain Range in Antarctica

Bremer K., Herpers U.: Abteilung Nuklearchemie, Universität zu Köln, Germany; Delisle G.: Bundesanstalt für Geowissenschaften und Rohstoffe, Hannover, Germany; Höfle H.C.: Niedersächsisches Landesamt für Bodenforschung, Hannover, Germany; van de Wateren D.W.: Rijks Geologischer Dienst, Haarlem, Netherland; Hofmann H.J., Wölfli W.: Institut für Mittelenergiephysik, ETH-Hönggerberg-Zürich, Switzerland

During the GANOVEX expedition in 1984/85 a meteorite trap in a valley SE of the Frontier Mt. was discovered and 42 meteorites were found with terrestrial ages from recent to 710000 years (1). More than 300 meteorites have been found at this trap and on the blue ice field to the NE of the Frontier Mt. until now (2). The ice that had overridden the Frontier Mt. during the previous glacial maximum had transported away any debris out of the valley and the meteorite trap became only functional after cessation of ice overridding the mountain chain. This and the high degree of weathering of glacial features on top of the Outback Nunataks (3) suggests a high, probably Upper Tertiary age of the last glacial maximum. This view is in opposition to the opinion of Denton et al. (4), who do not rule out a "late Wisconsin" glacial maximum in North Victoria Land.

In addition to this investigations several quartz grains from ice free rock surfaces from different locations and different elevations have been taken to determine the ^{10}Be-content produced by cosmic ray interaction. The ^{10}Be analysis was done by Accelerator Mass Spektrometry technique (AMS) which is described in detail elsewhere (5). From the ^{10}Be-content the exposure ages were calculated according to Nishiizumi et al.(6), Lal & Arnold (7) and Klein et al.(8). They are expected to be roughly equivalent to the time of removal of ice after the last glaciation. The results suggests that the last glacial maximum of the Frontier Mt. region was in the Upper Neogene and give evidence against a Pleistocene maximum wich would also be in conflict with the presence of a high meteorite concentration on a blue ice field NE of the Frontier Mountains.

(1) Delisle G. et al. (1989) Geol. Jb. **E38**, 483-513
(2) Delisle G. (1991) Polarforschung, Bremerhaven (in press)
(3) Höfle H.C. (1989) Geol. Jb. **E38**, 335-355
(4) Denton G. et al. (1986) Antarctic Research Ser.**46**, 339-375
(5) Suter M. (1990) Nucl. Instr. and Meth. **B52**, 211-223
(6) Nishiizumi et al. (1986) Nature **319**, 134-136
(7) Lal D., Arnold J.R. (1985) Proc. ind. Acad. Sci. **94**, 1-5
(8) Klein et al. (1986) Radiocarbon **28** No.2a, 547-555

"Space Weathering": Are Regolith Processes an Important Factor in the S-type Controversy?

D.T. Britt, Lunar and Planetary Laboratory, University of Arizona, Tucson, AZ 85721.

"Space weathering" or, more appropriately, regolith processes, in this case refers to the changes in the texture, form, mineralogy, spectral properties, and density of surface material as a result of exposure to the chemical, radiation, accretionary, and impact environment of space. There are two basic questions involved in the role of regolith processes in the S-type controversy: Can regolith processes alter ordinary chondrite spectral properties to those of S-type asteroids? And if not, where are the ordinary chondrite parent bodies and can regolith alteration explain the apparent absence of ordinary chondrite parent asteroids? Spectrally there are two principal differences between S-type asteroids and ordinary chondrites. The first and most important is that most S-type asteroids have overall strongly reddened spectral continuum (an increase in reflectance with increasing wavelength) in the visible and near-infrared [1]. In contrast the overall continuum of ordinary chondrites tends to be flat [2]. A spectral continuum can be reddened by concentrating additional metal in the regolith or, as in the lunar case, by the production of glassy agglutinates. However, there are actual samples of asteroidal regolith soil available in the gas-rich ordinary chondrites [3] and analysis of these meteorites shows that agglutinates are rare and the metal fraction is not enhanced. In addition, the spectra of gas-rich chondrites do not show the red continuum characteristic of S-type asteroids [4] and experiments with the vitrification of ordinary chondrites also fail to redden their spectra [5]. The second difference is in the mineralogy of S-type asteroids. The olivine/pyroxene ratio, as interpreted from reflectance spectra, shows a great deal more variation [1] than is seen in the range of ordinary chondrite mineralogy [2]. In order for ordinary chondrites to achieve these ratios the olivine fraction in the regolith would have to be significantly enhanced and/or the pyroxene component significantly suppressed. Impact experiments have shown that some minerals are more susceptible to comminution than others and these more easily comminuted minerals (principally feldspar) can be enhanced in the optically critical fine-grain fraction [6]. However, it is not clear that olivine would be enhanced by this process and experiments with the comminution of ordinary chondrite material have failed to significantly change spectral characteristics [5].

If regolith processes cannot alter ordinary chondrite spectra to match S-type spectra, then where are the ordinary chondrite parent bodies? Once again we have the advantage of actual samples of ordinary chondrite regolith material to draw upon. The gas-rich ordinary chondrites generally consist of two components, light colored gas-poor clasts set in a fine grained, dark, gas-rich matrix [3]. It is the dark matrix material that represents material that has actually been on the surface of a parent body and this material has been optically altered. The optical alteration consists of reduced reflectance (darkening) and attenuation of the spectral absorption features due to the shock/heating dispersal of micron-sized metal and troilite grains [7]. One of the major effects of shock and heating on ordinary chondrite material is to redistribute the opaque metal and troilite fraction, producing significant darkening and attenuation of spectral features. Britt and Pieters [8] have suggested that if ordinary chondrite parent bodies are covered by an optically darkened regolith soil, then these asteroids would have spectral characteristics more resembling the dark, low spectral contrast C-type asteroids than the bright, high-contrast S-types. It may be that some of the inner-belt C-type asteroids are actually the source of the ordinary chondrite meteorites.

References: [1] Bell J.F. et al (1989) *Asteroids II*, 921-945. [2] Gaffey M.J. (1979) *JGR 81*, 905-920. [3] Keil K. (1982) *LPI 82-02*, 65-83. [4] Bell J.F. and Keil K. (1987) *PLPSC 18th*, 573-580. [5] Clark B.E. and Fanale F.P. (1991) Preprint. [6] Cintala M.J. and Horz F. (1987) *PLPSC 18th*, 409-422. [7] Britt D.T. (1991) Ph.D. Thesis, Brown Univ. [8] Britt D.T. and Pieters C.M. (1991) *LPSC XXII*, 141-142.

Bidirectional Reflectance Spectra of the Divnoe Anomalous Achondrite.

D.T. Britt[1], C.M. Pieters[2], M.I. Petaev[3], and N.I. Zaslavskaya[3]. (1) Lunar and Planetary Laboratory, University of Arizona, Tucson, AZ 85721. (2) Brown University, Providence, RI 02912. (3) Vernadsky Institute of Geochemistry and Analytical Chemistry of the USSR Academy of Sciences, Moscow, USSR.

The Divnoe meteorite has a number of unusual characteristics. Its mineralogy and petrologic structure are roughly similar to that of ordinary chondrites, however, many of its major element ratios are strongly different from the patterns seen in ordinary chondrites and the meteorite has no chondrules[1]. The RRE's in Divnoe are depleted in most elements except Europium, which is similar to the pattern seen in differentiated meteorites such as diogenites and brachinites [2]. The oxygen isotope ratios are distinctly different from the range seen in ordinary chondrites. Ordinary chondrites plot above the terrestrial fraction line while Divnoe tends to plot below the line and in roughly the same area as the HED meteorites [3]. Divnoe has been classified as an anomalous achondrite and interpreted as a residue material that has been depleted in Si, Al, alkalies, and REE by the extraction of small amounts of partial melt [4]. These factors suggest that Divnoe may sample the depleted source material of differentiated meteorites and as such could represent an important link in the geochemical evolution of the asteroid belt.

In hand sample Divnoe is generally dark and metal-rich with an overall coarse-grained granoblastic texture. Small areas are fine-grained and these fine-grained areas tend to appear darker and are enriched in opaque mineral., principally troilite [1]. These two areas, the coarse-grained lighter material and the fine-grained darker material, are termed the light and dark lithologies respectively. Bidirectional reflectance spectra of chips from these two lithologies were measured at Brown University using the NASA RELAB facility. Both samples were prepared by crushing to a particle size of >250 μm using a clean ceramic mortar and pestle. The spectra of the two lithologies are shown in **Figure 1**. The most striking feature of these spectra are the reflectance similarity between the light and dark lithologies. Both samples are dark due to dispersed fine-grained metal and troilite. Although there are visible reflectance differences in hand sample, as crushed powders the two lithologies have essentially no reflectance differences. This reflectance similarity may be due to the redistribution of opaques during the crushing process. Both samples show identical spectral features, a modest absorption at approximately 1.0 μm and a drop-off in the UV. The UV drop-off is typical of mafic silicates and is probably enhanced by the terrestrial weathering of the sample. The 0.5/0.6 μm ratio is 0.87 indicating moderate terrestrial weathering [5]. The broad shallow absorptions centered at 1.05 μm and 1.25 μm are indicative of olivine which accounts for between 50-63 wt. % of the sample's normative mineralogy [2]. This band is much darker and weaker than is normal for olivine, but the presence of dispersed opaques strongly attenuates the band and reduces the overall reflectance. The remainder of the spectrum is essentially featureless with a modest red slope. This is remarkable since the normative mineralogy reports between 27-16 wt. % pyroxene [2]. With this pyroxene content there should be at least a modest 2.0 μm pyroxene band. Apparently the band has been suppressed by either shock or the opaque component.

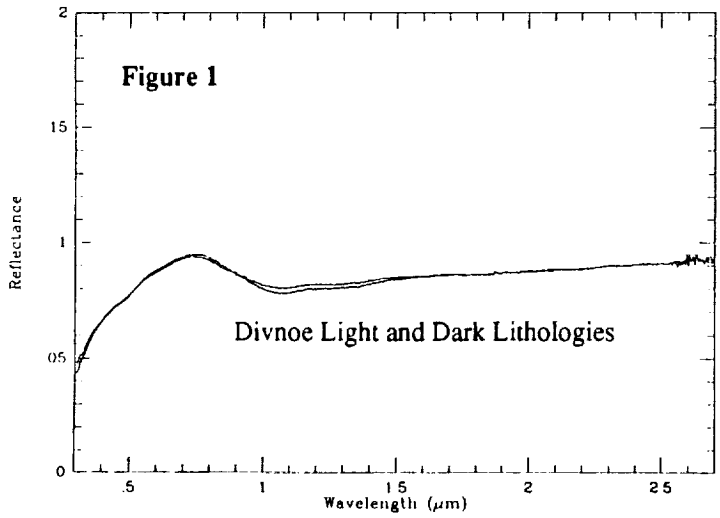

References: [1] Zaslavskaya N.I. and Petaev M.I. (1990) *LPS XXI*, 1369-1370. [2] Petaev M.I. et al. (1990) *LPS XXI*, 948-949. [3] Petaev et al (1990) *LPS XXI*, 950-951. [4] Petaev M.I. and Zaslavskaya N.I. (1990) *LPS XXI*, 946-947. [5] Salisbury J.W. and Hunt G.R. (1974) *JGR 79*, 4439-4441.

C-2

N92-12910

The Composition of Meteoroids Impacting LDEF- D.E. Brownlee[1], F.Horz[2], M. Laurance[1], R.P. Bernhard[2], J. Warren[2], and J.P. Bradley[3]. 1-Dept. of Astronomy, Univ. of Washington, Seattle, WA, 2-NASA Johnson Space Center, Houston, TX, 3-McCrone Associates, Westmont Ill

The Long Duration Exposure Facility (LDEF), recovered from a nearly 6 year exposure in low Earth orbit, has provided an unprecedentedly large number of meteoroid impact craters that can be studied in the laboratory to determine the composition of sub-millimeter meteoroids. We are currently analyzing the elemental composition of meteoroid residue found lining the interiors of craters in the high purity Al and Au exposure surfaces of the A-187-1 experiment. Although hypervelocity micrometeoroids impacting solid metal targets are usually severely altered during capture, space collection of this type provides unique information that cannot be obtained from more pristine particles collected in and below the atmosphere. One major advantage is that without bias all meteoroids produce craters that can be examined to detect meteoroid types that either do not survive atmospheric entry or are not recognized in atmospheric collections. For example, pure Halley CHON material would be difficult to distinguish from contaminants in stratospheric collections but could clearly be found in orbital collections. Another value of LDEF collections is that the spacecraft's fixed attitude relative to its velocity vector provides an important means of statistically distinguishing low velocity particles such as orbital debris and asteroid dust from high velocity cometary dust. Low velocity particles are highly concentrated on the leading edge while higher velocity particles produce a more even distribution on the leading and trailing edges. CI matrix and stratospheric IDPs of probable asteroidal origin often have large Ca depletions relative to bulk CI and we plan to test the hypothesis that Ca depletion is a common property of asteroidal dust by examining the relative abundance of chondritic composition impacts with abnormally low Ca meteoroids on the front and back of LDEF.

So far we have completed an initial SEM survey of craters in the 100μm to 1mm size range and done some quantitative analysis. Typical craters have only small amounts of residue and with variable matrix/residue geometry it is difficult to do more than semi-quanitative analysis. In these "typical" craters the residue appears to be a mixture of glass and FeNi and sulfide beads with an overall chondritic elemental compositon. In less than 10% of the craters there is a substantial amount of meteoroid debris that also contains unmelted mineral grains. The relatively high abundance of forsterite and enstatite among these irregular grains suggests that high melting point probably plays a role in surviving impact without melting. Some irregular sulfides up to several microns in size have also survived without melting. Unmelted olivine grains extracted from one crater contain faint linear defects consistent with their being solar flare tracks at a density similar to that commonly observed in stratospheric IDPs.

The initial EDX analyses of LDEF metal craters has shown that the composition of crater residues can provide valuable information on the meteoroid complex although it has also shown that impact velocity and projectile melting point provide bias in obtaining craters with abundant residue for analysis.

ZIRCONS IN *PADVARNINKAI* BRECCIATED EUCRITE. *M. Bukovanská*[1], *T.R. Ireland*[2], *and A. El Goresy*[3]. [1]National Museum in Prague, Czechoslovakia; [2]Research School of Earth Sciences A.N.U. Canberra, Australia; [3]Max-Planck-Institut für Kernphysik, Heidelberg, Federal Republic Germany

PADVARNINKAI, a Ca-rich eucrite (shergottite?), fell in 1929, on February 9, in Lithuania. A sample of 87 g (from the Meteorite Collection of the National Museum in Prague) was studied. The sample consists of three distinct parts: 1. fine- to coarse-grained eucritic clasts (pyroxenes and feldspars - bytownite), 2. a fine-grained lithology with quenched texture, presumably as a result of rapid cooling of a silicate liquid; 3. a partly glassy matrix between eucritic clasts with large pyroxenes, feldspars, and tridymites.

Pyroxenes in all parts are ranging in composition between Ca-rich augite (Wo_{45} Fs_{23} En_{32}) and Ca-low hypersthene (Wo_2 Fs_{63} En_{35}). Pigeonite is present in a small amount. Well pronounced high Ca- and low Ca- exsolution lamellae (as usual thin high Ca-lamellae in low Ca-pyroxene) indicate slow cooling within the eucritic well crystallized part 1 with the ophitic texture. Pyroxene in part 2 is only high Ca-augite, either higher in Mg (big laths) or higher in Fe. This distribution of Fe and Mg within pyroxenes shows some similarity with howarditic pyroxenes. High Al- and Ca-pyroxenes were found in part 3. *Bytownites* ($Ab_{9.33}$ $An_{90.36}$ $Or_{0.31}$) are the main phenocrysts in the eucritic clasts, and they are also present in other parts of the meteorite. *Maskelynite*, sometimes higher in Fe, is mainly present in parts 2 and 3. The high content of SiO_2-*tridymite* is typical of the brecciated and remelted parts. *Ilmenite, troilite,* metallic *iron*, and very few *apatite* are present as accessory minerals. The *chromite* chemistry differs largely. $Ti^{4+}/Cr^{3+}+$ $Al^{3+}+$ $V^{3+}+$ Fe^{3+} show a wide range of chromite chemistry and up to 3.8 atoms of Ti^{4+}.

Zircon in the ilmenite-chromite assemblage was found only in eucritic clasts in part 1. More than 10 grains of 4-25 μ were analyzed by electron microprobe. Average composition: SiO_2 32.05; TiO_2 0.91; Al_2O_3 0.09; FeO 1.46; MgO 0.03; CaO 0.11; V_2O_5 0.02; ZrO_2 64.42; HfO_2 1.15 (totals 100.22). Zr is present also in ilmenites (0.05% of ZrO_2). After the discovery of zircon in Vaca Muerta mesosiderite (Marvin and Klein, 1964), in Simmern H5 chondrite (Wlotzka, 1985), in Bouvante eucrite (Christophe Michel-Levy et al., 1987), and the recent studies of the chemistry and ion probe U-Th-Pb systematics (Wlotzka et al., 1990; Ireland et al., 1990), the U-Pb ages and rare element analyses by ion microprobe on zircons in Padvarninkai will be reported here.

References

Christophe Michel-Levy M.(1987), *Bull.Mineral.* **110**, 449-458
Ireland T.R. et.al. (1990), Abstract, *Meteoritics* Vol. **25**, No. 4, 373.
Marvin U.B. and Klein C.J. (1964), *Science* **146**, 919.
Wlotzka F.(1985), *Lunar Planet.Sci.* **XVI**, 918.
Wlotzka F. et al. (1990), Abstract, *Meteoritics* Vol. **25**, No. 4, 420.

COULD CHONDRULE RIMS BE FORMED OR MODIFIED BY PARENT BODY ACCRETION EVENTS?

T. Bunch, P. Cassen, R. Reynolds, S. Chang, NASA- AMES, Moffett Field, CA 94035
M. Podolak, Tel Aviv University, Ramat Aviv, Israel 69978
P. Schultz, Brown University, Providence RI 02912

The origin of rims on chondrules is controversial, i. e., did they form mostly from nebular or planetary processes? Although many observations of rims (e. g.,1-3), some experimental approaches (e. g., 4, 5) and a few theoretical efforts (e. g., 6) have been made over the last decade, no definitive model has appeared, possibly due, in part, to the fact that there are many different kinds of rims on chondrules in the various meteorite classes. In order to gain clearer perspective on the origin (s) of rims, a number of first-order questions should be systematically addressed: (1) What are the plausible processes responsible for isotopic differences between rims and host chondrule? (2) What is the source of Fe-enrichment and other compositional differences of rims? (3) What is the significance of rim thickness to chondrule size and the occurrence of coarse-grained rims to the formational mechanism? (4) What was the degree of rim heating? (5) What role did pro- and/or retrograde metamorphism play in the observed characteristics? (6) If rims formed by nebular processes alone, were modifications made by parent body processing (ablation, regolith impact)? (7) What is the relationship between opaque matrix and opaque rims?

We are presently addressing those questions that are testable by experimentation within our capabilities. Some of our observations on L3 (3.4-3.6) UOCs are consistent with a heating/ melting origin event for rim formation. Textures of opaque matrix and rims are similar to each other: porous to compact, fine-grained (<0.002 mm) assemblages of anhedral grains that have diffuse grain contacts suggestive of similar thermal /mechanical histories. Terrestrial ablation rinds on two of the chondrites are also similar in some textures, phase contents and compositions compared to opaque matrices and rims. In addition, very Fe-rich olivine ($Fa_{>65}$), present as crystals in the ablation rinds, contains large amounts of Cr, Na, Al, Ti, P, S, Ni and Ca similar to Fe-olivine found in Allende rim and matrix olivine (7) and in UOC rim olivine (5). Textures in some rims appear to show sintering or melt/reaction relationships with the host chondrule. Fe, Si, and Mg contents of opaque matrices and rims when projected onto the Fe-Si-Mg ternary diagram are confined within the field predicted for the crystallization of a rock melt (8). A computer code is bring used to model the thermal histories of chondrules as they pass through a gas/dust medium. Results show that chondrules with a radius > 0.2 cm and of thermal conductivity 2×10^4 ergs/°K cm, passing through a transient atm (scale height = 37 km and surface pressure of 1.53×10^3 dynes/cm^2) will begin to melt at velocities > than 3 km/s and will not reach total melting before they are stopped. Chondrules < 0.05 cm will not melt at $v < 3$ km/s, but will totally melt at $v > 4$ km/s which indicates a narrow survival window for smaller particles under these parameters. The results of sensitivity studies involving key parameters will be discussed. Finally, vertical gun experimental testing is being conducted by launching olivine/enstatite projectiles (at $v = 2$-6 km/s) into dusty atmospheres (to test ablation melting) and into low density targets (to test regolith penetration processing).

Whether or not rims are formed by parent body processes, the possibility remains for thermal and/or mechanical processing of objects with accretion velocities of 1-4 km/s.

(1) Huss G. R. *et al.* (1981) *Geochim. Cosmochim. Acta* **45**, 33-51. (2) Rubin A. E. (1984) *Geochim. Cosmochim. Acta* **48**, 1779-1789. (3) Alexander *et al.* (1989) *Earth and Planet. Sci. Lett.* **95**, 187-207. (4) Connolly H. C. and Hewins R. H. (1991) *LPSCXXII*, 233-234. (5) Bunch *et al.* (1991) *Icarus* - in press. (6) Podolak *et al.* (1990) *Icarus* **84**, 254-260. (7) Kornacki A. S. and Wood J. A. (1984) *Geochim. Cosmochim. Acta* **48**, 1663-1676. (8) Bowen N. L. and Schairer J. F. (1935) *Amer. J. Sci.* **38**, 151-217.

Al-Mg ISOTOPIC RECORD OF RECRYSTALLIZATION OF A REFRACTORY INCLUSION DURING ACCRETION INTO THE LEOVILLE PARENT BODY.

C. Caillet[1], G. J. MacPherson[1], and E.K. Zinner[2].
[1]Dept. of Mineral Sciences, Smithsonian Institution, Washington, D.C. 20560, USA.
[2]Physics Dept. and McDonnell Center for the Space Sciences, Washington University, St. Louis, MO. 63130, USA.

USNM 3537-1 is an unusual type B Ca-Al-rich inclusion (CAI), highly flattened in shape and ~3 cm in maximum dimension, from the Leoville CV3 chondrite. It has a predominantly metamorphic (porphyroblastic) texture, but elongate coarse-grained vestigial areas of "normal" type B texture occur within the CAI core. The long axes of both the inclusion and the relict coarse islands parallel the overall lineation of the meteorite. Meteorite matrix immediately adjacent to the inclusion appears in places to have been melted, with skeletal olivine crystals nucleating on the surface of the CAI. Refractory glass apparently derived from the CAI is intermixed with the matrix melt, and swirled mixtures of the two can be found intruded into fractures and crevasses on the CAI surface, but only along one side of the inclusion. The textural evidence suggests that deformation of the inclusion and melting of the adjacent matrix occurred as a result of accretion of a hot (partially molten) plastic inclusion into the Leoville parent body. Our preliminary isotopic studies of 3537-1 [1] suggested that this hot accretion of the inclusion occurred long after its initial formation with $^{26}Al/^{27}Al \sim 5x10^{-5}$. More detailed isotopic studies now clearly reveal two isotopic signatures in this inclusion (Fig. 1). Anorthites from the interior "vestigial" islands disperse near the canonical correlation line of $^{26}Al/^{27}Al \sim 5x10^{-5}$. Anorthites from the recrystallized outer parts of the inclusion disperse along a line of $^{26}Al/^{27}Al < 1.9 \times 10^{-6}$ (a line of zero slope is shown for reference in the figure), and this is especially true for those anorthites located near the zones of melted meteorite matrix. The clear association of relict "normal" type B textures with canonical initial $^{26}Al/^{27}Al$ and of recrystallized textures with essentially zero initial $^{26}Al/^{27}Al$ is compelling evidence that the isotopic systematics of 3537-1 records two major chronologic events separated by at least 3.3 million years. The lack of excess ^{26}Mg in neomineralic anorthites places the timing of recrystallization at least ~3.3 million years after formation of the original inclusion as represented by the vestigial islands. The low ^{26}Al abundance present during the inferred accretion of 3537-1 into the Leoville parent body raises anew the question of whether ^{26}Al was a viable heat source for planetary melting.

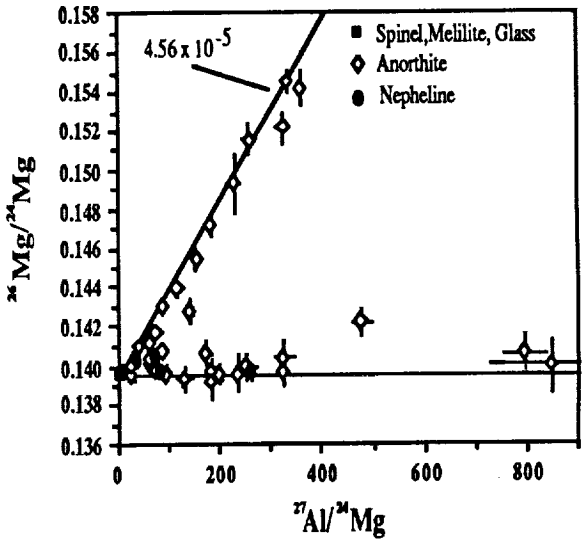

[1] Caillet *et al.* (1991) LPSC XXII, 167-8.

DISTRIBUTION OF SILICON BETWEEN KAMACITE AND TAENITE.

Ignacio Casanova. SN2, NASA-Johnson Space Center. Houston, TX 77058, USA.

Meteorites formed under highly reducing conditions can incorporate substantial amounts of Si in solid solution in their metallic phases. In enstatite meteorites, reduced Si appears in schreibersite, perryite and, in variable amounts, in the kamacite, taenite and tetrataenite[1]. Microprobe bulk analyses of Si in Fe,Ni particles of aubrites show a large variation from grain to grain (<0.02-1.4 wt.%); this large compositional range has been attributed to local equilibrium conditions in the specific T and/or fO_2 environments in which they formed[1,2]. Si concentrations are homogeneous in the kamacite; in contrast, the Ni-rich phases (taenite and tetrataenite) show a characteristic Si profile. Concentrations of this element in tetrataenite are substantially higher than in the adjacent kamacite, and decrease smoothly towards the center of the taenite grain, matching very closely the M-shaped profile of Ni (Fig. 1). Other elements with similar distribution patterns are Ge[3] and Cu[4]. A satisfactory explanation for this behavior cannot be given in the absence of experimental data for the diffusion of Si between α and γ-Fe alloys. However, two end-member possibilities can be envisioned: the distribution of Si between kamacite and taenite may be controlled by (1) the crystallographic structure or (2) the chemical composition (*i.e.*, Ni content) of the host phases. If the distribution is structurally controlled, the observed Si compositional profile would represent a higher affinity of this element for the structure of the high-Ni phases, rather than the kamacite. However, the addition of Si to the Fe (and Ge and Cu to their respective alloys) favors the formation of α-Fe, and not the γ phase, as interpreted from the sub-solidus phase equilibrium diagrams for the Fe-(Si,Ge,Cu) binary systems. This is in apparent disagreement with the observations that Si is concentrated in the taenite (γ) and tetrataenite (γ'). An additional problem to silicon distribution being controlled by structure arises from the fact that formation of tetrataenite occurs at low temperatures (~320 °C, 1 bar), at which appreciable diffusive equilibration may be difficult. On the other hand, the observed Si compositional profiles may denote a chemical effect and, consequently, the distribution of Si may depend on the Ni content of the kamacite and taenite.

Fig.1 - Ni and Si profiles in kamacite and taenite (Norton County aubrite)

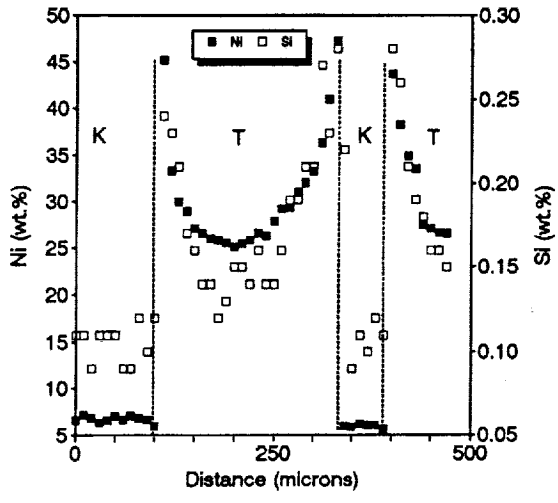

According to this, silicon and nickel would diffuse together during the sub-solidus cooling history of the metal. The main problem to this interpretation is that, while in the taenite the Ni/Si ratio is fairly constant over a wide variety of Ni contents, the $C^{\gamma'}/C^{\alpha}$ ratio is three times larger for Ni than for Si. This would suggest lack of linearity in the Ni/Si variation. Therefore, caution should be taken in assuming that Si and P may have similar effects in the growth rate of the kamacite[5,6] and, consequently, in the metallographic cooling rates of meteorites formed under reducing conditions. It should also be noted that germanium displays a very similar behavior[3] to that of Si, and the same kind of problems can be considered for both elements. Research currently in progress will be addressing this question in a systematic manner, with the aim to find further constraints to this apparently puzzling behavior.

References: [1] Casanova, I. 1990) Ph.D. Thesis. University of New Mexico. [2] Casanova I., Keil K. and Newsom, H.E. (1991) *LPSC* **XXII**, 185-186. [3] Goldstein, J.I. (1967) *JGR* 72, 4689-4696. [4] Clarke R.S., Jr. and Jarosewich E. (1978) *Meteoritics* 13, 418-420. [5] Okada A., Keil K., Taylor G.J. and Newsom H. (1988) *Meteoritics* 23, 59-74. [6] Keil K., Ntaflos Th., Taylor G.J., Brearley A.J., Newsom H.E. and Romig A.D. (1989) *GCA* 53, 3291-3307.

A GUIDE TO THE USE OF THEORETICAL MODELS OF THE SOLAR NEBULA FOR THE INTERPRETATION OF THE METEORITIC RECORD

Pat Cassen, NASA Ames Research Center, Moffett Field, CA 94035

Attempts to derive a theoretical framework for the interpretation of the meteoritic record have been frustrated by our incomplete understanding of the fundamental processes that controlled the evolution of the primitive solar nebula. Nevertheless, it is possible to develop qualitative models of the nebula that illuminate its dynamic character, as well as the roles of some key parameters. These models draw on the growing body of observational data on the properties of disks around young, solar-type stars, and are constructed by: (1) applying the results of known solutions of protostellar collapse problems; (2) making simple assumptions about the radial variations of nebular variables (e.g., that they are smooth on the large scale); and (3) imposing the integral constraints demanded by conservation of mass, angular momentum and energy. The models so constructed are heuristic, rather than predictive: they are intended to help us think about the nebula in realistic ways, but they cannot provide a definitive description of conditions in the nebula.

For instance, it is useful to know how such important physical quantities as the size of the nebula and its temperature and density depend on quantities associated with the initial conditions of star formation. It follows from the conservation of angular momentum that a disk's radius is proportional to $(J/f)^2$, where J is the angular momentum accumulated, and f is the fraction of accumulated mass retained in the disk. Neither of these quantities are well-constrained for the solar system. Current estimates of J (which cannot be determined by theoretical considerations alone) depend primarily on the amount of material believed to have been put into primordial comets. The determination of f is a major goal of dynamical theories; it is currently only weakly constrained by models of the structures of the outer planets and observations of T-Tauri star disks. For much of the nebula's lifetime, the temperature was determined by a balance between the rate at which energy was released as mass was transferred to the Sun and the rate at which energy was radiated from the nebula's surface. From this idea, and inferences drawn from the temperature distributions characteristic of T-Tauri star disks, it can be deduced that the temperature at any radius and time was proportional to (f/J). Corresponding dependencies on cloud collapse rate during the formation stage can be derived from similarly general considerations. In all cases, a sensitivity to poorly constrained parameters is revealed, which suggests that the expected range of initial conditions in the interstellar medium produces a rich variety of stellar outcomes. The derived relationships are useful for understanding evolutionary trends, generalizing the results of complex numerical simulations, focusing attention on the critical parameters, and delineating the predictive limits of current theoretical modeling.

Other results are not so sensitive to input parameters. The construction of simple models allows one to calculate the trajectories (defined as the radial positions as functions of time) of parcels of nebular gas. A general result is that much of the gas undergoes extensive radial excursions during the formation and post-accretion evolution the disk. Material that ultimately resides in the inner solar system might have previously spent considerable time in the cold outer regions. Moreover, gas from one part of the collapsing protostellar cloud is inevitably mixed with gas from other parts as it enters the nebula, even in the absence of turbulence. The degree of mixing is variable, but quantifiable in the context of the models. It may be that meteoritic evidence for the retention (on a macroscopic scale) of a degree of interstellar heterogeneity implies the rapid accumulation and decoupling of solids from nebular gas.

S-TYPE ASTEROIDS AND THE GASPRA FLY-BY; Clark R. Chapman, Planetary Science Inst., 2421 E. 6th St., Tucson, AZ 85719 USA.

The S-type asteroids are a diverse group of objects, mainly located in the inner half of the main belt and among the Earth-approachers. In some spectral parameters, the variation among S-types is nearly half the variation among all types. Although they have not been formally subdivided, the inferred mineralogies (of the silicate/iron assemblages) range from pyroxene with no olivine to the reverse, with major variations in inferred metal content.

By straightforward interpretation of reflectance spectra, most S-types seem related to stony-iron meteorites and, for a few of them, mineralogical heterogeneities strongly indicate differentiated mineralogies. However, other evidence (of variable weight) argues for a strong presumption that the parent bodies of ordinary chondrites must be found among the S-types. The evidence includes: (a) meteoritical inferences about sizes and locations of parent bodies, (b) physical models for collisional evolution of asteroids and dynamical evolution of fragment orbits, and (c) tentative but intriguing relationships between S-types and near-Earth streams.

Some researchers give weight to the remote-sensing data and believe S-types are all (or mostly) differentiated objects, while ordinary chondrite parent bodies are hiding among small, undiscovered/unmeasured objects. Others believe that the properties of asteroid regoliths (not yet well understood) may permit some or most S-types to be related to ordinary chondrites, after all. I will summarize some recent progress in these areas and comment on perspectives offered earlier in this special session.

Galileo's October 29th flyby of 951 Gaspra, an unusual olivine-rich S-type (of uncertain size, about 12 km diameter, and very irregular shape), will be the first-ever spacecraft encounter with an asteroid. Combined with a 1993 flyby of 243 Ida (a pyroxene-rich S-type in the Koronis family), *Galileo* promises to tell us much about this enigmatic class. Recent problems with *Galileo* degrade the capabilities of the camera and NIMS instruments, but nevertheless will result in (a) high resolution spectra for resolved regions, (b) mapping of compositional units to 200m resolution, and (c) pictures at reasonable phase angle of morphology below 100m. The data may be available for analysis in December 1992. I will describe the final observing sequence (still tentative at this time) and discuss Gaspra's and Ida's roles in resolving the long-standing S-type controversy. If Gaspra is a differentiated body, there is an excellent chance that *Galileo* will prove that. It will be harder to prove that it is undifferentiated.

The Positive Eu Anomaly and Sc Enrichment of Minerals A and B in Enstatite Meteorites

Yongheng Chen[1], Yangting Lin[1], Ernst Pernicka[2] and Daode Wang[1]
[1]Guangzhou Branch, Institute of Geochemistry, Chinese Academy of Sciences, Wushan, Guangzhou 510640, P. R. China
[2]Max-Planck-Institut fur Kernphysik, 6900 Heidelberg 1, Germany

Minerals A and B are unusual minerals that only occur in enstatite meteorites. Since they were identified by Ramdohr(1963, 1973), their compositions have not yet been determined. Up to date, there is no satisfactory results. On the other hand, there is no report about their trace element analysis. In this study, the contents of REE and some other trace elements in 3 grains of minerals A and B in Qingzhen(EH3, 2grains) and in Bustee(Aub, 1 grain) have been determined by INAA. The trace element abundances of minerals A and B indicate that they are all enriched in Sc(a refractory lithophile element, 10.5, 7.8 and 5.5 X CI respectively). The enrichments of Sc in them are corresponding to those in oldhamite and niningerite. Furthermore, minerals A and B in Bustee are unusually enriched in Eu(5700 X CI), other REE in them and all REE in Qingzhen minerals A and B are below the detection limit. The electron microprobe analysés of minerals A and B suggest that these minerals in Bustee are highly enriched in Ti(1.18% in A and 0.91% in B). Ti contents of minerals A and B in Qingzhen are very low(less than 0.08%, El Goresy et al., 1988). In contrast to large negative Eu anomalies in aubrites (Watters and Prinz, 1979; Walf et al., 1983) which are not found in E chondrites, it seems that the presense of extreme positive Eu anomaly and Ti enrichment indicate that aubrite was formed from magmatic differentiation of a melt. The REE pattern of minerals A and B in Bustee is consistent with that of the simulating fractionation of sulfide/silicate melt in the laboratory (Lodders and Palme, 1989). During the fractional crystallizing process, REE were strongly fractionated and Eu found its way into minerals A and B so that the large negative Eu anomalies in aubrites could be interpreted.

El Goresy A. et al., (1988) Proc. NIPR Symp. Antarct. Meteorites 1, 65-101.
Lodders K. and Palme H. (1989) Meteoritics, 24, 293-294.
Ramdohr P. (1963) J. Geophys. Res. 68, 2011-2036.
Ramdohr P. (1973) The opaque minerals in stony meteorites. London, Elsevier, p244.
Walf R. et al., (1983) G. C. A. 47, 2257-2270.
Watters T. R. and Prinz M. (1979) Proc. LPSC. 10th, 1073-1093.

The Trace Element Chemistry and Composition of Niningerite in Enstatite Meteorites

Yongheng Chen[1] Ernst Pernicka[2] and Daode Wang[1]
[1] Guangzhou Branch, Institute of Geochemistry, Academia Sinica, Wushan, Guangzhou, P.R.C.
[2] Max-Planck-Institut fur Kernphysik, 6900 Heidelberg 1, Germany.

Some authers have certified that oldhamite is indeed the principal carrier of REE in enstatite meteorites(Larimer and Ganapathy, 1987; Chen et al. 1989; Lundberg and Grozaz, 1988; Lundberg et al. 1989). In this work, the chemical composition and trace element concentrations of niningerite in Qingzhen(EH3) and some other enstatite chondrites, Abee(EH4), St. Marks(EH5), Atlanta(EL6), Hvittis(EL6), Pillistfer(EL6) and Bustee(Aub) have been determined by using electron microprobe and INAA techniques.

The chemical composition of Qingzhen niningerite varies over a very small range. In general, the contents of Fe and Mg are complementary and no obvious corrlation is noticed between Mg and Mn. The results of analysis for 10 Qingzhen niningerite grains show that some HREE(Yb and Lu) and Eu exist in 5 niningerite samples but LREE are below the detection limit in all samples. Fe-normalized REE patterns have similar shapes in which HREE are evidently enriched than LREE. There seems such a trend that the REE patterns betwwen oldhamite and niningerite are complementary. The mineralogical features of niningerite and thermodynamic calculation indicate that it is a high-temperature mineral as oldhamite(El Goresy et al. 1988; Kumura, 1988; Lattimer and Grossman, 1978). But the fact that it is only enriched in part of HREE reveals that there is some difference between oldhamite and niningerite in origin. These HREE are found in niningerite due to their small ionic radii like Mg. Similarly, Sc is more enriched in niningerite(4.5-28×CI, mean 16±7.4×CI)than in oldhamite because the properity of Sc is more similar to that of Mg. It replaces Mg into the crystal lattice of niningerite. The niningerite is also enriched in Hf in some samples.

Data of alabandite in the Atlanta chondrite(EL6) indicate that some REE exist in alabandite and the Fe-normalized pattern is similar to that of niningerite i.e., HREE are more enriched than LREE. But the REE abundances of alabandite in EL chondrites seem to be different from those of the niningerite in EH chondrites, but probably similar to those of oldhamite in EL chondrites. The abundances of Eu, Sc and Se in oldhamite and niningerite(alabandite) in enstatite meteorites obviously vary with metamorphic grade. They decrease monotonously with increasing metamorphic grade in EH chondrites, but there is an uncontinuous trend in EL chondrites. High Sc concentration of alabandite in Bustee aubrite suggests that Sc can find its way into alabandite again during the crystallizing process.

Chen Y. et al.(1989), Meteoritics, 24, 258. El Goresy A. et al.(1988), Proc. NIPR Symp. Antarct. Meteorites, 1, 65-101. Kumura M.(1988), Proc. NIPR Symp. Antarct. Meteorites. 1, 51-64. Larimar J. W. and Ganapathy R.(1987), EPSL, 84, 123-134. Lundberg L.L. and Grozaz G.(1988), Meteoritics, 23, 285-286. Lundberg L. L. et al. (1989), Meteoritics, 24, 296-297.

LEONARD MEDAL ADDRESS

METEORITICS AND THE ORIGINS OF ATOMIC NUCLEI

Donald D. Clayton, Department of Physics and Astronomy, Clemson U.

The science of nucleosynthesis was substantially inspired by chemical analyses of meteorites. In repayment that theory has imbued meteoritics with enlarged meaning. I will discuss the emergence of four great issues for nucleosynthesis--issues that have received decades of my own attention; and I will also describe unexpected abundance patterns within meteorites that were suggested by the resolutions of those issues. The latter have altered the information content of meteoritic science. The issues are:

1. a quantitative *s*-process theory
2. cosmoradiogenic chronology
3. explosive nucleosynthesis and gamma-ray astronomy
4. cosmic chemical memory

I will begin with historical origins for each issue, emphasizing both the broad cultural canvas in which they lay and my own work in their establishment. To each I will add an example of predicted (or rationalized) meteoritic measurements, emphasizing our surprised delight at the expansion of the range and power of meteoritic science.

TWO-STEP LASER MASS SPECTROMETRY: ANALYSIS AT HIGH SPATIAL RESOLUTION OF COSMOCHEMICAL SAMPLES.

S. J. Clemett, L. J. Kovalenko, C. R. Maechling, and R. N. Zare, Department of Chemistry, Stanford University, Stanford, CA 94305-5080

The capacity of laser desorption to volatilize intact neutral molecules and the high sensitivity and molecular selectivity of resonance-enhanced multiphoton ionization (REMPI) combine to make two-step laser mass spectrometry (L^2MS) a promising technique for the organic analysis of unique cosmochemical and geochemical samples. The utility of L^2MS has been demonstrated by the *in situ* analysis of polyaromatic hydrocarbons (PAHs) in both carbonaceous [1] and ordinary [2] chondrites, and our recent modifications to reduce the desorption laser spot size has allowed us to expand this technique to extra-terrestrial bodies of limited size and fine spatial heterogeneity. We have recently used L^2MS to analyze the acid (HF-HCl) insoluble residues of the interiors of the carbonaceous chondrites Murray (CM2) and Murchison (CM2), the unequilibrated ordinary chondrites Bishunpur (LL3) and Semarkona (LL3), and the ordinary chondrites Saratov (L4) and Barwell (L6). These residues, consisting of particles no larger than 200 μm in diameter, were individually mounted onto a sample platter for analysis.

In the L^2MS technique, the output of a pulsed CO_2 laser (10.6 μm) is focussed through a microscope objective onto the sample causing the rapid desorption of neutral molecules; the effective desorption region is a spot 40 μm in diameter. After a suitable time delay, the frequency-quadrupled output of a pulsed Nd:YAG laser (266 nm,) selectively ionizes the PAHs in the mixture of desorbing species by 1+1 REMPI. The ions are mass analyzed in a reflectron time-of flight mass spectrometer and detected by a microchannel plate.

Consistent with previous bulk chemical analyses, large PAH concentrations are found in the unequilibrated chondrites and undetectable amounts are found in the more equilibrated, thermally processed chondrites [3]. The acid residue of Bishunpur has the strongest signal, followed by Semarkona, Murchison, Murray, and Saratov. Barwell is absent of any detectable signal, which is consistent with its type-6 petrographic classification. This sample also serves as a reference for contamination introduced during sample preparation. Although great care was taken to ensure that we did not introduce contamination in our lab, the indigeneity of the organic material remains speculative, as the histories of the meteorites on Earth aren't well documented. In an effort to further classify the organic material, we have noted trends in the ratios of a set of PAHs in the meteorites. The ratios compare nicely between the Murchison and Murray samples and between the Bishunpur and Semarkona samples, while showing distinct differences between the LL3, CM2, and L4 chondrite samples.

[1] Zenobi et al. (1989) *Science* 246, 1026; [2] Zenobi, Philippoz, and Zare, unpublished results; [3] Hayatsu and Anders (1981) *Topics in Current Chemistry, vol. 99.*

THE EFFECT OF PRECURSOR GRAIN SIZE ON CHONDRULE TEXTURES

Harold C. Connolly Jr., Brian D. Jones and Roger H. Hewins. Dept. of Geological Sciences, Rutgers University, New Brunswick, NJ 08903

INTRODUCTION: Chondrule textures are controlled by the number of growth sites present when crystal growth commences and is directly related to initial temperature in traditional experiments. We report experiments that use short melting times and coarse initial particle size to reproduce chondrule textures for initial temperatures much higher than equilibrium liquidi in a dust free enviroment.

EXPERIMENTS: A fayalite analogue of a PO chondrule composition (calculated equilibrium liquidus 1288^{o}C; Herzberg, 1979) was made from mineral powder mixtures that were sieved to 20-45, 45-63, 63-125 and 125-250 micrometers size fractions. To simulate a flash heating event, cold samples were inserted into the furnace at initial temperature of 1400-1600^{o}C, cooled as rapidly as possible to the liquidus (melting times were 3 to 9.5 minutes) and then cooled from their liquidi to 900^{o}C at 500^{o}C/hr.

RESULTS: The 20-45 micrometer fraction charge produced glass textures at all initial temperatures at and above 1400^{o}C. The 45-63 and 63-125 micrometer fraction charge produced glass textures for initial temperature of 1500^{o} and 1600^{o}C, but produced BO textures at 1400^{o}C. The coarsest fraction (125-250 micrometers) produced BO at an initial temperature of 1600^{o}C but BO/PO textures at 1500^{o}C and 1400^{o}C.

DISCUSSION: BO texture can be formed from coarse grained material as much as 350^{o}C above the liquidus with short duration melting by olivine growth on relicts. Radomsky and Hewins (1990) also produced BO texture in experiments from superliquidus initial temperatures by incorporating large olivine seeds into charges but, argued that in the absence of coarse grained precursors and of dust in the nebula, the upper limit for BO chondrule formation would be 1750^{o}C. However, Connolly and Hewins (1990) produced BO texture by puffing mineral dust into totally molten droplets. Therefore, since large olivine relict grains occur in some chondrules and that the amount of dust in the nebula was probably great, it is difficult to argue that some chondrule precursors did not contain large grains or that crystal growth did not occur after molten chondrule- dust interactions. Therefore, the upper temperature limit 1750^{o}C for the formation of chondrules probably only applies in an "ideal" experimental case rather that in a dusty early nebula. BO chondrules may have formed at temperatures above their liquidus.

CONCLUSIONS: Precursor grain size and heating time have a profound effect on the formation of chondrule textures. Given precursor grains larger than 125 micrometers and superliquidus heating times of 9 minutes or less, classic BO textures can be produced with initial temperatures as much as 350^{o}C above the liquidus without dust interactions. The above experiments show that for short heating events the maximum temperature limit is presently unconstrained experimentally, and may be higher than the proposed 1750^{o}C. These short duration experiments make a true flash heating mechanism seem appropriate for the production of chondrule textures.

REFERENCES: Radomsky, Patrick M. and Hewins, Roger H. (1990) GCA 54, 3475-3490. Connolly, Harold C. and Hewins, Roger H. (1990) Meteoritics 25, 233-234. hewins, Roger H. and Radomsky, Patrick M. (1990) Meteoritics 25, 309-318. Herzberg, Claude T. (1979) GCA 43, 1241-1251.

Particle-Gas Dynamics in the Protoplanetary Nebula; J. N. Cuzzi (Ames Research Center, NASA), J. M. Champney (A. T. M. inc.), and A. R. Dobrovolskis (U. C. Santa Cruz)

During the stage of meteoroid parent body accumulation, the particulate elements attain sizes which allow them to settle vertically in the protoplanetary nebula into a particle layer which is quite thin (thousands of km at 1 AU) compared to the gas phase (ten million km at 1 AU), and which consequently reaches a mass density well in excess of that of the surrounding gas. The gas and particulate phases orbit the forming sun at different velocities because the gas is partially pressure supported. Because the gas and particle phases are coupled by gas drag, velocity gradients are set up in both phases, primarily in the vertical direction, which induce turbulence and hinder further settling of the particles. The viscosity resulting from the turbulence, acting across the various velocity gradients, transfers momentum and energy between the phases and induces a variety of mean relative radial and angular drift velocities in the gas and particulate phases throughout a boundary layer region of thousands of km thickness surrounding the nebula midplane. We have modeled this environment for a range of particle sizes up to tens of meters in order to help in understanding the meteorite parent body formation process. We find that, among other things, a steady-state particle layer is maintained and gravitational instability is forbidden until particles reach at least meters or tens of meters in size; during this stage objects must grow by collisional sticking. Differential (particle - gas) radial drift velocities (inwards) of a significant fraction of an AU during planetesimal growth times are found. Recent results will be presented.

ULTRAREFRACTORY INCLUSIONS AND THE NATURE OF THE GROUP II REE FRACTIONATION: Andrew M. Davis, Enrico Fermi Institute, University of Chicago, 5640 S. Ellis Ave, Chicago, IL 60637

Approximately 20% of the refractory inclusions in carbonaceous chondrites have group II REE patterns (Fig.). It has long been known that this pattern is caused by volatility fractionation in a two-stage process [1,2]. In the first stage, fractionation between gas and dust occurs at temperatures high enough to volatilize most of the condensible elements in the solar system, such that increasingly large fractions of Gd, Tb, Dy, Ho, Er and Lu are partitioned into the dust and the remaining REE are partitioned into the gas. In the second stage, all REE except Eu and Yb condense with other elements to form group II refractory inclusions. The second stage is clearly condensation, because the REE start out in the gas phase. It has not been clear whether the first stage fractionation was achieved by condensation or evaporation, because the dust fraction from the first stage is exceedingly rare. The dust fraction from this stage has now been recognized in three ultrarefractory inclusions and trace element and isotopic analyses of these by ion microprobe are reported here.

Ornans OSCAR [3] consists of Y-rich perovskite enclosed in fassaite with up to 50 mole% $CaScAlSiO_6$. Ornans 1105-42 [4] is an amoeboid olivine inclusion containing an enclave of Zr-Y-Ti-Sc oxide enclosed in Ca-,Al-,Si-glass. Mighei 3483-1-1 is an aggregate of spinel balls containing abundant Y-rich perovskite and minor hibonite and ZrO_2. Analyses of individual phases in each inclusion were combined with modal abundances to calculate bulk compositions. These three inclusions have extraordinary enrichments in the most refractory elements and have REE patterns closely resembling those of the component missing from group II inclusions (Fig.).

Experiments have shown that large enrichments in the heavy isotopes of Mg, Si and O accompany high temperature vacuum evaporation of liquid Mg_2SiO_4 [5]. The extreme chemical fractionations in the ultrarefractory inclusions allow a test of whether the fractionations were achieved by evaporation or condensation, as the latter process leads to little isotopic mass fractionation. The amount of mass fractionation expected for Ti was calculated for each inclusion, assuming that: (1) evaporation started with C1 chondrites; (2) no Zr evaporated; and (3) evaporation followed a Rayleigh process, where the gas/solid isotopic fractionation factor is determined by the inverse square root of the mass ratios of the evaporating species Ti, TiO or TiO_2. The fraction of Ti volatilized is ~99% and implies fractionations of 15-50‰/amu for Ti isotopes. Ion microprobe measurements show Ti fractionations of 0±10 ‰/amu for all three inclusions. Thus it appears that the first stage of gas-solid fractionation in the formation of group II inclusions involved condensation, not evaporation. The object with the most extreme chemical fractionation, Zr-rich oxide from Ornans 1105-42 appears to have been isolated from the solar nebula after only 10 ppm of condensible matter had condensed.

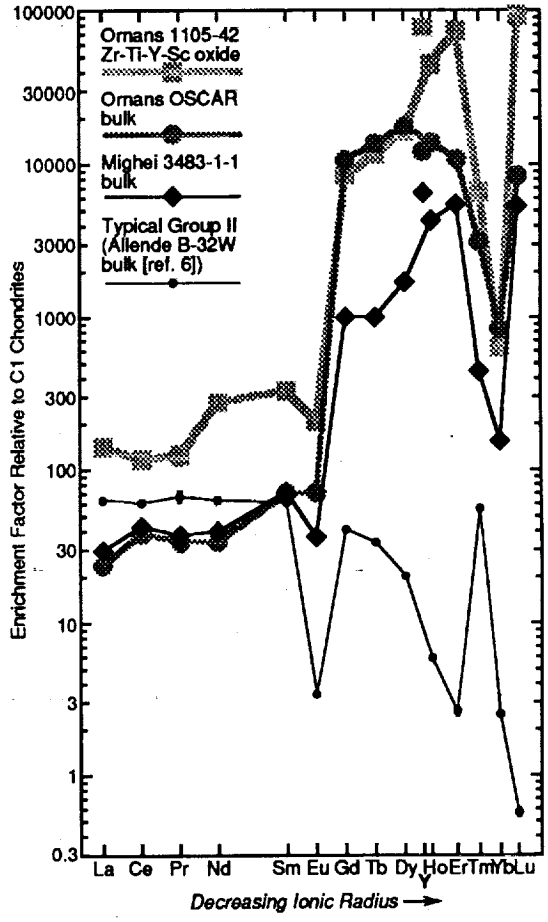

Refs. [1] Boynton W.V. (1975) *GCA* **39**, 569-584. [2] Davis A.M. & Grossman L. (1979) *GCA* **43**, 1611-1632. [3] Davis A.M. (1984) *Meteoritics* **19**, 214. [4] Noonan A.F. *et al.* (1977) *Meteoritics* **12**, 332-335. [5] Davis A.M. *et al.* (1990) *Nature* **347**, 655-658. [6] Conard R.L. (1976) M.S. Thesis, Oregon State Univ.

N92-12913

Low Temperature Annealing and Cathodoluminescence Studies of Type I Chondrule Compositions. J.M. DeHart and G.E. Lofgren, Mail Code SN2, Johnson Space Center, Houston, TX 77058

INTRODUCTION: Although there are many criteria available to determine if ordinary chondrites have been subjected to moderate and high temperatures during metamorphism, low level thermal alteration has been difficult to assess. It has been shown that the Cathodoluminescence (CL) properties of the minerals and glasses in ordinary chondrites change rapidly in response to low level thermal metamorphism (1). The refractory-rich mesostasis in type I chondrules appears to be especially sensitive to low level thermal alteration. These mesostases emit yellow CL in Semarkona (3.0) but produce white then blue CL in ordinary chondrites of increasing petrologic subtype. We have previously shown that yellow CL of type I chondrule mesostases forms during crystallization (2). It is still uncertain, however, whether the differences in CL properties of type I chondrule mesostases in meteorites of differing metamorphic subtype is a consequence of their metamorphic reheating or due to subtle differences in the chondrules' crystallization history. In order to determine if these types of mesostases can be altered by increasing temperatures, we have conducted a series of annealing experiments at low temperatures.

EXPERIMENTAL: Three series of experiments have been conducted using 1 mm slices of the previous experiments in (2) that produced yellow CL or from charges that have been heated and cooled under the same conditions. The first series of experiments consisted of samples annealed in a Thermolyne oven at 200°C and 500°C for 150 hours. In the second series of experiments, samples were sealed in gold capsules with 45 uL of deionized water and annealed at 100°C, 200°C and 350°C for 250 hours in externally heated pressure vessels. A third series of experiments were conducted with a solution of .1 M sodium metasilicate and annealed at the same conditions as the second series of experiments. CL photographs of the sections were made before and after each experiment using a Nuclide Luminoscope and a 35mm camera.

OBSERVATIONS: CL photos of the mesostases in the sections before annealing all had bright homogeneous regions of bright yellow CL. The first series of experiments failed to change the CL from the glasses. A sample from the second series of experiments did show changes in the CL. In the section annealed at 200°C with distilled water had changed from a bright, homogeneous yellow to a dull yellow to yellow brown luminescence. This sample also had small pockets of mesostases in the altered areas where the bright yellow luminescence remains.

CONCLUSIONS: These preliminary results indicate the yellow luminescing mesostases in type I chondrules can be altered by the effects of low level thermal metamorphism. Although heat alone was insufficient to alter the CL, reheating for geologically relevant periods could have the same results as we obtained in the second series of experiments with water present. It is known that both water and solutions of sodium metasilicate greatly accelerate the devitrification of glasses. The results of the experiments that will be repeated should further clarify how the CL changes with increased thermal alteration.

References: (1) DeHart J. M. and Sears D W G (1986) **LPS XVII**, pp 160-161. (2) DeHart J. M. and Lofgren G. E. (1991) **LPS XXII**, pp 291-292.

Fe/Mn ratios in basaltic achondrites and primitive meteorites.

Jeremy S. DELANEY, Department of Geological Sciences, Rutgers Univ., New Brunswick, NJ08903

Chemical analyses of unweathered stony meteorites (from 1) reveal Fe/Mn (molar) variation in nebular materials. Using Fe_{ox} (in FeO and Fe_2O_3), a systematic correlation of Fe/Mn with oxidized Fe is evident(Fig. 1). Both the carbonaceous and the ordinary chondrites (OC) define regular arrays of increasing Fe/Mn with increasing Fe_{ox}. The individual OC arrays overlap but have distinctly lower Fe/Mn than the carbonaceous chondrites. The basaltic achondrites, however, have lower Fe/Mn than any of the chondritic groups, as do the shergottites. High lunar values (e.g. MAC88105) plot close to the high Fe/Mn carbonaceous chondrite array. Unlike the chondrites, the basaltic achondrite samples define an array with almost constant Fe/Mn.

The slopes of these arrays in chondrites are generally consistent with mixing of low Fe/Mn components with oxidized iron within each chondrite class. This variability may reflect variations of fO_2, or physical mixing of primitive Mn-rich and Mn-free components. Mn-rich components, however, are rare in chondrites(2).

Fe/Mn in phases from basaltic achondrites differs from those in lunar samples (3) as there is little variation of Fe/Mn with Fe/(Fe+Mg). Thus, the partitioning of Fe/Mn in basaltic achondrites is distinct from that on the Moon and must result from Kd for Fe-Mn exchange of ~1. The low Fe/Mn ratios of basaltic achondrites indicate that they do not reflect the Fe/Mn systematics of any known chondritic precursor (Fig. 1) but have been modified on their parent body. Eucritic magmas must have experienced removal of a high Fe/Mn phase from their source prior to eruption. Plausible candidates are metal and olivine. Removal of metal would have depleted these systems in bulk Fe and is unlikely given the very iron rich character of eucrites. Olivine removal is, however, a requirement of any model deriving eucrites from chondritic presursors and can modify the Fe/Mn ratio without the extreme Fe depletion of metal loss. Thus the low Fe/Mn ratios of basaltic achondrites are compatible with derivation of these meteorites from a chondritic precursor after early removal of olivine from initial partial melting of the chondrites. Less olivine fractionation is required if that source had ordinary chondrite affinities.

Initial magma ocean type models of the basaltic achondrite parent body would result in the sinking of early olivine (c.f lunar 'magma oceanography') but no evidence exists for subsequent resampling of deep olivine rich mantle (cf mare basalts). Thus in both the Moon and the basaltic achondrite parent body variation of Fe/Mn ratios in silicate minerals reflect the influence of early planet-wide olivine fractionation and distinctive subsequent fractionation, probably reflecting fO_2, controls near surface magma compositions. In contrast, the primitive meteorites have variable Fe/Mn related to mixing of a high Fe/Mn (or pure Fe) component with a low Fe/Mn component.

Notes: (1) Jarosewich E., (1990) *Meteoritics* 25,323-327: (2) Rubin AE, (1984) Am Mineral. 69, 880-888: (3) Delaney JS. & SR Sutton (1991) LPSC 22 *Acknowledgement* NASA NAG9-304

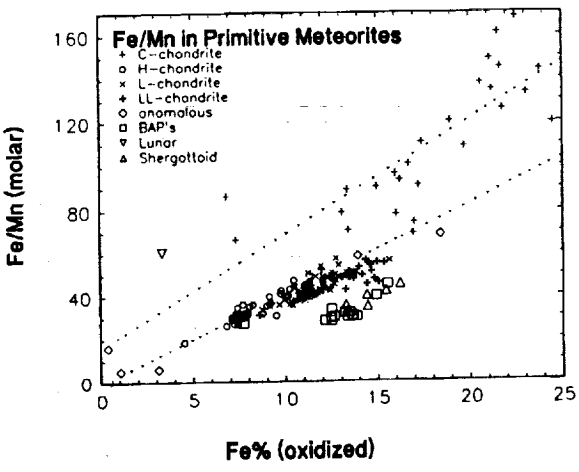

Figure 1: Variation of bulk Fe/Mn in chondritic and achondritic meteorites. Only unweathered samples and falls are plotted. Weathered meteorites extend these arrays to higher Fe/Mn. Fine dotted lines are regression plots for carbonaceous chondrites and H-chondrites

GLOBAL CHANGE, THE EAST ANTARCTIC ICE BUDGET AND THE EVOLUTION OF THE FRONTIER MOUNTAINS METEORITE TRAP, NORTH VICTORIA LAND, ANTARCTICA; G. Delisle, Bundesanstalt für Geowissenschaften und Rohstoffe, Postfach 510153, D-3000 Hannover 51, Germany

Shape and dynamics of the East Antarctic Ice Sheet depend on climatic conditions (primarily precipitation pattern and mean annual air temperatures over the continent) and their effect on ice-rheological parameters. A climatic change will cause the ice sheet to react eventually to the new conditions. What exactly the effect of climatic changes on meteorite traps are, has already been a matter of debate in the past (1,2,3).

A numerical model that simulates the response of the East Antarctic Ice Sheet to climatic changes typical for the last Glacial-Interglacial cycle will briefly be discussed. The model predicts a decreasing ice thickness in areas, where meteorite traps are known to exist today.

Field evidence suggesting a currently shrinking ice thickness in places near or with meteorite concentrations (Allan Hills, Griffin Nunatak, Brimstone Peak, Frontier Mountains) will be presented.

The meteorite concentration in the moraine of the "Meteorite Valley" of the Frontier Mountains has been described in (4). The results of the investigation of the area last season by EUROMET (supported logistically and scientifically by Italy by its "Programma Nazionale di Richerche in Antartide", PNRA) strongly suggest that the local meteorite trap has passed through several stages in response to thinning of the regional ice sheet. At one stage a melt-water lake has formed in the valley covering the moraine made up of granitic fragments. This would well explain the leaching process causing the high uranium content observed in all meteorites from the "Meteorite Valley".

About 80% of the 256 meteorites discovered by EUROMET were collected in a depression crossing the blue ice field to the NE of the "Meteorite Valley". All meteorites weigh less than 100 g (personal communication; Ian Franchi, Open University, UK) and were apparently wind-blown to the site. It will be argued that the on average 50 m deep depression is the result of an oblique collision of two local ice streams. Both of them have been exposed recently to ice thinning and, therefore, have become less mobile. Horizontal ice velocities near the collision zone are reduced to near zero values. A numerical model will be presented to show that the depression can be explained as the result of a balance between loss of ice by sublimation and lateral ice flow toward the depression attempting to compensate the mass loss.

REFERENCES: (1) Cassidy (1983) Proc. IVth Int. Symp. Antarctic Earth Sciences,Adelaide, 623-625; (2) Drewry (1986) LPI Tech. Rpt.86-01, Houston,37-47; (3) Schultz et al., (1991) Antarctic J. of the US, Review Issue 1990 (in press); Delisle et al., (1989) Geol.Jb. E38, Hannover, 483-513.

HOT SHOCKED BUSHVELD GABBRO (60 GPa - 630° C): MINERALOGY AND Rb - Sr SYSTEMATICS. Deutsch, A. & Langenhorst, F. , Inst. f. Planetologie, Wilhelm-Klemm-Str. 10, D-4400 Münster, F.R.G.

Target rocks at high temperatures certainly were involved in high-velocity collisions during the early solar system evolution or in large-scale impact processes on the earth's crust, *e.g.* at Vredefort (1) or Sudbury. In the Sudbury structure a maximum depth of excavation in the order of 25 km was calculated (2), obviously enough to reach lower crustal rocks. In order to recognize "hot shocked targets" in nature and to understand this different kind of shock metamorphism, we started a series of recovery experiments on preheated rocks and minerals (3).
To simulate shock effects occuring in extraterrestrial basaltic rocks, a medium-grained gabbro from the Bushveld complex was selected. This rock has quite a simple mineralogy with plagioclase, ortho-, and clinopyroxene, which are surrounded in certain areas by biotite flakes. The pyroxene is showing exsolution lamellae similar to those found in eucritic basalts. Disks of this Bushveld gabbro, preheated to 630°C were shocked to a peak pressure of 60 GPa and quenched to room temperature immediately. More detailed information about the set-up is found in a companion abstract (4).
In the *hot shocked gabbro* plagioclase is totally converted into a melt glass with bubbles and a fluidal texture. Pyroxen display manifold shock effects: Some are fragmented into small disorientated grains embedded in plag- glass. The more unfragmented, larger crystals show in part a slightly reduced birefringence and planar features on a small scale. It has not been cleared yet, whether these remarkable features represent mechanical twins or simply planar fractures.
An internal Rb-Sr isochron for the unshocked gabbro, using plag, two px-fractions, and the whole rock yields an age of 2043 $\pm$ 22 Ma (2σ) with I_{Sr} of 0.70739 $\pm$ 0.00002. The age is in excellent accordance with data published for the Bushveld area (5). For the hot shocked gabbro, a regression line defined by molten plag-glass, px, and a 20 mg "whole rock"-chip corresponds to an age of 2568 $\pm$ 140 Ma, the intercept is unchanged compared to the reference material. The hot shocked system is characterized by alkali-loss, and we interpret the obtained colinearity of the data in the isochron diagram as a random pattern.
These preliminary dating results corrborate our previous observations that shock alone do not reset isotope systems (6 - 9), moreover it extends this statement to the field of "high temperature" impact metamorphism.

(1) Tectonophysics **171**; (2) LAKOMY 1990, Meteoritics **25**, 195; (3) LANGENHORST et al. 1991, LPSC **XXII**, 777; (4) LANGENHORST & DEUTSCH 1991, this volume; (5) WALRAVEN et al. 1990, Tectonophysics **171**, 23; (6) DEUTSCH 1990 Habil.-Schrift math.-nat. Fak. Univ. Münster (7) DEUTSCH & SCHÄRER 1990, GCA **54**, 3427; (8) SCHÄRER & DEUTSCH 1990, GCA **54**, 3435; (9) STEPHAN & JEßBERGER 1989, Meteoritics **24**, 327.

ASTROBLEMES RECENTLY CONFIRMED WITH SHATTER CONES

Robert S. Dietz and John F. McHone, Geology Dept., Arizona State University, Tempe, AZ USA 85287-1404

Shatter cones are distinct conical fracture patterns formed in brittle rocks subjected to radiating shock waves. We accept unambiguously identified shatter cones as criteria for meteoroid impact and, due to their detection, one or two newly recognized sites are added to the world's growing inventory of impact structures each year. We present here a brief list of some of these sites.

Beaverhead, Montana, USA: 44°36'N; 112°58'W; estimated 60 km dia.
Recently discovered shatter cones in Paleozoic Belt rocks are spread over a 15 X 8 km area in Soutwestern Montana (2). These same shatter cones were noted, but not recognized, as early as 1966 (3).

Glasford, Illinois, USA: 40°36'N; 089°47.1'W; 4 km dia.
Originally mapped as an unusual domal structure in coals, this buried structure is presently utilized for underground gas storage. Shatterconed fragments occur in breccia veins within gas company core samples (4).

Glover Bluff, Wisconsin, USA: 43°58.2'N; 089 32.3'W; 8 km dia.
An isolated group of hills contains disturbed dolomite beds mined for agriculture. In 1983, Wm. Read found shatter cones in a reopened quarry (5). In spite of abundant shatter cones and contorted structure, this site is still ranked as "discredited" in at least one current listing of terrestrial impact sites (6).

Kara, USSR: 69° 10'N; 065°00'E; 60 km dia.
Originally described as a large volcanic complex, an impact origin was discovered when V. Masaitis found shatterconed samples in a Leningrad museum collection (7).

Lac de la Presquile, Quebec, Canada: 49°43'N; 074°48'W; 12 km dia.
Well developed shatter cone faces up to 60 cm long have recently been found associated with a roughly circular lake containing a peninsular central uplift (8).

Lawn Hill, Queensland, Australia: 18° 42'S; 138°39'E; 18 km dia.
Shatterconed Proterozoic siltsones and sandstones occur widely distributed within an 18 km diameter ring of brecciated limestone hills. Shatter cone fragments contain quartz grains with well developed decorated planar deformation lamellae (9).

Logancha, USSR: 65°30'N; 095°50'E; 20 km dia.
A 500 m deep crater in lower Triassic basalts and pyroclastics overlying Permian shales, coal beds, and limestones. Near the uplifted center, shatter cones up to 50 cm long are formed in basalts from lower trap units(10).

Marquez Dome, Texas, USA: 31°17'N; 096°17.5'W; 20 km dia.
Originally interpreted as one of several East Texas salt domes, shatterconed surface rocks first revealed its impact origin. Further work has now produced planar deformation features and other shock metamorphic effects (11).

Shangewan, China: 44°29'N; 126° 11'E; 30 km dia.
Detected on Landsat imagery as a discontinuous circular river pattern and central uplift, field work soon produced shatter cones in early Permian limestones. Subsequent studies yielded planar deformation features, impact melts and glasses, and breccias (12).

References: (1)Dietz, R.S. & J.F. McHone, 1988. *EOS*, 69, 1290 (2)Hargraves, R.B., et al., 1990. *Geology*, 18, 832-834 (3)Lucchitta, B.K., 1966. *Ph.D. Diss. Penn. State Univ.* (4)McHone, J.F., et al., 1988. *Meteoritics*, 21, 446-447. (5)Read, W.F., 1983.*Meteoritics*, 18, 241-242. (6)Graham et al., 1985. Catalogue of Meteorites, Ariz. State Press p.430 (7)Masaitis, V.L., Pers. Comm. (8)Higgins,M. & L. Tait, 1990. *Meteoritics*, 25, 235-236. (9)Stewart, A. & K. Mitchell, 1987. *Austr. Jour Earth Sci*, 34, 477-485. (10)Feldman et al., 1983. *Lunar and Planet .Sci. Conf. 14th*, 191 (11)Gibson,J. & V. Sharpton, 1989. *EOS*, 70, 383. (12)Siben, W.,1988. *Lunar & Planet .Sci. Conf., 19th*, 1296.

REE ABUNDANCE IN ACID RESIDUES OF UOC'S - A POSSIBLE INDEX FOR SUBCLASSIFICATION; Ebihara, M, Department of Chemistry, Faculty of Science, Tokyo Metropolitan University, 1-1 Minami-Ohsawa, Hachioji, Tokyo 192-03

Unequilibrated ordinary chondrites (UOC's) are subclassified in two different ways: TL sensitivity (Sears et al., 1980) and volatile element content (Anders and Zadnik, 1985). It is suggested that classification based on TL sensitivity reflects the difference in metamorphism, whereas volatile element contents are affected by metamorphism and/or nebular fractionation. These two classifications are not always correlated.

Studying the rare earth element (REE) distribution in ordinary chondrites, Ebihara (1989) pointed out that REEs are distributed in UOC's in a different manner from those in equilibrated ordinary chondrites (EOC's). In EOC's, most REEs, especially light REEs, are in Ca-phosphates, the remaining being in acid-residual phases, which consist of pyroxene and plagioclase for the most part. A REE abundance pattern of acid residues is characterized by a steep inclination and a large positive anomaly of Eu, which is attributable to the preferential migration of Eu in plagioclase. On the other hand, in UOC's, REEs were found to be allotted in acid residues to greater extent. Their abundance pattern shows a less steep inclination and a smaller positive anomaly of Eu (even a negative anomaly for some cases). Thus, REEs must have been largely redistributed between UOC's and EOC's, and even among UOC's. Thermal metamorphism could be a cause to make such a difference in REE distribution in acid residues.

Table 1 shows some values characterizing REE abundances in acid residues of Antarctic UOC's. It is notable that the relative abundance of light REE ($(La)_{C1}$ in Table 1), the degree of inclination ($(La/Lu)_{C1}$) and the degree of Eu anomaly (Eu/Eu^*) are closely correlated with subclass numbers based on volatile element contents. This suggests that these values can be used for the subclassification of UOC's. Among them, the degree of Eu anomaly seems to be the most promising. Considering that those values and subclass numbers based on TL are poorly correlated, it is suggested that TL sensitivity do not always reflect the degree of metamorphism.

REFERENCES: Anders E. and Zadnik M.G. (1985) Geochim. Cosmochim. Acta 49, 1281. Ebihara M. (1989): Proc. NIPR Symp. Antarct. Meteorites 2, 279. Sears D.W., Grossman J.N., Melcher C.L., Ross L.M. and Mills A.A. (1980): Nature 287, 791.

Table 1 Values characterizing REEs in acid residues of UOC's.

meteorites	chemical class	petrologic type TL	petrologic type volatiles	$(La)_{C1}$[a]	$(La/Lu)_{C1}$[a]	Eu/Eu^*[b]
ALH 77011[c]	L	3.5	3.0	2.16	0.98	0.72
ALH 78038[c]	L	3.4	3.0	1.56	0.83	0.86
Y 74191	L	3.6		1.85	0.69	1.04
ALH 77299	H	3.7	3.4	1.31	0.80	1.43
ALH 78084	H	3.9		1.10	0.59	1.67
ALH 77278	LL	3.6	3.9	1.19	0.66	2.00
ALH 77252[d]	L			0.46	0.35	3.33

[a] C1-normalized values, [b] Eu^*: interpolated values, [c] paired, [d] L3 or L4/L6 (possibly an EOC clast).

NANOPHASE METALS IN FREMDLINGE FROM ALLENDE: "SMOKES" FROM THE EARLY SOLAR SYSTEM?

D. D. Eisenhour and P. R. Buseck, Departments of Geology and Chemistry, Arizona State University, Tempe, Arizona 85287-1404

During a recent TEM study of a Fremdling from a Type B1 Ca-, Al-rich inclusion (CAI) in Allende, we noted the occurrence of several aggregates of extremely small (1-3 nm) metal grains [1]. The grains are randomly oriented and have a bulk composition (in atom %) of approximately Ni_{45} Fe_{40} Pt_{10} Ir_5. Subsequent TEM studies of other Fremdlinge and refractory metal nuggets (RMNs) have revealed additional aggregates of nanometer-sized grains with more complex bulk compositions. One such aggregate occurs within a 10-μm Fremdling in a rare, rhoenite-bearing Type A inclusion. This aggregate is unusual because it contains several percent Si, Al, and Ca in addition to a wide range of refractory siderophile elements (Os, Re, Ru, Ir, Rh, and Pt). The identification of multiple phases has been hindered by the small sizes and close packing of these grains. However, the high levels of Ca, Al, and Si as well as the presence of refractory siderophiles of two different structure types suggests that this aggregate is multiphase.

The grain sizes and textures of these aggregates are reminiscent of carbonaceous smokes that we have observed during TEM studies of air pollutants. Could these nanophase metals be unaltered "smokey" condensates from the early nebula? Sylvester *et al.* suggested that the refractory siderophile elements condensed into three separate alloys according to their crystal structures: Re, Os, and Ru forming a hexagonal close-packed (hcp) alloy; W, Mo, and Cr forming a body-centered cubic (bcc) alloy; and Ir, Pt, Rh, Co, Ni, and Fe forming a face-centered cubic (fcc) alloy [2]. If true, perhaps the aggregates represent mixtures in varying proportions of nanometer-sized hcp, fcc, and bcc condensates. Other origins are also possible, however. The pure fcc, nanophase aggregate in the Type B1 inclusion may be a low-temperature decomposition product similar to plessite. This possibility could provide new information about the low-temperature thermal histories of CAIs. The more complex nanophase aggregates that contain metals of two or more structural types may be the product of a rapidly quenched homogeneous liquid or high-temperature homogeneous solid. This origin would provide new constraints on CAI peak temperatures and cooling rates, or possibly on the pre-incorporation thermal histories of Fremdlinge and RMNs.

References: [1] Eisenhour D. D. and Buseck P. R. (1991) LPSC ***XXII***, 343-344. [2] Sylvester *et. al* (1990) GCA ***54***, 3491- 3508.

Negative Thermal Ionization and Isotope Dilution Applied to the Determination of Re and Os Concentrations and Os Isotopic Compositions in Iron Meteorites.

Tezer Esat and Victoria Bennett, Research School of Earth Sciences, The Australian National University, Canberra 2601, Australia.

The radioactive decay of ^{187}Re to ^{187}Os with a half-life of 4.45×10^{10} years combined with the refractory siderophile nature of these two elements, provide a unique opportunity for dating early events during the formation of the solar system. However, Os analysis also poses unique problems both for the chemical extraction and purification of Os as well as in obtaining the sufficiently intense ion beams for precise isotope ratio measurements. Techniques used previously include secondary ion mass spectrometry (Luck and Allegre [1,2]) ionization of Os using tunable dye lasers (Walker and Fasset [3]) and more recently inductively coupled plasma mass spectrometry [4].

Over the past year we have developed methods for more precise measurement of Os isotopic compositions by thermal production of an OsO_3^- ion beam. Our methods are based on further improvements of techniques suggested by Klaus Heumann of Regensburg University, Germany during a visit to the ANU. For analysis of standards, 1.0 - 1.5 ng of Os are loaded onto a Pt filament as a chloride with KOH and BaOH activators. At about 800°C, a 4×10^{-12} Ampere to 1.5×10^{-11} Ampere $^{192}OsO_3^-$ beam can be obtained and lasts for more than 6 hours, indicating an ionisation efficiency of about 25%. For Re the platinum filaments appear to be contaminated by a small amount of Re and a 4×10^{-14} ampere ReO_4^- beam can be obtained at about 1000°C when the filament is doped with BaOH+KOH. At Os running temperatures there is no indication of Re above the background noise level. The ANU 61-cm mass spectrometer is equipped with 3 Faraday cups each 11mm wide. They cannot be placed at 1 amu mass separation at masses of about 250; we have used ^{186}Os -^{188}Os -^{192}Os, ^{187}Os-^{189}Os-^{192}Os, ^{188}Os-^{190}Os-^{192}Os for measurements by peak jumping between each triplet to measure all (except ^{184}Os) of the Os isotopes relative to ^{192}Os. For normalisation we have used $^{189}Os/^{192}Os$=0.39593 [5]. The interferences from the minor oxygen isotopes and mass dependent instrumental fractionation are corrected for in a single step, in the first order approximation, by assuming that the oxygen reservoir is unfractionated. In Table 1 we show the results for two standard solutions. In Table 2 repeat runs for $^{187}Os/^{192}Os$ are given. The abundance of ^{187}Os can be determined to a precision of about ±0.3‰.

In Table 1 we have included a measurement on a directly loaded iridosmine grain from Tasmania. As reported by Creaser et al.,[6] there is no interference between the ReO_4^- and the OsO_3^- beams. We also report the first isotope dilution determinations of Os and Re concentrations extracted from the iron meteorite Cape York. Our methods of chemical extraction of Os are modified from Morgan and Walker [7]. Re is extracted using a small anion exchange column. Our preliminary data show excellent agreement between Re concentrations and Os isotopic compositions as compared with published values for these meteorites. However, the measured $^{187}Re/^{186}Os$ ratio for Cape York and two Henbury samples is lower than expected [1,8] with these samples plotting above the Re-Os isochron for iron meteorites. Comparison between 4 Gravimetric mixtures of Os spike-Os standard and measured values shows a total spread of 0.8‰ in the difference. The measured $^{187}Re/^{186}Os$ ratios in our meteorite samples differ from the expected values by more than 10%. We interpret this discrepancy as resulting from Os spike-sample disequilibrium during the dissolution/chemical extraction procedure rather than having age significance. Further work is in progress to eliminate this problem and extend the measurements to other iron meteorites.

References: [1]Luck,J-M.&Allégre,C.J.,(1983),*Nature* 302, 130-132. [2] Luck, J-M.&Allégre C.J.,(1980), *EPSL*, 48, 148-154. [3] Walker, R.J.,& Fassett, (1986) *Anal. Chem.* 58, 2923-2927.[4] Russ, G.P., *et al.*, (1987), *Anal. Chem.* 59, 984-989. [5] Völkening, J. *et al.*, (in press) *Int. J. Mass Spec.* [6] Creaser, R.A., *et al.*, (1991), *Geochim. Acta* 55, 397-401. [7] Morgan J.W.& Walker, R.J. (1989) *Anal. Chim. Acta* 222, 291-300.[8]Morgan, J.W. *et al.*, (1991) *LPSC XXII*, 919-920.

Table 1. Os and Re isotopic composition of standards spikes and samples determined by negative thermal ion mass spectrometry.

Osmium	$^{186}Os/^{192}Os$	$^{187}Os/^{192}Os$	$^{188}Os/^{192}Os$	$^{190}Os/^{192}Os$	$^{187}Os/^{186}Os$
standard 1	0.03886±5	0.04004±1	0.32428±8	0.64409±7	1.0305±5
standard 2	0.03895±5	0.03465±2	0.32449±10	0.64397±6	0.89166±5
spike	0.01242±6	0.01385±8	0.26354±10	50.696±30	
Iridosmine	Black Hill, Tasmania 40x30x30μm with 320ng of Os.				
		0.03896±1			1.0026±5
Cape York	Iron meteorite $^{187}Re/^{186}Os$=2.55 Re=0.35 ppm. Os=5.3 ppm.				
		0.04335±3			1.1147±6

Rhenium	$^{185}Re/^{187}Re$
Standard	0.5970±2
Spike	37.17±2

Table 2. Reproducibility of $^{187}Os/^{192}Os$ ratio for standards.

Osmium	$^{187}Os/^{192}Os$	$^{187}Os/^{186}Os$
standard 1	0.040034±7	1.0302±5
	0.040031±25	1.0301±5
	0.040050±4	1.0306±5
	0.040044±9	1.0305±5
standard 2	0.034653±10	0.8917±4
	0.034638±7	0.8913±4
	0.034661±5	0.8920±4
	0.034621±4	0.8909±4
	0.034671±8	0.8922±4

CONDENSATION OF GRAPHITE AND REFRACTORY CARBIDES IN STELLAR ATMOSPHERES

Bruce Fegley, Jr., LPI, 3303 NASA Road 1, Houston, TX, 77058, USA

Introduction. In this abstract I report preliminary results of condensation calculations for graphite and refractory carbides in a gas of solar composition but having a C/O ratio of 1.2. The condensation chemistry of these phases is of interest for interpreting the results of observational work on interstellar grains in meteorites, for predicting as yet unobserved mineral assemblages, and for guiding future experimental measurements.

Method. The condensation calculations are made using a modified version of the TOP20 code and the METKON code. The dual constraints of mass balance and chemical equilibrium are applied in both codes. The elemental abundances used in the calculations are from Anders and Grevesse (1989) and the thermodynamic data are from the JANAF Tables and other standard compilations. Initially, refractory carbides of elements more abundant than vanadium were considered. The results of the calculations are shown in the Figure.

Results. The new results confirm my prior calculations (Fegley 1982) for TiC, SiC, and graphite over the same pressure range. The curve labelled SiC in the Figure is for β-SiC; however, the condensation curves for α- and β-SiC are generally less than 10° apart over the entire pressure range shown. The curves for $VC_{.88}$ and SiC intersect at about 10^{-6} bars total pressure. The graphite and TiC curves intersect at about the same pressure. At high pressures, the SiC curve begins to level off and this phase becomes unstable at slightly higher pressures. Aluminum, which is not shown, does not condense initially as a carbide, but condenses as a nitride instead. Finally, it should also be noted that the intersections of the graphite and carbide condensation curves lead to different mineral assemblages produced by isobaric condensation at higher and lower pressures.

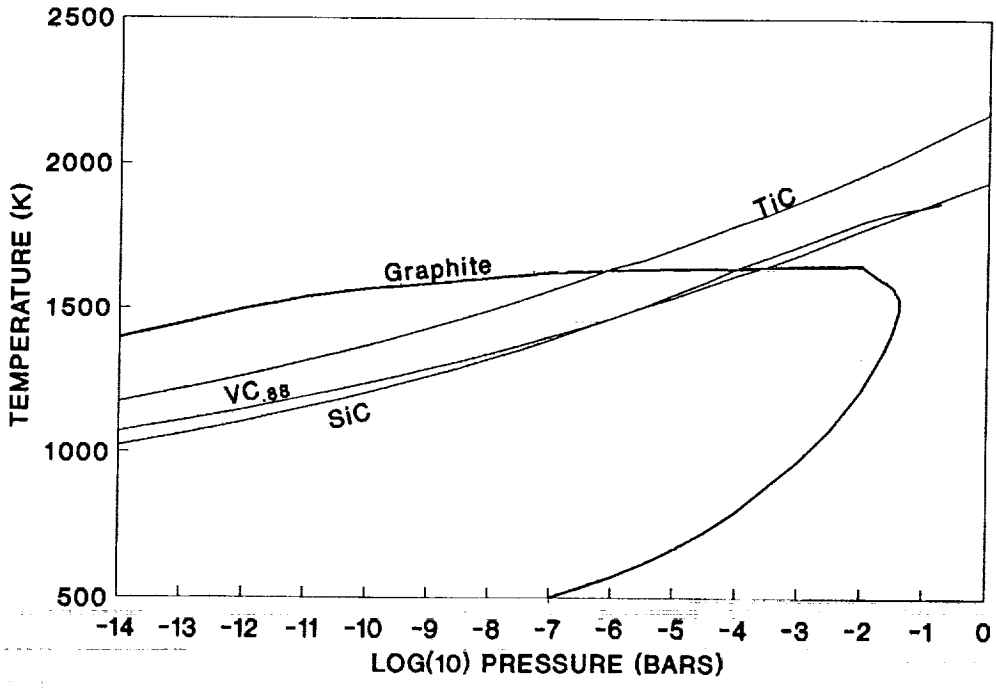

REE VARIATIONS IN OLDHAMITE FROM AUBRITES AND EL6 CHONDRITES Christine Floss and Ghislaine Crozaz. Department of Earth and Planetary Sciences and McDonnell Center for the Space Sciences, Washington University, St. Louis, MO 63130.

The use of rare earth element (REE) data to model the origin of the aubrites has been hampered by the heterogeneity of whole rock REE patterns and abundances. Whole rock REE abundances in the aubrites are dominated by oldhamite, the major REE host [1]; most other phases are extremely REE-depleted [1, 2]. Last year we presented results from the Bustee aubrite, which showed that REE patterns in oldhamite are highly variable with positive, negative or no Eu anomalies [3]. Here we report the results of ion microprobe measurements on oldhamite from two additional aubrites, Khor Temiki and Mayo Belwa, as well as from two equilibrated (EL6) enstatite chondrites.

Analyses of oldhamite from Khor Temiki and Mayo Belwa confirm previous results from Bishopville and Bustee: REE patterns and abundances in aubritic oldhamite are highly variable. 109 CaS grains have been measured in these four aubrites; 18 of these are unaltered oldhamite while the remainder are slightly to severely weathered. However, previous work has shown that, while weathering may leach REE, it does so uniformly, preserving the original REE pattern [1, 2, 3]. Ten distinct patterns have been observed. Pattern A is LREE-enriched with positive Eu and (sometimes) Yb anomalies. B is bow-shaped with a negative Eu anomaly. Pattern C also has a negative Eu anomaly, but the other REE are unfractionated. D is flat and exhibits no anomalies. Pattern E has LREE higher than HREE; positive Yb anomalies are common. Pattern F is strongly HREE-enriched, with a negative Eu anomaly. In contrast, pattern G is LREE-enriched and may or may not have a negative Eu anomaly. Patterns H and I are both bow-shaped and have LREE higher than HREE. The difference is that the break occurs at Eu in pattern H, whereas in pattern I, Eu remains high and the break occurs at Gd. Finally, pattern J has remarkably steep enrichments of both the LREE and HREE, as well as a positive Eu anomaly.

Four patterns (A, B, C, and D) account for 82% of the oldhamite grains measured. Of these, A is the most common (33 out of 109), followed closely by D (27 out of 109). The distribution of pattern types among the meteorites is random. Four of the patterns (A, C, D, and E) are similar to REE patterns found in oldhamite from the unequilibrated (E3-4) enstatite chondrites [4]. This observation, and the fact that these patterns are among the ones most commonly observed in aubritic oldhamite, suggests that many grains survived the melting event that produced the aubrites. A relict origin for oldhamite is also consistent with the extremely REE-depleted nature of most major silicates in these meteorites. However, not all oldhamite REE patterns are necessarily relict. Some have intermediate characteristics that may have formed through sintering of two or more CaS grains with different REE patterns. A few patterns are strongly fractionated, suggestive of igneous processing (e.g., pattern F). Apparently the role of oldhamite in aubrite formation was complex, and more than one process may be responsible for the REE patterns observed.

Twenty CaS grains were measured from the EL6 chondrites, Jajh deh Kot Lalu and Khairpur. In contrast to both aubrites and E3-4 chondrites, oldhamite grains from these two meteorites have nearly identical REE concentrations. All have flat REE patterns at about 100 x C1, with pronounced negative Eu anomalies, consistent with preliminary measurements of oldhamite from Jajh deh Kot Lalu [5]. The pattern is the same as C from aubritic oldhamite. If these results are characteristic of all CaS from Jajh deh Kot Lalu and Khairpur, then the positive Eu anomalies exhibited by whole rock REE patterns for these meteorites [6, 7] must be due to the presence of some other Eu-bearing phase, probably plagioclase.

[1] Floss *et al.* (1990) Geochim. Cosmochim. Acta **54**, 3553-3558. [2] Wheelock *et al.* (1990) LPSC XXI, 1327-1328. [3] Floss and Crozaz (1990) Meteoritics **25**, 364-365. [4] Lundberg *et al.* (1991) LPSC XXII, 835-836. [5] Lundberg and Crozaz (1988) Meteoritics **23**, 285-286. [6] Nakamura and Masuda (1973) Earth Planet. Sci. Let. **19**, 429-437. [7] Strait (1983) Ph.D. Thesis, Arizona State University, 172 pp.

AVERAGE MINOR AND TRACE ELEMENT CONTENTS IN SEVENTEEN "CHONDRITIC" IDPs SUGGEST A VOLATILE ENRICHMENT. Flynn, G. J.[1] and Sutton, S. R.[2] (1) Dept. of Physics, SUNY-Plattsburgh, Plattsburgh, NY 12901, (2) Dept. of Geophysical Science, The University of Chicago, Chicago, IL 60637.

Element abundances provide clues to the sources and formation conditions of interplanetary dust. Schramm et al. [1] determined that the major element abundances in 200 interplanetary dust particles (IDPs) most closely resemble those of CI carbonaceous chondrites, while van der Stap et al. [2] found the volatile minor and trace elements in 3 chondritic IDPs to be enriched over CI, suggesting the IDPs are late stage nebula condensates [2]. However, on the average S is observed to be depleted relative to CI in the 200 particles measured by Schramm et al. [1].

We have reported Synchrotron X-Ray Fluorescence (SXRF) minor and trace element abundance measurements on 20 C-type and 6 C?-type IDPs from the Johnson Space Center stratospheric particle collections. Elemental abundances in individual IDPs distribute about the CI values [3], but variations of a factor of 2 or 3 are frequently seen, possibly due to inhomogeneities in the small IDPs.

We have inferred the average composition of chondritic IDPs by averaging the element/CI ratios for the C-type particles we have measured by SXRF [3, 4, 5, 6]. We excluded 5 C-type particles, one so small that we only detected Fe, Ni, and Cr [6], and 4 low-Ni particles (one dominated by an olivine crystal [7], two exhibiting igneous mineralogies [7, 8], and one not yet examined by TEM [6]) all of which exhibited dramatically non-chondritic minor/trace element abundance patterns. Two C?-type particles which exhibited chondritic minor/trace element abundance patterns [6] were included, giving a total of 17 particles in the average.

The average abundance data (plotted in Figure 1 for all elements detected in 6 or more of the particles) range from 1 x CI to 19 x CI. Although most elements were within a factor of two of CI, Zn and Br, two of the most volatile elements detected, exhibited the largest enrichments, 3.2 and 19 x CI respectively.

Elements with condensation temperatures lower than that of Cr were enriched (with the exception of Ge). This is similar to the enrichment pattern reported in the three IDPs examined by van der Stap et al., though they also observed an enrichment in Ge (to ~1.8 x CI) [2]. For most elements, the difference between this average composition and CI is smaller than the particle to particle abundance variation (eg., Cu ranges from 0.4 to 6.9 x CI in the seventeen particles). Nonetheless, the overall average abundance pattern suggests the existence of a general volatile enrichment in the IDPs relative to CI composition.

REFERENCES: 1. Schramm, L. S. et al. (1989) Meteoritics, 24, 99-112. 2. van der Stap, C. C. A. H. et al. (1986) LPSC XVII, 1013-1014. 3. Flynn, G. J. and Sutton, S. R. (1988) Proc. Lunar Planet. Sci. Conf. 18th, 607-614. 4. Flynn, G. J. and Sutton, S. R. (1991) Proc. Lunar Planet. Sci. Conf. 20th, 335-342. 5. Flynn, G. J. and Sutton, S. R. (1991) Proc. Lunar Planet. Sci. Conf. 21st, 549-556. 6. Flynn, G. J. and Sutton, S. R. (1991) LPSC XXII, 395-396. 7. Sutton, S. R. et al. (1990) LPSC XXI, 1225 1226. 8. Rietmeijer, F.J.M. (1991) LPSC XXII, 1121-1122. 9. Wasson, J. T. (1985) Meteorites, W. H. Freeman, 250-252.

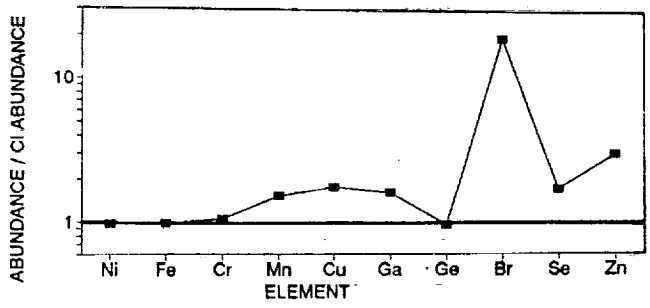

Figure 1: Average elemental abundances in 17 "chondritic" IDPs. Elements ordered with decreasing nebula condensation temperature [9] to the right.

VOLATILE TRACE ELEMENTS IN LARGE MICROMETEORITES FROM GREENLAND. Flynn, G. J.[1], Sutton, S. R.[2], and Klock, W.[3], 1) Dept. of Physics, SUNY-Plattsburgh, Plattsburgh, NY, 2) Dept. of Geophys. Sci., The University of Chicago, Chicago IL, 3) Inst. of Planetology, Westfalische Wilhelms-Universitat, Munster, Germany.

Micrometeors and micrometeorites in the range from 60 to 1200 micrometers constitute ~80% of the continuous meteoritic mass accreted by the Earth [1], thus their compositions determine that of the meteoritic material accreted onto inner solar system planets and moons. Unmelted micrometeorites in this size range have been recovered from ices in Greenland and the Antarctic. Noble gases with non-terrestrial isotopic compositions confirm an extraterrestrial origin for large particles having Mg, Al, Si, and Fe abundances which are approximately chondritic [2]. Maurette et al. report depletions of Ca, Ni, and S relative to CI meteorites in the large micrometeorites [2].

Four fine-grained, irregularly-shaped Greenland micrometeorites (#16, #20, #21, and #22) ranging from 50 to 160 micrometers in size were selected for Synchrotron X-Ray Fluorescence (SXRF) trace element analyses. Each exhibits roughly chondritic Mg, Al, Si and Fe, as well as detectable S in SEM EDX analysis. Two (#20 and #22) consist of olivine and pyroxene crystals embedded in glass.

The samples were analyzed as polished thin sections embedded in epoxy. A single SXRF analysis, using an 8 micron beam spot, was performed on each particle. The Fe abundance is approximately the CI value in all four particles (0.4 to 1 x CI). However, Ni is substantially depleted in all four particles with Fe/Ni ranging from 80 to over 3,000. Notwithstanding these low Ni contents, other trace elements (Cu, Zn, Ga, Ge) in three of the four particles scatter within about a factor of 3 range around the CI values, reminiscent of the range of compositions of individual stratospheric cosmic dust particles [3]. Of these elements, Zn and Ge are depleted from CI in all three particles, while Cu and Ga are present at or above CI abundances in two of the particles (#16 and #22). Cu, Zn, Ga, and Ge contents in the fourth particle (#20) are less than 0.1 x CI. Dramatically high concentrations of Pb were observed in all four particles (up to ~0.1% Pb). The fact that similarly high Pb contents have been seen in Deep Sea Spheres but not in stratospheric cosmic dust suggests the Pb may be incorporated through interactions with sea water/ice. The high Br content of the epoxy precluded measurement of this element in the samples.

Atmospheric entry heating calculations suggest most micrometeorites larger than 100 micrometers in diameter should be substantially heated during atmospheric entry [4, 5]. However, the presence of the volatile elements Cu, Zn, Ga, and Ge in three of these large particles at or near CI abundances suggests their abundances have not been substantially altered by atmospheric entry heating.

We have mapped the distributions of Fe, Ni, Zn, and Pb in particle #16 to search for chemical heterogeneities, particularly surface correlations. An 8 micrometer x-ray beam was used and stepped across the sample in 5 micrometer steps in a 2 dimensional grid pattern. This procedure divided the sample into about 400 individual measurements each acquired for 20 seconds. The Fe/Ni and Fe/Zn ratios were remarkably constant over the whole sample suggesting that although there is considerable fluctuation in the abundances of the elements from particle to particle, these elements are uniformly distributed in at least one particle (#16) on a 5 micrometer scale. Pb showed no evidence for a surface correlation suggesting that if it is a contaminant, it permeates the entire sample.

Acknowledgement: We thank M. Maurette for providing the samples.

REFERENCES: 1. Hughes, D. W. (1978), in Cosmic Dust (ed. J. A. M. McDonnell), Wiley, 123-185. 2. Maurette, M. (1991), Nature, 351, 44-47. 3. Flynn, G.J. and Sutton, S.R., Proc. Lunar Planet. Sci Conf 20th, 335-342. 4. Flynn, G.J. (1990) Meteoritics, 25, 365. 5. Love, S. G. and Brownlee, (1991), Icarus, 89, 26-43.

TO MAKE, PERHAPS, OR NOT TO MAKE CHONDRULES; K. Fredriksson, Smithsonian Institution, Washington, D.C. 20560, USA. F. Wlotzka and B. Spettel, Max-Planck-Institut für Chemie, Abteilung Kosmochemie, 6500 Mainz, Germany.

Ten chondrules from the Bjurböle chondrite were analyzed by INAA for Fe, Ca and minor and trace elements. The results are shown in Figure 1 and illustrate again the difference between Ca-rich ($>$ 1.3 wt%) and Ca-poor ($<$ 1.3 wt%) chondrules and the remarkable fact that their average equates that of the bulk [1].

Electron probe analyses of fragments from four of these chondrules showed the Fe/Mg to be constant. Remainders of these chondrules were melted under vacuum, $\sim$ 40 microns Ar, in a Leitz Heating Stage. Melting and boiling occurred between $\sim$ 1200 to 1370 degrees C with simultaneous, heavy condensation on the window*. The melting temperature was held less than 30 seconds before quenching at atmospheric Ar, 1000°/min. The condensate contained Na, K and Fe; essentially all of these elements volatilized. The analyses of the residual melt beads by INAA will be compared with the original composition of each chondrule.

In parallel studies the silicate-FeS portions (metal removed) from a few chondrules with extreme Ca/Al were analyzed by electron probe and INAA. The chondrule silicates from all petrographic groups overlap in composition.

We conclude that chondrules formed by melting of aggregates of pre-existing phases mixed in various proportions but with a common parent such that different chondrules in an essentially closed system could form chondrites of almost identical bulk composition but variable mineralogy and texture. However, the chondrules could not have formed under vacuum. Even heating individual aggregates in a low density nebula seems highly unlikely. Thus after 30 years we can now report how chondrules were not made; the nebular condensation theory is wrong.

References: [1] Fredriksson, K. (1983). In Chondrules and their Origins (E.A. King, Ed.), pp.44-52, Lunar & Planet. Inst., Houston.

* A brief video of heating experiments may be shown.

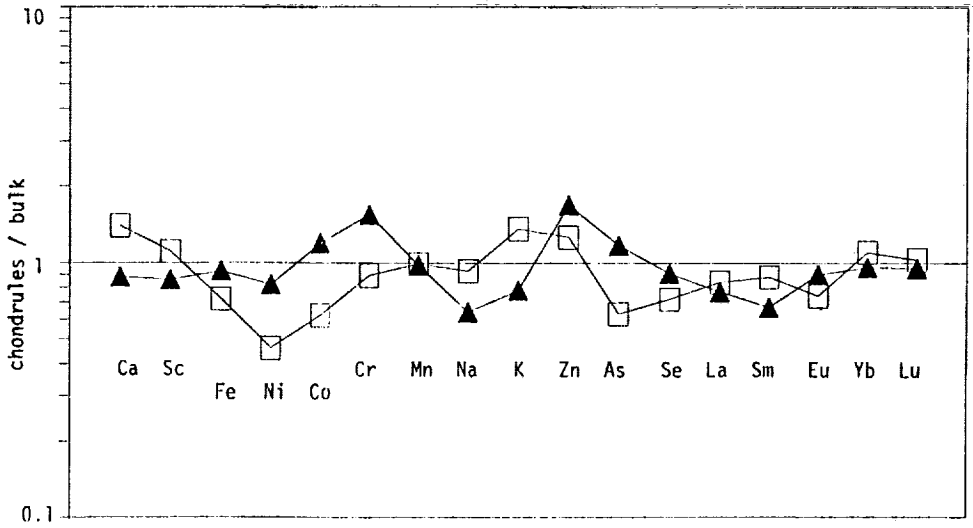

Fig. 1. Ave. composition of 10 Bjurböle chondrules, 4 lo Ca (▲) and 6 hi Ca (□) relative to bulk (1.3%Ca).

THE MINERALOGY OF S-TYPE ASTEROIDS: WHY DOESN'T SPECTROSCOPY FIND ORDINARY CHONDRITES IN THE ASTEROID BELT? M.J. Gaffey, Geology Dept., Rensselaer Polytechnic Institute, Troy, New York 12181 USA

Many meteorite and orbital dynamics investigators present strong but indirect arguments that a significant fraction of the asteroid belt must be composed of ordinary chondrite (OC) assemblages, and that the S-type asteroids are the best OC candidates. However, observational investigations have increasingly lead asteroid spectroscopists to conclude that no mainbelt asteroid studied to date (including the S-asteroids) can be identified as a probable OC assemblage. Resolving this seeming paradox should contribute significantly to our understanding of the conditions and processes in the late solar nebula and the early solar system. The present paper reviews the spectral evidence to help both meteorite and asteroid investigators better understand and evaluate the criteria for identifying or eliminating OC assemblages on individual S-asteroids and within the S-asteroid population.

Chondrites have approximately solar abundance ratios for the less volatile elements. Major element abundances vary somewhat between the individual chondrite types (EH,EL,H,L,LL,CV,CO,CI,CM) as a result of nebular processes during their formation, but all of the chondrites represent undifferentiated (non-igneous) assemblages. The major differences in mineralogy and phase abundance between and within the chondrite types are primarily a function of oxidation state. This can be expressed by the general formula:

$Fe + O + (FeO,MgO)SiO_2 \Leftrightarrow (FeO,MgO)_2SiO_2$ [Metal + Pyroxene <=> Olivine]

which proceeds to the left under more reducing conditions and to the right under more oxidizing conditions. Since this reaction occurs in an essentially closed chemical system, the phase abundances (olivine, pyroxene, metal) and the mafic phase compositions (Fs, Fa) do not vary independently. Fixing any one of these parameters determines all the others. The slopes of these parameters versus oxidation state varies somewhat between the different chondrite types, but the sign of the slope (positive or negative) is the same.

The S-class asteroids have spectra which indicate surfaces composed of various mixtures of olivine, pyroxene and metal. Their general similarity to OC assemblages lead to the early suggestion that S-asteroid were ordinary chondrites. Observational studies of individual S-asteroids and of the S-population has made this interpretation increasingly untenable. The following discussion outlines (in order of increasing rigor) six major lines of observational evidence which indicate that most of the studied (mostly large) S-type asteroids are not ordinary chondrite assemblages.

I. Metal Abundance: A general reddish spectral slope, which is interpreted as the signature of NiFe metal, is more pronounced in S-asteroids than in even the most metal-rich (H-type, 14-21%) ordinary chondrites. The S-asteroid surface materials either contain high metal abundances (near 50%) or have undergone some type of regolith process which greatly increases the spectral contribution of metal. Simple enrichment of chondritic metal does not appear to be a viable mechanism since OC metal grains are coated with a surface layer that suppresses the red slope. Preferential fragmentation of cold brittle metal has been proposed as a means to increase its surface area (spectral effect) relative to the silicates but this mechanism does not appear viable since metal is still stronger than silicate even when embrittled. Also many S-asteroids are olivine-rich [see below] and the metal in the equivalent OC assemblages (LL type) is not abundant (1.4-8%) and does not embrittle at low temperatures. Since there is no correlation between apparent S-asteroid metal abundance and silicate mineralogy, the metal fragmentation in the regolith

would have to produce the same effect over a wide range of initial metal abundances and in both the brittle and ductile fracture regimes. This seems improbable. No proposed regolith process for producing S-type spectra from ordinary chondrite substrates has yet survived testing. However, the physical abundance of metal on S-asteroids is poorly determined from reflectance spectra, so there is still room to postulate such mechanisms. Better metal abundance determinations may come from radar or thermal infrared studies.

II. Olivine Abundance: It has been long noted that many S-asteroids have higher olivine abundances than are commonly present in the ordinary chondrite suite. Based upon silicate mineralogy, if S-asteroids were chondrites, most would have to be extreme LL or even CV/O-types to match the olivine abundance.

III. Relative Olivine/Metal Abundances: If most S-asteroids were chondrites, then the metal abundance would favor H-types while the silicate mineralogy would simultaneously favor LL or CV/O-types for the same objects. Although one can postulate an unsampled OC group (e.g. a highly oxidized HH-type) to reconcile these observations, this does not solve the problem of parent bodies for the present ordinary chondrites. In addition, based upon the relationship of principle component score to mineralogy within the S-population, the general trend is for decreasing olivine/metal abundance ratios at larger heliocentric distances. This is opposite to the pattern expected for chondritic assemblages formed in standard solar nebula models, suggesting that the observed pattern was established by subsequent igneous differentiation.

IV. Pyroxene Chemistry: More than a third of the S-asteroids show absorption features indicating that calcic clinopyroxene (cpx) is a significant surface phase. The mere presence of a significant clinopyroxene component is a strong indication that those specific objects are achondrites rather than chondrites.

V. Range of Bulk Silicate Mineralogy: The S-asteroid mineralogies derived from the analysis of reflectance spectra have silicate assemblages ranging from dunite to basaltic, nearly four times the range present in OC silicates. More than 75% of studied S-asteroids have pyroxene compositions and/or mafic silicate abundances which fall outside the OC range. The 25% which meet OC-criteria for these two parameters are possible candidates for OC bodies but are as yet unproven. Many of these OC candidates appear to be metal-rich and may be analogous to the primitive achondrites (in which an Fe-FeS melt was added to an unmelted chondritic silicate assemblage). However if there are OC objects among the larger S-asteroids, they are probably to be found in this subset, and observational studies are proceeding to test each individually.

VI. Rotational Spectral Variations: Relative mineralogic variations between different surface regions observed as an asteroid rotates provides the most sensitive and robust diagnostic test of whether an object satisfies the fundamental chondritic criteria discussed above. The interdependence between phase abundances and compositions for the chondrites requires that any mineralogic differences observed across an OC asteroid surface must exhibit specific relative variations. Thus an olivine-rich region on an OC-body must show higher Fs and Fa contents in the mafic silicates and lower pyroxene and metal abundances relative to a region with a lower olivine abundance. Any body which shows variations that do not have the correct sense of these relative variations cannot be chondritic. The observations and analysis to apply this test are very time consuming but are also quite insensitive to uncertainties in spectral calibrations. Among the handful of S-asteroids so far tested by this technique (primarily selected as good OC candidates), all have failed.

This work was supported in part by NASA Planetary Geology and Geophysics Grant NAGW-642 and by NSF Solar System Astronomy Grant AST-9012180.

N92-12914

COSMOGENIC ^{36}Ar FROM NEUTRON CAPTURE BY ^{35}Cl IN THE CHICO L6 CHONDRITE: ADDITIONAL EVIDENCE FOR LARGE SHIELDING; D.H. Garrison, D.D. Bogard, (NASA, Johnson Space Center, Houston, TX 77058) & G.F. Herzog (Rutgers Univ., New Brunswick, NJ 08903).

The cosmic-ray-produced $^{36}Ar/^{38}Ar$ ratio measured in iron meteorites is ~0.65 but is not well determined for stone meteorites due to the common presence of trapped Ar or adsorbed atmospheric Ar in bulk analyses. Almost all single-extraction measurements of stones give $^{36}Ar/^{38}Ar$ ratios intermediate between the trapped and air values of 5.3 and the expected cosmogenic value of ~0.65 (1). Cosmic ray interactions produce ^{36}Ar directly and through the ^{36}Cl precursor (half-life, $3x10^5$ yrs). The high-energy production rate of ^{36}Cl in chondrites is predicted to be 3-8 atoms/min/kg (2), and virtually all of the limited ^{36}Cl measurements in chondrites are within this range (3). Theoretically, ^{36}Cl can also be produced in significant amounts in large meteorites by thermal neutron capture on ^{35}Cl (2). Except for Allende (4), significant excesses of ^{36}Cl and/or cosmogenic ^{36}Ar attributable to neutron capture have not been reported for any chondrite, including samples of variable shielding from large chondrites. The Chico L6 chondrite is a good candidate for observing cosmogenic ^{36}Ar produced by neutron capture because: 1) it had a long irradiation under very large shielding (5); 2) an impact ~0.5 Ga ago strongly degassed it of radiogenic ^{40}Ar and presumably any trapped Ar as well; 3) measurements of ^{37}Ar and ^{38}Ar by stepwise temperature degassing of neutron-irradiated Chico samples define the release of cosmogenic Ar produced from Ca in relation to neutron-capture Ar produced from Cl sites; and 4) we determined the [Cl] for the irradiated samples.

The isotopic composition of Ar was measured for stepwise temperature release of both chondritic and melt portions of Chico. For the neutron-irradiated samples, most of the ^{37}Ar and ^{38}Ar (produced in the reactor from Ca and ^{37}Cl, respectively), and most of the cosmogenic ^{36}Ar were released at relatively high extraction temperatures of 1100-1600°C, suggesting that Cl contamination is not significant. From the reaction ^{37}Cl ($n,\gamma\ \beta$) ^{38}Ar and a determination of [Cl] in our flux monitor, we calculate [Cl] for the chondrite and melt samples of Chico as 77ppm and 84ppm, respectively. For the two unirradiated Chico samples, cosmogenic ^{36}Ar and ^{38}Ar were also primarily released at 1100-1500°C. However, the cosmogenic $^{36}Ar/^{38}Ar$ ratio varied considerably during the releases, reaching high values around 1000°C of 4.4 and 9 for the chondritic and melt samples, respectively, and dropping to low values around 1400°C of 1.2-1.3. The variation in $^{36}Ar/^{38}Ar$ was essentially that expected from the relative releases of ^{38}Ar (from Cl) and ^{37}Ar (from Ca) in irradiated samples, and indicates the presence of both high-energy and neutron-capture components for ^{36}Ar. Values greater than ~5.3 can only be produced from Cl. The average cosmogenic $^{36}Ar/^{38}Ar$ for the chondritic and melt samples (after small corrections for low-temperature air Ar and ^{38}Ar from probable Cl weathering products) were 1.76 and 2.27, respectively. The maxima in $^{36}Ar/^{38}Ar$ for the unirradiated samples occurred at approximately the same extraction temperature as maxima in $^{38}Ar/^{37}Ar$ for the irradiated samples. These data demonstrate that the cosmogenic $^{36}Ar/^{38}Ar$ ratio in Chico is much higher than the typical value accepted for chondrites of ~0.65-0.7.

Assuming a high-energy spallation ratio of $^{36}Ar/^{38}Ar$ =0.65, we calculate excesses of ^{36}Ar produced by neutron capture on ^{35}Cl for the chondritic and melt samples of 2.6 $x10^{-8}$ and 3.4 $x10^{-8}$ ccSTP/g, respectively. For a cosmic ray exposure age for Chico of 63 My (5), these ^{36}Ar excesses correspond to a ^{36}Ar production rate by thermal neutron capture of ~300 atoms/minute/gram-Cl. By way of comparison, (4) observed an average excess of ^{36}Ar in their Allende samples of ~$2x10^{-8}$ ccSTP/g and an average [Cl] of 2800ppm, which yields an average ^{36}Ar production rate (with Allende exposure age = 5.2 My) of ~70 atoms/min/g-Cl. For chondrites this calculated production rate (2, 6) rises from essentially the spallation-produced value at no shielding to values of 200-275 atoms/min/g-Cl or more at shielding levels of ~300 g/cm^2 in large meteorites. Because bulk analyses of most chondrites yield measured $^{36}Ar/^{38}Ar$ ratios higher than the assumed cosmogenic value of ~0.65, the ^{38}Ar is corrected for trapped (or atmospheric) Ar using assumed end-member components and the lever rule. The Chico data suggest that for large chondrites the cosmogenic $^{36}Ar/^{38}Ar$ ratio may well be significantly higher than 0.65 and therefore such a procedure may underestimate the concentration of cosmogenic ^{38}Ar. In this context we note that in analyses of many Antarctic chondrites (7) observed that determined amounts of cosmogenic ^{38}Ar averaged ~13% too low in comparison to that expected from measurements of other cosmogenic species. Measurement of ^{36}Cl in Chico is planned.

1) L. Schultz & H. Kruse, Meteoritics 24, 1989; 2) M.Spergel et al, Proc. 16 LPSC, 91, 1986; 3) K. Nishiizumi, Nucl. Tracks Radiat. Meas. 13, 1987; 4) R.Goebel et al, GCA 46, 1982; 5) D.Garrison et al, LPS XXII, 1991; P.Eberhardt et al, Earth Sci. & Meteoritics, 1963; 7) L.Schutz et al, GCA 55, 1991.

EJECTA FROM LUNAR IMPACTS: WHERE IS IT ON EARTH?
Gault, D.E. , Murphys Center of Planetology, Murphys, CA 95247
Schultz, P.H., Department of Geological Sciences, Brown University, Providence, RI 02912

Apollo samples and Antarctica meteorites represent a trivial fraction of the mass of material that Earth is/has been accreting from the Moon every year. Crater production rates from Apollo sample age-dating for craters < 100 meters diameter provide a revised current influx rate for material from the Moon amounting to $3x10^8$ grams/year, almost an order of magnitude greater than previous estimates (1). Most of this mass comes from an Earth-orbiting cloud of debris that has a lifetime of about 30 years and a small fraction arriving from direct trajectories from the source crater(s). The total mass is equivalent to one 10-micron glass sphere per 20 sq. cm. on Earth.

Superimposed on this "background" rate there will have been periodic increased bursts caused by major impact events. Calculations indicate that the 100 million year old 90 km crater Tycho, for example, deposited more than 10^{16}g of ejecta on Earth. The 60 million year old Kepler (30 km diameter) sent more than 10^{14}g to Earth. But it is far more intriguing if, as suggested by Hartung (2, 3), the 20 km lunar crater Giordano Bruno was formed in the year 1178 AD. Then it would be only 813 years ago that Earth accreted more than 10^{13}g in a week following the impact and a total of 10^{14}g over the subsequent three decades, enough to have deposited a total of 10^4g 10-micron spheres per sq. cm.

Question: Why has none of this lunar debris been yet found/recognized/identified?

Answer (?): There are a lot of uncertainties. What should one look for: size, shape, and composition? Size and shape depend on the scale and chemistry of the source. Most of the ejecta will arrive as highly-shocked and/or melt material. Basic composition will enhance probability for small glass spheres, both at crater ejection and by ablation of larger pieces during atmospheric entry. Highly silicic ejecta should experience less melting during ejection and entry so that larger pieces and partial melt/crystalline material would survive.

Question: Where should one look? Sea cores, polar/glacial ice cores, and the LDEF, the latter two probably providing the best/easiest source for identification. And if Giordano Bruno was formed 813 years ago (2, 3), there absolutely has to be lunar material from the event stored some place in Earth's geologic record.

Conclusion: Earth has accreted over the past 100 million years more than 10^{17}g of lunar material, equivalent to a spherical mass more than 6 km in diameter. It is a challenge for search and discovery.

References:
(1) Gault, D.E. (1983) *LPSC XIV,* 243-244.
(2) Hartung, J.B. (1976) *Meteoritics,* 187-194.
(3) Hartung, J.B. (1981) *LPSC XII,* 401-403.

THE CK CHONDRITES - CONDITIONS OF PARENT BODY METAMORPHISM; T. Geiger and A. Bischoff, University of Münster, Institute of Planetology, Wilhelm-Klemm-Str.10, 4400 Münster, Germany.

Here we report on the results of a mineralogical study of the formerly called C4-6 chondrites. Mainly based on bulk chemical data these meteorites have been recently classified in a new carbonaceous chondrite group - the CK (Karoonda) group (Kallemeyn et al., 1991). Earlier Geiger and Bischoff (1990b) recommended based on their mineralogical observations and mineral chemical data to group these meteorites in an own carbonaceous chondrite group. The present study considers 19 different meteorites classified earlier as C4-6.

Mineralogy: The **olivines** are highly equilibrated. Mean Fa-contents of matrix-olivines vary from 28.6 mol% in ALH84038 to 33.9 mol% in Maralinga - with standard deviations (1σ) of 0.45-1.0 (PMD 1.2-3.3; Coolidge 14.6 ± 0.7, PMD 4.79). Except for Coolidge and ALH84096 all olivines contain high NiO-contents (0.33-0.72 wt.%). Their CaO-contents are mostly below 0.1 wt.%. In general chondrule olivines are equilibrated. Only in Karoonda we have found a Fo-rich core of an olivine within the center of a PO chondrule. In addition to the Fe-Mg zoning we observe also a distinct zoning of Ca and Ni (Ni is decreasing and Ca is increasing towards the core). Two types of **pyroxenes** could be found: Low-Ca pyroxenes with mean Fs-contents from 24.0 to 27.5 mol% (1σ: 0.74-2.00; Coolidge 11.3 ± 3.19). The second pyroxene is an augite (Fs $\approx$10 mol%). The paragenesis of low-Ca and high-Ca pyroxene was found in three meteorites. The calculated equilibration temperatures lead to 680°C for EET87507, 720°C for Maralinga, and 1000°C for LEW97009, the mean errors are $\pm$50°C (Lindsley and Andersen, 1983). **Plagioclase** compositions are heterogeneous in all samples investigated. They vary mostly from 20-75 mol% anorthite - in some cases even higher and lower An-values could be measured.

The most abundant opaque mineral within the CK chondrites is **magnetite** (Coolidge and ALH84096 do not contain magnetite but Fe,Ni metal). Geiger and Bischoff (1990a) described exsolution of ilmenite and spinel in magnetites from all CK-chondrites and the existence of different magnetite-populations. These magnetites contain up to 5.5 wt.% Cr_2O_3 and small amounts of MgO, Al_2O_3, and TiO_2. The dominating **sulfide** minerals are pyrite and pentlandite. Minor phases are pyrrhotite and chalcopyrite in some of the meteorites. In some CK chondrites we observe strong evidence that sulfides have been replaced by magnetite. **Platinum-group-minerals** (PGM) (e.g. $(Os,Ru,Ir)S_2$, $PtTe_2$, PtS) intergrown with sulfides and magnetites (Geiger and Bischoff, 1989) occur in all studied CK chondrites. As suggested by Keays et al. (1981) for the formation of these mineral phases in terrestrial environments we believe that the PGM must have been formed by sub-solidus exsolution during metamorphism under highly oxidizing conditions.

Compared with type 4-6 OC some mineralogical differences can be pointed out: 1) Occurrence of magnetite; 2) heterogeneity of plagioclase composition; 3) high NiO-contents in olivines; 4) occurrence of PGM. The metamorphic temperatures on the CK parent body are similar to those assumed for the parent body of the ordinary chondrites (Dodd, 1981). Based on the determined equilibration temperatures of coexisting pyroxenes and on the metamorphic temperature of the Karoonda meteorite of 580°C (Clayton et al., 1977) we conclude for type 4 $\approx$550-650°C, for type 5 $\approx$650-800°C, and for type 6 $\approx$800-1000°C. Based on mineralogical characteristics Coolidge and ALH84096 should not be classified as CK chondrites.

References: Clayton et al., EPSL 34, 209-224, (1977). Dodd R.T Cambridge Univ. Press, (1981). Geiger and Bischoff, LPSC XX, 335-336, (1989). Geiger and Bischoff, LPSC XXI, 409-410, (1990a). Geiger and Bischoff, 15th Symp. Antarctic Meteor., Natl Inst. Polar Res., Tokyo, 78-80, (1990b). Kallemeyn et al., GCA 55, 881-892, (1991). Keays et al., Nature 294, 5842, 646-648, (1981).

A NOBLE GAS STUDY IN ST SEVERIN CORE AIII AND KNYAHINYA SAMPLES: E. Gilabert, B. Lavielle; U.R.A. 451 of C.N.R.S. , C.E.N.B.G. , 33175 GRADIGNAN CEDEX, FRANCE

The purpose of this work is to improve the determination of the cosmogenic Kr and Xe component in meteorite sample by using a precombustion step in O_2 at 600°C. As previously observed [1], this procedure allows a low temperature extraction of a fraction of the trapped noble gas component, allowing an enrichment of the cosmogenic component during the melting of the sample. We have carried out noble gas analysis in St Séverin core AIII and Knyahinya gram-size samples by using the experimental procedure previously reported [2]. Concentration and isotopic composition of Ne, Ar, Kr and Xe were measured in 3 samples from St Séverin (1 from piece B, 2 from core AIII) and in 3 samples from Knyahinya. Figure 1 presents the release of ^{83}Kr versus the temperature step for a St Séverin core AIII sample located at 330 mm. It appears that more than 16% of the trapped Kr component is released during the 625°C combustion step with only 2% of the cosmogenic component. The isotopic composition of the trapped Xe in the combustion step is similar to the composition measured in Forest Vale by using the same method. On the figure 2, concentrations of cosmogenic ^{83}Kr are reported versus the location of the samples in the core AIII. The new measurements well agree with the previous determinations from the same laboratory [3] for cosmogenic krypton and with the results from Schultz and Signer [4] for cosmogenic neon.

According the calibrations by Eugster [5], ^{21}Ne and ^{83}Kr irradiation ages of St Séverin were found to be respectively (14.0 ± 0.4) and (12.6 ± 0.7)ma. Irradiation age using ^{81}Kr-Kr method has also been measured in the 2 core AIII samples leading to a value of (14.0 ± 1.4)ma. In Knyahinya, irradiation ages of (37.4 ± 1.5)ma for ^{21}Ne and (35.7 ± 2.0)ma for ^{83}Kr have been obtained.

References: [1] Lavielle and Marti (1988) Lunar Planet. Sci. Conf. (abstract) 19th, 667; [2] Lavielle et al. (1990) Meteoritics 25,378; [3] Lavielle and Marti; Proc. Lunar Planet. Sci. Conf. 18th (1988) 18,565; [4] Schultz and Signer (1976) Earth Planet. Sci. Lett. 30,191; [5] Eugster(1988) Geochim. Cosmochim. Acta 52,1649

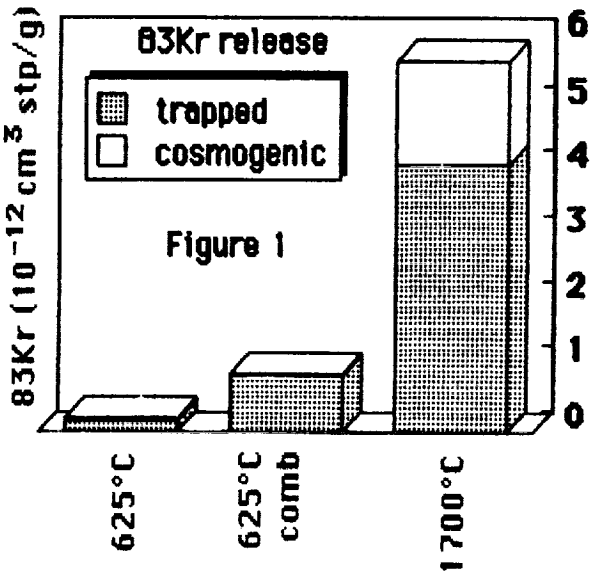

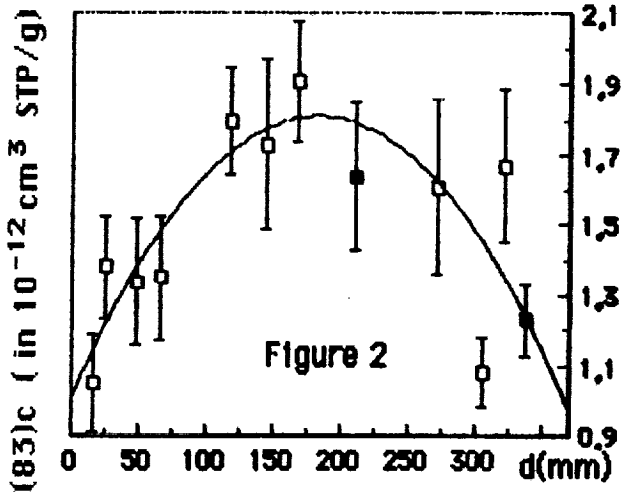

Cosmogenic 83Kr in St Séverin core AIII

□ Lavielle and Marti,1988

■ this work

COMPOUND SPECIFIC ISOTOPE ANALYSIS OF POLYCYCLIC AROMATIC HYDROCARBONS IN CARBONACEOUS CHONDRITES;

I. Gilmour, I.A. Franchi and C.T. Pillinger, Dept. Earth Sciences, Open University, Milton Keynes, U.K., P. Eakin and A. Fallick, S.U.R.R.C., East Kilbride, U.K..

The origins of the aromatic macromolecular material in carbonaceous chondrites remains a major goal in the study of meteoritic organic matter. It has been known for some time that it cannot simply be polymerized interstellar material as the D enrichment is 2 to 4 orders of magnitude below that observed for interstellar molecules (1). A putative structure of the macromolecular material consisting of bridged aromatic ring systems has been taken to imply formation temperatures similar to those of the solar nebula rather than molecular clouds (2). However, there is now convincing evidence for emission bands resembling those of PAH in interstellar infra-red spectra (3). These PAH are thought to occur in two forms; as free-molecule PAH and as amorphous carbon particles. It is therefore conceivable that the macromolecular material may be predominantly presolar.

Free PAH from the Orgueil and Murchison meteorites were analyzed for their carbon isotope compositions (Table 1). Previous compound specific isotope studies on saturated aliphatic material from the same meteorites have suggested that the straight chain hydrocarbons are largely terrestrial contamination and that there is no straight chain predominance thereby arguing against formation by a selective process such as Fischer-Tropsch type synthesis. Results for PAH of 3-5 aromatic rings suggest that they are largely indigenous with $\delta^{13}C$ values of between -9 and -24‰ with most having isotopic compositions of around -15 to -17‰, similar to that in the macromolecular material (1). These values are generally 10‰ heavier than typical carbon isotope ratios for petroleum which would appear to be the major contaminant in the Orgueil meteorite (4). However there does appear to be some level of contamination of specific molecules in Orgueil such as phenanthrene and chrysene. The similarities between the PAH and the macromolecular material as well as the inter-meteorite variation will be discussed.

REFS. (1) Kerridge J.F. (1983) EPSL **64**, 186-200; (2) Hayatsu R. and Anders E.(1981) Topics in Current Chemistry **99**, 1-37; (3) Allamandola L.J. *et al.* (1987), Science **237**, 56-59; (4) Franchi I.A. *et al.* (1990) Oral presentation at 53rd Meteoritical Society, Perth.

Table 1 - $\delta^{13}C$ of PAH in Murchison and Orgueil

PAH	No. Rings	Murchison	Orgueil
Anthracene	3	-10.7	nm
Phenanthrene	3		-23.8
Fluoranthene	3*	-9.4	-18.8
Pyrene	4	-16.1	-17.1
Chrysene	4	-	-23.2
Benzofluoranthene	4*	-	-15.4
Benzanthracene	4	-	-15.2
Dibenzanthracene	5	-	-17.0

* Also contains one five member ring.

THE PLESSITE STRUCTURE IN IRON METEORITES: J. I. Goldstein, D. B. Williams and J. Zhang, Dept. of Materials Science & Engineering, Lehigh University, Bethlehem, PA 18015, USA

Plessite is a two phase structure composed of a high Ni fcc precipitate phase and a low Ni bcc matrix phase. The morphology of the plessite varies with the local average Ni content in the "M" shaped profile of the parent taenite phase [1,2]. At Ni contents above about 25 wt% Ni, other low temperature structures such as clear taenite and the cloudy zone form. Fig. 1 shows a Ni profile across half of a plessite "M" profile in the Grant meteorite. The composition ranges of the two major structural types of plessite, high Ni black plessite and low Ni duplex plessite are shown. This paper presents the results of electron microscopy studies of plessite in two octahedrites, Carlton and Grant, in high Ni ataxites, and in carbon rich iron meteorites in order to develop an overall understanding of the plessite structure and its formation in the iron meteorites.

The two phase plessite structure forms during the slow cooling of the iron meteorites generally in a two step process [2,3]. During the development of the "M" Ni profile, taenite transforms to martensite in the lower Ni part of the Ni gradient. During further cooling, martensite decomposition occurs. In the low Ni region of the "M" profile, < 15wt%, duplex plessite forms. Precipitates of fcc taenite, 50 to 54 wt% Ni, nucleate at the original martensite grain boundaries and grow to a relatively large size (50 to >200 nm wide). These taenite precipitates are ordered and are in equilibrium with the kamacite matrix phase, containing 4 to 5 wt% Ni. The composition of the two phases is consistent with the current Fe-Ni phase diagram [4]. In the high Ni region of the "M" profile, > 15wt% to 25 wt% Ni, black plessite forms. Precipitates of fcc taenite, 57 to 60 wt% Ni, form inside the original martensite grains and their sizes are very small, typically 10 to 20 nm wide. These taenite precipitates are found in a matrix bcc phase of 10 wt % Ni or higher. Fig. 2 shows a Ni profile taken with the analytical electron microscope across a precipitate in a 17 wt% Ni black plessite region of the Grant meteorite. These taenite precipitates are ordered but are <u>not</u> in equilibrium with the kamacite phase. The growth of the taenite precipitates in the black plessite occurs at lower temperatures than in the duplex plessite because the martensite formation and subsequent decomposition occurs at lower temperatures. At the lower temperatures, <350°C, the growth process gradually changes from equilibrium diffusion control to interface control. Interface controlled growth no longer requires equilibrium between kamacite and taenite at the interphase interface as given by the phase diagram. In addition, composition gradients are no longer observed in the matrix bcc phase (Note Fig. 2) and the matrix composition changes (increases) to maximize the growth rate. These results are consistent with measurements of laboratory alloys heat treated from 300 to 450°C for periods of up to 370 days [3].

REFERENCES: 1. Buchwald, V.F. (1975) Handbook of Iron Meteorites, University of California Press. 2. Massalski, T.B., Park, F.R., and Vassamillet, L.F. (1966) Geochim. et Cosmochim. Acta, **30**, pp. 649-62. 3. Zhang, J. (1991) PhD Thesis, Lehigh Univ. 4. Reuter, K.B., Williams, D.B., and Goldstein, J.I. (1989) Met. Trans. **A20**, 719-25.

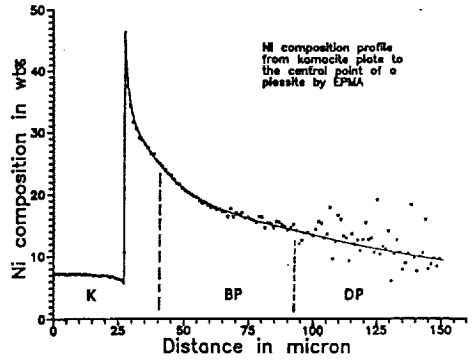

Figure 1

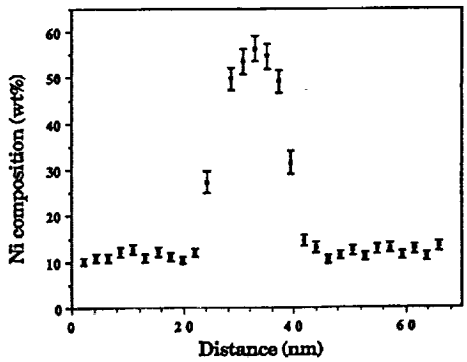

Figure 2

CONSTRAINTS ON THE TIME OF ACCRETION AND THERMAL EVOLUTION OF CHONDRITE PARENT BODIES BY PRECISE U-PB DATING OF PHOSPHATES; C. GÖPEL, G. MANHES, C. J. ALLEGRE
(Lab. Géochimie & Cosmochimie, I. P. G., 4, Place Jussieu, 75252 PARIS CEDEX 05)

We report new age data for phosphates separated from ordinary chondrites, thus expanding our data set on chondrites of metamorphic grade 4. The purpose of this U-Pb study of phosphates is to constrain the formation ages of equilibrated chondrites with a resolution of a few million years. This should contribute to a characterization of the effective heat sources which affected their parent bodies.

Phosphates are minor mineral phases in all classes of chondrites and apparently formed as secondary mineral phases during chondrite metamorphism by oxidation of the metal. Both phosphates (merrillite and apatite) present in chondrites, are enriched in U compared to the bulk rock and contain Pb with a highly radiogenic isotopic composition.

We analysed ~ 15 phosphates seperated from H-, L- and LL- chondrites. All meteorites were chosen for their non-shocked character. Most of them had been previously studied with Rb/Sr- and Ar/Ar isotopes or fission tracks (1-4). All Pb isotopic compositions for the phosphates are more radiogenic ($^{206}Pb/^{204}Pb$ = 3500 for Barwell) than the corresponding bulk fragments. Because of these radiogenic compositions, the Pb/Pb ages are independent from the composition of the nonradiogenic or initial Pb component. All phosphates are concordant, indicating that the U-Pb system stayed closed since ~4.55Æ, allowing us to interpret the Pb/Pb ages with the analytical precision of 1 x 10^6 y.

This precise U-Pb chronology allows us to constrain the thermal evolution of the chondrite parent bodies and to place it into an absolute time scale:

All measured phosphate ages lie between 4.50 and 4.56Æ. These ages are consistent with the time interval predicted for thermal metamorphism by other chronometers; the resolution of these Pb ages is, however, 20-30 times better than the other absolute chronometers (Rb/Sr, Ar/Ar).

Phosphates from H- chondrites represent the most favourable case. They preserved their U-Pb systematics, obtained during the cooling phase following thermal metamorphism. The minerals from the most highly metamorphosed H6 chondrites (Guarena, Kernouvé) are (30-50 x10^6y) younger than those from the H5 meteorites (Richardson, Nadiabondi, Allegan), clustering around ages of 4.55Æ. Phosphates from the H4 meteorites (Forest Vale, St. Marguerite) show the oldest ages with >4.56 Æ.

The most outstanding result of this age distribution is the confirmation of an onion shell structure and the relatively simple thermal evolution of the H chondrite parent body, which had already been proposed by studies of thermochronometry with ^{244}Pu and metallic cooling rates (3, 5). This is however, the first time that a correlation of ages versus metamorphic grade can be resolved using an absolute chronometer.

The ages indicate a lower limit for the formation age of the chondrite parent bodies. The U-Pb age of the H4 chondrites lies close to that of the Allende inclusions, estimated at 4.566± 0.002Æ. It situates the formation of the H chondrite parent body at a time when ^{26}Al could have still been alive in solar material and it renders plausible the idea that ^{26}Al may have played a role as a heat source.

References: 1) Minster, J. F. & Allègre, C. J. (1979) *Earth Planet. Sci. Lett.*. **42**, 333-347. 2) Turner, G., Enright, M. C. & Cadogan, P. H. (1978) *Proc. Lunar. Sci. Conf.* **9th**, 989-1025. 3) Pellas, P. & Störzer, D. (1981) *Proc. R. Soc. Lond. A* **374**, 253 -270. 4) Podosek, F. & Brannon, J. C. (1991) Meteoritics, in press. 5) Wood, J. (1979) in: Asteroids, ed. T.Gehrels (Tuscon: Univ. of Arizona Press), 849-891.

METEORITIC EVIDENCE FOR AN ACTIVE EARLY SUN: J.N.Goswami, Physical Research Laboratory, Ahmedabad-380 009, India

The pre-main-sequence evolution of sun-like stars is dominated by an active phase, the so-called T-Tauri phase, characterized by high mass-outflow at the rate of $\sim 10^{-7}$ to 10^{-8} solar mass per year. Planetary scientists have invoked the presence of a strong T-Tauri wind from the early sun which presumably cleared the residual nebular gas and dust following the formation of small objects, the precursors to the planetesimals/ planetary objects in our solar system. Even if the Sun was magnetically active during this phase and was the source of intense flare activity, self shielding by the nebular gas may not allow the solar energetic particles to effectively interact with the meteoritic components at 2-4 AU. Recent studies have however revealed that weak T-tauri stars, which are not prominent in optical emission and have weak mass-outflow, show variations in their emission in X-ray and radio-band over short time-scales. These variabilities have been attributed to magnetically driven intense flare-like activity in the weak T-Tauri stars [1]. If the Sun has also gone through such a stage, following the burst of the T-Tauri wind that cleared the residual nebular gas and dust, it will be logical to expect intense solar flare irradiation records in meteoritic components that were exposed to an active early Sun. Gas-rich meteorites, and the gas-rich carbonaceous chondrites in particular, seem to be the most ideal samples to look for such records. Several experimental approaches, both direct and indirect, have so far been attempted to address this problem [2]. The main uncertainty in interpreting the data is our lack of proper knowledge about (i) the exact epoch of the early irradiation of the meteoritic component and (ii) collision-controlled evolutionary time scales of the meteorite-parent-body surfaces. The present status of the work will be summarized and results from some recent effort will be presented.

References:

1. Feigelson E.D.*et al.*, in 'The Sun in Time' (in press), 1991. 2. Caffee M. *et al.*, Ibid, 1991.

TITANIUM, CALCIUM AND MAGNESIUM ISOTOPIC COMPOSITIONS IN A HIBONITE-RICH INCLUSION FROM EFREMOVKA. J.N. Goswami[1] , G.Srinivasan [1] and A.A.Ulyanov[2] . [1]Physical Research Laboratory, Ahmedabad – 380 009,India. [2]Vernadsky Institute of Geochemistry and Analytical Chemistry,Moscow 11795,USSR.

Studies of nuclear and radiogenic anomalies in different refractory phases within a given inclusion can provide insight about the processes leading to the incorporation and preservation of anomalous isotopic records in these early solar system objects. We have chosen an inclusion E-50 from the Efremovka CV3 chondrite for such a study. This multi-zoned hibonite rich inclusion has a spinel-rich core , followed by a hibonite rich zone, a melilite-spinel zone, a melilite zone and a melilite-perovskite zone near a multilayered complex rim and contains at least five distinct refractory phases(hibonite,perovskite,spinel,melilite and fassaite) that can be analysed for their isotopic composition by the ion-probe technique. It is a normal(non-FUN) inclusion and like most other Efremovka inclusions, it is characterized by the absence of secondary alteration products.

The Mg-isotopic composition measured in spinel,melilite and hibonite in representative samples from all the zones in this inclusion show the presence of non linear ^{26}Mg excess that correlates well with ^{26}Al and yields an initial $(^{26}Al/^{27}Al)$ of $(4.6 \pm 1.8) \times 10^{-5}$ and initial magnesium composition $(^{26}Mg/^{24}Mg)_i = (0.139385 \pm 0.00024)$ similar to the solar system value. These values are in agreement with those found by earlier work[1].

The Titanium isotopic composition was measured at a mass resolution $(M/\Delta M)$ of more than 10,000 so that isobaric interference at mass 48 was completely resolved. Several hibonite,perovskite and fassaite grains were analysed. The hibonite grains were sampled from the hibonite rich zone, the pyroxene grains from a melilite-spinel zone and the perovskites from the melilite-spinel and melilite zones. A positive anomaly in ^{50}Ti was found in hibonite and in perovskite from one region of the melilite zone. Ti composition in perovskite from another region of the melilite zone as well as both perovskite and fassaite from the melilite-spinel zone are normal within experimental uncertainty.

The Calcium isotopic studies were made extremely difficult due to the small size of the perovskite and hibonite phases and contribution to the signal from calcium present in melilite. No meaningful data could be obtained for the hibonite while the perovskite grain with ^{50}Ti anomaly showed a definite excess at ^{48}Ca. The presence of non uniform nuclear anomaly in micro-phases of the same inclusion, even though the magnesium systematics for the whole inclusion is well defined, raises new questions about the incorporation and preservation of nuclear anomaly in pristine solar system material.

REFERENCES:

1 Fahey A.J.(Thesis), Washington University. St Louis,1988.

ACFER 182: AN UNUSUAL CHONDRITE WITH AFFINITIES TO ALH 85085; Monica M. Grady, R. D. Ash, A. D. Morse and C. T. Pillinger, Planetary Sciences Unit, Department of Earth Sciences, The Open University, Walton Hall, Milton Keynes MK7 6AA, U.K.

Acfer 182 was returned from the Western Sahara in 1990 as two stones totalling 166 g in weight. Preliminary optical examination by the finder tentatively classed the meteorite as EH3 - 4. However, a more detailed petrographic study [1] recognized many similarities in Acfer 182 to the highly unusual chondrite ALH 85085, despite the heavy weathering which the former had undoubtedly undergone. ALH 85085 is distinguished by its high enrichment in ^{15}N [2], therefore if Acfer 182 is indeed related to ALH 85085, then it too should be similarly enriched in ^{15}N.

Both whole-rock nitrogen and carbon abundance data exhibit the same effect (see Table): Acfer 182 has only *ca.* one third the volatile abundance of ALH 85085. Whereas for carbon, total $\delta^{13}C$ is not substantially different despite its lower abundance, in the case of nitrogen, $\delta^{15}N$ of whole rock Acfer 182 is over 300‰ lighter than that of ALH 85085. Stepped combustion data indicate that it is not the minor component "N_C" of ALH 85085 with $\delta^{15}N$ *ca* +1500‰ [2] that is missing from Acfer 182, but rather that the major components "N_A" and "N_B" are reduced in both abundance and $\delta^{15}N$. Indeed, the abundance of N_C might be enhanced in Acfer 182 relative to ALH 85085: the yield of nitrogen is greater across the temperature range associated with N_C in the former specimen. In ALH 85085, N_A was interpreted as carbonaceous material and N_B as nitrogen associated either with fine-grained Fe-Ni metal or with the abundant matrix clasts. Weathering can certainly account for the depletion of N_B in Acfer 182: much of the Fe-Ni metal has been oxidized to limonite [1], imparting a reddish colour to the meteorite.

Acfer 182, like ALH 85085, contains abundant inclusions of CI-like material, veined with carbonates [1]. Dissolution in two steps in orthophosphoric acid (H_3PO_4) yields CO_2 successively from calcite and dolomite; the total carbonate concentration and isotopic composition are given in the table. Both meteorites contain similar abundances of carbonate, with differing isotopic compositions, however, $\delta^{13}C$ of the carbonates is more akin to that of CM than CI chondrites [3]. Additionally, 95% of the carbonate dissolves in the first acid extraction, implying calcite rather than dolomite: the former is more abundant in CMs, the latter in CIs. Hydrogen analysis of Acfer 182 and ALH 85085 gave similar quantities of water with low values of δD. The isotopic composition is more characteristic of terrestrial material than of CIs.

It is concluded that on the basis of carbon and nitrogen stable isotope geochemistry, Acfer 182 has affinities with ALH 85085, and that many of the differences which exist are due to differences in the weathering regimes which the two specimens have experienced.

	Whole Rock						H_3PO_4 Dissolution		
	[C] (wt.%)	$\delta^{13}C$ (‰)	[N] (ppm)	$\delta^{15}N$ (‰)	[H] (ppm)	δD (‰)	[C] (ppm)	$\delta^{13}C$ (‰)	$\delta^{18}O^*$ (‰)
ALH 85085	1.21	+0.7	280	+858	344	–79	746	+32.0	+23.4
Acfer 182	0.35	+0.3	102	+541	322	–135	623	+11.4	+29.2

*$\delta^{18}O$ relative to SMOW, calculated assuming the carbonate to be calcite.

References: [1] Bischoff, A. (1991) Paper presented at "Euromet Desert Meteorite Workshop", Cambridge, U.K., April 1991; [2] Grady, M.M. & Pillinger, C.T. (1990) *Earth Planet. Sci. Lett.* **97**, 29-40; [3] Grady, M.M. *et al.*, (1988) *Geochim. Cosmochim. Acta* **52**, 2855-2866.

EXPOSURE AGES OF LL- AND L/LL-CHONDRITES AND IMPLICATIONS FOR PARENT BODY HISTORIES. Th. Graf and K. Marti, Dept. of Chemistry, Univ. of Calif., San Diego, La Jolla, CA92093-0317.

We reported (1) that H- and L-chondrites show exposure age peaks at 33Ma and 40Ma, respectively, and sharp drop-offs towards higher ages. All petrographic types are represented in these peaks. Additional clusters were resolved for different petrographic types and for subgroups of distinct characteristics of radiogenic gases (retention of ^{4}He and ^{40}Ar). We report here the reevaluated cosmic-ray record of all LL-chondrites. The distribution of exposure ages is shown in Fig. 1. We observe the following systematics:

1) Exposure ages of about 30% of all LL-chondrites peak at ~15Ma. Despite the somewhat poor statistics, the peak shape corresponds to that expected for a break-up. The exposure age distribution is not consistent with the roughly exponential distribution expected for a quasi-continuous supply of meteorites. One (St. Mesmin) out of three solar gas bearing LL-chondrites is in this peak. The systematics of ^{40}Ar retention ages show that only minor heating occurred in the history of 15Ma LL-chondrites except for 2 strongly degassed members (Paragould and Oberlin). No clear differences are observed for petrographic types 4 to 6.

2) Small clusters of exposure ages are observed at about 10Ma, 28Ma, and 40Ma, respectively. The positions of the latter 2 clusters agree with clusters or peaks found in the exposure age distribution of L-chondrites. Moreover, a small cluster at ~15Ma is observed for the L-chondrites. One obvious interpretation comes to mind: It is possible that some L- and LL-chondrites are misclassified. In case this option can be rejected, then some striking similarities in the collisional history of L- and LL-chondrites will be indicated.

3) The postulated clan of L/LL-chondrites is small and about 1/3 of these reveal exposure ages of ~40Ma, more than 1/3 have ages <10 Ma, and no exposure age around 15Ma is observed. Therefore, the collisional histories of L/LL chondrites are similar to those of L-chondrites and do not reflect the break-up peak of the LL group at 15Ma. Wasson and Wang (2) note that the gas retention ages of L/LL chondrites are on average higher than those of L-chondrites, but this distinction does not necessarily apply to the members of the 40Ma peak, and certainly not to the group with T_e < 10Ma. In fact, it is interesting to note that among the short exposure ages, radiogenic gas losses are observed for more than half of the L/LL as well as the L-chondrites.

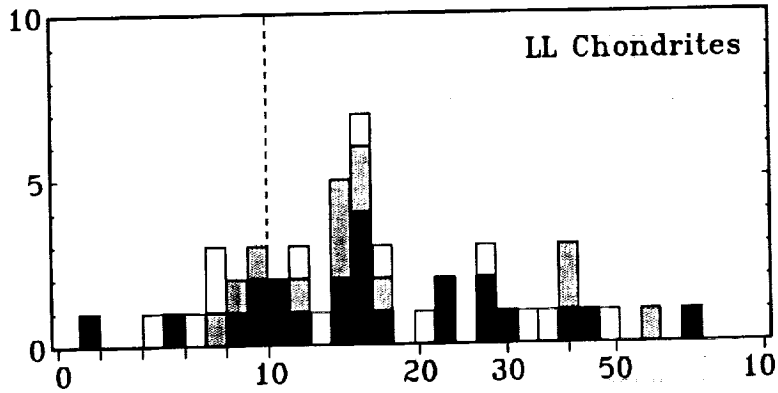

Fig. 1. Exposure age distribution of LL-chondrites. Data quality classes: high quality (black), intermediate (grey), and poor (white). Note scale change: linear between 0-10Ma (resolution 1Ma), logarithmic scale above 10Ma (resolution 10% of the age). Most of the data were compiled in (3).

References: (1) Graf Th. and Marti K. (1990) Meteoritics 23, 368. (2) Wasson J.T. and Wang S. (1991) Preprint. (3) Schultz L. and Kruse H. (1989) Meteoritics 24, 155-172.

SPINEL-BEARING REFRACTORY INCLUSIONS IN COLD BOKKEVELD (CM2). R.C. Greenwood, R. Hutchison, & G. Cressey. The Natural History Museum, London SW7 5BD, UK.

As part of a collaborative study with C.T. Pillinger's group (Open University), D.J. Barber and M. Lee (University of Essex), and J.W. Arden (Oxford University) spinel-bearing refractory inclusions in Cold Bokkeveld (CM2) were located *in situ* and characterized by S.E.M. and electron microprobe techniques. Three main inclusion types are recognised i) spinel-pyroxene inclusions, ii) spinel-perovskite (± hibonite) spherules, iii) anhedral spinel-perovskite (± hibonite) inclusions.

Spinel-pyroxene inclusions are irregular ovoids, up to 400μm long, with a complex internal geometry and variable porosity. In many examples ribbons of spinel are directly overgrown by pyroxene, zoned outwards from fassaite to diopside; in others pyroxene and spinel are separated by Fe-rich phyllosilicate. Spinel-perovskite spherules (1) are 30-100μm in diameter, have high internal porosity and are invariably overgrown by 2-6μm wide rims of Fe-rich phyllosilicate. Anhedral spinel-perovskite inclusions are a morphologically diverse group, which vary in form from nodular to banded. Nodular varieties are 40-100μm in diameter, have variable porosities and are often rimmed by Fe-rich phyllosilicates. Banded varieties are up to 300μm long, have elongate-sinuous shapes and are sometimes enclosed by complex rim sequences composed of Mg-rich phyllosilicates. Like other macroscopic components in Cold Bokkeveld, spinel-rich inclusions are enclosed by accretionary rims of matrix-like material (2).

In situ analysis demonstrates that spinels in most inclusions form a homogeneous population with a composition close to $MgAl_2O_4$. Minor elements in these spinels are FeO 0.2-2.0 wt%, V_2O_5 0.1-0.7 wt%, TiO_2 0-0.6 wt%, MnO 0-0.2 wt%; Cr_2O_3 is up to 1.1 wt% in some pyroxene-spinel inclusions and 0-0.4 wt% in the others. In a few nodular spinel-perovskite inclusions higher FeO values of up to 5.7 wt% have been determined. X.R.D. and microprobe analysis of residues confirm that 85% of the spinel in Cold Bokkeveld has less than 2.0 wt% FeO, with 6.7% in the range 2.0-10%. The remaining 8.3%, with FeO values in the range 10-20 wt%., has yet to be located *in situ*.

The textures displayed by spinel-rich inclusions in Cold Bokkeveld indicate a complex history subsequent to formation. Inclusions, like chondrules, experienced an early phase of disaggregation prior to the formation of accretionary rims. Subsequent to rim formation further disruption of the inclusions took place such that few examples are complete. Matrix material in the meteorite contains isolated spinel grains 1-10μm diameter apparently produced by dissagregation of inclusions. In addition to mechanical disruption inclusions experienced hydrous alteration and the growth of secondary calcite. Spinel-rich inclusions in Cold Bokkeveld are elongate parallel to a distinct planer fabric, which is believed to have formed during compaction in an asteroidal regolith (3). Disaggregation and aqueous alteration of inclusions were mainly the result of regolith processes taking place immediately prior to compaction.

(1) Macdougall, J.D. (1981). Geophys. Res. Lett. 8, 966-969. (2) Metzler, K. and Bishoff, A. (1987) Meteoritics 22, 458-459. (3) Fujimura, A., Kato, M. and Kumazawa, M. (1983) E.P.S.L. 66, 25-32.

THE CO-EVOLUTION OF CHONDRULES AND MATRIX IN ORDINARY CHONDRITES.
Jeffrey N. Grossman, U.S. Geological Survey, Mail Stop 923, Reston, VA, 22092, USA.

Chondrules probably formed in the solar nebula by the melting of pre-existing, low-temperature dust. Known samples of unmelted nebular materials that could be surviving chondrule precursors include CI chondrites, chondrite matrix, and some interplanetary dust particles, all of which are fine-grained and FeO-rich. Other candidates that cannot be examined in the laboratory include interstellar grains and direct condensates from high-temperature nebular gas, both of which are also likely to have been fine-grained and FeO-rich (at low temperature). Chondrules, however, have highly diverse bulk compositions and mineralogies that are difficult to reconcile with precursors such as these.

In my previous work, I concluded that nebular condensates could have the correct chemical properties to be chondrule precursors if they were coarse-grained enough to withstand low-temperature modification. In fact, some of the condensates would need a grain size approaching 100's of μm in order to produce heterogeneous mm-sized chondrules. While this model works mathematically, and may in fact turn out to be correct, there is no physical evidence that such precursors ever existed, and it is extremely difficult to believe that grains could grow to such large sizes during condensation. It is also difficult to account for the chemical and petrological properties of matrix in this model. Other workers have speculated that different types of chondrules came from different nebular locations. The huge local fractionations that the latter model requires are also difficult to explain.

I have devised an alternative mathematical model that allows the generation of heterogeneous chondrules from initially homogeneous, fine-grained, FeO-rich precursors. The model is based on the observation by Jones (1990) that type I chondrules can be derived from type II chondrules via reduction, metal loss and volatilization. In the new model, two types of endmember chondrules may form by batch melting of representative dust: (1) Chondrules that get reduced, experience partial evaporation of elements more volatile than Mg, and lose immiscible metal/sulfide; and (2) Chondrules that only lose metal/sulfide. Elements lost during chondrule formation are returned to the solid dust, and new chondrules are isolated from the system. In this way, the compositions of chondrules and dust evolve with progressive melting events.

This model can account for many chemical properties of chondrules and matrix in ordinary chondrites. Model parameters were adjusted within the bounds allowed by natural chondrules (the probability of forming type I chondrules, the fractions of volatiles lost, and the average amount of metal/sulfide loss). The range of olivine/pyroxene ratios and refractory element/Si ratios in chondrules, the difference in metal/sulfide ratio between matrix and chondrules, and the bulk composition of the final dust (i.e., matrix) were all successfully modelled. Like previous models, the new one seems to fail on several counts, some of which may be fatal. It incorrectly predicts an anticorrelation between volatiles and refractories in type II chondrules, provides no mechanism for producing the observed fractionation of Mg from refractory elements, and does not produce the ferroan-pyroxene normative compositions of many natural radial chondrules. Future refinements to the model may surmount some of these problems. Nevertheless the fact that no ad hoc assumptions are used makes the model worthy of careful consideration.

Ref: Jones, R.H. (1990) GCA 54, 1785-1802.

EVIDENCE FOR CRYSTALLIZATION OF THE IIIAB CORE BY INWARDS DENDRITIC GROWTH Henning Haack, Planetary Geosciences Div., Dept. of Geol. Geophys., SOEST, University of Hawaii, Honolulu, HI 96822, USA

It is generally believed that the compositional variations observed between members of the iron meteorite group IIIAB are due to fractional crystallization of a central molten core. The Cape York iron meteorite shower defines a trend in composition that is close, but not identical, to the 7.5-8.5 wt% Ni section of the IIIAB trend [1]. My modelling of both trends is not consistent with outwards plane front growth of the entire core but consistent with crystallization of the core by inwards dendritic growth.

The observed large ranges in compositions within group IIIAB indicate that the core was mixed during crystallization. Fractional crystallization of the core may be modelled using 1-dimensional models which assume that the liquid is homogenous throughout crystallization. In this work, results from a 1-dimensional model using a new set of experimentally determined distribution coefficients [2] are presented. Even when using the new set of distribution coefficients, there is still a substantial discrepancy between the IIIAB data and the model. This can either be attributed to the distribution coefficients or to the crystallization model. I argue that the distribution coefficients are well determined and that the discrepancy between data and model is due to the assumption of a homogenous liquid in the model.

The Cape York shower of iron meteorites apparently represents a fractional crystallization sequence from the IIIAB parent body. If so, the Cape York meteorites represents the only known sequence with a common origin within a limited space in the parental core. Presumably, the size of the Cape York meteoroid was less than 10m, whereas the total radius of the IIIAB core probably was of the order of 10km. It is shown that, in contrast to the general IIIAB trend, the fractional crystallization of the Cape York sequence may be modelled using a 1-dimensional model. This seems to indicate that the place where the Cape York meteorites crystallized was well mixed, and that the new set of distribution coefficients are well determined. The differences between the general IIIAB trend and the Cape York trend indicates that the Cape York meteorites crystallized from a melt which was not in equilibrium with the bulk IIIAB liquid.

These results are consistent with crystallization of the IIIAB by inwards dendritic growth [3]. In this scenario, the core develops into a stage where the upward concentration of sulfur results in a highly irregular crystallization front. Under these circumstances the dendritic growth is controlled by the convection pattern in the melt rather than liquid diffusion. The large dendrites which grow deep into the core from the base of the mantle separate sections of the core from one another. This type of crystallization could, therefore, explain why regions of the core may have experienced a different evolution. It could also explain the large magnitude of the compositional gradients observed in Agpalilik and the apparent vertical crystallization front [1].

[1] Esbensen et al. (1982) Geochim. Cosmochim. Acta, 46, pp. 1913-1920. [2] Jones, J.H. and D.J. Malvin (1990) Metall. Trans. A, 21B, pp. 697-706. [3] Haack, H. (1990) Meteoritics, 25, pp. 369.

N92-12915

^{135}Cs - ^{135}Ba: A NEW COSMOCHRONOMETRIC CONSTRAINT ON THE ORIGIN OF THE EARTH AND THE ASTROPHYSICAL SITE OF THE ORIGIN OF THE SOLAR SYSTEM;

C. L. Harper, H. Wiesmann, and L. E. Nyquist, SN2, NASA/JSC, NASA Road 1, Houston, TX 77058.

^{135}Cs is produced in the rapid neutron capture process (thought to occur in supernovae) with a production ratio of ~0.6 relative to stable ^{133}Cs, which is estimated to be about 85% *r* -process in the bulk solar system reservoir (BSS) [1]. Inferred *ab initio* BSS abundances of other unshielded extinct radionuclides, ^{107}Pd (τ_m = 9.4 Ma, [2]), ^{182}Hf (13 Ma, [3]), and ^{129}I (23 Ma, [4]) in the early solar system are consistent with a model in which most of these nuclides are contributed to the protosolar reservoir very near in time to the birth of the sun following a long *r* -process separation ("free decay") interval of ~10^8 yr, as expected if the solar system formed in the vicinity of a massive star association generated during the passage of a galactic spiral density wave. Because of its relatively short mean-life (3.3 Ma), ^{135}Cs is a critical test nuclide for this "late input" scenario. For a late input *r* -process fraction, $N_r^*/N_r = 1 \times 10^{-4}$, for Cs (inferred from ^{129}I, assuming constant $^iN_r^*/^iN_r$ in the mass region), the late-input model predicts $^{135}Cs/^{133}Cs \sim > 3 \times 10^{-5}$ for a decay interval of less than one half life (2.3 Ma) between synthesis and the origin of the solar system. Live ^{26}Al (1 Ma) in the early solar sytem suggests the possibility of an even shorter time-scale.

$^{135}Ba/^{138}Ba$ relative precisions of ±25 ppm ($2\sigma_m$), normalized to $^{136}Ba/^{138}Ba = 0.109540$, are achievable by averaging the results of 6 multiple 100 ng multicollector runs with ±60 ppm ($2\sigma_p$) external reproducibility (*fig.* 1). The use of ^{138}Ba in the normalization is justified at this level because $^{138*}Ba/^{138}Ba$ from the decay of ^{138}La is only 2.5 ppm in BSS, and because the meteorites included in this study have identical bulk La/Ba to within uncertainties of ~±25%. La/Ba in our terrestrial standard "1154", a Gorda ridge basalt, is 1.8 x CI: hence $\Delta^{138*}Ba/^{138}Ba$ relative to Orgueil is < 2 ppm, (probably << 2 ppm).

Six runs each of Ba separated from whole rock samples of the Orgueil (*fig.* 2) and LEW 86010 (*fig.* 3) meteorites, having $^{133}Cs/^{135}Ba$ ratios of 1.3 and 0.0 respectively, reveal a statistically resolved difference of 45±35 ppm (2σ) in $^{135}Ba/^{138}Ba$ (*fig.* 4). We interpret this difference as evidence for live ^{135}Cs in the early solar system at an *ab initio* level: $^{135}Cs/^{133}Cs$ ~(3±2) x 10^{-5}. Further higher-precision measurements are planned to evaluate this tentative conclusion.

The LEW 86010 data is in close agreement with the terrestrial normal (*fig.* 4). ^{53}Mn - ^{53}Cr chronometry indicates that the LEW 86010 angrite crystallized from a melt at the same time (to within ~2 Ma) as the formation of the refractory Ca, Al-rich inclusions in the Allende meteorite (at ~4566±2 Ma [5]) during a very early (essentially *"ab initio"*) period of solar system history. *If* ^{135}Cs was indeed present in the early solar system at the level inferred, then 2 major conclusions follow: (i) A supernova contributed newly synthesized *r* -process matter into the protosolar reservoir within ~5 Ma of the Cs/Ba fractionation recorded in LEW 86010; (ii) The strong Cs depletion in the bulk earth reservoir ($^{133}Cs/^{135}Ba$ ~0.1) took place very early in solar system history. If this volatile-loss was pre-accretionary (*viz.*, in the nebula or planetesimals), then the accretionary chronology of the earth is not constrained. However if it is a consequence of accretion, then a very tight time constraint of <~5 Ma (rel. to LEW 86010) is obtained for accretion of most of the earth's mass.

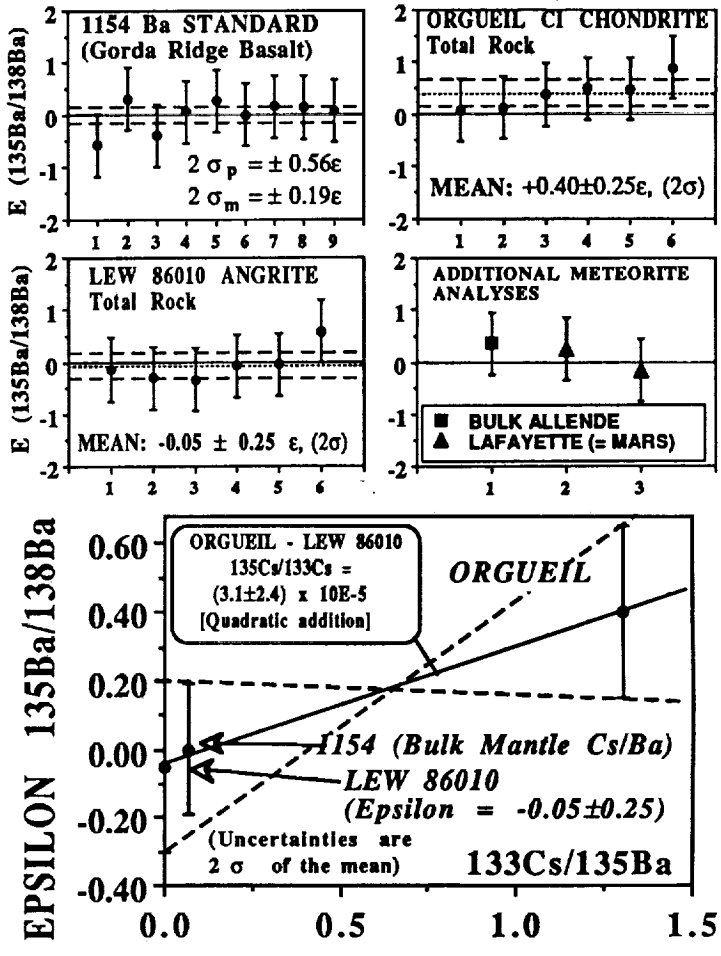

References: [1] F. Käppeler *et al.*, (1989). *Rep. Prog. Phys.*, 52: 945; R. Gallino, *pers. comm.*; [2] J. H. Chen and G. J. Wasserburg, *GCA*, 54: 1729; [3] C. L. Harper *et al.*, (1991). *LPSC XXII:* 515; [4] R. S. Lewis and E. Anders, (1975). *Proc. Nat. Acad. Sci. USA*, 72/1, p. 268; [5] G. Manhes *et al.*, (1986). *Terra Cognita*, 6/2: 173; C. Göpel, *pers. comm.*.

NUCLEOSYNTHESIS IN NEUTRON-RICH SUPERNOVA EJECTA; Hartmann, Dieter H.[1], Howard, W. Michael[2], and Meyer, Bradley S.[1]. [1]Dept. Physics and Astronomy, Clemson University, Clemson, SC 29634, [2] Lawrence Livermore National Laboratory, Livermore, CA 94550.

Certain meteoritic samples exhibit strongly correlated anomalies of the most neutron-rich isotopes of the elements Ca, Ti, Cr, Fe, Ni, and Zn. Extremely neutron-rich environments required for the synthesis of these species may exist in either the cores of Type I supernovae or near the neutron star mass cut in Type II supernovae. In both cases temperatures are sufficiently high for nuclear statistical equilibrium (NSE) to be achieved. It is possible in such cases to approximate the nucleosynthesis of the elements heavier than calcium by simple NSE calculations that are relatively independent of specific supernova models. This is important because supernova models make few reliable predictions of the thermodynamic history of their most dense and therefore most neutron-rich ejecta. The nucleosynthetic signature of these ejected stellar zones (1) is in relatively good agreement with correlated abundance anomalies observed in several meteoritic inclusions. No perfect fit has been found, but a number of uncertainties in the models remain. These are mainly due to uncertainties in the nuclear input physics, in particular from nuclear mass estimates (2), the unknown relative contributions of zones with different neutron enrichments η, and corrections due to the freeze-out of nuclear reactions in the cooling ejecta. Hartmann *et al.* (2) investigated freeze-out properties, but studied only matter with $\eta \leq 0.01$ because of their limited nuclear reaction network. We calculate these freeze-out corrections to nuclear abundances for an extended grid in η. To follow the dynamic evolution of abundances in the ejecta we employ a reaction network that includes all nuclei from the stability line to the neutron drip line for the elements H to Kr. We compare the final (frozen-out) abundances obtained from dynamic calculations with those of NSE calculations with effective freeze-out temperatures. The implications for isotopic excesses found in meteoritic inclusions are discussed. In this context we also consider abundance modifications due to β-delayed neutron emission (3). References: (1) Hartmann, D., Woosley, S. E., and El Eid, M. F. 1985, ApJ, 297, 837. (2) Hartmann, D. 1987, in *The Origin and Distribution o the Elements*, ed. G. J. Mathews, (World Scientific: Singapore), 361. (3) Thielemann, F.-K., Kratz, K.-L., Pfeiffer, B., Möller, P., and Hillebrandt, W. 1990, in *Nuclear Astrophysics: Nuclei in the Cosmos*, eds. H. Oberhummer and W. Hillebrandt, MPI publ. MPA/P4, 286.

Attempts to constrain the carbon isotopic composition of dispersed carbonate in EETA 79001. Hartmetz C.P., Wright I.P., Pillinger C.T. The Open University, Planetary Sciences Unit, Milton Keynes MK7-6AA.

Two types of Ca-carbonate have been identified in the Antarctic shergottite EETA 79001 (1). The first type, dubbed "white druse", was discovered in the sample's interior at the lithology A/C boundary. The druse has been described alternatively as a magnesium-rich granular calcite that contains dissolved phosphorus, or calcite with intergrown magnesium-bearing phosphate. Analyses of the druse has shown that it decrepitates from 400°-800° C; carbon and oxygen isotopic abundances were also determined ($\delta^{13}C = +6.8‰$, $\delta^{18}O = +21‰$) that are inconsistent with the isotopic composition of terrestrial carbonates (2,3). A second type of carbonate in EETA 79001 consists of small anhederal highly fractured grains (10-20μm), trapped within mafic glass and rapidly quenched pyroxene, that are associated with laths and needles of sulfate grains, probably gypsum (1). This textural relationship is compelling evidence for the existence of these salt minerals prior to the event that formed the glass and pyroxene.

Unfortunately, it has proved impossible thus far to separate sufficient quantities of the second type of carbonate for isotopic analysis. An alternative approach is to perform heating experiments of whole-rock samples, rather than the obvious druse deposits, in order to access the distribution and isotopic composition of any dispersed carbonate grains. Herein, we have started a series of analyses of EETA 79001 using a new high-sensitivity static mass spectrometer, capable of measuring <nanogram levels of carbon to precisions in $\delta^{13}C$ of ±0.4‰. A typical blank per step of 0.5±0.3ng is observed during stepped heating experiments performed on the extraction line used in conjunction with this instrument. Using high-resolution stepped combustion (25°-50° C steps depending on the amount of carbon released) we have analyzed band saw fines (split 351), and lithology A (split 115).

A previous analysis of EETA 79001 (4), suggested that carbonate in lithology A samples (split 115) decrepitates in the 600°-700° C step and had an isotopic abundance of $\delta^{13}C = -11‰$. However, the combustion of isotopically light carbon-bearing components over the same temperature interval is known to cause the observed isotopic value ($\delta^{13}C = -11‰$) to be somewhat compromised. A reexamination of lithology A using the refined technique described above constrains this component to the interval between 575° and 600° C with an observed $\delta^{13}C = -14.3‰$; unfortunately high-resolution stepped heating did not enable separation of the isotopically light component so the carbonate $\delta^{13}C$ value is artificially light. Acid digestion experiments are required to estimate the actual isotopic abundance of this component. An intriguing experiment involves analysis of band saw fines obtained from several saw cuts through all lithologies of EETA 79001. In this case carbonate appears to be released in two components over a temperature range of 450°-700° C: the first decrepitated from 450°-575° C ($\delta^{13}C = -16.1 \pm 1‰$), the other from 600°-700° C ($\delta^{13}C = -12.9 \pm 1‰$). Although the carbon isotopic compositions of these components are compromised by the co-release of light carbon it would seem that the experiment has given evidence for two types of carbonate that can be resolved on the basis of thermal stability. The carbonate observed in lithology A profiles is consistent with the higher-temperature component seen in band saw fines. More work is planned to both search for and characterize this dispersed form of preterrestrial carbonate.

References: 1) Gooding J.L. *et al.* (1988) *GCA* **52**, p. 909-915. 2) Wright I.P. *et al.* (1988) *GCA* **52**, p. 917-924. 3) Clayton R.N. and Mayeda T.K. (1988) *GCA* **52**, p. 925-927. 4) Wright I.P. *et al.* (1986) *GCA* **50**, p. 983-991. 5) Wright, I.P. *et al.* (1989) *Nature* **340**, p. 220-222.

ROTER KAMM CRATER AGE: 3.5 to 4.0 Ma

Hartung J.[1], M. Kunk[2], W. Reimold[3], R. Miller[4] and R. Grieve[5]

Roter Kamm, in southern Namibia, is a bowl-shaped impact crater 2.5 km across and 150 m deep. A comprehensive report on Roter Kamm is given by Reimold and Miller (Proc. Lunar and Planet. Sci. Conf. XIX, 711-732). The crater was formed mainly in granitic, dioritic and granodioritic-composition rocks of the Namaqualand Metamorphic Complex, the age of which is roughly 1000 Ma. An upper limit to the age of the crater, based on the presence of ejecta fragments on top of calcrete formed at the end of the Miocene, is about 5 Ma.

The sample selected for $^{39}Ar/^{40}Ar$ analysis, designated URK-41, is a vesicular melt bomb with many clasts. It was crushed, sieved and subjected to repeated application of heavy liquid and magnetic separation procedures to obtain two sub-samples. One was gray and contained light glass, some probably diaplectic; the other appeared black, but was not opaque, and consisted of dark brown glass.

Results of analysis of 15 temperature fractions released from the dark glass are shown in figure 1. The mean for the 15 fractions is 3.7 Ma. An overall uncertainty in the age measurement, +-0.3 Ma, is one standard deviation from the mean age. The range of ages shown for each fraction corresponds to +-2 standard deviations from the mean, the uncertainty being due only to analytical procedures. If the slightly-high 7th fraction is excluded, the resulting mean age would be 3.6 Ma. Had the accumulated radiogenic ^{40}Ar been released all at once, the total gas age would be 3.7 Ma.

Results of analysis of the light glass are given in figure 2. The shape of the spectrum is that expected when a heating event does not cause 100% loss of previously accumulated radiogenic ^{40}Ar. In this case the age for the lowest temperature fraction is an upper limit for the age of the heating event, 3.6 Ma for this sample. We conclude the best age for the Roter Kamm crater is 3.7 +- 0.3 Ma.

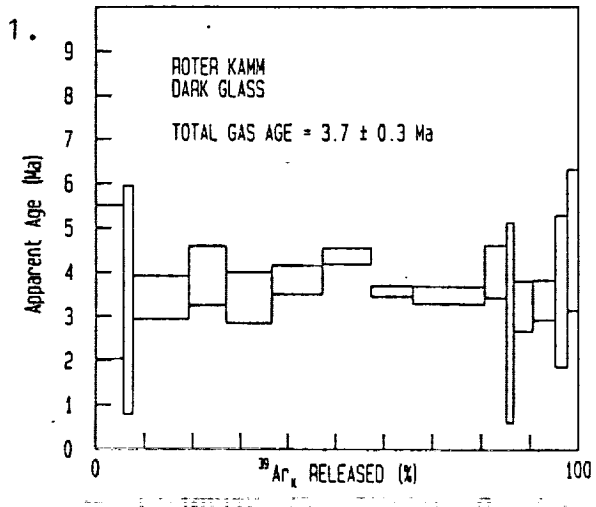

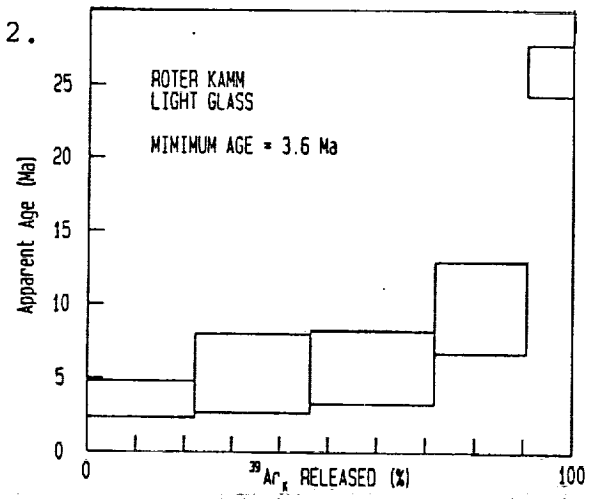

1. Box 101, APO NY 09128, USA, or Auf der Stelle 11/1, 7032 Sindelfingen, Germany.
2. U. S. Geological Survey National Center, Mail Stop 981, Reston, VA 22091, USA.
3. Department of Geology, Univ. of the Witwatersrand, P.O. WITS 2050, Johannesburg, RSA.
4. Geological Survey of Namibia, P.O.Box 2168, Windhoek, 9000, Namibia.
5. Geological Survey of Canada, Dept. of Energy, Mines and Resources, Ottawa, Canada.

PARENTAL MAGMAS OF THE NAKHLITES: CLUES FROM THE MINERALOGY OF MAGMATIC INCLUSIONS. R.P. Harvey and Harry Y. McSween Jr., Department of Geological Sciences, University of Tennessee, Knoxville, TN 37996-1410 USA.

The nakhlite meteorites (Nakhla, Governador Valadares and Lafayette) are members of the SNC group whose parent body is thought to be Mars; therefore, unravelling the petrogenesis of the nakhlites will also provide clues to martian igneous processes. Unfortunately, calculating parental magma compositions for the nakhlites is difficult, because of the cumulate nature of the rock and persistent questions about the parentage of the major cumulate phases [1-4]. Luckily, large olivine grains in all three nakhlites, and in particular Governador Valadares, often contain partially crystallized melt inclusions which presumably are representative of an early or intermediate liquid coexisting with the cumulus phases. This study represents our detailed analyses of magmatic inclusions in the nakhlites, and includes identification of some previously undetected phases (kaersutitic amphibole and hercynitic spinel) and new constraints on parental magma compositions.

Typical melt inclusions within nakhlite olivine are sub-rounded and between 50 and 200 μm in diameter. Most inclusions consist predominantly of augite; the other major phases are an interstitial Si-rich glass (58-72% SiO_2) and an Fe-Ti oxide (either Ti-magnetite or ilmenite). Unlike the mesostasis of the nakhlites, these inclusions do not contain any feldspar minerals. The presence of minor phases varies dramatically from inclusion to inclusion and includes pigeonite, Fe-sulfides, chlor-apatite, and notably kaersutitic amphibole and hercynitic spinel.This is the first identification of a hydrous mineral and spinel in a nakhlite, both of which were found in separate Governador Valadares inclusions. The presence of a hydrous mineral in the nakhlites reinforces the idea that H_2O may have played a role in martian igneous processes; it also allows a more controlled calculation of the compositions of the parental magma from which these rocks were generated [5].

Studies of zoning of olivine in the nakhlites have indicated that olivine was the first phase to crystallize from the nakhlite parent magma [1,2]. Given that the inclusions studied were centered within the olivine it was assumed that a mixture of the enclosing olivine and the inclusion phases would represent possible parental magmas. Parental magma compositions were calculated using a system of linear mass-balance equations that were then solved by regression methods using both exact and inexact constraints [6]. The primary phases used in the regression were olivine, augite, Ti-magnetite or ilmenite, and the inclusion glass, and minor phases were also included when present. The results of previous experimental and theoretical studies of SNC meteorites [3,5] allowed the use of measured partition coefficients for several major oxides as partial constraints to the calculations. The equations were weighted appropriately and initial solutions were introduced to constrain final results to physically realistic possibilities. Both the sum of the oxides and the sum of the phases were constrained to total 100%, and thus the proposed parental compositions are approximations rather than unique solutions. In spite of the fact that the calculated and visually estimated proportions of the phases differ significantly, the solutions chosen were convergent on a single parent of composition near SiO2 (49.7%), TiO_2 (0.67%), Al_2O_3 (2.65%), MgO (8.10%), CaO (11.67%), FeO (25.21%), K_2O+Na_2O (2.0%), implying that all three inclusions were produced by a single basaltic parental magma. This parent is intermediate to those proposed by previous authors [3,4]. The presence of small volumes of highly evolved liquids in the nakhlites and the other SNC meteorites suggests that magmas evolved beyond primitive basaltic compositions may have existed on Mars.

References: [1] Harvey & McSween (1991) LPSC 22, p. 527-528.[2] Treiman (1990) *Proc. 20th LPSC*, p.273-280, Pergamon. [3] Longhi & Pan (1989) *Proc. 19th LPSC*, p.451-464, Pergamon.[4] Treiman (1986) *Geochim. Cosmochim. Acta,* **50**, p. 1061-1070. [5] Johnson, Rutherford & Hess (1991) *Geochim. Cosmochim. Acta,* **55**, p. 349-366. [6] Reid, Gancarz & Albee (1973) *Earth. Plan. Let.* **17**, p.433-445.

Direct Evidence of In-Ice or Pre-ice Weathering of Antarctic Meteorites.
Ralph P. Harvey* and Roberta Score** *Dept. of Geological Sciences, U. of Tennessee, Knoxville, TN 37996-1410. **Solar Sytem Exploration Department, Lockheed-ESC C-23, 2400 NASA Rd. 1, Houston, TX 77058.

Currently the most accepted theory of meteorite stranding surface formation is the Whillans-Cassidy model [1]. In this model, meteorites which fall into accumulation areas on the Antarctic ice cap are incorporated into the ice and transported seaward; occassionally, in areas where ice-flow is interrupted by sub-ice or above-ice barriers and ablation is high, meteorites are exhumed from the ice by the forces of sun and wind, and begin to pile up. Most versions of this theory have assumed that the meteorites themselves are not substantially weathered, deformed or broken up while in the ice. Burial of the meteorite in the snow of the accumulation zone is assumed to be rapid.

Only two meteorites have been found in the process of ablating out of the ice. When these two meteorites, LEW87295 and ALH82102, were discovered they still had the majority of their mass within the ice, and in both cases a large block of ice containing the meteorite was exhumed. This ice was subsequently brought to CRREL laboratories for ice-fabric analysis [2,3]. During these investigations it was determined that the fabric of the ice had deformed around the meteorite, rather than vice-versa, and that the meteorites had not melted into the ice to form clear, cryoconite envelopes. In addition, both meteorites were small, whole, rounded specimens, and had not evidently been fractured in the ice

At the time these blocks of ice were initially studied, the weathering stage of the meteorites was not noted. We have observed that both of the exhumed meteorites have been classified as type C, indicating that these meteorites have experienced severe weathering. LEW87295, a eucrite, shows only 40-50% fusion crust, large rust stains and severe pitting, characteristic of having been severely weathered [4]. ALH82102, an H5 chondrite, had an "almost" complete fusion crust, but also exhibited many cm-sized oxidation haloes and was a uniformly reddish-brown on exposed interior and fracture surfaces, indicating severe weathering had occurred [5].

It is apparent that these two meteorites, our only samples that are not thought to have spent much time exposed on the ice surface after transport, have been substantially weathered during some previous stage. Gooding has examined ALH82102 in detail and found weathering products indicative of aqueous precipitation [6]. This weathering occurred either while encased in ice during transport, or prior to burial and incorporation into the ice while on the surface in the accumulation zone (weathering in laboratory conditions is discounted). In either case, substantial exposure to liquid water is suggested. It seems probable, therefore, that only in extremely rare circumstances could an Antarctic meteorite escape weathering. If burial in the accumulation zone is rapid, as has been suggested, then weathering during transport is the culprit, and only direct fall meteorites escape. If burial in the accumulation zone is not rapid, then meteorites spend a much longer amount of time on the surface of the Antarctic ice-sheet than has previously been thought, and their arrival at stranding surfaces in a pristine condition is unlikely. Detailed studies of the behavior of meteorites encased in ice might reveal the source of in-ice or pre-ice weathering.

References: [1] Whillans & Cassidy (1983) Science 222, p.55-57. [2] Gow (1990) LPI Tech. Rep. 90-03, p. 85. [3] Gow & Cassidy (1989) Smith. Contr. Earth Sci. 28 p. 87-92. [4] Score (1991) Ant. Met. Newsl. 14 p. 13. [5] Mason, et al. (1989) Smith. Contr. Earth Sci. 28 p. 29-60. [6] Gooding (1986) Geochim. Cosmochim. Acta. 50, 2215-2223.

EVAPORATION OF MELILITE; A. Hashimoto, Center for Astrophysics, Cambridge, MA 02138, U.S.A.

Melilite is the most abundant mineral in Type A and B Ca,Al-rich inclusions in carbonaceous chondrites. Does melilite evaporate congruently or incongruently? If the latter, how does the chemical composition of the residue evolve during evaporation? Can other CAI minerals such as spinel and anorthite form from melilite evaporation residues?

I have carried out Langmuir (vacuum) evaporation experiments on pure gehlenite, pure akermanite, and a 50/50 (mol%) mixture of them, in the molten state. The experimental procedure has been reported previously [1]. Pure gehlenite (~180 mg) was partially evaporated at 2000°C for 40 min and 15 min, yielding residues "G1" (64 wt% of the original weight remained) and "G2" (78 wt%), respectively. Pure akermanite (~160 mg) was partially evaporated at 1800°C for 40 min ("A1": 87 wt% remained), and at 2000°C for 15 min ("A2": ?% remained). Both the molten gehlenite and akermanite were transparent at visible wavelengths when the evaporation degree was small (<25 wt% evaporation), but they became opaque at larger degrees of evaporation.

Previous experiments on pure SiO_2 had indicated that the effective temperature of the (transparent) molten silica was ~70°C lower than the black body temperature inside the furnace. This problem was solved by doping the sample with Ir black (ultrafine-grained Ir metal). The same technique was used for 50/50 melilite. Vacuum evaporations of this mixture produced "GA1" (1900°C for 9 min; initially ~160 mg, 88 wt% remained) and "GA2" (1800°C for 120 min; initially ~200 mg, ?% remained).

G1 and G2 became depleted in Si (G1: SiO_2 0 wt%, Al_2O_3 60 wt%, CaO 40 wt%; G2: 4, 48, 48 wt%) relative to the initial composition (gehlenite: 22, 37, 41 wt%). G1 consists of $CaAl_2O_4$ and an interstitial phase (probably a mixture of more than two Ca-aluminates). G2 was recovered as a transparent glass. The evaporative loss of Al_2O_3 was negligible. SiO_2 evaporated ~9 times as fast as CaO. The compositions of both G2 and G1 show that pure gehlenite evolves to Ca, Al-oxides by evaporation.

A1 became depleted in both Mg and Si (SiO_2 42 wt%, MgO 10 wt%, CaO 48 wt%) relative to the initial composition (akermanite: 44, 15, 41 wt%). A1 consists of $(Ca_{1.5}Mg_{0.5})SiO_4$ (*i.e.*, a solid solution of nearly equal mols of monticellite with Ca-olivine) and interstitial glass. Evaporation of CaO was negligible. MgO evaporated ~2 times as fast as SiO_2. A2, which evaporated more than A1, was not recovered as a single droplet; it crumbled into powder shortly after it cooled to low temperature. This is characteristic of Ca-olivine (Ca_2SiO_4), whose phase transition at ~700°C involves a large volume change. Presumably the composition of A2 is close to that of Ca_2SiO_4.

GA1 became depleted in Mg and Si (SiO_2 29 wt%, MgO 2 wt%, Al_2O_3 23 wt%, CaO 46 wt%) relative to the initial composition ($Ge_{50}Ak_{50}$: 33, 7, 19, 41 wt%). Evaporation of Al_2O_3 was negligible. The relative evaporation rates of Mg:Si:Ca were 17:8:1. GA1 consists of Ca_2SiO_4 and a very fine-grained (<1 μm) mixture of two phases whose composite composition shows a slight excess of $CaSiO_3$ after subtraction of normative melilite. GA2, which probably evaporated more than GA1, again crumbled into powder, possibly due to a larger degree of Ca_2SiO_4 crystallization in the residue.

These experiments show that molten melilite evaporates incongruently in a vacuum, and that the partial evaporation of melilite does not produce other major CAI minerals such as spinel, anorthite, and diopside, but instead Ca-aluminates.

REFERENCE: [1] Hashimoto, A. (1990) *Nature 347*, 53-55.

THE CORRELATION BETWEEN THE PRIMORDIAL ARGON AND NITROGEN IN UOCs;

Ko Hashizume and Naoji Sugiura, Department of Earth and Planetary Physics, University of Tokyo, Tokyo 113, JAPAN.

Primordial rare gases heavier than argon in primitive chondrites are known to be concentrated in the so called *phase "Q"* which is insoluble in HF/HCl but soluble in oxiding reagents. In case of carbonaceous chondrites, the amount of the heavy rare gases in the Q-phase accounts approximately 80% of the total amount. The Q-type rare gases are also observed in the unequilibrated ordinary chondrites (UOCs), although their amount accounts only 20-40% (in case of argon) of the total amount, which suggest the existence of some other phases where the major portion of the heavy rare gases is trapped.

We have measured isotopes of nitrogen and argon in UOCs by a mass-spectrometer with a high sensitivity. The gases are extracted stepwisely from 200° C up to 1200° C in an oxygen atmosphere. Among the UOCs, some nitrogen components whose $\delta^{15}N$ values were well distinguishable from those of the air-like components (including organic contamination) were observed. Extreme cases were observed in Y74191 (L3.7) and ALH77214 (L3.4) whose typical $\delta^{15}N$ values in bulk samples were +750 and $-200\,‰$, respectively. The remarkable point observed is that the release profile of the anomalous nitrogen and the primordial argon generally correlates during the stepwise combustion, especially well in case of Y74191. The proportion between the amount of the anomalous nitrogen (which is expressed by the index, excess-$^{15}N \equiv \delta^{15}N_{AIR} \times [N] \times (^{15}N/^{14}N)_{AIR}$) and that of the primordial argon is observed to be kept almost constant throughout various chemical treatments. The correlation was also observed in other UOCs, presently, Chainpur (LL3.4) and Mezö Madaras (L3.4/3.7). The case of Chainpur is shown in the figure. A negative "excess-^{15}N" means a nitrogen component isotopically lighter than air is released. The lowest $\delta^{15}N$ value of $-62\,‰$ was observed at 800°C fraction of the H_2O_2 treated sample. A significant portion of the anomalous nitrogen and the primordial argon was lost by the HCl treatment, however the correlation is still observed.

The observed correlations suggest that a significant portion of the primordial argon in these UOCs is possible to be trapped in sites identical to or very close to those of the anomalous nitrogen.

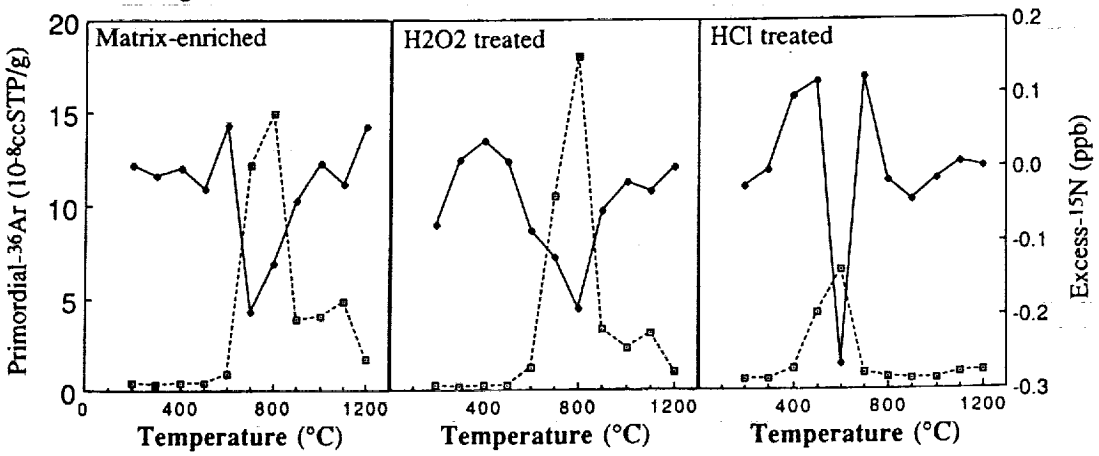

Fig. The release profile of the anomalous nitrogen and the primordial argon in Chainpur. The amount of the anomalous nitrogen is expressed by excess-^{15}N. The filled marks connected with solid lines and the open marks connected with broken lines represent nitrogen and argon, respectively. The Matrix-enriched fraction is the non-magnetic portion after chondrules hand-picked from the bulk sample (chondrules: 25.1wt%, magnetic (metal-enriched): 15.9wt%, matrix-enriched: 59.0wt%). 10.2wt% of the matrix-enriched fraction was dissolved by H_2O_2 treatment. 45.2wt% of the matrix-enriched fraction was dissolved by HCl treatment.

SIMULATION OF THE INTERACTION OF GALACTIC PROTONS WITH METEOROIDS: ON THE PRODUCTION OF ^{7}Be, ^{10}Be AND ^{22}Na IN AN ARTIFICIAL METEOROID IRRADIATED ISOTROPICALLY WITH 1.6 GeV PROTONS; U. Herpers[1], R. Rösel[1], R. Michel[2], M. Lüpke[2], D. Filges[3], P. Dragovitsch[3], W. Wölfli[4], B. Dittrich[4], H.J. Hofmann[4],1 Abteilung Nuklearchemie, Universität zu Köln, F.R.G., 2 Zentraleinrichtung für Strahlenschutz, Universität Hannover, F.R.G., 3 Arbeitsgruppe Strahlungstransport, IKP/KFA Jülich, F.R.G., 4 Institut für Mittelenergiephysik, ETH Hönggerberg, Zürich, Switzerland

Depth profiles for the production of ^{7}Be, ^{10}Be and ^{22}Na were measured by gamma-spectrometry and accelerator mass spectrometry in targets located inside an artificial meteoroid irradiated isotropically by 1.6 GeV protons in the course of the experiment LNS 172 at Laboratoire National Saturne. The target elements C, N, O, Mg, Al, Si, Ti, Mn, Fe, Co and Ni were investigated. In order to analyze the experimental depth profiles, theoretical production rates were derived on the basis of Monte Carlo calculations of the depth-dependent spectra of primary and secondary protons and of secondary neutrons using the HERMES code system [1] and of experimental and calculated cross sections of the underlying nuclear reactions. For the proton-induced production these calculations are based on a consistent set of thin-target excitation functions, which was measured recently by our group from threshold up to 2.6 GeV [2,3]. There is, however, a problem with respect to the availability of cross sections for the neutron-induced production. The three product nuclides are produced from the various target elements by a wide variety of nuclear reactions covering low-energy reactions (^{7}Be and ^{10}Be from C, N, O and ^{22}Na from Mg, Al, Si) as well as deep spallation (^{22}Na from elements with $Z \geq 22$) and fragmentation (^{7}Be and ^{10}Be from elements with $Z \geq 22$). Only for some of the low-energy reactions the necessary cross sections can be calculated with some confidence by the hybrid model [4] of preequilibrium reactions using the code ALICE LIVERMORE 87 [5]. For fragmentation and spallation reactions it is usually adopted that the cross sections for proton- and neutron-induced production are equal. A comparison of the experimental depth profiles with those calculated under this assumption demonstrates the limitations of this approach, which mostly results in an underestimation of the neutron-induced production. On the basis of the results from the simulation experiment a set of excitation functions for the neutron-induced production of these isotopes is proposed. With these cross sections the calculations describe excellently the production rates measured in the present experiment and in earlier simulation experiments with 600 MeV protons [6]. Using these cross sections, production rates of ^{10}Be and ^{22}Na in stony meteoroids and in lunar surface material are calculated by an analogous physical model of GCR interactions with extraterrestrial material [7]. The new production rates are compared with experimental data from meteorites and lunar samples. **Acknowledgement:** This work was supported by the Deutsche Forschungsgemeinschaft and partly by the Swiss National Science Foundation. **References:** [1] P. Cloth et al., Juel-2203 (1988). [2] B. Dittrich et al., Nucl. Instr. Meth. Phys. Res. B52, 588 (1990). [3] R. Bodemann et al. and M. Lüpke et al., in S.M. Qaim (ed.) Proc. Int. Conf. Nuclear Data for Science and Technology, May. 13-17, 1991, Jülich, in press. [4] M. Blann, Phys. Rev. Lett. 27, 337 (1971). [5] M. Blann, priv. comm. (1987). [6] R. Michel et al., Nucl. Instr. Meth. Phys. Res. B16, 61 (1985) and B42, 76 (1989). [7] R. Michel et al., LPS XX, 693 (1989); LPI Techn. Rep. 90-05, 86 (1990); Meteoritics (1991) in press.

PROXIMAL EJECTA OF THE CHICXULUB CRATER, YUCATÁN PENINSULA, MEXICO, A.R. Hildebrand and W.V. Boynton, Department of Planetary Sciences, University of Arizona, Tucson, Arizona 85721-0001.

The Chicxulub crater, the largest probable impact crater on Earth and a possible K/T boundary crater, is buried on the Yucatán Peninsula, Mexico (1). Discovery of shock metamorphic features in proximal ejecta (2) and an intracrater breccia (3) established an impact origin for this structure. Sharpton et al. (4) have questioned an impact origin for this structure, and the identification of the ~90-m-thick K/T boundary breccia in the Y-2 oil well as its proximal ejecta blanket. We describe a newly-discovered, 5-cm-long clast of impact ejecta from this breccia that further substantiates an impact origin for this deposit and the nearby crater.

We studied a sample of this breccia using optical microscopy and X-ray diffraction techniques. Sample Y2 N6 is composed of core fragments taken from 301 to 303 m in well Y-2, which is ~50 km southeast of the crater margin. The core is from the lower part of a 90-m-thick bentonitic breccia, which is the uppermost Cretaceous unit in the well (5). The rock is a poorly-sorted, polymict breccia with angular to rounded fragments in which subangular clasts dominate. The breccia fragments contain varicolored clasts ranging from a few tens of microns to ~5 cm across. Clasts are predominantly calcareous and dolomitic limestones (sometimes fossiliferous), anhydrite, and marl, with a trace amount of small silicate clasts. One 5-cm-diameter, coarsely-laminated, disc-shaped clast of very poorly ordered smectite also occurs. Veins of gypsum up to 1 cm wide crosscut the breccia. Two mineral separates from two different samples of the breccia contain abundant quartz grains (up to 1.1 mm long) with rare examples of single and multiple planar lamellae typical of shock deformation. The large smectitic clast contains 1.7% quartz and feldspar (low-temperature albite) grains which also show single and multiple planar lamellae typical of shock deformation. Debye-Scherrer XRD studies of individual grains confirm the visual identification of shock deformation.

The large smectitic clast is probably altered glassy impact ejecta which may be analogous to Muong Nong tektites or the suevite bombs in the Ries crater ejecta. At this distance from the crater the predicted thickness of ejecta (6) is only ~10 m compared to the 90 m observed, suggesting that the ejecta must have been mixed with locally-derived material. Mixing could have occurred when the ejecta blanket was deposited, was disturbed by impact-waves, and/or was modified by the back surge filling the crater.

The presence of the shock-metamorphosed grains within the large ejecta clast establishes that the grains are not reworked from a thin, distal K/T boundary layer as suggested by Sharpton et al. (4).

We thank D.A. Kring for help with shocked mineral studies, and A. Weidie and G.T. Penfield for supplying samples.

References: (1) Hildebrand, A.R., Penfield, G.T., Kring, D.A., Pilkington, M., Camargo Z., A., Jacobsen, S., and Boynton, W.V., manuscript in review; (2) Hildebrand, A.R. and Penfield, G.T., 1990, Eos 71, No. 43: 1425; (3) Kring, D.A., Hildebrand, A.R. and Boynton, W.V., 1991, L.P.S.C. XXII: 755-756; (4) Sharpton, V.L., Schuraytz, B.C., Ming, D.W., Jones, J.H., Rosencrantz, E. and Weidie, A.E., 1991, L.P.S.C. XXII:1223-1224; (5) Weidie et al., unpublished cross section; (6) McGetchin, T.R., Settle, M., and Head, J.W., 1973, E.P.S.L. 20: 226-236.

CALCALONG CREEK: A KREEPY LUNAR METEORITE; D.H. Hill, W.V. Boynton*, Lunar & Planetary Laboratory, University of Arizona, Tucson, AZ 85721 USA, and R.A.Haag, P.O.Box 27527, Tucson, AZ 85726 USA. *also Department of Planetary Sciences

Calcalong Creek is shown to be lunar based on the diagnostic Fe/Mn ratio=73-78 and other elemental abundances determined by instrumental neutron activation analysis (INAA) [1]. Abundances of rare-earth elements (REE) and other incompatible elements in Calcalong Creek and several other lunar samples are shown in fig. 1. It is readily apparent that these samples have KREEP abundance ratios. The lower abundance (0.2x) of the incompatibles in Calcalong Creek compared to typical KREEP indicate that it contains other components as well. This is to be expected since Calcalong Creek is a clast-laden impact melt according to the Stoffler[2] et al. classification of lunar rocks. For example, its abundances plot in the highland field of Wood's Ti vs. Ca/Al diagram[3] yet, it just meets the CaO/Al_2O_3 criterion Naney et al.[4] established for mare glasses, suggesting it contains a mare component. Note that other lunar meteorites shown to contain mare material, such as bulk samples of EET 87521 [5,6], plot in both highland and mare fields. Both Calcalong Creek and Y 793274 [6,7] plot in the *highland* field **and** near the demarcation line defined by the polymict breccias 15558 and 79135 (fig.2). This is partly due to the fact that all three meteorites are breccias in which each chip analyzed may contain different proportions of highland and mare components.

The bulk composition of the new lunar meteorite appears to follow the trend that mare basaltic clasts and components in all lunar meteorites are of the low-titanium (LT) or very-low-titanium (VLT) varieties [6,7]. This is in contrast to the abundant hi-titanium mare basalts sampled and mapped by gamma-ray spectrometry and ground-based reflectance spectroscopy by the Apollo missions [8,9]. Only one-third of the basalts on the near side have been sampled [8]; since lunar meteorites are more representaive samples of the moon, VLT and LT mare basalts may be more abundant than previously identified [7].

Mixing calculations indicate that Calcalong Creek is consistent with a composition of 50% anorthosite, 20% KREEP, 15% Luna-16 type LT mare basalt and 15% SCCRV (Sc-Cr-V) components. It contains the highest KREEP component of any lunar meteorite and is remarkably similar in KREEP content to samples collected at the Apollo 14 and 16 sites.

REFERENCES: [1] Hill, D.H., Boynton, W.V. and Haag, R.A. (1991) *Nature* (in press). [2] Stoffler, D. et al. (1980) *Proc. Conf. Lunar Highlands Crust, pp. 51-70.* [3] Wood, J.A. (1975) *Proc. 6th Lunar Sci. Conf.*, pp. 1087-1102. [4] Naney, M.T. et al.(1976) *Proc. 7th Lunar Sci. Conf.*, pp. 155-184. [5] Warren, P.H. and Kallemeyn, G.W. (1989) *Geochim. Cosmochim. Acta* **53**, pp. 3323-3300. [6] Lindstrom, M.M et al. (1990) *Proc. 4th NIPR Symp. Antarctic Met.* (in press). [7] Warren, P.H. & Kallemeyn G.W. (1990) *Proc. 4th NIPR Symp. Antarctic Met.*(in press). [8] Pieters C.M. (1978) *Proc. 9th Lunar Planet. Sci. Conf.* pp. 2825-2849. [9] Metzger A.E. et al. (1979) *Proc. 10th Lunar Planet. Sci. Conf.* pp. 1719-1726. [10] Laul, J.C. & Schmitt, R.A. (1973) *Proc. 4th Lunar Sci. Conf.* pp. 1349-1367. [11] Warren, P.H. & Wasson, J.T. (1979) *Rev. Geophys. Space Phys.* **17**, pp. 73-88. [12] Warren, P.H. (1989) in *Workshop on Moon in Transition: Apollo 14 KREEP, and Evolved Lunar Rocks* pp. 149-152.

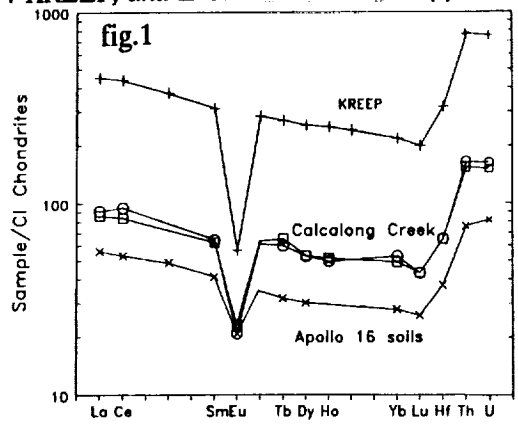

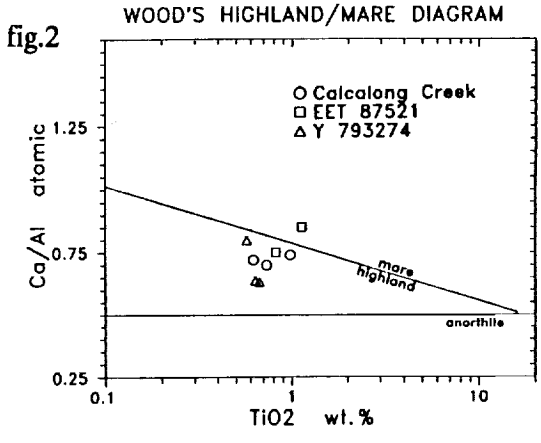

SIZE AND COMPOSITION EFFECTS TO COSMOGENIC NUCLIDES IN METEORITES

M.HONDA[1], H.NAGAI[1], M.IMAMURA[2] and K.KOBAYASHI[3]
1) Deptment of Chem.,Coll.Hum.Sci.,Nihon Univ., Setagaya, Tokyo.
2) Inst. Nucl. Study, Univ.Tokyo, Tanashi,Tokyo.
3) Res. Center, Nucl.Sci. & Techn., Univ.Tokyo,Tokyo

By AMS and RNAA methods, cosmogenic ^{10}Be, ^{26}Al and ^{53}Mn were measured in various samples of meteorites which contain silicates, carbon and metal simultaneously in one fragment. The samples were, Landes(IA), Zagora(IA), Y790981(Ureilite), Tsarev(L5), Odessa(IA), Campo del Cielo(IA) and Brenham (Pallasite). These nuclides were measured in the separated phases of composing targets as well as in the bulk. The contents of above nuclides found in the fractions were interpreted as the functions of two shielding parameters, k_1' and k_2', applying the (effective) delta A values. According to a systematic treatment reduced from the other data, the production rates can be estimated in terms of the radius and depth, equivalent to chondrite, in the preatmospheric body. Fig.1 illustrates those of ^{10}Be in chondritic targets as indicated by current results, and shows a wide range of irradiation conditions for ^{10}Be production in these meteorite samples covering 3 orders of magnitude.

Ref. Honda, Meteoritics,23,3(1988); Nagai et al, Meteoritics,22, 467 (1987); ibid,25,390(1990); Nagai et al, "Workshop on cosmogenic nuclides production rates",p.91, Vienna(1989)

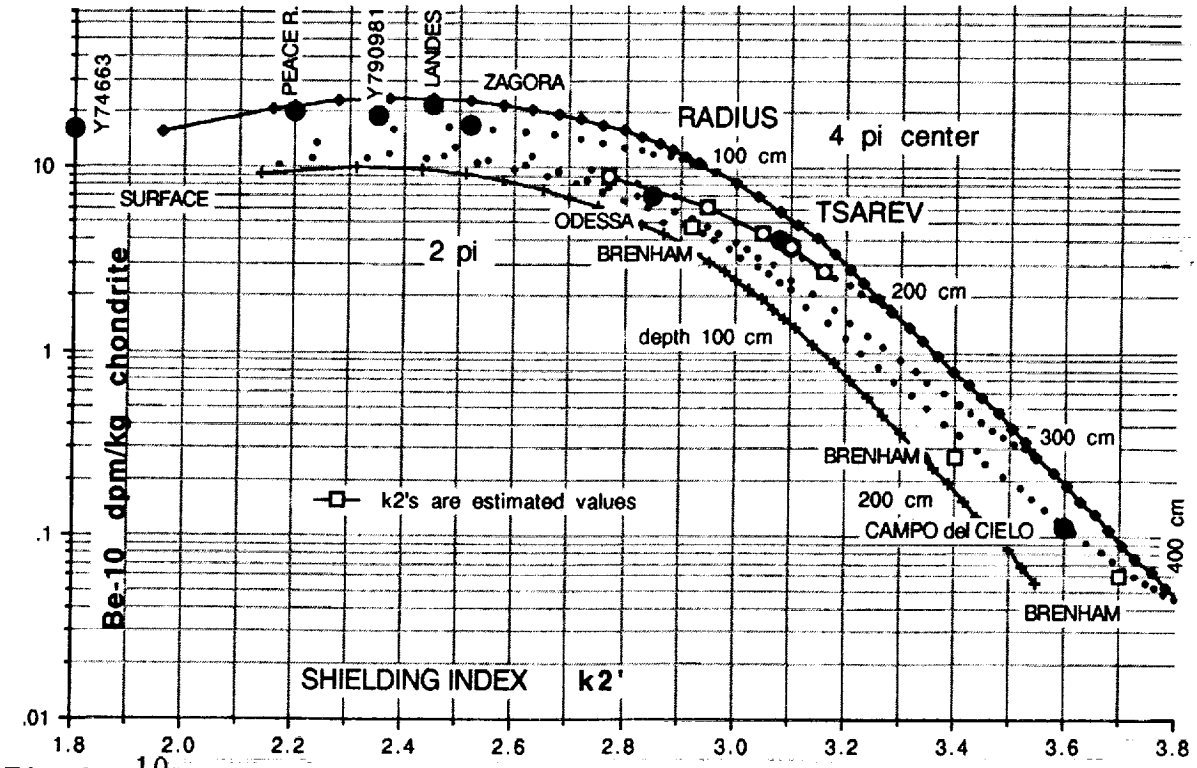

Fig.1 ^{10}Be in chondritic targets as a function of shielding parameter, or effected by the assumed radius and depth.

CARBON, NITROGEN AND SILICON ISOTOPES IN SMALL INTERSTELLAR SiC GRAINS FROM THE MURCHISON C2 CHONDRITE; P. Hoppe[1,2], J. Geiss[1], F. Bühler[1], J. Neuenschwander[1], S. Amari[3,2] and R.S. Lewis[3]. [1]Physikalisches Institut der Universität Bern, Sidlerstr. 5, CH-3012 Bern, Switzerland. [2]McDonnell Center for the Space Sciences, Washington University, One Brookings Drive, St. Louis, MO 63130, USA. [3]Enrico Fermi Institute, University of Chicago, Chicago, IL 60637-1433, USA.

The isotopic compositions of carbon, nitrogen and silicon in interstellar SiC grains varies over a broad range (1, 2, 3). The isotopic anomalies of C and N in SiC can be associated mainly with two nucleosynthetic processes in stellar sources: hydrostatic H-burning via CNO-bicycle in C-rich Red Giants and explosive H-burning in Novae (2). Analyses of large individual interstellar SiC grains (2-20 μm) have shown that the isotopic compositions of C and Si for some separates fall into several discrete clusters (1, 2).

We report here the results of C, N and Si isotopic measurements on small SiC grains (0.2-2.4 μm) from the Murchison C2 chondrite. Analyses were made on agglomerates of various sizes from fraction HN (0.2-1 μm) and on 14 individual grains (1.3 - 2.4 μm) from fraction KJF (nominal: 0.8-1.5 μm) with the University of Bern ion probe (modified Cameca IMS 3f). The aim of this work can be described as follows: 1) Are the total ranges of C-, N- and Si isotopic compositions of small SiC grains comparable to those of larger individual grains? 2) Are there discrete clusters (by analogy to larger grains) for the isotopic compositions of C, N and Si?

Fig. 1 shows C- and N-isotopic compositions of the smallest agglomerates (defined by their C^- count rate) from fraction HN and of individual grains from fraction KJF. Most data points fall into two regions (HN1, KJF1). Based on Fig. 1 and those measurements for which only C isotopes were analyzed, data points for the smallest agglomerates from fraction HN with $\delta^{13}C > 2000$ ‰ tend to form two clusters (HN2, HN3). Total ranges of C- and N-isotopic ratios (including those measurements made on fraction HN which are not shown in Fig. 1) are fairly similar for both fractions ($-200 < \delta^{13}C < +30000$ ‰, $-900 < \delta^{15}N < +2000$ ‰). All measurements made on the smallest agglomerates from fraction HN exclusively give $\delta^{15}N < 0$, whereas about 30 % of measurements made on large agglomerates give $\delta^{15}N > 0$. This could be a hint that heavy nitrogen is predominantly present only in larger grains from fraction HN (which would not fulfill the criterion for "smallest" agglomerates) or that there is a rare component having very heavy nitrogen ("grain X"; ref. 4). The observed range for the silicon isotopic composition is $-152 < \delta^{29}Si < +141$ ‰ and $-216 < \delta^{30}Si < +104$ ‰ without having clearly distinct clusters. Aside from the very rare SiC-component found in larger grains ("grain X"; ref. 4) the total ranges of C-, N- and Si-isotopic ratios observed in small SiC grains are comparable to those of larger grains.

Acknowledgements: We thank Edward Anders for his advice and Tang Ming for the preparation of sample HN.

References: (1) Wopenka et al. (1989) Meteoritics 24, 342. (2) Zinner et al. (1989) Geochim. Cosmochim. Acta 53, 3273-3290. (3) Zinner et al. (1991) Nature 349, 51-54. (4) Zinner et al., this volume.

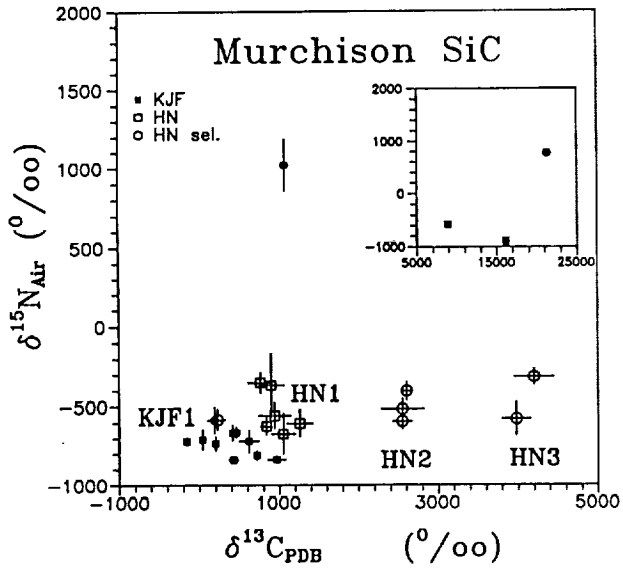

Fig.1: SiC isotopic compositions of C and N for smallest agglomerates from fraction HN and for individual grains from fraction KJF. "HN sel." is a selected group ($\delta^{13}C > +2000$ ‰ or $\delta^{13}C < +300$ ‰) whose true abundance is only approx. 10 % of all small agglomerates from fraction HN.

DISSEMINATION AND FRACTIONATION OF PROJECTILE MATERIAL IN IMPACT MELTS FROM THE WABAR CRATER, SAUDI ARABIA.

Friedrich Horz, NASA JSC, SN2, Houston, TX 77058. D.W. Mittlefehldt and T.H. See, Lockheed ESC, C23, Houston Tx 77058.

We previously analysed spheres, teardrops, dumbells and other small (<5mm) glass objects that were ejected ballistically from the Wabar crater, Saudi Arabia (1) to complement our analyses of large, irregular glass chunks representing the major melt volume and which lack evidence for ballistic flight (2). We thus characterized a representative, if not complete, suite of Wabar melts and present now some implications regarding dissemination and elemental fractionation of projectile materials.

The ballistic beads have higher siderophile contents (frequently 10-15%) than the massive melts (<5%). The small beads also contain fewer vesicles, fewer clasts, fewer Fe-Ni spheres and less pronounced schlieren, all indicating hotter liquids compared to the massive main melts. We suggest that these differences relate to stratigraphic position. The hottest and most siderophile rich melts that demonstrably underwent ballistic transport derive from near-surface positions, while the least contaminated materials [= "white" glass variety of (2)] originated from the deepest sections within Wabar's melt zone.

The relative siderophile concentrations in the melt beads compared to the Wabar and Nejed group IIIA irons (Wasson; pers. comm.) indicate substantial fractionation (see Figure 1). The same depletion-sequence exists at the Henbury and Wolf Creek craters (3). Lithophile elements in the melt beads are not fractionated relative to their progenitor sandstones. Siderophile element fractionation occured therefore at conditions unlike those prevailing during the melting of the sandstones. This then suggests that most fractionation must have been completed before intimate mixing and dissemination of projectile residues and silicate melts commenced.

We do not know of any materials at Wabar that contain the complementary fraction of siderophiles (Ni, Ir and Au rich; Co and Fe poor). We therefore postulate that vaporized species were lost to the atmosphere. However, the relative sequence of depletion seems unrelated to vapor pressure and heat of vaporization of elements or their oxides, therefore precluding simple vapor fractionation. Also the Wabar trend is unrelated to ion-radius (4). The trend is approximately consistent with partitioning between molten metals and silicates (5; Jones, pers. comm). This mechanism, however, depends on intimate mixing and partial equilibration of metal and silicate melts with subsequent, physical separation of the fractionated products; this seems difficult to accomplish during impact processes.

We prefer the view that fractionation occured before Wabar's major meltzone was established and that fractionated siderophiles were lost to the atmosphere, yet we are unable to specify the detailed process(es).

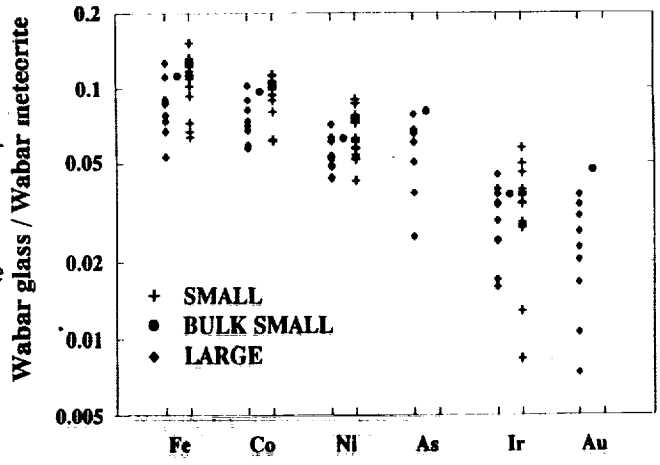

(1) See, T.H. et al. (1989), LPSC XX, Abstr., 980-981; (2) Horz, F. et al. (1989), Proc. LPSC, 19th, 697-710; (3) Attrepp, M. et al. (1991), LPSC XXII, Abstr., 39-40; (4) Engelhardt, W. et al. (1987), Geochim. Cosmochim. Acta, 46, 1913-1920; (5) Jones, J.H. and Drake, M.J., (1986), Nature, 322, 221-228.

Xe-H AND Ba-H FROM WEAK NEUTRON BURST; Howard, W. Michael[1], Clayton, Donald D.[2], and Meyer, Bradley S.[2] . [1] LLNL, Livermore CA 94550, [2] Dept. Physics, Clemson University, Clemson SC 29634

Following the discovery(1) of isotopically anomalous Ba accompanying Xe-HL in diamonds from Allende, we have undertaken a survey of the entire chart of heavy elements to calculate the isotopic compositions expected from the idea of a rapid weak burst of neutrons in the He shells of Type II supernovae(2,3). The tool is a large nuclear network constructed at Livermore that contains accurate (n,gamma) cross sections. Following (3) we suppose a weak s process tau=0.02 mb^{-1} is followed during the shock with a rapid burst tau=0.06 mb^{-1}. Table 1 gives calculations (Xe_n and Ba_n) for non-p isotopes . First two entries are on scale Si=10^6; second two (mix of Xe_n with $4N_\odot$; Xe-H) are overabundances normalized to ^{130}Xe. Rough agreement between the last two lines for Xe suggests (3) that this supernova-burst model may indeed be the nuclear origin of Xe-H .

Table 1. non-p anundances of Xe and Ba

	^{128}Xe	^{129}Xe	^{130}Xe	^{131}Xe	^{132}Xe	^{134}Xe	^{136}Xe
$N_\odot$(Si=10^6)	0.103	1.28	0.205	1.020	1.240	0.459	0.373
Xe_n (calc. N)	0	0.220	2.7(-4)	0.570	0.794	1.90	2.12
$Xe_n+4N_\odot/4N_\odot$	1	1.03	1	1.11	1.13	1.83	2.14
$N^i/N_\odot$ "Xe-H"	1.139	1.059	1	1.073	1.046	1.60	2.10

	^{134}Ba	^{135}Ba	^{136}Ba	^{137}Ba	^{138}Ba
$N_\odot$(Si=10^6)	0.109	0.296	0.353	0.504	3.22
Ba_n (calc.N)	0	1.16	0.048	0.534	5.62
$Ba_n+4N_\odot/4N_\odot$	1	1.78	1.03	1.21	1.38
delta "Ba-H" %	=0	12.2	0	6.0	=0

The last line enters for Ba the deviation from normal in parts per thousand, which was quoted (1) after defining $^{134}Ba/^{138}Ba$ to be normal. That normalization is seen to be suspect if this physical model is correct, because ^{138}Ba has the second largest excess for this model. Almost all Ba goes to 138. The odd-A Ba excesses, $^{135,137}Ba$ made as ^{135}Xe and ^{137}Cs respectively, but both implanted as Cs, agree in spirit but are about 50 times smaller than Xe-H, a puzzling contradiction to this model. Precondensation of Ba_n before gas implantation (1) seems likely to reduce concentration of anomalous Ba; but then the measured Ba-H must be contamination that coincidentally equals Xe-H concentration. The p isotopes and other elements in our full work may clarify this impasse.

References: (1)Lewis,R.S. *et al.*(1991)Lun.Planet.Sci.22,pp.807. (2) Clayton,D.D. (1981)Proc.Lun.Planet.Sci.12B,pp1781.(3) Clayton,D.D. (1989)Astrophys. J. 340,pp. 613-619.

USING NEURAL NETWORKS TO CLASSIFY ASTEROID SPECTRA;
E. S. Howell, E. Merényi, and L. A. Lebofsky, Lunar and Planetary Laboratory, University of Arizona, Tucson, AZ 85721

Asteriods have been placed in broad classes based on their spectral appearance by many different groups. Starting with Chapman *et al.* (1), the classes have been refined and expanded to the present widely used taxonomic system developed by Tholen (2). This system is based on the results of the eight-color asteroid survey (3) covering the visible and very near-infrared spectral region, and the asteroid albedo, in most cases determined by IRAS (4). Similar attempts to classify asteroids using the 52-color survey (5), which produced near-infrared spectra in the 0.8–2.5 μm region, has supported the classes defined by Tholen. The only minor modification is the addition of a small sub-class of S-type asteroids, the K class, first suggested by Bell.

We have attempted to use the combined surveys to classify asteroids using a neural network, which is able to recognize patterns to determine the similarities between spectra. The primary method used in earlier classification schemes is that of principal components, which uses the variance of the data to define a new basis set of orthogonal vectors to group the objects best. Even the combined eight-color and 52-color surveys produce only four significant principal components (6), which are related to general characteristics of the spectra. Instead, we used a Kohonen-type self organizing map (7), to explore the cluster structure in an unsupervised mode, presenting the full 60-dimensional information to the neural network so subtle features can be recognized. We also trained the above neural network with a categorization-learning output layer in a supervised mode to group the established clusters into the Tholen classes. After training, additional spectra were presented to the network for class-membership prediction.

Preliminary results show that all of the Tholen classes are formed by the network in the unsupervised classification mode. After supervised training, the network correctly classifies both the training examples, and additional spectra into the correct Tholen class. Objects such as 308 Polyxo (T) which is known to be anomalous within the T class is similarly anomalous in this system, usually classifying between two classes. The results of the unsupervised training phase suggest possible separation between the E, M, and P classes in the absence of albedo information, which was previously thought to be the only discriminant between these spectrally degenerate classes. There is a good deal of structure and variation within the S class, and the possibility of two broad sub-classes of S-type asteroids. The separation of the K class from the S class is supported in our classification scheme, although the number of samples is small. Further results and implications will be presented.

References: (1) Chapman, C.R., Morrison, D., and Zellner, B., 1975, *Icarus*, 25, 104. (2) Tholen, D.J., 1989, *Asteroids II*, U. Arizona Press, 1139. (3) Zellner, B., Tholen, D.J., and Tedesco, E.F., 1985, *Icarus*, 61, 355. (4) Tedesco, E.F., 1989, *Asteroids II*, U. Arizona Press, 1090. (5) Bell, J.F., Owensby, P.D., Hawke, B.R., and Gaffey, M.J., 1988, *LPSC XIX*, 57. (6) Burbine, T.H., and Bell, J.F., 1991, *LPSC XXII*, 155. (7) Kohonen, T., 1988, Self-Organization and Associative Memory, *Springer-Verlag.*, New York.

FAYALITIC HALOS AROUND FeNi INCLUSIONS IN FORSTERITE IN THE KABA CARBONACEOUS CHONDRITE

X. Hua[1,2], P. R. Buseck[1], and A. El Goresy[3]. [1]Depts. of Geology & Chemistry, Arizona State University, Tempe, AZ 85287 USA. [2]Central Laboratory, China University of Geosciences, Wuhan, PRC. [3]Max-Planck-Institut f. Kernphysik, Heidelberg, FRG.

Petrography and mineral chemistry: We have found spindle-shaped fayalitic halos in Kaba forsterites. All halos (1) have round bleb-like inclusions containing Ni-rich metal and sulfide in their centers, (2) are ellipsoidal rather than round, and (3) have their long axes parallel, suggesting crystallographic control by their olivine hosts. The halos are 4 to 6 μm wide, 14 to 20 μm long, and surround central inclusions approximately 5 μm across. The olivine composition along the long axes next to the inclusions is $Fa_{40.64}$, and it is $Fa_{26.63}$ along the short axes. The Fa content drops gradually towards the host olivine, which has a composition of $Fa_{0.11}$. EDS measurements of the metal-sulfide inclusions show a much higher Ni than Fe peak. A line scanning profile of the Fe content along the long axis of the spindle confirms that the fayalite increases toward the inclusion (see figure).

Discussion: Fa-rich halos in olivine can provide information regarding the relationship between the metal inclusions and the surrounding olivine. We believe that *in situ* oxidation provides an explanation for these halos: (1) the Fa concentrations increase toward the metal inclusions; (2) the halos do not contain measurable Ni; (3) the metal inclusions are rich in Ni. Therefore, we propose that the halos formed by oxidation of FeNi metal and subsequent Fe^{2+} diffusion into the adjoining forsterite. The expected and observed Fa-concentration profiles match such an origin. Furthermore, the shapes of the halos suggest more rapid diffusion along the long axes of the spindles than along their short axes. Buening and Buseck (1973) showed that the diffusion coefficient of Fe^{2+} along the olivine **c**-direction is roughly four times faster than along **a** and five times faster than along **b**. Our results from the longest symmetric halos suggest their long axes are close to the olivine **c**-direction and their short axes are near the **a**- or **b**-directions, inferences compatible with a diffusion origin. The development of the halos by oxidation must have involved mass transport, either by the introduction of SiO_2 or the removal of MgO, consistent with the calculations of Palme and Fegley (1987). Transport presumably occurred via a gas phase.

Conclusions: (1) Fayalitic halos around metal inclusions in forsterites of the Kaba CV3 chondrite formed by the oxidation of Fe; (2) Fe^{2+} subsequently diffused into adjoining forsterite to form the halos; (3) the development of fayalitic halos required either the introduction of SiO_2 or removal of MgO.

References: (1) Boland J. N. and Duba A. (1981) *Nature* **294**, 142-144; (2) Buening D. K. and Buseck P. R. (1973), *J. Geophys. Res.* **78**, 6852-6862; (3) Hua X. *et al.* (1988) *GCA.* **52**, 1389-1408; (4) Palme H. and Fegley B., Jr. (1987) *LPS XVIII* 754-755.

Two distinct 'normal planetary' noble gas carriers in chondrites.

Gary R. Huss and Roy S. Lewis , Enrico Fermi Institute, Univ. of Chicago, Chicago, IL 60637

'Planetary' noble gases are severely depleted in light elements with respect to solar system abundances [1]. 'Planetary' noble gases in chondrites are dominated by gases with 'normal' isotopic ratios, similar to those of solar wind or Earth's atmosphere, although interstellar diamonds have 'planetary' abundances and highly anomalous isotopic ratios. Using noble-gas data for acid residues from 14 meteorites of 7 chondrite classes, we find evidence for two distinct 'normal planetary' gas carriers. For historical continuity, we adopt the labels P1 and P3 from [2].

Component P1 is closely analogous to 'Q' gases [2]. The carrier is carbonaceous, thermally resistant, and is largely oxidizable in HNO_3 or chromic acid. However, the properties of the carrier and the elemental and isotopic ratios of the noble gases vary depending upon thermal history. The Table shows ratios for unaltered P1, which differs from measurements of 'Q' gases obtained by closed system chemical oxidation [3]. The 'Q-Xe' measured by [3] appears to be a mixture of P1 plus Xe-S plus Xe-HL.

The gas-release temperature of P1 differs significantly between meteorite classes. While essentially all gases were released from Orgueil (CI) residues by 1550 C, the Qingzhen (E3) HF/HCl residue retained 30 % of its P1 gas to 1800 C and was not fully degassed even at 2000 C! P1 content decreases with metamorphic grade, but more slowly than do contents of exotic components [4]. Julesburg (L3.6), which now contains almost no SiC or diamond [4], has about 45 % of the Xe-P1 found in LL3.0-3.2 chondrites. Metamorphism also affects chemical and thermal resistance of the P1 carrier. In Abee (E5), about 35 % of the Xe-P1 survives chromic-acid etch (vs <1 % in Qingzhen), and >80 % is retained to 1500 C. The elemental and isotopic ratios of P1 gases in Julesburg and Abee reflect the addition of gases released by other phases during metamorphism (Table).

P3 accompanies Xe-HL in interstellar diamond and is released at 250 to 800 C [2]. It is only observed in quantity in CI, CM2, and LL3.0-3.2 chondrites. P3 has less He and Ne and more Ar and Kr (relative to Xe) than does P1, and the Xe apparently contains less Xe-S and Xe-HL (Table). About 70 % of the P3 and 34 % of the Xe-HL in the Orgueil HF/HCl residue are removed by chromic-acid etch, and only 17 % of the P3 and 51 % of the Xe-HL survive perchloric acid. This Xe-HL loss rate is much higher than for ordinary and CV chondrites and apparently reflects chemical destruction of 'reactive diamond' that cannot survive accretion-disk processing or metamorphism. The higher loss rate of P3 is consistent with it being located in more reactive and thermally labile portions of the same diamond or diamond-like material that hosts Xe-HL and does not require an additional carrier (e.g., organic polymer [2]).

Acknowledgements: This work was supported by NASA grant NAG 9-52 to E. Anders.

Table: Ratios in P1 and P3 compared to gases from diamond, 'Q', and 2 chondrite samples.

Component	$\frac{^{22}Ne}{^{132}Xe}$	$\frac{^{36}Ar}{^{132}Xe}$	$\frac{^{84}Kr}{^{132}Xe}$	$\frac{^{20}Ne}{^{22}Ne}$	$\frac{^{130}Xe}{^{132}Xe}$	$\frac{^{136}Xe}{^{132}Xe}$
P1	>0.36	≤71	≤0.79	>10	0.1617	0.3165
P3	<0.25	≥375	>2.9	>10	0.1597	0.3120
'Q' [ref. 3]	0.47	90	0.96	10.7	0.1629	0.3188
Diamond (w/o P3)	44	112	0.58	8.468	0.156	0.642
Julesburg bulk res.	0 49	48	0.61	10.1*	0.1624	0.3186
Abee bulk res.	0.48	186	1.05	9.7*	0.1625	0.3211

* Corrected for spallation.

[1] Ozima, M. and Podosek, F. A. (1983) Noble Gas Geochemistry, Cambridge. [2] Tang, M. and Anders, E. (1988) GCA, **52**, 1245-1254. [3] Wieler, R., Anders, E., Baur, H., Lewis, R. S., and Signer, P. (1991) GCA, **55**, submitted. [4] Huss, G. R. (1990) Nature, **347**, 159-162. [5] Crabb, J. and Anders, E. (1982) GCA, **46**, 2351-2361.

Cr ISOTOPIC COMPOSITION OF SULFIDES IN THE QINGZHEN ENSTATITE CHONDRITE; I. D. Hutcheon[1], M. Bar-Matthews[1,2] and P. K. Carpenter[1], [1] Lunatic Asylum, Division of Geological & Planetary Sciences, California Institute of Technology, Pasadena, CA 91125; [2] Geological Survey of Israel, Jerusalem, Israel.

Studies of the Cr isotopic composition of uncharacterized, soluble phases in carbonaceous and enstatite(E) chondrites [1] and of individual phosphate minerals in IIIAB iron meteorites [2] have provided evidence of ^{53}Mn ($\tau_{½} \sim 3.7 \times 10^6$y). Inferred initial ^{53}Mn/^{55}Mn ratios range from 8×10^{-7} to 4.4×10^{-5} and evidence for disturbed Mn-Cr isotopic behavior is apparent in several meteorites. We initiated a petrographic and isotopic study of Mn-rich sulfides in E-chondrites to determine if ^{53}Mn was present in regions of the nebula characterized by very low oxygen fugacity and to gain new clues to the behavior of the Mn-Cr system in response to metamorphic processes. More than 30 Mn-rich sulfides, 20 to 60μm in size, were located in a polished section of Qingzhen (EH3) using the electron probe in an automated "point" counting mode. Most of the sulfides are niningerite (Nin), although a few small (10-20μm), angular crystals of daubreelite (Dau) and one large (150μm) rounded oldhamite (CaS) were also found. Nin occurs (1) in the matrix surrounded by enstatite or adjacent to troilite, (2) in multi-phase sulfide-metal aggregates and (3) within chondrules embedded in enstatite or associated with troilite. Chemical compositions (Table 1) are fairly uniform and differ from those reported previously [3] primarily due to higher Mn (up to 12.7%) and lower Mg. Nin contains up to 0.09% Ga and Ge.

The Cr isotopic compositions of 4 Nin and 1 Dau were determined with the PANURGE ion probe. All Nin exhibit enrichment of the lighter Cr isotopes relative to Dau and chromite, $F_{Cr} \sim 8$‰/amu; data are corrected for ^{50}Ti overlap on ^{50}Cr and normalized to ^{50}Cr/^{52}Cr=0.051859. Two Nin show small but well resolved ^{53}Cr excesses (δ^{53}Cr$\sim$5.2‰); the other two Nin and the Dau contain isotopically normal Cr within the analytical uncertainty (Fig. 1). No correlation between the isotopic composition of Nin and petrography is apparent. A correlation line fitted to the data from Nin and Dau has slope corresponding to ^{53}Cr*/^{55}Mn$\sim 7 \times 10^{-6}$. However, ^{53}Cr/^{52}Cr ratios for niningerite alone do not correlate with Mn/Cr ratios and the data do not allow a firm conclusion regarding *in situ* decay of ^{53}Mn. The Nin have different textural occurrences and may not derive from a common source with uniform ^{53}Mn/^{55}Mn. Evidence of Ca isotopic heterogeneity among Qingzhen oldhamite [4] suggests the presence of several, isotopically distinct nebular components. The 4 Nin analyzed occur in different lithologies and may not share a common source. If sulfides in Qingzhen preserve a record of the isotopic composition of precursor dust aggregates, Cr isotope heterogeneity among Nin should not be unexpected.

Refs: [1] J-L. Birck & C.J. Allegre (1988) *Nature* **33**, 579; [2] I.D. Hutcheon & E. Olsen (1991) *LPSC XXII*, 605; [3] A. El Goresy *et al.* (1988) *Proc. NIPR Symp. Antarc. Meteorites* **1**, 65; [4] L.L. Lundberg *et al.* (1991) *LPSC XXII*, 835.

Table 1. Qingzhen sulfides

	1.	2.	3.	4.
Mg	27.76	26.73	27.12	0.52
Fe	11.69	12.51	14.65	0.20
Mn	12.23	12.65	11.18	0.19
Ca	0.36	0.35	0.31	55.41
Cr	0.13	0.14	0.13	----
S	47.86	47.27	46.95	42.14
Total	100.08	99.65	100.39	98.46

1-3: niningerite; 4: oldhamite.

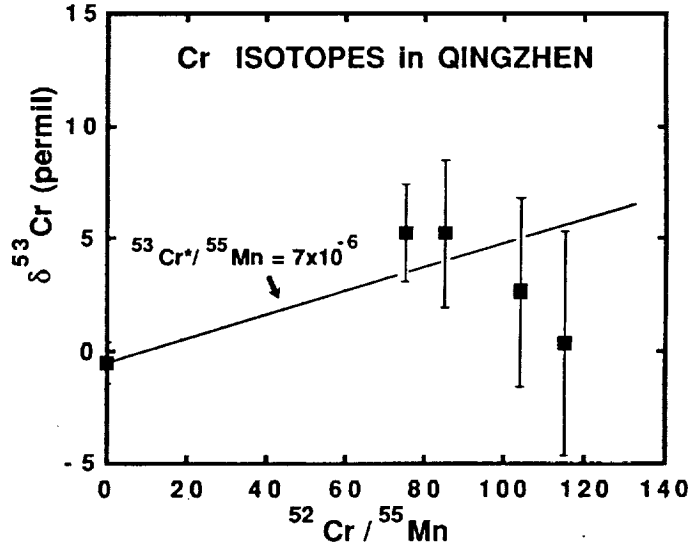

THE L6 CHONDRITE FALL AT GLATTON, ENGLAND, 1991 MAY 5. R. Hutchison, Mineralogy Department, The Natural History Museum, London SW7 5BD, UK., J.C. Barton, Physics Department, Birkbeck College, Malet St., London WC1E 7HX and C.T. Pillinger, Earth Sciences Department, The Open University, Milton Keynes MK7 6AA, UK. plus various colleagues.

A single stone of 0.767 kg fell in the garden of 80 year old Mr. A. Pettifor in the village of Glatton, 15 km SSW of Peterborough, England. The co-ordinates of Glatton are 52° 28" N, 0° 19" W. At about 12.30 pm British Summer Time on May 5th (11.30 hours GMT), Mr. Pettifor was startled by a whining noise as he worked in his garden. He immediately heard something crash through a hedge, some 20 metres from where he stood. The meteorite was found beneath damaged shrubs in a shallow pit about 2 cm deep. The stone was warm, not hot, when picked up. The circumstances indicate that the stone came from a northerly direction. It was overcast at the time, so no fireball was seen and no sonic booms have been reported. The stone was polyhedral and completely crusted; a secondary crust covered one tiny face (3 cm^2) caused by shearing of one corner in atmospheric flight.

On 9 May, R. Hutchison and C.T. Pillinger were alerted to the possibility of a new fall by Mr. Howard Miles of the British Astronomical Association and news media respectively. A visit to Mr. Pettifor that evening confirmed that his stone is a meteorite. On Sunday 12 May, volunteers searched E-W swathes of farmland both north and south of the place of fall, looking for more stones; none was found. The stone was loaned to The Natural History Museum, and after 37 grams were broken from it, low-level counting began on 13 May. The Museum should shortly acquire the main mass.

In reflected light, a polished mount revealed a granular texture with few chondrules. The olivine is close to $Fo_{75.5}$ and the pyroxene is about En_{79}. Areas tens of micrometres across have low reflectivity consistent with plagioclase; two analyses gave $Ab_{86}Or_5An_9$. Texture and mineral compositions indicate a L6 classification.

A preliminary figure for the ^{26}Al content, 50 disintegrations/min/kg, indicates that the stone was close to the saturation value. This yields a minimum cosmic ray exposure age of about 2 Ma.

Data that become available over the next few months will be presented at the Meeting.

ADRAR 003: A NEW EXTRAORDINARY UNEQUILIBRATED ORDINARY CHONDRITE. R. Hutchison, Mineralogy Department, The Natural History Museum, London SW7 BBD, S.J.B. Reed, Earth Sciences Department, University of Cambridge, Downing St., Cambridge CB2 3EQ, R.D. Ash & C.T. Pillinger, Earth Sciences Department, The Open University, Milton Keynes MK7 6AA, UK.

A 287g stone found in southern Algeria proved to be a highly unequilibrated ordinary chondrite. Abundant chondrules ranging from over 3 mm to less than 50 μm are set in opaque matrix. Metal-sulphide objects are smaller; discrete inclusion in the matrix are up to 500 μm in diameter, whereas those within silicate chondrules, or situated along their margins, range down to micrometre-size. Reflected light microscopy indicates that many metal-sulphide objects have rims with layering on a 10 μm scale where they abut interchondrule matrix. Veins of highly reflecting material up to about 10 μm wide cross cut the matrix. These are texturally similar to the Fe-carbide veins in Semarkona. Again, like Semarkona (1), some chondrules and irregularly shaped inclusions contain crystalline feldspar. A barred olivine chondrule almost 2 mm across has olivine dendrites, Fo_{95}, sometimes rimmed by pigeonite, $Wo_{12}En_{83}Fs_5$, or in contact with interstitial granular pigeonite, $Wo_{10}En_{84}Fs_6$. Plagioclase, An_{86-89} is intergrown with the olivine bars.

Mineral analyses by Bischoff (2) and this work indicate that olivine ranges from Fo_{93-69}, and pyroxene from En_{95-76}. These ranges are reminiscent of Semarkona, in which the more Fe-rich silicates have been preferentially altered to smectite (3,4). Further mineralogical work will be undertaken on Adrar 003 to determine whether its opaque mineral assemblages closely resemble those of the unique chondrite, Semarkona. If so, we shall have a new, highly unequilibrated sample of a hydrously altered ordinary chondrite parent body on which to work.

A distinguishing feature of Semarkona is the greatly enhanced D/H ratio of water released by pyrolysis of bulk samples (5) and chondrules (6); this meteorite affords one fraction with δD almost a factor of six higher than SMOW during a stepped pyrolysis. The bulk samples of Adrar 003 analysed for D/H ratio show quite low amounts of water with no δD values > +42‰. In this respect, Adrar 003 resembles Krymka which previously, alone amongst low petrologic type 3 ordinary chondrites, failed to show substantial D enrichments. Results from hydrogen isotope studies of highly unequilibrated ordinary chondrites have been notoriously variable, possibly because of heterogeneity of the samples. In reality this variability may be a clue to the carrier of the D anomaly; it might well be located in a very minor component and be truly astronomical in magnitude. Further studies of Adrar 003 can contribute to the understanding of D/H systematics.

(1) Hutcheon and Hutchison (1989) Nature 337, 238-241. (2) A. Bischoff, priv. comm. and Meteorit. Bull., in press. (3) Hutchison *et al.* (1987) GCA 51, 1875-1882. (4) Alexander *et al.* (1989). 53, 3045 - 3057. (5) McNaughton *et al.* VGR. 87, A297 - A302 (1982). (6) Morse *et al.* Meteoritics 23, 291 (1988).

NA-CR SULFIDE PHASES IN THE INDARCH (EH4) CHONDRITE

M.L. Hutson, Lunar and Planetary Lab., Univ. of Arizona, Tucson, Az, 85721

Two hydrated Na-Cr-sulfides (mineral A and mineral B, with about 10 and 20 wt% oxygen, respectively [1]) have been observed in many E-chondrites [2]. A new Fe-Cr sulfide with about 5 wt% water has also been observed in 4 E-chondrites, including Indarch [3]. Indarch (USNM 334-1) contains several Na-Cr-S phases. I have studied numerous grains optically and with an SEM, and 14 of the largest with an electron microprobe, analyzing for K, Na, Fe, Cr, S and O.

All of the hydrated Na-Cr-S grains observed in Indarch are < 60 microns across, and are in contact with troilite. Of the 14 grains analyzed with the microprobe, 10 have approximately 10 wt% O (mineral A). Some of the grains have uniform compositions, while others vary from 8-13 wt% O. These variations correlate with Z-variations observed with BSE and with color variations seen in reflected light. In general, the darker the color in reflected light, the higher the O content. Two of the 14 grains have O content in the range of 18-20 wt% (mineral B). Neither of these 2 grains is associated with mineral A; they both appear to be primary minerals. Two grains (one mineral A and one mineral B) were examined with an ion probe. In addition to oxygen and hydrogen, both grains contain noticeable amounts of lithium.

An additional grain has a uniform composition of 15.6 wt% O (3 analyses). No compositional variation was apparent in either BSE of reflected light, so it seems clear that this grain does not represent a fine-grained mixture of minerals A and B. The remaining grain has about 5 wt% O. Although about 5 wt% H_2O has been reported previously for Fe-Cr-S grains in Indarch [3], that phase contained approximately 20-21 wt% Fe and no Na. The grain in this study contains only 1.5 wt% Fe and is not the same phase described by [3]. This grain also contains 8.2 wt% Na, much more than reported for other hydrated Na-Cr-S phases (<3 wt% Na).

Despite the variability in O content, all of these grains have a Cr:S ratio of approximately 1:2, suggesting they are members of a single phase consisting of CrS_2 units, perhaps layers, that can accomodate variable amounts of O, Na and Fe. A phase fitting this structural description, a weathering product of Caswellsiliverite, is known [4]. However, the phases in Indarch are compositionally dissimilar to this weathering product, as they contain approximately an order of magnitude less alkalis. In addition, the grains in Indarch grains appear to have been unaffected by terrestrial weathering.

[1] Rambaldi, E.R., Housely, R.M., Rajan, R.S., Cirlin, E., El Goresy, A., and Wang, D. (1983) Meteoritics 18, 380-381. [2] Ramdohr, P. (1973) The Opaque Minerals in Stony Meteorites, Amsterdam, Verlag. [3] Lin, Y.T., Kimura, M. and El Goresy, A. (1990) Meteoritics 24, 379. [4] Schollhorn, R., Arndt, R., and Kubny, A. (1979) J. Sol. State Chem. 29, 259-265.

OXYGEN ISOTOPIC COMPOSITIONS OF INDIVIDUAL METEORITIC MAGNETITE GRAINS FROM CARBONACEOUS CHONDRITES; M. Hyman[1], E. K. Zinner[2] and M. W. Rowe[1], [1]Dept. of Chemistry, Texas A&M University, College Station, TX 77843, USA, [2]McDonnell Center for the Space Sciences and the Physics Dept., Washington University, St. Louis, MO 63130, USA.

Magnetite in Cl chondrites occurs in several distinct morphologies. We isolated individual magnetite grains with characteristic structures from Alais, Ivuna, Orgueil and Revelstoke and examined their oxygen isotopic compositions. The values, obtained on the Washington University Cameca IMS 3f ion microprobe, cluster near the intersection of the ^{16}O-rich mixing line (defined by the Allende refractory inclusions) with the terrestrial mass fractionation line as seen in Figs. 1-3. The center of mass of the cluster for all meteorites lies somewhat above the terrestrial mass fractionation line. δO-values for all grains are consistent with a mass fractionation line with a slope of 1/2. What is striking is the extreme range in mass fractionation covered by the meteoritic magnetite grains, which is much larger than that for terrestrial magnetite standard grains of similar size measured under the same conditions. The errors for measurements on individual meteoritic grains include the scatter measured in grains of the terrestrial standard. A majority of the particles analyzed were plaquettes and spherulites. Of the outlying data points in the Figures, three (one crystal from Alais and two grains of nondescript morphology from Orgueil) have $\delta^{18}O$ values of −30 and −20 ‰ respectively (Figs. 1 and 2); seven (plaquettes and sperulites from Alais and Ivuna) lie near +20 ‰ (Figs. 1 and 3), while one plaquette from Ivuna plots at ~+40 ‰ (Fig. 3). Two framboidal particles from Orgueil were measured; one with $\delta^{18}O = -4$ ‰ and one measured simultaneously with a spherulite, with $\delta^{18}O = 0$ ‰. Only Revelstoke, with just one plaquette measured (Fig. 3), is not represented among these outlying oxygen compositions.

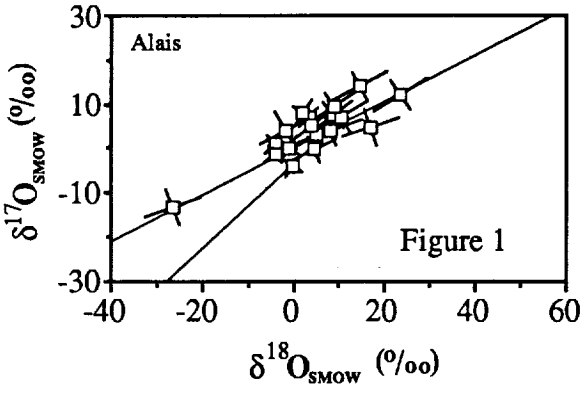

Figure 1

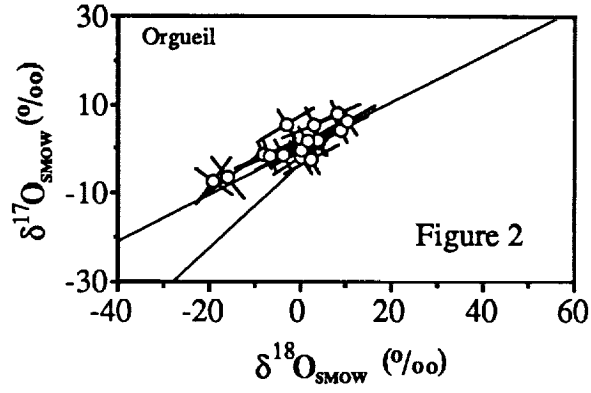

Figure 2

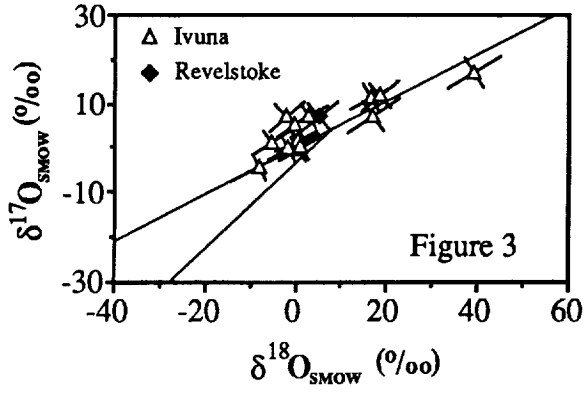

Figure 3

MORE Ti ISOTOPIC COMPOSITIONS OF PRESOLAR SiC FROM THE MURCHISON METEORITE; T. R. Ireland[1], E. K. Zinner[2], S. Amari[2,3] and E. Anders[3], [1]Research School of Earth Sciences, ANU, Canberra ACT 2601, Australia, [2]McDonnell Center for the Space Sciences and Physics Dept., Washington University, One Brookings Drive, Saint Louis, MO 63130-4899 USA, [3]Enrico Fermi Institute and Dept. of Chemistry, University of Chicago, 5630 S. Ellis Ave., Chicago, IL 60637-1433 USA.

We extended Ti-isotopic measurements of individual interstellar SiC grains from large sizes (separate LU; 8-20 μm) to smaller ones (separate KJH; 3-5 μm). The LU grains have ^{13}C excesses, ^{15}N depletions, ^{29}Si and ^{30}Si excesses, and low Al and Ti concentrations [1,2]. The KJH grains have higher Al and Ti concentrations, making it possible to measure Ti isotopes in smaller grains. In addition, their C-, N-, and Si-isotopic compositions scatter much more.

The majority of the KJH SiC grains have Ti-isotopic compositions similar to those of the LU grains: they have valley-shaped isotopic abundance patterns (grain 071 in Fig. 1), qualitatively consistent with neutron-capture synthesis such as in AGB [3] or Wolf-Rayet [4,5] stars. The $\delta^{50}Ti$ is correlated with $\delta^{29}Si$ (Fig. 2). For the KJH grains this correlation extends to depletions in ^{29}Si and ^{50}Ti: grain 081 has an inverted pattern relative to the majority. The other exceptional grain is 166; it has very unusual C-, N-, Si-, Mg-, and Ca-isotopic compositions (≡ grain X2 of [6]). It also has an unusual Ti isotopic composition with a smoothly fractionated pattern from a positive anomaly at ^{46}Ti to a deficient ^{50}Ti abundance, except that ^{49}Ti is overabundant by 220 ‰. This excess of ^{49}Ti could be due to the decay of ^{49}V ($t_{1/2}$ = 331 days) that (originally as ^{49}Cr) is the precursor of ^{49}Ti in explosive nucleosynthesis [7].

References: [1] Ireland *et al.* (1991) *Ap. J. Lett.*, in press; [2] Zinner *et al.* (1991) *Nature* **349**, 51; [3] Gallino *et al.* (1990) *Nature* **348**, 298; [4] Busso and Gallino (1985) *Astron. Astroph.* **151**, 205; [5] Prantzos *et al.* (1987) *Ap. J.* **315**, 205; [6] Zinner *et al.* (1991) This volume; [7] Woosley *et al.* (1973) *Ap. J.* **26**, 231.

Figure 1

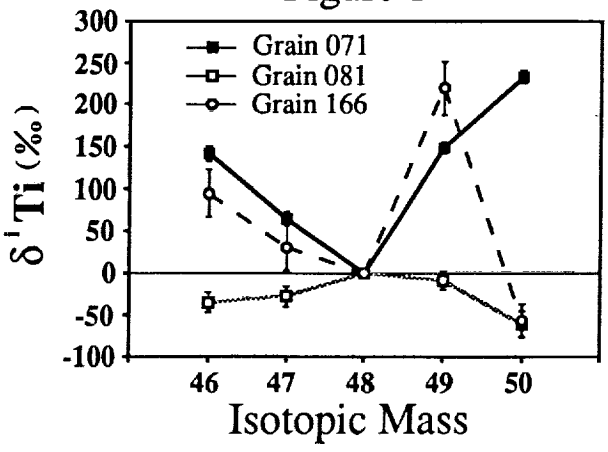

Figure 2

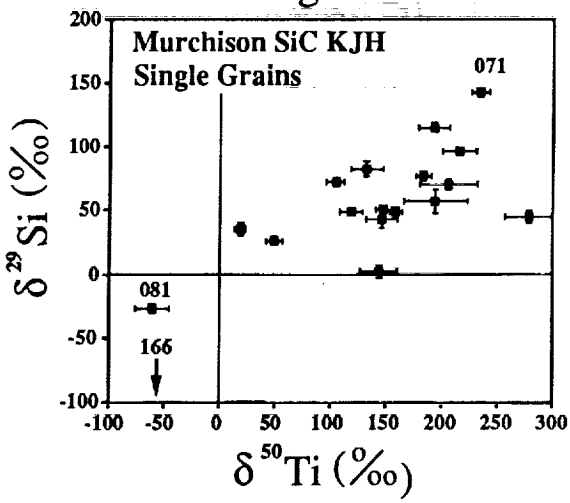

SILICATE MELT STRUCTURES, PHYSICAL PROPERTIES, AND PLANETARY ACCRETION.
P. Jakes [1,2], S. Sen [2], and K. Matsuishi [3]; 1. Lunar and Planetary Institute, 3303 NASA Rd. # 1, Houston TX 77058; 2. Department of Geosciences, University of Houston, Calhoun Rd. 4800, Houston TX 77204; 3. TSCUH - University of Houston, Houston, TX., 77204

Raman spectroscopy of natural, experimentally remelted, highly siliceous melts/glasses indicates the existence of at least two different structural states of silicate melts above the solidus: (1) fully polymerized structures with Si4, Si3Al, and Si2Al2 unit environments characteristic of near liquidus temperatures; and (2) depolymerized structures are characterized by the decreasing proportion of Si4 units and increased proportin of Si2Al2 and Si(M2) and Si(M3) environments. Such structures were observed in experimental runs quenched from temperatures about 350°C higher than liquidus.

The composition of the melt has been considered to be a major factor controlling the viscosity of the melts, and temperature was believed to have only minor influence [1] on polymerization and depolymerization. We are finding that the structural state of melts of the same composition is significantly temperature dependent and that the change from a low-temperature, fully polymerized state to a high-temperature depolymerized state is rather sudden[2].

In order to examine the relationship of structural state and physical properties of melts we have modified the falling sphere method to measure viscosities high above the liquidus at atmospheric pressures. The X-ray tube was mounted on vertical quenching furnace and the sphere falling through the melt was traced at specific time intervals using a consecutive series of photographs.

The change of physical properties of melts (viscosity) could be related to the structural state of melts; however no significant changes were recorded, in viscosity measurements in the temperature region above the liquidus. Glasses quenched from the near-liquidus region do have structures of melts characteristic of the liquidus-solidus region (fictive temperatures are much lower than liquidus), whereas glasses formed by quenching from temperatures 350°C higher than liquidus reflect the structures of near liquidus melts. We were unable to measure the structures of qeunched melts and viscosities from temperatures higher than 1650°C.

There is yet another enigma in the melt/glass properties. If the measured viscosities between 1250°C and 1550°C are linearly extrapolated into the superheated region (above 2000°C), the viscosities of the siliceous melts are still extremely high and do not explain the differences between "geologically" observed "low" viscosities (coatings, homogeniety, thin veins). We suggest therefore, that yet another structural "transition", similar to that observed above liquidus, takes place in silicate melts in the region high above liquidus. In this structural state silicate melts are completely depolymerized and drastically change physical properties and hence behavior.

The implication for planetary science of the existence of different high-temperature depolymerized structural states of silicate melts for the planetary science is in the interpretation of impact induced (nonequilibrium) melting. Extremely high temperatures are expected in scenarios of planetary origins advocating late large impacts leading to the superheating of melts in impact and adjacent regions[3]. Physical properties of melted rocks change accordingly: extremely fluid melts, vigorous mixing, and hence easy volatilization (otherwise protected by low convective mixing) are first order implications. Independent chemically distinct reservoirs, depleted in the volatile elements, and regions of different redox states (depending on composition e.g. the carbon content of the projectile) could be created at this accretionary or later "cataclysmic" stages of early planetary evolution.

References: 1. Mysen B.O., Finger, L.W., Virgo D., and Seifert F. A. (1982) Amer. Miner. 67, 686-695; 2.Jakes P., Sen S., and Matsuishi K., (1991) Nature, submitted; 3.Ahrens T.J.(1990): in Origin of the Earth. Newsom and Jones eds., Oxford.Univ.Press,211-227.

FeO and MgO trends in the plagioclases of two Apollo 15 mare basalts. Odette B. James and James J. McGee, U. S. Geological Survey, Reston, VA 22092, USA.

We have begun a study of lunar mare basalts to define the nature of igneous variations of FeO and MgO in lunar plagioclases. Our recent studies of plagioclases in lunar ferroan anorthosites (1,2) identified pronounced negative correlations of FeO and MgO with anorthite (An) content. We interpreted these trends as igneous, but our interpretation has been questioned by Phinney (3), because the FeO and MgO contents of the ferroan-anorthosite plagioclases, when used with distribution coefficients determined experimentally and from natural terrestrial systems, yield unrealistically low contents of FeO and MgO in the parent melt(s). We argued that these distribution coefficients may not be appropriate for ferroan-anorthosite plagioclase (1), whereas Phinney (and others (4)) suggested that the low FeO and MgO contents in the ferroan-anorthosite plagioclases are the result of metamorphic reequilibration. Our current study of basalts, in which the FeO and MgO distributions are clearly the result of igneous processes, should help resolve this controversy over the origin of the trends in the ferroan anorthosites.

The two basalts we have studied are 15384 and 15388. Basalt 15384 is a medium-grained olivine-normative mare basalt (5). There are local patches of coarsely variolitic intergrowths of pyroxene and plagioclase, but most of the rock has hypidiomorphic-granular texture. Basalt 15388 is a feldspathic microgabbro (5). Most of this rock consists of early crystallized, coarse-grained variolitic intergrowths of pyroxene and plagioclase and late crystallized, coarse-grained intergrowths of plagioclase laths and equant pyroxene grains.

The plagioclase in the early crystallized variolitic intergrowths in 15388 and all the plagioclase analyzed in 15384 show identical trends of variation of FeO and MgO with An: there is a strong negative correlation of both these oxides with An (Fig. 1), but mg' (100 x molar Mg/Mg+Fe) is nearly constant and relatively high (Fig. 2). The late crystallized plagioclase in 15388 shows a different trend (Fig. 1,2): as the edges of grains are approached, An content decreases, MgO is constant or decreases slightly, FeO increases markedly, and thus mg' decreases greatly. The relationship of the two trends in 15388 indicates that the first plagioclase to crystallize in this rock had relatively low An, high FeO, and the highest MgO. Subsequent plagioclase was reversely zoned: An increased and both FeO and MgO decreased. The last plagioclase to crystallize was zoned normally: An and MgO decreased and FeO increased.

We interpret the two trends shown by the plagioclases as indicating two different crystallization regimes. The trend shown by the plagioclase in 15384 and the early crystallized, reversely zoned plagioclase in 15388 may be the product of nonequilibrium crystallization of a melt undercooled with respect to plagioclase nucleation (6,7). The trend shown by the last crystallized plagioclase in 15388 is probably the product of equilibrium crystallization.

Our data also demonstrate that the FeO and MgO contents of the plagioclases in the lunar ferroan anorthosites can indeed be the result of igneous processes. On Fig. 1, the compositions of the ferroan-anorthosite plagioclases lie on the extensions of the FeO and MgO variation trends observed in the basalt plagioclases. References: (1) James O.B., Lindstrom M.M. and McGee, J.J. (1991) *PLPSC* **21**, 63. (2) McGee J.J. (1990) *LPS* **XXI**, 761. (3) Phinney W.C. (1991) *PLPSC* **21**, 29. (4) Hansen E.C., Steele I.M. and Smith J.V. (1979) *PLPSC* **10**, 627. (5) Ryder G. (1985) Catalog of Apollo 15 Rocks, NASA Cur. Branch Pub. 72. (6) Lofgren G. (1974) in "The Feldspars", eds. W.S. MacKenzie and J. Zussman, Manchester Univ. Press, 362. (7) Crawford M.L. (1973) *PLSC* 4, 705.

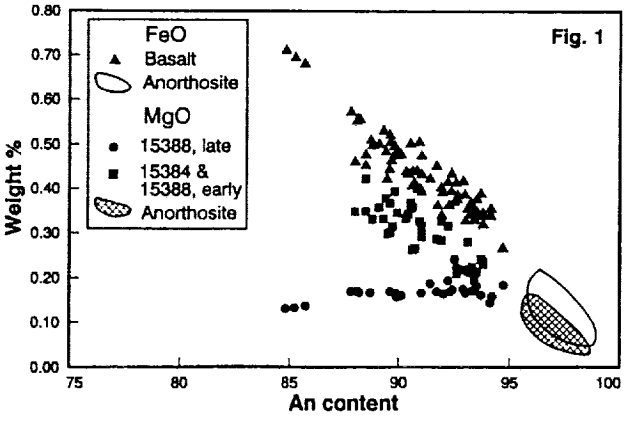

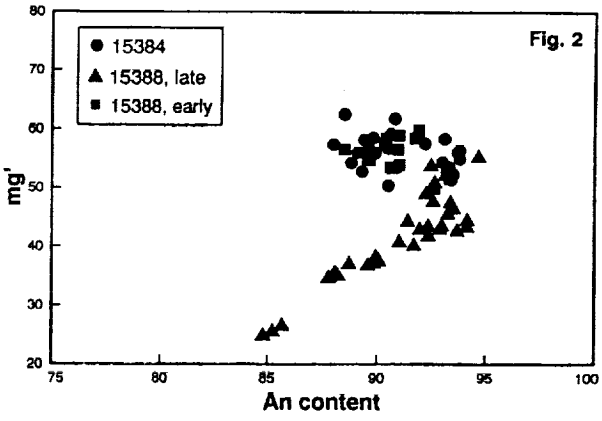

NEW PIXE ANALYSES OF INTERPLANETARY DUST PARTICLES; Elmar K. Jessberger, Jörg Bohsung, Sepideh Chakaveh, Max-Planck-Institut für Kernphysik, P.O. Box 103980, 6900 Heidelberg, Germany. Kurt Traxel, Physikalisches Institut der Universität, Heidelberg, Germany

The genetic classification of meteorites is based on their bulk chemical composition. With this in mind, we set out to explore if also for interplanetary dust particles (IDPs) a classification scheme based on bulk chemical composition could be established with the ultimate goal to reveal their sources, histories, and origins. Because of the smallness of IDPs and the necessity of follow-up studies, the bulk analytical technique has to be non-destructive. It also has to be highly sensitive since minor and trace element variations are crucial. Both requirements are fulfilled by Proton-Induced X-Ray Emission (PIXE).

We performed two tests of the validity of PIXE results obtained on these complex, small (≈ 10 μm), irregular grains: Firstly, after our PIXE measurements, we re-analyzed two particles with Synchrotron X-Ray Fluorescence (SYXFA) and found agreement for the 19 mutually accessible elements [1]. Secondly, we re-analyzed with PIXE 11 stratospheric particles that had before been studied also with PIXE by other experimenters [2], and again found agreement for the 13 commonly determined elements. Thus, we have confidence in our PIXE data.

There are now major, minor and trace element data of eleven IDPs on hand (eight analyzed by us with PIXE and SYXFA, three analyzed by [3] with SYXFA). Keeping in mind the uncertainties of $\approx 15-20\%$ and the small number of analyzed IDPs, the principal findings are as follows (after normalization to Fe and CI abundances):

- Refractory and moderately volatile elements (Al, Si, S, Cr, Mn, Ni) are chondritic with the exception of a ubiquitous Ca-depletion. The latter also had been found in matrices of carbonaceous chondrites [4] and Antarctic micrometeorites [5].
- Some volatile elements (Cℓ, K, Cu, Zn, Ga, Ge, Se) and Co are enriched by factors of 2 to 7, and Br by a factor of up to 80.
  In CM-chondrites, which contain layer lattice silicates, Br-enrichments (relative to elements of similar volatility) are common [6]. In IDPs, however, this enrichment can be explained by atmospheric contamination judged from the Cℓ/Br ratio. Global fractionation of the solar nebula as proposed by [2] is not mandatory.
- With most elements being similar, different enrichment factors of Cℓ, Zn, Ga, and Se distinguish two groups of four IDPs each.
- One IDP with low S, K, Ca, Cr, Mn, Ni, and Zn resembles Antarctic micrometeorites [5].

The similarities of this suite of IDPs with chondrites prove their extraterrestrial nature, the dissimilarities, however, suggest that they typify a different class of planetary bodies. Possibly the volatile-rich IDPs represent a reservoir which is the complement of the volatile-depleted chondrites.

[1] R. Wallenwein et al. (1989) Lunar Planet. Sci. XX, 1171, The Lunar and Planetary Science Institute, Houston
[2] C. van de Stap et al. (1986) Lunar Planet. Sci. XVII, 1013, The Lunar and Planetary Science Institute, Houston
[3] S.R. Sutton and G.J. Flynn (1988) Proc. 18th Lunar Planet. Sci. Conf., 607
[4] H.Y. McSween and S.M. Richardson (1977) Geochim. Cosmochim. Acta 46, 1145
[5] M. Maurette et al. (1991) Nature, in print
[6] G.W. Kallemeyn and J.T. Wasson (1981) Geochim. Cosmochim. Acta 45, 1217

LARGE NB-TA FRACTIONATIONS IN ALLENDE CA, AL-RICH INCLUSIONS.

K. P. Jochum, H. Palme and B. Spettel
Max-Planck-Institut für Chemie, W-6500 MAINZ, GERMANY

After the first analyses of fine-grained spinel rich Allende inclusions it became clear that volatility played an important role in establishing the refractory element patterns of Ca, Al-rich inclusions (CAIs) in carbonaceous chondrites (1).

Most analyses of these inclusions were performed with INAA. Data for elements which are difficult to determine with this technique are rare (e. g., Nb and Y). These elements can be analysed by the spark source mass spectrometry (SSMS) technique (2). To obtain a maximum of information we have combined both techniques by analysing Allende CAIs with SSMS that were previously analysed by INAA. The analyses of three fine grained (spinel rich) and six coarse grained CAIs reported here represent the first determinations of Ta and Nb on the same inclusions.

In this report we will focus on pairs of elements with similar geochemical properties, such as Zr-Hf and Nb-Ta. Both element pairs show almost no fractionation in terrestrial rocks, SNC-meteorites and eucrites despite huge variations in absolute concentrations (3). A limited but parallel fractionation of Zr/Hf and Nb/Ta is observed in lunar rocks (3). Our analyses show that the Zr/Hf ratios in Ca,Al-rich inclusions are essentially chondritic as are Zr/Y ratios confirming earlier findings (2). However, Nb/Ta ratios are in all cases (except one) below the chondritic ratio, sometimes by as much as a factor of 30, in one group II inclusion. As Ta abundances are essentially constant most of the scatter is due to variable and low Nb contents. The large fractionation between Ta and Nb is surprising since the difference in condensation temperatures is small. At 10^{-4} bar the 50 % condensation temperature for Ta is 1540 K and for Nb 1500 K considering condensation in solid solution with perovskite and compared to the condensation temperatures of pure Ta_2O_5 of 1271 K and 1211 K for Nb_2O_5.

In group II inclusions the behaviour of Ta is similar to that of other refractory lithophile elements of intermediate volatility: Th, Tm, Nd, Pr, Sm, La and Ce (average CI-normalized abundances 30). According to calculated condensation temperatures (4) Ta is the most volatile of these elements. Niobium is the most refractory of the group of volatile refractory elements: Yb, Eu, Sr, U and Ba (with lower and more variable CI-normalized abundances). The break in the abundance patterns occurs exactly between Ta and Nb indicating a sharp temperature cut between Ta and Nb condensation temperatures. Either removal of the condensed phases at that temperature or appearance of a new phase that would take up some of the Nb must have occurred. In both cases efficient removal of Ta atoms from the gas is required while the major fraction of the much more abundant Nb atoms (there are 35 times more Nb than Ta atoms) remains uncondensed in the gas. This clearly indicates the dominant factor of volatility and the unimportance of kinetic effects in establishing these patterns.

Lit.: (1) Boynton, W. V. (1975) Geochim. Cosmochim. Acta **39**, 569-584; (2) Mason, B. and Martin, P. M. (1977) Smith. Contr. Earth Sci. **19**, 84-95; (3) Jochum, K. P., Seufert, H. M., Spettel B. and Palme H. (1986) Geochim. Cosmochim. Acta **50**, 1173-1183. (4) Kornacki, A. S. and Fegley, B., Jr. (1986) Earth Planet. Sci. Lett. **79**, 217-234.

A LIQUIDUS PHASE DIAGRAM FOR A PRIMITIVE SHERGOTTITE. J.H. Jones, SN2, NASA-JSC, Houston, TX 77058; A.J.G. Jurewicz and L. Le, Lockheed ESC, C23, 2400 NASA Rd. 1, Houston, TX 77058.

Shergottites are members of the SNC meteorite suite, which are thought to be samples of Mars. Of the shergottites in our collections, the meteorite most likely to represent a primitive liquid from the martian mantle is EETA79001. EETA79001 has the Nd isotopic signature of a long-term depleted mantle [1], has a relatively high Mg# [2], and is slightly olivine normative [2].

Actually, these primitive characteristics do not apply to the EETA79001 whole-rock, which is an assemblage of lithologies, but to the groundmass of a particular lithology, EETA79001A. The composition of this groundmass (Eg) has been estimated by [2]. To see if there is any relationship between "primitive" shergottites such as Eg and "evolved" shergottites such as Shergotty and Zagami, we have performed one-bar experiments on an Eg composition.

A synthetic Eg glass was prepared by fusing a mixture of oxides and carbonates. Excess Fe_2O_3 (2.4 wt.%) was added to correct for FeO loss to Pt. Charges were placed on Pt loops and equilibrated at temperature (f_{O_2} of QFM) for 10-12 hours. Quenched charges were analyzed using the electron microprobe. At 1175°C we have FeO mass balance to within 0.6 wt.% (3% relative). Our experiments range from 1300 to 1100°C, at ~25°C intervals. We report preliminary results.

The Eg liquidus is approximately 1300°C, with Fo_{78} olivine as the liquidus phase. Sub-calcic pyroxene (~En_{78}, Wo_3) joins olivine between 1275°C and 1250°C. By 1100°C, plagioclase has appeared (~An_{63}). Changes in liquid composition (Figure 1) imply that, in the interval 1200-1150°C, either the pigeonite starts to become more calcic or that a second pyroxene appears. Projections onto OL-SI-PL and mass balance calculations suggest that the olivine-pigeonite boundary is a peritectic (Figure 2). The 1100°C liquid has probably been modified during quenching and should probably plot nearer the ol-pig-plag±cpx pseudo-invariant point (Figure 2).

We compare these results with the calculated phase relations predicted by [3]. The predicted liquidus is 1304°C, with the first olivine being Fo_{79}. Low-Ca pyroxene (En_{73}, Wo_4) is predicted to appear at 1245°C. Augite (En_{49}, Wo_{36}) is calculated to appear at 1174°C. Plagioclase (An_{73}) is predicted to appear at 1098°C. Broadly, our experimental results compare favorably with prediction, although there is a systematic difference in normative silica. This difference is probably because the calculation treats the Ol-Pig boundary as a cotectic. Our inferred phase diagram (Figure 2) and a comparison to the Shergotty and Zagami melting experiments of Stolper and McSween [4] are given below (Figure 1). It does not appear possible to derive bulk Shergotty or Zagami by either equilibrium or fractional crystallization of Eg. However, if Shergotty and Zagami are cumulates, it may be possible to derive the inferred interstitial liquid [4] from a composition such as Eg.

References: [1] Jones (1989) *Proc. Lunar Planet. Sci. Conf. 19th.*, pp. 465-474. [2] Longhi and Pan (1989) *Proc. Lunar Planet. Sci. Conf. 19th.*, pp. 451-464. [3] Longhi (1991) pers. comm. [4] Stolper and McSween (1979) *Geochim. Cosmochim. Acta* **43**, 1475-1498.

Figure 1

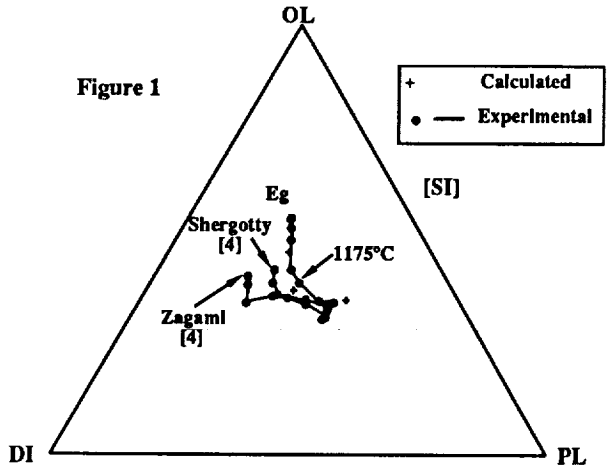

Figure 2

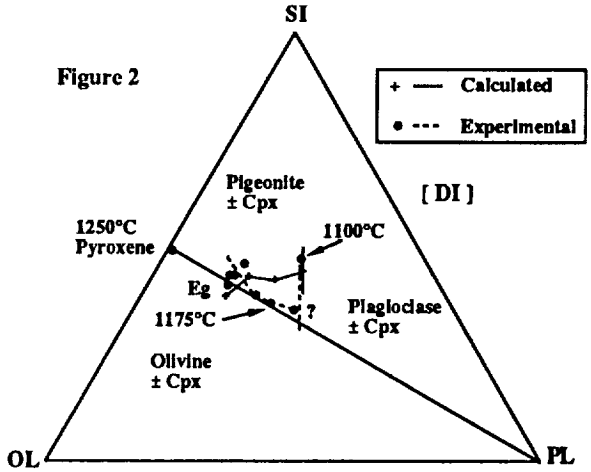

EFFECT OF METAMORPHISM ON ISOLATED OLIVINE GRAINS IN CO3 CHONDRITES. Rhian H. Jones, Institute of Meteoritics, Department of Geology, University of New Mexico, Albuquerque, NM 87131, USA.

A sequence of increasing degree of metamorphism has been described in the CO3 chondrite group [1,2]. Studies of changes in properties of chondrule silicates and bulk matrix have shown that thermal metamorphism *in situ*, after accretion, is the most likely environment for metamorphism [2,3]. The effects of metamorphism on isolated olivine grains in these chondrites have not been discussed previously. If metamorphism occurred *in situ*, isolated olivine grains should have participated in equilibration of the chondrite, and some of their properties should be attributable to metamorphism. In order to determine the effects of metamorphism I have examined minor element compositional variations and zoning profiles in isolated olivine grains and olivines from chondrules in Lancé and Isna (subtypes 3.4 and 3.7 respectively). These grains may be compared with their counterparts in ALH A77307 (subtype 3.0) in which no effects of metamorphism are observed [4].

Three types of isolated olivines are observed in ALH A77307: (a) forsteritic, (b) fayalite-rich and (c) "complex" olivine grains with forsteritic cores and fayalite-rich rims [4]. All three types have counterparts in chondrules, and textural and compositional evidence strongly suggests that they are derived from chondrules by fragmentation. In Lancé and Isna three distinct types have also been identified: (a) grains showing strong Fe/Mg zoning from core to rim, (b) Fa-rich grains with relatively limited Fe/Mg zoning and (c) grains with strong Fe/Mg zoning similar to (a), with a wider Fa-rich zone on one or more edges. These three types are very similar in composition and zoning characteristics to (a) olivine grains in type I chondrules, (b) type II chondrules and (c) relict grains in type II chondrules respectively in each chondrite. This evidence strongly suggests that they are the metamorphosed counterparts of (a)-(c) in ALH A77307, with Fe diffusing from matrix into isolated grains during metamorphism. Complex grains in ALH A77307 (c) and strongly zoned isolated grains in Isna (a), are apparently very similar in BSEI, both having Fo-rich cores and Fa-rich rims. However, detailed zoning profiles show that the properties of the core/rim interface and minor element characteristics in both are distinct. The different processes responsible for formation of these fayalite-rich rims (igneous and metamorphic processes, respectively) may therefore be readily identified.

Minor element compositions of isolated grains show identical ranges to those of corresponding chondrule olivines. The sequence from ALH A77307 to Lancé to Isna shows the following effects. For type I chondrules and isolated forsterite grains, FeO contents increase, FeO and MnO become very strongly correlated, Cr_2O_3 shows a pronounced decrease and CaO, Al_2O_3 and TiO_2 are virtually unchanged. For type II chondrules and isolated fayalites, FeO and MnO become increasingly homogeneous, CaO and Cr_2O_3 decrease significantly, and Al_2O_3 and TiO_2 are virtually unchanged. The difference in behaviour of Ca between the two groups of olivines suggests that the diffusion rate of Ca is strongly dependent on Fa content, and increases with increasing Fa [5]. The decrease in Cr_2O_3 content of all olivines with increasing degree of metamorphism is consistent with an increase in the bulk Cr_2O_3 content of matrix with petrologic subtype in the CO3 group [1,2].

Observed changes in major and minor element compositions of isolated olivines are consistent with the hypothesis that isolated grains participated in equilibration of the various chondrite components. Changes in composition in isolated grains are very similar to those in chondrule olivines, and progressive changes are observed in all olivines with increasing petrologic subtype. This is additional evidence for metamorphism *in situ*, and equilibration of subtype 3.0-like material to form higher petrologic subtypes.

References: [1] McSween HYJr (1977) GCA 41, 477-491 [2] Scott ERD and Jones RH (1990) GCA 54, 2485-2502 [3] Jones RH and Rubie DC (1990) LPSC XXI, 583-584 [4] Jones RH (1991) LPSC XXII, 659-660 [5] Morioka M (1981) GCA 45, 1573-1580.

RAMAN SCATTERING AND LASER-INDUCED LUMINESCENCE FROM MICRO DIAMONDS IN UREILITES; H. Kagi[1], K. Takahashi[2] and A. Masuda[1]
1) Department of Chemistry, Faculty of Science, University of Tokyo, Hongo, Bunkyo-ku, Tokyo 113, Japan. 2) Earth Science Laboratory, Institute of Physical and Chemical Research (RIKEN), Hirosawa, Wako-shi, Saitama 351-01, Japan.

Optical property of diamond particles found in ureilites was investigated by means of microprobe photoluminescence and Raman measurement. The ureilites studied here were Allan Hills (ALH)-77257, Yamato (Y)-791538 and Novo Urei. Y-791538 was chemically decomposed with HCl and HF at room temperature. ALH-77257 and Novo Urei were transferred to RAMANOR U-1000 as the polished thin section. Furthermore, a natural irradiated diamond aggregate, carbonado, was investigated for evaluating temperature dependence of the photoluminescence.

Raman spectra and incidental photoluminescence spectra of the diamond particle collected from Y-791538 are shown in Fig. 1. Sharp lines at 552 nm observed in all spectra derive from Raman active lattice vibration excited by the incident 514.5 nm green laser light. On the other hand, profiles of photoluminescence band at 585 nm differ from each other within a small (10 mg) chip of the sample, which implies that the diamond particles collected from a small portion of ureilite reflect the wide range of their formation condition.

On the analogy of heating experiment on carbonado (see Fig. 2), the maximum temperature which the meteoritical diamonds have suffered can be estimated to be not lower than 500 °C. The optical property can give a new clue to the thermal history of diamonds in ureilites independently of the surrounding silicate minerals.

Reference:

Kagi, H., Takahashi K. and Masuda, A.: Naturwissenschaften, 77, 531-532, 1990.

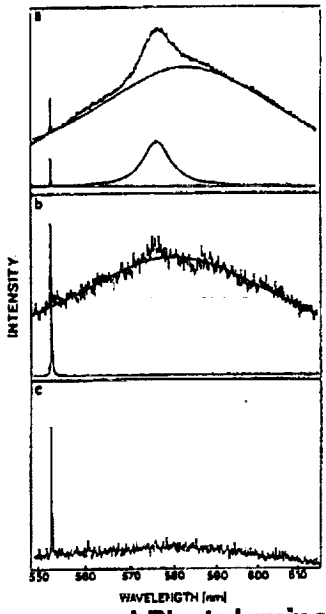

Fig.1 Raman and Photoluminescence spectra of diamonds in Y-791538

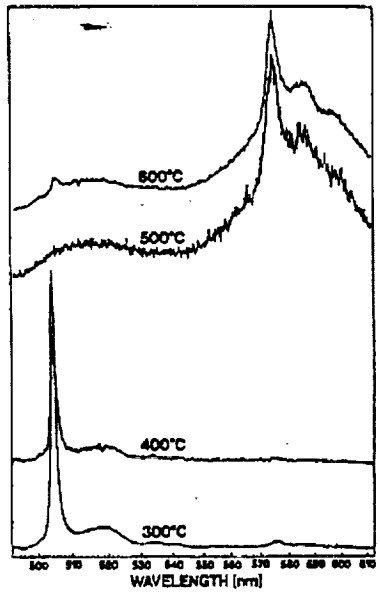

Fig.2 Photoluminescence spectra of the heated carbonado

COMPOSITIONAL STUDIES OF ANTARCTIC CARBONACEOUS CHONDRITES POSSIBLY RELATED TO AL RAIS AND RENAZZO; G.W. Kallemeyn, Institute of Geophysics and Planetary Physics, University of California, Los Angeles, CA 90024, USA.

Several carbonaceous chondrites from Antarctica are noted as texturally similar to Renazzo and Al Rais. These include Elephant Moraine 87747, 87770 and 87847, MacAlpine Hills 87320, and Yamato 793495. Multielement compositional analyses by instrumental neutron activation analysis can be used to help determine any strong relationships with either the Al Rais or Renazzo chondrites. These analyses are complete for MAC87320 and Y793495, while analyses of the other chondrites are still underway. Two other carbonaceous chondrites (MacAlpine Hills 87300 and 87301) listed as texturally similar to CM chondrites may also be related, and are also undergoing INAA analyses to help elucidate the situation.

Although Al Rais and Renazzo may be members of the same compositional 'clan' (similar refractory abundances), Renazzo has distinctly lower volatile abundances (≤CV chondrites) than Al Rais (mid CM-CV range), thus precluding their being members of the same compositional group. CI-normalized refractory (Al, Sc, Ca, REE, V) and common nonvolatile (Mg) lithophile abundances in Y793495 are very similar to those of Al Rais and Renazzo, close to CI levels. MAC87320 seems to have slightly higher refractory lithophile element abundances, especially Ca and Sc, than either Renazzo or Y793495. Refractory siderophile (Os, Ir, Ru) and common nonvolatile siderophile (Fe, Ni) abundances in Y793495 are also similar to both Al Rais and Renazzo.

Yamato 793495, like Renazzo, is relatively volatile-poor compared to Al Rais. With the exception of an anomalously high As abundance in Renazzo and a low Na abundance and high Br abundance in Y793495, the lithophile and nonlithophile volatile element abundances are quite similar in the two chondrites. Volatile element abundances, especially Se and Zn, are somewhat lower in MAC87320 than the other chondrites. The Na and Br anomalies could be explained by the mobility of those elements and may be affected by terrestrial weathering processes.

A very useful method for distinguishing between all known chondrite groups is a comparison of Zn/Mn and Al/Mn atom ratios. On such a plot MAC87320, Renazzo and Y793495 group together closest to the CO chondrites (to which they have no petrographic similarity) and are quite distinct from the CM and CV chondrites. Al Rais plots close to the CM group.

Preliminary data of two other carbonaceous chondrites currently being analyzed, MAC87300 and MAC87301, appear to be compositionally unlike CM chondrites, but possibly similar to Renazzo. It is also hoped that complete analyses of EET87747, EET87770, EET87847, MAC87300 and MAC87301 will be available by meeting time.

Extraterrestrial water of possible Martian origin in SNC meteorites: Constraints from oxygen isotopes. H. R. Karlsson[1], R. N. Clayton[2], E. K. Gibson[1], T. K. Mayeda[2] and R. A. Socki[1,3]. [1]SN2, NASA/JSC, Houston, TX 77058, [2]EFI, Univ. of Chicago, Chicago, Il. 60637, [3]LESC, Houston, TX 77058, all USA.

Many lines of evidence suggest that the "SNC" group of meteorites (Shergotty-Nakhla-Chassigny) are derived from the planet Mars (1). Because SNC meteorites have water, they may contain information on the origin and fate of water on the planet Mars.

Previous stable isotopic studies of SNC water have concentrated on measuring the D/H ratios using either combustion or pyrolysis techniques. The results are conflicting and none thus far demonstrates conclusively whether the water is extraterrestrial (2, 3, 4).

We present the first measurements of $\delta^{18}O$ and $\delta^{17}O$ of water extracted from SNC's. After overnight room temperature evacuation, powdered samples of Chassigny (2.0 g), Lafayette (3.0 g), Nakhla (2.1 g) and Zagami (2.9 g) were heated under high vacuum and the volatiles evolved were condensed into a cold-trap at liquid nitrogen temperatures. Each sample was heated step-wise to 150°C, 350°C, 600°C and 1000°C, and held at those temperatures for 1hr. Water was then cryogenically separated from other volatiles by raising the cold-trap temperature to that of dry ice. Water was converted to O_2 using BrF_5 and isotopically measured on a double collecting ratio mass spectrometer. Yields (wt%) were: Chas., 0.102; Laf., 0.387; Nak., 0.114; Zag., 0.042.

Clayton and Mayeda (5) have shown that SNC whole rocks lie on a mass fractionation line parallel to the terrestrial line on a three isotope plot, with an average $\Delta^{17}O$ excess ($\Delta^{17}O = \delta^{17}O - 0.52\delta^{18}O$) of +0.3‰ relative to Earth. Our ability to resolve samples from the terrestrial line is at the ± 0.1‰ level (2σ). The water analyses are displayed in Figs. 1-3, where each meteorite is designated by its initial letter. Fig. 1 shows the isotopic composition of the SNC waters relative to the SNC whole rocks (WR) and the terrestrial line. It is clear that the waters as a whole cover a much wider range than the bulk rocks, and that there is a wide variation within waters from individual meteorites. Fig. 2 shows the ^{17}O excess of the SNC water as a function of pyrolysis temperature. Waters entirely of origin on the SNC parent body should have $\Delta^{17}O$ the same as the rocks (dotted line); water of partial terrestrial origin should have $\Delta^{17}O$ between zero and the whole-rock value. In every case the $\Delta^{17}O$ increases with increasing temperature, and is equal to or greater than the whole-rock value for all extractions at ≥ 600°C, implying only a minor terrestrial component in these fractions.

Fig. 3 displays the $\delta^{18}O$ values of the waters as a function of pyrolysis temperature for the four SNC meteorites. Except in the case of Lafayette (find), which probably has a major terrestrial component, similar downward trends are observed. These variations have some interesting implications. One might expect that the highest temperature water would have values close to that of bulk rock (~+5‰) which is not the case for Chassigny, Zagami, and Nakhla (falls). A possible explanation is that the low $\delta^{18}O$ water in Chassigny and Zagami represents samples of trapped Martian atmosphere.

References: (1) Laul J.C. (1986) GCA **50**, 875. (2) Fallick A.E. et al. (1983) LPSC XIV, 183. (3) Kerridge, J.F. (1988) LPSC XIX, 599. (4) Watson et al. (1991) LPSC XXII, 1473. (5) Clayton, R. N. and Mayeda T. K. (1983) EPSL **62**, 1.

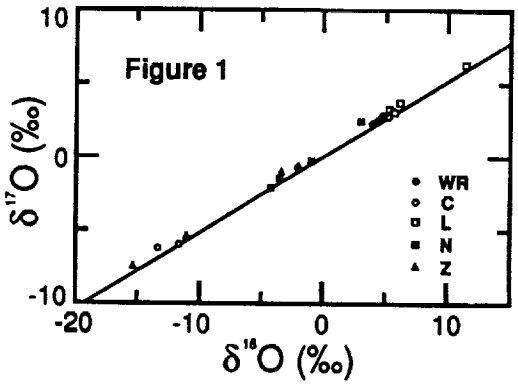

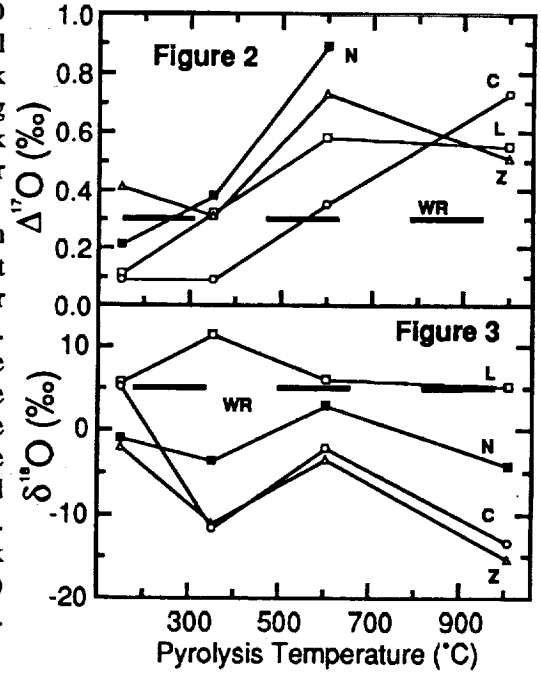

N92-12918

THE ORIGIN OF AMORPHOUS RIMS ON LUNAR PLAGIOCLASE GRAINS: SOLAR WIND DAMAGE OR VAPOR CONDENSATES?

Lindsay P. Keller and David S. McKay, SN14, NASA-Johnson Space Center, Houston TX 77058.

Introduction. A distinctive feature of μm-sized plagioclase grains from mature lunar soils is a thin (20- to 100-nm) amorphous rim surrounding the grains. These rims were originally described from high voltage electron microscope observations of lunar plagioclase grains by Dran *et al.* [1], who observed rims up to 100 nm thick on plagioclase grains from Apollo 11 and Apollo 12 soils. These rims are believed to be the product of solar wind damage [*e.g.*, 2, 3].

We studied the amorphous rims on μm-sized plagioclase grains from a mature Apollo 16 soil using a JEOL 2000FX transmission electron microscope (TEM) equiped with an energy-dispersive x-ray spectrometer. We found that the amorphous rims are compositionally distinct from the the interior plagioclase and propose that a major component of vapor condensates is present in the rims.

Experimental. We prepared TEM specimens by diamond knife ultramicrotomy of the <20 μm fraction of Apollo 16 sample 61181. The density of solar flare tracks was determined by counting the number of tracks present in 100 nm^2 areas of similar contrast in dark field TEM images and extrapolating upwards to cm^2 areas. Quantitative energy-dispersive x-ray spectroscopy (EDS) analyses were obtained using a probe ~20 nm in diameter, and a detector live time of 400 s. The accuracy for routine analyses of major elements is ~10% relative based on counting statistics and the errors associated with the determination of k-factors.

Results. We analyzed a number of μm-sized plagioclase grains with prominent amorphous rims in sample 61181. The rims are variable in thickness, from 20- to 60-nm, and share an abrupt interface with the interior plagioclase. In TEM images, the plagioclase exhibits strain contrast adjacent to the plagioclase-amorphous rim interface. We have not observed any crystalline inclusions in the rims. The interior of the plagioclase grains are characterized by high track densities (~10^{10}) as determined from dark-field TEM images.

A major result of this study is that all of the amorphous rims that we analyzed are compositionally distinct from the interior plagioclase. EDS analyses show that the rims are Si- and Fe-rich as compared to the plagioclase (Table 1). The ratio of Ca/Al in the rims is significantly different from that in the bulk plagioclase.

Discussion. The origin of amorphous rims is controversial, and two opposing models have been proposed for their formation. In the first hypothesis, originally proposed by [1] and subsequently developed by others [2, 3], it was suggested that amorphous rims are a product of solar wind damage, whereas the second hypothesis holds that the rims represent deposits of impact-generated vapor that condensed on nearby grains [*e.g.*, 4]. The latter hypothesis was disputed by [2,3] who showed that rims could be produced by exposing fresh material to a high flux of low-energy ions.

A major process affecting materials at the Moon's surface is impact vaporization, inferred from the presence of surface deposited volatiles [5-7] and from the compositions of impact glasses [*e.g.*, 8, 9]. The chemical fractionation that occurs during the vaporization process has been elucidated by experiments on lunar rocks and lunar analogs [e.g. 10, 11]. The vapors are rich in volatile elements, Si, and Fe, and are very poor in refractory elements. The same chemical trend (an enrichment in volatile elements) is observed in the rims. Thus, we believe that the composition of all the amorphous rims that we analyzed is consistent with the condensation of vapor on nearby grains as proposed by [4]. The Si- and Fe-enrichment in the rims is inconsistent with rim formation by sputtered ion deposition, which is a mass-dependent process [12].

Borg *et al* [3] noted that grains with the highest solar flare track densities also had the thickest rims and inferred that these grains had been exposed on the lunar surface for long periods of time. We propose that these grains would also tend to accumulate the greatest build-up of vapor condensates on their surfaces.

TABLE 1. EDS analyses of plagioclase and amorphous rims (average of 3 grains with rims).

	Plag.	Rim
Na2O	1.4	0.9
MgO	0.0	0.8
Al2O3	34.	27.
SiO2	47.	60.
K2O	0.2	0.1
CaO	16.	8.4
TiO2	0.0	0.2
FeO	0.4	2.6
Total:	100.0	100.0

Conclusions. We observed amorphous rims on μm-sized plagioclase grains that are Si- and Fe-rich compared to the interior plagioclase. We propose that rims are formed through a combination of solar wind damage and a significant accumulation of impact-generated vapor deposits.

References. [1] Dran, J. C. *et al.* (1970) *EPSL* 9, 391. [2] Bibring, J. P. *et al.* (1973) *IV LPSC*, 72. [3] Borg, J. *et al.* (1980) *Proc. Conf. Ancient Sun*, 431. [4] Kerridge, J. F. and Kaplan, I. R. (1978) *Proc. 9th LPSC*, 1687. [5] McKay, D. S. *et al.* (1972) III LPSC,529. [6] Walker, R. J. and Papike, J. J. (1981) Proc. 12th LPSC, 421. [7] Devine, J. M. *et al.* (1982) *JGR* 87, A260. [8] Chao, E. C. T. *et al.* (1972) *Proc. 3rd LPSC*, 907. [9] Naney, M. T. *et al* (1976) *Proc. 7th LPSC*, 155. [10] Ivanov, A. V. and Florensky, K. P. (1975) *Proc. 6th LPSC*, 1341. [11] De Maria, G. *et al.* (1971) *Proc. 2nd LPSC*, 1367. [12] Haff, P. K. *et al.* (1977) *Proc. 8th LPSC*, 3807.

N92-12919

TRANSMISSION ELECTRON MICROSCOPY OF AN INTERPLANETARY DUST PARTICLE WITH LINKS TO CI CHONDRITES.

Lindsay. P. Keller[1], Kathie. L. Thomas[2], and David. S. McKay[1]. [1]SN14, NASA-Johnson Space Center, Houston, TX 77058, [2]Lockheed 2400 Nasa Rd. 1, Houston, TX 77058.

Introduction The majority of hydrated interplanetary dust particles (IDPs) have compositions that resemble CI and CM chondrites [1], however, their mineralogies are most similar to the fine-grained material in certain altered type-3 carbonaceous and ordinary chondrites [2,3]. During our transmission electron microscope (TEM) studies of hydrated IDPs, we discovered a unique particle whose mineralogy is very similar to that reported from CI chondrites.

Experimental. W7013F5 is a smooth particle (9 X 14 μm) with a chondritic bulk composition. We prepared microtomed thin sections (<100 nm thick) for study in the TEM. Our sample preparation techniques and TEM procedures (both imaging and analytical) are described elsewhere [2].

Results. The mineralogy of W7013F5 is dominated by phyllosilicates, carbonates, and sulfides. Trace phases include magnetite, kamacite, a Zn-bearing Fe sulfide, and a fibrous mineral with a 0.5 nm layer spacing.

The phyllosilicates exhibit a bimodal size distribution. Coarse-grained phyllosilicates up to 500 nm in length are common and occur in μm-sized clusters. Fine-grained phyllosilicates (typically <10 nm) are intergrown with carbonates and sulfides. High resolution (HRTEM) images show that the coarse phyllosilicates consist of intergrowths of 1- and 0.7-nm layers on the unit cell scale. EDS analyses combined with high-resolution images suggest that the coarse phyllosilicates are Fe-bearing saponite intergrown with Mg-Fe serpentine. The fine-grained phyllosilicates are poorly crystalline and show only 1-nm layer spacings in HRTEM images. Several curled flakes of a fine-grained layered mineral with a 0.5 nm periodicity (brucite?) occur with the coarse phyllosilicates but were too small to quantitatively analyse.

Mg-Fe carbonates are abundant in W7013F5 and occur in two morphologies, rhombohedral crystals up to 400 nm on edge, and rounded aggregates up to 200 nm in diameter. Molar Mg/Mg+Fe ratios in the carbonates range from 0.3 to 1. Ca and Mn occur as minor components. No correlation of carbonate morphology with composition was observed.

Rounded grains of pyrrhotite and pentlandite up to 200 nm in diameter are dispersed throughout the particle and are equally abundant. The maximum Ni content of the pentlandite is 26 wt.%. Rod-shaped grains (in cross-section) of pyrrhotite are also present.

Discussion. The distinctive unit cell scale intergrowth of saponite and serpentine has previously been reported only from the Orgueil CI chondrite [4]. Mg-Fe carbonates are common in CI chondrites and in other hydrated IDPs [5], but are not observed in other chondrite types. The compositions of the phyllosilicates, carbonates, and sulfides in W7013F5 overlap with those in CI chondrites but tend to be more Fe-rich. A major difference between W7013F5 and CI chondrites is the oxidation state recorded by the mineral assemblages. Fe-Ni sulfides and kamacite occur in W7013F5, whereas ferrihydrite (a Fe oxyhydroxide with adsorbed S) and magnetite are the major Fe bearing phases in CI chondrites.

Conclusions. W7013F5 is the first IDP whose mineralogy and chemistry approximates that of CI chondrites. The similarity in mineralogy and mineral chemistry suggests that W7013F5 was altered under conditions similar to those that existed on the CI parent bodies.

References. [1] Schramm, L. S. *et al.* (1990) *Meteoritics* 24, 99. [2] Thomas, K. L. *et al.* (1991) *XXII LPSC*, 1395. [3] Keller, L. P. and Buseck, P. R. (1990) *Geochim. Cosmochim. Acta*, 54, 2113. [4] Tomeoka K. and Buseck, P. R. (1988) *Geochim. Cosmochim. Acta*, 52, 1627. [5] Tomeoka, K. and Buseck, P. R. (1986) *Science*, 231, 1544.

TRACE ELEMENT PARTITIONING WITHIN MESOSIDERITE CLASTS

A.K. Kennedy, B.W. Stewart, I.D. Hutcheon & G.J. Wasserburg, The Lunatic Asylum, Division of Geological and Planetary Sciences, Caltech, Pasadena, CA 91125

Mesosiderites are polymict silicate and metal breccias resulting from magmatic differentiation, brecciation, metal-silicate mixing, and metamorphic recrystallization in early planetary bodies. Petrographic and trace element studies have documented the great diversity of differentiated silicates, with eucritic basalt, gabbroic cumulate and diogenite clasts and trace element disequilibrium between phases [1-4]. Isotopic studies using long-lived systems (U/Pb, Rb/Sr, Sm/Nd and K/Ar) suggest (1) silicate formation within 10^7 yr of the formation of the solar system, (2) mixing of metal and silicates, recrystallization and isotopic homogenization by 4.47AE [4-6] and (3) metamorphism at 3.4-3.8 AE [7]. At present little is known about trace element partitioning within clasts, between matrix and clasts, and the effect of partial re-equilibration of trace elements on isotope systematics [4]. To address this deficit we used the Panurge ion microprobe to measure Ba, Sr, Hf, Ti and Cr and REE concentrations in plag, opx and phosphate in: (1) Vaca Muerta pebbles 5 and 12 [8], and (2) a phosphate-rich (25%) lithic clast, a phosphate-opx corona surrounding troilite, groundmass phosphate, and a plag clast from Patwar. In addition we measured Ba, Hf and the REE in phosphate, plag, cpx and opx from Morristown. Vaca Muerta and Patwar are slightly recrystallized and Morristown is highly recrystallized and pyroxene poikiloblastic [1]. The trace element data reflect the diversity of mesosiderite silicates. Vaca Muerta pebble 5 contains LREE-depleted pyroxene (La 0.3xchondritic (ch); Lu 15xch), LREE-enriched plag (La 3-20xch; Lu 0.05-0.6xch) and phosphate (La 400xch; Lu 95xch). Pebble 12 has much greater depletion of REE, especially the LREE, with plag having a relatively flat REE pattern (La and Yb are 0.02-0.03xch); pyroxene is highly LREE-depleted (La 0.01xch; Lu 4xch). The partitioning of trace elements in both pebbles is similar to igneous partitioning in terrestrial and lunar cumulates. If both pebbles are cumulates, pebble 5 requires a melt with a relatively flat REE pattern and ≈20xch [4] and pebble 12 a LREE-depleted melt with ≈0.04xch La and ≈0.4xch Lu. In contrast to the equilibrium trace element partitioning in the Vaca Muerta pebbles, Patwar and Morristown contain abundant evidence of disequilibrium, with little consistency of REE patterns. Phosphates in the opx-phosphate clast in Patwar are LREE-enriched with a +ve Eu anomaly (La 90xch; Lu 40xch; Eu 130xch). Groundmass and corona phosphates have flat REE patterns (La and Lu 80-110xch) with or without a -ve Eu anomaly. A small plag enclosed by troilite has lower REE abundances (La 0.9xch; Er 0.1xch) than plag clasts (La 6xch; Er 0.4xch) with identical major element compositions. Orthopyroxene is LREE-depleted and the corona opx has 6x lower HREE (Dy 0.01xch; Lu 0.09xch) than the opx in the opx-phosphate clast. Morristown phosphate, cpx and opx are LREE-depleted and have +ve Eu anomalies. Phosphate has La 25xch, Eu 115xch and Lu 130xch, and cpx and opx have La <0.02xch and Lu 0.9-2.5xch. The cpx, opx and phosphate would be in equilibrium with a LREE-depleted melt which has a +ve Eu anomaly. In contrast neither plag clast would be in equilibrium with such a melt. Plagioclase 1 is LREE-enriched and has a large +ve Eu anomaly (fig. 1) and would be in equilibrium with a melt with a flat REE pattern or a slightly LREE-enriched pattern. Plagioclase 2 has an unusual REE pattern (fig. 1), with (1) enrichment of La and Sm relative to Ce, Pr and Nd, (2) the usual large +ve Eu anomaly, (3) a decrease from Gd to Dy, (4) a rapid increase from Dy to Tm, and (5) an overall HREE enrichment. Both plag 1 and 2 have much higher Sm/Nd (0.29-4.9) than plag separates (0.11-0.13) [4], requiring at least two distinct plag components. The presence of unequilibrated components may explain why one Morristown plag separate lies off the best-fit isochron [4] and suggests that variation of initial ϵ_{143} may be responsible for inconsistencies between the ^{147}Sm-^{143}Nd and ^{146}Sm-^{142}Nd isotope chronometers, rather than partial re-equilibration of phosphate and plag [4]. If plag 2 is a relict of the source that melted to produce the mesosiderite silicates, the high Sm/Nd may explain the unsupported initial ϵ_{143} of Morristown [4].

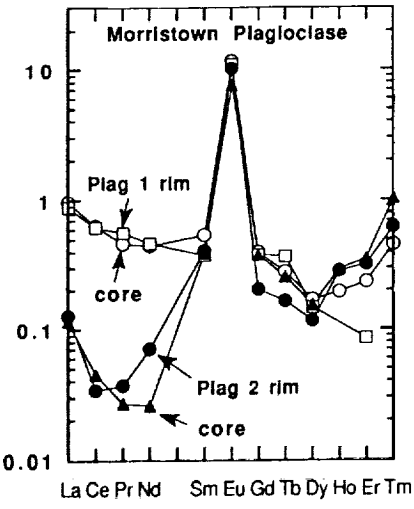

[1] Rubin and Mittlefehldt (1991) preprint; [2] Floran (1978) Proc. LPSC IX, 1053; [3] Mittlefelhdt (1979) GCA 43, 1917; [4] Prinzhofer et al. (1991) submitted GCA; [5] Stewart et al. (1991) LPSC XXII, 1333; [6] Brouxel & Tatsumoto (1991) GCA 55, 1121; [7] Bogard et al. (1990) GCA 54, 2549; [8] Rubin & Jerde (1987) EPSL 84, 1.

INTERSTELLAR PRECURSORS IN SYNTHESIS OF METEORITIC ORGANIC MATTER

J.F.Kerridge, Inst.Geophysics, UCLA, Los Angeles, CA 90024

High D/H ratios measured in meteoritic organic matter are commonly attributed to presence of molecules enriched in D by isotopic fractionation during ion-molecule reactions at low temperatures in interstellar clouds. However, it has not been clear whether the putative interstellar component represents a minor fraction of the present molecular population of the meteorites or whether the meteoritic molecules were synthesised from precursors that included an interstellar component. This issue is still not resolved, but existing evidence favors the latter alternative.

The nature of the precursors that led to formation of the organic acids in carbonaceous meteorites can be constrained by three separate lines of reasoning. First, their aliphatic groups contained H with δD values at least as high as $+2400^{o}/oo$ [1]. Second, those aliphatic groups were apparently derived from aldehyde and/or ketone precursors [2]. Third, the $\delta^{13}C$ values of the aliphatic groups in monocarboxylic acids decrease systematically with increasing C number, and the same phenomenon is observed in light alkanes trapped in the meteorites [3]. These observations lead to the following conclusions.

The light alkanes and aldehydes/ketones apparently shared related, possibly common, origins. Those origins permitted acquisition of substantial D enrichment, presumably generated in an interstellar cloud. Because aldehydes, and presumably ketones, would not have been stable reaction products in a nebula of solar composition [4], interstellar production of both aldehydes (ketones) and alkanes is implied. Formaldehyde is a well-established interstellar molecule; methane cannot be observed directly but is inferred to be present in some molecular clouds [5].

Although the above arguments point towards identification of meteoritic alkanes as interstellar molecules, there are several problems with this scenario. These include the difficulty of preserving such volatile species during the collapse phase of nebula formation, and the fact that their $\delta^{13}C$ values are typical of "normal" solar-system material. However, *ad hoc* arguments can be constructed to deal with these problems, so that the scenario cannot be ruled out on that basis. On the other hand, if the scenario is correct, these "problems" become important constraints on the thermal history of the solar nebula and the distribution of C isotopes in the early solar system, respectively. Furthermore, preservation of interstellar methane for incorporation into primitive solar-system objects could explain the high CH_4/CO ratio inferred for comet Halley [6].

[1] Pizzarello S. *et al.* (1991) Geochem.Cosmochem.Acta 55, 905.
[2] Peltzer E.T. *et al.* (1984) Adv.Space Res. 4, 69.
[3] Yuen G. *et al.* (1984) Nature 307, 252.
[4] Fegley B. & Prinn R. (1989) In: The Formation and Evolution of Planetary Atmospheres, p.171.
[5] Irvine W.M. & Knacke R.F. (1989) In: Origin and Evolution of Planetary and Satellite Atmospheres, p.3.
[6] Weaver H.A. (1989) In: Highlights of Astronomy, p.387.

XENON IN CHONDRITIC METALS; J. S. Kim[1], K. Marti[1], C. Perron[2], and P. Pellas[2], [1]Department of Chemistry, University of California, San Diego, La Jolla, CA 92093-0317. [2]Museum National d'Histoire Naturelle Mineralogie 61, Rue de Buffon, Paris 53, France

We report and discuss argon and xenon isotopic abundances as observed in the stepwise release of noble gases from high-purity metal separates obtained from the chondrites Dhajala (H3.8), Forest Vale (H4), Ste. Marguerite (H4) and Estacado (H6). The purity of most samples was estimated from microscopic inspection of grain surfaces to be > 99.5 %. Chondritic metals contain several types of inclusions and one of these has a composition similar to the fine-grained matrix (1).

We identify Xe isotopic signatures of a ^{244}Pu-derived fission component, both due to in situ decay and due to recoils into the metal, cosmic-ray-produced spallation component, FVM-Xe (2), radiogenic ^{129}Xe and FVC-Xe (3). Chondritic metals also contain small amounts of trapped ^{36}Ar, a spallation Ar component and radiogenic ^{40}Ar, due to inclusions. FVM-Xe is apparently surface-correlated and generally is released at intermediate temperatures. The source is clearly not the solar wind, because of $^{36}Ar/^{132}Xe = \sim 100$ (solar ratio is $\sim 60{,}000$). The FVM-Xe concentrations in the metal depend on the petrologic types. Dhajala (H3.8) contains more FVM-Xe than do the H4 chondrites, and this component was not observed in Estacado (H6). We have monitored the gas release from metal using spallation $^{38}Ar_s$ which is mainly produced by cosmic rays in Fe-Ni. There is no correlation between $^{38}Ar_s$ and FVM-Xe. FVM-Xe cannot be obtained from any of the known solar system reservoirs by either mass dependent fractionation or by the addition of HL-Xe. We have postulated several possible sources: addition of Xe due to ^{248}Cm spontaneous fission or ^{235}U neutron induced fission, or a distinct early solar Xe plus ^{244}Pu fission Xe(2). Using precise solar-type Xe data (4), we evaluate the possible origins of the FVM-Xe isotopic signature. Solar Xe plus $^{235}U_{nf}$-Xe is a viable option which requires an external neutron source.

FVC-type Xe is released during low temperature combustion steps, which is a general characteristic of this component. The finest grain-size fraction of Dhajala (<38μm) reveals large concentrations of FVC-Xe apparently from a C-rich carrier which is still present in the metal. One type of inclusion in the metal must contain iodine, since excesses of radiogenic $^{129}Xe_r$ are clearly resolved. Release patterns of radiogenic $^{129}Xe_r$ are similar to those of spallogenic $^{38}Ar_s$. This may simply indicate the characteristics of diffusion in metal. The amounts of $^{38}Ar_s$ in different grain sizes are agree and this component is released mainly in the melting steps.

References: (1) Perron C., Bourot-Denise M., Pellas P., Marti K., Kim J.S., and Lavielle B. (1989) *Lunar and Planet. Science XX*, 838-839. (2) Marti K., Kim J.S., Lavielle B., Pellas P., and Perron C. (1989) *Z. Naturforsch. 44a*, pp 963-967. (3) Lavielle B. and Marti K. (1988) *Lunar and Planet. Science XIX*, 667-668. (4) Kim J. S. and Marti K. (1991).*Lunar and Planet. Science XXII*, 715-716.

MUONG NONG-TYPE AND SPLASHFORM-TYPE TEKTITES FROM HAINAN, CHINA

Elbert A. King, Dept. Geosciences, Univ. Houston, Houston, TX 77004 and
Christian Koeberl, Inst. Geochemistry, Univ. Vienna, A-1010, Austria

ABSTRACT - A small collection of tektites from Hainan, China, consists of one Muong Nong-type tektite (weight 44 grams) and seven smaller splashform-types. Because of the location from which these tektites were collected, at the extreme northeast edge of the Australasian strewnfield, it may be that a study of the petrography and geochemistry of these specimens could contribute to a better understanding of the parent materials and the location of the source crater for this strewnfield. Tektites with optically apparent layering were first described by LaCroix (1) from western Laos near Muong Nong. New localities were documented by Barnes (2) who also published detailed petrographic work (3,4) as did Futrell and Fredriksson (5). Muong Nong-type tektites have now been reported from Thailand, Laos, Cambodia, Vietnam and China within the Australasian strewnfield. In all southeast Asian localities reported to date, the Muong Nong-type tektites tend to be considerably larger than the associated splashform-types. Two Muong Nong-type tektites recently displayed in a shop in Bangkok weigh more than 24 kilograms each (6).

Light and dark schlieren are readily visible in sections of the Muong Nong-type specimen (HMN-1). The dark schlieren contain numerous spherical bubbles ranging in size from a fraction of a micron to more than half a millimeter in diameter. Thicknesses of the schlieren range from a few millimeters to only a few microns and the contacts between the light and dark schlieren are quite sharp. Electron microprobe analyses of the light and dark schlieren show substantial major element differences in composition (Table 1).

Table 1. Comparison of average major element compositions of light and dark glass schlieren in Hainan Muong Nong-Type tektite (HMN-1) with glass in ordinary splashform tektites (HSF-1, HSF-2). All values in weight percent. Electron microprobe analyses by Anne McGuire.

	HMN-1 (a) (light glass)	HMN-1 (b) (dark glass)	(c) HSF-1	(c) HSF-2
SiO2	67.38	77.69	76.09	75.54
TiO2	0.83	0.65	0.70	0.70
Al2O3	16.20	10.62	11.18	11.53
FeO*	5.65	3.77	4.01	4.06
MgO	2.65	1.52	1.62	1.66
CaO	3.05	1.63	1.62	1.76
Na2O	1.05	0.81	1.09	1.13
K2O	2.30	2.53	2.37	2.46
Totals	99.11	99.22	98.68	98.84

(a) Average of seven analyses.
(b) Average of eight analyses.
(c) Average of five analyses.
(*) Total iron as FeO.

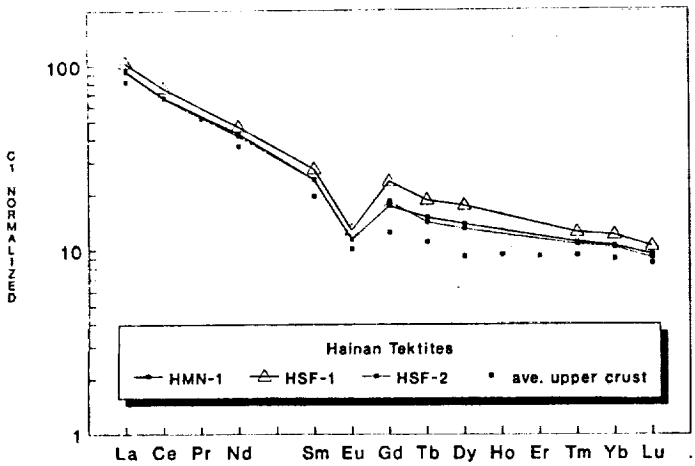

It is interesting to note that the dark schlieren are the relatively silica-rich glass, an observation that was previously reported by Futrell and Fredriksson (5). Trace element analyses by neutron activation analysis shows only small differences between the Muong Nong-type tektite and the normal splashform specimens. This is illustrated by the plot of rare earth elements (Fig. 1, at bottom left).

Refs.: (1) LaCroix, A (1935) Compt. Rend. Acad. Sci.Paris 200, 2129; (2) Barnes, V. E. (1963) in Tektites, O'Keefe, Ed., Chicago 25;(3) Barnes, V. E. (1964) GCA 28, 1267; (4) Barnes, V. E. (1971) Chem. Erde 30, 13; (5) Futrell, D. & Fredriksson, K. (1983) Meteoritics 18,15; (6) King, L. M. (1990) pers. communication.

^{41}Ca IN THE JILIN (H5) CHONDRITE: A MATTER OF SIZE. J. Klein, Fink D., Middleton R.[1], Vogt S., Herzog G.F.[2] 1)Dept. Physics, Univ. of Pennsylvania, Philadelphia PA 19104 USA. 2) Dept. Chem., Rutgers Univ., New Brunswick, NJ 08903 USA.

The size of Jilin is exceptional for a stone, making it particularly useful for studying the systematics of shorter-lived cosmic-ray-produced nuclides. It has been estimated that its pre-atmospheric radius was 85 cm [1,2], and that it had a two-stage irradiation history: the first stage at the surface of a parent body (2π irradiation) lasting 10 Ma; the second as a nearly spherical body in space (4π), lasting ~0.4 Ma.

^{41}Ca has a saturation value in the iron phase of meteorites of ~24 dpm/kg-Fe where it is produced by spallation initiated by high-energy protons. Like that of ^{36}Cl [3], the production rate of ^{41}Ca changes only slowly with depth [4]. In the stone phase, ^{41}Ca is produced by thermal neutrons through the reaction, ^{40}Ca(n,γ)^{41}Ca. The saturation value is expected to be ~2000 dpm/kg-Ca based on measured values in the long-core from Apollo 15 [5], but is affected by the attenuation of the thermal-neutron flux by other elements with large thermal-neutron cross sections. Using accelerator mass spectrometry [6], we measured the ^{41}Ca in metallic and stone separates in four samples of Jilin (see Figure 1). As expected, ^{41}Ca in the stone phase (after correcting for the fraction produced by spallation in the non-metallic iron) is well correlated with ^{60}Co produced in the iron phase—both are produced predominantly by thermal neutrons.

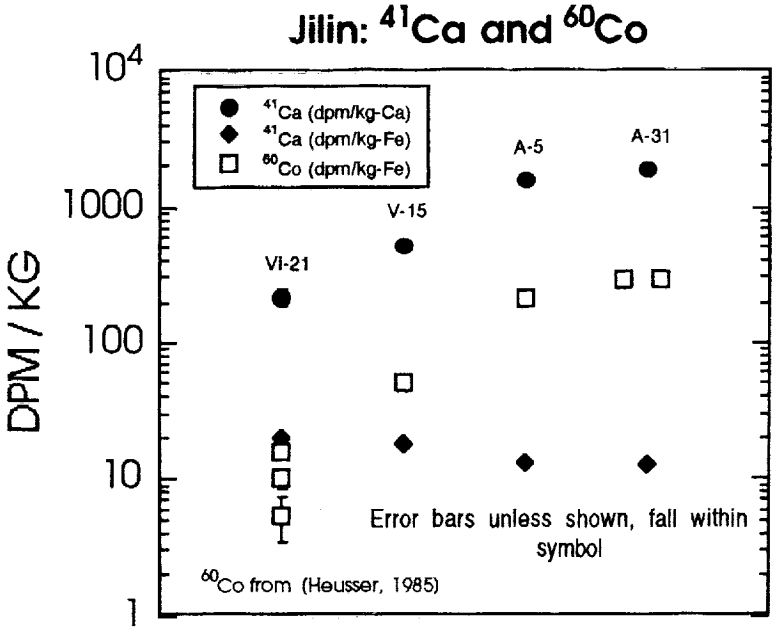

Figure 1. ^{41}Ca in metallic and stone phases, ^{60}Co in iron phase in Jilin.

Coupled with noble gases or other cosmogenic nuclides sensitive to shielding, ^{41}Ca can be used to determine the pre-atmospheric sizes of meteorites, in much the same way the ^{60}Co is now used. ^{41}Ca has an advantage: its long halflife (103±7 ka) [7] means that it can be used on finds as well as falls.

We can use the profiles of ^{59}Ni in meteorites of different radii reported in Spergel [8], to calculate ^{41}Ca concentrations as a function of radius if we scale the concentrations of ^{59}Ni by the relative production cross sections to produce ^{41}Ca. Doing this, we obtain lower and upper limits for the size of Jilin of 54 cm and 135 cm assuming a density of 3.7 g/cm^2.

References: 1) Heusser G., *et al.* (1985) *Earth Planet. Sci. Lett.* **72**, 263-272. 2) Pellas, P. and Bourot-Denise,M. (1985) *Earth Planet. Sci. Lett* **72**, 286-298. 3) Nishiizumi K., *et al.* (1989) *Earth Planet. Sci. Lett.* **93**, 299-313. 4) Fink D., *et al.* (1989) *Meteoritics* **24**, 266. 5) Nishiizumi K., *et al.* (1990) *Abs. Lunar and Planet. Sci.* **XXI**, 893-894. 6) Fink D., *et al.* (1990) *Nucl. Instr. Meth.* **B47**, 79-96. 7) Klein J., *et al.* (1991) *Earth Planet. Sci. Lett.* **103**, 79-83. 8) Spergel M. S., et al. (1986) Proc. Sixteenth Lunar and Planet. Sci. Conf., J. of Geophys. Res. **91**, D483-D494.

BEAVERHEAD IMPACT STRUCTURE, MONTANA: GEOCHEMISTRY OF IMPACTITES AND COUNTRY ROCK SAMPLES. *Christian Koeberl*[1] *and Peter S. Fiske*[2]. [1]Institute of Geochemistry, University of Vienna, Dr.-Karl-Lueger-Ring 1, A-1010 Vienna, Austria; [2]Dept. of Geology, Stanford University, Stanford, CA 94305-2115, USA.

Introduction. The Beaverhead impact structure is a newly discovered impact feature in Montana. The structure was identified by the presence of shatter cones in outcrops of Proterozoic sandstones of the Belt Supergroup in and northwest of Island Butte in Beaverhead County, southwestern Montana [1]. The geology of the area is complicated and involves Precambrian gneisses, Belt sandstones, Paleozoic carbonate and clastic sedimentary rocks, Cretaceous-Tertiary extrusive rocks, Paleocene sediments, Pleistocene glacial deposits, and Quaternary gravel and alluvium. The shatter cones point steeply upward and are abundant in sandstones of the Belt Supergroup, covering an area of about >100 km^2. The absence of shatter cones in younger sedimentary units suggest a late Precambrian-early Paleozoic age for the impact structure. No distinct surface expression of the crater has remained, which requires detailed geological and petrological studies to determine the size and structure of the feature.

Samples and Methods. We have studied the chemical composition of a series of deformed and crushed sandstones from the Belt Supergroup which show a fluidal texture. Several slabs of sandstones with veins that closely resemble melt flows have been selected for major and trace element analysis. In addition, a sample of a shatter cone was analyzed. For the vein-sandstone associations, chips of the vein material, the vein-sandstone boundary (which often shows different colors), and the adjacent sandstone were broken off the original slab. Major element analyses were done on larger bulk samples by XRF, trace element analyses on individual chips and powders by neutron activation analysis.

Results and Conclusions. The vein material is situated in brecciated sandstone and has a greenish color and shows a structure similar to melts and has a cryptocrystaline matrix. Some veins contain small clasts of (deformed) sandstone. Shock features and planar lamellae have been found in minerals from such clasts. The major element composition of the sandstone is relatively uniform. The trace element composition shows some interesting variations between the vein material and the adjacent sandstone. For example, a vein/sandstone pair from sample PF90-BH1b shows the following trends: Compared to the sandstone, the vein sample is depleted in Na by a factor of about 5, but enriched in, e.g., K, Sc, Fe, Co, As, Se, Sb, Rb, Cs, the REEs, Th, and U. Almost the same pattern was found for a second pair of samples from the same rock, but for a vein/sandstone pair from another sample, PF90-BH1d, no such characteristic enrichments or depletions are found. A clast within a vein of sample IB-89-8c shows also high K, Sc, Fe, Co, REE, etc., and lower Na than the surrounding vein and sandstone. The enrichment in K, Rb, and (to a lesser extent) Cs, and the depletion in Na, as well as slight differences in the REE patterns, are a strong indication for extensive weathering and hydrothermal alteration. Similar observations have been made for impactites from the Rochechouart impact structure [2]. We interpret the veins as previous impact melts that have been injected into the basement sandstone and were later subjected to extensive (impact-induced?) hydrothermal alterations and weathering.

References: [1] R.B. Hargraves, C.E. Cullicott, K.S. Deffeyes, S. Hougen, P.P. Cristiansen, and P.S. Fiske (1990) Geology **18**, 832-834. [2] P. Lambert (1982) Geol. Soc. Am. Spec. Paper 190, 57-68.

THERE ARE TOO MANY KINDS OF MAFIC IMPACT MELT BRECCIAS AT APOLLO 16 FOR THEM ALL TO BE BASIN PRODUCTS

Randy L. Korotev, Department of Earth and Planetary Sciences and the McDonnell Center for the Space Sciences, Washington University, St. Louis, MO 63130

The most mafic, common rock type acquired from the Apollo 16 mission to the Central Highlands of the Moon were crystalline impact melt breccias with noritic compositions such as samples 60315 and 65015. Rocks of very similar composition were found at most Apollo sites. NIMBs (noritic impact melt breccias, alias "LKFM") are usually thought to be melt produced during very large impacts, probably basin-forming events [1-3]. Although the Apollo 16 NIMBs are usually regarded as a compositional "group," compositional scatter among different samples is large compared to that of the DB melt (melt phases from dimict breccias, e.g., sample 61015), thus some have argued that they cannot all derive from a single impact event [4,5]. However, others have suggested that they represent a single melt sheet [6], possibly that of Imbrium [2].

New data for a large number of melt breccias show that *intrasample* variation is larger for Apollo 16 NIMBs than it is for the DB melt, thus the large *intersample* variation of the NIMBs itself does not eliminate the possibility that they are all the product of a single impact. However, two compositionally distinct subgroups can be recognized on the basis of several geochemical parameters, suggesting at least two melting events. The 60315 group (includes also 60526, 63558, 64816, and 69945) has higher concentrations of Mg and Cr, alkali elements (Na, Cs, Rb), and siderophile elements (Ni, Co, Ir, Au), and lower concentrations of Al and Ca compared to the 65015 group (includes also 60525, 61247, 62235, 64575, 65357, 65358, 65778, 65905). The 60315 group may also have a lower Ir/Au ratio (80% confidence level, based on samples with >10 ng/g Au), supporting the suspicion that 60315 represents a different "ancient meteorite group" (1LL) than that represented by 65015 (1H) [3].

It is unlikely that the Apollo 16 NIMBs are products of basin formation. The compositional dichotomy implies two impacts. The DB melt, which is only slightly more feldspathic, represents a third melt group. A fourth mafic melt group is represented by several samples from North Ray Crater and possibly samples 62245 and 64515. Three compositionally unique ('ungrouped') mafic samples (61568, 64815, 68525) may each represent separate impacts of large objects. All of these samples share the characteristic of having higher siderophile-element concentrations (2-5X) and generally lower Ir/Au ratios than similarly mafic melt breccias from other Apollo sites. They probably formed from impact into the Central Highlands of several large, metal-rich meteorites [7].

References

[1] Taylor G. J. *et al.* (1991) Lunar rocks. Chapter 6 in *Lunar Sourcebook* (G. H. Heiken, D. T. Vaniman, and B. M. French, eds.), pp. 183-284. Cambridge Univ. Press, Cambridge.
[2] Spudis P. D. (1984) *Proc. Lunar Planet. Sci. Conf. 15th*, pp. C95-C107.
[3] Hertogen *et al.* (1977) *Proc. Lunar Sci. Conf. 8th*, pp. 17-45.
[4] McKinley J. P. *et al.* (1984) *Proc. Lunar Planet. Sci. Conf. 14th*, pp. B513-B524.
[5] Ryder G. and Seymour R. (1982) Abstract in *Lunar and Planetary Science XIII*, pp. 673-674.
[6] Floran R. J. *et al.* (1976) Abstract in *Lunar and Planetary Science VII*, pp. 263-265.
[7] Korotev (1987) *Proc. Lunar Sci. Conf. 17th*, pp. E491-E512.

MICRODISTRIBUTION OF CHROMIUM IN METAL AND SULFIDE OF IAB SILICATE INCLUSIONS AND WINONAITES. ***Alfred Kracher***, Geological Sciences, Iowa State University, Ames, IA 50011-3212.

At oxygen fugacities characteristic of IAB silicate inclusions and winonaites, the partitioning of Cr between oxidized (mostly Cr^{3+}) and reduced states is a strong function of temperature [1]. The microdistribution of Cr may therefore contain information about the genetic history of these meteorites.

In IAB silicate inclusions, the main carrier of Cr^{3+} is chromian diopside and, in some meteorites, chromite. Reduced Cr occurs mostly in troilite; sometimes daubréelite is also present [2]. Where chromite is absent, a fictive "chromite activity" can be estimated from the Cr_2O_3 content of chromian diopside. The latter ranges from 0.38 to 1.27% in different IAB meteorites, the higher values corresponding to chromite-bearing samples. Chromium contents of troilite vary between 500 and 6000 ppm.

Texturally the distribution of metal and sulfide within IAB silicate inclusions varies. Some inclusions, e.g., Four Corners, are transsected by veins that are either all sulfide or all metal. Other silicates, e.g., in Udei Station, contain abundant small metal inclusions where metal and sulfide coexist. The metal:sulfide ratio suggests that they may be derived from isolated pockets of eutectic. This is reminiscent of winonaites such as Acapulco and Allan Hills A77081. From the limited amount of material studied so far it is not certain whether different inclusion textures occur in the same meteorite, or whether each meteorite has its own peculiar inclusion texture.

High-sensitivity microprobe analyses reveal minor variations in the Cr content of sulfide within a given silicate inclusion. However, none of the IAB inclusions studied so far shows the pronounced heterogeneity in Cr contents previously found in A77081 [1]. The Cr content of isolated metal grains in IAB silicates is usually <100 ppm. This is also different from A77081, where some metal grains contain up to 900 ppm Cr. A metal concentrate from Acapulco was reported to contain about 1000 ppm Cr [3].

In IAB silicates, the excess of metal and sulfide may have effectively buffered the activity of reduced Cr, erasing some of the genetic evidence. In addition, subtle differences in thermal history may be responsible for the somewhat different microdostribution of Cr in IAB inclusions on the one hand, and Acapulco and A77081 on the other.

---

[1] Kracher A. (1987) *Meteoritics 22*, 431. [2] Bunch et al. (1970) *Contrib. Mineral. Petrol. 25*, 297. [3] Palme et al. (1981) *Geochim. Cosmochim. Acta 45*, 727.

PETROLOGIC DESCRIPTION OF EAGLES NEST: A NEW OLIVINE ACHONDRITE

-- D.A. Kring†, W.V. Boynton†, D.H. Hill†, and R.A. Haag‡ -- †The Lunar and Planetary Laboratory, University of Arizona, Tucson, AZ 85721 USA, ‡P.O. Box 27527, Tucson, AZ 85726 USA.

Eagles Nest is an oriented meteorite with a complete fusion crust. The 154 g mass has a sienna-colored, coarsely-crystalline interior, and is moderately friable. It is dominated by cumulate olivine (Mg/(Mg+Fe) = 0.68) without significant Fe-Mg or minor-element zoning. Individual olivine crystals contain inclusions of Cr-spinel, a Ca-phosphate, and sulfides, but apparently lack melt inclusions. Cr-spinel (Cr/(Cr+Al) = 0.82, Mg/(Mg+Fe) = 0.18) and sulfides also occur interstitially between olivine crystals. Eagles Nest contains a limited amount of equilibrated high-Ca pyroxene ($Wo_{45}En_{45}Fs_{10}$) which sometimes encloses small grains of olivine. Low-Ca pyroxene and plagioclase were not observed. The textures suggest that olivine and Cr-spinel crystallized first, followed by the coprecipitation of these phases with high-Ca pyroxene.

Olivine crystals are generally subequant, form triple junctions, and are up to 1.5 mm in length. Pyroxene, Cr-spinel, sulfide, and Ca-phosphate crystals have maximum dimensions of 1.5, 0.5, 0.3, and 0.5 mm, respectively. Olivine and pyroxene crystals are crosscut with a network of Fe-rich veins, <10 μm wide, which seem to be related to the very small amount of intercumulus material which occupies zones that are <50 μm wide. A single fracture, ≤ 1 mm wide, contains loosely-packed grains of quartz and orthoclase which may represent terrestrial contamination.

Other olivine achondrites with which Eagles Nest might be related include Chassigny, Brachina, and ALH84025 [*e.g.*, 1, 2, 3]. The olivine in all four of these achondrites have moderately high concentrations of MnO (0.42 to 0.60 wt. % in Eagles Nest), but at the same time, have high Fe/Mn ratios (50 to 70 in Eagles Nest). However, Eagles Nest and ALH84025 do not contain plagioclase and are thus mineralogically unlike Chassigny and Brachina. Other similarities between Eagles Nest and ALH84025 include their textures and the major element compositions of olivine, high-Ca pyroxene, and Cr-spinel in them. In addition, the olivine in Eagles Nest has abundances of Cr_2O_3 and CaO (0.01 to 0.06 and 0.06 to 0.13 wt. %, respectively) which are comparable to those in ALH84025. Similarly, high-Ca pyroxene in Eagles Nest has abundances of MnO (0.16 to 0.31 wt. %), Al_2O_3 (0.62 to 0.91 wt. %), TiO_2 (0.15 to 0.40 wt. %), and Na_2O (0.40 to 0.53 wt. %) which are comparable to those in ALH84025. The Cr-spinel in both achondrites have $\sim$1.4 wt. % TiO_2. Thus, Eagles Nest appears to be related to ALH84025.

Previously, a relationship between ALH84025 and Brachina has been suggested [3,4], while a relationship between ALH84025 and Chassigny (and other SNC's) has been discounted. Because the petrologic properties of Eagles Nest are similar to those of ALH84025, we tentatively conclude that Eagles Nest is also related to Brachina.

References: [1] Nehru C.E. *et al.* (1983) *Proc. Lunar Planet. Sci. Conf.*, **14th**, B237-B244. [2] Prinz M. *et al.* (1986) *Lunar Planet. Sci. XVII*, 679-680. [3] Warren P.H. and Kallemeyn G.W. (1989) *Proc. Lunar Planet. Sci. Conf.*, **19th**, 475-486. [4] Ott U. *et al.* (1987) *Meteoritics* **22**, 476-477.

MARALINGA (CK4): RECORD OF HIGHLY OXIDIZING NEBULAR CONDITIONS; G.Kurat and F.Brandstätter, Naturhistorisches Museum, Postfach 417, A-1014 Vienna, Austria. H.Palme and B.Spettel, Max-Planck-Institut für Chemie, Saarstraße 23, D-65 Mainz, Germany. M.Prinz, American Museum of Natural History, New York, NY 10024, USA

The Maralinga carbonaceous chondrite is a member of the newly defined CK(Karoonda) group of carbonaceous chondrites (1). However, Maralinga is depleted in Ni, Co, Se, and Zn relative to the other members of the CK group (1,2), in some respect similar to LEW86258. These depletions were considered being the result of pentlandite weathering by (1). We analyzed a 198.41 mg sample of Maralinga (provided by D.New) by INAA. Our results grossly confirm the previous findings. In addition, our analysis revealed significant depletions in the refractory siderophile elements Mo and Re. In the Figure we compare the Maralinga bulk data with data obtained by (3) in heating experiments at high fO_2 using homogenized Allende powder samples. As is evident, the experimental data match the Maralinga data perfectly for the refractory elements. We conclude that the depletion pattern must be due to a heating event under highly oxidizing conditions in an open system. The high degree of oxidation is well documented in Maralinga (and the other CK chondrites) by their fayalitic olivines (Fa 28-33), which also contain NiO (0.4-0.6 wt.%), and the absence of metal in these meteorites (4).

A low Mo content was previously reported for Karoonda, an observed fall (5), perhaps also reflecting loss of volatile Mo-oxide. W loss is not expected in Maralinga since experiments with CAIs have shown that, although W is oxidized under similar conditions as Mo, it is trapped in the silicates preventing its loss form the system. The data of (3) also show that Na and K are not significantly lost under oxidizing conditions, in agreement with the Maralinga data. Losses of Se, Au and As are, however, expected at an fO_2 above Ni-NiO. All three elements are depleted in Maralinga.

Magnetites are dispersed throughout CK rocks. The large ones fill cavities and have been considered being the product of oxidation of former metal (1,5). However, the composition and texture of magnetite suggest a primary origin. Magnetites typically contain 3-6 wt.% Cr_2O_3, 1-2.6% Al_2O_3, 0.15-0.5 (sometimes even more) TiO_2, but only about 0.17-0.30% NiO. The high contents of TiO_2 and Al_2O_3 - which lead to the exsolution of ilmenite and spinel (6) - are not compatible with the metal oxidation model. The mode of occurrence of large magnetites, similar to primitive metal in Forest Vale and Chela (7,8) suggests precipitation into pre-existing voids, usually as a single crystal, presumably from the vapor phase.

In conclusion we suggest that Maralinga (and perhaps other members of the CK group) collected the refractory siderophile elements mainly together with the main silicates, lost the ones volatile under oxidizing conditions (Re, Mo), was metasomatized during that event (FeO and NiO introduced into olivine) and magnetite precipitated into existing voids from the vapor. Possibly, Maralinga never contained the full share of common siderophile elements (Ni, Co) because of being processed in an oxidizing environment.

References: (1) Kallemeyn G.W., Rubin A.E. and Wasson J.T.(1991) Geochim.Cosmochim.Acta 55, 881. (2) Geiger T. and Spettel B.(1991) LPS 22, 433. (3) Wulf A.-V.(1990) Dissertation, Johannes Gutenberg-Universität Mainz, 177 pp. (4) Geiger T. and Bischoff A.(1989) Meteoritics 24, 269. (5) Palme H. and Rammensee W.(1981) Earth Planet.Sci.Lett. 55, 356. (6) Geiger,T. and Bischoff A.(1990) LPS 21, 409. (7) Perron C., Bourot-Denis M., Pellas P., Marti K., Kim J.S. and Lavielle B. (1989) LPS 20, 838. (8) Kurat G., Brandstätter F., Mayr M. and Hoinkes G.(1990) Meteoritics 25, 378.

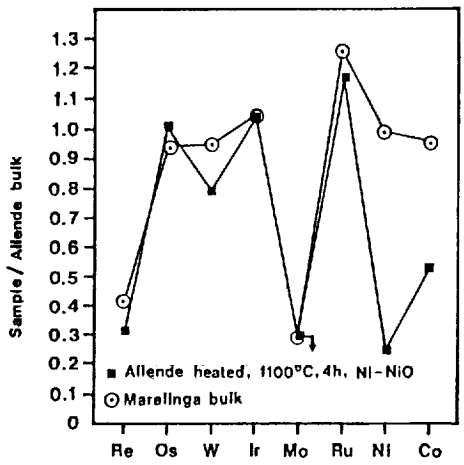

Figure: Heated Allende bulk and Maralinga bulk compositions normalized to untreated Allende bulk composition. Allende data are from (3).

MAGNESIOWÜSTITE - A NEW HIGH-TEMPERATURE MINERAL IN K/T BOUNDARY SEDIMENTS; Frank T. Kyte, Lei Zhou (Inst. Geophys. Plan. Phys, University of California, Los Angeles CA 90024) and Bruce F. Bohor (U.S. Geological Survey, Box 25046, MS 972, Denver, CO 80225).

High-temperature relict minerals, which crystallized during the K/T impact event, record the chemical and physical evolution of impact-derived melt and vapor. Although abundant K/T spheroidal material is likely from high-temperature, originally molten, impact debris, it is almost invariably composed of authigenic phases that replaced the original spheroid mineralogy. Notable exceptions include magnesioferrite spinel, which has been found in spherules from many localities, clinopyroxene in spherules from one Pacific locality[1], and tektite glass in Haiti[2].

Analyses of magnesioferrite from DSDP Site 596, a So. Pacific pelagic clay locality[3] indicate compositions similar to those measured at other localities showing considerable variability, but with a magnesioferrite composition approximated by $(Mg_{.85}Ni_{.08}Fe_{.07})O(Al_{.15}Cr_{.02}Fe_{.83})_2O_3$ (68 analyses on 22 grains). The high Fe_2O_3/FeO ratio is diagnostic for K/T spinel. Within three large magnesioferrite grains we found oval-shaped regions up to 10μm in diameter which consisted of fine-grained intergrowths between magnesioferrite and another oxide. Good analyses obtained from one specimen yielded a composition of $(Mg_{.85}Ni_{.11}Fe_{.04})O$ which we will call Ni-rich magnesiowüstite. Given its chemical similarity to periclase (MgO), this phase should be prone to diagenetic alteration and probably survived here only because it was enclosed in magnesioferrite. We observed texturally similar growths of magnesioferrite on other grains which may reflect regions where magnesiowüstite has been lost following alteration.

Phase relations of silicate systems with coexisting magnesioferrite and magnesiowustite are reasonably well understood. If we assume crystallization from a silicate liquid under conditions approaching equilibrium, we can infer some physical and chemical conditions of the crystallization environment. In the experimentally-observed system MgO-FeO-Fe_2O_3-SiO_2[4], the only univariant boundary with mangnesioferrite and magnesiowüstite also includes olivine, liquid, and vapor. Oxygen fugacities inferred from Fe_2O_3/FeO ratios are high, probably indicating crystallization in air near 1 atm. Liquidus temperatures in this system exceed 1600°C. In a more realistic system including additional components (probably principally Al_2O_3), liquidus temperatures would be lower, but other relationships are unlikely to change. The mineral chemistry of these relict phases indicate crystallization in air of a molten silicate droplet, more mafic than inferred in other studies [1], and probably with olivine and glass as the principal silicate phases.

[1]Smit J., Montanari A. and Alvarez W. (1991) Lunar Plan. Sci. Conf. **XXII**, 1277. [2]Sigurdsson et al. (1991) Nature **349**, 482. [3] Zhou L., Kyte F.T. and Bohor B.F. (1991) Geology (in press). [4] Muan A. and Osborn (1956) J. Am. Cer. Soc. **39**, 121.

HOT SHOCK EXPERIMENTS: SIMULATION OF AN IMPORTANT PROCESS IN THE EARLY SOLAR SYSTEM AND IN MULTI-RING CRATERING . Langenhorst, F. and Deutsch, A., Inst. f. Planetologie, Wilhelm-Klemm-Str. 10, D-4400 Münster.

Introduction. Previous shock experiments on rocks and minerals were performed only at room temperature (1). Today, we know that dynamic compression by hypervelocity collision affects lithologies at elevated temperatures. For example, for the Sudbury structure, a maximum depth of excavation in the order of 25 km was calculated (2), obviously enough to reach lower crustal rocks. Based on geothermometric results (3), it is assumed that the proposed shock event at Vredefort affected "hot" target rocks. Up to now, any knowledge about "high temperature" shock-metamorphism is lacking.

Recovery experiments. In order to detect special shock effects in hot targets, we performed shock-loading experiments on externally preheated single crystal quartz as well as on the ordinary chondrite Holbrook (L6) using a high-explosive set-up. Preheated quartz was shocked in the pressure range from 20 to 48 GPa; on the preheated Holbrook meteorite only one 60 GPa-shot was carried out. The actual preheating temperature directly before the passage of the shock wave was at least 630°C.

Results. *QUARTZ*: On SEM-images of hot shocked quartz, fractures are diagnostic for the structural state: ß-quartz shocked up to 25 GPa is still crystalline and displays mosaicism, whereas glassy-like fractures and grooves in samples of higher shock pressure (> 25 GPa) indicate a total transformation to diaplectic glass. X-ray data corroborate this abrupt transformation: back reflection is totally absent for preheated shocked quartz above shock pressures of 25 GPa, but is gradually fading out between 25 and 34 GPa for cold shocked quartz. Spindle stage measurements on *hot shocked quartz* yield in comparison to *cold shocked quartz* (4,5) to the following results: (*i*) *Below 25 GPa*, they both display a similar optical behaviour equivalent to characteristics of unshocked quartz. (*ii*) In the pressure range from *25 to 26 GPa*, refractive indices and birefringence of hot shocked quartz decrease abruptly down to values for melt glass, whereas the equivalent change for cold shocked quartz takes place smoothly from *25 to 35 GPa*. (*iii*) The complete transformation to diaplectic glass is achieved at *26 GPa* for hot shocked, but not before *35 GPa* for cold shocked quartz. U-stage determinations on cold shocked quartz confirm results by (6), namely that {1012} is the predominant orientation of planar features above 20 GPa. In contrast, hot shocked quartz does not show this orientation, but contains complex sets of planar elements of higher MILLER indices. *HOLBROOK*: This hot shocked *L6* chondrite shows a distinct blackening, and was heavily fragmented in the experiment. Olivine and pyroxene display shock-induced undulatory extinction but birefringence is not reduced; plag-grains are totally converted into maskelynite.

Implications. Recovery experiments on preheated quartz indicate that during shock metamorphism hot samples behave quite different to "cold" specimens. Usually, refractive index data of cold shocked quartz is used for shock wave barometry at natural impact sites. Concerning our data for hot shocked quartz, this application is only correct as far as the target temperature is accurately known. The shock experiment on the preheated chondrite Holbrook yields a texture similar to naturally shocked meteorites. This demonstrates that hypervelocity collisions with hot meteorite parent bodies might be important processes in the early solar system.

REFERENCES: (1) STÖFFLER ET AL. (1988). In Meteorites and the Early Solar System (eds. Kerridge & Matthews), pp. 165. (2) LAKOMY (1990). Meteoritics 25, p. 195. (3) SCHREYER (1983). J. Petrol. 24, pp. 26. (4) GROTHUES ET AL. (1989). LPSC XX, p. 365. (5) REHFELDT-OSKIERSKI ET AL. (1986). LPSC XVII, p. 697. (6) HÖRZ (1968). In shock metamorphism of natural materials (eds. French & Short), pp. 243.

CHARACTERIZATION OF LOW ALBEDO ASTEROIDS; L. A. Lebofsky[1], E. S. Howell[1], and D. T. Britt, Lunar and Planetary Laboratory, Univ. of Arizona, Tucson, AZ 85721 USA.

Three asteroid classes were defined from the early spectral surveys of the asteroids: C for carbonaceous, M for metallic, and S for stony. Subsequent spectral studies have defined new asteroid classes and have shown that the original classes can be divided into a number of additional types. The low albedo asteroids are now classified as types B, C, D, F, G, K, and P. These types are concentrated in the middle asteroid belt and out to the Trojan asteroids at the distance of Jupiter. Their visible and near-infrared spectra are generally dark and featureless, with a red slope in the ultraviolet. Some of them show water absorption features in the mid-infrared, indicating the presence of bound water.

The lack of absorption features in the telescopic reflectance spectra, especially in the visible and near IR, has made it difficult to determine mineralogy of the low albedo asteroids. The spectra of some asteroid classes, concentrated primarily in the middle of the asteroid belt, closely resemble laboratory spectra of carbonaceous chondrite meteorites, implying similar mineralogy. These meteorites are chemically primitive, composed of fine-grained matrix material which includes hydrous silicates, complex carbon compounds, olivine, and pyroxene, combined with olivine and/or pyroxene chondrules. This disequilibrium mineralogy has led Jeff Bell to place these asteroids in his primitive superclass. The outer belt low albedo asteroids are probably very similar to these asteroids, but no meteoritical analogues exist for most distant asteroid types.

The mineralogic interpretation is complicated by two problems. Phobos and Deimos spectrally resemble the C asteroids. However, the theory for the formation of these asteroids does not allow their condensation that close to the Sun. This requires that Phobos and Deimos be captured, but dynamicists have difficulty postulating a plausible mechanism for the capture. The spectral interpretation has also been complicated by the recent work of one of us (DTB) with shocked ordinary chondrites. These meteorites are also spectrally similar to the C asteroids, but they are mineralogically different than the carbonaceous chondrites. Further work needs to be done to determine whether it is possible for shocked material to spectrally dominate the surface of a large asteroid.

Since the taxonomic classes are determined solely on they visual spectra, concerns have been raised as to the relationship of classes to mineralory and the possibility that an individual class may contain asteroids of greatly differing mineralogy. Our asteroid studies in the 3-μm spectral region have found that about half of the C asteroids have surfaces composed of hydrous silicates. Most D asteroids are concentrated in the Trojan region and have not shown the presence of hydrous silicates. However, we have recently detected hydrous silicates on a mainbelt D asteroid. This variation in hydration may imply major mineralogical differences among the Cs and Ds.

---

[1] Visiting astronomer at the Infrared Telescope Facility which is operated by the University of Hawaii under contract to the NASA

FORMATION AND ALTERATION OF REFRACTORY INCLUSIONS WITHIN THE CM CHONDRITES COLD BOKKEVELD, MURCHISON AND MURRAY.

Lee, M.R. and Barber, D.J. Department of Physics, University of Essex, Colchester, Essex CO4 3SQ, U.K.

A detailed scanning and transmission electron microscopy study of thin sections from three CM chondrites has revealed over 350 individual calcium- and aluminium-rich inclusions (CAI). These inclusions differ significantly in abundance between the three meteorites and within each one there are very variable morphologies and mineralogies. However, consistent mineralogical associations characterise all CAI and many had similar formational histories.

The core of most CAI comprises iron-poor spinel which encloses accessory perovskite and twinned hibonite laths. Hibonite formed first and was followed by perovskite, then spinel. This core is successively rimmed by iron-rich phyllosilicate, pyroxene (diopside ± fassaite) and occasionally forsterite. Both phyllosilicate and pyroxene may additionally occlude primary intracrystalline pores within the core. This texture grades into CAI solely comprising an intergrowth of equidimensional granular spinel and pyroxene crystals. Following rim formation the outer pyroxene layer of many inclusions was abraded, being removed from prominences but preserved within embayments. Lastly, CAI were rimmed by one or more phases of fine grained, fragmentary material prior to incorporation into the final parent body.

Many CAI contain evidence of aqueous alteration, most distinctively the iron-rich phyllosilicate rim that comprises 7Å serpentine and occasionally PCP, both of which are common within the matrices of CM chondrites. The sharp interface between phyllosilicate and adjacent phases in the rim indicates that the phyllosilicate formed by fine scale alteration of an iron-rich precursor. Occasionally, rim phyllosilicates of Cold Bokkeveld CAI are intergrown with calcium sulphate which also occludes fractures within the meteorite as 'satin spar' gypsum. This unequivocally demonstrates aqueous processes in the final parent body. Additionally, calcite is present in many CAI from all three meteorites. Calcite may occur within the rim of the CAI or the core where it has formed, at the expense of spinel, although both hibonite and perovskite are unaffected. This style of alteration is comparable with that of calcitized forsterite within type 1 chondrules of Cold Bokkeveld. Both CAI and chondrules are most heavily calcitized in the same areas of the meteorite which is possibly due to fabric-related porosity and permeability inhomogeneities.

COMPOUND CHONDRULES IN ORDINARY CHONDRITES. Min Sung Lee, Alan E. Rubin and John T. Wasson, Institute of Geophysics and Planetary Physics, University of California, Los Angeles, CA 90024, USA.

A few percent of the chondrules in ordinary chondrites (OC) consist of one chondrule or chondrule fragment physically attached to another. Most of these pairs are similar chemically and petrographically [1], although compound chondrules composed of dissimilar objects have been reported previously [2]. Statistics on the occurrence of different types of compound chondrules potentially offer important clues regarding nebular conditions at the time that chondrules were molten.

Two related types of radial pyroxene (RP) chondrules are among the most common varieties of compound chondrules. The first consists of optically continuous pyroxene fans that propagate from one chondrule to another; the second appears to have several lumps of RP material adhering to its surface. Such chondrules may be siblings that reflect collisions among objects formed at the same time and microlocation by the same heat pulse. A rarer group of compound chondrules consists of a barred olivine (BO) chondrule (with devtrified mesostasis) enclosed within a larger porphyritic olivine (PO) chondrule. We suggest that unmelted precursor dust accreted around the pre-existing BO chondrule, then a second heat pulse melted the PO material and devitrified the glassy mesostasis of the BO. The refractory character of the forsteritic pyroxene of the BO chondrule facilitated its survival during the heating event. There is a selection effect operating here: if a less-refractory PO chondrule had been reheated, it would have been completely melted.

Gooding and Keil [3] found only 33 compound chondrules in their petrographic survey, too few to allow significant statistical inferences. We are assembling statistics on a much larger population of compound chondrules by concentrating on massive type-3 OC.

References: [1] Lux G., Keil K. and Taylor G.J. (1981) Geochim. Cosmochim. Acta **44**, 841-855; [2] Scott E.R.D. and Taylor G.J. (1983) Proc. Lunar Planet. Sci. Conf. **14th**, B275-B286; [3] Gooding J.L. and Keil K. (1981) Meteoritics **16**, 17-43.

SHAPE-DIFFERENTIATED SIZE DISTRIBUTIONS OF CHONDRULES IN TYPE 3 ORDINARY CHONDRITES. James M. Leenhouts and William R. Skinner, Department of Geology, Oberlin College, Oberlin, OH 44074.

Ordinary chondrites contain an intimate mixture of nearly spherical "drop-formed chondrules" (DFCs) and angular "clast-formed chondrules" (CFCs) (1). This study was initiated to determine (a) if two discrete populations of chondrules exist based on shape, and (b) how the chondrule size distributions within a given chondrite differ between DFCs and CFCs.

The data were derived from 42x photographic enlargements of thin sections Bishunpur 418-2, Khohar 4245-1, Chainpur 4020-2, and Tieschitz 560-1 from the American Museum. Tieschitz yielded the most chondrules with 280 objects measured. For each chondrule selected, the long axis, the longest axis perpendicular to the long axis, the perimeter, and the cross-sectional area were measured with a digitizing tablet. Chondrules were selected individually using a petrographic microscope with the requirement that each have an identifiable dust rim. Thus only those objects existing as DFCs or CFCs before accretion were measured, and CFCs produced by breakage on the parent body were excluded.

To quantify chondrule shape, a surface roughness index (SRI) was determined for each chondrule. (SRI is defined as the ratio of the measured perimeter of a chondrule to the perimeter of a smooth ellipse with the same axial ratio and the same cross-sectional area as the chondrule). Histograms of the shape data revealed a unimodal population distribution from low SRI values for DFCs to high values for CFCs.

Both the long axis and the average of the two measured axes for each selected chondrule were plotted as cumulative frequency percents. Each of the four thin sections yielded results for long axis only data that were similar to the data for averaged axes values indicating that long axis measurements are sufficient to characterize size frequency distributions in chondrites as previously done by Dodd (2). The CFCs and DFCs exhibited very similar mean and median diameters and grain size distributions, the CFCs being slightly better sorted. The mean phi value for the average of the axes of Tieschitz' DFCs = 1.3016 and for CFCs = 1.3330; the median phi values are 1.3285 and 1.3793, respectively. Except for Bishunpur, the largest CFCs were as large or larger than the largest DFCs in these sections. Chainpur 4020-2 yielded mean long axis values (in mm) comparable to those determined by Hughes (3) with DFCs = 0.708 and CFCs = 0.683 vs. Hughes values of 0.714 and 0.705, respectively.

Many of the CFCs have an arcuate face that suggests they were once part of much larger DFCs. Reconstruction of the most evident examples yielded maximum parent DFCs of about 3.3 mm. CFCs derived from even larger DF parents may exist, but it is difficult to identify very open arc segments.

The evidence strongly suggests that DFCs formed in a wider range of sizes than now observed, that larger DFCs were broken up to yield CFCs, and that DFCs and CFCs were mixed together and sorted primarily by size. Larger DFCs like the 5.7 mm chondrule in Bishunpur 418-2 are rare.

References: 1) Dodd R.T. (1981) Meteorites. Cambridge Univ. Press. 2) Dodd R.T. (1976) EPSL 30, 289-291. 3) Hughes D.W. (1978) EPSL 38, 391-400.

EVALUATION OF THE STRECKER SYNTHESIS AS A SOURCE OF AMINO ACIDS ON CARBONACEOUS CHONDRITES

N. R. Lerner, E. Peterson, and S. Chang
NASA-Ames Research Center, Moffett Field , CA 94035

The Strecker synthesis, $R_2CO + HCN + NH_3 \leftrightarrow R_2C(NH_2)CN + H_2O \rightarrow R_2C(NH_2)CO_2H$, has been proposed as the source of amino acids formed during aqueous alteration of carbonaceous chondrites (Cronin et al. 1988). It is postulated that the aldehyde and ketone precursors (R_2CO) of the meteoritic amino acids originated in interstellar syntheses and accreted on the meteorite parent body along with other reactant species in cometesimal ices. Formaldehyde is observed in the interstellar medium and in comets, and if produced by ion-molecule reactions would be expected to be D-enriched. The amino acids found in Murchsion are D-rich with δD=1370 ‰ (Epstein et al. 1987, Pizzarello et al. 1991). Any proposed synthesis of amino acids must be capable of preserving the D-enrichment of the interstellar precursors during synthesis and aqueous alteration and accounting for the relative abundances of amino acids.

The Strecker synthesis has been run with formaldehyde, acetaldehyde, proprionaldehyde, acetone and methyl ethyl ketone as starting materials. The concentrations studied ranged from 0.003M to 0.3M in NH_4Cl and HCN and from 0.0045M to 1 molar in aldehyde or ketone. In the case of aldehydes, the Strecker synthesis is very efficient in producing amino acids: the yields of amino acids in basic solution at room temperature ranged from 15-95% of theoretical. Yields were decreased by decreasing the temperature to 278K, the concentration of starting materials, or the pH of the solution. In addition to the expected α-amino acids, compounds such as α-iminodiacetic acid were formed which could be sought in Murchison samples as an independent chemical indicator of the Strecker synthesis. With acetone as the starting material, less than 1% α-amino-isobutyric acid formed in basic solution and in solutions buffered at pH 6.5. An improvement in yield to 15% was achieved by acidifying the basic solutions to a pH of 6 to 7 and allowing them to stand for several days. The yields ranged from 8 to 70% when the basic solutions were hydrolyzed in concentrated hydrochloric acid. It is noteworthy that roughly equivalent amounts of glycine and α-amino-isobutyric acid are observed in Murchison. The low yields of α-amino-isobutyric acid from the Strecker synthesis, except when pH was drastically lowered in the reaction medium, suggest that if such synthesis had occurred, a similar change in pH would have been necessary during aqueous alteration on the parent body.

To study the effect of minerals on the reaction, the Strecker synthesis was run in the presence and absence of dust from the Allende meteorite using deuterated aldehydes and ketones as starting materials. The products were investigated by GC/MS. With the exception of glycine the retention of deuterium in the amino acids was greater than 90%. Some D-exchange with water does occur, however, and determination of the rate of exchange as a function of pH and temperature may allow some bounds to be placed on the duration of parent body aqueous alteration. For glycine, $NH_2CD_2CO_2H >> NH_2CH_2CO_2H > NH_2CHDCO_2H$, which indicates that some of the glycine might have been formed from HCN and water. The retention of deuterium by the amino acids under conditions studied thus far is consistent with the model that a Strecker synthesis starting from interstellar aldehydes and ketones led to the production of meteoritic amino acids. Additional work is required to strengthen this conclusion.

Cronin, J. R. and Pizzarello, S. (1988) *Meteorites and the Early Solar System*, The U. of Arizona Press, Tucson, 808-853. Epstein et al. (1987) *Nature*, **326**, 477-479. Pizzarello et al. (1991) *Geochimica Cosmochemica Acta* **55**, 905-910.

Elemental abundance patterns in presolar diamonds

Roy S. Lewis[1], Gary R. Huss[1], Edward Anders[1], Y.-G. Liu[2] & R. A. Schmitt[2,3]

[1] Enrico Fermi Inst. & Dept. of Chem., Univ. of Chicago, Chicago, IL 60637-1433
[2] The Radiation Center & Depts. of Chem. and [3] Geosciences and College of Oceanography, Oregon State University, Corvallis, Oregon 97331

Presolar microdiamonds (1) with highly anomalous Xe-HL as well as N of $\delta^{15}N \sim -300‰$, are the most abundant presolar grains identified in primitive meteorites. Although the Xe-HL suggests a supernova connection (2), the details of this connection are unknown. This may be contrasted with SiC grains, with isotopic compositions of major, minor, and trace elements in general agreement with theoretical predictions for carbon stars (e.g. 3, 4, 5). Isotopic and abundance measurements have come more slowly for the diamonds. First He, Ne, Ar, Kr, Xe (6), & N (7) by pyrolysis or combustion, then H & Si by ion probe (8), and oxygen by ion probe and titration (9). After learning how to combust diamonds at low temperature we measured Rb, Sr, & Ba by solid source mass spectrometry (10). Now we present INAA results for Sc, Cr, Fe, Co, Ni, Ru, Os, & Ir in specially purified micro-diamond separates. Extra effort was made to remove silicates, other oxides, oxidizable materials, noble metals, and any grains > 0.1 μm in size by repeated cycles of treatment with HF-HCl, H_2SO_4 at 200°C, $HClO_4$ at 200°C, aqua regia, and colloidal separation. Fine grained SiC (<200 ppm of the diamonds) may have survived. Plotted in figure 1 are the depletion factors = $(X_A/C)_{Diamond}$ / $(X_A/C)_{Solar}$, where X_A/C = the atomic ratio to C. The open symbols are upper limits. In fact, even the good measurements are upper limits in the sense that a small contaminating phase may overwhelm the quantity of a particular trace element in the diamonds. An example may be Ir, which at 300ppm in the diamond fraction accounts for 30% of the Ir in bulk Allende. This Ir in large part survives both aqua regia and NaOCl and hence is either specially resistant or protected. However, putting the Ir inside the diamonds implies that this 30% is carried in surviving presolar grains, a real stretch. Other potentially special cases are carbon, of course, and the cosmically abundant or especially volatile elements such as H, He, Ne, and perhaps O & N. However, the cluster of values between 0.0001 and 0.01 over a wide range of elements may partly represent nearly unfractionated trapping in, and the true indigenous content of, these elements in the diamonds. Additional elements may clarify this, but cannot yet be done by INAA due to the overwhelming Ir activity. Work continues on attempts to further purify these diamonds and to measure additional elements.

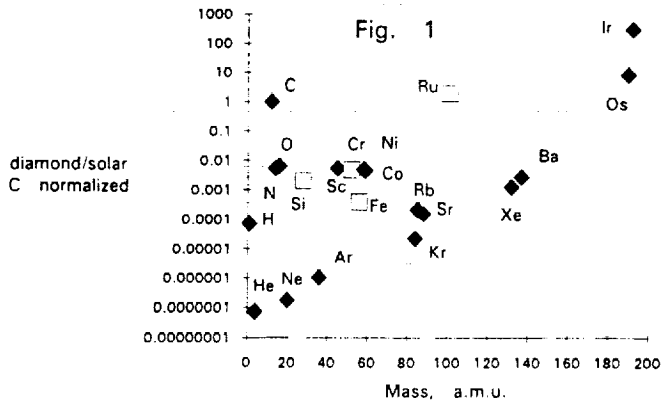

References: (1) Lewis, R. S., *et al.* (1987) *Nature* **326**, 160-162. (2) Clayton, D. D. (1981) *Proc. Lunar Planet. Sci. Conf.* **128**, 1781-1802. (3) Lewis, R. S., *et al.*, (1990) *Nature* **348**, 293-298. (4) Amari, S., *et al.*, (1991) *this volume*. (5) Zinner, S., *et al.*, (1991) *this volume*. (6) Huss, G. R., Lewis, R. S., and Anders, E., *in prep.* (7) Ash, R.D., *et al.*, (1987) *Meteoritics* **22**, 319. (8) Virag, A., *et al.* (1989) *Lunar Planet. Sci.* **20**, 1158-1159. (9) Lewis, R. S. *et al.* (1989) *Nature* **339**, 117-121. (10) Lewis, R. S., *et al.* (1991) *Lunar Planet. Sci.* **22**, 807-808.

THE DISCOVERY OF FOUR CONCENTRIC RING GROWTH PATTERN OF Fe-Ni METAL NUCLEATION AND CRYSTALLIZATION IN SPACE

Li Zhaohui, Xie Xiande (Institute of Geochemistry, Academia Sinica, Guangzhou Branch) and Zhang Datong (South China University of Technology)

The new meteorite fall of Yanzhuang H6 is a rare type due to heavily shocked features and the thick veins of molten materials. The black phase contains a lot of recrystallized Fe-Ni particles of 10um to 7mm in size, and with relatively uniform Ni content (11.41%). The SEM studies of the surface of the large metal grains have revealed rather specific features of nucleation and crystallization of Fe-Ni metal in the form of round, needle-like, spear-like and petal-like microcrystals. They form the dentritic, bears-shaped and network surface structure of the grains. Our detailed SEM studies have firstly discovered the four separeted concentric ring growth pattern on the head of each of the recrystallized Fe-Ni metal microcrystals (Fig.1 and Fig.2). This pattern is different from the spiral growth pattern for the most natural and synthetic crystals on the Earth. Each of the concentric rings looks like the water wave propogating form (Fig.3), so we deduce that the four concentric ring pattern is a possible fundamental nucleation and crystallization form for the Fe-Ni metal recrystallization from shock melt under the microgravity enviroment.

Fig.1 The structure of four concentric ring growth pattern of Fe-Ni metal crystallization in Yanzhuang meteorite.

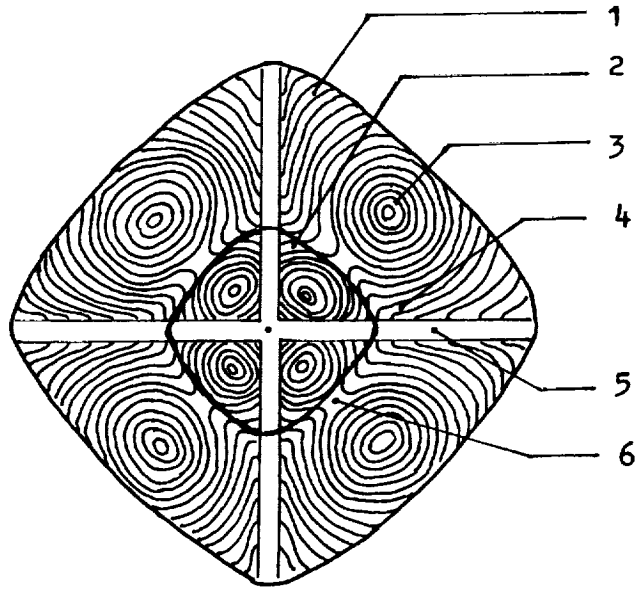

Fig.2 Sketch of the four concentric ring growth pattern of Fe-Ni metal crystallization in space. 1-Lower layer, 2-Upper layer, 3-Circular growth lines, 4-Arc-bridge like lines, 5-Crystal edge of skeletal octahedra, 6-Hollow rhomb area.

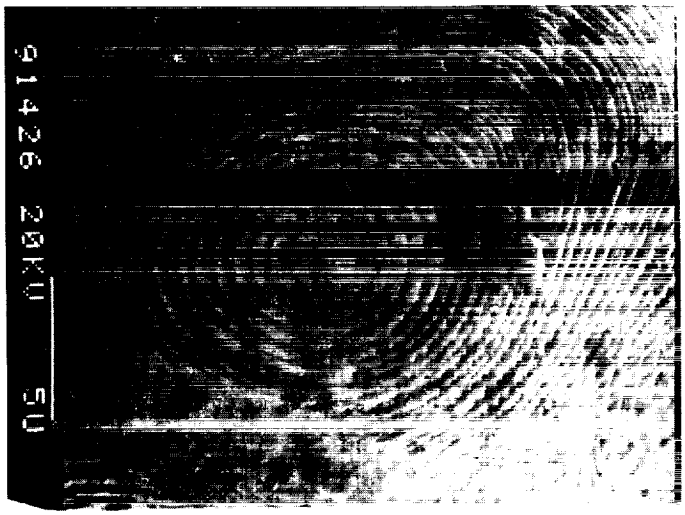

Fig.3 The close view of one of the four circular growth lines of Fe-Ni metal crystallization in Yanzhuang meteorite.

Ca-Al-RICH INCLUSIONS IN NINGQIAN (CV3) CHONDRITE: EVIDENCE FOR PRIMORDIAL HIGH ENRICHMENT IN Re IN Pt-GROUP ELEMENT NUGGETS. Lin Y.T.[1], El Goresy, A.[2], and Fang, H.[3].
[1]Institute of Geochemistry, Academia Sinica, Guiyang, P.R. China. [2]Max-Planck-Institut fur Kernphysik, Heidelberg, FRG. [3]Institute of High Energy Physics, Academia Sinica, Beijing, P.R. China.

Ningqian (anomalous CV3) is a recent meteorite fall (25 June 1983) from P.R. of China [1]. It contains few Ca-, Al-rich inclusions (0.5-1.5% by volume). Only one coarse-grained CAI resembling Allende type C and low in bulk refractory lithophiles (~ 0.82 x CV) was reported so far [1]. Our investigations revealed the presence of two subgroups of CAIs.

Type I: Four of these CAIs (0.4 μm-0.87 mm in diameter) consist of gehlenitic melilite (G_{86-100}), Fe-bearing spinel (FeO < 6.10 wt.%), and perovskite. The largest of these displays delicate and highly convoluting mineral layers. The core is occupied by melilite, perovskite, and spinel. The convoluting mantle consists of layers of spinel + idiomorphic hibonite (6.89-9.27% TiO_2; 3.08-4.26% MgO) + perovskite and a thin rim of melilite + perovskite. Several Pt-metal nuggets (RPMN) are confined to the outer rim.

Type II: Three CAIs (15 μm-1 mm in diameter) majorily consist of spinel and fassaite (3.91-13.% Al_2O_3; 0.31-1.77% TiO_2), or diopside. Minor phases are: gehlenitic melilite, perovskite, and forsterite. RPMN, FeNi, and a NiCu alloy were also found. A few very small grains ($\leq$ 1 μm) of thorianite (ThO_2) occur in the largest CAI. The Th/U ratio of thorianite is > 76.

Microprobe analyses of 10 RPMN in the CAIs of the two groups revealed that only one nugget displays a cosmic (CI normalized) Re/Os ratio of 0.9. All other nuggets are strikingly enriched in Re (Re enrichment factor > 10^7; Re/Os ratios > 6-10^3 x CI). There are two groups of Pt-element patterns: a) High Re with flat patterns and chondritic Os/Ir ratios; b) enrichment in Re accompanied by Os-depletion (Figure 1). Some nuggets are depleted in Mo and Pt, and others are in W. Patterns with W-depletion display no negative Mo anomaly, thus excluding condensation at high fo_2 (Figure 1).

The very high enrichment in Re in 9 RPMN is difficult to reconcile with either the one phase equilibrium condensation model [2, 3, 4] or a three phase model [5]. No metal with a CI-normalized Re/Os ratio > 1.5 is predicted by these models. The unique high Re/Os ratios cannot have resulted from fractional crystallization, since Re and Os display complete solid solutions [6]. Enrichment of Re, due to condensation under oxidizing conditions or a late-stage oxidation episode, is very unlikely because the Re-enrichment is always present, regardless if the patterns are flat or display W or Mo depletions. We consider the unique Re-enrichment as an evidence for a primordial addition of an almost pure Re component. This is manifested in the flat patterns and the chondritic Os/Ir ratios. Patterns with Os-depletion in addition to enrichment in Re indicate an Os/RPM fractionation process in material originally enriched in Re. The very high abundance of Re in RPMN in the CAIs of Ningqian places these CAIs as premium candidates for NTIMS $^{187}Re/^{187}Os$ dating.

References: [1] Rubin *et al.* (1988), *Meteoritics* ***23***, 13-23. [2] Palme, H. and Wlotzka, F. (1976), *Earth Planet.Sci.Lett.* ***33***, 45-60. [3] Blander, M. *et al.* (1980), *Geochim.Cosmochim. Acta* ***44***, 217-223. [4] Fegley, B. and Palme, H. (1985), *Earth Planet.Sci.Lett.* ***42***, 311-326. [5] Sylvester, P.J. *et al.* (1990), *Geochim.Cosmochim. Acta* ***54***, No.12, 3491-3508. [6] Hansen, P.M. (1958), *Constitution of Binary Alloys.* 2nd Edition.

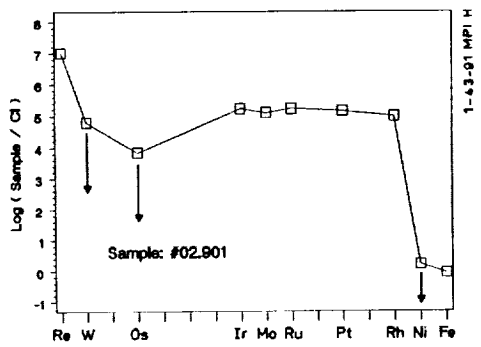

Figure 1

N92-12921

MICROPROBE STUDIES OF MICROTOMED PARTICLES OF "WHITE DRUSE" SALTS IN SHERGOTTITE EETA 79001; D. J. Lindstrom, Code SN2, NASA/JSC, Houston, TX 77058.

The "white druse" material in Antarctic shergottite EETA 79001 [1,2] has attracted much attention as a possible sample of Martian aqueous deposits [3,4]. Instrumental Neutron Activation Analysis (INAA) has been used to determine trace element analyses of small particles of this material (0.03-2.9 ug) obtained by hand-picking of likely grains from broken surfaces of the meteorite [5]. Unfortunately, the analyses show quite clearly that the "druse" samples actually contained substantial amounts of igneous phases (mostly pyroxene), and that the druse material itself is essentially barren of trace elements; with the exception of Na, Br, and Zn, all analyzed elements fall on mixing lines on two-element plots between zero and typical matrix values [5].

INAA is a nondestructive technique, apparently even for these rather thermally fragile samples, so after INAA, they were mounted in epoxy and partially sliced with a diamond knife microtome. The intent was to analyze the microtome slices in the transmission electron microscope, but the quality of the sections obtained was very poor due to the friability of the material and the large size of the particles compared with the cosmic dust particles for which the microtoming procedures have been developed. After partial slicing, the material remaining in the epoxy (the "potted butt") had a good surface, so electron microprobe work was attempted on areas as large as about 150x120 um. Backscattered electron images show a few mineral grains as large as 10 um, which are invariably pyroxenes. The surrounding druse is extremely fine-grained, below the resolution obtainable under normal microprobe conditions. Nonetheless, backscattered electron images show considerable variations in brightness (different average atomic numbers), and botryoidal structures have been observed. Recognizing that the surfaces were likely to be uneven, we rastered the beam at magnifications of 20-80kX (areas about 6 to 1.5 um square) during microprobe analysis. Analyses showed considerable variability, both within single particles and between different particles. In order to interpret these analyses, normative abundances of minerals observed in the druse [3,4] have been calculated. After the usual simplifications (e.g., grouping of minor Mn, Ni, and Fe with Mg), the calculations assumed: 1) all P is present as $Mg_3(PO4)_2$, 2) remaining Mg and Si are dominantly in pyroxene, with any excess Si appearing as silica, 3) all S is as $CaSO_4$, and 4) remaining Ca (plus any remaining Mg, alkalies, etc.) is present as carbonates. Analytical totals based on these calculations range from 96-108%. Data shown on the figure are renormalized after subtraction of the pyroxene, which is considered to be igneous meteorite material. Some particles (9 and 7) are quite homogeneous, and contain a very high proportion of carbonates. Separate regions in the other particles vary widely, e.g. sulfate in particle 3 ranges from less than 1% to nearly 70%. Silica contents are also quite variable, silica being present in major amounts in some analyses of particles 12 and 15, but not at all in particle 3. Phosphate abundances display a much narrower range, all but one analysis falling between 3-8 %.

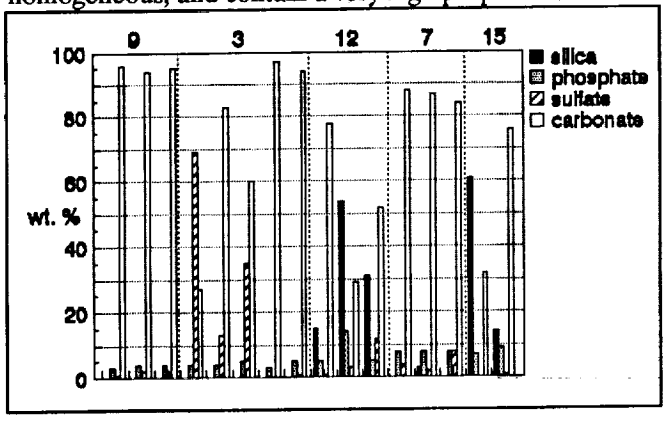

Microtomed surfaces of small selected particles have been shown to be very useful in obtaining information on the texture and composition of rare lithologies like the white druse of EETA 79001. This material is clearly heterogeneous on all distance scales, so a large number of further analyses will be required to characterize it. Further characterization of these sections is in progress.

References: [1] Martinez R. and Gooding J. L. (1986) Antarctic Meteorite Newsletter 9(1), 23-29. [2] Gooding J. L. (1990) Antarctic Meteorite Newsletter 13(2), 4. [3] Gooding J. L., Wentworth S. J., and Zolensky M. E. (1988) Geochim. Cosmochim. Acta 52, 909-915. [4] Gooding J. L. and Wentworth S. J. (1991) Lunar Planet. Sci. XXII 461-2. [5] Lindstrom D. J. and Martinez R. R. (1991) Lunar Planet. Sci. XXII, 813-4.

RELATIONSHIPS AMONG BASALTIC LUNAR METEORITES; Marilyn M. Lindstrom, SN2 NASA Johnson Space Center, Houston TX 77058.

During the past two years four meteorites of dominantly mare basalt composition have been identified in the Japanese and US Antarctic collections. Basalts represent a much higher proportion of the lunar meteorites than is expected from photogeologic mapping of mare and highland regions. Furthermore, the basaltic lunar meteorites are all described as VLT mare basalt, which is a relatively uncommon type among returned lunar samples. The significance of the basaltic meteorites to our understanding of the lunar crust depends on the evaluation of possible relationships among the individual meteorites. None of the specimens are paired meteorites. They were collected in three different areas of Antarctica and differ from each other in petrography and composition. It is important to determine whether they might be paired ejecta which were ejected from the same mare region by the same impact.

The question of paired ejecta must be addressed using a combination of exposure histories and petrographic/compositional characteristics. For two meteorites to be paired ejecta it is necessary that they were ejected from the moon at the same time. To date exposure studies have been done only for EET87521 and Y793274, and are consistent with the two meteorites being paired ejecta (1). To demonstrate that any two meteorites came from the same region of the Moon, they should exhibit some petrologic relationship.

The four meteorites are easily distinguished from each other petrographically. Asuka-31 and Y793169 are coarse-grained mare gabbros, but Asuka-31 is distinctly coarser than Y793169 (2). EET87521 and Y793274 are breccias, but EET87521 is a fragmental breccia consisting almost entirely of mare basalt (3,4), while Y793274 is a regolith breccia containing 1/4-1/3 highland material (5,6). Could the mare gabbros represent the basaltic components of the mare breccias?

Major and trace element compositional data are incomplete for the two mare gabbros, but sufficient data are available to make some comparisons. EET87521, Asuka-31, and Y793169 are all Fe-rich VLT basalts similar to those from Luna 24, while Y793274 contains Mg-rich VLT basalt similar to those from Apollo 17 (5). Compatible trace elements are highly variable (7). Some of this variation may be attributed to modal heterogeneity, but magmatic differentiation of Mg-rich basalts like Y793274 can produce Fe-rich basalts like those in the other basaltic lunar meteorites (8).

Variations in incompatible trace element contents, such as the REE, seem to be dominated by a different process. REE patterns in the basaltic breccias are LREE-enriched similar to that of KREEP (4,8), while those of Asuka-31 (7) and clasts in EET87521 (9) are LREE-depleted as are typical mare basalts. The REE patterns of the breccias appear to reflect the addition of a small amount of KREEP component to these dominantly basaltic rocks (9).

It is possible that the basaltic lunar meteorites are paired ejecta from the same region of the Moon. However, the relationships among them are more complicated than the basaltic breccias being simply brecciated mare gabbros. Both magmatic differentiation and KREEP mixing are required. Further studies, especially exposure histories of the mare gabbros, are required to evaluate these complicated relationships, and may prove that the meteorites are unrelated.

REFERENCES: (1) Nishiizumi K. et al. (1991) *Lunar Planet. Sci. XXII*, LPI, 977-978. (2) Yanai K. (1991) *Proc. Lunar Planet. Sci. 21*, 317-324. (3) Delaney J. (1989) *Nature 342*, 889-890. (4) Warren P. and Kallemeyn G. (1989) *Geochim. Cosmochim. Acta 53*, 3323-3330. (5) Lindstrom M. et al. (1991) *Proc. NIPR Sym. Ant. Met. 4*, in press. (6) Warren P. and Kallemeyn G. (1991) *Proc. NIPR Sym. Ant. Met. 4*, in press. (7) Lindstrom M. et al. (1991) *Papers Submitted to 16th Sym. Ant. Met.*, NIPR, in press. (8) Lindstrom M. et al. (1991) *Lunar Planet. Sci. XXII*, LPI, 817-818. (9) Delaney J. et al. (1991) *Lunar Planet. Sci. XXII*, LPI, 301-302.

ORDINARY CHONDRITE CLASSIFICATION AND METEORITIC EVIDENCE REGARDING PARENT BODIES, M. E. Lipschutz, Dept. of Chemistry, Purdue University, W. Lafayette, IN 47907.

Data from ordinary chondrites strongly constrain the properties of their parent bodies. Meteorites provide a biased sampling of the known asteroids and derive from a comparatively small number of possible parents. Chronometers and barometers indicate parent bodies in the 100-km range. Contradictory views have been presented on the internal structures of ordinary chondrite parent bodies.

Antarctica is a very rich source of meteorites that fell 0.1-1 Myr ago. Many properties of ordinary chondrites recovered from there differ, on average, from those of modern falls, with increasing evidence that these reflect preterrestrial thermal history differences for the populations. These differences lead to the highly controversial suggestion that the meteoroid sources sampled by the Earth have varied on the Myr time scale. This suggestion continues to be tested (e.g. Wolf and Lipschutz, 1991): the recent identification of near-Earth asteroid streams (Drummond, 1991) and meteorite streams (Halliday et al., 1990) also seem relevant to the question of meteorite flux variations.

The similarities of the surface reflectance properties of certain meteorite and asteroid types imply that the nature of asteroid surfaces can be approximated by meteorite analogues. However, spectral properties of ordinary chondrites (the most common meteorite types) differ from those of the abundant S asteroids, like Gaspra, and no known process can reconcile these. The closest asteroidal analogues to mildly shocked ordinary chondrites are near-Earth Q asteroids – which may be parts of Group I and III asteroid streams (Drummond, 1991). Why abundant meteorite types have rare asterodal analogues, and why an abundant asteroid type has rare meteorite analogues are open questions that clearly will be studied further.

This paper is adapted from the chapter by Lipschutz, Gaffey and Pellas in the Asteroids II volume (pp. 740-777) and was supported by NASA grant NAG 9-48.

REFERENCES

J. D. Drummond (1991) Earth-approaching asteroid streams. Icarus 89, 14-25.

I. Halliday, A. T. Blackwell and A. A. Griffin (1990) Evidence for the existence of groups of meteorite-producing asteroidal fragments. Meteoritics 25, 93-99.

S. F. Wolf and M. E. Lipschutz (1991) Labile trace element comparisons in H chondrites from Victoria Land and Queen Maud Land: A progress report (abstract) 54th Ann. Mtg., Meteoritical Soc.

PRIME LAB: A DEDICATED AMS FACILITY FOR EARTH AND PLANETARY SCIENCE RESEARCH, M. E. Lipschutz*, S. Vogt*, D. Elmore†, F. A. Rickey† and P. C. Simms†, Depts. of Chemistry (*) and Physics (†), Purdue University, W. Lafayette, IN 47907.

A dedicated Accelerator Mass Spectrometry (AMS) facility based on an existing 8 MeV tandem Van de Graaff accelerator is being developed at Purdue University for the measurement of cosmogenic radionuclides – mainly ^{10}Be, ^{26}Al, ^{36}Cl, ^{41}Ca and ^{129}I – in terrestrial and extraterrestrial samples, including meteorites. The primary activity of PRIME Lab will be AMS, which is planned to use ~90% of the beam time. Elmore and Phillips (1987) have previously described the AMS technique.

The facility start-up phase is being funded by Purdue and the National Science Foundation. In this phase, the first 3 cosmogenic radionuclides will be measured at 3-5% precision in a few hundred samples. With additional funding, we plan to provide rapid isotope cycling, and fully automate the AMS measurements. This will enable us to add additional cosmogenic radionuclides to our suite, improve precision to $\leq$1%, and increase capacity to several thousand samples annually.

We describe the facility and report the results of measurements of cosmogenic radionuclides in a suite of Canyon Diablo meteorites from known recovery sites at the Barringer Crater. The shock histories and cosmogenic noble gas contents of these samples had previously been determined by Heymann et al. (1966). At the preparation time of this abstract, only ^{36}Cl has been measured and in but a few samples. The data exhibit a strong inverse dependence on (^{3}He or ^{4}He)/^{21}Ne – i.e. depth – as expected from nuclear processes.

This work was supported by NSF grant EAR 89-16667.

REFERENCES

D. Elmore and F. M. Phillips (1987) Accelerator mass spectrometry for measurement of long-lived radioisotopes. Science 236, 543-550.

D. Heymann, M. E. Lipschutz, B. Nielsen and E. Anders (1966) Canyon Diablo meteorite: Metallographic and mass spectrometric study of fifty-six fragments, J. Geophys. Res. 71, 643-661.

THE ROLE OF SULFUR IN PLANETARY CORE FORMATION

K. Lodders and H. Palme, MPI für Chemie, Saarstr.23, 6500 Mainz, Germany

Formation of a metal or metal-sulfide core in a planet or asteroid will cause removal of siderophile and/or chalcophile elements from the silicate mantle into the core. The absolute and relative abundances of siderophile and chalcophile elements in the residual mantle are, therefore, sensible indicators for the type and extent of core formation. To determine the involvement of sulfides during core formation, Fe-sulfide/silicate liquid partition coefficients of Mo, W, As, Sb, Co, Ga, Cu, Zn, Mn, Cr, Na, K and Br were experimentally studied.

Experimental: Experiments were conducted in a similar way than reported previously for Mo and W (Lodders & Palme 1991). Sulfide compositions varied from Fe-metal saturated sulfides (three coexisting phases Fe-metal, sulfide liquid and silicate melt) to S-rich sulfides (two coexisting phases, no solid metal).

Results:

(1) Mo, W, Ga, As, Sb, Co: Partition coefficients (D) decrease with increasing S-content of the Fe-sulfides reflecting the more siderophile than chalcophile character of these elements. The increasing D can be explained by increasing amounts of Fe-metal. This allows to calculate metal/silicate partition coefficients (see Table 1).

(2) Cu, Zn, Cr, Mn, Na, K, Br: Partition coefficients increase with increasing S-content of the Fe-sulfides. These elements show more chalcophile than siderophile tendencies, although low absolute partition coefficients indicate their strongly lithophile behavior (except for Cu).

If only two phases coexist (sulfide liquid and silicate melt) fO_2 and fS_2 increase with increasing S-content of sulfides. However, in both groups of elements variations of D with increasing S-content of Fe-S cannot be ascribed to increasing fO_2 and fS_2 alone, but must also reflect changes in the activity coefficients of the elements dissolved in Fe-S.

Implications: The results of this study show, that chalcophile (and siderophile) element abundances in residual mantles will depend on the composition of sulfide removed during core formation. E.g., if during accretion conditions change from reducing to oxidizing, the composition of sulfides will change from Fe-rich to S-rich because of progressive oxidation of Fe. Extraction of elements with siderophile and only weakly chalcophile behavior (W, Mo, Ga) requires the presence of metal or Fe-rich sulfides. These elements are not affected by separation of metal-free, S-rich sulfides. Cu shows the opposite behavior. S-rich sulfides will extract Cu more efficiently than Fe-rich sulfides. Hence, the ratio of the chalcophile element Cu to the siderophile element Mo is a good indicator for the amount of S in the core formation process. The Cu/Mo partition coefficient ratios vary from 6.2 for the S-rich system to 0.42 for the S-free system. The Cu/Mo ratio in the martian mantle (as derived from SNC meteorites, Dreibus & Wänke 1990) is about 0.16 (normalized to CI) reflecting the sulfur rich nature of the martian core. In contrast, the Cu/Mo ratio is about 4 in the Earth's upper mantle indicating the predominant influence of metal separation.

Table 1: $Fe\text{-}S_{liq}/silicate_{liq}$ partition coefficients at 1200°C for variable sulfide compositions

X_S	0.5	0.385	0		0.5	0.385	0
log fO_2	-11.4	-13.8	-13.8		-11.4	-13.8	-13.8
log fS_2	- 2.7	- 5.8	- 5.8		- 2.7	- 5.8	- 5.8
	(a)	(b)	(c)		(a)	(b)	(c)
Sb	100	440	2150	Cu	400	300	150
As	180	420	970	Zn	1.2	0.5	-
Mo	65	150	360	Cr	1.0	0.5	-
W	0.5	2.5	35	Mn	0.35	0.08	-
Co	20	55	180	Na	0.045	0.007	-
Ga	0.13	0.65	5.4	K	0.040	0.006	-
				Br	0.55	<0.1	-

$X_S + X_{Fe} = 1$, (a) $S\text{-rich sulfide}_{liq}/silicate_{liq}$, (b) $Fe\text{-rich sulfide}_{liq}/silicate_{liq}$, (c) $solid\ metal/silicate_{liq}$

Ref.: Dreibus G. and Wänke H. (1990), Adv. Space Res., 10, (3)7-(3)16., Lodders K. and Palme H., Earth Planet. Sci. Lett. (1991), in press.

DYNAMIC CRYSTALLIZATION CHARACTERISTICS OF ENSTATITE CHONDRITE CHONDRULES

Gary E. Lofgren, John M. DeHart, SN-2, NASA Johnson Space Center, Houston, TX 77058 A.B. Lanier, C23, Lockheed ESC, 2400 NASA Rd. 1, Houston, TX 77058.

Although the chemical properties of enstatite and ordinary chondrites are distinctly different (1), they both contain chondrules with a similar array of textures. This similarity suggests like origins. Textural studies using chondrule compositions from ordinary chondrites suggest that these chondrules have an igneous origin: either by crystallization from melts or from partial melts of crystalline material, probably nebular dust. In contrast, the cathodoluminescence (CL) properties of the enstatite from enstatite chondrites have been interpreted to mean that mechanical aggregation played an important part in their formation (2). An alternative interpretation of these CL properties, however, suggests that variations in the minor element content of the enstatite, a probable result of igneous fractionation processes, could also produce different CL colors (3). We will attempt to evaluate the two models by performing dynamic crystallization experiments on an average enstatite chondrule composition and by looking at the resultant CL.

The crystallization characteristics of this E-chondrite chondrule composition are broadly similar to the pyroxene rich (radial pyroxene) composition studied previously (4). The liquidus phase is olivine which is in a peritectic relationship with enstatite. Thus, depending on the nucleation conditions, the resulting crystalline material may or may not have olivine as a significant phase. There are several typical textures for both olivine and pyroxene. For olivine, the barred dendrite is common for melts which experienced temperatures above the liquidus. These textures are not like the barred dendrite in the olivine rich compositions which dominate the entire charge, but sparse dendrites enclosed in a matrix of enstatite, usually spherulitic or dendritic. At melt temperatures at or just below the liquidus, skeletal or hopper olivine microphenocrysts and/or large phenocrysts prevail. These olivines can be quite large and grow beyond nominal modal proportions of the melt. Pyroxene textures dominate if pyroxene nuclei are present in near liquidus or subliquidus melt runs because enstatite will crystallize readily. Slightly skeletal enstatite which encloses rounded olivine, whose growth preceded the enstatite, dominate at the slower cooling rates (5-50°C/hr). At the faster cooling rates the enstatite is dendritic and/or barred and may also contain barred olivine dendrites. If large numbers of nuclei are present, the texture becomes granular and the crystals decrease in size in proportion to the increase in the number of nuclei. Olivine crystals are mixed with the enstatite if the melting occurs reasonably close to the liquidus.

The CL of the experimentally grown enstatite is mostly red to purplish red with blue intermixed in a striated pattern. The CL color was determined under the electron microprobe beam at a potential of 15KeV and a current of 300na. The bluish areas have slightly lower Cr and Mn contents. The Cr in the bluish enstatite is approximately .15 wt % as opposed to >0.2 for the red. The Mn is typically 0.05 wt. % in the blue and 0.1 in the red enstatite. There is overlap in these values, but they do correspond to the approximate values reported for naturally occurring red and blue enstatite (2,3). The close association of the red and blue enstatite must be a growth phenomena. It has the superficial appearance of exsolution lamellae or an intergrowth of ortho (blue) and clinoenstatite (red), but the only compositional differences are in the minor elements.

The textures grown experimentally crystallized E-chondrite melts confirm that formational processes are similar to those for the ordinary chondrites with the obvious exception of the oxidation state. A first look at the CL of these enstatites suggests that mixed blue and red CL colors in a single chondrule or grain could result from growth processes.

REFERENCES: (1) Keil K. (1989) Meteoritics **24**, 195-208. (2) Leitch C.A. and Smith J.V. (1982) Geochim. Cosmochim. Acta **46**, 2083-2097. (3) McKinley S.G. et al. (1984) Jour. Geophys. Res. **89**, B567-B572. (4) Lofgren G.E. and Russell W.J. (1986) Geochim. Cosmochim. Acta **50**, 1715-1726.

RELATED COMPOSITIONAL AND CATHODOLUMINESCENCE TRENDS IN CHONDRULES FROM SEMARKONA Lu Jie[1], D.W.G.Sears[1], P.H.Benoit[1], M.Prinz[2] and M.K.Weisberg[2]
[1]Cosmochemistry Group, Univ. Arkansas, Fayetteville, AR 72701. [2]Amer. Mus. of Nat. Hist., NY, NY 10024.

Because of their dependence on mineral composition and texture, cathodoluminescence (CL) properties are very useful in sorting out the variety of chondrule types (1). Here we report on our continuing study of the CL of chondrules from the most primitive ordinary chondrite, Semarkona. We call chondrules which display CL Group A, and those without CL Group B; these groups are not necessarily related to textural types. Group A are subdivided into A1 (yellow CL mesostasis, red CL ol/px) and A2 (yellow CL mesostasis, dull red or non-CL Ol/Px). Table 1 lists the data for the 23 chondrules studied. Group A1 chondrules include type IA and others, A2 are mostly PP, while Group B include type II and others (2).

Normalized INAA data for Group A1 and A2 chondrules show depletions which increase with volatility from Mg to K, whereas group B chondrules show a flat pattern for all lithophiles (Fig. 1). Group A chondrules all have a positive Eu anomaly and a slight enrichment in Yb and Lu, especially in A2, while the anomaly is weak or absent in Group B (Fig. 2). The differences in REE behavior are related to the composition and oxygen fugacity of the different groups; Eu tends to be higher in CaO-rich, low fO_2 melts.

This study demonstrates that the unusual volatile-depletion patterns and Eu enrichments in some Semarkona chondrules are not rare phenomena since Group A chondrules constitute 35% of the chondrules present (4). Such chondrules cut across all textural types. The data appear to suggest that chondrules within Groups A and B are genetically related, but that the two CL groups are fundamentally distinct from each other. These results may be applicable to other type 3 chondrites, since similar CL subdivisions are present, although metamorphism has changed the details.

Table 1.

Chond.	CL Color mesos.	CL Color grains	Text.	Mesos. CaO(%)	Fa	Fa
Group A1						
31-1	yellow	red	POP	16.6	0.6	1.4
23-5	yellow	red	PO	20.0	0.5	--
22-4	yellow	red	PO	18.9	0.5	--
30-6	yellow	red	POP	15.8	0.5	0.8
28-12	yellow	red	BO	17.0	0.8	0.8
2-12	yellow	red	POP	16.6	0.6	2.2
2-8	yellow	red	POP	14.0	0.4	0.8
24-6	yellow	red	--	--	--	--
Group A2						
3-10	yellow	d. red	PP	10.5	--	2.0
26-5	yellow	d. red	PP	9.3	3.3	4.8
20-5	yellow	d. red	PP	12.5	--	3.7
23-18	yellow	d. red	PP	10.8	1.7	2.8
22-10	yellow	none	PP	8.9	7.9	4.0
22-3	yellow	none	PP	10.0	3.5	5.0
23-2	yellow	none	--	--	--	--
23-8	yellow	none	POP	1.6	8.3	8.1
28-1	yellow	none	POP	18.6	20.8	13.8
20-1	yellow	none	BO	10.4	23.2	19.2
Group B						
7-3	none	none	POP	6.4	22.3	12.9
29-11	none	none	PO	0.83	10.3	--
30-5	none	none	POP	2.28	12.8	11.8
22-12	none	none	POP	1.05	15.3	27.8
10-2	none	none	C	--	--	--

Fig. 1

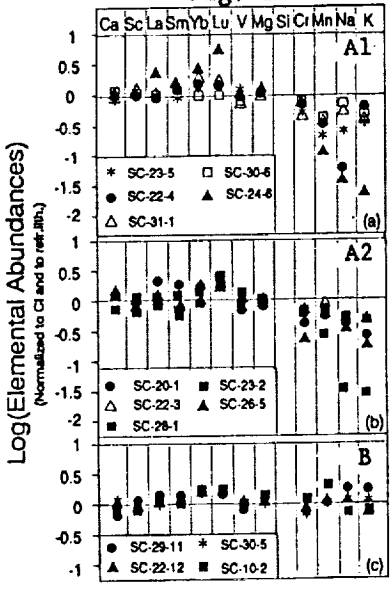

Fig. 2

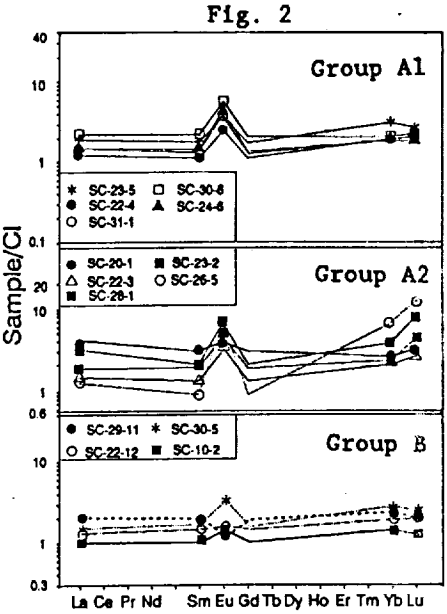

1. Sears et al. (1990) In Spectroscopic Characterization of Minerals and their Surfaces, (Coyne et al., eds.), 190. 2. Scott and Taylor (1983) Proc. LPSC 14th, B275. 3. Lu et al (1990) LPSC XXI 720. 4. DeHart (1989) PhD Thesis.

ABUNDANCE RATIOS OF MOLYBDENUM ISOTOPES IN SOME IRON METEORITES

Qi Lu[1,2] and Akimasa Masuda[1]. [1] Department of Chemistry, Faculty of Science, the University of Tokyo, Hongo 7-3-1, Bunkyo-ku, Tokyo, 113, Japan.
[2] Department of Chemistry, Inner Mongolia University, Huhhot, China.

Investigations of the isotopic compositions of elements in meteorites supply important chronological clues to the early solar system and some of its planetary members. Potentially, Mo is a very interesting element. However, few studies of isotopic abundances of Mo have been performed with some success in a search for isotopic abundance anomalies in Mo from iron meteorites. In this study, the procedures have been developed so that microgram quantities of Mo can be cleanly and efficiently separated from gram quantities of iron meteorite. The isotopic abundance of Mo in iron meteorites can subsequently be determinated with high accuracy by using thermal ionization mass spectrometry.

First, the chemical separation of Mo, Zr and Ru from Fe, Ni, Cu and Cr was undertaken by application of anion exchange (AG 1-X8, 100-200 mesh). It was found that the separation of Mo from Zr and Ru in meteorite can not be achieved under the conditions of previous work (1,2). The result of this study indicates that Mo, Zr and Ru can be separated cleanly with the elutions of 6 M HCl and 7 M HNO_3 after removal of Fe, Ni, Cu and Cr by 1 M HF-0.01 M HCl. A further purification of Mo was performed by extracting Mo into HDEHP-cyclohexane phase, and then back-extracting Mo using 3% H_2O_2 in 7 M HNO_3 (3).

The abundance ratios of Mo isotopes were measured by a thermal ionization mass spectrometer, and normalized against $^{94}Mo/^{98}Mo = 0.3802$, based on our high accuracy measurement of isotopic abundances of molybdenum in some terrestrial molybdenites (3). The iron meteorites selected here are Canyon Diablo, Odessa and Hardesty. The data thus obtained are not in agreement with those available in literature (1,2). In comparision of the meteoritic ratios of this study with the means of the terrestrial values, we found that all three Mo^{96}/Mo^{98}, Mo^{97}/Mo^{98} and Mo^{100}/Mo^{98} ratios agree, respectively, with the means of the terrestrial values. Thus far, there appears no evidence for a significant deviation of the meteoritic values from the terrestrial ones except for Mo^{92}/Mo^{98} and Mo^{95}/Mo^{98}. The ratio of Mo^{92}/Mo^{98} in Canyon Diablo is significantly high (about 3ε) for which there is at present no satisfactory explanation. However, the small depleption (about -1ε) of Mo^{95}/Mo^{98} might result from strong neutron irradiation during the early history of the solar system due to the effect that the isotopes Mo^{95} and Mo^{96} have some resonance peaks with high absorption cross sections for neutrons in the 100 eV range (1).

(1) V. Rama Murthy (1963) Geochim. et Cosmochim. Acta, pp. 1171-1178.
(2) G. W. Wetherill (1964) J. Geophysical Research, pp. 4403-4408.
(3) Qi Lu and A. Masuda, in preparation.

ISOTOPE SYSTEMATICS OF CUMULATE EUCRITE EET-87520.

G.W. Lugmair[1], S.J.G. Galer[1,2], R.W. Carlson[3]; [1]Scripps Inst. of Ocean., Univ. of Calif. San Diego, La Jolla, CA 92093; [2]Max Planck Inst. fuer Chemie, Mainz, Germany; [3]Carnegie Inst. of Washington, 5241 Broad Branch Rd. N.W., Washington, DC 20015.

Sm-Nd, Rb-Sr and U-Pb isotopic data were obtained on unwashed whole rock (*WR*) and high purity washed mineral separates - plagioclase (*Plag*), pigeonite (*Pig*), augite (*Aug*) and troilite (*Tro*, Pb only) - from the cumulate eucrite EET-87520.

Rb-Sr: The Rb-Sr system is highly disturbed and does not yield useful information for dating purposes. The $^{87}Sr/^{86}Sr$ ratios for the main mineral phases are high for a cumulate eucrite and range from 0.69925 for *Aug* to 0.69945 for *Pig* with *Plag* being intermediate. The (unwashed) *WR* ratio is higher still (0.69971) and indicates severe contamination. In spite of thorough washing of the mineral separates Rb/Sr ratios are also high and yield initial $^{87}Sr/^{86}Sr$ far below reasonable values.

Pb-Pb, U-Pb: A large amount (0.2-1.0 ppm) of slightly radiogenic modern terrestrial Pb (MT-Pb) was removed by the 2N HCl wash from the mineral phases. Concentrations of Pb in the washed mineral phases are extremely low, being 22 ppb in *Plag*, 19 ppb in *Pig*, 16 ppb in *Aug* and 12 ppb in *Tro*. The small *Tro* separate contains mostly MT-Pb even after washing, indicating that *Tro* is not a major Pb carrier in eucrites. When corrected for MT-Pb the *Tro* and *WR* Pb isotopic compositions are indicative of an indigenous highly radiogenic component similar to the two pyroxenes. *Plag* has an isotopic composition of $^{206}Pb/^{204}Pb$ = 29.07 and $^{207}Pb/^{206}Pb$ = 1.196 which is quite exceptional; this reflects a history of radiogenic Pb growth at an enormous μ before isotopic closure. The *Plag-Pig* pair yields a relatively imprecise Pb-Pb age of 4.42±2 Ga which is slightly discordant with its respective U-Pb age. Like the Rb-Sr system, U-Pb appears to have been disturbed, questioning the true significance of the Pb-Pb age. The model two-stage μ_1 of 222 and radiogenic initial $^{206}Pb/^{204}Pb$ = 19.0 and $^{207}Pb/^{206}Pb$ = 1.52 appear fairly robust, however. The Pb-Pb age is decidedly younger than the Sm-Nd age, a result that has not been observed with other cumulate eucrites. The high μ_1 is broadly consistent with the inferred *WR* μ_1 indicating that the Pb-Pb system may reflect a "cooling" age, with the older Sm-Nd age giving the time of formation. None the less, it is not clear whether cooling could reasonably have taken as long as ~140 Ma.

Sm-Nd: In contrast to the other isotope systems the Sm-Nd data are much more coherent, though not totally undisturbed. If all data from *Plag, WR, Aug,* and *Pig* are used an age of 4.598±7 Ga is calculated, but with *Pig* slightly above and *Aug* below the best fit isochron line. If the *Pig* data are omitted the age becomes 4.547±9 Ga, but with a slightly elevated initial $^{143}Nd/^{144}Nd$. However, this small disturbance has no significant effect on the ^{146}Sm-^{142}Nd system. The latter yields $^{146}Sm/^{144}Sm$ = 0.00694±45 with an initial $^{142}Nd/^{144}Nd$= -2.71±0.23 ϵ units. These values are in excellent agreement with our recent data for the angrite LEW 86010, which has a Sm-Nd age of 4.55±3 Ga and a very precise Pb-Pb age of 4.5577±4 Ga. Thus, both the slightly disturbed Sm-Nd isochron for this exceptional cumulate eucrite EET 87520 and the precise $^{146}Sm/^{144}Sm$ point towards a very early differentiation of its parent body and may help clarify the history of other cumulate eucrites exhibiting ~100 Ma younger ages.

OXYGEN ISOTOPES IMPLANTED IN THE LDEF SPACECRAFT; I C Lyon, J D Gilmour, J M Saxton and G Turner, Geology Department, Manchester University, Manchester M13 9PL, UK.

The elemental and isotopic composition of the atmosphere is well mixed below 110 km, but above this height atoms separate out according to the scale height, RT/mg. By 330 km, the height at which much of LDEF's exposure occurred, $^{18}O/^{16}O$ is only half its value in the lower atmosphere. Depth profiles of ^{16}O and ^{18}O have been measured in stainless steel nuts and copper sheet (from a grounding strap) recovered from the leading surface of LDEF. The material encountered an estimated oxygen fluence of around 10^{21} ^{16}O atoms m^{-2}. Depth profiles were measured using a VG Isolab 54 multicollector ion probe. 10 to 100 um spots were analysed using a Cs^+ primary ion beam to generate O^- secondaries. ^{16}O was measured on a Faraday collector, at a mass resolution of 500, and ^{18}O by counting on a micro channel plate with a resolution of 2000 (to resolve ^{16}OD interference). Ratios were normalised to an oxygen 'standard' obtained by oxidising copper sheet in air with a heat gun. Typical experimental conditions were; primary ion current, 1-5 nA; secondary ion currents, ^{16}O $2x10^{-12}A$, ^{18}O $1\text{-}2x10^4$ cps.

Plots of $^{18}O/^{16}O$ as a function of time (equivalent to depth) show large depletions, up to a factor of 2, in ^{18}O relative to ^{16}O at the surface, and return to normal values in the interior. The ^{16}O current decreases by two orders of magnitude in the interior and the corresponding profile of anomalous ^{16}O, is strongly peaked in the outer few tens of nanometres of the surface (fig 1). The depth scale in fig.1 is a tentative one based on an estimated sputtering rate.

Plots of $^{18}O/^{16}O$ against $1/^{16}O$ (figs 2 and 3) should be straight lines if two isotopically distinct components, one of variable concentration (orbital oxygen) and one of fixed concentration (normal oxygen) are mixed. The observed departures from a straight line may result from variability in the background concentration of normal oxygen. This may be the case for the leading surface which is darkened, possibly as a result of spacecraft outgassing. Curvature may also arise from variations in the isotopic composition of the anomalous oxygen (as might arise from different implantation depths). Oxygen in the unexposed surfaces of the stainless steel nuts is normal, but leading and trailing surfaces of the Cu both contain anomalous oxygen, possibly due to scattering. The observations show that isotopic composition may be used as a clear and sensitive fingerprint of exposure to oxygen in near Earth orbit. Implications for micrometeoroid and other measurements will be discussed at the meeting.

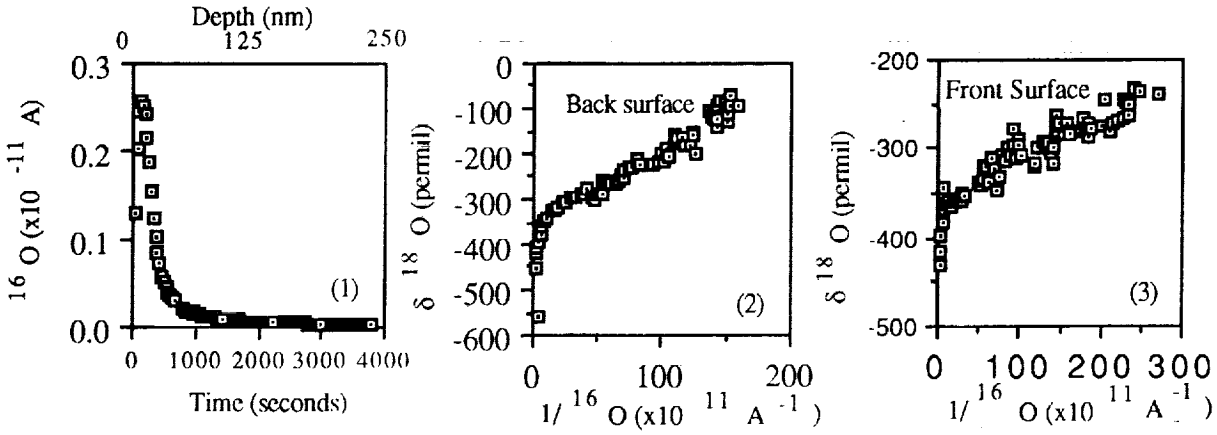

THE 1095 AD METEOR EVENT AS DESCRIBED IN THE ANGLO SAXON CHRONICLE; E. G. Mardon, A. A. Mardon, Red Deer College, Red Deer, Canada, Texas A & M University, College Station, Texas, USA.

This research paper is a critical examination of the one reference found in the various manuscripts of the Anglo Saxon Chronicle between 538 AD and 1140 AD that refers to a Meteor shower event [1095 AD]. Thirty five astronomical events are described in the Anglo Saxon Chronicle, which is also referred to as the Old English Annals. The Anglo Saxon Chronicle is an Old English history of events begun under the direction of King Alfred the Great in the 9th Century and containing earlier material in adapted form. It was written from records kept by various English Monasteries. After the account of King Alfred's wars which started with the invading Danes, the Chronicle was officially kept up year by year until the last entry dated for 1154 AD It survives in seven manuscripts, although the Anglo Saxon Chronicle contains non-factual material and legends, and references the eclipse of the Sun and the Moon being often verifiable through other contemporary or near contemporary sources, for example, the Bayeux Tapestry contains a panel of the 'long-haired comet', that appeared in 1066 AD, and few months prior to the invasion of England by William the Conqueror.

The following is the text entry of the 1095 AD meteor event:

ANNO MXCV "and ſa uppon Eastron on sce Ambrosius mæsse niht. *ƒ* is ii nõ Apr' wæs gesewen for neah ofer eall ſis land swilce for neah ealle ſa niht swiðe mæni fealdlice steorran of heofenan feollan. naht be anan oððe twam." [original Anglo Saxon]

1095 AD...there was on the second night before the none of April was across the land such stars falling from the heavens, not as individual but in groups of two.

The 1095 AD reference to a meteor shower only appeared in the Parker manuscript. No other meteor references exist in the Anglo Saxon Chronicle. The Lyrids meteor shower currently peak on April 21st. Chinese medieval chronicles state that the Lyrids were very intense. No actual linking has been successfully achieved by the author between this Western European astronomical reference in 1095 AD and contemporary Chinese meteor shower references.

Bibliography

The Parker Chronicle. Edited A. H. Smith. New York: Appleton-Century- Croft, 1966.

PROGRESS IN THE ACAPULCO CONSORTIUM; K. Marti[1], J. S. Kim[1], Y. Kim[1], B. Lavielle[1], and M. Prinz[2], [1]Department of Chemistry, University of California, San Diego, La Jolla, CA 92093-0317. [2]American Museum of National History, New York 10024-5192

The Acapulco meteorite, an exceptional object with chondritic bulk composition, a high degree of recrystallization and abundances of some volatiles close to CI chondrites, has received much attention and is currently studied by a consortium. Recrystallization under redox condition intermediatebetween those of H and E chondrites was inferred (1), but the O and N isotopic compositions of Acapulco (2, 3) are inconsistent with an origin from either H- or E- chondrite parent bodies. An old ^{147}Sm-^{143}Nd internal isochron age of 4.60 ± 0.03 Ga was determined (4), but the coupled chronometers ^{146}Sm-^{142}Nd and ^{147}Sm-^{143}Nd seem to reflect some internal inconsistences. At least two distinct N isotopic signatures (3) show that their carriers were not equilibrated and similar evidence has been observed in an Acapulco metal concentrate (5). Another unusual feature is the frequent occurrence of swarms of Fe-Ni blebs in the cores of orthopyroxene crystals which reveal the composition of normal metal grains, rather than Ni-free Fe expected from reduction reactions.

We have measured Xe and Ar in bulk and in separates (magnetic, nonmagnetic and high-purity metal), as well as Xe and N in HCl-treated silicates. The observed concentrations of trapped heavy noble gases are significantly larger than in equilibrated ordinary chondrites and they are enriched in a magnetic separate. Fission Xe compositions due to ^{244}Pu are observed in both, the magnetic and the non-magnetic fractions. In contrast to the trapped noble gases which are predominantly released at high temperature, the distribution of radiogenic ^{129}Xe is interesting. Major release peaks are observed in the low-temperature (600 °C) fractions of bulk Acapulco, the magnetic fraction (pyrolysis and combustion steps) and the nonmagnetic separate. Although the carrier(s) of extinct ^{129}I have not been identified, we can rule out major silicate phases and metal. A stepwise release of N in the silicates, in pyrolysis and combustion steps, does reproduce the pattern of "heavy" N observed in bulk Acapulco, but no evidence for the presence of "light" N has been obtained. This component so far was observed only in the metal separate (5)

References: (1) Palme H., Schultz L., Spettel B., Weber H. W., Wänke H., Michel-Levy C. M., and Lorin J. C. (1981) *Geochim. Cosmochim. Acta 45*, pp 727-752. (2) Mayeda T. K and Clayton R. N. (1980) *Proc Lunar Planet. Sci. Conf. 11th*, pp 1145-1151. (3) Sturgeon G. and Marti K. (1991) *Proc. Lunar Planet. Sci. Conf. 21th*, pp 523-525. (4) Prinzhofer A., Papanastassiou D. A., and Wasserburg G. J. (1990) *Lunar and Planet. Science XXI*, 981-982. (5) Becker R. (1991) *Lunar and Planet. Science XXII*, 69-70.

BARRINGER MEDAL ADDRESS

IMPACT CRATERS: ARE THEY USEFUL?

V.L.Masaitis, All-Union Geological Research Institute,Leningrad

Impact craters as a special group of natural objects interesting not only for different scientific researches, but for using in industrial and other aims, were determined in relatively recent time. The considered structures may comprice commercial minerals directly connected with the thermodynamic transformations of target rocks (including primary forming ores) or located in craters and controlled by some morphological, structural or lithological factors. In impact craters iron and uranium ores, nonferrous metals, diamonds coals, oil shales, hydrocarbon, mineral waters and some other raw materials occur. Impact diamonds in impactites represent the special variety, they are synchronous to the impact and originated in graphite- or coal-bearing rocks transformed by shock wave. Buried impact morphostructures may be used as natural underground gas storages or storages of liquid waste materials,the crater s depressions on the surface also as storage reservoirs. The possibility of using the geothermal resources from recent impact craters should not be excluded.

The assesment of the global biotic extinctions caused by impact events and evaluation of the influx of crater-forming bodies in geological past gives a possibility to forecast the asteroid threat and permits to compare such cosmic catastrophes with the expected consequence of large-scale use of nuclear weapon or of ecologic pollution.

Investigations of deep structure of impact craters, of their filling and ejecta are exceptionally important for the development of comparative planetology, they are necessary for planning some of the space experiments too. The study of the distribution and the preservation of impact structures and their populations permits to get the significant information concerning the accretion of planets and formation of their crusts, to evaluate the duration of exposure of some types of surfaces, the relations between impact cratering and different exogenic and endogenic processes etc.The investigation of mineral matter and character of its mode of occurence in the craters allows to understand the geological role of rock-forming and structure-forming impact processes with different intensity and essentially distinquished by their parameters from any endogenic processes. Some theoretical models of behavior of mineral matter subject to shock compression, evaporation, melting, brecciation, jetting, moving and subsequent cooling are built up on these results. The possibility of ejection of fragments near to the escape velocity explained the origin of tektite strewn fields, and in case of exceeding such a velocity - the appearance of meteorites from the moon. Some of above mentioned models have applied significance.

The impact cratering research promotes the dismissal of dogmatic ideas of an exclusive role of evolutionary processes in geological history of the Earth and its satellite and of the outer shells of the Earth (including the biosphere) and stimulate the development of notions on the role of stochastic events in such evolution.

SPINEL-BEARING, Al-RICH CHONDRULES: MODIFIED BY METAMORPHISM OR UNCHANGED SINCE CRYSTALLIZATION ? T.J. McCoy[1,2], Aurora Pun[2], and Klaus Keil[1] [1]Planetary Geosciences Div., Dept. of Geology and Geophysics, SOEST, Univ. of Hawaii, Honolulu, HI 96822 USA [2] Inst. of Meteoritics, Dept. of Geology, Univ. of New Mexico, Albuquerque, NM 87131 USA

Al-rich chondrules are rare, yet ubiquitous, components of ordinary chondrites (1). While Al-rich chondrules from unequilibrated ordinary chondrites have received considerable attention, those from metamorphosed chondrites are less well studied. We have studied two spinel-bearing, Al-rich chondrules in metamorphosed chondrites from Roosevelt County, New Mexico - RC 071 and RC 072. Compositional variabilities within Al-rich spinels of ordinary chondrites may reflect chondrule crystallization (2) or subsequent metamorphism (3). We have determined the effect of metamorphism on Al-rich chondrule spinels and further elucidated the diversity of materials and processes present during chondrule formation.

These two Al-rich chondrules are dominated by large (100 μm), picotitic Al-Cr-rich spinels (14.2 and 21.1 vol. %), which are strongly and asymmetrically zoned. Cr_2O_3 and FeO are enriched at the grain edge closest to the chondrule exterior and decrease steadily to the grain edge nearest the chondrule interior. Al_2O_3, MgO and ZnO show the reverse behavior. These chondrules have undergone metamorphism, which homogenized the chondrule olivines. The formation of the asymmetric zoning in the spinels is inconsistent with diffusional modification during metamorphism, which produces symmetric zoning, as seen by Fe-Mg diffusion in olivines and Ni diffusion in taenite grains in metamorphosed chondrites. Further, chromites (which are present in both chondrules) are nearly absent in zones around the picotitic spinels. Such a depletion would not result from any metamorphic process. Instead, we support the idea of (1) that the spinels depleted the surrounding melt of Cr_2O_3 as they grew inward from the chondrule edge, forming the asymmetric zoning. The composition and zoning of these spinels was largely established during crystallization, although we cannot rule out some diffusive modification for minor elements.

The bulk compositions of these chondrules suggest affinities with the subgroup of Na-Al-Cr-rich chondrules (1), as expected from the abundance of Al-Cr-rich spinels, but extend the lower limit of Na contents of this subgroup. Formation of these chondrules by melting of rare and unusual precursor components is indicated. One of these precursors must have included abundant Cr_2O_3, suggesting a spinel-rich precursor. Despite nearly identical bulk compositions with other Na-Al-Cr-rich chondrules, these two chondrules have a much higher modal content of spinels than other members of this group (1). This suggests that factors other than bulk composition, such as peak temperature and cooling rate during crystallization, control the chondrule mineralogy. These two chondrules cooled rapidly, as evidenced by the presence of glass, localized chromite depletions and spinel sizes (4). Cooling from above the liquidus is suggested by spinel location within the chondrule (4) and the radiating texture of one of the chondrules (5). Since other Na-Al-Cr-rich chondrules exhibit different modal mineralogies, but have similar bulk compostions, a range of peak temperatures and cooling rates is indicated. We see no reason to believe that this range of thermal conditions is fundamentally different from those experienced by "normal" Fe-Mg-rich chondrules.

References: (1) Bischoff A. and Keil K. (1984) *GCA* 48, 693-709. (2) Fudali R.F. and Noonan A.F. (1975) *Meteoritics* 10, 31-40. (3) Wlotzka F. (1985) *LPSC XVI*, 918-919. (4) Stolper E. and Paque J.M. (1986) *GCA* 50, 1785-1806. (5) Hewins R.H. (1988) In *Meteorites and the Early Solar System*, 660-679.

OLIVINES IN ANGRITE LEW87051: PHENOS OR XENOS? G. McKay (SN2, NASA-JSC, Houston, TX,77058) L. Le, and J. Wagstaff (Lockheed ESCO, 2400 NASA Rd. 1, Houston, TX 77058)

Nyquist et al. [1] recently reported the presence of live ^{53}Mn in angrite LEW 86010 when it crystallized. Hence, melting must have occurred within ~10Ma of accretion of the angrite parent body, and LEW 86010 is the oldest known differentiated meteorite. This discovery has made it even more desirable to understand the petrogenesis of angrites, which presumably were all formed at a similar time. As part of our continuing work on angrite petrogenesis, we have conducted crystallization experiments on LEW 87051, the other antarctic angrite, to clarify its petrogenesis. This abstract reports several aspects of our experimental results.

LEW 87051 consists of coarse subhedral to euhedral zoned olivine crystals (~Fo60-90, typical grainsize ~0.5mm) set in a fine-grained intergranular matrix composed primarily of elongate anorthite and interstitial olivine, kirschsteinite, and fassaitic pyroxene [2,3]. The groundmass clearly represents a crystallized melt. Groundmass ferromagnesian minerals are zoned to nearly Mg-free compositions, indicating fairly rapid cooling with nearly perfect fractional crystallization.

The large olivine crystals in LEW 87051 consist of volumetrically minor Cr-enriched cores, in which Cr decreases with decreasing Fo, and volumetrically dominant rims, in which Cr increases with decreasing Fo (Fig. 1). A major question concerning the petrogenesis of this sample is the relationship of these large olivine crystals to their host melt. At LPSC XXI, Prinz and co-workers [2] suggested that the large olivines are xenocrysts, grossly out of equilibrium with the melt, while we [3] interpreted at least the rims as phenocrysts whose fractional crystallization from a more primitive, olivine-rich melt produced the groundmass. To clarify this relationship, we have conducted experiments to determine the phase relations and major, minor, and trace element partitioning behavior for LEW 87051.

At fo_2=IWx10 (the value we prefer for angrite crystallization [4]) a synthetic LEW 87051 analog (L7) crystallizes olivine alone from 1420-1320°C, where Al,Cr-rich spinel appears. At 1220°C, after crystallization of ~25% olivine and a trace of spinel, plagioclase appears. Olivine/Liquid values for D_{Ca} and D_{Cr} are shown in Fig 2. D_{Ca} is constant, while D_{Cr} increases slightly over the crystallization interval (1420-1220°C). Note that the behavior of Cr changes from incompatible to compatible over this interval.

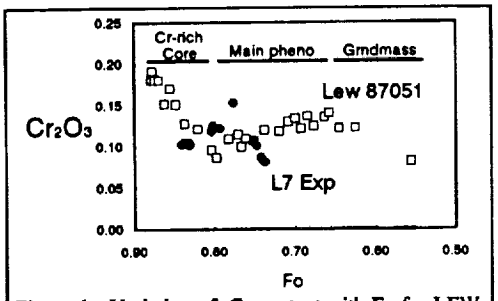

Figure 1, Variation of Cr content with Fo for LEW 87051 natural olivines and olivines from our L7 experiments.

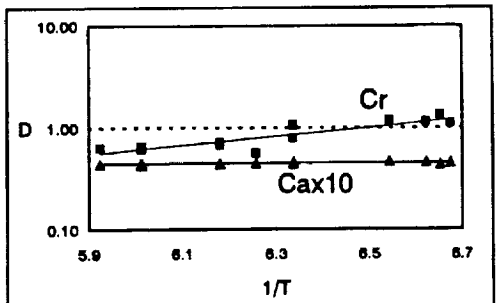

Figure 2. Variation of olivine D(Cr) and D(Ca) with 1/T along crystallization path of LEW 87051 (IWx10). D(Ca) is essentially constant, while D(Cr) increases with falling T. Note that Cr changes from slightly incompatible to slightly compatible over this crystallization interval.

Comparison of compositional trends in the synthetic olivine crystals with those in LEW 87051 olivine phenocrysts (Fig. 1) reveals some interesting contrasts. Except for the Cr-rich cores (~Fo_{90} - Fo_{80}), Cr in the natural olivine phenocrysts increases continuously from core to rim (~Fo_{65}), and then falls again in the groundmass olivines (Fig 1). We had earlier modeled this continuous increase as resulting from normal fractional crystallization, with D_{Cr} increasing from about 0.6 at the outer edge of the Cr-rich cores to about 0.8 at the phenocryst rims. However, our experimental values for D_{Cr} are closer to unity (Fig. 2), and are too high to explain the gradual increase in Cr in the olivine. Nevertheless, despite these high D values, our more Fo-rich synthetic olivines also show an increase in Cr with decreasing Fo, followed by a decrease at about Fo_{75}. Although we do not yet understand the details, it is clear that the Cr abundance in our experimental olivines must be controlled by spinel crystallization. We plan future experiments to work out the details of the spinel stability field and the Cr mass balance over a range of oxygen fugacities. For now, the relationship of the large olivines to the groundmass remains ambiguous.

References: [1] Nyquist *et al.*(1991) LPS XXII 989. [2] Prinz *et al.* (1990) LPS XXI 979. [3] McKay *et al.* (1990). LPS XXI, 771. [4] McKay *et al.*(1989) LPS XX 677.

OXIDATION DURING METAMORPHISM: ANOTHER ARGUMENT AGAINST S-ASTEROIDS HAVING CHONDRITIC COMPOSITIONS

McSween, Harry Y. Jr., Department of Geological Sciences, University of Tennessee, Knoxville, TN 37996-1410, USA.

New calculations using the normative mineral abundances of ordinary chondrites (1) reveal that, within each ordinary chondrite group (H, L, and LL), mineral proportions vary systematically with increasing petrologic type. Specifically, the ratio of olivine/orthopyroxene increases and the proportion of metal decreases in the sequence type 4 - type 5 - type 6. The mean FeO contents of olivine and pyroxene also increase in this sequence (2). These differences in mineral proportions and mineral compositions reflect progressive oxidation during thermal metamorphism on chondrite parent bodies.

It has generally been assumed, perhaps incorrectly, that metamorphic changes in chondritic asteroids would not result in changes in spectral reflectance. However, metamorphic variations in olivine/pyroxene ratio, as well as in the compositions of these phases, might be observable in spectral data. Variations in the rotational spectra of S-asteroids have been cited previously as evidence that they are igneous bodies (3). In light of the newly documented mineral changes during chondrite metamorphism, we should also explore another possibility: impacts into onion-shell asteroids could locally expose materials of different metamorphic grade and hence with different spectral properties. However, the predicted spectra appear to be inconsistent with this idea as an explanation for S-asteroid spectral variability. Asteroid rotational spectra define a line with positive slope on a plot of band II wavelength versus band II/band I area ratio (2). The latter parameter is a function of the relative abundances of olivine and pyroxene, whereas the former is primarily a function of pyroxene FeO content. Ordinary chondrites of various petrologic types should define a line with negative slope on this diagram, because type 6 chondrites (with higher olivine/pyroxene ratios) have more FeO-rich pyroxenes than type 4 chondrites. Although ordinary chondrite metamorphism might result in observable spectral shifts in both parameters, they would be in the opposite sense from the correlation observed in S-asteroids. Thus the recognition of oxidation during metamorphism does not provide a way to link S-asteroids with ordinary chondrites. References: (1) McSween, H.Y., Bennett M.E. and Jarosewich E. (1991) Icarus 90, 107. (2) Scott E.R.D., Taylor G.J. and Keil K. (1986) Proc. Lunar Planet. Sci. Conf. 17th, E115. (3) Gaffey M.J. (1990) Origin of the Earth, Oxford Univ. Press, 17.

ABLATION OF AUSTRALIAN TEKTITES SUPPORTIVE OF A TERRESTRIAL ORIGIN. W.L. Melnik, Aerospace Engineering Dept., University of Maryland, College Park, Maryland 20742, USA.

The amount of ablation together with the wavelength of concentric rings imprinted on the melt layer when it solidified would normally serve to define the entry conditions of tektite trajectories. Previous studies of tektite ablation (1-5) supported a lunar origin in contrast to the geochemical argument that tektites must be the result of meteorite impact on the earth.

In the previous calculations of ablation of tektites, the estimates of aerodynamic heating were based on correlations of measurements on a surface which catalyzed the recombination of oxygen or nitrogen atoms, whereas tektite glass is essentially inert to such reactions. Consequently the estimated aerodynamic heat transfer rates were higher than those actually encountered by the tektites. The previous results would, at first glance, appear to understate the case for a lunar origin.

Starting from prescribed entry conditions, the trajectories of initially spherical tektites were obtained from numerical integration of Newton's second law using a fourth-order Runge-Kutta method. The rate of ablation, shape and instantaneous mass of the tektite were obtained from numerical solutions of the governing equations, using appropriate estimates of the aerodynamic heating (6). Entry conditions were varied to achieve matching in the ablation depth with the field observations. Trajectories representative of a lunar origin were modeled using a parabolic entry speed. For the terrestrial scenario, tektites were presumed to originate from entrainment of splash ejecta by the vapor cloud produced by impact. It was assumed that they were launched into space along ballistic (suborbital) trajectories, where upon they cooled by radiation and solidified prior to reentry to the earth's atmosphere.

RESULTS: Ablation depths comparable with the maximum value of 10 mm observed on the tektites found at Port Campbell, Victoria (7) required rather shallow entry angles for speeds representative of both lunar and terrestrial origins. However, for these trajectories, the stagnation pressure at the instant ablation ceased would result in no ring waves according to (1), in contrast to the field observations. Adams and Huffaker (3) gave some arguments that question the validity of Chapman's criterion for the occurrence of ring waves on tektites that are subjected to large decelerations.

Although recent results (6) still marginally favored a lunar origin, the latest findings based on just the duplication of ablation depths observed in australites are not entirely conclusive in the identification of tektite trajectories. However, comparisons with the limited data on striae displacement, especially the section of an australite from Pine Dam, unmistakenly require a terrestrial origin for australites. The internal striae pattern appears to be that of a torroidal vortex. The evidence of internal flow structure suggests that the tektite was subjected to external drag prior to its solidification by the time of reentry to the earth's atmosphere.

REFERENCES: (1) D.R Chapman and H.K. Larson (1963), *J. Geophys. Res.*, **68**, 4305. (2) D.R. Chapman (1964), *Geochim. Cosmochim. Acta*, **28**, 841. (3) Adams E.W. and Huffaker R.M. (1964), *Geochim. Cosmocchim. Acta*, **28**, 881-892. (4) D.R. Chapman (1971), *J. Geophys. Res.*, **76**, 6309. (5) J.A. O'Keefe, E.W. Adams, J.D. Warmbrod, A.D. Silver, and W.S. Cameron (1973), *J. Geophys. Res.*, **78**, 3491. (6) Melnik W.L. and O'Keefe J.A. (1990) *Lunar and Planetary XXI*, 783-784. (7) G. Baker (1955), *Proc. Roy. Soc. Victoria*, **67**, 165.

DOUBLET CRATERS AND THE TIDAL DISRUPTION OF BINARY ASTEROIDS; H. J. Melosh and J. Stansberry, Lunar and Planetary Laboratory, University of Arizona, Tucson, AZ 85721.

Out of approximately 28 known terrestrial impact craters with diameters greater than 20 km[1], at least 3 are doublets created by the nearly simultaneous impact of objects of comparable size (See Table 1). The large size and separation of these doublets rule out atmospheric breakup as the agent of dispersion[2,3]. Previous investigations of fragmentation within the Roche Limit are similarly unable to account for the dispersion of the doublets[4,5,6,7,8]. Both the frequency of occurrence and the morphology of the craters and their ejecta blankets make very low angles of impact highly improbable. The recent discovery of an unexpectedly large number of contact binary asteroids[9,10] suggests the possibility that tidal disruption of contact binary asteroids just before impact on Earth might account for doublet craters. After detailed orbital integrations for both equal-size binary components and components of ten times different diameters (as suggested by Table 1), we find that although such asteroids are often disrupted by tidal forces well outside the Roche Limit, the magnitude of the separations Δ, averaged over a random population of impactors, is too small to account for the observed doublet craters. In the most favorable case for large tidal separations ($v_\infty = 0$, density = 2600 kg/m^3) only 3% of the impacts occur with normalized separation $\Delta/a \geq 7$ (and of these, all strike at angles less than 10°). Using the binomial theorem, the probability that the observed occurrence of 3 doublet craters out of a population of 28 impacts is due to a statistical fluctuation is 4.1%. In the least favorable case ($v_\infty \geq 5$ km/sec) with a 0.8% probability of finding $\Delta/a \geq 7$ (all at angles less than 5°), the probability that the observed occurrence is a statistical fluctuation is only 0.14%. In either case, the likelihood that the observed doublets are the result of tidally separated contact binaries is very low. The only rational explanation we can find for the occurrence of doublet craters is an initial population of kilometer-size Earth-crossing objects containing about 20% of binaries separated by 5 times or more of the largest component's diameter. We offer this result as a prediction that may be tested by future radar observations of Earth-approaching asteroids.

Table 1. Terrestrial Doublet Craters

Crater Pair	Crater Age Myr	Crater Diameter D, km	Projectile Diameter* L, km	Separation Δ, km	Normalized Separation** Δ/a
W. Clearwater Lake[1]	290±20	32	3.3		
E. Clearwater Lake	290±20	22	2.1	28.5	11
Ries[11]	14.8±0.7	24	2.3		
Steinheim	14.8±0.7	3.4	0.20	46	37
Kamensk[1,2]	65	25	2.4		
Gusev	65	3	0.16	15	7.5

* Computed from L(km) = 0.039 $D^{1.28}$(km) ** $a = (L_1+L_2)/2$

1. Grieve, R.A.F. (1987) *Ann. Rev. Earth Planet. Sci.* **15**, 245-270. 2. Passey, Q. & Melosh, H.J. (1980) *Icarus* **42**, 211-233. 3. Melosh, H.J. (1981) in *Multi-ring Basins* (eds. Schultz, P.H. & Merrill, R.B.), 29-35. 4. Sekiguchi, N. (1970) *The Moon* **1**, 429-439. 5. Oberbeck, V.R. & Aoyagi, M. (1972) *J. Geophys. Res.* **77**, 2419-2432. 6. Aggarwal, H.R. & Oberbeck, V.R. (1974) *Astrophys. J.* **191**, 577-588. 7. Noerdlinger, P.D. (1980) *Bull. Amer. Astron. Soc.* **12**, 829-830. 8. Dobrovolskis, A.R. (1990) *Icarus* **88**, 24-38. 9. Ostro, S.J., *et al.* (1990) *Science* **248**, 1523-1528. 10. Ostro, S.J., *et al.* (1990) *Astron. J.* **99**, 2012-2018. 11. Movshovich, E. V. & Milyavskii (1986) *Meteoritika* **45**, 112-118.

ACCRETIONARY DUST MANTLES IN CM CHONDRITES: CHEMICAL VARIATIONS AND CALCULATED TIME SCALES OF FORMATION; K. Metzler[1], A. Bischoff[1] and G. Morfill[2]. [1]Institut für Planetologie, Wilhelm-Klemm-Str. 10, 4400 Münster, Germany; [2]Max-Planck-Institut für Physik und Astrophysik, Karl-Schwarzschild-Str. 1, 8046 Garching, Germany

Most CM chondrites represent fragmental or regolith breccias that consist of pristine accretionary rock fragments, embedded in a clastic matrix (1). All coarse-grained chondritic components of these pristine rock fragments (chondrules, CAIs, PCP-rich objects, mineral fragments) are coated by accretionary, protoplanetary dust. The rock fragments consist of roughly 50 vol% of dust (2). The *whole* dusty matter sticks to the surfaces of coarse-grained components in the form of dust mantles; no other type of fine-grained "matrix" was found within these rock fragments. The dust mantles must have formed in dust-rich regions within the solar nebula by the sticking of fine-grained matter to the surfaces of coarse-grained components like chondrules, CAIs, etc.. During the sticking process these components moved independently through the solar nebula as individual objects. During their passage through dust-rich regions chondrules, CAIs, etc. encountered different dust reservoirs with distinct chemical and mineralogical compositions. This successive sampling of different protoplanetary dust reservoirs resulted in the formation of stratified dust mantles consisting of different dust layers. The chemical compositions of these layers directly reflect the chemical variations of the dust reservoirs. Chondrules with up to 5 different dust layers with sharp contacts can be observed. Variations in the Fe/Mg-ratio are the main chemical difference between the different layers. These chemical variations are the result of different modal abundances of Fe-rich minerals like cronstedtite and tochilinite. There is a strong tendency for an increasing Fe/Mg-ratio from the inner layers to the outer ones. Due to modal variations of different dust layers around individual coarse-grained components dust mantles in a single meteorite show considerable chemical variations (3). Nevertheless, the mean chemical composition of dust mantles in various CM chondrites is different (3,4).

A roughly linear dependency between the thickness of an individual dust mantle and the diameter of the corresponding mantled component can be observed (2,3,5). This very important fact seems to be a key to understand the physical conditions of dust mantle formation. The thickness of dust mantles and the diameter of the corresponding cores in several CM chondrites were measured using back-scattered electron images (2,3). On average, the thickness of a dust mantle reaches 22% of the diameter of the enclosed component. These data were used to calculate the time scale of dust mantle formation. Two different models were calculated. The first model assumes a turbulent protoplanetary disk with a fully developed Kolmogorov type frequency power spectrum. The chondrules spend some time in this turbulent environment until they are finally absorbed into the meteorite parent body. During this time small fine-grained material collides with and sticks to the surface of the chondrules. The relative velocity between the grains was calculated according to the expressions given in (6) and (7). For this particular scenario we obtain the result that the thickness of the accreted dust mantle, Δa, should vary proportional to $a_0^{1/2}$, i.e. the square root of the original chondrule radius. If we interpret the measurements in such a way that the scatter of the data points permits such a law, this scenario predicts a lifetime of the chondrule in the dust of $\sim 2 \times 10^4$ years. This assumes subsonic turbulence to exist at a level of 0.1 of the thermal gas speed, cosmic abundance of the elements, a disk column density of 400 g/cm^2 and a chondrule formation region located at 5 A.U..

The second model assumes gravitational settling in a quiescent disk with accretion of dust due to sweeping up of the more slowly settling fine-grained material. In this scenario we obtain the result that Δa varies proportional to a_0, as suggested by the measurements. Again the life time of the chondrules in the dust can be calculated. For cosmic abundances and a formation region located at 5 A.U. we obtain $1{,}4 \times 10^7$ years, clearly much too long! The sedimentation time under these conditions is only about 3000 years. This implies that either some level of turbulence exists in the gas, which allows accretion of dust mantles in a shorter time, or that the dust disk has already become compacted such that the abundance of heavy elements in the central disk region has increased by a factor 1000 over the cosmic level.

(1) Metzler K. and Bischoff A. (1989a), Meteoritics 24, 303-304; (2) Metzler K. and Bischoff A. (1989b), LPS XX, 689-690; (3) Metzler K. (1990) Ph.D. dissertation, University of Münster; (4) Metzler K. and Bischoff A. (1990), 15th Symp. Antarc. Met.,198-200; (5) Metzler K. and Bischoff A. (1991), Geochim. Cosmochim. Acta (submitted); (6) Morfill G. (1985), In *Birth and Infancy of Stars*, Elsevier Sci. Publ. B.V., 693-792; (7) Mizuno H. (1988), Astron. Astrophys. 195, 183.

SIMULATION OF THE INTERACTION OF GALACTIC PROTONS WITH METEOROIDS: ISOTROPIC IRRADIATION OF AN ARTIFICIAL METEOROID WITH 1.6 GeV PROTONS;

The Collaboration of the Experiment LNS 172: R. Michel[1] (Spokesman): J. Audouze[2], F. Begemann[3], P. Cloth[4], B. Dittrich[5], P. Dragovitsch[4], D. Filges[4], U. Herpers[6], H.J. Hofmann[5], B. Lavielle[7], M. Lüpke[1], R. Michel[1], S. Richardt[1], R. Rösel[6], E. Rüter[1], M. Schnatz-Büttgen[1], P. Signer[8], G.N. Simonoff[7], H. Weber[3], R. Wieler[8], W. Wölfli[5], B. Zanda[2,9]; 1 Zentraleinrichtung für Strahlenschutz, Universität Hannover, F.R.G., 2 Institute d'Astrophysique de Paris, France, 3 Max Planck Institut für Chemie, Mainz, F.R.G., 4 Gruppe Strahlungstransport, IKP/KFA Jülich, F.R.G., 5 Institut für Mittelenergiephysik, ETH-Hönggerberg, Zürich, Switzerland, 6 Abteilung Nuklearchemie, Universität zu Köln, F.R.G., 7 CEN Bordeaux-Gradignan, Bordeaux, France, 8 Institut für Kristallographie und Petrographie, ETH Zürich, Schweiz, 9 Muséum National d'Histoire Naturelle, Paris, France

In order to simulate the interactions of galactic protons with meteoroids an artificial meteoroid with a diameter of 50 cm made out of gabbro was irradiated with 1.6 GeV protons, which is the mean energy of galactic protons during times of a quiet sun, e.g. during the Maunder Minimum. A realistic isotropic irradiation of the artificial meteoroid was achieved by superposition of two translational and two rotational movements during a two weeks irradiation at maximum intensity of the Saturne cyclotron at Laboratoire National Saturne/CEN Saclay.

The flux of primary protons was determined by measuring ^{22}Na in a thin 50 cm * 50 cm Al-foil, which shadowed the artificial meteoroid during irradiation and which followed both translational movements. A proton-dose of $1.32 * 10^{14}$ cm^{-2} was accumulated, which is equivalent to 1.4 Ma exposure of a meteoroid in space. The artificial meteoroid had two perpendicular bores, which contained more than 1400 individual targets consisting of pure elements, suitable chemical compounds, natural minerals and degassed meteoritic materials. After irradiation these individual targets inside the artificial meteoroid were distributed to the collaborating laboratories, where the residual product nuclides are investigated by X- and gamma-spectrometry, low-level counting as well as by conventional and accelerator mass spectrometry.

Up to now, depth profiles for more than 200 target/product combinations have been measured. The measurements of stable and long-lived nuclides are still going on. The complete experimental results will provide a comprehensive survey on the production of all relevant cosmogenic nuclides from all contributing target elements. In order to interpret the experimental data, the depth dependent spectra of primary and secondary particles were calculated by Monte Carlo techniques using the HERMES [1] code system. Theoretical production rate depth profiles were calculated from these spectra using experimental and theoretical thin-target cross sections of the underlying nuclear reactions. The model calculations excellently describe the production depth profiles in the artificial meteorite, if reliable cross sections are available. A detailed analysis of all the measured depth profiles allows to distinguish still existing shortcommings of the underlying data base and to improve models describing the production of cosmogenic nuclides extraterrestrial matter. **Acknowledgement**: This work was supported by the Deutsche Forschungsgemeinschaft and the Swiss National Science Foundation. [1] P. Cloth et al., Juel-2203 (1988)

DETERMINATION OF THE ^{81}Kr SATURATION ACTIVITY AND Kr PRODUCTION RATES FOR VARIOUS METEORITE CLASSES; APPLICATION TO EXPOSURE AGES AND TERRESTRIAL AGES; Th. Michel, O. Eugster, and S. Niedermann, Physikalisches Institut, University of Bern, CH-3012 Bern, Switzerland.

In the framework of our study of meteorite exposure ages we determined the concentrations of the radionuclide ^{81}Kr. Until now ^{81}Kr concentrations are known in 9H-, 9L-, 3LL-, and 1E-chondrite, 6 eucrites, 2 howardites, 5 diogenites, 1 aubrite, 2 angrites and 5 anorthositic lunar meteorites. In meteorites, whose terrestrial age is known, the equilibrium concentration ($^{81}Kr_{equ.}$) and the corresponding activity can be measured. The table gives the data for some meteorites.

	$^{81}Kr_{equ.}$		P_{83}	$P_{83}(4\pi)$
	10^{-12}cc/g	dpm/kg	P_{81}	10^{-12}cc/g Ma
H, L, LL-chondrites[1)]	0.023	0.0038	1.66	0.124
E-chondrites (Qingzhen)	0.0113	0.0019	-	0.061
Eucrite (Millbillillie)	0.129	0.0215	1.75	0.74
Eucrite (Stannern)	0.202	0.0337	1.61	1.06
Howardites (Kapoeta, Bholghati)	0.058	0.0097	1.53	0.29
Diogenite (Garland)	0.0135	0.0022	1.58	0.070
Diogenite (Ibbenbühren)	0.0019	0.00032	-	0.0098
Aubrite (Khor Temiki)	0.0089	0.0015	1.84	0.053
Lun. anorth. met. (Y-82192)[2)]	0.221	0.037	1.68	1.21
Angrite (ADOR, pyroxene) [1]	0.43	0.072	1.65	2.31

Errors for ^{81}Kr 10-30%. 1) For shielding corresponding to $(^{22}Ne/^{21}Ne)_c$ = 1.11. 2) 80'000 a terr. age from ^{26}Al and ^{36}Cl [2] corrected.

$^{81}Kr_{equ.}$ depends (among other parameters) on the shielding within the meteoroid and on the concentrations of the target elements. For ordinary chondrites $^{81}Kr_{equ.}$ varies from about 0.03 (at $(^{22}Ne/^{21}Ne)_c$ = 1.07) to 0.015 x 10^{-12} cc/g (at 1.25). For other meteorite classes the shielding dependency could not yet be derived.

The ^{83}Kr production rate P_{83} is calculated from $P_{83} = (P_{83}/P_{81})(^{81}Kr/\tau)$, where $P_{81}/P_{83} = 1.262\ (^{78}Kr/^{83}Kr)_c + 0.381$ [3] and τ = 0.307 Ma. From P_{83} of the different classes the yield factors for ^{83}Kr production from Rb, Sr, Y, and Zr are determined and will be given. The $P_{83}(4\pi)$ values in the table are a factor of 3-4 higher than $P_{83}(2\pi)$ at 40 g/cm^2 (close to peak production) calculated from Regnier et al. [4] and up to 50% lower than P_{83} (4π) calculated from Marti et al. [5].

Exposure ages calculated from $^{83}Kr_c$ and the proposed production rates generally agree with those calculated from cosmogenic ^{21}Ne, ^{38}Ar, and ^{126}Xe. Knowledge of the 4π equilibrium concentration of ^{81}Kr for the various meteorite classes allows us to derive terrestrial ages of antarctic meteorites using Kr data alone from $t_{terr} = \tau \ln (^{81}Kr_{equ.}/^{81}Kr_{meas})$.

Acknowledgements: This work was supported by the Swiss NSF.

References: [1] Lugmair G. and Marti K. (1977) EPSL 35, 273. [2] Vogt S. et al. (1991) GCA, in press. [3] Finkel R.C. et al. (1978) GCA 42, 241. [4] Regnier S. et al. (1979) Proc. LPSC 10th, 1565. [5] Marti K. et al. (1966) Z. Naturforsch. 21a, 398.

PETROLOGY AND GEOCHEMISTRY OF THE EETA79002 DIOGENITE David W. Mittlefehldt, *Lockheed Engineering and Sciences Co., 2400 NASA Rd. 1, Houston, TX 77058* and Ben Myers, *Dept. of Agronomy, University of Arkansas, Fayetteville, AK 72701*

INTRODUCTION. EETA79002 is a brecciated diogenite with a pronounced light-dark structure. Earlier study of 2 clasts indicated that it contains pyroxenes with a range of compositions (1), in contrast to the generally uniform pyroxenes typical of most diogenites (2). We therefore decided to undertake a more detailed study of EETA79002 in order to further define the petrogenetic history of diogenites. We have analyzed 4 whole rock and 10 additional clast samples selected from the interior of the meteorite. Samples were selected to represent the entire range of macroscopically observed lithologic variation.

PETROLOGY. EETA79002 is composed dominantly of orthopyroxene, with minor olivine and chromite. Ubiquitous, but inhomogeneously distributed, 5-50 micron-sized troilite and metal grains are present. Petrographic observations indicate that the metal and troilite grains are more prevalent in the dark samples. They occur in the breccia matrix, as minute spherical inclusions decorating healed fractures in pyroxene and olivine, and in 300-500 micron-sized symplectic intergrowths with pyroxene. Trace amounts of silica and diopside are also found. Pyroxene compositions form a bimodal distribution with most compositions in the range $Wo_{2.1-2.9}En_{71.7-75.6}$ with a peak between $Wo_{2.2-2.4}En_{74.0-75.6}$. A few magnesian pyroxenes are present with compositions of $Wo_{1.7-2.3}En_{78.0-80.2}$. Olivine compositions are Fo_{75-77}. Metal grains have been found with 3 distinct compositions: 1.6% Ni - 0.86% Co; 1.8% Ni - 0.67% Co; and 2.5% Ni - 0.73% Co.

GEOCHEMISTRY. The 16 samples are remarkably uniform in trace lithophile element composition when compared to Johnstown. For example, Yb concentrations in 12 of 16 samples are identical to the mean (0.138 ppm) within analytical uncertainties. For Johnstown, only 10 of 23 Yb literature analyses are within uncertainty of the mean. The REE patterns for EETA79002 samples are parallel with limited dispersion of the LREE (La 5-12 ng/g). In Johnstown, La varies from 7-2680 ng/g (1,3). As La is very sensitive to the amount of trapped liquid component (1), the uniformity of the EETA79002 data indicates little variation of this component. The siderophile and chalcophile element concentrations confirm that the light-dark structure is due to the distribution of metal and troilite grains. Dark samples contain 40-180 ppm Ni, 20-60 ppm Co, and 0.5-3 ppm Se, while light samples contain 10-60 ppm Ni, 10-30 ppm Co, and ≤0.7 ppm Se. There is no enhancement in Cr in dark relative to light samples. The Ni and Co concentrations of the dark samples are consistent with the admixture of ≤1% metal with compositions similar to those measured. Troilite is modally more abundant, but we cannot calculate its abundance in the dark samples.

REFERENCES. (1) Mittlefehldt & Lindstrom (1989) *LPSC XX*, 697-698. (2) Harriott & Hewins (1984) *Meteoritics 19*, 15-23. (3) Floran et al. (1981) *Geochim. Cosmochim. Acta 45*, 2385-2391.

ANOMALOUS SHOCKED QUARTZ IN AUSTRALIAN IMPACT CRATERS. Yasunori MIURA and Toshio KATO, *Department of Mineral Science and Geology, Faculty of Science, Yamaguchi University, Yoshida, Yamaguchi 753, Japan.*

Anomalous quartz with multiple sets of lamellae reveals the following characteristics [1]:

1) Tiny fragments of fine grains (less than 1 mm in size).
2) Higher density (ca. 1% of density deviation):
3) Diffuseness of X-ray intensity peak (ca. 0.3% in cell-dimensions).
4) Pseudo-monoclinic features of structural discrepancy (ca. 0.3% between original a- and b-axes).
5) Anomalous quartz with higher density is mainly caused by shrinkage of the shock planes of quartz, m(10 $\bar{1}$0) and π (10 $\bar{1}$ 2).

Anomalous quartz with higher density can be found in all types of impact craters which is used for indicator of shock metamorphism on the remained target rocks of the impact craters.

Density-deviations of anomalous shocked quartz grains are obtained in eight Australian impact craters, as follows (cf. Table 1).

1) Wolfe Creek crater shows the most deviated anomalous shocked quartz with more diffuse peaks.
2) Shattercone of the Gosses Bluff shows intermediate density-deviation of anomalous quartz between the matrix and clast quartz of the brecciated sample.
3) Small meteoritic impact crater of the Dalgaranga reveals typical density-variatuon of anomalous quartz. The place found the meteorite includes the highest density of anomalous shocked quartz.
4) Lake Acraman shows the simialr small density-deviation to that of the clast fragments of breccias from the Gosses Bluff.

Table 1. Anomalous shocked quartz data in Australian Impact craters.

Sample No.	Density-deviation (ρ / ρ_0)	Sample No.	Density-deviation (ρ / ρ_0)
Dalgaranga(DR4)	+0.27(8)*	Teague Ring(TRC1P)	+0.30(6)
Gosses Bluff(GB3S)	+0.21(10)	Connolly Basin(CB1WP)	+0.24(5)
(GB4C)	+0.14(27)	Veevers(VR2P)	+0.27(4)
(GB4M)	+0.26(9)	Henbury(HC71P)	+0.31(4)
Wolfe Creek(WCR1)	+0.32(11)	Lake Acraman(AC7RP)	+0.14(5)

* Numbers in parentheses are standard deviation refering to the last decimal place of the data used for discussion.

References:

[1]Miura Y., Ashida, T. and Okamoto M. (1990): Intern. Workshop on Meteoritic Impact on the Early Earth, LPI Contribution, 746, 34-35.

[2]Miura Y. (1991): Shock Waves, an International Journal, 1, 35-41.

[3]Miura Y. (1991): LPSC XXII (NASA, LPI), 905-908.

ANOMALOUS QUARTZ FROM POSSIBLE IMPACT CRATERS IN JAPAN

Yasunori MIURA, Toshio KATO and Makoto OKAMOTO
Department of Min. Sci. & Geology, Fac. of Sci., Yamaguchi University
Yoshida, Yamaguchi 753, Japan.

From complicated characteristics of Japanese island, possible impact craters in Japan are considered as follows.

1) Iron meteorites are found as projectiles of small impact craters,
2) Almost all circular impact structures are destroyed by progressive plate tectonic movements and volcanic activities except small craters, and
3) Shocked minerals and rocks can be found as impact indicators [1-3].

Tektites and diaplectic glasses could not found in Japan.

From the main three evidences of impact craters (i.e. projectile of iron meteorites, small circular impact structure, and shocked minerals), possible impact craters in Japan are discussed in this study as follows.

1) Among 14 iron meteorites 7 iron meteorites (Tanokami, Shirahagi, Okano, Sakauchi, Kuga, Saotome, and Tendo) are exceeded the weight by 1kg to make small impact craters which evidences are applied from data of Australian impact craters.

2) Origins of circular structures in Japan are difficult to determine by existing the volcanic and tectonic activities.

3) Impact indicators of shocked metamorphism (anomalous shocked quartz, high-pressure silica minerals, anomalous cristobalite, and anomalous feldspar) should be checked in the possible impact craters in Japan.

4) Anomalous quartz grains are obtained in Kuga iron meteorite (ca. 6kg) with probable semi-circular impact crater. Hoshinoko-Zan impact crater [4,5] without iron meteorites shows semi-circular structure. But few shocked data have been obtained so far. Ohtaki small circular impact structure with anomalous shocked data and cristobalite have no meteorite so far. Very small impact crater (ca. 30 cm in diameter) formed by Kokubunji L6 chondrite (total ca.11 kg) has no distinct shocked data of target rock.

From shocked mineral data, Kuga and Ohtaki target rocks are probable impacted target rocks in Japan.

References:

[1] French B. (1968): Shock metamorphism of natural materials, 1-17.
[2] Miura Y. et al. (1990): Intern. Workshop on Meteoritic Impact on the Early Earth (Perth), LPI Contribution, No. 746, 30-35.
[3] Miura Y. (1991): Shock Waves, an International Journal , 1, 35-41.
[4] Graham A., Bevan A. and Hutchison R. (1985): Catalogue of Meteorites (British Museum), 423-454.
[5] Classen J. (1977): Meteoritics, 12, 61.

COOLING HISTORIES OF PRIMITIVE ACHONDRITES YAMATO 74357 AND MAC88177; M. Miyamoto, Dept. of Pure and Applied Sci., Univ. of Tokyo, Komaba, Tokyo 153 and H. Takeda, Mineralogical Inst., Faculty of Sci., Univ. of Tokyo, Hongo, Tokyo 113, Japan.

Primitive achondrite is the group name suggested for all of the ungrouped chondritic meteorites and clasts. Yamato(Y)74357 and MAC88177 have many chemical and mineralogical characteristics of primitive achondrites and are closely related to lodranite [1]. Similarity of the primitive achondrites to ureilite is also pointed out [1]. Y74357 and MAC88177 consist mainly of olivine (ol), orthopyroxene (opx), augite (aug), Fe-Ni metal and troilite. We discuss cooling rates of the primitive achondrites on the basis of chemical compositions and zoning profiles of ol and opx.

The chemical compositions of ol and opx in MAC88177 are uniform within and between the crystals and the mg numbers (=100xMg/(Mg+Fe)) of olivine 87, opx 87, and augite 90 are in equilibrium and the opx-aug pair gives equilibrium temperatures of 1100 to 900 °C. The CaO contents of opx decrease toward the rims. The CaO contents of ol is 0.01 to 0.03 wt%.

The chemical compositions of ol and opx in Y74357 are not an equlibrium pair. Ol is uniform (mg=92) and is more Mg-rich than opx mg=86. Opx shows a reverse chemical zoning at the rim of a few tens microns in width like olivine rims in ureilites. The mg number of 92 at the edge of the reduced rim of opx is equal to that of ol. Higher mg number of ol than that of the core of coexisting opx in Y74357 and the chemical zoning of opx at the rim distinguish it from MAC88177. These results suggest that ol in Y74357 was completely reduced during a subsolidus annealing episode, but cooling of Y74357 was slow enough to homogenize ol, but too fast to homogenize entire opx. The CaO contents in ol gradually decrease from core to rim (Fig. 1). The CaO contents in opx rapidly decrease at the rim. The MnO contents in opx slightly increase at the rim probably due to effects of the reduction. Reduction rims were not detected in aug with a microprobe.

We assume that these compositional gradients of the mg number of opx and CaO contents of ol in Y74357 are controlled by atomic diffusion and fit diffusional calculation profiles to the observed zonings to obtain cooling rates. The diffusion coefficients of Fe and Ca in ol and opx and details of calculation are given in [2]. A cooling rate of 1.5 °C/year from 1000 to 600 °C gives the best fit for the observed CaO profile of ol in Y74357 (Fig. 1). This cooling rate corresponds to a burial depth of about 70 m under solid rock (thermal diffusivity = 0.004 cm^2/s). For Fe-Mg profile at the rim of opx in Y74357, a cooling rate of 1.5 °C/year also gives the best fit for the observed profile [2]. The cooling rate obtained by Fe-Mg zoning of opx agrees well with that by the CaO profile. At this cooling rate, any primary Fe-Mg zoning in ol will be homogenized because of diffusion coefficient of Fe greater than that of Ca, in agreement with observation. The cooling rate will be useful in deducing their formation conditions. We thank the Natl. Inst. Polar Res. for the consortium meteorite sample.

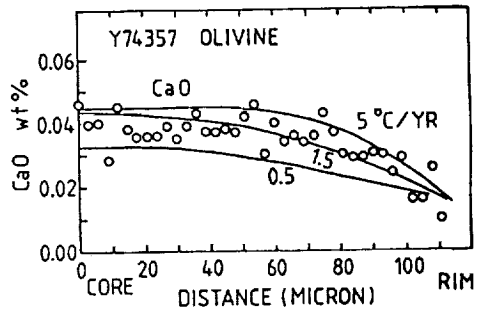

Fig. 1 CaO zoning of Y74357 olivine

References: 1. Takeda H., Saito J. and Miyamoto M. (1991) Lunar Planet. Sci. XXII, 1375-1376. 2. Miyamoto M. and Takeda H.(1991) 16th Symp. Antarct. Meteorites(in press).

A new mechanism for the formation of meteoritic kerogen-like material. W. A. Morgan, Jr.[1,2], E. D. Feigelson[1], H. Wang[3], and M. Frenklach[3]. [1]Department of Astronomy and Astrophysics, The Pennsylvania State University, University Park, PA 16802, USA. [2]Space Telescope Science Institute, Baltimore, MD 21218, USA. [3]Department of Material Sciences and Engineering, The Pennsylvania State University, University Park, PA 16802, USA.

Most of the carbon-bearing material in carbonaceous chondrite meteorites resides in the matrix as a hydrocarbon composite similar to terrestrial kerogen, an acid-insoluble cross-linked structure of aromatic and aliphatic hydrocarbons. In meteoritic kerogen-like material, about 75% of the carbon is contained in the aromatic component. Recent analysis of the Allende meteorite matrix shows most of its polycyclic aromatic hydrocarbons (PAH) molecules have 3 or 4 rings, but can have as many as 7 rings (1).

Attempts to explain the origin of meteoritic kerogen-like material generally assumed that it formed in the early solar nebula, though recent evidence for PAH molecules in the interstellar medium permits inheritance from the parent interstellar cloud. The formation mechanism which has attracted the most attention is the reaction of CO and H_2 on the surface of mineral catalysts through Fischer-Tropsch-type (FTT) reactions (2). The FTT synthesis, however has several drawbacks (e.g. 3). Of interest here is that the FTT process under terrestrial conditions produces almost exclusively aliphatic hydrocarbons (4). There is thus considerable motivation to investigate alternative mechanisms which can efficiently produce aromatics.

We propose here that aromatic hydrocarbon formation takes place in the gas phase by pyrolysis of simple hydrocarbons present in the solar nebula, in particular acetylene (C_2H_2) and methane (CH_4). Our model is based on the detailed non-equilibrium chemical kinetic mechanism developed recently by Frenklach and colleagues to explain the early stages of soot formation in hydrocarbon pyrolysis and combustion (5). The first aromatic ring can be formed through one of several possible pathways. The principal growth pathway of the mechanism is the abstraction of hydrogen atoms, followed by the addition of acetylene molecules to the resulting aromatic radical. We have applied essentially the same mechanism to investigate PAH formation in the dense atmospheres of carbon-rich red giant stars (6).

This chemical mechanism has been applied to a range of possible solar nebula conditions. We find aromatic hydrocarbon yields greater than 10% are obtained when the initial $[C_2H_2]/[H_2]$ ratio is greater than 10^{-7}, the pressure ranges from 10^{-6} to 10^{-7} atm, the temperature ranges between 900 K and 1100 K, and the reactions continue for at least 10^6 yr. Aromatic formation occurs only in the 900 K $\leq$ T $\leq$ 1100 K temperature window. Therefore, pyrolysis of C_2H_2 and CH_4 in the solar nebula may account for meteoritic aromatic hydrocarbons. This study is discussed in detail in (7). References: (1) Zenobi R. *et al.* (1990) *Science* **246**, 1026. (2) Studier M. H. *et al.* (1972) **36**, 189 and Hayatsu R. and Anders E. (1981) *Top. Curr. Chem.* **99**, 1. (3) Yuen G. U. *et al.* (1990) *LPSC* **21**, 1367. (4) Sneeden R. P. A. (1982) in *Comprehensive Organometallic Chemistry: The Synthesis, Reactions, and Structures of Organometallic Compounds*, pp. 19-100. (5) Frenklach M. *et al.* (1985) in *20th Symp. (Intl.) on Combustion*, p. 887 and Frenklach M. (1989) in *22nd Symp. (Intl.) on Combustion*, p. 1075. (6) Frenklach M. and Feigelson E. D. (1989), *Astrophys. J.* **341**, 372. (7) Morgan W. A. *et al.* (1991), *Science* **252**, 109.

HIGH-TEMPERATURE MASS SPECTROMETRIC DEGASSING OF ENSTATITE CHONDRITES: IMPLICATIONS FOR PYROCLASTIC VOLCANISM ON THE AUBRITE PARENT BODY.

D.M. Muenow[1], K.Keil[2], and L. Wilson[2,3]. [1]Chemistry Dept., Hawaii Instit.Geophys., [2]Planetary Geosci. Div., Dept. Geol. Geophys; SOEST, University of Hawaii-Manoa, Honolulu, HI 96822, USA. [3]Environmental Sci. Div., Lancaster University, Lancaster LA1 4YQ, United Kingdom.

Wilson and Keil (1) argued that a few hundred ppm of expanding volatiles present in early partial (basaltic) melts on the aubrite parent body (or on other differentiated asteroids < 100 km in radius), upon ascent of the magma to the surface of the body, would cause disruption into a spray of droplets moving with velocities in excess of the escape velocities of small asteroidal-sized bodies and, thus, escape and be lost into space 4.55 Ga ago. Hence, no such basaltic rocks exist as individual meteorites nor as clasts in brecciated aubrites. We report measurements of volatiles in reasonable analogs of the precursor rocks of the aubrites [Qingzhen (EH3); Indarch, Abee (EH4); St. Mark's (EH5); Hvittis, Pillistfer (EL6, sinoite-bearing); Khairpur (EL6, no sinoite)] and address in detail the nature and origin of volatile phase(s) driving this pyroclastic volcanism. **Results and discussion:** 1. Volatiles measured by high-temperature mass spectrometric degassing (2) and released at < 780°C are contaminants from terrestrial weathering, handling and cutting; those released at > 950°C (principally CO, 1580-2830 ppm, N_2 110-430 ppm, Cl 120-450 ppm) are indigenous (Fig. 1). 2. N_2 release appears to be associated with the melting of the Fe,Ni-sulfide cotectic at ~950°C, although amounts of gas released exceed by several orders of magnitude the N_2 solubility in metallic Fe,Ni. CO release at T>1025°C is violent and results in pronounced vesiculation of the residue; CO appears to be trapped in microvesicles and cracks in silicates. Cl release beginning at 950°C (EH's) and 1025°C (EL's) appears not to be associated with lawrencite, which should sublime at T as low as 325°C (3); some may be released from djerfisherite. 3. Gas release and textural studies suggest that metamorphic reheating of EH and EL chondrites was to <950°C. 4. Sinoite present in some EL6's did not form by condensation from the solar nebula, but during parent body metamorphism at T<950°C via the reaction of SiO_2, gaseous N_2, and Si (in solid solution in the metallic Fe,Ni). 5. As little as 1 % by volume partial melting in an asteroid of any size will generate excess pressures in the melt much greater (10's of MPa) than the tensile strength of silicate materials and will initiate formation of cracks. This process will be enhanced by expansion of any exsolved or trapped gas phase in the asteroid and will lead to the formation of pathways (cracks growing into dikes) for melt migration. 6. The pressure gradients implied when these pathways intersect the asteroid surface, coupled with the observed amounts of indigenous volatiles released from EH and EL chondrites, are easily sufficient to drive the pyroclastic volcanic eruptions envisaged by (1).

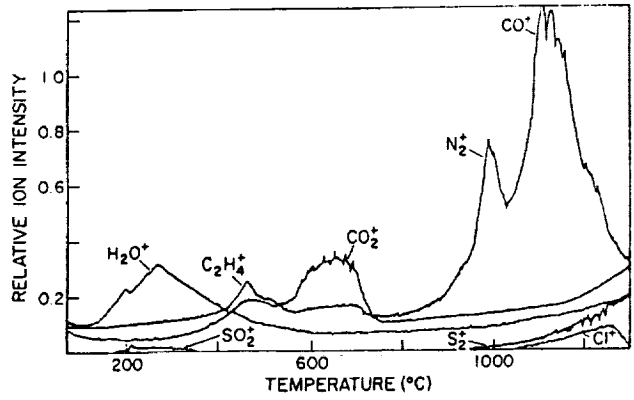

Fig. 1: Mass pyrogram for Indarch (EH4), showing release of principal volatiles from 50-1300°C (background uncorrected).

References: (1) Wilson L. and Keil K. (1991) EPSL (in press). (2) Muenow DW. (1973) GCA 37, 2523-2528. (3) Schoonmaker R.C and Porter R.F. (1958) J. Chem. Phys. 29, 116-121.

PRODUCTION RATE OF COSMOGENIC NITROGEN FROM NORTON COUNTY AUBRITE. S.V.S. Murty and Varun Sheel, Physical Research Laboratory, Navrangpura, Ahmedabad 380 009, INDIA

Oxygen is the principal target element for the production of ^{15}N and ~45% of most of the silicate minerals is made of oxygen. Inspite of its ubiquitous production in all silicate material that were exposed to cosmic rays, it has not been easy to decipher the cosmogenic N component, due mainly to a prepondarance of large indegenous N which is most often ill-defined. One approach that has been adopted to circumvent this difficulty was to theoritically calculate the production ratios $^{15}N/^{21}Ne$ or $^{15}N/^{38}Ar$ and use the measured ^{21}Ne or ^{38}Ar to derive the cosmogenic ^{15}N (Murty and Marti, 1990). But it is desirable to independently derive ^{15}Nc in order to confirm and improve the calculated production rates. Aubrites which have a well defined indegenous N component with $\delta^{15}N = -33^{o}/oo$, are good candidates to independently obtain the ^{15}Nc.

We studied N, Ne and Ar in Norton County, an aubrite with a high exposure age. A 400°C combustion in ~100 m Torr O_2 to get rid of surficial contamination followed by pyrolysis at temperatures (^{o}C) 800, 1000, 1200, 1400, 1500 and 1600 are carried out and Ne, Ar and N have been analysed by standard procedures (Murty 1990). Most of the N is released in the 1400 and 1500°C steps. The 1200°C fraction gave the lowest $\delta^{15}N = -33\pm2\ ^{o}/oo$ characteristic of enstatite meteorites and subsequent steps showed +ve $\delta^{15}N$ excursions due to release of cosmogenic nitrogen. We calculated the ^{15}Nc, assuming the nitrogen to be a two component mixture (indegenous + cosmogenic) and taking the $\delta^{15}N$ of 1200°C step as the indegenous value. Our results are as follows: N = 11.8 ppm, the cosmogenic components (in 10^{-8}ccSTP/g) $^{15}N = 236\pm30$; $^{21}Ne = 62\pm6$ $^{38}Ar = 2.1\pm.2$. Both ^{21}Ne and ^{38}Ar gave an exposure age of 121±15 Ma, resulting in a production rate $P_{15} = (1.95\pm.35)\ 10^{-8}$ccSTP/g Ma.

Becker et al. (1976) have obtained an emperical production rate $P_{15} = 3.6\pm.8$ pg/g Ma for lunar samples, assuming that all the cosmogenic nitrogen is released in the highest temperature fraction, which is equivalent to $(1.08\pm.24) \times 10^{-8}$ccSTP/g Ma for 4π exposure while Reedy (1981) production rates give $P_{15} = 1.42\times10^{-8}$ccSTP/g Ma for a shielding depth of 40 g/cm^2 and 4π exposure. Partial release of ^{15}Nc at lower temperatures in case of Becker et al. (1976) and the lower value of $^{15}N/^{15}O = 0.55$ used for estimating the direct ^{15}N production by Reedy (1981) might be the reasons for the lower values as compared to ours.

Becker R.H. et al. (1976) Proc. 7th LPSC, 441; Murty S.V.S. (1990) 21st LPSC, 829; Murty S.V.S. and Marti K (1990), Mateoritics 25, 227; Reedy R.C. (1981) Proc, 12th LPSC, 1809.

EVAPORATION OF PEROVSKITE: H. Nagahara and B. O. Mysen, Geophysical Laboratory, Carnegie Institution of Washington, 5251 Broad Branch Road, N W., Washington, D. C. 20015, U. S. A.

Mysen and Kushiro [1] showed that spinel and hibonite evaporate congruently at a fairly oxidizing condition (at the Mo-MoO_2 buffer which lies about 1.5 to 2 orders of magnitude above the Iron-Wustite buffer in the present experimental condition) and incongruently to corundum and a Ca-rich gas at a fairly reducing condition (at the C-CO-CO_2 buffer which lies about 1.5 to 2.5 orders of magnitude lower than the IW buffer). They also suggested that perovskite evaporates incongruently to rutile and a gas at reducing condition. Perovskite is a direct condensates from gases with solar and non-solar compositions [2], and it is a problem if perovskite evaporates incongruently. In order to investigate the evaporation of perovskite further, high temperature phase relation was studied on the basis of vapor pressure measurement.

Experimental technique is the same as that described in [3]. Finely powdered synthetic perovskite was put in a Mo or C Knudsen cell and kept at a desired temperature in a vacuum chamber. The total pressure of the chamber was kept constant at 1.8×10^{-8} bar by bleeding hydrogen gas.Vapor pressure was calculated from the measured weight loss by using the previously determined correction factor [3]. Experimental temperature ranged from 1450 to 1900°C and the duration from 30 min to 4 days. The weight loss was from several % to less than 40%.

Residues of partial evaporation of perovskite are perovskite alone in most cases except above 1800°C, which have small amount of melt. Thus it appears that perovskite evaporates congruently at least within the f_{O_2} range of the Mo-MoO_2 and C-CO-CO_2 buffers.

Mode of evaporation seems to change at about 1700 to 1750°C regardless of f_{O_2}; both ΔSv and ΔHv of evaporation become larger above 1750°C than below 1700°C. Although the difference might have been due to a difference in mode of evaporation, based on the SEM observation there is no visible change in the residues below and above 1750°C. With increasing temperature, degree of recrystallization of perovskite proceeds and the area of surface decreases. The apparent increase of both ΔHv and ΔSv are not, however, due to decrease of surface area which would cause a decrease of those numbers. One possible explanation for the change of heat and entropy of evaporation at higher temperatures is partial reduction of Ti oxide to Ti in the gas. The data below 1750°C gives $\Delta Hv = 266 \pm 64$ KJ/mol and $\Delta Sv = 10.9 \pm 2.5$ J/K•mol for evaporation of perovskite for the C-CO-CO_2 buffer. These values are much lower than those for forsterite, SiO_2, CaO, MgO, and Al_2O_3 [1,3] . At temperatures below 1700°C and at the Mo-MoO_2 buffer, the estimated ΔHv is 270 KJ/mol and ΔSv is 8.4 J/K•mol. These values have, however large uncertainty. Above 1750°C and at the C-CO-CO_2 and Mo-MoO_2 buffers, the vapor pressure data give ΔHv is 406 and240 KJ/mol and ΔSv is 87 and 24 J/K•mol, respectively. These values are from non-melted samples. The estimated vapor pressure at the C-CO-CO_2 buffer is higher than that at the Mo-MoO_2 buffer, which is consistent with the previous works on spinel, hibonite, and CaO [3], and was ascribed to partial reduction of oxides to metal in gases.

Some charges melted above 1800 °C. It is still not clear whether they melted in equilibrium or not because the melting point of perovskite at 1 atm is 1915°C [4]. The amount of the liquid is very small, and it is difficult to know the precise composition. Semiquantitative analyses indicate an approximately 1:1 ratio of Ca and Ti for the liquid, suggesting congruent melting.

[1] B. O. Mysen and I. Kushiro (1989) *Ann. Rep. Geophys. Lab. Carnegie Inst.* **1988-1989**, 33 [2] Lattimer, et al. (1978) *Astrophys. J.* **219**, 230 [3] Mysen, B. O. and Kushiro, I. (1988) *Amer. Min.* **73**, 1 [4] R. S. Roth (1958) *J. Res. Natl. Bur. Stand.*, **61**, 440.

GAS – SOLID PHASE DIAGRAM OF OLIVINE AND ITS APPLICATION TO CHONDRITES: H. Nagahara[1], I. Kushiro[2], and B. O. Mysen[1], (1) Geophysical Laboratory, Carnegie Institution of Washington, 5251 Broad Branch Road, N.W., Washington, D.C. 20015, U.S.A., (2) Geological Institute, University of Tokyo, Hongo, Tokyo 113 Japan

Partial evaporation of olivine forms highly magnesian olivine residue and a ferrous gas with the olivine stoichiometry [1]. The genetic relationship between highly magnesian chondrules and highly ferrous matrix are well explained as partial evaporation residue of chondritic precursor and recondensates from the gas generated during chondrule formation [2]. Although many evaporation and condensation experiments have been carried out for forsterite [e.g., 3-5], few data exist for olivine with intermediate to ferrous compositions. We have measured the vapor pressure of fayalite and made the gas-solid phase diagram for the olivine solid solution system. These data enables us to predict the composition of coexisting gas and solid during a partial evaporation process.

The Knudsen method was used to measure the vapor pressure of fayalite; fine-grained powder from synthesized singe crystal of fayalite was put in a molybdenum Knudsen cell and kept at a constant temperature from 1050 to 1175 °C for 1530 to 20160 minutes in a vacuum chamber. The pressure in the vacuum chamber was at about 10^{-10} to 10^{-9} bar. The oxygen fugacity (f_{O_2}) inside the cell was at the Mo-MoO_2 buffer, which is about 1.5-1.9 orders of magnitude higher than the Iron-Wustite buffer in the experimental conditions. The measured evaporation rate was calibrated against vapor pressure by using an empirical correction factor [3]. The heat and entropy of evaporation were calculated from the relationship between vapor pressure and temperature.

The vapor pressure (P_V) of fayalite is related to temperature by the equation $\ln P_V=(-\Delta G_V/RT) = (-\Delta H_V/RT)+(\Delta S_V/R)$, where $\Delta H_V=608\pm60$ (KJ/mol) and $\Delta S_V=273\pm9$ (J/K•mol). These values are identical, within experimental errors, to those for forsterite at the same f_{O_2} (640±36, 210±54, respectively) [3]. Assuming that melting points of forsterite and fayalite at lower pressures are the same as those at 1 atm, that their Cp are independent of pressure and temperature, and that both solid olivine and gas are ideal solutions, the equilibrium solidus and vaporous for olivine are calculated. The phase diagram is a loop with an extremely large difference in the Fe/(Mg+Fe) ratio between coexisting gas and solid. This difference is much larger than that between liquid and solid. There is almost no stability field of olivine solid solution in the coexisting region of solid and gas. The Fe/(Mg+Fe) ratio of olivine is nearly constant at zero from the melting temperature of forsterite (2163K) to 1700K and increases rapidly from 0.02 to unity from 1600 to 1478K (melting temperature of fayalite); on the contrary, the Fe/(Mg+Fe) ratio of the gas increases rapidly from zero to 0.94 from 2163 to 2000K.

The phase diagram implies that residue after partial evaporation of intermediate olivine is forsterite at most temperatures unless kinetic control is not effective. Forsteritic isolated olivine grain could have easily been formed as a residue by heating both in a fairly low pressure of the nebular condition and in a higher pressure region for chondrule formation. When equilibrium was not achieved because of slow cation diffusion in an olivine crystal and short heating duration, iron-bearing olivine could survive after partial evaporation.

[1] Nagahara, H. et al. (1989) *Nature* **313**, 516 [2] Nagahara, H., *Meteoritics* **26**, (in press) [3] Mysen, B. O. and Kushiro, I. (1988) *Ame. Miner.* **73**, 1 [4] Hashimoto, A. (1990) *Nature* **347**, 53 [5] Uyeda, C. et al., *Meteoritics* **26** (in press).

HIGHLY FRACTIONATED REE IN CHONDRULES AND MINERAL FRAGMENTS FROM MURCHISON (CM2): ALTERATION OR IGNEOUS ?

Noboru Nakamura and Mutsuo Inoue, Dpartment of Earth Sciences, Kobe University, Nada, Kobe 657, Japan

The chondrules (true and fragments) and mineral fragments [1] from the MURCHISON (CM2) chondrite were analyzed for trace elements by isotope dilution [2,3]. **MC-9** is an olivine (Fa38) fragment carrying abundant inclusions of glass, phosphate and Fe,Ni-sulfides. **MC-7** is a porphyritc olivine (Fa≤1)-pyroxene chondrule with round Fe-Ni metal grains in olivines. **MC-5** consists of numerous Fe metal grains (≤~1um), anhedral olivines (Fa1-8), Mg-rich pyroxene and matrix materials with near olivine compositions. **MC-2** appears to be a chondrule carrying fresh olivine grains (Fa1) in the core but the other part were severely altered.

REE PATTERNS: **MC-9** indicates a REE pattern with a gradual decrease from light (La=6.2xCI) to heavy REE (Lu=2.1xCI) and a large negative Eu anomaly (Eu/Eu^*=0.33). **MC-5** shows a light REE depleted pattern (1.4~3.0xCI) with a negative Eu anomaly (Eu/Eu^*= 0.43). **MC-7** has REE abundances lower than but quite similar relatively to those in MC-5. **MC-2** also indicates a light REE depleted, smoothly fractionated pattern (1.1~1.6xCI).

DISCUSSION: It is surprising that all the chondrules and mineral fragments from the "primitive" chondrite analysed here indicate such a pattern that light to heavy REE (except for Eu) are smoothly fractionated and the Eu anomaly associates with Sr. This type of pattern would be the first case for chondrules, even for other inclusions of unequilibrated chondrites. The similar REE patterns have been known for enstatite achondrites and well documented for differentiated planetary materials, typically lunar basalts, but never so for chondrules and CAI's. They have flat or fractionated patterns with more or less irregularities of Ce and Yb (Tm) as well as Eu, typically Group II REE pattern [2,3,4], which is a marker signiture of the volatility control in the nebular processes [5]. It may be possible that the observed low abundances of alkalis were due to leaching during the alteration processes on the parent body. However, it seems questionable that the abundances of most immoble elements REE were also significantly changed by the same event, having resulted in the observed REE fractionations. These patterns are well explained as being due to the mineral (plagioclase and orthopyroxene) control in an igneous process. We, therefore, suggest that the precursors of the MURCHISON "chondrules" formed by the igenous processes.

REFERENCES: [1] Fuchs L.H., Olsen E. and Jensen K.J. (1973) Smithsonian Contrb. Earth Sci. 10, 39pp. [2] Nakamura N. et al. (1989) Anal. Chem. 61, 755-762. [3] Misawa K. & Nakamura N. (1988) GCA 52, 1699-1710. [4] Misawa K. & Nakamura N. (1988) Nature 334, 47-50. [5] Tanaka T. & Masuda A. (1973) Icarus 19, 523-530. [6] Boynton W.V. (1975) GCA 39, 569-584.

SHOCK-INDUCED DEFORMATION RECORDED IN THE LEOVILLE CV CARBONACEOUS CHONDRITE; Tomoki Nakamura, Kazushige Tomeoka and Hiroshi Takeda, Mineralogical Inst., Faculty of Sci., Univ. of Tokyo, Hongo, Tokyo 113, Japan.

Leoville is a unique CV(3) carbonaceous chondrite that shows foliation defined by alignment of elongated chondrules and inclusions with high aspect ratios. The texture is strongly suggestive of deformation. However, whether the deformation resulted from shock-induced pressure [2] or static compaction due to overburden [3] remains inconclusive. We studied mineralogy and petrology of chondrules and matrix in Leoville by using an optical microscope, an SEM, and a TEM in order to find out what caused its deformation.

Chondrules in Leoville consist mostly of Mg-rich olivine, pyroxene, kamacite, taenite, troilite, and mesostasis glass. Olivine and pyroxene grains in chondrules show fine fractures in high density, when they are observed by an optical microscope; fracture domains range in size from 10 to 50 μm. Almost half of the chondrules display wavy or mosaic extinction. Many large olivine grains show subparallel fractures with spacings of 10 to 30 μm in orientations oblique to the elongation axis of deformation. As Muller et al. [3] reported, we observed, by using TEM, many dislocations with Burgers vector b=[001] in olivines and stacking faults in orthopyroxenes in the chondrules.

The matrix of Leoville consists mainly of Fe-rich olivine (Fo_{40-55}) and minor enstatite, kamacite, and troilite. Those grains are strongly compacted. TEM observations reveal that olivines in the Leoville matrix occurs in discrete grains ranging in size from 0.1 to 2 μm and exhibit many cracks and screw dislocations with Burgers vector b=[001]. Many screw dislocations bend in various directions. There are many areas in the matrix consisting of very small olivine grains (100 to 1000 Å in diameter) with random orientations and almost free of dislocations, in which amorphous material, probably glass, fills interstices of those olivine grains.

Wavy or mosaic extinction and fine subparallel fractures observed in the Leoville chondrules are characteristic of shock-induced deformation [4]. Roughly similar orientations of subparallel fractures in olivines of different chondrules suggest that those fractures were produced simultaneously after accretion. High densities of screw dislocations with Burgers vector b=[001] and many cracks of olivines in the Leoville matrix are similar to those found in the olivines in shocked ordinary chondrites [5].

Leoville may have experienced local, mild heating caused by impact. Olivine grains in the matrix show many bended dislocations; the bending probably resulted from recovery by shock-induced heat [6]. The areas of fine-grained olivines in the matrix also resemble the recrystallized olivines that were produced by shock-induced heating [7].

Based on these observations and interpretations, we suggest that the deformation experienced by Leoville was due to shock-induced pressure.

REFERENCES: [1] J. T. Wasson (1985) in Meteorites, 164-165 (Springer-Verlag). [2] P. M. Cain, and H. Y. McSween (1984) Lunar Planet. Sci. XV, 116-117. [3] W. F. Muller and F. Wlotzka (1982) Lunar Planet. Sci. XIII, 558-559. [4] W. U. Reimold and D. Stoffler (1978) Proc. Lunar Planet. Sci. Conf. 9th, 2805-2824. [5] J.R. Ashworth and D. J. Barber (1975) Luner Planet. Sci. Let. 27,43-50. [6] R. Jeanloz (1980) J. Geophys. Res. 85, 3163-3176. [7] J. R. Ashworth (1985) Earth and Planet. Sci. Let. 73, 17-32.

MATRIX LUMPS IN DHAJALA AND MEZO-MADARAS: IMPLICATIONS FOR CHONDRULE-MATRIX RELATIONSHIPS IN ORDINARY CHONDRITES. C.E. Nehru[1,2], M. Prinz[1], M.K. Weisberg[1,2], R.N. Clayton[3] and T.K. Mayeda[3]. (1) Amer. Mus. Nat. Hist., NY, NY 10024. (2) Brooklyn College, CUNY, Brooklyn, NY 11210. (3) Enrico Fermi Inst., Univ. Chicago, Chicago, IL 60637

Introduction. The nature and origin of fine-grained opaque matrix in ordinary chondrites has received considerable study in recent years but no consensus has emerged as to its nature and origin. Matrix lumps in ordinary chondrites have been noted, but few have been studied adequately. Matrix lumps in Semarkona have oxygen isotopic compositions relatively near their host rock, but are aqueously altered [1]. A well-studied matrix lump in ALHA 77299 (H3.7) [2] has a composition below the terrestrial fractionation (TF) line, but to the left of the Equilibrated Chondrite Line (ECL) of Clayton et al. [3]. A matrix lump in ALHA 76004 (LL3.2) has a composition which is highly ^{16}O-rich, lies well below the TF line, and is exactly on the ECL line. Sometimes matrix-rich lumps have been interpreted as unusual microchondrule-bearing chondrites (e.g. Piancandoli, Krymka, Mezo-Madaras) [5-7] but we suggest that these are matrix lumps requiring more study. In this study we have examined matrix lumps from Dhajala (H3.8) and Mezo-Madaras (L3.7), petrologically and oxygen isotopically, in order to determine their relationship to the chondrules and whole rock, as well as nebular processes.

Dhajala. Matrix lumps in Dhajala are angular, sharply bounded, and up to 4mm across. They have a clastic texture, with clasts mainly 5 μm or less across, but up to 200 μm. They contain up to 4 vol% chondrules, which range from 75-300 μm; very few microchondrules (<100 μm) are present. Chondrules in the matrix lumps are mostly granular olivine and generally smaller in size than those in the host chondrite. Modally, the clasts contain (in vol%) 20 olivine, 71 opx, 5 cpx, 1 plag, 0.5 chromite, 2 FeNi, and trace FeS. Mineralogically, ol is equilibrated at Fa 19 (same as the host chondrite), opx is highly variable, at Fs 3-23 (as in the host), devitrified plag has highly variable Ca/Na, and FeNi has 6-51% Ni. The bulk composition of the clasts (in wt%, recal. to 100%) is 48.3 SiO_2, 0.16 TiO_2, 6.0 Al_2O_3, 0.49 Cr_2O_3, 12.2 FeO, 0.40 MnO, 27.8 MgO, 1.87 CaO, 1.78 Na_2O, 0.12 K_2O, 0.13 P_2O_5, 0.59 Ni, and trace S. This is similar in composition to the host Dhajala matrix; the lumps are also similar to the matrix texturally, mineralogically and modally. The oxygen isotopic composition of the clasts are: $\delta^{18}O=1.67$; $\delta^{17}O=0.30$. This composition is precisely on an extension of the ECL line to the other side of the TF line. The sized Dhajala chondrules are systematically enriched in ^{16}O toward the TF line, and the matrix lumps continue in this direction across the TF line. Thus, the Dhajala matrix lumps and chondrules are on a nebular mixing line between ^{16}O-rich and ^{16}O-poor components.

Mezo-Madaras. A single matrix lump (5 x 7mm) in Mezo-Madaras was studied. It consists mainly of clasts that are mainly 10 μm or less across, but contains clasts up to 200 μm; there are two chondrule clasts 250 μm across. Microchondrules (3-100 μm) make up <1 vol%, but larger clasts (often broken microchondrules) make up 10 vol%. Most are glassy to cryptocrystalline, with chondrule fragments mostly barred olivine. Modally, the clast has (vol%) 38 ol, 44 opx, 5 cpx, 0.6 plag, 1.8 chromite, 6 FeS, 4 FeNi. Mineralogically, the clast is unequilibrated and Mg-rich (Fa 1-30), whereas the host chondrite opaque matrix is Fe-rich (Fa 32). The bulk composition reflects the Mg-rich character of the clast. The oxygen isotopic composition of the clast is: $\delta^{18}O=2.97$; $\delta^{17}O=1.01$. This composition is also below the TF line and near the extension of the ECL line. Thus, the Mezo-Madaras lump is primitive (^{16}O-enriched) matrix material, and related to the chondrules; the host chondrite matrix has experienced a more oxidized environment.

Conclusions: Matrix lumps in ordinary chondrites contain an important source of primitive matrix component. They are often on or near the ECL line between ^{16}O-rich and ^{16}O-poor components. Chondrules and matrix lumps are on opposite ends of this line, with chondrules above and matrix below the TF line. Matrix lumps are more primitive than the host chondrite matrix which may have exchanged oxygen with nearby host chondrules. Matrix lumps often contain microchondrules and small chondrules and microchondrule-bearing clasts (e.g., Piancandoli) may be matrix-rich lumps rather than new types of chondrites.

References. (1) Grossman, J.N. et al. (1987) Meteoritics 22, 395-396. (2) Brearley, A.J. et al. (1989) GCA 53, 2081-2093. (3) Clayton, R.N. et al. (in press) Oxygen isotope studies of ordinary chondrites, GCA (4) Mayeda, T.K. et al. (1980) Meteoritics 15, 330-331. (5) Rubin, A.E. et al. (1982) GCA 46, 1763-1776. (6) Rubin, A.E. (1989) Meteoritics 24, 191-192. (7) Michel-Levy (1988) Meteoritics 23, 45-48 (8) Huss, G.R. et al. (1981) GCA 45, 33-51

^{22}Ne-E(H) AND ^{4}He MEASURED IN INDIVIDUAL SiC GRAINS USING LASER GAS EXTRACTION; R. H. Nichols, Jr.*, C. M. Hohenberg*, S. Amari*† and R. S. Lewis†; *McDonnell Center for the Space Sciences, Physics Department, Washington University, St. Louis, MO 63130 USA; †Enrico Fermi Institute and Department of Chemistry, University of Chicago, Chicago, IL 60637 USA.

We have successfully measured ^{22}Ne-E(H) and ^{4}He in individual SiC grains from the Murchison CM2 chondrite using a laser extraction technique. The parent SiC grain size fraction (KJG, 1.5 - 3.0 μm) was previously analyzed for noble gases [1] and for Si, N, Mg and C isotopic compositions [2,3]. Two single grains (possibly 4) out of 54 have significant ^{22}Ne-E(H) with accompanying ^{4}He, *confirming both that SiC is the carrier of Ne-E(H) and that the noble gases are carried in a small subset of the SiC grains [1].* The noble gas results for these grains are given in Table 1.

Grain size and morphology was determined with the SEM prior to noble gas extraction. Vaporization of individual grains was confirmed with the SEM following gas extraction. During several extractions grains adjacent to the one in question were slightly heated due to their proximity to the focused laser beam, as evidenced by a thin carbon deposition surrounding each heated grain. This spurious heating occurred for two of the four grains (1093, 3003) with ^{4}He and ^{22}Ne signals in excess of spectrometer background. The other two single grains with excess ^{4}He and ^{22}Ne (1216, 2010) were relatively isolated on the gold substrate and were vaporized without heating any adjacent grains. We were unable to detect any ^{3}He, ^{20}Ne or ^{21}Ne significantly above spectrometer background.

The percentage of SiC grains in fraction KJG with gas amounts greater than 1×10^{-14} ccSTP ^{22}Ne and 4×10^{-12} ccSTP ^{4}He (roughly our detection limits) is ~ 4-8%. Thus, given the nominal grain size (1.5 - 3.0 μm) and the average gas concentrations for bulk KJG (Table 1) this 4-8% fraction apparently carries more than 50% of the ^{22}Ne-E(H) and ^{4}He in KJG. (The error on this percentage is potentially quite large due to the difficulties in estimating the masses of the individual grains.) Although it is still possible for each of the gas-poor grains to carry on average $\leq 0.5 \times 10^{-14}$ ccSTP ^{22}Ne-E(H), our results strongly suggest that only a small fraction of the SiC contributes to the ^{22}Ne-E(H) and ^{4}He. This implies that the remaining SiC were degassed or that they formed later than (or were not exposed to) the event(s) producing the anomalous Ne component [1]. The ^{4}He / ^{22}Ne-E(H) ratios for the single grains (Table 1) are consistent at the 2σ level with the ratio for bulk KJG [1]. None of the grains studied has excess ^{4}He without accompanying ^{22}Ne-E(H) and vice versa. This suggests that both gases originate from the same source, possibly the He-burning shell of AGB stars [1].

References: [1] Lewis *et al.* (1990) *Nature*, **348**, 293. [2] Zinner *et al.* (1991), *Nature*, **349**, 51. [3] Zinner *et al.* (1991), this volume.

TABLE 1. Single Grain Noble Gas Results from Murchison KJG SiC

Sample	^{22}Ne-E(H)[a] (10^{-14} cc)	^{4}He[a]	^{22}Ne-E(H) (10^{-3} cc/g)	^{4}He (cc/g)	^{4}He/^{22}Ne-E(H) (×10^{2})	Size[b] (μm)	Type
1216	24.8(2.3)	7150(70)	~ 2.5(0.6)	~ 0.74(0.20)	~ 3.0(1.0)	4.0×2.5	fluffy
2010	2.1(0.3)	1020(30)	~ 0.2(0.1)	~ 0.11(0.05)	~ 5.0(1.5)	4.0×3.0	platy
3003[c]	1.6(0.5)	1460(80)	~ 0.2(0.1)	~ 0.24(0.12)	~ 9.0(3.0)	2.5×2.5	fluffy
1093[c]	9.0(0.8)	—	~ 1.0(0.5)	—	—	3.0×3.0	platy
KJG[d]	—	—	0.29	0.07	2.5	1.5-3.0	—

[a] Blanks have been subtracted of ~ 1.0 and 400 × 10^{-14} ccSTP at masses 22 and 4, respectively. Blank uncertainty is less than 50% of these amounts. Errors on amounts are given in parentheses. [b] Mass of grains (used for concentrations) estimated from SEM photograph. [c] Multiple grains heated; see text. Helium was not measured on 11 grains including 1093. [d] See reference [1].

TERRESTRIAL Kr AND Xe IN EXTRATERRESTRIAL ROCKS: CHEMICAL ADSORPTION OF NOBLE GASES? S. Niedermann[1] and O. Eugster, Physikalisches Institut, University of Bern, CH-3012 Bern, Switzerland. [1]Present address: Dept. of Chemistry, University of California, San Diego, La Jolla, CA 92093-0317, USA

In several anorthositic lunar rocks trapped Xe with isotopic composition similar to that in the terrestrial atmosphere was observed [1,2]. In a subsequent investigation Niemeyer and Leich [3] found that their samples had been contaminated by terrestrial air. However, they pointed out that such a conclusion could not unequivocally be drawn for other lunar rocks containing a terrestrial-like Xe component.

We found such a component in anorthositic breccias 60018 and 65315 [4,5]. In order to elucidate the problem whether atmospheric contamination is the only source of terrestrial-like Xe in lunar samples, and if so, what the nature of the contamination process is and whether it affects other noble gases as well, we crushed samples of 60018 and 65315 in atmospheres enriched in ^{86}Kr and ^{129}Xe [6,7]. These experiments showed clearly that anorthositic samples can be contaminated by Kr and Xe, and maybe also by Ar, from the ambient atmosphere. Kr and Xe concentrations are grain size anticorrelated, indicating adsorption of the gas atoms on the grain surfaces. Furthermore, the amount of gas adsorbed by a sample is approximately proportional to the partial pressure as described by Henry's law. Activation energies for adsorption of Kr and Xe at room temperature lie between 10 and 20 kJ/mole, which is typical for ordinary physical adsorption.

At 600°C, however, only a minor portion of Kr and Xe atoms (less than 25%) are desorbed again, therefore much higher activation energies must be effective at this temperature. They can be estimated to be approximately 200 kJ/mole both for Kr and Xe, indicating chemical adsorption of the noble gas atoms on the anorthositic material. The kind of adsorption at room temperature seems thus to be fundamentally different from the one at higher temperatures. Obviously a potential barrier exists for the transition from physical to chemical adsorption, which cannot yet be overcome at 20°C. However, it is not clear whether the gas atoms are in fact chemically bound or rather trapped, e.g. buried beneath the surface due to chemical reactions of mineral components or occluded in internal pore labyrinths. Therefore, we prefer the term "anomalous adsorption" instead of chemisorption for the phenomenon.

Contamination by anomalously adsorbed terrestrial Kr and Xe has also been observed for some meteoritic samples, in particular diogenites, which are composed mainly of pyroxene [8,9]. Anomalous adsorption may explain the incorporation of certain noble gas components into extraterrestrial material, e.g. the planetary trapped gases or the surface correlated components of ^{129}Xe and fission-type Xe in some lunar breccias.

Acknowledgement: This work was supported by the Swiss National Science Foundation.

References: [1] Lightner B.D. and Marti K., Proc. Lunar Sci. Conf. 5th, 2023 (1974). [2] Leich D.A. and Niemeyer S., Proc. Lunar Sci. Conf. 6th, 1953 (1975). [3] Niemeyer S. and Leich D.A., Proc. Lunar Sci. Conf. 7th, 587 (1976). [4] Eugster O. and Niedermann S., Lunar Planet. Sci. XVIII, 275 (1987). [5] Eugster O. and Niedermann S., Meteoritics 22, 373 (1987). [6] Niedermann S. and Eugster O., Lunar Planet. Sci. XX, 788 (1989). [7] Niedermann S. and Eugster O., Lunar Planet. Sci. XXI, 881 (1990). [8] Rowe M.W. and Bogard D.D., J. Geophys. Res. 71, 4183 (1966). [9] Michel Th. et al., Meteoritics 25, 387 (1990).

Re-Os CHRONOLOGY OF IAB, IIE, AND IIIAB IRON METEORITES; S. Niemeyer and B.K. Esser, Lawrence Livermore National Laboratory, P.O. Box 808, L-232, Livermore, CA 94550

The IAB iron meteorites are likely to be among the oldest iron meteorites because they have many chondritic affinities and their silicate inclusions are 4.5 Ga old. We have analyzed a set of four IAB irons in order to determine whether the iron phase is contemporaneous with the silicate. Two different dissolution techniques were used due to the difficulties we have encountered in achieving isotopic equilibration between Os from the spikes and the samples. Our acid dissolution procedure involves dissolving the iron with 4-6N HCl, then heating with ethanol prior to distillation. In our second procedure the samples are decomposed by alkaline fusion (1), the same technique employed in a previous study of iron and carbonaceous meteorites (2). In three out of four meteorites, the model age determined for the acid-dissolved sample is younger than for the peroxide-fused sample. We favor the acid-dissolution results, and suggest that our peroxide fusion procedure either gives Re contents that are too low or it leads to a slight disequilibrium for Os during distillation due to slightly different distilling conditions.

Relying upon the results given by the acid-dissolution technique, three of the four IAB irons yield model ages (calculated using 0.0965 for the initial $^{187}Os/^{188}Os$) that are the same within the uncertainties. The average model age is 4.58 Ga, in excellent agreement with the Ar-Ar ages for their silicate inclusions. The outlier, Pitts, has a model age of only 4.0 Ga. We then explored the possibility of using minor non-metallic phases in these meteorites to either give an internal isochron, or alternatively, to investigate the extent of disequilibrium within the meteorite. Non-metallic fractions were extracted from Landes and Woodbine by scraping inclusions with a dental pick and selecting the material with the least silicate. In both cases, the $^{187}Os/^{188}Os$ ratios are the same for non-metal and metal, so an internal isochron cannot be determined. The smaller non-metal sample from Landes agrees with the model age for its metal, albeit the uncertainties are relatively large; for Woodbine, the non-metallic fraction indicates a somewhat older model age. Although these results suggest that there may be some disequilibrium in IAB meteorites, the disequilibrium is small enough that it is not a likely candidate to explain variability between pieces of the same meteorite.

The other silicate-bearing iron meteorite class, the IIE irons, have silicates that range in age from 3.8 to 4.6 Ga. Analyses of metal from three IIE irons are in progress in order to determine whether the Re-Os model ages agree with the previously determined Rb-Sr and Ar-Ar ages. Finally, for comparison to the silicate-bearing iron meteorites, we are studying IIIAB irons since they clearly formed in a planetary core by fractional crystallization. Two high-Ni meteorites give model ages significantly less than 4.0 Ga, so we are currently focusing on the lower-Ni IA meteorites to determine whether the model ages correlate with the Ni fractionation trend.

This work was performed under the auspices of the U.S. Dept. of Energy by LLNL under contract No. W-7405-Eng-48.

(1) Morgan J.W. and Walker R.J. (1989) Anal. Chim. Acta 222, 291-300.
(2) Morgan J.W. and Walker R.J. (1989) Science 243, 519-522.

EXTRACTION OF ^{4}He FROM IDPs BY STEP-HEATING. A.O. Nier and D.J. Schlutter, School of Physics and Astronomy, University of Minnesota, Minneapolis, MN 55455, USA

We have reported on the isotopic composition of helium and neon extracted from 16 individual interplanetary dust particles (IDPs) collected in the earth's upper atmosphere (1). In further experiments, step-heating was performed on ten more particles and the extraction of ^{4}He studied with the hope that differences observed might provide clues to the thermal history of the particles (2). Flynn (3) has pointed out that dust particles from asteroids or high perihelia comets enter the earth's atmosphere with less energy than particles from low perihelia comets, and consequently would be heated less in their deceleration in the atmosphere. This should be reflected in the presence or absence of solar flare tracks or in differences in amounts of volatile elements or minerals observed.

We have now performed step-heating on ten more particles, and for comparison, on lunar soil grains of size comparable to that of the IDPs (< 20 μm). Our IDPs were actually fragments of somewhat larger particles, other fragments of which are being studied for elemental and mineralogical composition by other investigators.

Of the 20 particles investigated, 12 contained amounts of ^{4}He falling between 10^{-11} and 10^{-10} cm^{3}STP, almost all of which was released in the approximate temperature range 450 to 650°C, the same general range as found for the lunar particles. There was no systematic relation between the amount of ^{4}He observed and the temperature at which it was released. In NASA's Johnson Space Center's Catalog, these particles are identified as fragments from U2034*A3, W7029*C3, W7029*B10, W7031*C4, L2005-C27, -C29, -C20, -C23, -D26, -D29, -E35, and -E38. For four of the particles (W7010*A7, W7026*A3, W7031*A4, L2005C25) the amount of ^{4}He was substantially less, and, within the accuracy of the measurements, appeared to be released at higher temperatures. In the remaining four cases (W7031*B5, W7071*A4, W7028*C4, L2005E32) the amount present was too small to measure.

While real differences were observed which could be related to thermal history, the full significance of the finding may not be known until the comparison studies of the companion fragments are completed. The experience gained in conducting the present measurements indicates that modest changes in the procedures followed will lead to greater precision.

References: (1) Nier, A. O. and Schlutter, D. J., 1990, *Meteoritics* **25**, 263; (2) Nier, A. O. and Schlutter, D. J., 1990, *Meteoritics* **25**, 392; (3) Flynn, G. J., 1989, *Icarus* **77**, 287.

^{41}Ca PRODUCTION PROFILE IN THE ALLENDE METEORITE ; K. Nishiizumi[1], J. R. Arnold[1], D. Fink[2], J. Klein[2] and R. Middleton[2] ; (1) Department of Chemistry, University of California, San Diego, CA 92093-0317, (2) Department of Physics, University of Pennsylvania, Philadelphia, PA 19104

This study is an extension of our series of ^{41}Ca measurements in the Apollo 15 lunar core [1]. ^{41}Ca ($t_{1/2}$=1.0x10^5 years), like ^{36}Cl ($t_{1/2}$=3.0x10^5 years) is produced by spallation and by thermal neutron capture reactions in meteorites. Previous measurements [2-7] of thermal-neutron produced nuclides, ^{60}Co, ^{36}Cl, and noble gases, have shown that Allende had one of the largest pre-atmospheric sizes known for stony meteorites. We measured ^{41}Ca in 7 fragments of Allende which are aliquots of samples used previously for ^{36}Cl measurements [6]. The ^{41}Ca concentrations were determined using the University of Pennsylvania tandem accelerator [8]. Figure 1 shows observed ^{41}Ca and ^{36}Cl vs. depth from the surface of the meteorite. The preatmospheric depths were estimated by P. Pellas using cosmic ray track densities [9]. ^{41}Ca and ^{36}Cl activities increase with increasing depth except for one sample, USNM3512-C3A. Probably the depth estimation for this sample is somewhat in error, since ^{41}Ca and ^{36}Cl data agreed well. The neutron capture production rates for both ^{41}Ca and ^{36}Cl were calculated by subtraction of spallation contributions to Ca and Fe from the observed activities. Figure 2 shows neutron capture ^{41}Ca and ^{36}Cl concentrations (dpm/g target element) vs. ^{60}Co which is produced almost entirely by a neutron capture reaction. The figure also shows the previous low-level counting measurements of ^{36}Cl by Nakamura [5]. Both types of measurements are in agreement within errors except for ^{41}Ca in USNM3529 [4]. Mabuchi's value of (2.2±0.4) dpm^{41}Ca/g Ca (not shown in Fig. 2) is more than 70% higher than our value for the same specimen. We compared our observed neutron capture profiles of ^{41}Ca and ^{36}Cl to two theoretical models [10, 11]. Experimental results fit relatively well with the model of Eberhardt et al. [10] using a preatmospheric radius of 60-65 cm. Spergel et al. [11] predicted slightly lower values than those observed especially at deeper depths. Observed neutron capture production for both ^{41}Ca and ^{36}Cl at the surface is measured to be nearly zero which is in agreement with the former model [10] ; Spergel et al. [11] predicted somewhat higher production at the surface. ^{41}Ca is one of the most useful nuclides for depth and size estimation in large meteorites since ^{60}Co has a short half-life and comparatively low sensitivity for measurement by γ-ray counting.

We thank P. Pellas for providing documented Allende samples.

References: [1] Nishiizumi K. *et al.* (1990) *Lunar and Planetary Science XXI*, 893-894. ; [2] Cressy P. J. (1972) *J. Geophys. Res. 77*, 4905-4911. ; [3] Evans J. C. *et al.* (1982) *J. Geophys. Res. 87*, 5577-5591. ; [4] Mabuchi H. *et al.* (1975) *Meteoritics 10*, 449. ; [5] Nakamura Y. (1978) *Personal communication* . ; [6] Nishiizumi K. *et al.* (1986) *Lunar and Planetary Science XVII*, 619-620. ; [7] Göbel R. *et al.* (1982) *Geochim. Cosmochim. Acta 46*, 1777-1792. ; [8] Fink D. *et al.* (1990) *Nucl. Inst. Meth. B47*, 79-96. ; [9] Bourot-Denise M. and Pellas P. (1982) *Meteoritics 17*, 186. ; [10] Eberhardt P. *et al.* (1963) in *Earth Science and Meteoritics* 143-168. ; [11] Spergel M.S. *et al.* (1986) *Proc.16th Lunar Planet. Sci. Conf., J. Geophys. Res. 91*, D483-D494.

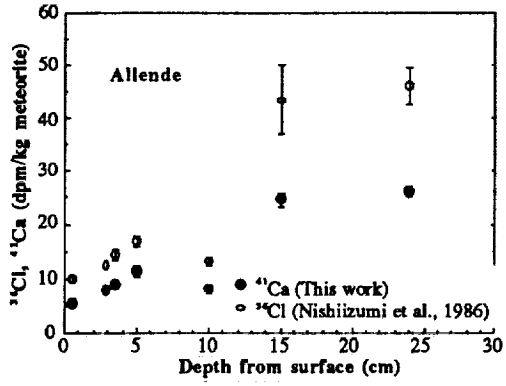

Figure 1.
^{36}Cl and ^{41}Ca vs. depth

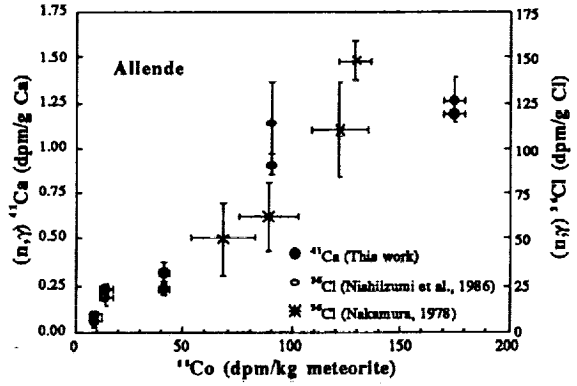

Figure 2.
Neutron produced ^{36}Cl and ^{41}Ca vs. ^{60}Co

^{10}Be AND ^{53}Mn IN NON-ANTARCTIC IRON METEORITES

K. Nishiizumi[1], M. W. Caffee[2], R. C. Finkel[2] and J. R. Arnold[1] ; (1) Department of Chemistry, University of California, San Diego, CA 92093-0317, (2) Nuclear Chemistry Div., Lawrence Livermore National Lab., Livermore, CA 94550

Clarke (1986) observed that the iron meteorite population in Antarctica contained a higher percentage of ungrouped meteorites than has been observed in non-Antarctic iron meteorites [1]. Wasson (1990) pointed out that this difference seems to be related to the median mass of Antarctic irons, which is about 1/100 that of the non-Antarctic population and hypothesized that this population difference could be explained by differences in the orbital dynamics between small and large pre-atmospheric iron meteoroids [2]. Wasson (1990) further suggested that the high efficiency of our collection of small meteorites in Antarctica is responsible for the high abundance of ungrouped Antarctic iron meteorites [2]. Cosmogenic nuclides can be used to determine both the preatmospheric size and the terrestrial age of iron meteorites. We have started a systematic survey of cosmogenic nuclides in both non-Antarctic and Antarctic iron meteorites in order to study the dynamics of iron meteorite transport between their parent bodies and the earth and to gain information about the history of the cosmic ray flux.

We have measured ^{10}Be, ^{36}Cl, and ^{53}Mn in the same sample of each object, calculated the terrestrial age of the object, and estimated the minimum preatmospheric size (depth) for both grouped and ungrouped iron meteorite populations. The ^{10}Be was measured at the new LLNL AMS facility. Since these were the first ^{10}Be measurements in natural samples made on this instrument we have also measured three lunar meteorites (MAC88104,9, MAC88105,19, and MAC88105,25) that were previously measured at the University of Pennsylvania AMS facility [3, 4]. For all three samples the ^{10}Be concentrations agree within 1 σ. For the iron meteorites the ^{10}Be/^{9}Be ratios were measured between (1-180)x10^{-13}. The errors on these measurements were between 2-5 %. The ^{53}Mn in the same samples was measured by NAA. The results of these measurements are shown in Table 1. The ^{36}Cl measurements were performed at the University of Rochester (unpublished) and will be reported elsewhere.

Chang and Wänke (1969) obtained terrestrial ages of about 30 iron meteorites using the ^{36}Cl/^{10}Be ratio [5]. We measured ^{10}Be in four of the iron meteorites also measured by Chang and Wänke. Our measured ^{10}Be activities are a factor of 3-12 lower than these previous measurements. We believe this discrepancy can be explained by the difficulty in using conventional β counting techniques for measuring ^{10}Be and ^{36}Cl. AMS provides a more reliable means of measuring these nuclides. A complete listing of these terrestrial ages will be published elsewhere. The ^{53}Mn and ^{10}Be together can be used to determine the depth in the preatmospheric body at which the meteorite was exposed to galactic cosmic rays. From this information one can obtain the preatmospheric size of the meteoroid. The preatmospheric size distribution of ungrouped and grouped iron meteorites, both Antarctic and non-Antarctic, is an important constraint in evaluating the transport of material from asteroids to Earth-crossing-orbits. From our preliminary measurements we do not see any correlation between minimum preatmospheric size and recovered mass for objects weighing more than 100 kg, excepting Gibeon.

References : [1] Clarke R.S.Jr. (1986) *International Workshop on Antarctic Meteorites LPI Tech Rpt. 96-01*, 28-29. ; [2] Wasson J.T. (1990) *Science 249*, 900-902. ; [3] Klein J. *et al.* (1982) *Nucl. Inst. Meth. 193*, 601-616. ; [4] Nishiizumi K. *et al.* (1991) *Geochim. Cosmochim. Acta* in press. ; [5] Chang C. and Wänke H. (1969) in *Meteorite Research* 397-406.

NAME	GROUP	^{10}Be (dpm/kg)	^{53}Mn (dpm/kg)	NAME	GROUP	^{10}Be (dpm/kg)	^{53}Mn (dpm/kg)
Toluca	IA	0.176 ± 0.005	52 ± 2	Gibeon	IVA	0.0076± 0.0004	
Filomena	IIA	0.674 ± 0.021	224 ± 7	Santa Clara	IVB	2.914 ± 0.055	
Mount Joy	IIB	0.166 ± 0.007	66 ± 2	Tlacotepec	IVB	2.769 ± 0.074	
Old Woman 1	IIB	2.576 ± 0.060	441 ± 20	ILD 83500,1	UNGR	0.519 ± 0.014	225 ± 8
Old Woman 2	IIB	2.846 ± 0.048	453 ± 19	Mundrabilla II-1	UNGR	0.704 ± 0.021	179 ± 11
Old Woman 3	IIB	1.736 ± 0.039	376 ± 16	Mundrabilla II-23	UNGR	0.690 ± 0.019	144 ± 9
Old Woman 4	IIB	2.216 ± 0.047	407 ± 17	Mundrabilla IX-1-1	UNGR	0.870 ± 0.023	188 ± 12
Old Woman 5	IIB	2.226 ± 0.045	412 ± 17	Pinon	UNGR	4.093 ± 0.066	
Old Woman 6	IIB	2.049 ± 0.040	353 ± 15	Santa Catharina	UNGR	0.201 ± 0.006	81 ± 4
Santa Luzia	IIB	0.082 ± 0.004	50 ± 2	Twin City	UNGR	1.616 ± 0.036	438 ± 18
Sao Juliao de Moreira	IIB	0.283 ± 0.014	89 ± 4	Waverly	UNGR	3.292 ± 0.070	560 ± 24
Cape York D4	IIIA	0.116 ± 0.003	23 ± 1	Pavlodar (metal)	Pal	5.73 ± 0.11	416 ± 14
Dayton	IIICD	4.267 ± 0.097	583 ± 25				

^{36}Cl TERRESTRIAL AGES OF ANTARCTIC METEORITES

K. Nishiizumi[1], P. Sharma[2], P.W. Kubik[2], and J. R. Arnold[1] ; (1) Department of Chemistry, University of California, San Diego, CA 92093-0317, (2) Nuclear Structure Research Lab. University of Rochester, Rochester, NY 14627

We continue to study cosmogenic nuclides in Antarctic meteorites. The major objective is to measure terrestrial ages using ^{36}Cl concentrations determined using the University of Rochester tandem accelerator. We have measured ^{36}Cl in over 40 Antarctic meteorites since our previous publication [1]. In general we measured ^{36}Cl in the metallic phase, since its production rate is expected to be nearly independent of depth and size in small meteorites. In some cases, such as heavily weathered chondrites or achondrites, it is impossible to get a clean metallic phase for the measurements. Thus ^{36}Cl was measured instead in the weathered meteorites ALH77026 (^{36}Cl terrestrial age = 800,000 years) and ALH85118 (670,000 years) meteorites, in separated magnetic and non-magnetic fractions. The results agree well with other data by normalizing the activities to the production rate in metallic phase using the elemental production rate ratio (P_{Ca}:P_{Fe} = 8:1) [2, 3]. This normalization method was also applied for terrestrial ages of bulk samples of the unique meteorites ALH85085 (<60,000 years) and LEW86010 (290, 000 years).

Although the data are still preliminary, there are a few interesting points. (1) Many of the Lewis Cliff meteorites are as old as Allan Hills (Main Icefield) meteorites. Although we have measured only five Lewis Cliff meteorites, four out of five meteorites have more than 200,000 years terrestrial age. No clear correlation was yet found between the terrestrial ages and the locations (Lower Ice Tongue and Upper Ice Tongue) of meteorites. Fireman measured the age of one dust-containing ice sample from Lewis Cliff Ice Tongue using a U-Th dating method [4]. The terrestrial ages of Lewis Cliff meteorites which we have measured are significantly longer than the age of this Lewis Cliff ice, 25,000 years. If we accept the young age of Lewis Cliff ice, ice from Law Glacier flowed continuously into the Lewis Cliff Ice Tongue for more than a few hundred thousand years. (2) Four Allan Hills meteorites, ALH77026, 77248, 85048, and 85118 have terrestrial ages ≥ 400,000 years. (3) Four Allan Hills meteorites (ALH84243, 85037, 85048, and 85123) were collected on soil or on bedrock. Three of them have terrestrial ages less than 100,000 years but one, ALH 85048, has a 920,000 years terrestrial age. The outcrop southeast of the Allan Hills Main Icefield and the west side of Allan Hills were essentially ice free for at least 1.4 to 2.5 million years based on in-situ produced cosmogenic nuclides, ^{10}Be, ^{26}Al, and ^{21}Ne, in quartz [5, 6]. We do not yet understand the relationship between the terrestrial ages and the history of the outcrops on which the meteorites were found. (4) ALH85118 was collected from a steeply sloping ice surface. If the meteorite was recently exposed from inside the ice, the age of the ice should be same as the terrestrial age of the meteorite, 650,000 years. However, the meteorite age is much older than the measured age of ice at Allan Hills Main Icefield (~100,000 year) based on U-Th [4] and ^{81}Kr dating [7] and age of ice at Allan Hills Cul de Sac (~300,000 years) [4]. (5) So far old meteorites have been found only at Allan Hills Main Icefield, Elephant Moraine, and Lewis Cliff Ice Tongue. Although some trends were found in the Allan Hills Main Icefield, both old and young meteorites were found there. The oldest terrestrial ages of these meteorites are far older than the age of the ice. If these meteorites fell on the snow accumulation area and transferred to the present location by the current accepted mechanism [8, 9], the Allan Hills, Elephant Moraine, and Lewis Cliff Icefields have been in steady state condition (nearly same ablation and uplift rates of ice) for at least a few hundred thousand years.

References : [1] Nishiizumi K. *et al.* (1989) *Earth Planet. Sci. Lett. 93*, 299-313. ; [2] Begemann F. *et al.* (1976) *Geochim. Cosmochim. Acta 40*, 353-368. ; [3] Nishiizumi K. *et al.* (1991) *Lunar and Planetary Science XXII*, 979-980. ; [4] Fireman E.L. (1988) *Antarctic Journal of the U.S. 23*, 49-50. ; [5] Graf T. *et al.* (1991) *Geophys. Res. Lett. 18*, 203-206. ; [6] Nishiizumi K. *et al.* (1991) *Earth Planet. Sci. Lett.* in press. ; [7] Craig H. *et al.* (1990) *Trans. Am. Geophys. Union 71*, 1825. ; [8] Yanai K. (1978) *Mem. Natl. Inst. Polar Res., Spec. Issue 8*, 1-37. ; [9] Whillans I.M. and Cassidy W.A. (1983) *Science 222*, 55-57.

DELIVERY OF METEORITES FROM THE ASTEROID BELT; Michael Nolan and Richard Greenberg, Lunar and Planetary Laboratory, University of Arizona, Tucson, Arizona 85721 USA

The study of asteroid formation and composition is of keen interest, since the processes that formed our own Earth and the other planets may have been similar in some important ways. Also, the numerous objects in the main asteroid belt and elsewhere help us avoid the "sample of one" problem so common in planetary science. Unfortunately, asteroids are very difficult to study directly: we have relatively noisy, low resolution optical spectra of their disk-averaged surfaces in reflected sunlight or thermal emission, and even then we see only their "dirty" surfaces. Meteorites, on the other hand, can be studied in great detail at high resolution by a wide array of techniques with much lower noise. Thus it would aid our understanding to know how asteroids and meteorites are connected, even if only statistically.

Transport processes for bringing asteroids from the asteroid belt to the Earth have been critically reviewed by Greenberg & Nolan [in *Asteroids II*, R. Binzel, T. Gehrels & M. S. Matthews, eds., 1989, 778–804]. According to most current models, asteroidal material is transported to the Earth by way of Jovian and secular resonances. We do not know for certain how asteroids get into the resonances, which are now fairly clear of asteroids (probably due to the same processes that bring material to the Earth). We understand in general some dynamical delivery mechanisms, but not their relative efficacy, or what regions of space they sample.

As an alternative to using a variety of poorly understood processes to analyze the meteorite delivery process from the main belt, we can look at the process from the other end: meteorites arriving at the Earth. Networks of cameras operating since the early 1950s have photographed several thousand meteor trails. From these photographs, it was possible to determine the orbits of the asteroids which fell as meteors. Wetherill & ReVelle [*Icarus* **48** (1981), 308–328] identified 27 meteors which they believed to be of ordinary chondritic composition (including Lost City, a recovered meteorite). Their orbital elements in a, e space show clusters near several Jovian resonances zones. The orbits of 42 496 meteors collected by the IAU Meteor Data Center show only weak evidence of clustering. The low accuracy of many of the orbits [D. Steele, pers. comm.] is a critical factor. There is a fairly strong concentration of orbits with perihelia near 1 AU. The published orbits, however, are based on a two-body treatment of the the gravitational attraction of the Earth. We are numerically integrating the orbits of these meteors, to determine whether the two-body results are sufficiently precise. These results will help constrain how many came to Earth-crossing by each of the possible routes.

$^{142}Nd/^{144}Nd$ IN SNCs AND EARLY DIFFERENTIATION OF A HETEROGENEOUS MARTIAN (?) MANTLE;

L.E. Nyquist, SN2/NASA Johnson Space Center, Houston, TX, 77058; C.L. Harper, National Research Council, SN2/NASA Johnson Space Center, Houston, TX, 77058; H. Wiesmann, B. Bansal, C.-Y. Shih, Lockheed ESC, C23, 2400 NASA Road 1, Houston, TX, 77258.

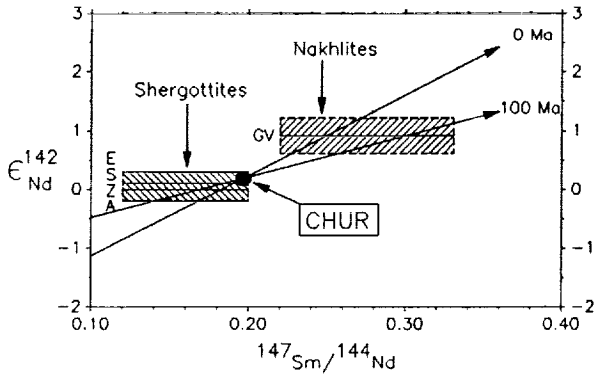

Figure 1. $^{142}Nd/^{144}Nd$ in SNC meteorites compared to the correlation with $^{147}Sm/^{144}Nd$ observed by (4) for the LEW86010 Angrite (0 Ma isochron) and that 100 Ma later.

Sm/Nd correlated variations in $^{142}Nd/^{144}Nd$ have been observed for mineral phases of achondrites from decay of live ^{146}Sm ($T_{1/2}$ = 103 Ma) in the early solar system (1,2,3,4). Crystallization ages of SNC meteorites are $\leq$1.3 Ga, so variations of $^{142}Nd/^{144}Nd$ among mineral phases of the SNCs are not expected. However, if SNCs were derived from source reservoirs of differing Sm/Nd ratios, established while ^{146}Sm was still alive, and which remained isolated except for magma extraction, then variations in $^{142}Nd/^{144}Nd$ would exist among individual SNC meteorites. Rb-Sr (5) and U-Pb (6) isotopic data for the shergottites imply differentiation of their parent planet ~4.6 Ga ago. Although the crystallization ages of the shergottites are uncertain, Shih et al. (5) considered it probable that all of them came from sources having undergone similar $^{143}Nd/^{144}Nd$ evolution. In this case, the Sm-Nd whole rock age, 1.3 Ga, approximates the crystallization age and the average $^{147}Sm/^{144}Nd$ required in the source between 4.56 Ga and 1.3 Ga is 0.165, corresponding to initial ϵ_{Nd} = -13. Nakamura (7) measured the Sm-Nd age, 1.26$\pm$0.07 Ga, and ϵ_{Nd} = +16 for Nakhla. Several authors (8,9,10) assumed shergottites and nakhlites came from a common parent body (SPB=Mars?) and considered the isotopic systematics of the SNCs together. Jones (9) concluded that SNCs were derived from an approximately homogeneous mantle having depleted LREE and $^{147}Sm/^{144}Nd$ ~0.234. These estimates of Sm/Nd in the source(s) of SNCs are sufficiently different from one another to suggest variations in $^{142}Nd/^{144}Nd$ among the SNC meteorites might be detectable.

Figure 1 shows $^{142}Nd/^{144}Nd$, expressed as ϵ^{142}_{Nd}, for shergottites, Shergotty, Zagami, ALHA77005, and EETA79001, and nakhlite Governador Valadares (T_{Rb-Sr} = 1.3 Ga (11)). No detectable $^{142}Nd/^{144}Nd$ anomalies were found for the shergottites. Nakhlite Governador Valadares, however, shows an apparent enrichment of +0.9$\pm$0.3ϵ in $^{142}Nd/^{144}Nd$. When these results are compared to values expected from the correlation of $^{142}Nd/^{144}Nd$ and $^{147}Sm/^{144}Nd$ observed for the LEW86010 angrite (4), the magnitude of the $^{142}Nd/^{144}Nd$ excess found for Governador Valadares is seen to correspond to $^{147}Sm/^{144}Nd$ ~0.25 in the nakhlite source if it formed contemporaneously with LEW86010. This Sm/Nd ratio agrees satisfactorily with that inferred by Jones (9) for the SPB mantle. A delay of ~100 Ma in establishing the source reservoir would require a higher value of $^{147}Sm/^{144}Nd$ ~0.3. The $^{142}Nd/^{144}Nd$ data do not support derivation of shergottites and nakhlites from a homogeneous depleted mantle source. In the Jones (9) and similar models, Nd in Shergotty and Zagami is assumed to be dominated by "crustal" Nd (ϵ_{Nd}<0), whereas Nd in the Antarctic shergottites is dominated by mantle Nd (ϵ_{Nd}>0). $^{142}Nd/^{144}Nd$ for the Antarctic shergottites is indistinguishable from that for Shergotty and Zagami, suggesting similar chondritic or slightly subchondritic Sm/Nd ratios in the primordial sources of the shergottites. The amount of mixing of Nd from different reservoirs inferred from $^{142}Nd/^{144}Nd$ is independent of the exact age of the shergottites. Thus, the conclusion that the nakhlites and shergottites were derived from different source regions and that, consequently, the SPB mantle was heterogeneous, seems firm.

REFERENCES: (1) Lugmair G.W. et al. (1975) EPSL 27, 79–84. (2) Prinzhofer A. et al. (1989) Ap. J. Lett., 344, L81–L84. (3) Lugmair G.W. and Galer S.J.G. (1989) Meteoritics 24, 296. (4) Nyquist L.E. et al. (1991) LPSC XXII, 989–990. (5) Shih et al. (1982) GCA 46, 2323–2344. (6) Chen J.H. and Wasserburg G.J. (1986) GCA 50, 955–968. (7) Nakamura N. et al. GCA 46, 1555–1573. (8) Wood C.A. and Ashwal L.D. (1981) PLPSC 12B, 1359–1375. (9) Jones J.H. (1989) PLPSC 19, 465–474. (10) Jagoutz E. (1989) GCA 53, 2429–2441. (11) Wooden et al. (1979) LPS X, 1379–1381.

SILICON, CARBON AND TITANIUM ISOTOPES IN SIC FROM AGB STARS : Obradovic, M., Brown, L.E., Guha, S. and Clayton, D.D. Dept. Physics and Astronomy, Clemson University, Clemson SC 29634.

We report models of the evolution of isotopic abundances in the envelopes of AGB stars. We now have more than one model of the evolution of these stars, and will attempt to choose those most consistent with observations of the Magellanic Clouds. We continue to regard the neutron fluence per pulse $\Delta\tau$ to be an unknown. Our first report (1) erred in judging the $^{33}S(n,\alpha)^{30}Si$ cross section to be unimportant; measurements show it to be much larger than the (n,γ) branch. Inclusion in the pulse-and-mix algorithm results in considerably larger ^{30}Si excesses in the He shell than for ^{29}Si, and hence smaller slope for the $\delta(29)$ *vs.* $\delta(30)$ correlation line generated in the mixed envelopes . Fig.1 shows this calculated slope for models of differing mass as a function of the fluence per pulse $\Delta\tau$. Fig.1 shows that if the initial composition was indeed solar, that slope is well less than unity, in contrast to the values observed near 1.4. Apparently the presolar AGB stars must be more deficient initially in ^{30}Si than in ^{29}Si and/or have a larger Si/S elemental ratio, both of which are astrophysical possibilities. We will illustrate some of them.

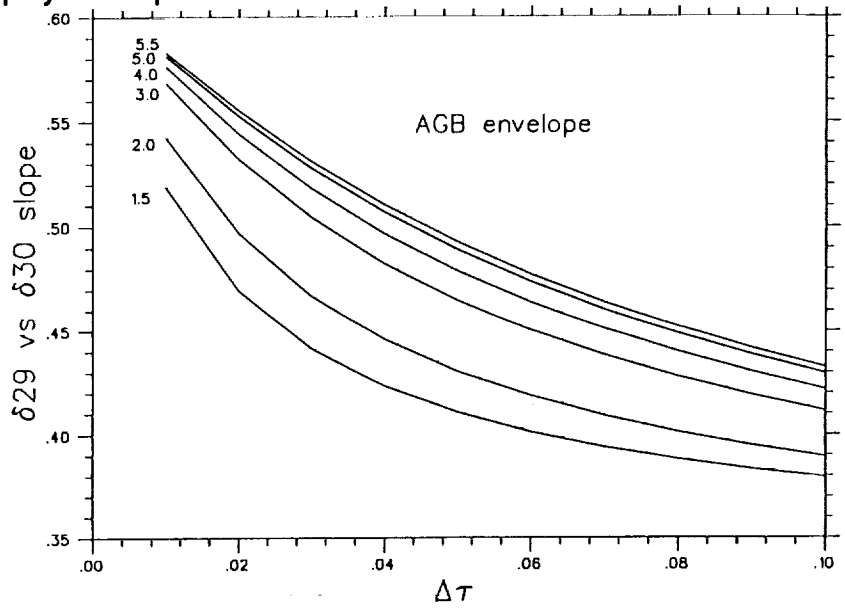

We have implemented a time-dependent convective envelope to study hot-bottom burning in AGBs. Surface $^{12}C/^{13}C$ rises to a maximum value during dredgeups and then declines at the end as $^{12}C(p,\gamma)$ elevates ^{13}C. The Ti isotopes of interest depend strongly on $\Delta\tau$ as major *s*-process adjustments (2) occur. We also show these results. *References*: Clayton, D.D. *et al.*(1991) Lunar PLanet.Sci. **22**,pp.221-222. (2) Clayton, D.D. (1981) Meteoritics **16**, 303.

RADAR CONSTRAINTS ON ASTEROID METAL ABUNDANCES AND METEORITE ASSOCIATIONS, S. J. Ostro, Jet Propulsion Laboratory/Caltech, 300-233, Pasadena, CA 91109

Radar observations can shed light on asteroid-meteorite relations because metal, which is much more abundant in iron/stony-iron meteorites than in chondrites, influences radar reflectivity dramatically. In principle, one can make measurements of an asteroid's radar reflectivity, interpret the measurements within the framework of our empirical and theoretical understanding of the electrical properties of mineral assemblages, and constrain the asteroid's surficial metal concentration (and set of plausible meteorite analogs). However, it is important to be aware of the technical difficulties, sources of uncertainty, and possible pitfalls encountered in the various stages of this idealized logical sequence. Some of the more important considerations mentioned here are discussed in more detail in (1).

In most asteroid radar experiments, one transmits a circularly polarized signal and then uses twin receivers to record echoes in the same circular polarization as transmitted (the SC sense) and the opposite (OC) sense. Measurements of the radar cross sections σ_{OC} and σ_{SC} normally have absolute uncertainties between 20% and 50%, and relative uncertainties of ~15%. The OC component includes echoes due to single reflections from large, smooth surface elements. Inferences of metal abundance rest on estimates of the radar albedo, $\hat{\sigma}_{OC} = \sigma_{OC}/A_{proj}$, with A_{proj} the asteroid's apparent projected area. Absolute uncertainties in A_{proj} are $\leq$ 20% for most of the 35 radar-detected mainbelt asteroids, but the uncertainties are considerably larger for most of the 28 radar-detected near-Earth asteroids (NEAs).

If $\sigma_{OC} >> \sigma_{SC}$, the albedo can be thought of as the product of the Fresnel power-reflection coefficient R and a gain factor, G, that depends on the target's shape at scales $\geq \lambda$. Large mainbelt objects are expected to be covered with regoliths more than 15 m thick. In light of expectations about such objects' shapes and surface slope distributions, G is probably within a few tens of percent of unity, so $\hat{\sigma}_{OC}$ is a reasonable first approximation to R. For the smaller, more irregularly shaped NEAs, G might be a strong function of orientation, causing radar cross section to vary much more dramatically than A_{proj} as the object rotates. NEA albedos derived from observations with thorough rotation-phase coverage might tend to "average out" variations in G, but possibly not enough to justify treating $\hat{\sigma}_{OC}$ as an approximation to R.

For dry, unconsolidated powders of meteoritic minerals, R depends primarily on bulk density *d*, and predictions of R(*d*) based on empirically determined functions probably are reliable to ± 25%. The radar absorption length in dry, powdered rocks is about 10 wavelengths, so a regolith more than one meter thick would "hide" underlying bedrock from the radar. A much thinner regolith can act similarly if it has a density gradient that matches the bedrock's impedance to that of free space, or if it has stratifications containing lossy layers that create certain resonance effects. For solids, small volume concentrations V of metal particles in a silicate matrix can raise R above the value for V = 0 by an amount that depends on the electrical properties of each phase, the metal particles' dimensions and packing geometry, and V. Predictions of the (rather large) ranges of R for several meteorite types on the basis of laboratory investigations of "loaded dielectrics" are consistent with available measurements of R for solid meteorite specimens. Solids are more reflective than powders. Clearly, inferences of metal concentration and meteoritical association from radar albedos necessarily involve assumptions about regolith depth and porosity.

(1) Ostro et al. (1991). Asteroid 1986 DA: Radar Evidence for a Metallic Composition. *Science*, in press.

NE-E(H) AND KR-, XE-S IN INDARCH AND KRYMKA: ARE THEY A MEASURE OF THE SIC ABUNDANCE? U. Ott, H.P. Löhr, and F. Begemann. Max-Planck-Institut für Chemie, Saarstr. 23, D-6500 Mainz, F.R.G.

Silicon carbide by now is well established as a phase of interstellar origin being present in primitive meteorites with an abundance in the range of a few ppm (e.g. [1]). Attempts have been made to infer its abundance in meteorites from different types and classes from the observed abundance of Ne-E(H) [1]. Here we report data obtained for Ne-E(H), Kr-S, and Xe-S in a primitive ordinary chondrite (LL 3.0 Krymka) and an enstatite chondrite (E3-4 Indarch) which indicate that the elemental and (at least in the case of Kr) isotopic composition of these gases is different for different meteorites and, hence, that trying to infer the abundance of SiC from the abundance of any of these trace elements is dubious at best.

We have reported abundances of Ne-E(H) and Xe-S in Krymka previously [2]. The ratio ^{22}Ne-E(H)/^{130}Xe-S of ~2000 is a factor of two higher than that for CM2 Murray [3]. Another ordinary chondrite, Inman (L/LL3.4) shows an even higher ratio of 3700 [4]. The same ratio in Indarch (~430), on the other hand, is significantly lower. Hence, there is at least a factor ~10 variation in this ratio among bulk meteorites, and, at present, we do not know which, if any, of these two gas abundances is a good measure for the abundance of SiC.

Previous work on Murchison has shown that the $(^{86}Kr/^{82}Kr)_s$ ratio is variable [5,6]. Our Kr data for Indarch (Fig.1) clearly show that this ratio is very low for the main combustion steps at 900°C and 1100°C (extrapolated to ~ 0.5±0.3 and 0.7±0.2, resp.), even lower than what has been observed in Murchison grain size fractions [6]. The correlation of this isotopic ratio with the Ne-E(H)/Xe-S ratio observed in Murchison [7,6] seems to hold also for bulk meteorites, since in Indarch both ratios are low (Fig.2). S-process Kr measured in our Krymka residue is less pure and the inferred $(^{86}Kr/^{82}Kr)_s$ ratios have large uncertainties. They are not shown in Fig.2; they are, however, compatible with the trend there.

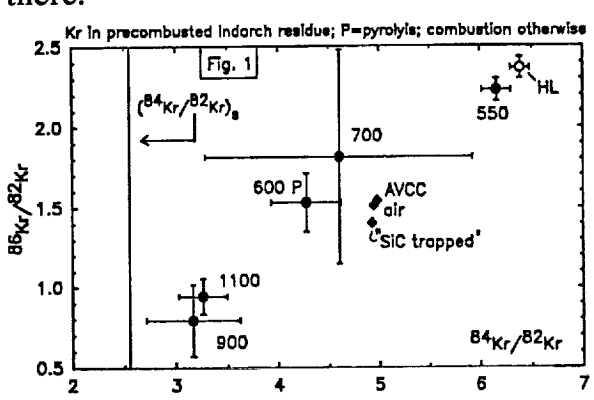

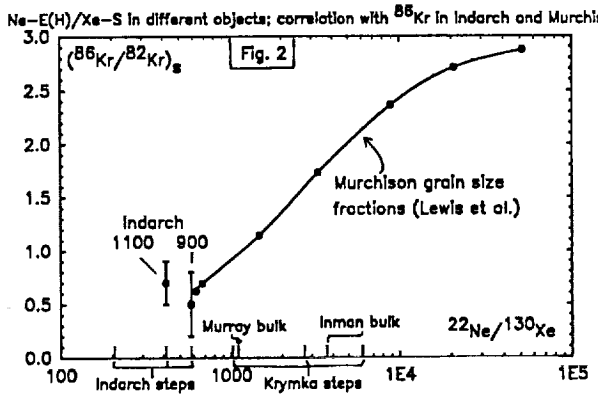

By comparison with the Murchison results in [6] these data might mean that enstatite chondrites contain a relatively higher fraction of fine-grained SiC, ordinary chondrites to contain a relatively higher fraction of coarse SiC than carbonaceous chondrites. This seems to contradict the observations of [8], however. The abundance, size distribution, and trace element contents of SiC in different meteorite types should be able to give us clues to its introduction into and/or history within the early solar system. But clearly more work is needed before we reach the stage of unambigous answers.

Acknowledgements: We thank L.K. Levsky for the Krymka sample and S.S. Russell and C.T. Pillinger for the precombusted Indarch acid residue.

References: [1] Huss G.R. (1990) Nature 347, 159. [2] Levsky K.L. et al. (1989) Meteoritics 24, 292. [3] Tang Ming and Anders E. (1988) GCA 52, 1235. [4] Alexander C.M.O'D. et al. (1990) EPSL 99, 220. [5] Ott U. et al. (1988) Nature 332, 700. [6] Lewis R.S. et al. (1990) Nature 348, 293. [7] Ott U. et al. (1988) LPSC XIX, 895. [8] Alexander C.M.O.D. et al. (1989) Meteoritics 24, 247.

Palaeoclimate Cycles due to Impacts by Extraterrestrial Bodies ---- A Study on the Possibility

Ouyang Ziyuan Guan Yunbin Cheng Hongde Zhang Yanhong
(Institute of Geochemistry, Chinese Academy of Sciences)

This paper deals with the characteristic features of six well-documented extraterrestrial-body impact events in the past 65 Ma (Cenozoic) and the possibility to cause the palaeoclimate cycles. K/T and T/Q boundary impact events occurred at 65 Ma and 2.4 Ma, respectively. Other four global impact events responsible for the formation of tektites took place at 34±1 Ma (E/O boundary), 15±1 Ma, 1.3±0.2 Ma(Q_1/Q_2 boundary) and 0.7±0.1 Ma, respectively.

Studies of the anormalies of iridium and other platinum-group elements, the characteristics of soot-bearing layers formed as a result of global fire, the variation trends of $\delta^{13}C$ and $\delta^{18}O$ and other palaeoenvironmental features at the K/T boundaries have shown that the impact events brought about serious consequences: highly concentrated fine dusts and soot particles were spread all over the stratosphere, hence solar radiation was shielded, photosynthesis was inhibited, the temperature on the Earth's surface went down drastically, ice sheets were enlarged and thickened and a new glacial epoch was ushered in, accompanied by regressions and acid rain fallout. As a result, a dark, cold winter came into being. In addition, quite a great number of species were extinct and geomagnetic polarity reversals occurred.

As viewed from variations in carbon and oxygen isotopic composition at the K/T boundary, the evolution of palaeoclimate cycles caused by impact events may be devided into three stages: 1. the temperature-decrease and new glacial stage; 2. the temperature-increase and greenhouse effect stage; and 3. the palaeoclimate turning normal stage.

Radiation-induced diamond (carbonado): a possible mechanism for the origin of diamond in some meteorites

Ozima, M.[1] and Zashu, S.[2], (1)Department of Earth and Space Science, Osaka University, Toyonaka City, 560 (2)Department of Geophysics, University of Tokyo, Bunkyo-Ku, Tokyo, 113, Japan

There are three major ways to synthesize diamond: (i) application of high hydrostatic pressure and temperature, (ii) application of shock, and (iii) crystallization from vapour phase at a relatively low pressure (CVD method). Each process has been called for the origin of diamond in meteorites by different authors. Recently we reported (1) that carbonado can be produced from carbonaceous matter through irradiation of high energetic particles. This new type of a diamond formation process may be relevant to the origin of diamond in some meteorites.

Carbonado is an aggregate of micrometer-size diamond crystals. We have analysed four carbonados from different localities for noble gas isotopic composition ,U content, and $\delta^{13}C$. All the carbonados showed enormous amount of fission Xe and Kr which far exceeded the expected in-situ produced amounts. They were also characterized by a large amount of atmospheric noble gases which were degassed mainly at the highest temperature fraction (graphatization temperature) in the step-heating degassing. The incorporation of a large amount of unsupported fission Xe and Kr, and the very tightly trapped atmospheric noble gases indicate that the carbonados crystallized in the crust in an intimate contact (i.e. within the range for fission particles which is about 20 micrometers) with U and Th. The noble gas experimental results support the speculation by Kaminskii (2) that carbonado was formed by high energetic particle irradiation from decaying U and Th in uranium enriched phase in coal.

Diamonds in undifferentiated meteorite are characterized by the presence of Xe-HL which is supposed to be implanted into the diamond during supernova explosion (3). The characteristic association of the high energetic Xe particles in the diamond can be easily understood in terms of the above radiation induced diamond formation. Extremely small grain size and low density of the diamond are also consistent with the radiation induced origin.

References.

(1) Ozima,M.,S.Zashu,K.Tomura, and Y.Matsuhisa (1991) Nature (in press)
(2) Kaminsky,F. (1987) Dokl.Akad.Nauk USSR 294, 439-40
(3) Anders,E. (1989) in Interstellar Dust, eds. L.J.Allamandola and A.G.G.M.Tielens, 389-402, published by the IAU

PLASMA CHEMICAL INERT GAS RELEASE FROM THE ALLENDE METEORITE; R. L. Palma, Department of Physics, Sam Houston State University, Huntsville, TX. 77341; S. Chaffee, M. Hyman, and M. W. Rowe, Department of Chemistry, Texas A&M University, College Station, TX. 77843.

Recent advances in plasma chemistry (1, 2, and 3) have yielded impressive results and hold great promise for meteoritic studies. Our preliminary experiments (4 and unpublished data) indicate that low temperature oxygen plasmas will be effective in extracting inert gases from cosmological samples. Notable advantages are first, that inert gases are effectively extracted at temperatures of less than or equal to 250 °C. This reduces the background problems associated with high temperatures necessary for complete gas extraction in ultra-high vacuum heating. Furthermore, it alleviates problems of diffusive mixing of component gases caused by the high temperatures. In addition, the oxygen plasma totally converts carbonaceous material to CO(g) and/or CO_2(g) and H_2O(g) before significant gas release from the other components of the sample begins. This allows the separation and measurement of the inert gases from the carbonaceous carrier as well as the rest of the meteorite in a single sample. A study of the extraction conditions necessary for efficient gas removal from important minerals may allow selective gas removal from complex mineral systems.

The conditions required for the removal of the inert gases from the Allende meteorite will be reported along with the data on the individual gases. The conditions to be discussed, among others, include the plasma power, the length of the reaction time, the position of the sample in the plasma, and the sample gas clean up procedures. References: (1) Veprek S. and Elmer J. Th. (1985a) *Zeitschr. Schweizer. Archaol. und Kunstgesch.* **42**, 61-63. (2) Veprek, S., Patscheider, J. and Elmer, J. Th. (1985b) *Plasma Chem. Plasma Proc.* **5**, 201-209. (3) Patscheider, J. and Veprek, S. (1986) *Stud. in Conserv.* **31**, 29-37. (4) Cocke, D. L. and Rowe, M. W. (1986) *Meteoritics* **21**, 315-317.

REHEATING OF ALLENDE COMPONENTS BEFORE ACCRETION

H. Palme[1], S. Weinbruch[1,2], and A. El Goresy[2]
[1]Max-Planck-Institut für Chemie, Mainz; [2]Max-Planck-Institut für Kernphysik, Heidelberg.

A late heating event affected all major components of Allende before they accreted to form a parent body. Evaporation of earlier, condensed material resulted in an oxygen rich vapor that deposited, on condensation, FeO and Cr_2O_3-rich layers around preexisting chondrules, inclusions and mineral fragments. At the same time redistribution of volatiles occurred. The ubiquitous presence of Ni-rich metal and Ni-rich sulfide in lithologies originally formed under very different conditions (CAIs, chondrules, fragments, mineral grains) may be the result of reaction with the oxidized, sulfur-rich gas. Formation of pyrrhotite, commonly found in Allende, instead of troilite is expected from such a gas, but not from the reduced solar nebula.

Deposition of FeO-rich and occasionally Cr_2O_3-rich layers in veins and rims of chondrules, forsterite grains and CAIs occurred, most likely, by condensation from a gas phase (1). A chromite crystal inside a fayalitic rim yields an equilibration temperature with olivine of 1300-1370 K (2), indicating rim formation at this temperature. Such high temperatures can only have lasted for several hours, considering the steep compositional gradient between forsterite and fayalite (1). Fayalitic rims were also found around rare, large FeO-rich olivines formed by metal-silicate equilibration at 700 K according to the chromite-olivin thermometer (2). This and other evidence demonstrates that rim formation is a late event.

FeO-rich spinels in fine grained Ca, Al-rich Allende inclusions and in rims of coarse grained inclusions were formed under the same conditions. There is a corresponding enrichment of volatile elements in the same phases (Na, K, Ga, Zn, Cl, Br, I), suggesting incorporation of FeO and the volatiles by condensation from a gas phase (3). The paucity and poor development of FeO-rich rims in chondrules and mineral grains and the low contents of FeO and volatile elements (Ga, Zn etc.) in fine grained spinel-rich inclusions of members of the reduced sub-group (Efremovka, Vigarano etc.) compared to members of the oxidized subgroup (Allende, Grosnaja etc.) indicates a higher intensity of the late reheating event in the formation location of the oxidized subgroup of CV-chondrites.

There is some evidence for inhomogeneous distribution of the vaporized cloud: Variable widths of faylitic rims and the adjacent transition zone to forsterite and large differences in the extent of sulfurization. On the other hand, the similar bulk composition of all C3V-chondrites and the uniform chemical composition of Allende indicates a closed system behavior, i.e. the late evaporation did not lead to a net-loss of volatiles, large lateral temperature gradients were absent during heating and subsequent cooling, and evaporation and recondensation occurred on a fast time scale.

Radiogenic clocks involving volatile elements may have been reset by the event. Fine-grained spinel rich Allende inclusions are rich in I and ^{129}Xe. Their I-Xe ages indicate two events separated by 3.7 my. The younger age may be associated with condensation after the reheating event (4).

In summary, the late heating hypothesis is able to explain a variety of otherwise apparently unrelated observations. The alteration must have occurred after CAI and chondrule formation but before accretion since there is no textural evidence for high temperature heating event of bulk Allende.

Lit.: (1) X. Hua *et al.* (1988) GCA **52**, 1389; (2) S. Weinbruch *et al.* (1991) this volume; (3) H. Palme and D. Wark (1988) LPSC XIX, 897; (4) A. Zaikowski (1980) EPSL **47**, 211.

EXCEPTIONALLY UNFRACTIONATED SOLAR NOBLE GASES IN THE H3-H6 CHONDRITE AÇFER 111.

A. Pedroni and H. W. Weber, MPI für Chemie, Saarstrasse 23, D-6500 Mainz, Germany.

Among a few hundred meteorites recovered in the past two years in the desert highland AÇFER (Algeria) we find an exceptional stone, AÇFER 111, weighing 987 g. In a petrographic investigation (1) this stone was classified as polymict, H3-H6-chondritic regolith breccia. A preliminary noble gas analysis of the bulk matrix revealed a trapped gas composition of $(^4He/^{20}Ne)_{trap} \approx 600$ and $(^{20}Ne/^{36}Ar)_{trap} \approx 40$. These values are the highest ever seen in any regolithic material. Compared to $(^4He/^{20}Ne)_{sw} = 540 \pm 70$ and $(^{20}Ne/^{36}Ar)_{sw} = 45 \pm 10$ obtained in the solar wind composition (SWC)-experiments (2), trapped gases of AÇFER 111 look virtually unfractionated. The isotopic compositions $(^4He/^3He)_{trap} \approx 3000$ and $(^{20}Ne/^{22}Ne)_{trap} = 12.1 \pm .2$ of AÇFER 111 are distinctly heavier than $(^4He/^3He)_{sw} = 2350 \pm 120$ and $(^{20}Ne/^{22}Ne)_{sw} = 13.7 \pm .3$ obtained in the SWC-experiment.

Noble gases released by stepped etching of Fayetteville (H-chondrite), Kapoeta (howardite) and lunar samples (3,4) showed that solar energetic particles (SEP), that are implanted deeper than solar-wind (SW)-particles, have the isotopic composition $(^4He/^3He)_{SEP} = 4400 \pm 250$ and $(^{20}Ne/^{22}Ne)_{SEP} = 11.3 \pm .1$. The elemental composition of SEP was undistinguishable from that of SW-particles. The trapped gas composition measured for AÇFER 111 can thus be explained as a mixture of nearly equal amounts of SW and SEP. This SW/SEP ratio does not necessarily reflect the SW/SEP flux ratio of the ancient sun, because the mineral grains of AÇFER 111 may have lost the uppermost solar wind bearing layer by some regolith process (sputtering by solar ions, lithification) or by weathering on earth. More detailed results will be presented at the meeting.

REFERENCES: (1) A. Bischoff (1991) pers. comm. (2) P. Bochsler (1987) Solar wind ion composition. Physica Scripta T18, 55-60. (3) J. -P. Benkert et al. (1988) Lun. Planet. Sci. XIX Houston, 59-60. (4) A. Pedroni et al. (1991) Lun. Planet. Sci. XXII Houston, 1049-1050.

EXOTIC CLASTS IN METEORITIC BRECCIAS. P. Pellas. Equipe Météorites (CNRS), Lab. de Minéralogie du Muséum, 61 rue Buffon, 75005 Paris (France).

In recent years, through detailed petrological and oxygen isotope investigations, a large number of foreign clasts have been detected in meteoritic breccias (1, 2). The majority of them are of carbonaceous chondrite parentage (mostly CM2, but some of them CI or even not represented in our meteorite collections), while the OC-like clasts represent about 1/3 of the total. Among the rest, it is of some interest to note the near absence of exotic metal clasts (not easy to detect them in OCs, one possibility being the metal fraction of Bencubbin, according to H.E. Newsom, personal communication, 1988), and of igneously differentiated ones (f.i. similar to eucrites and/or aubrites). For the latter, most Ca-plagioclase bearing clasts in OCs of petrological types 3 and 4 may simply be explained by volatile element losses from chondrule and chondrule fragments (3). Apparently, five distinctly differentiated exotic clasts have been found to date in meteoritic breccias. These are : A) an igneous inclusion of H-parentage in L5-Barwell (4); B) a noritic clast or chondrule fragment (with excess 26Mg) in LL3-Semarkona (5); C) a diabase like inclusion in LL3-Parnallee which apparently shows a strong affinity with the eucrites (6); D and E) andesitic clasts (An40-50) detected in H3-Study Butte and H4-Beddgelert chondrites (7).

At the first glance, such a scarcity, of "differentiated" clasts might reflect in some way the rarity of basaltic achondrite asteroids, and/or the difficulty to detect with naked eyes such alien fragments among the normal clast population of types 3 and 4 OCs. Nevertheless it must be recognized that if (at 2.5-3.0 AU) the abundance of C-like clasts in meteoritic breccias resembles more or less the distribution of "primitive" (carbonaceous) asteroids(8), a strong contradiction exists between the abundance of "igneous" (mantle shattered) asteroids (8) and the paucity of their equivalent differentiated (mantle derived) counterparts as exotic clasts in meteoritic breccias. This has to be explained.

Moreover, the fundamental contradiction between the large abundance of OC-like clasts (coming from more than 3 parent-bodies) and the apparent total absence of OC-type asteroids in the main belt remains a major challenge for future studies.

The author himself has to confess, after having carefully read all explanations given by most spectroscopists, to have found them short, and that he is far from being convinced by their arguments (8, 9, 10).

References. (1) Pellas P. (1988) Meteoritics 23, 293. (2) Lipschutz et al. (1989) Asteroids II, 740-777. (3) Grossman J.N. and Rubin A.E. (1986) LPSC XVII, 293. (4) Hutchison R. et al. (1988) EPSL 90, 105. (5) Hutcheon I.D. and Hutchison R. (1989) Nature 337, 238-241. (6) Kennedy A.K. et al. (1990) Meteoritics 25, 376. (7) Fredriksson et al. (1989) Z. Naturforsch. 44a, 945-962. (8) Bell J.F. et al. (1989) Asteroids II, 921-945. (9) Gaffey et al. (1989), Asteroids II, 98-127. (10) Bell J.F. (1991) LPSC XXII, 81.

MODIFICATION OF AMINO ACIDS AT SHOCK PRESSURES OF 3 TO 30 GPA: INITIAL RESULTS.

Etta Peterson, N-239-4, NASA-Ames Research Center, Moffett Field, CA 94035
Friedrich Horz, SN2, NASA-Johnson Space Center, Houston, TX 77058
Gerald Haynes and Thomas See, Lockheed-ESC, Houston, TX 77058

Since the discovery of amino acids in the Murchison meteorite, much speculation has focused on their origin and subsequent alteration, including the possible role of secondary processes, both terrestrial and extraterrestrial. As collisional processes and associated shock waves seem to have affected the silicate portions of many primitive meteorites, a mixture of powdered Allende (125-150 m grain size) and nine synthetic amino acids (six protein and three non-protein) were subjected to controlled shock pressures from 3 to 30 GPa to determine the effect of shocks on amino acid survivability. This report presents preliminary characterizations of the recovered shock products.

The shock experiments employed a powder propellant ballistic range, and the samples containing amino acids were encased in metal jackets; the latter and the flat-plate projectile were manufactured from materials of known equation-of-state, such that the peak pressures could be calculated from only a measured impact velocity (Gibbons, et al, 1975; and Schaal, et al, 1979). Temperature measurements cannot be made during such experiments, however, the metal container was recovered within one minute and equipped with a thermo–couple while simultaneously being placed on a pre-cooled aluminum block. The highest temperature recorded was 58°C at 30 GPa, and all samples cooled to ambient room temperature within 10 minutes. The unshocked control sample underwent all target preparation and recovery procedures, including milling and lathe operations, save the actual impact. The retrieved test samples were prepared for analysis to determine the extent of destruction of amino acids and the extent of their racemization. The general procedure followed was extraction of amino acids from the mineral matrix with dilute acid; separation of amino acids from other ions by ion exchange chromatography; and derivatization and analysis of amino acids gas chromatographically as described by Kvenvolden, et al (1972).

Results were as follows: (a) amino acids decreased as a function of increased pressure (e.g., aspartic acid was three orders of magnitude less at 30 GPa vs. the control sample and the 3 GPa sample). (b) Racemization increased as a function of increased pressure (e.g., aspartic acid increased from D/L = 0.011 for the control sample to D/L = 0.68 (equilibrium = 1.0) at 30 GPa). Evidence of secondary amino acid formation was insignificant. In terms of recovery, the acidic amino acids , aspartic acid and glutamic acid, survived better than the other amino acids. This result parallels findings in organic geochemistry in which the acidic acids survive longer in the sediment column. Perhaps the interaction of the carboxyl groups with the mineral matrix insures greater stability. Aromatic acids, such as phenylalanine, do not survive as well.

Gibbons, R.V., Morris, R.V., and Horz, F. (1975) Proc. Lunar Sci. Conf. 6th, 3143-3171.
Kvenvolden. K.A., Peterson, E., and Pollock, G.E. (1972) Adv. in Org. Geochem., 387-401.
Schaal, R.B., Horz F. , Thompson, T.D., and Bauer, J.F. (1979) Proc. Lunar Sci. Conf. 10th, 2547-2571.

VIS/NEAR IR REFLECTANCE SPECTRA OF CI/CM ANTARCTIC CONSORTIUM METEORITES: B7904, Y82162, Y86720: Carlé M. Pieters, Dan Britt, and Janice Bishop (Dept. Geological Sciences, Brown University, Providence, RI 02912)

A consortium to study a group of unusual Antarctic carbonaceous chondrites with CI affinities is being led by Y. Ikeda of Ibaraki University. Reported here and in a companion abstract (Bishop and Pieters) are initial results of reflectance measurements of B7904, Y82162, and Y86720. These carbonaceous chondrites have been variously classified as CI, CM, C1 and C2, but when both chemical and petrographic characteristics are considered, they do not easily fall into the current classification scheme (Fourth Consortium Circular by Ikeda, 1989). They may represent distinct differences in thermal history and pre- and post-accretionary processes of their respective parent bodies (Paul and Lipschutz, Proc. NIPR Symp. Antarct. Met. 3, 80-95, 1990).

Binocular microscope inspection of representative chips received for reflectance measurements revealed these low albedo samples exhibit a variety of alteration. Sample **B7940** appears unaltered throughout. Several areas of **Y86720** chips exhibit red-yellow alteration, a presumed weathering product. Chips of **YB2162** are unusual; almost all exhibit a thin coating (< 10 μm) of a brighter substance but little, if any, red-yellow weathering.

Reflectance spectra were first obtained for small areas on the meteorite chips. Samples Y86720 and B7940 were then ground and dry sieved to <125 μm and spectra were obtained for the powder form. [Chips of Y82162 will not be ground until the origin and character of the coating is better known and, if possible, the coating removed.] Near-infrared spectra obtained from 0.3 to 2.7 μm with the RELAB bidirectional spectrometer set at i=30°, e=0° are shown below. Although similar in general character to other carbonaceous chondrites (low albedo, almost featureless spectra), these Antarctic meteorites do not exhibit the 0.74 μm phyllosilicate absorption that is common to Murchison and Meghei CM meteorites (Moroz and Pieters, 1991, *Lunar and Planetary Sci. XXII*, 923). On the other hand, the 0.5 μm feature seen in Y86720 also occurs in spectra of Orgueil (Moroz, unpublished spectra; Gaffey, 1976, *JGR*, 81,905), but this feature is most likely a ferric absorption due to weathering processes.

The distinctively "blue" spectrum for Y82162 is characteristic of a thin transparent coating over a dark substrate. The shorter wavelengths interact more with the coating and reflectance is higher than the longer wavelengths which pass through the coating and are absorbed by the substrate. The Y82162 spectrum is indicative of the presence of a coating, but it does not provide mineralogical information in this part of the spectrum. When these data are combined with the mid-infrared, however, the character of the coating becomes more obvious (see Bishop and Pieters abstract, these volumes). The Y82162 coating exhibits exceptionally strong water absorptions at 3 and 6 μm and a distinctive feature at 6.8 μm attributed to carbonates (Sanford, 1984, *Icarus* 60, 115; Miyamoto, 1987, *Icarus*, 70, 146).

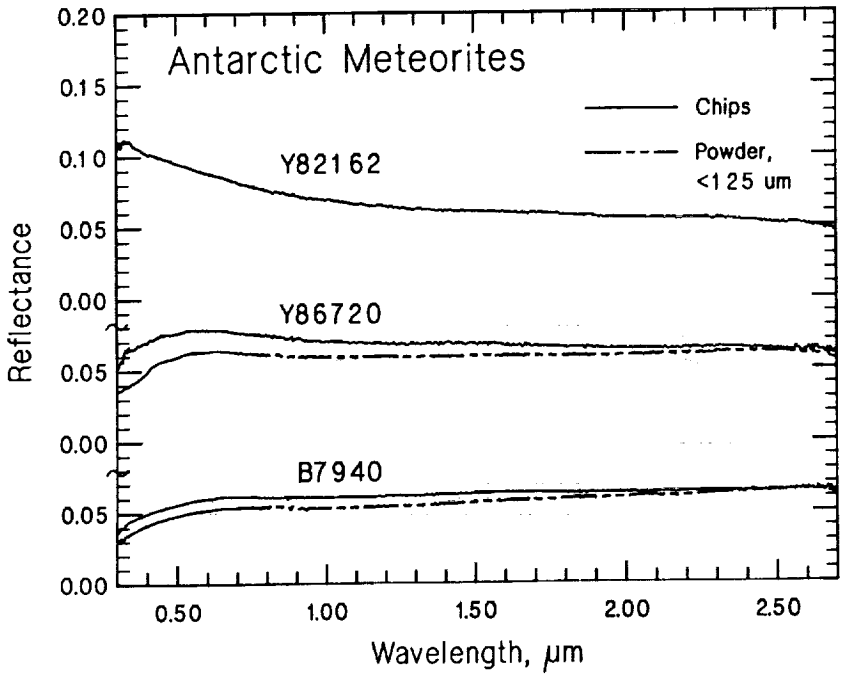

CHROMIUM ISOTOPIC COMPOSITIONS OF INDIVIDUAL SPINEL CRYSTALS FROM THE MURCHISON METEORITE;

F. A. Podosek[1], C. A. Prombo[1], L. Grossman[2] and E. K. Zinner[1]. [1]McDonnell Center for the Space Sciences, Washington University, One Brookings Drive, St. Louis, MO 63130-4899, USA [2]Enrico Fermi Institute, University of Chicago, 5630 S. Ellis Ave., Chicago, IL 60637-1433 USA.

Kuehner and Grossman [1] have described an unusual suite of spinels separated from Murchison by freeze-thaw disaggregation, density separation and hand picking. These spinels are large (≥ 100 μ) and rich in FeO and Cr_2O_3 [1] ; their O isotopic compositions are close to normal [2] , much less anomalous than spinels in Murchison dissolution residues [3, 4]. Esat and Ireland [5] studied Cr isotopic compositions in Murchison spinels which, judging by separation technique, size, color and mineral chemistry, appear to represent a population indistinguishable from that prepared by Kuehner and Grossman [1] ; they [5] found striking Cr isotopic anomalies at both ^{53}Cr (up to 3 ‰) and ^{54}Cr (up to 5 ‰), larger even than anomalies in Allende FUN CAIs [6]. Here we report Cr isotopic data for individual Murchison spinel crystals previously studied by Kuehner and Grossman [1] and Grossman *et al.* [2] , with the objective of extending the survey of Cr anomalies in these grains and seeking possible correlations with mineral chemistry.

We used a direct-load procedure in which solid grains (cf [5]) were loaded on V-shaped Re filaments with boric acid and silica gel. For calibration, we examined terrestrial (Burma) spinel [2] loaded the same way, and also reagent Cr solution. Isotopic analyses were performed in a VG-354 thermal ionization mass spectrometer, using a Daly detector in pulse-counting mode for ion collection. Corrections for instrumental discrimination were based on $^{50}Cr/^{52}Cr$ normalization assuming the "exponential" mass-dependence law; data for ^{53}Cr and ^{54}Cr are reported as ε-unit (parts in 10^4) deviations from the normal composition of Papanastassiou [6] . Data are organized into "sets," each comprising five cycles integrating the ion signal of each isotope for 5 sec, with the ^{52}Cr beam at 2×10^5 cps. For about half the data, set-to-set reproducibility is consistent with the limit dictated by Poisson statistics (standard deviations of 18ε for ^{53}Cr and 34ε for ^{54}Cr); for the other half, set-to-set variability was larger because of beam instabilities. Results to date (see Table) are reported as the mean and error of the mean for all sets obtained for a given sample, including the Burma spinel and reagent Cr. Data are of variable quality according to beam stability and duration for each sample.

A first order observation is that our results indicate no anomalies beyond error limits. In particular, we do not observe anomalies that would be expected on the basis of the size and frequency of anomalies observed by Esat and Ireland [5]. Our results also suggest (weakly) that this population of spinels may lack the "endemic" 5-10 ε ^{54}Cr anomaly of refractory inclusion spinels [6, 7] , a result which parallels the small (negligible?) O anomalies [2] in this population.

References: [1] Kuehner S. M. and Grossman L. (1987) *Lunar Planet. Sci. XVIII,* 519; [2] Grossman L. *et al.* (1988) *Lunar Planet. Sci. XIX,* 435; [3] Clayton R. and Mayeda T. (1984) *Earth Planet. Sci. Lett.* **67**, 151; [4] Virag A. *et al.* (1991) *Geochim. Cosmochim. Acta*; in press. [5] Esat T. M. and Ireland T. R. (1989) *Earth Planet. Sci. Lett.* **92**, 1-6; [6] Papanastassiou D. A. (1986) *Ap. J. Lett.* **308**, L27; [7] Birck J.-L. and Allègre C. J. (1988) *Nature* **331**, 579.

Cr Isotopic Analyses

Sample [a]	Group[a]	ε_{53}[b]	ε_{54}[b]
Reagent		2 ± 3	3 ± 5
Burma spinel		0 ± 2	−2 ± 4
SP 27	B	7 ± 10	
SP 28	A	6 ± 6	14 ± 16
SP 29	A	2 ± 5	−6 ± 10
SP 31	B	−1 ± 1	3 ± 2
SP 34	A	−3 ± 2	−10 ± 9

(a) Sample and group designations as in [1,2].
(b) Deviations from normal [6] composition in parts in 10^4; two-sigma errors.

ARE CHONDRULES PRECURSORS OF SOME COSMIC SPHERULES?

T. Presper and H. Palme, MPI f. Chemie (Abteilung Kosmochemie), Saarstraße 23, D - 6500 Mainz, Germany.

Twenty one arctic cosmic spherules, collected by M. Maurette (Orsay, France) in Greenland, were analysed by Instr. Neutron Activation Analysis (INAA). All samples were round spherules, apparently droplets melted through atmospheric heating. Weights of the spherules were in the range of 20 - 50 µg, diameters were >100 µm.

(1) Most spherules showed large depletions of the moderately volatile elements Na, Zn, Se when compared with their abundances in chondritic meteorites. In all particles Fe/Mn ratios are essentially chondritic (100:1 +/- 10%). A major volatility-ralated loss of Mn can therefore be excluded. (2) Refractory lithophile elements occur mostly in chondritic relative abundances. More or less flat REE-patterns are typical (except positive and negative Eu-anomalies). This implies a lack of igneous fractionation. Ca-depletions by a factor of 0.4 to 0.8 were found. (3) Siderophile elements are fractionated in most cases. Several compositional groups are observed: A) no depletion of siderophiles relative to lithophile refractory elements (Sc) and more or less chondritic ratios (2 particles); B) typical pattern resulting from metal-silicate-fractionation with increasing depletions from Fe through Co, Ni to Ir, Au (5 particles); C) Ir- enrichment relative to Ni but chondritic Ni/Au-ratios (this is the most common case, 14 particles). Type-A-pattern represents unfractionated chondritic material. Type-B-particles may have lost metal during melting in the atmosphere. Type-C-particles are more difficult to explain. Two distinct groups are observed: particles with Ni-contents similar to those of chondritic meteorites and particles with much lower Ni-concentrations. Variations of Ir-contents in both groups are similar. It is unlikely that the siderophile element pattern is influenced by remelting of the spherules in the Earth's atmosphere. Also, a simple metal-silicate-fractionation is insufficient to explain the observed patterns because loss of a metal phase would imply proportionally higher losses of Ir than of Ni which is against the observed trends. Also, the depletion of Ni is not affected by weathering or metamorphic processes /1/. Therefore we conclude that the low Ni-contents and variable Ni/Ir ratios are characteristic of the original cosmic particles. Bulk chondritic meteorites show very little variation in Ni/Ir-ratios (ca. 20 - 30 * 10^3). However, chondrules have lower and more variable Ni/Ir ratios that are comparable to the spherules (10^2 - 10^3). The depletion of iron and the essentially chondritic Ni/Au ratios found in our particles are also typical of chondrules in carbonaceous and unequilibrated ordinary chondrites. We, therefore, suggest that the cosmic spherules with low Ni/Ir-ratios were once chondrules that were remelted in the Earth's atmosphere.

Ref: /1/ Maurette, M., personal communication 26.04.91

LEW88055: AUBRITIC INCLUSIONS IN A SI-FREE IRON METEORITE. M. Prinz[1], M.K. Weisberg[1,2], N. Chatterjee[1,2] (1) Dept. Mineral Sci., Amer. Museum Nat. History, NY, NY 10024. (2) Dept. Geology, Brooklyn College, CUNY, Brooklyn, NY 11210.

LEW88055 is a 1.7g iron meteorite which contains several mm-sized silicate inclusions. The host iron meteorite is Si-free kamacite with a high concentration of Neumann bands, many of which are distorted [1]. Some small taenite areas contain martensitic plessite and are associated with schreibersite along grain boundaries. These observations suggest it is an anomalous iron [1].

The silicate inclusions are angular, and range in size from 1-3mm. Modally, the inclusions consist mainly of ortho - and clinoenstatite. Coexisting minor phases include diopside, K-spar, ferroan alabandite, Ti-bearing troilite, daubreelite, schreibersite and tiny particles of FeNi too small to analyze with an electron microprobe. Forsterite, albitic plagioclase and oldhamite, usually present in aubrites, were not found. Oldhamite may have been dissolved due to cutting the sample in water. This is the first occurrence of K-spar in an aubrite. Mineralogically, enstatite has no detectable FeO; some FeO when present is due to minor rust. Clinoenstatite twinning is often distorted, in a manner similar to that of the Neumann bands in the host iron. Enstatite is highly clouded with fine phases (too small to analyze) in selected areas; this is probably due to subsolidus heating. Diopside has (in wt%) 0.2 FeO, 0.13 Al_2O_3, 20 MgO and 24 CaO. K-spar has 64.7 SiO_2, 19.6 Al_2O_3, 0.56 Na_2O, 16.7 K_2O. Troilite has 0.9-3.1 Ti, similar to that found in aubrites [2]. Ferroan alabandite has 11-15 FeO, 0.4-1.2 MgO, 0.1-0.7 Cr, similar to aubrites. Daubreelites have 0.15 Ti, whereas the average in aubrites is 0.3 Ti [2]. Schreibersites have 47-52% Ni. The bulk composition of the aubritic inclusions (in wt%, by broad beam electron microprobe analysis) is 59.8 SiO_2, 0.03 TiO_2, 0.11 Al_2O_3, 38.9 MgO, 0.50 CaO, 0.03 Na_2O; Cr_2O_3, K_2O, P_2O_5, S and Ni are below detection, and FeO is difficult to analyze due to minor rust and is very low.

Conclusions. The host iron meteorite is clearly out of equilibrium with the aubritic silicate inclusions since the host consists of Si-free metal. Thus, this is the first example of aubritic silicate inclusions in an unrelated iron. The only other meteorite which has aubritic silicates mixed with metallic FeNi is Mt. Egerton, but it consists primarily of enstatite encrusted with, and in some cases included within, the metal [3,4]. Also, the metal is Si-bearing. LEW88055 appears to be still another example of an unusual iron meteorite with silicate inclusions that is part of the small population of iron meteorites from Antarctica. Wasson [5] has already noted that 39% of the iron meteorites from Antarctica are ungrouped, and LEW88055 will join this group. Prinz et al. (1991) described chondritic and modified chondritic silicate assemblages in two ungrouped Antarctic irons (LEW86211 and ALH84233); these types of silicates are usually found in IAB-IIICD irons. The LEW88055 iron meteorite and its aubritic inclusions clearly formed in different portions of the solar system and presumably came together by impact collision. The presence of distorted Neumann bands in the metal and distorted clinoenstatite twinning in the aubritic inclusions indicates a severe shock history during or after the collision. Larger samples of this type of meteorite would be helpful for future studies.

References. (1) Clarke, R.S. (1990) Antarctic Meteorite Newsletter 13, No.3 14-15. (2) Watters, T.R. and Prinz, M. (1979) LPSC X, 1073-1093. (3) McCall, J.G.H. (1965) Min. Mag. 36, 241-249. (4) Cleverly, W.H. (1968) J. Roy. Soc. W. Austr. 51, 83-88. (5) Wasson, J.T. (1990) Science 249, 900-902.

S-PROCESS Ba IN SiC FROM MURCHISON SERIES KJ;

C.A. Prombo[1], F.A. Podosek[1], S. Amari[1,2], E. Anders[2], and R.S. Lewis[2]. 1.McDonnell Center for Space Sci., Washington U., St. Louis MO 63130, 2.Enrico Fermi Inst., U. of Chicago, Chicago, IL 60637.

Ott and Begemann [1] have shown that Murchison SiC, a carrier of Ne-E, Kr-s and Xe-s [2,3,4], is enriched in s-Ba. Zinner et al. [5] reported ion probe Ba isotope measurements of size fractions separated from the parent residue KJ [3], but did not measure the low abundance p-process isotopes ^{130}Ba and ^{132}Ba.

Here we report Ba isotope measurements for all isotopes for the parent residue KJ. The sample was direct loaded on a V shaped Ta filament with 1 µl of 1 N H_3PO_4. Barium isotope analysis was performed in a VG-354 thermal ionization mass spectrometer using a Daly detector in single collector pulse counting mode. Te, La and Ce were of negligible interference, as determined by monitoring masses 129, 139 and 140.

Figure 1 shows an average of the first 5 blocks of our data (uncorrected for instrumental discrimination), along with the Ba isotope composition of R1CPF of Ott and Begemann [1] and that of KJB of Zinner et al.[5]. The agreement of our data with those of Zinner et al. [2] is gratifying, but perhaps not too surprising since KJB constitutes about 33% of the bulk parent KJ.

Figure 2 is a three isotope plot of our preliminary data for δ^{138}Ba vs δ^{135}Ba relative to ^{136}Ba for the individual blocks of bulk Murchison KJ SiC residue data. The isotope variations indicate admixture of at least two components, one presumably s-process Ba, whose composition can be determined by extrapolation to zero p-process (^{130}Ba and ^{132}Ba) contribution, and a second which could be blank (and therefore normal) or could be another meteoritic component (possibly, but not necessarily normal) e.g. as contained in hibonite present in the sample [6]. Murchison hibonites contain up to 120 ppm Ba [7]. Or the variations in measured compositions may be due to early release of distinctive Ba from the smaller SiC grains. Measurements on the size separated fractions will hopefully clarify this. Figure 2 illustrates two alternative calculations of the p-process free composition. Case A uses the mean of our first 5 blocks of data and assumes mixing with normal Ba. Case B uses all the data without assuming mixing with normal Ba. "Case 2" of Ott and Begemann [1] is consistent with either of the A and B compositions.

References: [1] Ott U. and Begemann F. (1990) Ap. J. **353**, L57. [2] Tang M. and Anders E. (1988) GCA **52**, 1235. [3] Lewis R.S. et al. (1990) Nature **348**, 293. [4] Ott et al. (1988) Nature **333**, 700. [5] Zinner E. et al. (1991) Lunar Planet Sci. **XXII**, 1553. [6] Ireland T.R. et al. (1991) Lunar Planet Sci. **XXII**, 613. [7] Ireland (1990) GCA **54**, 3219.

Figure 1

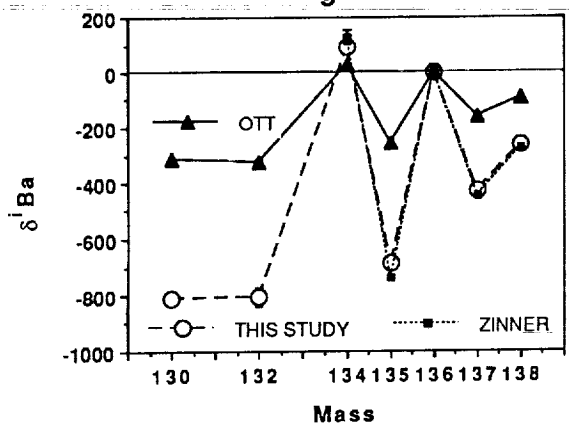

Figure 2

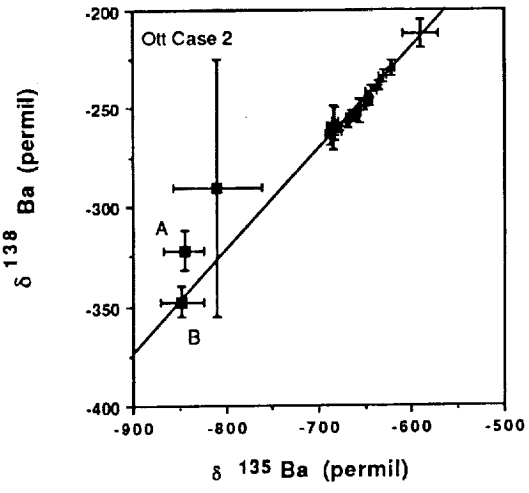

N92-12927

IMAGING ANALYSIS OF LDEF CRATERS: F. Radicati di Brozolo, D.W. Harris, J.A. Chakel, R.H. Fleming, C. Evans & Associates, 301 Chesapeake Dr., Redwood City, CA 94063; T.E. Bunch, NASA Ames Res. Ctr., Moffett Field, CA 94034.

We have analyzed two small craters in Al from LDEF experiment tray A11E00F (#74, 119 μm and #31, 158 μm diameter), using Auger electron spectroscopy (AES), time-of-flight secondary ion mass spectroscopy (TOF-SIMS), low voltage scanning electron microscopy (LVSEM) and SEM EDS. High resolution images and sensitive elemental and molecular analysis have been obtained with this combined approach.

Both craters exhibit residues on the bottom (Figure 1) indicating that impact craters on LDEF may be another source of information on extraterrestrial particles. The impactor for the two craters was C-rich, as elemental maps show C distributed near the bottom and around the raised rim. SEM EDS also reveals the presence of Si, Mg, S, Ca, Fe and Ni suggesting a chondritic composition for the impactor. TOF-SIMS images indicate the presence of numerous surface contaminants, including organics, Ag and I (Figure 2). A small spot containing locally elevated levels of Cl was observed on the walls of crater #31 (Figure 3).

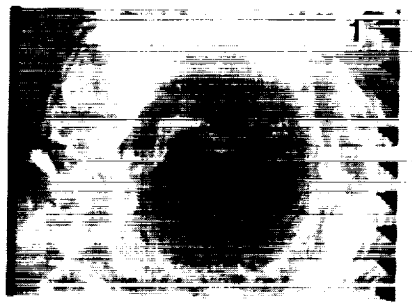

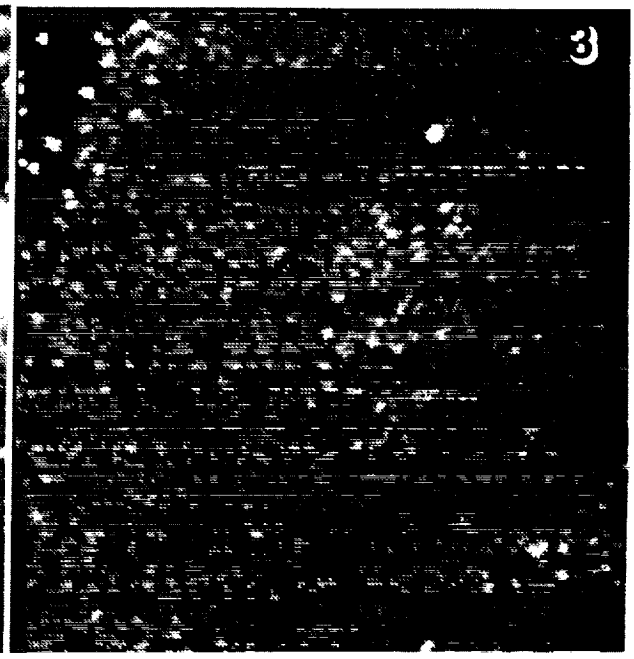

TWO RELATIVELY YOUNG IMPACT CRATERS NEAR WAUPUN, WISCONSIN.

W. F. Read, 1905 N. Alexander St., Appleton, WI, 54911.

A pair of relatively young impact craters has been found about 10 km NE of Waupun, Wisconsin. Both are surrounded by a rim of ejecta. Though overridden by glacial ice, the rim deposits are still visible as discontinuous circles of low hills. The two craters are nearly the same size--about 2.5 km in diameter--and so close together that they touch each other. The crater interiors are filled with drift and, presumably, lake deposits. It is not clear whether they were formed during, or immediately before, the Pleistocene epoch.

In all probability the craters are several hundred meters deep. This follows from theoretical considerations and is supported by geological evidence. A train of glacially-transported red rhyolite boulders begins at the craters and fans out to the SSW. No red rhyolite is exposed anywhere near them. The surface bedrock, though drift-covered at the craters, is presumed, from a quarry at Waupun, to be Middle Ordovician dolomite. This is underlain by something like 70 m of other Ordovician sediments plus about 170 m of Cambrian sandstone--all more or less flat-lying. The red rhyolite boulders, which are usually angular or subangular, almost certainly came from the Precambrian basement. How far the bottoms of the craters cut down into the Precambrian is not yet known.

In addition to the rhyolite, which is conspicuous, other types of Precambrian rocks were excavated--notably granite. Pebbles of battered-looking granite picked up in or near the craters were found to contain glass or microcrystalline material presumably derived from glass. Glass, or its microcrystalline derivative, has been found also in pebbles of altered sandstone and rhyolite. No quartz grains showing multiple sets of shock lamellae have yet been observed in thin sections and no shatter cones have been found.

I propose the names Waupun East and Waupun West for these craters. The center of Waupun East is located at Lat. 43° 42.3', Long. 88° 36.7'. The center of Waupun West is at Lat. 43° 41.9', Long. 88° 38.2'.

COSMOGENIC-NUCLIDE PRODUCTION IN VERY LARGE METEORITES*

Robert C. Reedy, Space Science and Technology Division, Mail Stop D438, Los Alamos National Laboratory, Los Alamos, NM 87545 USA.

For meteorites, most models for the production rates of cosmogenic nuclides have concentrated on GCR production in "normal" (pre-atmospheric radii $\sim$ 10–40 cm) meteoroids. The model of Reedy and Arnold (1) has worked well for the Moon, and Reedy (2) extended it to meteoroids. Reedy (2) concentrated on the normal-sized objects, using meteorites like St. Severin and Keyes (R $\sim$ 25 cm) in deriving the spectral-shape parameters for most meteorites. Production rates in such objects increase the most near the pre-atmospheric surface and tend to be relatively flat in the central parts of the meteoroid. Recently, results have been measured for meteorites that were larger in space, such as Jilin, Chico, and others. At some depth and radius, production rates drop near the center of meteoroids. The question in interpreting measurements for potentially large meteoroids is for what shielding conditions do various nuclides start to show such central decreases and by how much. Good models are needed to separate effects due to shielding from those due to complex exposures.

The Reedy model (2) was found not to work well for ^{22}Na near the center of Jilin (R = 300 g/cm^2) and was revised (3). The new model reproduced the basic trend for ^{36}Cl in Jilin's metal phase (a steady drop in rates from the surface to the center) but didn't match well the observed concentrations (3). This revised model was used to examine the systematics of nuclide production in an 85-cm radius meteoroid. High-energy products, like ^{3}He and spallation-produced ^{41}Ca, showed strong decreases in production as a function of depth and had rates that were much lower in than those in normal-sized meteoroids. The decreases for medium-energy products like ^{10}Be and spallation ^{36}Cl in stony phases, were less. Most nuclides, like ^{14}C, ^{22}Ne, ^{26}Al, ^{38}Ar, and ^{53}Mn show no pronounced drop near the center and are similar in rates to normal meteoroids. The only nuclide with an increase all the way to the center was ^{21}Ne. While the absolute values could be in error, the trend from high-energy to very-low energy products is probably in the right order.

These calculated profiles have much less drop for an 85-cm radius meteoroid than do those of Graf *et al.* (4). Michel *et al.* (5) only went to radii of 65 cm, where their ^{26}Al and ^{21}Ne profiles near the center were flat and their ^{21}Ne rates lower than for R = 40 cm. Some detailed comparisons among these models are being done. Additional tests are being done for the Reedy model as revised for larger meteoroids, especially for absolute rates. Additional measurements in samples from large meteoroids with known shielding conditions are needed for testing these models. Measurements of neutron-capture products would help to determine a sample's shielding. A problem in such comparisons is to get depths on a common scale, preferably in g/cm^2 and not in length.

References: (1) Reedy R. C. and Arnold J. R. (1972) *J. Geophys. Res.* **77**, 537. (2) Reedy R. C. (1985) *PLPSC15*, in *J. Geophys. Res.* **90**, C722. (3) Nishiizumi K. *et al.* (1989) *PLPSC19*, 305. (4) Graf Th. *et al.* (1990) *Geochim. Cosmochim. Acta* **54**, 2521. (5) Michel R. *et al.* (1990) *Meteoritics*, submitted. * Work supported by NASA and done under the auspices of the US DOE.

DYNAMIC PYROMETAMORPHISM OF INTERPLANETARY DUST PARTICLES COMPARED TO ATMOSPHERIC ENTRY MODEL TEMPERATURES.

Frans J.M. Rietmeijer, Department of Geology, University of New Mexico, Albuquerque, NM 87131, U.S.A.

Interplanetary dust particles [IDPs] are collected in the lower stratosphere at 20 km altitude following their descend through the atmosphere upon reaching a terminal velocity at ~80 km altitude. During deceleration in the upper atmosphere incoming IDP micrometeoroids experience flash-heating that may cause melting or vaporisation. Some fraction of IDPs survive intact and experience minor dynamic pyrometamorphism (1). The physics of the entry process are well-understood and models for time-temperature regimes of atmospheric deceleration are used to predict IDP survival. The models predict a near-Earth enhancement of asteroidal over cometary particles due to gravitational focusing and a higher probablity of intact (i.e. unmelted) survival of IDP-sized asteroidal micrometeroids (2,3). These results appear to contradict laboratory studies of IDPs that convincingly show a cometary origin for the chondritic porous [CP] subset of IDPs that is a common type of particles in the lower stratosphere (4,5). The survival of CP IDPs shows that dynamic pyrometamorphism does not seriously affect cometary dust. For example, the dynamic pyrometamorphic regime for CP IDP W7029A23/A24 is 575 °K to 875°K based on thermodynamic stability of layer silicates and ordering in poorly-graphitised carbon [PGC] as measured on a geological timescale (1). Using industrial heating rates, PGC ordering in this CP IDP would take place at ~3,000°K (6) and cause complete micrometeoroid evaporation. The example illustrates that the kinetics of mineral reactions in decelerating micrometeorites are important to determine the degree of survival. Dynamic pyrometamorphism of Bi to Bi_2O_3 in CP IDP W7029A23/A24 is kinetically favorable at ~575°K (7). This CP IDP also contains sub- to euhedral platey layer silicate grains that are on average one micron in size and that include kaolinite, $Al_2Si_2O_5(OH)_4$. Data on kaolinite dehydroxylation kinetics are available as a function of mean grain diameter (9) to calculate the stability of kaolinite during dynamic pyrometamorphism of CP IDP W7029A23/A24.

CP IDP KAOLINITE DEHYDROXYLATION. The entry heating temperature/time regime for this CP IDP, that is ~60 μm in diameter, was calculated asuming ρ = 1.0 g.cm^{-3} and initial velocity = 10 km.sec^{-1} (*Flynn, written comm.*). This velocity is consistent with a cometary particle source (2). The peak entry heating temperatures are used to calculate the rate of kaolinite dehydroxylation [TABLE 1]. The time for kaolinite dehydroxylation is invariably a small fraction of the time the temperature in CP IDP W7029A23/A24 is within 100°K of the peak temperature.

CONCLUSION. The survival of kaolinite in CP IDP W7029A23/A24 implies that dynamic pyrometamorphic temperatures never reached the theoretically values predicted for this particle that contains carbon-rich compounds including PGC and lonsdaleite (1,8). Accepting a model for the survival of carbon-rich micrometeorites (10), I suggest that carbonaceous compounds in CP IDPs offer protection against dynamic pyrometamorphism which results in a higher than calculated intact survival rate for solid cometary debris.

REFERENCES: 1 Mackinnon IDR & Rietmeijer FJM (1987) Reviews Geophys. 25, 1527; 2 Flynn GJ (1989) Proc. 19th LPSC, 673; 3 Flynn GJ (1990) Proc. 20th LPSC, 363; 4. Schramm et al (1989) Meteoritics 24, 99; 5 Rietmeijer FJM (1989) Proc. 19th LPSC, 513; 6 Rietmeijer FJM & Mackinnon IDR (1985) LPSC XVI, 700; 7 Mackinnon IDR & Rietmeijer FJM (1984) Nature 311, 135; 8 Rietmeijer FJM (1991) EPSL 102, 148; 9 Johnson HB & Kessler F (1969) J. Am. Ceram. Soc., 52, 199; 10 Bonny Ph et al (1988) LPSC XIX, 118;
This work is supported by NASA Grant NAG 9-160.

Peak T (°K)	T_{100} (sec)	$T_{dehydox.}$ (sec)	%
1563	0.7	8.9×10^{-4}	0.13
1509	0.9	1.4×10^{-3}	0.16
1433	1.2	2.9×10^{-3}	0.25
1326	1.7	9.4×10^{-3}	0.53
1114	3.9	1.8×10^{-1}	4.62

TABLE 1: Entry peak temperatures and thermal regime for normal to grazing incidence (top to bottom) for CP IDP W7029A23/A24 calculated by Flynn (1990) and kaolinite dehydroxylation time and its fraction of the time at 100°K within peak temperature (T_{100}).

CHROMIUM ISOTOPIC COMPOSITION IN THE ENSTATITE CHONDRITE QINGZHEN AND IN MAGNETITE OF ORGUEIL ;

M. Rotaru, J.L. Birck, and C.J.Allegre, Laboratoire de Géochimie, IPG, 4, place Jussieu, 75252 Paris Cedex 05.

Large Cr isotopic heterogeneities have been observed in the major phases of carbonaceous chondrites matrices, using a stepwise dissolution procedure (1,2). The magnitude of the observed 54Cr variations decreases with increasing metamorphic grade, reflecting the effect of secondary metamorphism in the parent bodies. CI1 and CM2 chondrites display the largest Cr isotopic diversity, with both negative and positive 54Cr effects ; they contain no measurable amount of normal Cr. Thus, the mean solar composition is interpreted as a mixture of different nucleosynthetic components of non-normal isotopic signatures. In addition, there is no correlation between the 53Cr and 54Cr effects, and the variations observed in 53Cr may be attributed to the in-situ decay of 53Mn (3).

In order to investigate the other classes of chondrites, we analyzed the Cr isotopic composition of the EH3 chondrite Qingzhen, one of the less metamorphosed enstatite chondrites. The stepwise dissolution procedure showed satisfactory reproducibility, but it may introduce some mixing between mineral phases. To locate more precisely the Cr carriers of the extreme isotopic components encountered in the CI1 Orgueil, we analyzed magnetite from Orgueil, isolated using its magnetic properties. Data are quoted in the table in part per 10000.

RESULTS AND DISCUSSION :

QINGZHEN : Isotopic effects in 53Cr and 54Cr are clearly resolved, but at a few ε-unit scale. The Cr isotopic pattern is similar to that of Allende (4), probably reflecting the metamorphism intensity. Investigation of the 53Mn-53Cr systematics on this meteorite require Mn-Cr concentration measurements.

ORGUEIL MAGNETITE : Magnetite was isolated using a hot NaOH bath and a stirring bar (5), from a powder obtained with a freeze-thaw procedure. A first etch of the bulk magnetite gave a component highly enriched in 53Cr. However, a duplicate of this same sample, and the leachates obtained from the magnetite never reproduced this result. Cr hydroxides, enriched in radiogenic 53Cr, adsorbed on the grain surfaces, may be responsible for the 53Cr excess. To isolate this component, a replicate of the whole separation was undertaken, and the new magnetite was subjected to a slightly different chemical treatment. The fractions enriched in 53Cr (6.5ε) or 54Cr (72.2ε) , obtained from the first experiment, could not be reproduced. The diversity obtained in the results for the magnetic fraction may be attributed to : 1- differences in the size of the grains obtained with the freeze-thaw procedure; 2- small differences in the procedure; 3- the presence of different types of magnetite grains : the hydrophobic grains may have been partly lost during one of the experiments. Hand magnet separations on bulk powders have also provided isolation of Cr isotopic component, but small variations in the applied field give irreproducible results. Further experiments, combined with other mineral separation methods may be more efficient in separating the microcrystalline phases.

In conclusion, physical enrichment of the carriers of the Cr isotopic anomalies appears possible, but due to the microcrystalline nature of the sample, it is not reproducible so far.

References : [1] M. Rotaru et al. (1989) LPSC XX, 924. [2] M. Rotaru et al. (1990) LPSC XXI, 1037. [3] J.L. Birck et al. (1990) Abstr. 53rd Met. Soc. Meet. Perth, 8. [4] M. Rotaru et al. (1989) Meteoritics 24, 321 [5] P.M. Jeffery & E. Anders (1970) G.C.A. 34, 1175.

QINGZHEN	53/52Cr	54/52Cr
WR	0.21±0.19	0.02±0.43
L1	2.96±0.33	0.27±0.67
L2	0.93±0.26	1.33±0.60
L3	0.34±0.30	1.14±0.64

	first exp.		2nd exp.	
Magnetite	53Cr/52Cr	54Cr/52Cr	53Cr/52Cr	54Cr/52Cr
bulk	6.54±0.33	21.30±0.71	-0.25±0.27	8.04±0.55
L1,2-acetic acid diluted	0.27±0.28	-4.90±0.60	-0.08±0.35	-3.38±0.74
L3-nitric acid diluted	0.11±0.26	8.37±0.57	-0.27±0.18	7.58±0.42
L4-HCl/HF	1.10±0.24	72.20±0.53	1.61±0.50	0.57±1.03
L5-HBr/HF	-1.36±1.31	30.70±2.62		
non-magnetic fraction	-0.77±0.27	61.60±0.60	0.75±0.18	5.01±0.41

SILICATE DARKENING AND HETEROGENEOUS PLAGIOCLASE IN CK AND ORDINARY CHONDRITES. Alan E. Rubin, Institute of Geophysics, University of California, Los Angeles, CA 90024, USA.

Silicate darkening in ordinary chondrites (OC) is caused by tiny grains of metal and troilite occurring mainly within curvilinear trails that traverse silicate interiors, and decorate or, in some cases, cut across silicate grain boundaries. Highly shocked OC (characterized by olivine grains with undulose to mosaic extinction) tend to have greater degrees of silicate darkening than lightly shocked OC; this indicates that silicate darkening is probably a product of shock metamorphism. The low Fe-FeS eutectic temperature (988°C) renders metal and troilite susceptible to melting and mobilization during shock heating. Silicate darkening is also evident in CK carbonaceous chondrites; in these meteorites, tiny magnetite and pentlandite grains form the curvilinear trails. Darkened CK silicates include olivine, pyroxene and plagioclase. In general, chondrules and chondrule fragments have been darkened less than isolated or groundmass silicates. It is possible that magnetite and pentlandite in CK chondrites were mobilized during shock metamorphism and dispersed through silicate interiors. Alternatively, because magnetite is not readily compressed, it is possible that silicate darkening in CK chondrites was caused by the shock-induced dispersal of metal and troilite; if so, these phases must have been transformed into magnetite and pentlandite during subsequent oxidation.

Unshocked OC tend to have plagioclase with uniform compositions (e.g., An 12.1-12.9 in H6 Ogi); shocked OC tend to have heterogeneous (albeit still stoichiometric) plagioclase (or maskelynite) (e.g., An 8.5-23.9 and 8.7-44.5 in H5 Rose City and LL5 Paragould, respectively). The low impedance of plagioclase to shock compression makes it probable that shock events are responsible for plagioclase heterogeneity, although the exact mechanisms are poorly understood. CK chondrites also have compositionally variable plagioclase (e.g., An 20-56 in CK5 EET87860). Because shocked OC that exhibit silicate darkening tend to have heterogeneous plagioclase, it seems likely that plagioclase heterogeneity in CK chondrites (all of which exhibit silicate darkening) is also a product of shock metamorphism.

Some OC and most CK chondrites were probably annealed after being shocked: e.g., H5 Allegan contains olivine with sharp optical extinction, but exhibits major silicate darkening and has moderately heterogeneous plagioclase (An 12.4-27.7). Most CK chondrites exhibit light shock effects in olivine that are consistent with shock pressures that are too low to account for silicate darkening or heterogeneous plagioclase; the shock veins in CK5 EET87507 are also inconsistent with this meteorite's apparently low degree of shock. It seems likely that, prior to annealing, most CK chondrites were shocked to sufficient degrees to cause silicate darkening and compositionally variable plagioclase. A few CK chondrites that contain olivine with undulose or mosaic extinction (e.g., CK6 LEW87009 and CK5 EET83311) may have been shocked again, after annealing.

A NEW KIND OF METEORITIC DIAMOND IN ABEE.

S.S. Russell, C.T. Pillinger, Planetary Sciences Unit, The Open University, Milton Keynes, MK7 6AA and J.W. Arden, Department of Earth Sciences, The University of Oxford, Oxford, OX1 3PR.

Our recent survey of microcrystalline diamond (Cδ) from primitive chondrites involved a comparison of meteorite types for the purpose of recognising whether the diamond has a common provenance. Both carbon isotopic composition and nitrogen abundance (but not as yet isotopic characteristics) show significant differences between meteorites. The $\delta^{13}C$ values encountered are however well constrained between about -32 and -38‰ whilst nitrogen concentrations fall in the range 2000 ppm to 1.2 wt % (1).

During the course of the investigation, a unique result has been obtained from the enstatite chondrite Abee (EH5). A residue (134.5 ppm of the meteorite) from HF/HCl, $Cr_2O_7^{2-}$ and $HClO_4$ treatment was found to contain > 85 % carbon with an average $\delta^{13}C$ of -1.8 ‰ which produced the x-ray pattern of diamond, and contained less than 50 ppm nitrogen. This diamond has a higher combustion temperature than typical Cδ suggesting a coarser grain size, a conclusion in keeping with the x-ray pattern and scanning electron microscope observation, although the diamond forms a milky suspension in ammonia solution suggesting the presence of some very small grains. Abee is Xe HL free (2) and along with the nitrogen content and carbon isotopic composition this demonstrates that the diamond is unrelated to the interstellar component Cδ . Whilst the Abee diamond has a $\delta^{13}C$ not dissimilar to some ureilites, it is much more easily combusted.

Unfortunately the sample of Abee from which the residue was obtained was one which had saw cut faces, and so the possibility that the diamond is simply a contaminant from the saw blade must be considered. Anticipating potential contamination of any Cδ residue, the slab was pre-etched in HF/HCl twice followed by washing with acetone and water, so that approximately 1.5g of surface material was removed prior to the crushing and extraction of the main residue. The solutions were discarded, hopefully along with any extraneous diamondiferous material from the saw. Another argument can also be used to refute the interpretation that the diamond is of terrestrial origin. A $\delta^{13}C$ of -1.8‰ is not impossible for kimberlitic/lamproitic diamond but consideration of data from *ca.* 750 analyses of individual minerals by ourselves and in the literature gives only 11 examples of diamond with carbon heavier than -2‰. It is unlikely that the saw used to cut Abee contained diamond from an unusual stone; terrestrial diamond would be recognised by a $\delta^{13}C$ of ≤ -5.5‰.

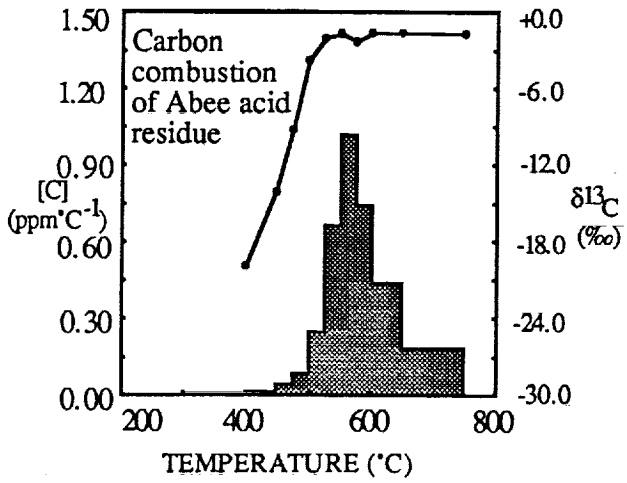

The discovery of diamond in Abee is the first observation of chondritic diamond which is not apparently associated with any isotopic anomalies, and its formation mechanism is not yet clear. Whilst we have not completely ruled out contamination, diamond with a $\delta^{13}C$ heavier than Cδ and virtually no nitrogen, if present in other (Cδ containing) meteorites, would begin to explain some of our results, which show a relationship between increasingly heavy carbon and a decrease in nitrogen content. However, the Abee diamond alone cannot explain all the observed differences in diamond between primitive chondrite types.

We thank Ed Olsen of the Chicago Field Museum for the sample of Abee.

References: (1). S.S Russell *et al.* (1991), LPSC **XXII** 1151-1152 (2). G.R. Huss and R.S. Lewis (1990), LPSC **XXI** 542-543.

METEORITIC SILICON CARBIDE - SEPARATE GRAIN POPULATIONS AND MULTIPLE COMPONENTS REVEALED BY STEPPED COMBUSTION. S.S. Russell, R.D. Ash, and C.T. Pillinger, Dept. of Earth Science, Open University, Milton Keynes, MK7 6AA UK., and J.W. Arden, Dept. of Geology, Parks Road, Oxford, UK.

Analysis of meteoritic silicon carbide has been dominated by ion probe measurements, a technique which has revealed the rich diversity of carbon and nitrogen isotopic composition in discrete grains. However, it is a selective process, since only the larger grains can be measured individually. To obtain a dataset that is independent of grain size, silicon carbide residues have been investigated by stepped combustion, which enables mean $\delta^{15}N$ and $\delta^{13}C$ values to be determined, and allows comparisons to be made between meteorite groups. Samples composed mainly of diamond, spinel and silicon carbide were prepared by acid dissolution, and then combusted slowly up to 550°C, to remove the diamond (1), before analysis by high resolution carbon stepped combustion and by nitrogen/carbon conjoint experiments. The results from this suite of experiments are summarised below.

Type	Meteorite	Temperature range of major carbon release	$\delta^{13}C$ (mean)	$\delta^{13}C$ (maximum)	$\delta^{15}N$ (peak)	C/N
CI1	Orgueil	600-1000°C	+329.4	+1344.8	-576.5	30
CM2	Cold Bokkeveld	950-1125°C	+963.9	+1398.6	-407.1	33
	Murchison	950-1125°C	+1101.9	+1429.4	-365.7	12
	ALH83100,78	900-1000°C	+885.3	+1402.9	-594.6	36
	Murray	1000-1200°C	+1160	+1384.1		
CV3	Allende	900-1100°C	+34.7	+503.6	-24.1	33
	Efremovka	625-775°C	+13.3	+134.2		
L3	Inman	675-800°C	+78.6	+993.7	+204.5	4
EH4	Indarch	1175-1350°C	+1010.5	+1432.8	-51.7	3

The temperature range of the high temperature carbon release varies between meteorites, indicating some differences in the grain populations. The maximum $\delta^{13}C$, however, recorded at temperatures between 950 and 1300°C, is almost constant for all the SiC rich samples at around +1400‰, a $^{12}C/^{13}C$ ratio of 35 - the mean value of many co-combusting silicon carbide grains. The samples in which the maximum was <1400‰ were silicon carbide poor and so the values quoted are subject to blank effects. The isotopic profiles also suggest the presence of several isotopically anomalous minor components whose identity is unknown.

The high temperature nitrogen associated with the SiC in the CM2s and CI is isotopically light, with values recorded as low as -595 ‰ ($^{14}N/^{15}N$ = 676) for ALH83100. Their C/N ratios are between 30 and 36. Inman differs from the carbonaceous chondrites: the nitrogen released at high temperatures is ^{15}N enriched, an effect also observed in other ordinary chondrites (2). The C/N associated with this release is only ~4 and so it seems unlikely that this nitrogen can be contained in the silicon carbide. The enstatite chondrite Indarch has a $\delta^{15}N$ of -52‰, again with a low C/N ratio, possibly indicating nitride decomposition (3).

Whereas analysis of individual grains reveals information about the parent stars of the silicon carbide, step combustion techniques, which combust tens of thousands of grains during each experiment, indicate the average isotopic value of grains within the dust cloud from which the Solar nebula condensed. The data may also reflect processing of the grains within the meteoritic parent body by metamorphic and hydrothermal events. Thus the two isotopic measuring techniques (ion probe and gas source mass spectrometry) afford complementary information.

References: (1) Russell *et al.*,(1990) Meteoritics **25**, 402. (2) Alexander *et al.*,(1990) Earth Planet. Sci. Lett. **99**, 220-229. (3). Grady *et al.*, (1986) Geochim. Cosmochim. Acta. **50** 2799-2813.

A SURVEY OF CAIs IN LEOVILLE AND VIGARANO: RIM LAYERS, BRECCIATION, METAMORPHISM, AND ALTERATION; A. Ruzicka and W.V. Boynton, Dept. of Planetary Sciences, University of Arizona, Tucson, AZ 85721

An optical and SEM survey of Ca,Al-rich objects in the CV3 chondrites Leoville and Vigarano was performed to serve as a basis of comparison with the much better-studied Allende chondrite. A total of 66 Ca,Al-rich objects were found in two sections each of Leoville (ASU, USNM 3535-2) and Vigarano (USNM 6295-2, USNM 6295-4). In Leoville, 44 of 55 Ca,Al-rich objects are fine-grained inclusions with wormy or nodular textures that appear to be relatively unaltered variants of fine-grained inclusions in Allende. Many of the spinel-rich nodules have pyroxene rims, but the inclusions themselves are not surrounded by classic Wark-Lovering rims [1]. Coarse-grained ($\geq$ 100 μm) inclusions are relatively rare: only one Type B2, one "compact" Type A, and two Type B1 CAIs have been found in the two Leoville sections examined. All of these inclusions are melilite-rich and have Wark-Lovering rims. Many microfaults have displaced the rim layers and often two or more essentially complete rim sequences have become stacked upon one another. Melilite in the CAIs shows undulatory extinction and kink-banding indicative of strain. The microfaulting and deformation of melilite probably arose during shock metamorphism, possibly during the same process that caused Leoville to become foliated [2]. Three additional objects contain melilite- and spinel-cored nodules surrounded by pyroxene rims, and the objects are surrounded by semi-continuous Wark-Lovering rims; these inclusions are interpreted to be relatively unaltered versions of "fluffy" Type A CAIs in Allende. Unlike Leoville, the two Vigarano sections show a brecciated (clastic) texture, and many of the CAIs are obviously broken fragments of slightly larger inclusions [3,4]. The CAIs tend to be smaller (typically $\sim$0.5 mm across) and contain a higher proportion of melilite-rich CAIs compared to Leoville. Of the eleven Ca,Al-rich objects found in Vigarano, seven are recrystallized, melilite-rich objects that have granoblastic textures indicative of slow cooling or a reheating episode. All of these objects have partial Wark-Lovering rims. They may represent metamorphosed equivalents of compact or fluffy Type A inclusions in Leoville and Allende [4]. Two fine-grained CAIs were found in Vigarano and these resemble the ubiquitous fine-grained objects in Leoville except for being coarser-grained and apparently recrystallized.

The observations of Leoville and Vigarano show that classic Wark-Lovering rim layers are best developed on medium-to-coarse grained ($\geq$ 50-100 μm), melilite-rich objects. The CAIs in Leoville and Vigarano are much less altered than their Allende counterparts. However, alkali-halogen alteration strongly affected one Type B2 CAI in Leoville, and the general absence of such alteration elsewhere suggests that alkali-halogen alteration pre-dated the final compaction of Leoville. The presence of matrix in direct contact with the interiors of CAIs across microfaults shows conclusively that rim layers could not have formed by an *in situ* reaction. Thus, in at least those inclusions now in Leoville, both rim layer formation and alteration appear to have occurred at an early stage. CAI interiors are also in direct contact with matrix in Vigarano, and many Vigarano CAIs were clearly fragmented in a relatively late episode of brecciation.

[1] Wark D.A. and J.F. Lovering (1977) Proc. Lunar Planet. Sci. Conf. **8**, 95-112. [2] Sneyd *et al.* (1988) Meteoritics **23**, 139-149. [3] Armstrong J.T. (1989) Lunar Planet. Sci. Conf. **XX**, 23-24. [4] MacPherson G.J. (1985) Meteoritics **20**, 703-704.

ZONE SEQUENCES, WIDTHS AND COMPOSITIONS OF OLIVINE CORONAS IN MESOSIDERITES; A. Ruzicka and W.V. Boynton, Dept. of Planetary Sciences, University of Arizona, Tucson, AZ 85721

Olivine coronas in thin-sections of the Emery (AMNH 4441-2, 4441-4) and Morristown (AMNH 305-1) mesosiderites were studied by optical and SEM microscopy to place constraints on the kinetic parameters and metamorphic conditions that prevailed during the formation of these coronas. All isolated olivine grains in these mesosiderites are surrounded by coronas. The coronas in both meteorites contain an optically distinctive orthopyroxene + chromite inner zone adjacent to olivine. In Emery, this inner zone is surrounded by fine-grained zones that are rich in orthopyroxene, merrillite and plagioclase; clinopyroxene exsolution lamellae and blebs are concentrated in the outermost portion of the corona adjacent to matrix. In Morristown these additional zones (if present) are difficult to optically discern from matrix. On flat portions of the coronas in Emery, the inner zone is typically 20-40% of the total thickness of the corona. One dunite clast was found in Morristown but it lacks an obvious corona, suggesting that the coronas (at least in Morristown) were formed *before* the final incorporation of olivine into mesosiderite matrix.

The modal compositions of various corona zones on the two largest olivine grains (Object 1: ~1 x 2 mm; Object 7: ~0.5 x 2.9 mm) in Emery 4441-4 were determined from backscattered-electron images of 5-11 representative areas from each zone on the flat edges of each object. Image processing of these areas enabled all phases except ortho- and clinopyroxene to be readily distinguished and the modes to be determined to an estimated precision of 0.1-0.5 vol% within each imaged area. The coronas on both objects are similar. The distinctive inner zone (~0.3 mm thick) is rich in pyroxene (~70-85 vol%) and chromite (~3-20%), but also contains minor (<5%) merrillite and ilmenite, and rare (generally <1%) metal, sulfide, and plagioclase. An intermediate or middle zone (~0.3 mm thick) is rich in merrillite (~9-22%), pyroxene (~54-62%) and plagioclase (~9-28%), contains less chromite than the inner zone (<10%), and has minor ilmenite, metal, and sulfide. Plagioclase and merrillite tend to vary inversely in this zone, and a thin (<0.1 mm thick) plagioclase-free, merrillite-rich zone is locally present immediately adjacent to the inner zone. An outer zone (~0.4-0.5 mm thick) adjacent to matrix is generally similar to the middle zone except that it contains less merrillite (~7-10%), and more metal (to a few %) and sulfide.

The layer sequence and zone compositions of the coronas in Emery are consistent with a 5-component (MgO-$AlO_{3/2}$-CaO-SiO_2-$PO_{5/2}$) steady-state kinetic model that assumes reaction and diffusion between olivine and a mesosiderite-like, silicate-phosphate assemblage [1]. The coronas formed during thermal metamorphism after (and in Morristown possibly also before) brecciation episodes in the respective parent bodies. A comparison of model and actual coronas in Emery suggests that the diffusivities of MgO, CaO, SiO_2 and $PO_{5/2}$ during metamorphism were generally similar to one another, but that the diffusivity for $AlO_{3/2}$ was especially low. Moreover, the presence of merrillite in the outer zone of the coronas suggests that an additional source of $PO_{5/2}$ was added to the coronas besides that now present in the matrix; most likely this source was an earlier generation of P-rich metal that was initially present in mesosiderites.

[1] Ruzicka A. and Boynton W.V. (1990) Meteoritics **25**: 403.

PLAGIOCLASE, ILMENITE, LUNAR MAGMA OCEANS, AND MARE BASALT SOURCES; G. Ryder, Lunar and Planetary Institute, 3303 NASA Road One, Houston, TX 77058, USA.

Lunar mare basalt source depletions in both europium and alumina are consensually attributed to complementary plagioclase floating from a magma ocean. However, the connection cannot be simple or direct: in contrast to the magma that crystallized to produce the mare basalt sources, the ferroan anorthosite parent magma was *more evolved* by virtue of its lower Mg/Fe ratio and Ni abundances, although *less evolved* in its poverty of clinopyroxene constituents, flat rare earth patterns, and lower incompatible element abundances (e.g., [1,2]). To crystallize plagioclase requires about 15% Al2O3 in a magma. Starting from a bulk Moon with less than about 5% Al2O3 requires crystallization of 70% Al-free phases before plagioclase can crystallize: even a whole-Moon melt would be less than 200 km deep before plagioclase could crystallize (Fig. 1); a half-Moon melt would be as shallow as 100 km before anorthosites would be forming. Some mare sources, and their contained europium anomalies, are inferred (from phase equilibria exeriments) to be at depths of 400 km, too deep to have been directly influenced by plagioclase crystallization; nearly all mare sources are inferred to be deeper than 200 km. Ilmenite, also required in some mare sources, would not have crystallized until a whole-Moon ocean was little more than 50 km deep.

Global overturn of a hot, gravitationally unstable mantle following crystallization of a magma ocean would have carried down clinopyroxene, ilmenite, and phases with fractionated rare earths with Eu anomalies. These would have mixed with deeper olivines to form mare sources ([1,2]; Fig. 2). Upward-moving magnesian mafic minerals, decompressing, would have melted to be the prime component, with assimilated plagioclase, of the ancient Mg-suite that intruded the crust (Fig. 2). Mechanical mixing of a once stratified lunar interior creates considerable ambiguity and free parameters in numerical chemical modelling of supposed igneous processes of mare evolution.

References: [1] Ryder, G. (1982) Trans. Am. Geophys. Un. 63, 785-787. [2] Ryder, G. (1989) Lun. Plan. Sci. XX, 554-555.

Figure 1.

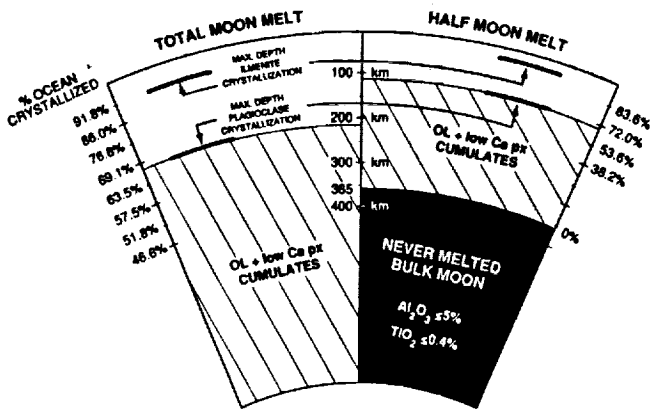

Figure 2.

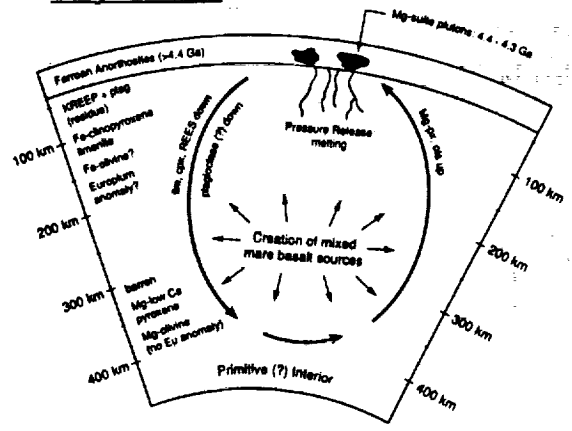

Mineralogical Study of metals in MAC88177 with reference to S-type Asteroids; Jun Saito and Hiroshi Takeda, Mineralogical Institute, Faculty of Science, Univ. of Tokyo, Hongo, Tokyo 113, Japan

MAC88177 was described as "carbon-free" ureilite by Mason (1). Prinz et al. (2) proposed that it may be a new type of achondrites on the basis of oxygen isotope and Takeda et al. (3) emphasized its link to primitive achondrites-lodranite.

We investigated metallic grains in MAC88177,17 polished thin section using electron probe microanalyser (EPMA) and scanning electron microscope (SEM) equipped with EDS with chemical map analysis (CMA) utilities.

The metallic grains of MAC88177 consist of kamacites (about 5 to 7 Wt% Ni), and taenites (about 10 to 30 wt% Ni). Taenite has not been described in ureilites except for the tiny blebby grains as described in Kenna by Berkley et al. (4). Troilite grains are also larger (about 100-300 microns in diameter) than those of ureilites, such large troilite grains had not been found in ureilites either. The troilites are in contact with metal in one grain.

Takeda, et al. (3) mentioned that the "primitive achondrites" including lodranites might have been produced by planetesimal-scale collision model as proposed for ureilite, but many "primitive achondrites" preserved more Ca,Al-rich and Fe-Ni-S components than ureilites. The different degree of partial melting and removal of its low-melting silicates can produce a variety of primitive achondrites.

Large amounts of FeNi metals and sulfides, and large variations of Ni contents of MAC88177 metals may indicate that Fe-Ni-S eutectic melts had not been removed from source materials. If a part of Fe-Ni-S partially melted had been removed, the metals have lower Ni contents, and the meteorite contains less taenite grains.

Differences between MAC88177 and other primitive achondrites are mainly Mg/(Mg+Fe) ratios of mafic silicates, olivine/pyroxene ratios and silicate/(metal + troilite) ratios. The same differences have been proposed for those among the S-type asteroids. On the basis of similarity between reflectance spectrums of "primitive achondrites" and S-type asteroids presented by Hiroi and Takeda (5), we conclude that a formation mechanism proposed for primitive achondrites can explain the variabilities among S-type asteroids. The data of MAC88177 metals may be consistent with the proposal of Takeda et al. (3).

We thank Antarctic Meteorite Working Group (AMWG) for meteorite samples.

References:

(1) Mason, B. (1990) Antarctic Meteorite Newsletter, 13,
(2) Prinz, M. et al. (1991) LPS XXII, 1099
(3) Takeda, H. et al. (1991) LPS XXII, 1375
(4) Berkley, J.L. et al. (1976) Geochim. Cosmochim. Acta, 40, 1429-1437
(5) Hiroi, T. and Takeda, H. (1990) Abst. 15th Symp. Antarctic Meteorites, 104-106, NIPR, Tokyo

OBSERVATIONAL EVIDENCE FOR PROTO-PLANETARY DISKS; A. I. Sargent and S. Beckwith, California Institute of Technology

Recent technological advances have allowed the imaging of gas and dust structures around very young, solar-mass stars on scales between 100 and 1000 AU. About 50% of these structures are disk-like, with masses and dimensions compatible with those frequently ascribed to the pre-solar nebula. The evidence that these disks may be the precursors of other planetary systems is reviewed. Possible disk evolution is discussed, along with relevant time-scales. The effects of differing star formation environments and varying central stellar masses are also considered.

The determination of platinum group elements (PGE) in target rocks and fall-back material of the Nördlinger Ries impact crater (Germany)

G. Schmidt and E. Pernicka, *Max-Planck-Institut für Kernphysik, Postfach 103980, D-6900 Heidelberg, FRG*

Most samples from the Ries crater studied so far to infer the nature of the projectile were derived from the surface. No indication of extraterrestrial material was found with the exception of one sample from the crater bottom which contained metal veinlets (1) and 0.21 ppb Ir (2). We analyzed systematically samples of the drill core from the research borehole Nördlingen 1973 to better characterize the indigenous Ir concentrations of the target rocks and to check, if there was indeed a spike of extraterrestrial PGE at the crater bottom. Samples from the saw-cut and mechanically crushed drill stems from the borehole were scratched from the interiors of the core segments and analyzed for platinum group elements, rhenium and gold. Altogether we have analyzed 10 samples of the so called Graded Unit (GU), which comprises 17.2 m of the core from the research borehole Nördlingen 1973 and is thought to represent fall-back material, which has been sorted to similar to tephra. In addition 21 samples of suevite, 15 samples of amphibolite, 5 samples of granite from the crater bottom and 4 samples of ultrabasic rocks from the basement were studied. We have found that ultrabasic rocks (peridotite) must also be taken into consideration, because 8 % of all rocks in the research borehole Nördlingen 1973 are of ultramafic composition (3, 4). These rocks have Ir concentrations of 0.5 ppb Ir, which are the highest ever measured in the target rocks and form an additional, indigenous source of siderophile elements. Therefore the indigenous level for Ir of 0.015 ppb estimated by Morgan et al. (2) is probably too low. Our measurements rather indicate an indigenous level in the order of 0.015 - 0.030 ppb Ir for the target rocks (Fig. 1). Our results show that no extraterrestrial contamination is indicated neither in the crater ejecta nor at the crater bottom confirming the view that low siderophile element concentrations seem to be typical for the Ries ejecta (2). This can now be extended to the crater bottom and the Graded Unit. Therefore we suggest that the observed metal veinlets at the crater bottom were formed by in situ reduction of the target rocks rather than by condensation of material from the projectile. Also there seems to be no significant enrichment of Ir in the fall-back sediments as has been suggested before (5).

References: (1) El Goresy and Chao (1976) *EPSL* **31**, 330-340. (2) Morgan et al. (1979) *Geochim. Cosmochim. Acta* **43**, 803-815. (3) Bauberger et al. (1974) *Geol. Bavarica* **72**, 33-34. (4) Matthes et al. (1977) *Geol. Bavarica* **75**, 231-253. (5) Pernicka et al. (1987) *EPSL* **86**, 113-121.

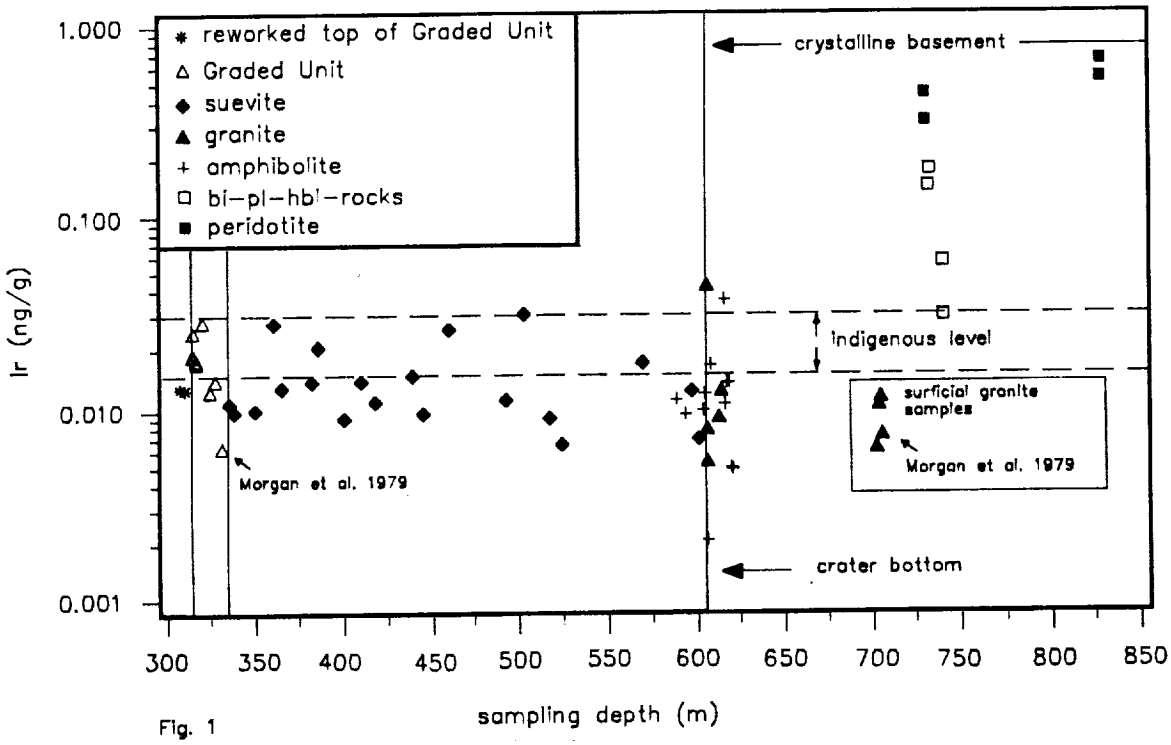

Fig. 1

A POSSIBLE MECHANISM FOR OUTBURSTS OF COMET P/HALLEY AT LARGE HELIOCENTRIC DISTANCES

by B. Schmitt, S. Espinasse and J. Klinger

A model of a porous comet nucleus containing amorphous water ice and CO or CO_2 ice has been developped. The model is based on the simultaneous solution of the heat conduction equation and the equation of gas diffusion in the pore system. Every equation contains a source term. The equations are coupled via these source terms. This model has been applied to comet P/Halley. The gas production rates obtained with this model showed in some cases an unexpected increase at large heliocentric distances. It also showed up that at heliocentric distances close to 12 AU, the temperature in several meters depth under the surface of the nucleus can attain values on the order of 130 K. This behavior is explained by the combined action of the thermal inertia of the nucleus and the crystallization of amorphous ice. When the comet surface is heated by the sun close to the perihelion, the penetration of the heat wave to deeper layers shows an important time lag. When the heat wave reaches the amorphous ice layers, the crystallization is triggered. The excess energy due to the crystallization may produce outbursts at rather large heliocentric distances.

ARE TWIN CRATERS CAUSED BY DOUBLE IMPACTORS?

Schultz, P.H., Department of Geological Sciences, Brown University, Providence, RI 02912
Gault, D.E., Murphys Center of Planetology, Murphys, CA 95247

Twin craters on Earth such as the Clearwater Lake, Kamensk, and Kara structures are commonly cited as possible simultaneous impacts by a tidally disrupted body or companion asteroids. Recent laboratory experiments and evidence from the planetary cratering record (1, 2), however, may provide an alternative explanation. Most cratering studies focus on impact excavation rather than the impactor's fate. As impact angles decrease below about 30° (referenced to the horizontal), internal energy losses (heat, fragmentation) in the impactor decrease as it retains an increasing fraction of its initial kinetic energy (2, 3). Hypervelocity impacts below 15° into a wide range of targets result in literal decapitation with fragments continuing downrange at 50-90% of the original impact velocity. Decapitation reflects two processes: spallation as the shock wave reflects off the projectile free surface and shear failure as it penetrates the target. Peak shock pressures in the projectile and target decrease with decreasing impact angle. The decapitated portion of the projectile survives as an ensemble of fragments ("siblings") with minimal dispersion in lateral velocities that re-impact downrange at hypervelocity. As a result, the primary crater in strength-controlled targets exhibit a deep uprange pit, a shallow overlapping sibling impact crater downrange (sheared fraction), and downrange pits (spalled fractions).

Downrange distance to the sibling craters is largely controlled by the degree of projectile penetration at the time of failure and hence depends on impactor physical properties and impact velocity. For impact velocities less than about 20 km/s, failure occurs before the projectile has penetrated to its radius, r_p, into the target (1). If this height above the target surface corresponds to $k \cdot 2r_p$, then the distance (in projectile radii) to the downrange sibling crater will occur at $2k \cdot \cot \theta$ for a minimal vertical velocity component. Impact angles of 15°, therefore, should lead to a sibling crater at $7.5r_p$ for $k = 1$. For strength-controlled excavation at laboratory scales, the sibling crater occurs as a separate pit at 15°. Although later stages of gravity-controlled growth at laboratory scales consume this impactor fate, scaling relations at larger scales (4) reveal that it would overlap the transient crater rim for impactors 2 km in diameter and occur as a companion crater for impactors > 10 km. Relatively small topographic relief or irregular shaped bodies can significantly extend these distances.

The well-preserved cratering record on the planets provide numerous examples of oblique impacts with downrange sibling companions, otherwise masked on the Earth. The siblings are invariably smaller and shallower except where an unusual topographic setting changes the impact angle. The Crisium, Moscoviense, and Orientale basins on the Moon and Bach on Mercury all exhibit clear evidence for origin by an oblique impact with sibling companions overlapping the downrange ring. Over fifty examples can be documented on Mars. With this proposed mechanism, twin craters on Earth may not be evidence for co-orbiting asteroids or tidal break-up but an expected signature of impactor fate for impact angles less than 15°, representing about 7% of the cratering record.

References:
(1) Schultz, P.A. and Gault, D.E. (1991) in *Geol. Soc. Amer. Sp. Paper 247*, pp. 239-261.
(2) Schultz, P.A. and Gault, D.E. (1991) *Lunar and Planet. Sci. XXII*, pp. 1195-1196.
(3) Gault, D.E. and Wedekind, (1978) *Proc. Lunar. Planet. Sci. Conf. 9th*, pp. 3843-3875.
(4) Schmidt, R. and Holsapple, K. (1982) in *Geol. Soc. Amer. Sp. Paper 190*, pp. 93-102.

IMPACT HEATING OF SHOCKED CHONDRITES; Edward R.D. Scott[1], Klaus Keil[1], and Dieter Stöffler[2] (1) Planetary Geosciences Division, Department of Geology and Geophysics, SOEST, University of Hawaii, Honolulu, HI 96822, (2) Institut für Planetologie, Westfälische Wilhelms-Universität, D-4400 Münster, Germany.

To understand how and where chondrites were heated by impacts and to elucidate the geological evolution of asteroids and the production of meteorites from asteroids, we are studying metallic Fe,Ni and troilite in a suite of H and L chondrites with diverse degrees of shock metamorphism. Petrographic studies of equilibrium shock effects in olivine and plagioclase allow these chondrites to be assigned to one of six stages of progressive shock metamorphism, S1 to S6 [1]. Thus we can compare directly the thermal history recorded in the metal with the shock history recorded in the silicate.

Chondrites of shock stages S1 and S2 have virtually undisturbed kamacite and taenite on the micron scale, consistent with normal slow cooling, maximum shock pressures of 5-10 GPa and mean shock-induced temperature increases of <100° C. A few of these (e.g., Menow and Ambapur Nagla, both S1) and some S3 and S4 chondrites have mosaicized troilite and micron-sized metal-troilite intergrowths ('fizzed' troilite [2]) at metal-troilite boundaries caused by rapid localized melting which we attribute to impact-induced heat pulses. Chondrites of shock stage S6 show extensive melting of metallic Fe,Ni (and silicate), no traces of the original kamacite-taenite structures and extensive blackening due to injection of melted troilite into silicate fractures following shock-induced heating. These observations confirm and strengthen the correlation between reheating and shock intensity discovered by Taylor and Heymann [3].

For chondrites of intermediate shock stages S3 to S5 the correlation between reheating and shock intensity is weaker, probably because of diverse degrees of localized shock melting of metal and silicates caused by jetting at pores and open cracks and frictional melting by shearing. Thus chondrites like Alfianello (S5) and Bruderheim (S4) in which melt pockets and shock veins are absent or rare tend to show only locally disturbed metallic microstructures and Ni profiles. Kamacite is polycrystalline, zoned taenite is largely replaced by micron-sized intergrowths of pearlitic plessite, and troilite is generally polycrystalline but not melted and injected into silicate fractures. This is consistent with the temperature increases of 100-600°C that are measured in non-porous silicates shocked to pressures of 20-50 GPa [4]. But for stage S3 to S5 chondrites that contain significant amounts of shock induced melt such as Orvinio (S3) and Walters (S4), the matrix grains of metallic Fe,Ni show evidence for more intense reheating: coarser plessite or martensite formed because of reheating to temperatures of 600-800°C [5,6]. In these more intensely reheated S3-S5 chondrites, silicate fractures around melt veins are filled with troilite causing localized shock-blackening. Thus moderatedly and heavily shocked ordinary chondrites show wide ranges in their optical and metallographic properties that are not correlated simply with equilibrium peak pressure even though most apppear to have experienced a single intense shock event.

Our observations suggest two major sources of heat for shocked chondrites: residual heat due to equilibrium shock pressures and localized impact melting that forms veins and pockets. We also recognize that some shocked chondrites like the LL granulitic breccia St. Severin were probably affected by an additional heating event, viz. metamorphism at 4.5 Ga. The similarity of shock veins and dikes in heavily shocked chondrites to those in terrestrial crater basements suggests that chondrite parent bodies did not form impact melt sheets in craters or retain much melted material in their ejecta blankets [7]. Thus heavily shocked chondrites were typically heated once beneath large craters on their parent bodies, not in ejecta blankets, impact melt sheets, or during impacts that exposed them to cosmic rays.

References. [1] Stöffler D. et al. (1991) this volume. [2] Scott E.R.D. (1982) Geochim. Cosmochim. Acta 46 813-823 [3] Taylor G.J. and Heymann D. (1969) Earth Planet. Sci. Lett. 7, 151-161. [4] Raikes S.A. and Ahrens T.J. (1979) Geophys. J. Roy. Astron. Soc. 58, 717-747. [5] Smith, B.A. and Goldstein, J.I. (1977) Geochim. Cosmochim. Acta 41, 1061-1072. [6] Taylor G.J. and Heymann D. (1971) J. Geophys. Res. 76, 1879-1893. [7] Stöffler D., et al. (1991) this volume.

VOLATILE LOSS DURING CHONDRULE FORMATION. D.W.G.Sears, Lu Jie and P.H.Benoit. Cosmochemistry Group, Dept. Chem.& Biochem., Univ. of Arkansas, Fayetteville, AR 72701.

The question of Na-loss from chondrules has been controversial for over two decades. Many chondrules contain their cosmic complement of Na, which is surprising in view of the ease with which Na is lost in laboratory experiments (1). Either these chondrules were heated under very unusual conditions (2), or they were heated too briefly for Na loss. Many contain relict grains indicating the lack of complete melting (3). However, 35% of the chondrules in the essentially unmetamorphosed Semarkona chondrite not only show major depletions in Na, but also show volatility-related depletions in at least 6 moderately volatile elements (4,5). They have distinctive cathodoluminescence (CL), which enables sorting into Group A1 (yellow CL mesostasis, with red CL ol/py, includes type IA, 4) and Group A2 (yellow CL mesostasis, little or no CL from the ol/py, includes PP). The better known 'Na-rich' chondrules, Group B (which include type II, 10), actually have flat CI-normalized abundance patterns, and none of their phases are cathodoluminescent (7).

Fig. 1 shows liquidus temperatures, calculated by the method of ref. 8,9, as a function of Na content for the chondrules from refs. 4,7 and 10. A negative correlation between liquidus temperature and Na is clearly present among the Group A chondrules, which also implies a relationship between FeO and Na content since A2 generally have higher Fa than A1 (7). The two chondrules furthest from the line have unusual characteristics, chondrule 28-12 is the only BO in Group A1 and chondrule 23-8 has atypically low CaO in its mesostasis. As expected, the Group B chondrules 10) show no evidence for a Na-liquidus temperature trend. In fact, since these chondrules probably did not reach the liquidus, their calculated temperatures are physically meaningless.

We have argued that the reduction of silicates accompanied loss of volatiles during chondrule formation (5). Others have argued that the redox state and volatile content reflect precursor composition (e.g. 4, 10). Hewins (9, quoting R.Jones) has suggested that if Na was lost during chondrule formation, then there would be negative correlation between liquidus temperature and Na, as we have observed for the Group A chondrules. The inverse zoning occasionally observed in the chondrule olivines, their small size relative to Group B chondrules and their elemental abundance patterns, which are volatility controlled, are additional evidence that, unlike Group B chondrules, Group A chondrules suffered reduction and devolatilization during chondrule formation.

1. Tsuchiyama et al. (1981) GCA 45, 1357. 2. Wood (1988) Protostars & Planets II, 687. 3. Nagahara (1983) Chondrules 211. 4. Jones & Scott (1989) PLPSC 19, 523. 5. Lu et al. (1989) LPS XXI 720. 6. DeHart (1990) PhD Thesis. 7. Lu et al., this volume. 8. Herzberg (1979) GCA 43, 1241. 9. Hewins (1991) GCA 55 935. 10. Jones (1990) GCA 54 1785.

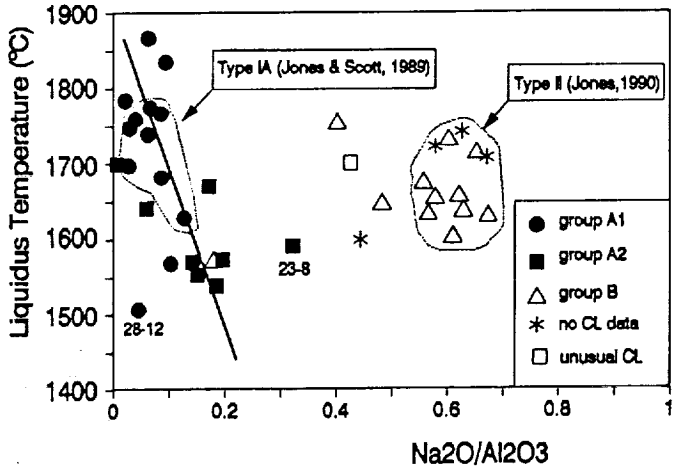

Fig. 1. Liquidus temperature vs. Na_2O/Al_2O_3 for chondrules from refs. 4,5,10.

AN EXPERIMENTAL STUDY OF Mg SELF-DIFFUSION IN SPINEL. Y.J. Sheng, I.D. Hutcheon, and G.J. Wasserburg. The Lunatic Asylum, Div. of Geol. and Planet. Sci., Caltech, Pasadena 91125.

Mg isotope heterogeneity, both between coexisting spinel and silicates and among spinels, is a prominent feature of Plagioclase-Olivine Inclusions (POIs) [1]. The preservation of isotopic heterogeneity and relict spinel (Sp) in inclusions with igneous textures indicates that the thermal event which partially melted the precursor material either had too low a temperature or was too brief to allow Mg isotope homogenization between Sp and the melt. Since the temperature history required to homogenize Mg isotopes depends on the diffusion rate of Mg in Sp, we designed experiments using an isotope tracer method to determine this critical rate [2]. The diffusion couple consists of a gem quality $MgAl_2O_4$ Sp wafer and ^{25}Mg-doped glass of POI composition. The bulk compositions of starting glasses were chosen from phase equilibria data [3] to be Sp-saturated at the run temperature of a given experiment. The presence of chemical equilibrium between glass and Sp for each run ensures that Mg diffuses only in response to the isotopic disequilibrium. Glasses were verified to be chemically and isotopically homogeneous and were then equilibrated at a temperature slightly below the spinel saturation temperature of the melt to ensure chemical equilibrium. Polished Sp wafers were pre-annealed for 24 hrs. at 1500°C. The polished surfaces of the Sp wafer and glass were placed together and held at temperatures between 1260 and 1550°C for 20 to 0.5 hr. Mg isotope profiles in Sp and glass were measured with the PANURGE ion microprobe [4,5] across a traverse perpendicular to the diffusion interface. Measured $^{25}Mg/^{24}Mg$ ratios were corrected for differences in isotopic fractionation between Sp and glass by normalizing to $^{26}Mg/^{24}Mg=0.13955$. The diffusion coefficients (D) were calculated from the measured isotope profiles using a model that includes the complimentary diffusion of ^{24}Mg, ^{25}Mg and ^{26}Mg in both phases with the constraint that the Mg content of each phase is constant. Diffusion profiles measured in Sp and glass for the experimental run at 1553°C are shown in Fig.1,2. The temperature dependence of D for Mg self diffusion in Sp is obtained from an Arrhenius relation. The activation energy and pre-exponential factor are, respectively, 397 ± 21 kJ and 199.4 ± 1.2 cm^2/s. This is somewhat different to the numbers previously reported [2] due to the inclusion of new data. For a maximum melting temperature for POIs of ~1500°C [3] these results show that a 10 μm diameter Sp would equilibrate isotopically with a melt within 60 min. To preserve isotopic heterogeneity, the POIs must have initially cooled faster than 50 to 250°C/hr. References. [1] Sheng Y. *et al.* (1991) GCA 55, 581; [2] Sheng Y. *et al.* (1991) LPSC XXII, 1233; [3] Sheng Y. *et al.* (1991) LPSC XXII, 1231; [4] Huneke J. *et al.* (1983) GCA 47, 1635; [5] Hutcheon I. *et al.* (1987) GCA 51, 3175; Captions. Variation of $^{25}Mg/\sum Mg$ across a traverse in glass (Fig.1) and Sp (Fig.2) for the experimental run at 1553°C. The fitted curve is the calculated diffusion profile.

Fig.1

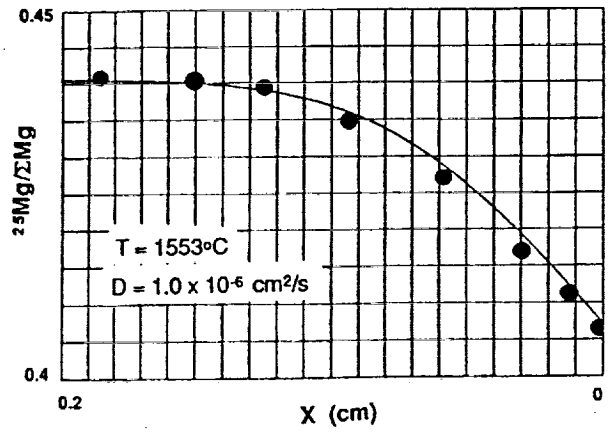

Fig.2

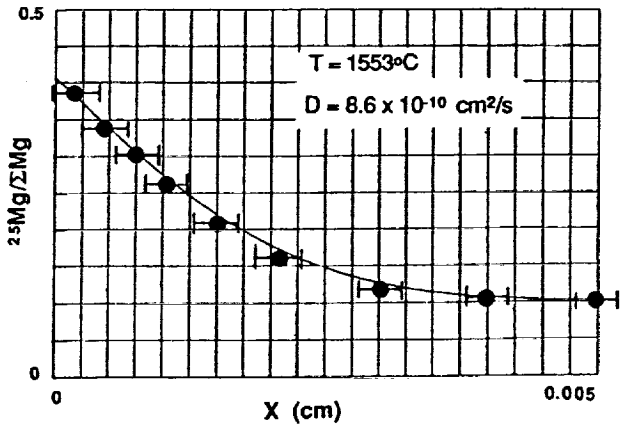

PROFILES OF Ti^{3+}/Ti^{tot} RATIOS IN ZONED FASSAITE IN ALLENDE REFRACTORY INCLUSIONS; S.B. Simon[1] and L. Grossman[1,2], [1]Dept. of Geophysical Sciences, [2]Enrico Fermi Institute, The University of Chicago, Chicago, IL 60637

In the fassaite found in Allende Type B, Ca-, Al-rich inclusions (CAI's), Ti is compatible and decreases in abundance from crystal cores to rims. This trend reflects crystallization-induced depletion of Ti in the residual liquid. $D^{fas/L}_{Ti^{3+}}$, the fassaite crystal/liquid distribution coefficient for Ti^{3+}, is greater than $D^{fas/L}_{Ti^{4+}}$, and Allende fassaite generally has $Ti^{3+}/Ti^{tot} > 0.5$, where $Ti^{tot} = Ti^{3+} + Ti^{4+}$ per six oxygen ions. Crystallization of fassaite from a CAI melt might therefore be expected to have depleted the residual liquid in Ti^{3+} relative to Ti^{4+}, *if* the residual liquid did not re-equilibrate with a reducing gas to restore the original Ti^{3+}/Ti^{tot} ratio. To investigate whether buffering occurred, we conducted electron probe traverses across two subliquidus fassaite crystals in TS22 (Type B2) and one each in TS23, TS33 and TS34 (all B1's). Because of the large uncertainty in Ti^{3+}/Ti^{tot} at low TiO_2^{tot} contents, we restrict our discussion to the parts of the traverses with $TiO_2^{tot} > 4$ wt %, but all are between 500 and 1000 μm long. One traverse, TS34, shows a gradual core-rim decrease in Ti^{3+}/Ti^{tot} from 0.790 ± .018 to 0.623 ± .063. Three traverses, in TS22 and TS33, are flat except for sharp drops at the points nearest the rims where $TiO_2^{tot} > 4$ wt %. In TS22 traverse A, the ratio drops from 0.726 ± .046 to 0.581 ± .071; TS22 traverse B drops from 0.738 ± .047 to 0.616 ± .076; and TS33 drops from 0.709 ± .030 to 0.516 ± .058. Fractional crystallization models (with $D^{fas/L}_{Ti^{3+}} \sim 3$ and $D^{fas/L}_{Ti^{4+}} \sim 1$) predict slight, gradual decreases in Ti^{3+}/Ti^{tot} during most of the interval of fassaite crystallization, with sharp drops toward the end of crystallization. Although the trends in TS22, TS33 and TS34 do not quantitatively match the models, they are generally consistent with control by fractional crystallization without re-equilibration of the residual liquid with the surrounding, solar nebular, reducing gas. This is not surprising, especially in the case of TS34. This inclusion has reversely zoned melilite, indicating a minimum cooling rate of 0.5 °C/hr and a maximum of ~ 50 °C/hr [1]. Fassaite crystallizes over a temperature range of ~ 30 °C [2], giving the liquid a maximum of ~ 60 hr, but as little as 1-2 hr, in which to re-equilibrate with the gas. Also, in Type B inclusions, fassaite crystallizes late, and isolation of liquid from the gas might be expected, especially toward the end of fassaite crystallization when the inclusions would have been almost completely solidified. The sharp drops in Ti^{3+}/Ti^{tot} correspond to this part of the crystallization history. One pattern, however, is flat: TS23, at 0.545 ± .068, suggesting that gas-liquid equilibrium was maintained throughout the interval of fassaite crystallization. This is not easily explained, because this inclusion is a Type B1 with reversely zoned melilite. The melilite mantle should have isolated the residual melt, and re-equilibration was subject to the same time constraint as described above. Perhaps parts of the mantle remained liquid long enough to allow communication with the reducing gas until after the TiO_2^{tot} of fassaite dropped below 4 wt %.

[1] G.J. MacPherson *et al.* (1984) *J. Geol. 92,* 289-305. [2] E. Stolper (1982) *GCA 46,* 2159-2180.

C-4

CROSS SECTIONS FOR PRODUCTION OF CARBON-14 FROM OXYGEN AND SILICON: IMPLICATIONS FOR COSMOGENIC PRODUCTION RATES;

J. M. Sisterson[1], A. J. T. Jull[2], D. J. Donahue[2], A. M. Koehler[1], R. C. Reedy[3] and P. A. J. Englert[4]. [1] Harvard Cyclotron Laboratory, Harvard University, Cambridge, MA 02138. [2] NSF Accelerator Facility for Radioisotope Analysis, University of Arizona, Tucson, AZ 85721. [3] Space Science & Technology Div., Los Alamos National Laboratory, Los Alamos, NM 87545. [4] Dept. of Chemistry, San Jose State University, San Jose, CA 92521.

The study of radioisotopes of differing half-lives in lunar rocks and cores gives valuable information about the constancy of the solar cosmic-ray (SCR) and galactic cosmic-ray fluxes and about the samples' recent histories. Determinations of SCR fluxes in the past depend on the accuracy of the cross sections. The cross sections for production of many radioisotopes from particles of SCR energies are often not well known (1). One such set of cross sections is that for $^{16}O(p,3p)^{14}C$; these data are important for interpretation of the 14C depth-profile data from Apollo 15 cores (2), lunar rocks (3) and some meteorites. Some re-evaluated or previously unpublished cross section measurements for the reaction $^{16}O(p,3p)^{14}C$ in the proton energy range 25-160 MeV were recently reported (4).

In this paper, we report on some new measurements for the cross sections for ^{14}C production from oxygen and silicon in the proton energy range of 58.5 to 158 MeV. Nine sets of SiO_2 (quartz) and silicon targets were irradiated at the Harvard Cyclotron Laboratory and the number of protons through each target ranged from about 0.7 to about 1.3 X 10^{14}. The samples were analysed at Arizona, where the samples were crushed and melted in an RF furnace with iron in a flow of oxygen (5). The resulting gas was oxidized to CO_2, and diluted to about 1 cm^3 volume. The diluted gas is reduced to graphite (5) and pressed into an accelerator target. Analysis for 14C was performed by accelerator mass spectrometry (6). The data from the quartz samples have been analysed and give preliminary values of about 2.1 to 2.8 mb for the $^{16}O(p,3p)^{14}C$ cross section in the energy range 58-158 MeV. After the analysis of the silicon targets is completed, these values will be corrected for the contribution to the cross section from $natSi(p,x)^{14}C$. Measurements at lower proton energies, down to threshold, are planned using the Davis cyclotron. The results appear to confirm the magnitude of previous estimates (7,8) of the production cross sections for ^{14}C from oxygen with reduced errors. Details of the measurements and their importance to lunar sample and meteorite studies will be presented.

(1.) R. C. Reedy and K. Marti (1991) in "The Sun in Time" (ed. C. Sonett and M. S. Matthews), Univ. of Arizona Press. (2.) A. J. T. Jull et al. (1991). Lunar Planet. Sci. XXII, 665. (3.) R. S. Boeckl (1972), Earth Planet. Sci. Lett., 16, 289. (4.) J. M. Sisterson et al (1991), Lunar Planet. Sci. XXII, 1267. (5.) A. J. T. Jull et al. (1989) Geochim. Cosmochim. Acta, 53, 2095. (6.) T. W. Linick et al. (1986), Radiocarbon, 28, 522. (7.) M. Tamers and G. Delibrias, Compt. Rend., 253, 1202. (8.) J. Audouze et al. (1967), in "High-Energy Nuclear Reactions in Astrophysics (ed. B. S. P. Shen), p. 255.

IMPLICATIONS OF CHONDRULE SORTING AND LOW MATRIX CONTENTS OF TYPE 3 ORDINARY CHONDRITES. William R. Skinner and James M. Leenhouts, Department of Geology, Oberlin College, Oberlin, OH 44074

Although chondrules span five orders of magnitude in size (1), the ordinary chondrites are characterized by chondrule populations with small size ranges and large chondrule to matrix ratios. This could result from a very restricted size range of chondrules formed during an efficient chondrule-making event, or it could be the result of sorting prior to accretion into parent bodies (2). Dodd (3) first quantified size distributions of chondrules and concluded that they had been aerodynamically sorted. Rubin and Keil (4) proposed size sorting of precursor "dustballs" to account for their observations of chondrules in CO chondrites. Others have considered chondrule size distributions (see references in 1): some included all chondrules, some only droplet chondrules, and some examined size differences among textural types within specific meteorites or meteorite groups. Comparisons of size distributions of droplet vs. clast-formed chondrules are now available for type 3 ordinary chondrites (5), and clast-formed chondrules prove to have size ranges and size distributions similar to those of droplet chondrules in the same chondrite. Many clast-formed chondrules are obviously fragments of broken droplet chondrules, some of which were much larger than any of the droplet chondrules now associated with these fragments.

The implication is clear: Whole droplet chondrules and fragments have been mixed and sorted by size, not created in the restricted size ranges observed in individual chondrites. Type 3 chondrites (and probably all ordinary chondrites) thus represent "size-bins" into which chondrules were sorted. As noted by others (e.g., 1,4), the range of chemical, isotopic, and textural characteristics exhibited by chondrules cannot be accounted for in a single population. The observed size distributions in chondrites must therefore be the result of at least three factors: 1) formation of chondrules in a wide range of sizes, 2) energetic events that fragmented chondrules, including large droplet chondrules rarely preserved as whole objects, and 3) sorting in the nebula (after formation and breakage) by some aerodynamic process that mixed whole droplet chondrules and fragments into closely sized fractions. Because of sampling problems and the limited preservation of primitive material in the solar system, the particular "size-bins" we observe must be a very restricted portion of those that once existed in the solar nebula.

The low matrix contents of ordinary chondrites (3) may also be related to sorting. Textural evidence suggests that much of the matrix fraction was acquired by type 3 ordinary chondrites as dust rims on chondrules; other small particles attached to chondrules at the time of accretion may now be part of the matrix. If the energy in the sedimentary environment prevented fine-grained material from settling out directly, then the low matrix content of these ordinary chondrites is not determined by the amount of dust present at the time of sedimentation (accretion), nor does it reflect the efficiency of the chondrule-forming process.

References: 1) Rubin A.E. (1989) Meteoritics 24, 179-189. 2) Wasson J.T. (1985) Meteorites. W.H. Freeman & Co. 3) Dodd R.T. (1976) EPSL 30, 289-291. 4) Rubin A.E. and Keil K. (1984) Meteoritics 19, 135-143. 5) Leenhouts J.M. and Skinner W.R., this volume.

High Sensitivity Survey Chemical Analysis of Metal-rich Meteorites by Secondary Ion Mass Spectrometry and Glow Discharge Mass Spectrometry.

Stephen P. Smith and John C. Huneke
CHARLES EVANS & ASSOCIATES
301 Chesapeake Drive, Redwood City, CA 94063

Both SIMS and GDMS are capable of providing major and trace element analyses of iron meteorites (1,2) and meteoritic metal phases with sub-ppm to sub-ppb detection limits for virtually all elements of the periodic table. The two techniques provide complementary information. SIMS analysis provides spatially-resolved measurements (on the order of 0.15 mm spot size for high-sensitivity bulk or depth profile analysis, 1 micron lateral resolution for SIMS imaging), with material consumption of a few tens of micrograms for complete survey analyses. GDMS analysis is non-selective on the scale of the required sample pin (1-2 mm in diameter and 10-20 mm long), with material consumption of a few hundred micrograms over a surface area of about 10 mm^2. While the larger amount of material analyzed by GDMS results in generally lower detection limits for many elements, SIMS analysis can provide better detection limits for certain elements that exist as contaminants in the glow discharge or whose GDMS analysis is hindered by argon-containing molecular ion interferences. We have analyzed six fine-grained iron meteorites (three group IIA and three group IVB) using both techniques.

Compared to SIMS, GDMS analysis has the distinct advantage of matrix-independent sensitivity factors for the analyte elements (due to the fact that ionization occurs post sputtering in a dominantly argon plasma). In addition, the GDMS sensitivity factors are relatively similar for all elements, unlike SIMS sensitivity factors which vary over several orders of magnitude. In practice, these differences mean that a typical GDMS analysis is completed in a single session, while separate SIMS analyses using both cesium and oxygen primary bombarding ions are required for full coverage. Also, quantitative SIMS analysis of unknowns requires careful standardization using reference materials of very similar major element composition. We have used a combination of the GDMS analyses on the same samples and literature values for major and trace elements to derive SIMS sensitivity factors.

SIMS analysis of trace elements heavier than the matrix species (Fe, Ni, P, Co in this case) is complicated by abundant molecular ion interferences involving the matrix species combined mutually and with the primary ion species (or residual vacuum impurities). High mass resolution on current instruments ($M/dM < 10000$) is frequently not useful, as well as being time consuming in a survey mode. A partial solution to this problem (on CAMECA magnetic-sector SIMS instruments) used here is selective energy-filtering of the secondary ions to minimize the molecular ion interferences. This technique is not very effective for dimer interferences (e.g. FeP^+ and NiP^+ at masses 85-95), in which case spectral peak stripping is useful.

For lighter elements, SIMS detection limits of 1ppbw or less (e.g. Be, B, Mg, ^{39}K, ^{41}K) and measured isotopic compositions suggest that the observed concentrations may contain significant or dominant contributions from cosmic-ray spallation reactions. Thus simultaneous measurements of a range of spallation products in iron meteorites may be practical using SIMS.

(1) Engstrom E.U. (1990) Meteoritics, p361.
(2) Chryssoulis S.L. and Weisener C.G. (1990) Secondary Ion Mass Spectrometry SIMS VII (Wiley), pp389-392.

N92-12928

CARBON AND OXYGEN ISOTOPE COMPOSITION OF CARBONATES FROM AN L6 CHONDRITE: EVIDENCE FOR TERRESTRIAL WEATHERING FROM THE HOLBROOK METEORITE

R. A. Socki[1], E. K. Gibson[2], A. J. T. Jull[3], and H. R. Karlsson[2]. [1]LESC and [2]SN2, NASA-JSC, Houston, TX 77058, [3]NSF Facility for Radioisotope Analysis, Univ. of Arizona, Tucson, AZ 85721, all USA.

Introduction. Terrestrial weathering in meteorites is an important process which alters pristine elemental and isotopic abundances. The Holbrook L6 chondrite fell in 1912. Material was recovered at the time of the fall, in 1931 and 1968. The weathering processes operating on the freshly fallen meteorite in a semi-arid region of northeastern Arizona have been studied after a ground residence of 19 and 56 years by (1). Karlsson, et al. (2) showed that a large portion of the carbonate material in 7 Antarctic ordinary chondrites either underwent extensive isotopic exchange with atmospheric CO_2, or formed recently in the Antarctic environment. In fact (3) demonstrated that hydrated Mg-carbonates, nesquehonite and hydromagnesite, formed in less than 40 yrs. on LEW 85320.

In order to help further constrain the effects of terrestrial weathering in meteorites, we have examined the carbon and oxygen isotopes extracted from carbonates of three different samples of Holbrook: a fresh sample at the time of the fall in 1912, a specimen collected in 1931, and a third specimen collected at the same site in 1968 (4). The effects of weathering on the chemical and noble gas isotopic compositions in the three Holbrook samples was shown by (1). Total carbon concentration increases up to a factor of three from the fresh fall to samples collected 19 years later. Carbonates in Holbrook are particularly well-suited for examining terrestrial weathering effects since their stable isotopes exchange readily at low temperatures. Furthermore, C-14 data will allow us to confirm both a pre- and post-bomb component.

Experimental Methods. Four powdered bulk meteorite samples from Holbrook (duplicate 1912 samples, a 1931 sample, and a 1968 sample) were reacted with 100% phosphoric acid releasing CO_2 for isotopic analysis. The reactions were carried out at 50°C for five days. The oxygen isotope fractionation factor of 1.00903 from (5) was assumed for this reaction. An additional step to remove H_2S involved passing the LN_2 condensible gasses over Ag_3PO_4, precipitating Ag_2S. After stable isotope analyses, the CO_2 was retrieved, reduced to graphite over hot iron and the ^{14}C abundances analyzed by accelerator mass spectrometry.

Results and Discussion. The ^{13}C and ^{18}O data for carbonates extracted from the 4 Holbrook samples are plotted as a function of recovery age in Figs. 1 and 2. Carbon isotope composition ranges from $-6.7^{o}/_{oo}$ to $-2.2^{o}/_{oo}$ PDB, becoming steadily enriched in ^{13}C with increasing residence time on the ground. Carbon isotopic composition approachs the theoretical composition of calcite in equilibrium with atmospheric CO_2 (6) (dashed line). Oxygen isotope composition of the 1931 and 1968 samples are essentially identical at $\sim+33^{o}/_{oo}$, and elevated relative to the 1912 duplicate (mean $+27.3^{o}/_{oo}$). A low CO_2 yield from the 1912 samples, indicating the absence of appreciable carbonate, is consistant with bulk carbon data from (1). The data indicate that a significant amount of carbonate probably formed in the Holbrook meteorite between the 1912 and 1931 interval. These results show that the carbon and oxygen isotopic abundances can be significantly altered in remarkably short periods of time on earth, similar to what is inferred for the Antarctic meteorites(2,3). ^{14}C analyses are underway and will be presented.

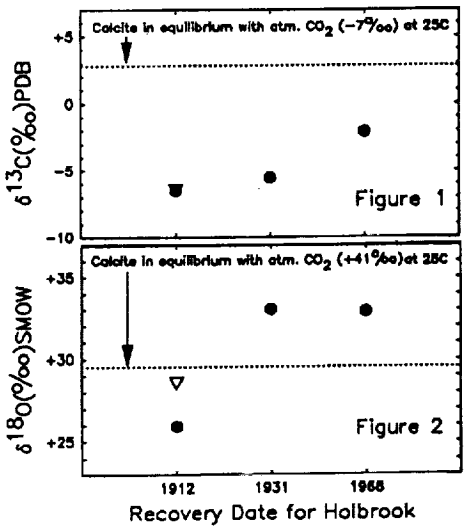

References. (1) Gibson, E.K, Jr. and Bogard, D.D. (1978) *Meteoritics* **13**, 277. (2) Karlsson, H.R., et al. (1991) *LPSC XXII*, 689. (3) Jull, A.J.T., et al. (1988) *Science* **242**, 417. (4) Gibson, E.K. Jr. (1970) *Meteoritics* **5**,57. (5) Clayton, R.N. and Mayeda, T.K. (1988) *GCA* **52**, 925. (6) Bottinga, Y. (1968) *J. Phys. Chem.* **72**, 800.

MAGNESIUM ISOTOPIC FRACTIONATION IN REFRACTORY INCLUSIONS: INDICATIONS FOR A MINERALOGIC CONTROL. G.Srinivasan[1], A.A.Ulyanov[2] and J.N.Goswami[1]. [1]Physical Research Laboratory, Ahmedabad–380 009, India. [2]Vernadsky Institute of Geochemistry and Analytical Chemistry, Moscow 11795, USSR.

A detailed study of magnesium isotopic fractionation in three petrographically well characterized coarse-grained refractory inclusions from Efremovka(CV3) was undertaken to infer their plausible formation scenarios. Intrinsic Mg isotopic fractionation $F(Mg)=[\Delta(25)_{sample}-\Delta(25)_{standard}]$ in melilite, spinel and hibonite was determined in the inclusions E-2(compact type A), E-40(type B1) and E-50(hibonite-rich) by the ion-probe. The inclusion E-40 shows clear indication of volatalisation loss during its solidification from a melt, as evident from the F(Mg) trend in melilite, the major mineral phase [1]. The spinel data, however, do not show a clear trend. The fractionation in spinel is nearly the same across the inclusion and is characterized by a heavier isotopic composition than in melilite. The spinels in the periphery of the inclusion were apparently not affected by the volatalisation event and the higher value of F(Mg) in spinel relative to melilite is a primary signature produced during crystallisation of this inclusion. Earlier data for E-2 [2] do not suggest any difference in F(Mg) values for spinel and melilite in the inclusion interior. However, our present data do show a signature for a systematically higher F(Mg) values for spinels compared to melilite. The rim spinel in this inclusion is isotopically much lighter compared to the interior spinel which is in agreement with earlier observation. The fractionation trend in the multi-zoned hibonite-rich inclusion E-50 is somewhat complicated with different F(Mg) values for the same phases in different zones. However in the spinel-hibonite dominant zone the F(Mg) values for spinel and hibonite are very similar but higher than that for melilite in the same zone. Earlier studies of F(Mg) trend in FUN inclusions[3, 4] suggest similar F(Mg) values for different mineral phases except when secondary processes have affected the inclusion. The present data for Non-FUN inclusions seem to suggest that there could be a primary control on F(Mg) seen in different mineral phases in coarse-grained refractory inclusions which may perhaps be related to the crystallisation sequence of these phases.

REFERENCES:

1. Goswami J.N. *et al.*, LPSC XXII, 1991. 2. Fahey A. *et al.*, GCA 51, 3215 (1987). 3. Clayton R.N. *et al.*, GCA 48, 535 (1984). 4. Davis A.M. *et al.*, GCA 55, 621 (1991).

TOF–SIMS, Applications in Meteorite Research, First Results

Thomas Stephan
Physikalisches Institut und Institut für Planetologie der Universität Münster
Wilhelm–Klemm–Straße 10, D–4400 Münster, Germany

Recent developements in microanalytical techniques for the analysis of extraterrestrial material demonstrate that increasing spatial resolution combined with increasing sensitivity mostly results in increasing knowledge about the formation of the solar system. The *in situ* registration of every single atom seems to be possible in the future. To reach this goal, high–resolution TOF–SIMS (Time–Of–Flight Secondary–Ion–Mass–Spectrometry) represents a big step foreward into the right direction.

In contrast to conventional ion microprobes with double focusing magnetic mass spectrometers, TOF–SIMS offers the possibility of a simultaneous detection of all masses with the same sign of charge in a single experiment. For the measurement of isotopic ratios or any quantification of the results linearity of the detection unit over a large dynamic range is a prerequisite. Dead time corrections play a major role for the quantification of TOF–SIMS results because the identification of an ion species depends on the exact registration of the time where the specific ion reaches the detector. A big signal on one mass may influence the detection probability of any ion which reaches the detector a short time later. Based on Poisson's statistical law, a procedure to correct the results for these dead time effects has been developed.

The corrected TOF–SIMS data allow the calculation of isotopic ratios with a high precision. Up to now the literature values for some elements like O ($^{18}O/^{16}O$), Mg, S ($^{34}S/^{32}S$), Cl, Cu, Ag, and Sb have been reproduced in different matrices with deviations between less than one permill and a few permill.

Besides probing a single spot on one sample, the *Münster TOF III Instrument* offers the possibility to produce *secondary ion images* of the sample by scanning the primary ion beam over the sample surface. One big problem here is to handle the large amount of data because every spot of the sample delivers a total mass spectrum. Up to now a spatial resolution of $\sim$10 μm has been reached with a gas primary ion source (mass resolution: $m/\Delta m \leq 20000$ FWHM) and $\sim$1 μm ($\sim$0.2 μm in the near future) with a Ga primary ion source ($m/\Delta m \leq 3000$ FWHM).

First results of isotopic measurements and secondary ion images of meteorite samples will be presented.

MAGNETIZATION OF METEORITES BY DYNAMO-GENERATED MAGNETIC FIELDS IN THE SOLAR NEBULA

T.F. Stepinski, Lunar and Planetary Institute, 3303 NASA Road 1, Houston, TX 77058

The residual magnetization of carbonaceous chondrites, which are generally assumed to be virtually unaltered relics from the nebular epoch of the Solar System and thus owning their magnetization to nebular magnetic fields, has been used to estimate the intensity of such fields and values of about 0.1 to 1 Gauss are most often quoted (1,2). Levy (3) originally presented nebular dynamo hypothesis to account for measured meteoritic magnetic remanence. Using order of magnitude estimations, he concluded that magnetic fields of magnitude of the order of 1 Gauss at the distance of few A.U. from the protosun could be maintained by $\alpha\omega$ dynamo. I have recently examined the feasibility of dynamo-generated field existence in the solar nebula. Calculations have been carried out for the nebula in the stage II (4), and the stage III (5), when the formation of meteorites and their subsequent magnetization are most likely to take place.

Nebular electrical conductivity σ_e is calculated by balancing ionization sources such as cosmic rays (6), decay of radioactive nuclei ^{40}K and ^{26}Al (7), and thermal ionization (where applicable) with electron losses due to reactions with positively ionized species, and recombination upon grains surfaces (7). Magnetic field is generated by differential rotation (ω_k) and local, turbulent motions (α) of nebular gas, and is diffused by ohmic dissipation $\eta_r = c^2/4\pi\sigma_e$ and turbulent dissipation $\eta_{turb} = h^2 M_{turb}^2 \omega_k$. Here ω_k is the Keplerian angular velocity, c is speed of light, h is nebula half-thickness, and M_{turb} is turbulent Mach number. The quantity α measures the helicity of turbulence. The ability of $\alpha\omega$ dynamo to maintain the magnetic field in the nebula is measured by dimensionless dynamo number $D = \alpha\omega_k h^3/(\eta_r + \eta_{turb})^2$, which characterizes the strength of regeneration mechanisms as compared to total diffusion. There exist a magnetic field generation threshold D_{crit} below which the dynamo mechanism is unable to maintain a magnetic field. Magnetic field can be generated only in those regions of the nebula where $D > D_{crit}$.

Figure 1. shows dynamo number D as a function of a distance from the protosun. Assuming uniform ionization of nebular gas along the entire disk thickness, numerical calculations (8) put the value of $D_{crit} = D_1$ at about 10. Thus magnetic field can be maintained by means of $\alpha\omega$ dynamo only beyond about 5 A.U. This model do not predict the existence of magnetic field at the region between 2 A.U. and 4.5 A.U., from which meteorites are believed to originate. However, the layers of nebular gas away from the midplane are more exposed to ionization by cosmic rays and have higher electrical conductivity. Numerical calculations taking this nonuniform σ_e into account yields $D_{crit} = D_2 \approx .01$ and magnetic field could be maintained throughout the entire radial extend of the nebula. Such field would have the significant toroidal magnetic field only in those exposed surface layers, the poloidal field, however, would penetrate to the midplane in much the same way that the Earth's magnetic field protrudes out of the planet's electrically conducting core. Thus a dynamo magnetic field generated in a canonical nebula model seems to be a plausible source of primitive meteorites magnetization, regardless of where in the nebula meteorites actually formed.

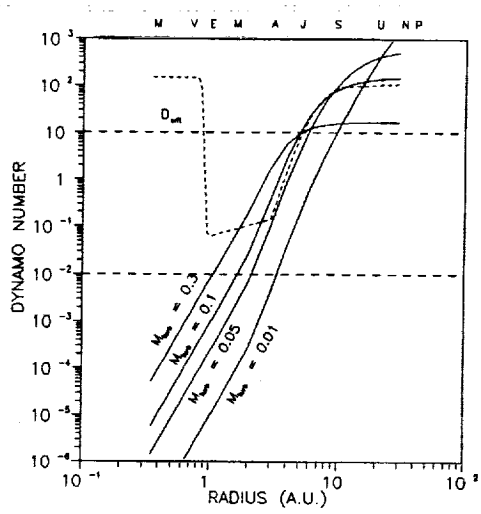

Figure 1 - Dynamo number D as a function of distance from the protosun. Short-dashed curve corresponds to the stage II nebula model with $M_{turb} = 0.1$. Labeled solid lines corresponds to different values of M_{turb} in the stage III nebula model. Long-dashed lines correspond to the generation thresholds D_1 and D_2.

References: [1] Butler, R.F. (1972), *Earth Planet. Sci. Lett.*, **17**, 120. [2] Brecher, A. (1972), in *Origin of the Solar System*, Reeves, H. ed. (Paris:C.N.R.S.) [3] Levy, E. H. (1978), *Nature*, **276**, 481. [4] Wood, J.A., and Morfill, G.H. 1988, in *Meteorites and the Early Solar System*, Kerridge, J.F., and Matthews, M.S. eds. (Tucson: University of Arizona Press), p. 329. [5] Hayashi, C. (1981), *Prog. Theor. Phys. Suppl.*, **70**, 35. [6] Umebayashi, T. and Nakano, T. (1988), *Prog. Theor. Phys. Suppl.*, **96**, 151. [7] Consolmagno, G.J. and Jokipii, J.R. (1978), *The Moon and the Planets*, **19**, 253. [8] Stepinski, T.F. and Levy E.H. to appear in Sep. 20 issue of *Ap.J.*

NEW SHOCK CLASSIFICATION OF CHONDRITES: IMPLICATIONS FOR PARENT BODY IMPACT HISTORIES; D. Stöffler, Institut für Planetologie, Westfälische Wilhelms-Universität, D-4400 Münster, Germany, K. Keil, and E.R.D. Scott. Planetary Geosciences Division, Dept.Geol.& Geophysics, SOEST, University of Hawaii, Honolulu, HI 96822, USA

Ordinary chondrites (77 samples) and carbonaceous chondrites (42 samples) have been assigned to 6 stages of progressive shock metamorphism S1 - S6 (1, 2), as defined in a revised shock classification system based on equilibrium shock effects in olivine and plagioclase (1, 3). Meteorites shocked above S3 (> 10 GPa) contain localized melt products such as melt veins, melt pockets and melt dikes.

Within each chemical group (H, L, LL), of ordinary chondrites the frequency statistics of shock stages is rather similar, with S3 being most abundant. Carbonaceous chondrites are predominantly unshocked and rarely reach S3 except for the metamorphic CK-suite (4). Among chondrites of different petrologic type, the frequency of the higher shock stages increases with increasing petrologic type. Stages S5 and S6 are lacking among type 3 and type 4 ordinary chondrites and are entirely absent in C3-4 chondrites. For C2-chondrites, all stages above S2 are missing. It is most likely that this effect is due to the differences in the physical properties of thermally unmetamorphosed type 2 and 3 target material (porous, volatile-rich) and recrystallized type 5 and 6 targets (coherent, dry rocks). The former reacts by total melting at shock pressures as low as 30 GPa, at which the latter starts to transform to shock stage S5 in the solid state.

As noted previously the noble gas content is positively correlated with shock intensity (e.g., 5, 6). Our study shows that the noble gases (data from (7)) are largely lost above ca. 35 GPa (i.e. stages S5 and S6) and completely retained below ca. 10 GPa (S1 and S2). This suggests that the loss of gases is related to the effect of localized melting. The scatter of data in S3 and S4 samples may be due to the lack or presence of melt products.

The type of shock metamorphism observed in all groups of chondrites is compatible with their formation in hypervelocity impacts which occurred on parent bodies with minimum sizes of probably kilometers (allowing the formation of sizeable craters), at a range of minimum impact velocities of less than 1 to about 5 km/sec. These conditions are required in order to explain the presence of polymict breccias and impact melt lithologies. Since highly shocked crater ejecta may not reach the size required for direct transfer to Earth as a meteoroid, it is reasonable to assume that most shocked chondrites originate from the inner impact formations and the subcrater basement of hypervelocity craters from which they were dislodged by later impacts. Shock veins and melt dikes are very characteristic of crater basements on Earth. The scarcety of genuine impact melt rock meteorites of the type expected in large impact melt sheets indicates that the largest craters on chondrite parent bodies were too small to form melt sheets, i.e., smaller than a few kilometers. The chondrites with extensive melt portions originate very probably from crater basements dissected by melt dikes and veins. Also, most of the small impact melt rock clasts in chondritic breccias may be derived from this basement by multiple impact reworking of preexisting craters.

References. (1) Stöffler D. et al.(1991) Proposal for a revised shock classification of chondrites (abstract), this volume. (2) Scott R.D.et al.(1991) Lunar Planet.Sci.XXII, The Lunar and Planetary Institute, Houston, pp.1205-1206. (3) Stöffler D., Keil K. and Scott E.R.D. (1991) Shock metamorphism of ordinary chondrites, submitted to Geochim.Cosmochim. Acta. (4) Scott E.R.D.et al.(1991) Lunar Planet.Sci.XXII, The Lunar and Planetary Institute, Houston, pp.1207-1208. (5) Bogard D.D. and Hirsch W.C. (1980) Geochim.Cosmochim.Acta 44, 1667. (6) Dodd R.T. and Jarosewich E. (1979) Earth Planet. Sci.Lett. 44, 335. (7) Schultz L. and Kruse H. (1989) Meteoritics 24, 155.

PROPOSAL FOR A REVISED PETROGRAPHIC SHOCK CLASSIFICATION OF CHONDRITES; D. Stöffler, Institut für Planetologie, Westfälische Wilhelms-Universität, D-4400 Münster, Germany, K. Keil, and E.R.D. Scott. Planetary Geosciences Division, Dept. Geol. & Geophysics, SOEST, University of Hawaii, Honolulu, HI 96822, USA

Based on the study of 119 ordinary and C-chondrites, we propose a revised petrographic shock classification of chondrites. Six stages of shock metamorphism (S1 to S6) are defined on the basis of characteristic shock effects in olivine and plagioclase: S1 (unshocked) - sharp optical extinction of olivine; S2 (very weakly shocked) - undulatory extinction of olivine; S3 (weakly shocked) - planar fractures in olivine; S4 (moderately shocked) - mosaicism in olivine; S5 (strongly shocked) - isotropization of plagioclase (maskelynite) and planar deformation features in olivine; S6 (very strongly shocked) - recrystallization of olivine and phase transformations of olivine (ringwoodite and/or phases produced by dissociation reactions). Shock effects of stage S6 are always restricted to regions adjacent to shock melted portions of a sample which otherwise is only "strongly shocked". Completely shock-melted chondrites with igneous and not chondritic textures are not included in this scale, because they should be classified as "impact melt rocks (breccias)". The symbol for the shock stage may be used in combination with the symbol for the chemical and petrologic type of a chondrite, e.g. L5(S4).

In shock stages S3 to S6, regions of localized shock-induced melts are present which result from local peaks of pressure and temperature deviating from the equilibrium (average) shock intensity of the sample. These melting effects are (a) opaque melt veins (shock veins), (b) melt pockets with interconnecting melt veins, (c) melt dikes; and (d) troilite/metal deposits in fractures. The melting effects, although important additional shock indicators, are not used as primary criteria for the proposed shock classification, in contrast to previous classifications (1, 2, 3).

A shock pressure calibration of the 6 progressive stages of shock metamorphism of chondrites is proposed on the basis of data from shock recovery experiments. The best estimates of the shock pressure for the transitions S1/S2, S2/S3, S3/S4, S4/S5, and S5/S6 are < 5, 5-10, 15-20, 30-35, and 45-55 GPa. Whole rock melting and formation of impact melt rocks or melt breccias occurs at about 75-90 GPa.

We propose this new classification system to replace previous systems (1,2,3,4) which are either restricted to one type of chondrite, e.g. L (2), or out-of-date with respect to pressure calibration (1,2,3), or based on incomplete and, in part, ill-defined sets of shock effects (1,2,3,4). Although we use some of the major principles of (2), a reclassification of the previously classified chondrites (shock facies a through f) is not possible in all cases without additional thin section studies as the proposed system uses some shock effects that have not previously been used for classification.

References. (1) Carter N.L., Raleigh R.B. and DeCarli P.S. (1968) J.Geophys.Res. 73, pp.5439-5461. (2) Dodd R.T. and Jarosewich E. (1979) Earth Planet.Sci.Lett. 44, pp.335-340. (3) Sears D.W.G. and Dodd R.T. (1988) In Meteorites and the Early Solar System, Kerridge J.F. and Matthews M.S. eds., Univ.of Arizona Press, pp. 3-31. (4) Stöffler et al. (1988) In Meteorites and the Early Solar System, Kerridge J.F. and Matthews M.S. eds., Univ.of Arizona Press, pp. 165-202.

NITROGEN ISOTOPE IN A EUCRITE YAMATO-792510;N.Sugiura and K.Hashizume, Geophysical Institute, Univ. of Tokyo, Tokyo, Japan

Nitrogen isotopic composition is quite variable for various groups of meteorites. The only previous nitrogen isotopic data on eucrites (1) was obtained for Pasamonte. The datum (8 ppm, delta ^{15}N=+5.4 permil relative to the terrestrial air) was obtained by single step heating. Since the abundance of indigenous nitrogen in achondrites is expected to be small, contributions of organic contamination and cosmogenic nitrogen to the datum may be significant.

We measured nitrogen isotopic composition of an eucrite Yamato-792510. The result of the stepwise combustion experiment is shown in the figure. At low temperatures, nitrogen due to organic contamination is dominant. At high temperatures, cosmogenic nitrogen is dominant. Thus indigenous nitrogen is observed only at a few temperature steps around 700 C. (Even at these steps, the indigenous nitrogen may be mixed with either organic or cosmogenic nitrogen and the obtained isotopic ratio is probably an upper limit.) The abundance of nitrogen extracted at T>600 C is about 0.32 ppm. The lowest delta ^{15}N value is about -60 permil at 700 C although the estimated error is relatively large due to the small abundance. The second lowest value at 800 C (-40 permil) is more reliable. A second sample was measured to confirm this result. Unfortunately, the sample seems to be more heavily contaminated with organic materials, and the lowest delta ^{15}N value is about -30 permil. Nevertheless we can conclude that the nitrogen in this eucrite is isotopically light.

Although the high temperature data are dominated by cosmogenic nitrogen, we can make another estimate of the isotopic composition of indigenous nitrogen by subtracting the contribution of the cosmogenic nitrogen from the high temperature data. The cosmic ray exposure age of this eucrite is calculated to be 18.8 m.y. from the measurement of cosmogenic neon (2) and the production rate. (Our own neon data suggest that the exposure age may be a bit longer, while the exposure age obtained from cosmogenic ^{38}Ar (2) is somewhat shorter.) We can calculate the abundance of the cosmogenic nitrogen using the production rate (3) and the oxygen abundance in eucrites. Subtracting the cosmogenic ^{15}N from the high temperature (>600 C) data, we estimated the delta ^{15}N value for the indigenous nitrogen to be -106 permil. Although the cosmogenic nitrogen may be incompletely extracted, this result is consistent with our direct observation shown above that the indigenous nitrogen is isotopically light.

The present data on a eucrite together with previously published data on primitive achondrites and iron meteorites suggest somehow differentiated meteorites tend to have light nitrogen.

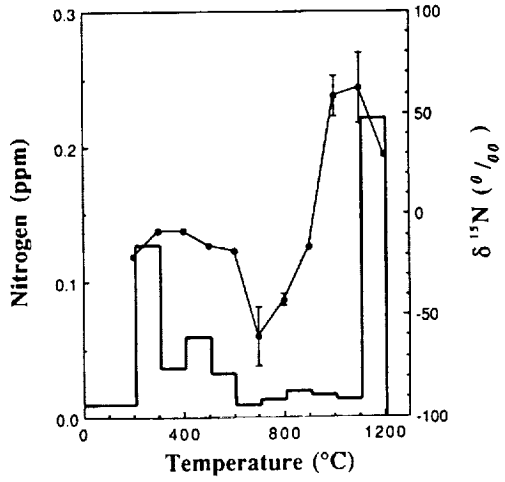

REFERENCES
C.Kung and R.N.Clayton (1978) Earth Planet. Sci. Lett. 38, 421.
K.Nagao and A.Ogata (1989) 14th Symp. Antarctic. Meteo. 119.
R.H.Becker, R.N.Clayton and T.K.Mayeda (1975) Proc. Lunar Planet. Sci. Conf. 7th, 441.

NOBLE GASES IN THE MONTICELLO HOWARDITE. T. D. Swindle and M. K. Burkland, Lunar and Planetary Laboratory, University of Arizona, Tucson, AZ 85721.

Monticello is a recently found howardite (1) which is rich in impact glass (2). As a part of an effort to understand the processes affecting noble gases in meteoritic regolith breccias (3), we have analyzed the noble gases extracted by stepwise heating of a 95.6 mg sample of Monticello. This report represents the first data from the new University of Arizona VG5400 noble gas mass spectrometer.

Although Monticello is glass-rich, the sample analyzed is not gas-rich: there does not seem to be any solar wind implanted ^{4}He, ^{20}Ar or ^{36}Ar. Although most howardites (13 of 18 tabulated in (4)) are not gas-rich, most of the glass-bearing howardites studied by Olsen et al. (2) are (3 of the 4 other than Monticello for which noble gases have been measured). Since howardites are regolith breccias, they are undoubtedly heterogeneous, and so there could be gas-rich portions of Monticello even if our sample, consisting of two fragments from the same 1g piece, is not.

Monticello also appears to have a short recent exposure history. Cosmogenic ^{3}He, ^{21}Ne, ^{38}Ar, ^{83}Kr and ^{126}Xe are all present at levels comparable to the lowest amounts observed in howardites (e.g., 5). Assuming that our sample has the same bulk chemistry as that analyzed by (1), we obtain a cosmic-ray exposure age of 2-3 Ma.

Further work on howardites will include analyses of Xe in gas-rich samples, in search of further evidence for excess fission Xe in meteorite breccias (3). We also plan to analyze another sample of Monticello after finishing installation of an ion-counting system, which should make determination of an accurate ^{81}Kr-Kr cosmic-ray exposure ages possible.

References: 1) E. J. Olsen et al. (1987) Meteoritics 22, 81. 2) E. J. Olsen et al. (1990) Meteoritics 25, 187. 3) T. D. Swindle et al. (1990) Geochim. Cosmochim. Acta 54, 2183. 4) L. Schultz and H. Kruse (1989) Meteoritics 24, 155. 5) R. Ganapathy and E. Anders (1969) Geochim. Cosmochim. Acta 33, 775.

NATURAL THERMOLUMINESCENCE AND ANOMALOUS FADING: TERRESTRIAL AGE, TRANSIT TIMES AND PERIHELIA OF LUNAR METEORITES. S. **Symes**, P.H. **Benoit**, H. **Sears**, and D.W.G. **Sears**. Cosmochemistry Group, Dept. of Chemistry and Biochemistry, University of Arkansas, Fayetteville, AR 72701 USA.

The last few years have seen the identification of no less than 11 meteorites which are almost certainly from the moon. Several of these meteorites (Y-791197, Y-82192 and ALHA81005) have been studied by Sutton (1-3) using thermoluminescence (TL). We have recently completed a detailed study of the natural and induced TL properties of MAC88104/5 and four achondrites (Kapoeta, LEW85303, PCA82502, and Serra de Mage). We here discuss these data, with special regard to the terrestrial and space history of lunar meteorites, as revealed by TL.

In general, the level of natural TL of all the lunar meteorites measured thus far is lower (at a glow curve temperature of ~250 C) than most ordinary chondrites and achondrites. Possible explanations for this are 1) longer than average terrestrial ages 2) recent reheating (e.g. by a low perihelion orbit) 3) short transit/exposure times or 4) high rates of anomalous fading. There is a fair degree of disagreement on terrestrial ages for lunar meteorites, MAC88104/5 in particular (4-6), but these ages are, in general, no greater than those of most achondrites.

We have experimentally determined rates of anomalous fading for MAC88104/5, four basaltic achondrites, and a chondritic control (Bruderheim). We found, as expected (7), that Bruderheim, with predominately disordered feldspar, showed only slight degrees of thermal fading in the low temperature portions of its glow curve. The other samples, containing predominately ordered feldspar, faded significantly throughout their glow curves. Most samples, including MAC88104/5, faded faster in lower temperature portions of their glow curves, but LEW85303 and Kapoeta appear to fade at the same rate throughout their glow curves. Absolute rates of fading are fairly similar at higher glow curve temperatures for all our samples.

We have found, after extrapolating our fading rates to long time spans, that the natural TL level of MAC88104/5 is too low to be caused solely by anomalous fading without requiring a terrestrial age in excess of 10^7 years, which is far higher than all the isotopic ages. However, anomalous fading is probably the major factor giving achondrites and lunar meteorites slightly lower average natural TL levels than chondrites. We conclude therefore that either MAC88104/5 has experienced a recent low perihelion orbit/reheating or that is has a short transit/radiation exposure history. If the latter is the case, our data show that the transit times are 2.0 and 1.8 ka for MAC88104/5, respectively. This compares well with the short exposure times (2.5 ka, ALHA81005; 19 ka Y791197) found by Sutton (1-3) for other lunar meteorites, and we suggest that, despite their compositional and textural differences, MAC88104/5 and ALHA81005 may have been ejected from the moon in the same event.

We will also report new data for two other lunar meteorites: Y82192 and a lunar mare meteorite EET87521.

1) Sutton (1986) Proc. 10th Symp. Ant. Met., NIPR Spec. Pub. 41, 133. 2) Sutton (1986) Meteoritics 21, 520. 3) Sutton and Crozaz (1983) Geophys. Res. Lett. 10, 809. 4) Eugster (1989) Science 245, 1197. 5) Vogt et al. (1991) GCA, submitted. 6) Nishiizumi et al. (1991) GCA, in press. 7) Hasan et al. (1986) J. Lumin. 34, 327.

Supported by NASA grant 9-81 and NSF grant DPP8817569.

REMNANT OF WATER-ROCK INTERACTION ON THE LUNAR SURFACE; K.Takahashi[1] and A. Masuda[2], [1]Earth Sciences Laboratory, The Institute of Physical and Chemical Research (RIKEN), Wako-shi, Saitama 351-01, Japan, [2]Department of Chemistry, The University of Tokyo, 7-3-1 Hongo, Bunkyo-ku, Tokyo 113, Japan

Since 1981, more than 10 antarctic meteorites have been recognized to belong to lunar meteorites and most of them except EET-875211 have been considered to have been derived from lunar highlands. Lunar highland rocks, including lunar meteorites, have been known to show various degree of positive Ce anomaly on their REE (rare earth element) abundance patterns [1]. We have performed the measurements of REE abundances, major element contents and Rb-Sr isotopic systematics for some lunar meteorites, to discuss the genesis of the Ce anomaly.The Ce anomaly could be considered to have been formed on the lunar surface, since the Rb-Sr systems of these lunar meteorites keep the ages of 3.9 Gyr. According to our geochemical (major elements and REE abundances) study and chronological (Rb-Sr systematics) study for some lunar meteorites, the degrees of Ce anomalies seem to increase with decreasing Al_2O_3 and CaO contents, as shown Fig. 1. Furthermore, the samples, which form an isochron with the relatively high initial ratio, show smaller degrees of positive Ce anomalies than the lunar meteorite samples forming an isochron with relatively low initial ratio as shown in Fig. 2. These correlations between major element contents, REE abundances, initial $^{87}Sr/^{86}Sr$ ratios and the degrees of Ce anomaly suggest that H_2O (possibly as ice) had taken part in the alteration which had brought Ce anomaly, and it is considered that there might have existed some ice at least locally on the surface of the moon in an early stage of lunar history (possibly on the pole like Mars).

References: [1] Masuda, A., Nakamura, N., Kurasawa, H. and Tanaka T. (1972) Proc. Lunar Sci. Conf., 3rd, 1307-1313.

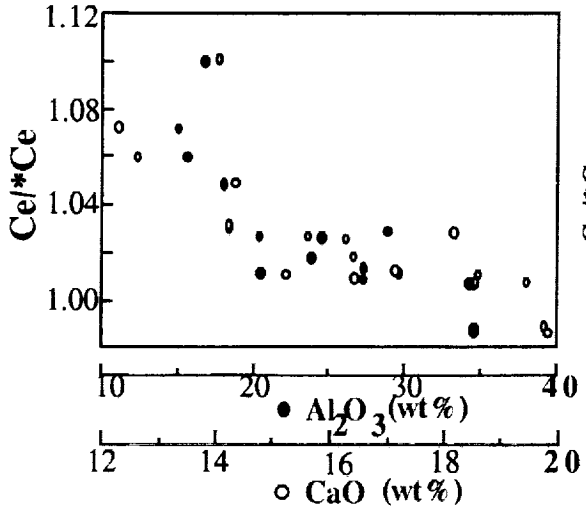

Fig.1 The degrees of Ce anomalies *vs.* the Al and Ca contents

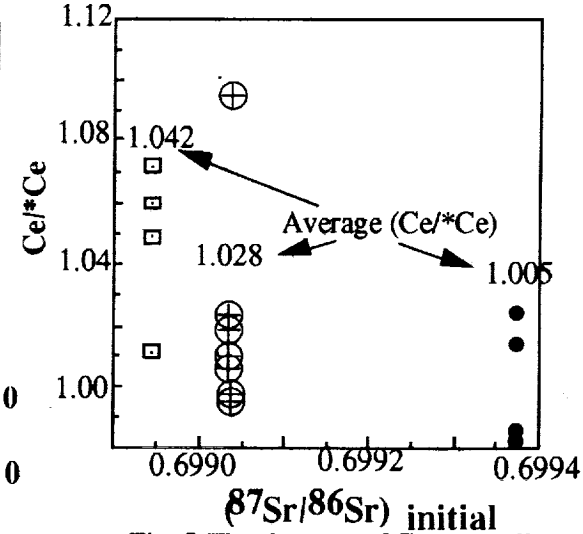

Fig. 2 The degrees of Ce anomalies *vs.* initial Sr isotope ratios

NOBLE GASES IN Y-74063(UNIQUE); N. Takaoka, Dept. Earth & Planet. Sci., Kyushu Univ., Hakozaki, Fukuoka 812, Japan; K. Nagao & Y. Miura, Inst. Study Earth Interior, Okayama Univ., Misasa, Tottori 682-01, Japan.

Unique meteorite Y-74063, similar to Acapulco and Lodran in texture, mineralogy and chemistry (Yanai & Kojima, 1990), contains large amounts of trapped Ar, Kr, Xe, whereas depleted in trapped He, Ne. Enrichment of Xe overwhelms E- and C-chondrites, and even ureilites with a few exceptions. The planetary gases reside in C for C-chondrites and ureilites, and in enstatite or some phase closely associated with enstatite for E-chondrites. Concentration of C has not been reported in Y-74063 except for accessory graphite(Nagahara et al.,1990). Therefore the first guestion is what is the noble gas carrier. Since the sample for noble gas analysis was not enough to carry out chemical etching, gas extraction by a laser beam was used. A preliminary result by the laser extraction shows that all grains pittd, which include silicate, troilite, Fe-Ni grains, released large amounts of Ar, Kr, Xe, suggesting that the gases are not enriched in a special mineral but reside rather ubiquitously, or that the carrier disperses in mineral grains. The first laser experiment was undertaken with large spots of ca. 100 μm in diameter. The experiment using small beam spots is planned.

The second question is concerning the heavy enrichment of Xe. $^{36}Ar/^{132}Xe$ is 32 for bulk, lower than for any meteorites reported, and ranges from 16 to 140 for the individual grains pitted. Some fractionation process should work to lower $^{36}Ar/^{132}Xe$ from solar 10^4 or planetary 90 to 32 or less. Ar loss by a factor of 300 from the solar gas should accompany appreciable isotopic fractionation in Ar. Measured $^{38}Ar/^{36}Ar$(0.190) does not show such isotopic fractionation. Preferential Ar loss or Xe trapping of the planetary gas is probable. An alternative explanation is to assume an Ar-poor gas (Takaoka & Yoshida, 1991) as a complementary component to the Ar-rich (or subsolar) component (Crabb & Anders, 1981; Wacker & Marti, 1983).

Ref:Crabb & Anders (1981), Geochim. Cosmochim. Acta, 45, 2443-2464.
Nagahara et al.(1990), Abstr. 15th Symp. Ant. Met. NIPR, Tokyo, 92-94.
Takaoka & Yoshida (1991), Proc. NIPR Symp. Ant. Met., 4, (in press).
Wacker & Marti, (1983), Earth Planet.Sci. Lett., 62, 147-158.
Yanai & Kojima (1990), Abstr. 15th Symp. Ant. Met. NIPR, Tokyo, 95-96.

RECRYSTALLIZATION AND SHOCK TEXTURES OF OLD AND NEW SAMPLES OF JUVINAS IN RELATION TO ITS THERMAL HISTORY; Hiroshi Takeda and Akira Yamaguchi, Mineralogical Inst., Faculty of Sci., Univ. of Tokyo, Hongo, Tokyo 113 Japan

Many monomict eucrites show petrographic evidence of secondary subsolidus reheating events. We proposed that their pyroxenes would have been equilibrated during post-shock thermal annealing, at or near the floor of an impact crater or along the crater wall(1). We have studied ten old thin sections of Juvinas preserved at the Muséum National d'Histoire Naturelle in Paris, and new ones made from chips sampled at six distant locations of the main mass by mineralogical techniques, to detect variability of the textures within a large sample such as Juvinas. In two old sections, we observed textures previously not well documented.

In one area, minerals except for the core portion of a large pyroxene crystal are replaced by fine-grained minerals, particularly aggregates of fine accicular plagioclase crystals (up to 0.2 mm). A similar texture was observed at fine-grained (FG) areas of many brecciated crystalline portions from the main mass. There are more Ca-rich pyroxenes ($Ca_{43}Mg_{29}Fe_{28}$) than low-Ca ones filling interstices of the accicular plagiocalses. The difference in crystal growth condition in two areas implies that the FG area is recrystallized from a shock partial melt. In some pyroxene-rich areas adjacent to the accicular plagioclase areas, small glanoblastic pyroxenes with opaque inclusions are observed. The texture indicates that this area was originally larger pyroxenes and experienced shock and reheating, but not melting. The chemical compositions of shock modified areas and large pyroxene crystals ($Ca_6Mg_{37}Fe_{57}$) show the same trend as an exsolution trend, which covers from the host pigeonite ($Ca_{1.8}Mg_{37.5}Fe_{60.7}$) to lamella augite ($Ca_{40.1}Mg_{31.3}Fe_{28.6}$) due to incomplete resolution of the lamellae by electron probe microanalysis. The fact suggests that Mg-Fe homogenization took place without modifying the previous shock and crystal growth textures. An content of the plagioclase crystals still preserve variations of the initial zoning during crystal growth because of slow diffusion of Al-Si. A large plagioclase shows variation from An_{93} to An_{83} with some high alkali spots (up to $An_{70}Ab_{25}Or_4$) and the fine accicular ones from An_{93} to An_{80}.

In another section, there is a heavily brecciated area with angular to subangular mineral fragments set in a dark brown glassy matrix. This area represent the last shock event after the homogenization of Mg-Fe took place, because the heat sourse for the Mg-Fe homogenization converts glassy materials to crystalline ones. This area has not been found in newly sampled portions. A newly chipped large mass (40E) includes vuggs with euhedral crystals of dark brown pyroxene and transparent white plagioclase and yellowish plate-like materials composed of fine glanoblastic pyroxene and minor plagioclase. The origin of vugg is not clear at present.

Variability of the textures and uniform chemistry at different portions of a large sample are the same as those found in Millbillillie (2) and suggest that heat sources due to impacts may be important factors for homogenization of Mg-Fe at low temperature without modifying their variations of shock-related textures except for the glassy matrix.

We thank Prof. Paul Pellas of Muséum National d'Histoire Naturelle for observation of Juvinas and Ministry of Education and JSPS of Japan for financial supports.

(1) Takeda H. and Graham A. L. (1991) Meteoritics, 26, in press.
(2) Yamaguchi A. and Takeda H. (1991) Abstract in this volume.

THERMAL RELEASE PATTERN OF Hg ISOTOPES IN CHONDRITES

Alakh N Thakur
California space Institute, M/C 0317 La Jolla, CA 92093

Hg is extracted from a neutron irradiated chondrite sample by stepwise heating. The activated nuclides are measured by gamma ray spectrometry. While most of the samples give $^{196}Hg/^{202}Hg$ ratios within 10% of normal , in some cases large anomalies are observed. A number of control experiments have been devised, including the re-irradiation experiments [1]. These experiments show the absence of experimental artifacts, during sample preparation, neutron irradiation, chemical separation and counting stages. In order to find the carrier phase of these anomalies several experiments were performed. Most promising of all these was the temperature profile studies and are being presented here.

There are variation in the abundances as well as ratios with temperature (Fig 1). Ratios are below normal in the RT-100 ^{o}C fraction. As the temperature increases the ratio increases and nearly equals (or even exceeds) the monitor value. It again comes down gradually. Sometimes , however, the first low value is masked from normal Hg of second fraction. The mass balance calculations demonstrate that if one were to make a one temperature measurement one may get almost normal value due to over abundance of the normal low temperature mercury.

These results put foreword some constrains on the formation history of stone meteorites. Presence of extrasolar grains at the time of condensation and / or collision of meteoritic parent body with a cometary object having isotopically different thermal components are the suggested mechanisms [2].

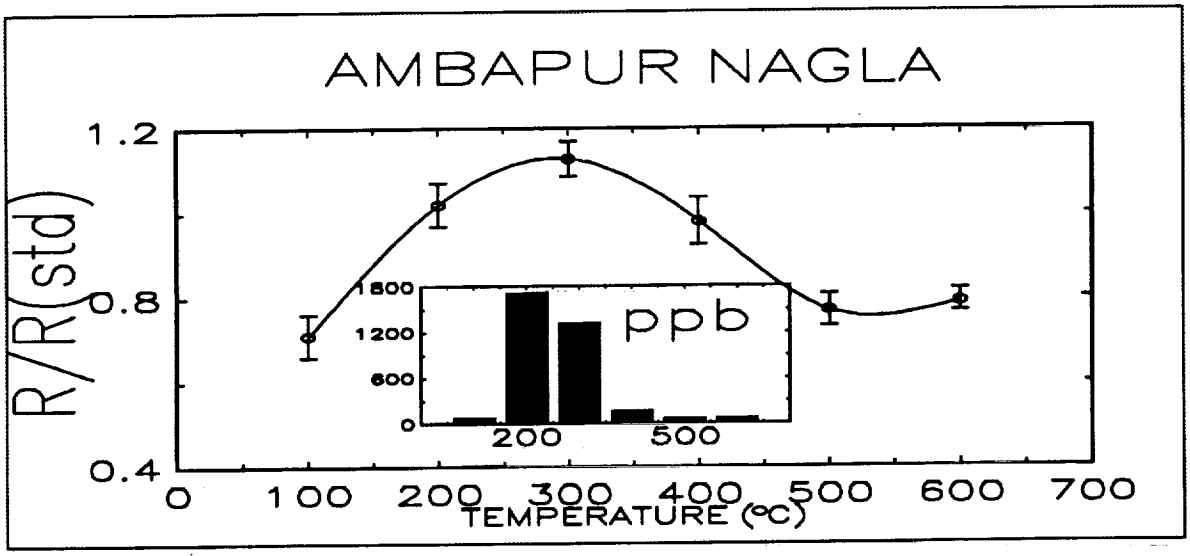

Fig 1. Hg isotopic ratio and abundance vs Extraction temperature.

References [1]. Thakur A N and Goel P S (1989) Earth Planet. Sci. Lett. 96, 235-246. [2]. Jovanovic S and Reed, Jr. G W (1990) Chem. Geology (Isotope Geoscience Section) 80, 181-191.

DUST INVESTIGATION OF INSOLATED COMET NUCLEUS ANALOGUES

K. Thiel and G. Kölzer
Abteilung Nuklearchemie, Universität zu Köln, Zülpicher Str. 47, D-5000 Köln 1

In a series of experiments using the satellite testing facility at DLR/Köln, comet nucleus analogue material is investigated under simulated space conditions (~77 K, ~10^{-4} Pa) at 0...2 solar constants artificial insolation intensity[1]. The objective of this interdisciplinary project (Kometensimulation KOSI) carried out by 8 German teams of scientists is to study processes that occur near the surface of ice-dust bodies (up to 0.6 m in diameter) under insolation in view of similar processes on comet nuclei.

Besides energy budgeting, material alteration and mobilization studies, optical, and mechanical measurements, great emphasis is laid on the investigation of dust properties and dynamics. A variety of diagnostics is used including active and passive dust collectors, Piezo impact sensors, ice particle detectors, optical and SEM microscopy, as well as image analyzing techniques to establish the relevant textural, structural and dynamical parameters of the ice/dust particles[2]. By employing a technique of spraying aquous suspensions of mineral dust into liquid nitrogen kilogram amounts of comet analogue material is produced that resembles fluffy type stratospheric particles (mass density 0.4-0.5 g/cm^3). The material, being irradiated in different sample holders (up to 0.6m x 0.3m) by 10 high pressure Xe-lamps under space conditions is investigated with respect to phenomenology and emission parameters of residual dust particles.

The results of the first 6 KOSI-experiments reveal a pronounced dust emission characteristics parallel to the surface normal. A significant interrelation of particle size (typically 10...500 μm), starting angle and velocity (~0.2...>5 m/s) of the emitted dust is observed. The frequency of ice free particles decreases with increasing particle size. The emitted particle stream exhibits an internal structure of a central low-speed flux of large agglomerates, superimposed by a high-speed background of small grains. The variation of the dust emission activity with time can be interpreted in terms of the removal or buildup of a dust mantle depleted in volatiles that covers the sample surface. This dust mantle may form a heat insulating "regolith" layer that quenches further rapid ice sublimation and dust emission. The results are compared with the latest experiment KOSI 7 that is characterized by an extremely low dust content. Possible implications for the near surface dust dynamics of a comet nucleus are discussed.

[1]**E. Grün et al.**, in: *Comets in the Post-Halley Era*, Vol.1, (Eds. R. L. Newburn et al.), Kluwer Academic Publishers, Dortrecht 1991, pp. 277-297
[2]**K. Thiel et al.**, *Proc. of Lunar Planet. Sci.*, Vol. 21, Cambridge University Press, Houston 1991, pp. 579-589

IDDINGSITE IN THE NAKHLA METEORITE: TEM STUDY OF MINERALOGY AND TEXTURE OF PRE-TERRESTRIAL (MARTIAN?) ALTERATIONS.

Allan H. Treiman and James L. Gooding, SN21, NASA/JSC, Houston TX 77058.

Rusty-colored veinlets and patches in the Nakhla meteorite, identified as "iddingsite" [1], are pre-terrestrial [2]. The rusty material is iddingsite (smectites + hematite + ferrihydrite); like terrestrial iddingsites, it probably formed during low-temperature interaction of olivine and water.

Fragments of rusty material with host olivine were removed from thin sections of Nakhla (USNM-426, Smithsonian Institution) with a tungsten needle. Fragments were embedded in epoxy, microtomed to 100 nanometers thickness and mounted on Cu grids. Phase identifications were by Analytical EM/EDX 'standardless' chemical analyses (for silicates), electron diffraction (hematite and ferrihydrite), and lattice fringe imaging [2].

The rusty material contains hematite, ferrihydrite, iron saponite, and a distinct "iron-bearing smectite"; the name iddingsite is consistent with this mineral assemblage [3,4]. Some serpentine is also present. The amorphous material found by [5] may be ferrihydrite or a smectite, which appear poorly crystalline in electron diffraction. Hematite and ferrihydrite (two-ring) were identified by composition and by electron diffraction.

Chemical analyses identified as iron saponite have little Al and normalize to 4 Si+Al and 3 Fe+Mn+Mg per 11 O; alkali content is variable. Interlayer spacings are 11-13 nm [2]. Areas identified as "iron-bearing smectite" are similar to iron saponite in CTEM imagery; their analyses show little Al, atomic (Fe+Mg+Mn)/(Si+Al) = 0.5, and variable alkali contents. They may represent a dioctahedral smectite. Analyses identified as serpentine have little Al and approximate, and average to, atomic (Fe+Mg+Mn)/(Si+Al) = 1.5. Individual analyses have this ratio significantly larger or smaller than 1.5.

Many analyses contain excess Ca, Na, K, S, P, and Cl, suggesting admixture of other phases. For a few analyses, the admixed phases can be tentatively identified as K-sulfate (jarosite?), Ca-sulfate [2], or KCl; other analysis contain equimolar K and Na, suggesting admixture of a stoichiometric mixed-alkali phase.

Textural relations suggest that the olivine altered in three stages: serpentine first; then smectites; and then hematite + ferrihydrite. Serpentine is found adjacent to olivine and as isolated patches in the iddingsite; it was probably the earliest alteration, as it normally forms at higher temperature and lower redox state than iddingsite. Two assemblages occur in the iddingsite. The smectites occur intermixed in patches and veins (down to 100 nm width) cutting olivine and possibly serpentine, as larger patches, and as coatings on mineral fragments [2]. The smectites are cross-cut by patches and veinlets, down to 40 nm width, of intergrown ferrihydrite and hematite (average grainsize 20 nm). Areas of pure ferrihydrite are present, but their paragenetic position is unknown.

This iddingsite in Nakhla is nearly identical to some formed on Earth [6], suggesting similar conditions of formation on the SNC parent planet. To permit formation of iddingsite, Nakhla must have been penetrated by oxidizing water at temperatures of weathering or of deuteric alteration, 50-150°C [4].

Assistance from K. Thomas, R. Barrett and L. Keller is gratefully acknowledged.

[1] Bunch and Reid (1970) Meteoritics 10, 303. [2] Gooding et al. (1991) Meteoritics 26, in press. [3] Deer et al. (1966) Intro. to Rock-Forming Minerals; Longman Gp. [4] Delvigne et al. (1979) Pedologie XXIX, 247. [5] Ashworth and Hutchinson (1975) Nature 256, 714. [6] Banfield et al. (1990) Contrib. Min. Petrol. 106, 110.

A NEW XE COMPONENT IN DIAMOND-RICH ACID RESIDUES FROM EFREMOVKA CV3 CARBONACEOUS CHONDRITE. A. Verchovsky, U. Ott, Max-Planck-Institut für Chemie, Saarstr. 23, D-6500 Mainz, F.R.G.

Preliminary analysis of the noble gas data obtained for a diamond-rich separate from Efremovka CV3 meteorite allowed us to argue that there are four isotopically distinct components in the residue: cosmogenic, common solar system (planetary) and two presolar ones: Xe-HL and Xe-S [1].

Now we report data for three more separates prepared from two different bulk specimens (23 g and 59 g) using similar chemical procedures as have been used for the previous samples except for the final stage of separation. In the case of the largest sample instead of a combination of three acids (H_3PO_4, H_2SO_4 and $HClO_4$) only $HClO_4$ was used. This sample was also separated into several grain size fractions. All samples were analysed by a combination of stepwise pyrolysis and combustion for all noble gases, two samples were, in addition, analysed for nitrogen isotopic composition.

In Xe three-isotope diagrams high-temperature fractions for all samples form correlation lines which can be regarded as mixing lines between Xe-HL and a component which in turn could be a mixture of Xe-S and a kind of Xe close to, but distinctly different from, planetary or solar Xe.

Moreover, analogous data for Allende [2] and Inman [3] form similar correlations which suggests this new component to be present in different meteorites (Figs. 1 and 2). The most important question arising in this connection is whether or not this Xe is indeed a mixture of two (or more) components and, if so, where the mixing took place: during the experiment as a result of the simultaneous release of several components from their respective host phases [3] or in an environment before trapping of the Xe mixture by its host phase.

If Xe-S were present in the released gases there are arguments against it being sited in SiC: (1) while its signature is observed only in high-temperature fractions of the combustion experiments, most of the new low-$^{136}Xe/^{130}Xe$ component is released between 500 and 600 ^{o}C which is lower than what is known for the combustion of SiC [4],
(2) nitrogen isotopic data show no sign of the presence of SiC in the Efremovka samples [S.S. Russell, private communication],
(3) the calculated amounts of the apparent Xe-S in Efremovka, Allende and Inman residues are similar ($2x10^{-10}$ - $5x10^{-10}$ cc/g) though only Inman is known to contain a noticeable amount of SiC [5].

The isotopic composition of carbon which we plan to measure in the Efremovka residues may give additional arguments concerning the possible presence of SiC in the samples.

Acknowledgement: We thank C.T. Pillinger and S.S. Russell for the nitrogen isotope analysis.

References: 1. A.B.Verchovsky et al. (1991), LPSC XXII, 1439-1440; 2. R.S. Lewis and E. Anders (1988), LPSC XIX, 679-680; 3. R.H. Nichols Jr. et al. (1991); GCA submitted, 4. E. Anders (1988), in: Meteorites and the early solar system. Univ. Arizona Press, 927-955; 5. C. M. O'D. Alexander et al. (1990), EPSL 99, 220-229

High-temperature fractions for Efremovka-•, Allende-□, Inman-Δ

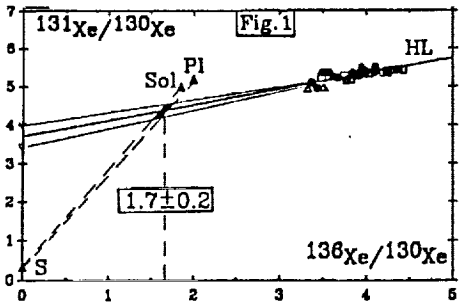

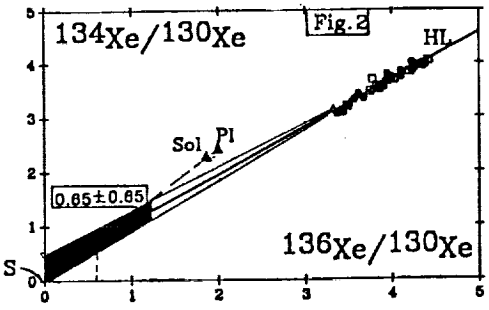

Water Depletion in Tektites. A. M. Vickery[1] and Lauren Browning[2]. [1]Lunar and Planetary Laboratory, [2] Department of Geological Sciences, both at The University of Arizona, Tucson, Az 85721 USA

The scientific consensus is that tektites were formed as the result of terrestrial impacts, largely because their overall compositions most closely resemble those of terrestrial sediments (Taylor, 1973). O'Keefe (1976), however, argues against a terrestrial impact origin, in part because of the very low water content of tektites. A recent semi-analytic model for droplet formation in impact-generated ejecta plumes (Melosh and Vickery, 1991) predicts droplet sizes that are of the same order of magnitude as observed tektite sizes. In this study, we couple the cooling history calculated from a 1D hydrocode (Vickery, 1986) and droplet sizes predicted by the Melosh-Vickery model with estimates of the diffusion coefficients at the relevant temperatures to estimate the relative depletion of water in the droplets. It is assummed that at high temperatures, water dissociates into H_2 plus O_2 or into H^+ and O^{-2}, so that hydrogen diffusion is the rate-controlling process. Two sets of calculations were done: in the first, data on the diffusion of H_2 through fused silica (Lee, 1963) are extrapolated to high temperatures, and in the the second, diffusion coefficients are estimated using the Lorentz model for the diffusion of a light species through a much heavier one (Lifshitz and Pitaevskii, 1981). The relative depletions as a function of radius within a sphere and of time are calculated with an explicit algorithm (Crank, 1975). The cooling history used is that for the outermost (fastest cooling) portion of the impact plume generated by the impact of a 10-km diameter projectile at 20 km/sec, for which the estimated droplet size is ~ 600 μm. The diffusion calculations are carried out from the highest temperatures (~34,000 °K) to approximately the melting temperature, for a total time of just over 100 sec. Both sets of diffusion coefficients gave consistent results; the final, volume-averaged concentration of hydrogen (and therefore by assumption, water) is of order 10^{-6} times the initial concentration -- more than sufficient to account for the observed depletions in tektites. Furthermore, the concentration gradients within the sphere are extremly low, so that the concentration is essentially uniform. We plan further calculations of the relative depletions in the larger droplets expected in the more slowly cooling interior portions of the plume, as well as using the results of impact calculations for smaller projectiles, for a more complete analysis. Based on the current results, however, we tentatively conclude that there is no inconsistency between the water depletions observed in tektites and the hypothesis that tektites are formed in terrestrial impacts.

The diffusivity of an ion varies, to first order, inversely with with its radius. If the depletion of other species depends on their diffusivity more strongly than on their volatility, then smaller ions in tektites should be more depleted relative to their concentrations in the presumptive source material. This is precisely what is observed for a wide variety of elements when their concentrations in moldavites are compared to those in the Middle Miocene sands, which formed a thin veneer at the surface in the Ries area at the time the Ries Crater was formed (von Engelhardt, *et al.*, 1987).

References:

Crank, J. (1975) *The Mathematics of Diffusion*, Clarendon Press, Oxford.
von Engelhardt, W. *et al.* (1975) *Geochim. Cosmochim. Acta* **51**, 1425 - 1443.
Lee, R. W. (1963) *J. Chem. Phys.* **38**, 448-455.
Lifshitz, E. M. and Pitaevskii, L. P. (1981) *Physical Kinetics*, Pergamon, New York.
Melosh, H. J. and Vickery, A. M. (1991) *Nature*, in press.
O'Keefe, J. A. (1976) *Tektites and Their Origin*, Elsevier, New York.
Taylor, S. R. (1973) *Earth Sci. Rev.* **9**, 101 - 123.
Vickery, A. M. (1986) *J. Geophys. Res.* **91**, 14139 - 14160.

COSMOGENIC NUCLIDES IN SHORT-LIVED METEORITES: Vogt S., Albrecht A., Herzog G.F.[1], Klein J., Fink D., Middleton R.[2], Weber H. and Schultz L.[3] 1) Dept. Chemistry, Rutgers Univ., New Brunswick, NJ 08903; 2) Dept. Physics, Univ. Penn., Philadelphia, PA 19104; 3) Max-Planck-Inst. für Chemie, D6500 Mainz, Fed. Rep. Germany.

A ^{21}Ne production rate, P_{21} (10^{-8} cm^3 STP/g-Ma), in meteorites is given by the expression ^{21}Ne/t where ^{21}Ne is the concentration of ^{21}Ne in a sample and t the exposure age. Exposure ages inferred from ^{10}Be and ^{53}Mn measurements give P_{21}(H-chondrite) of about 0.31 compared to values greater than 0.40 from ^{26}Al measurements [1]. To test proposed explanations for the difference we have examined more closely the irradiation histories of seven ordinary chondrites with ^{21}Ne contents less than 0.8×10^{-8} cm^3 STP/g (Table 1). Cosmogenic radionuclides were measured by accelerator mass spectrometry at the University of Pennsylvania; noble gases were measured by static mass spectrometry at the Max-Planck Inst. für Chemie.

The ^{41}Ca contents of the metal phases in five chondrites are normal [2] and indicate exposures of ~0.3 Ma or more. The ^{41}Ca contents of the silicate phases are comparable to values measured by us in small meteorites and near-surface samples from larger ones. In a well-behaved meteorite, exposure ages based on ^{26}Al, ^{10}Be, and ^{21}Ne would agree. Table 1 shows ages based on conventional H-chondrite production rates (P_{21}=0.31 [1], P_{10}=20 and P_{26}=56 dpm/kg, and P_{53}=434 dpm/kg Fe[3]); the application of shielding corrections would change the ages but not the conclusions that follow. In two cases, ***Cullison*** and possibly ***Ladder Creek***, the high values of P_{21} implied by the low ^{26}Al and ^{10}Be ages could reflect either 1) errors in the ^{21}Ne concentrations adopted, 2) the inappropriate pairing of data from different specimens, 3) uncorrected shielding effects (the ^{22}Ne/^{21}Ne ratios are low), or 4) the effects of prior irradiations; new noble gas analyses will help us check the possibilities. ***Guenie and Shaw*** appear to have had complex exposure histories and warrant further study. The large size of ***Tsarev*** (>1 tonne found; minimum radius ~ 40 cm) is suggested by the variations in its activities (Table 1; [4,5]). We note that the discrepancies between the various ages may also require a two-stage irradiation like Bur Gheluai's [6]. Three of the seven meteorites studied (***Ladder Creek, Sena and Timochin***) might be described as well-behaved.

Table 1. Cosmogenic nuclides in short-lived meteorites.

Meteorite	^{26}Al	^{10}Be	^{21}Ne	^{22}Ne/^{21}Ne	^{41}Ca (met)	^{41}Ca (sil)	t_{26}	t_{10}	t_{53}[1]	t_{21}
Cullison (H4)	39	8.6	0.55	1.04[2]	23.2	170	1.2	1.1		1.8
Guenie (H4)	22	5.4	0.67	1.07[2]			0.5	0.6		2.2
Ladder Cr. (L6)	38	7.1	0.3-0.4	1.07-1.17[2]	21.1	235	1.0	0.8	1.1	1.0-1.3
Sena (H4)	30	7.0	0.33	1.14	21.0	150	0.8	0.9	1.1	1.0
Shaw (L6)	15	2.6	0.28	1.11	19.9	120	0.3	0.3	0.5	0.85
Timochin (H5)	19	4.0	0.11	1.16	20.2	145	0.4	0.4		0.35
Tsarev (L5)	14	3.7					0.3	0.4	0.6-	
	20	6.1	0.71	1.09			0.4	0.7	1.0	2.1

Notes: Units - ^{26}Al & ^{10}Be (dpm/kg); ^{21}Ne [10^{-8} cm^3 STP/g]; ^{41}Ca(met) [dpm/kg Fe]; ^{41}Ca(sil) [dpm/kg Ca]; t [Ma]. 1) ^{53}Mn from [5]. 2) Gas data from [7].

References: **1)** Eugster O. (1988) *Geochim. Cosmochim. Acta 52*, 1649-1659. **2)** Fink D. et al. (1989) *Meteoritics 24*, 266. **3)** Vogt S. et al. (1990) *Rev. Geophys. 28*, 253-275. **4)** Nagai H. et al. (1990) *LPI Tech. Rep. 90-05*, Lunar Planet. Inst., Houston, 91-95. **5)** Nishiizumi K. (1987) *Nucl. Tracks Radiat. Meas. 13*, 209-273. **6)** Wieler R. et al. (1990) *Lunar Planet. Sci. XXI*, 1335-1336. **7)** Schultz L. and Kruse H. (1989) *Meteoritics 24*, 155-172.

^{41}Ca and ^{36}Cl DEPTH PROFILES IN THE IRON METEORITE GRANT

S.Vogt[1], D.Fink[2], J.Klein[2], G.Korschinek[3], R.Middleton[2] and G.F.Herzog[1]; 1. Dept. of Chemistry, Rutgers University, New Brunswick, NJ 08903; 2. Dept. of Physics, University of Pennsylvania, Philadelphia, PA 19104; 3. Dept. of Physics, TU München, 8046 Garching, Germany.

For systematic investigations of cosmogenic nuclide production rate patterns, iron meteorites offer two basic advantages over stony meteorites: fewer target elements and higher resistance to secondary break-up. On the debit side, as irons are often larger than stones, a knowledge of the depth dependent production of various cosmogenic nuclides is even more fundamental than for such studies on stony meteorites. The cosmogenic radionuclides ^{41}Ca ($T_{1/2}$=0.1Ma) and ^{36}Cl ($T_{1/2}$=0.3Ma) are two nuclides that have been steadily gaining importance in reconstructing exposure histories of meteorites [1,2]. We report the ^{41}Ca contents of seven samples in the main slab of the iron meteorite Grant (Zürich samples); two additional samples (USNM "surface" and "center") have been analyzed for their ^{41}Ca and ^{36}Cl concentrations. The Zürich samples are from positions adjacent to those reported in [3]; ^{36}Cl measurements for these samples are in progress.

The ^{41}Ca activities show a slight decrease from the surface towards the center (17.8±1.1 dpm/kg down to 14.8±1.0 dpm/kg, Figure 1.), reflected in the weak anticorrelation with the shielding indicator ^{4}He/^{21}Ne [4]. The small variation of the ^{41}Ca activities with depth clearly illustrates the significance of contributions from secondary particles as well as other potential reaction modes. The role of secondary particles is even more pronounced when considering the depth profiles of the lighter product nuclei ^{26}Al, ^{21}Ne, ^{10}Be, and ^{4}He [3]. The attenuation of the ^{4}He, ^{41}Ca, and ^{26}Al production parallel each other and their concentrations exhibit only a weak depth dependence; ^{21}Ne and ^{10}Be concentrations show a strong variation with depth by the same relative amount. Absolute activities of the radionuclides change as anticipated on account of the mass differences between target and product nuclei (ΔA value). The systematics of the experimental data in the Grant meteorite (preatmospheric radius R≈40 cm [3]) give no evidence that the conventional classification into typical "high- and low-energy products" is useful for small and medium sized iron meteorites.

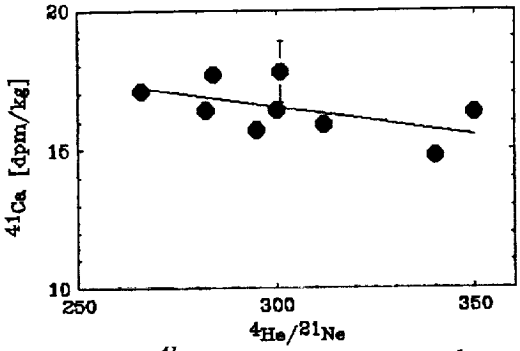

Figure 1: ^{41}Ca contents versus the shielding indicator ^{4}He/^{21}Ne.

The ^{36}Cl results of the two USNM samples (17.2±1.5 dpm/kg and 15.2±1.3 dpm/kg, respectively) suggest an equal attenuation of ^{36}Cl and ^{41}Ca production in Grant. The analyses of ^{41}Ca and ^{36}Cl in small iron meteorite falls corroborate the resemblance of their attenuation and also point towards very similar equilibrium concentrations for these two radionuclides [2]. If the ^{36}Cl analyses of the Zürich samples confirm the shielding independence of the ^{41}Ca/^{36}Cl ratio, then the simultaneous determination of these two radionuclides will be an excellent aid for several applications, for instance, improved determinations of terrestrial ages for meteorites found in Antarctica (see also [5]). In order to apply the ^{41}Ca/^{36}Cl method, the corresponding production rate ratio has to be known. At present, as the two nuclides have not been measured in true aliquots of a larger set of samples from meteorites with varying sizes, we adopt the respective average production rates of P_{41}=23.8±0.9 dpm/kg [2] and P_{36}=22.8±3.1 dpm/kg [6]. We infer from the ^{41}Ca/^{36}Cl ratios in Grant a terrestrial age of $T_{ter.} \leq 0.05$ Ma, in agreement with an age of 0.043±0.015 Ma [2].

Samples of the iron meteorite Grant were graciously provided by P. Signer (ETH-Zürich).

References: **[1]** Vogt et al. (1991), *Geochim. Cosmochim. Acta*, in press; **[2]** Fink et al. (1991), *Earth Planet. Sci. Lett.*, submitted; **[3]** Graf et al. (1987), *Nucl. Instr. Meth.* B29, 262-265; **[4]** Voshage and Feldmann (1979), *Earth Planet. Sci. Lett.*, 45, 293-308; **[5]** Nishiizumi (1986), *LPI Tech. Rep.* 86-01, 71-73; **[6]** Nishiizumi et al. (1989), *Earth Planet. Sci. Lett.*, 93, 299-313.

Cosmogenic ^{26}Al Activities in Antarctic and Non-Antarctic Meteorites

John F. Wacker
Battelle, Pacific Northwest Laboratories
P.O. Box 999, Mailstop P7-07
Richland, WA 99352

We have measured the activity of ^{26}Al ($t_{1/2}$ = 705,000 years; Norris *et al.*, 1983) in over 600 Antarctic meteorites as part of an on-going program to characterize the U.S. Antarctic meteorite collection. ^{26}Al assay is well suited for survey work since bulk meteorite specimens are analyzed rapidly and non-destructively using multi-parameter gamma-ray spectrometry. The ^{26}Al data have been used to search for pairs, to identify specimens with either very low activities (*e.g.*, due to long terrestrial residence times or short exposure ages) or usually high activities (by unusual cosmic ray exposure histories, *e.g.*, SCR exposure), and to estimate terrestrial ages.

Data on specimen pairing mostly confirms previously identified pairings (Score and Lindstrom, 1990), however, the ^{26}Al results contradict some pairing groups. New pairings have been tentatively identified using the ^{26}Al data, including a group of L6s recovered from the Elephant Moraine region. Specimens with high or low activities (*i.e.*, above 70 dpm/kg or below 30 dpm/kg) number about 20. Some of the high activity specimens (*e.g.*, ALHA 83101) have a probable SCR component. These specimens should be analyzed for other radionuclides and noble gases. Generally, the terrestrial ages calculated from the ^{26}Al data agree with those from ^{36}Cl (Nishiizumi *et al.*, 1989). The average terrestrial age of Antarctic chondrites based on our ^{26}Al data is ~200 kyr, but the ^{26}Al distribution has more structure than the average age implies. L chondrites display a bimodal ^{26}Al distribution, with one peak at ~40 dpm/kg, corresponding to an average terrestrial age of ~350 kyr and containing contributions from all L chondrite subclasses, with the other peak at ~55 dpm/kg, containing mainly L6s. The second peak has specimens with relatively high ^{26}Al activities but long terrestrial ages (Nishiizumi *et al.*, 1989), suggesting that these specimens may belong to a single shower whose parent meteoroid underwent an unusual exposure history. The data for Hs shows only one peak at centered at 50-55 dpm/kg. Surprisingly, when compared to non-Antarctic Hs (data from Nishiizumi, 1987), the two ^{26}Al distributions are nearly identical, as also seen by Alexeev (1991), indicating that most of the Hs recovered from the Antarctic fell within the last ~50,000 years. Thus, interpretations based on the ^{26}Al results do not point to preterrestrial origins for the differences between Antarctic and non-Antarctic Hs, in agreement with Cassidy and Harvey (1991), Wetherill (1986), Huss (1991), Schultz *et al.* (1991) and others, and contradicting suggestions by Dennison *et al.* (1986), Dennison and Lipschutz (1987), Lipshutz and Samuels (1991) and others.

REFERENCES

Alexeev, V.A. (1991) *LPSC* **XXII**, 7-8.
Cassidy W.A. and Harvey R.P. (1991) *Geochim. Cosmochim. Acta* **55**, 99-104.
Dennison J.E., Lingner D.W. and Lipschutz M.E. (1986) *Nature* **319**, 390-393.
Dennison J.E. and Lipschutz M.E. (1987) *Geochim. Cosmochim. Acta* **51**, 741-754.
Huss G.R. (1991) *Geochim. Cosmochim. Acta* **55**, 105-112.
Lipschutz M.E. and Samuels S.M. (1991) *Geochim. Cosmochim. Acta* **55**, 19-34.
Nishiizumi K. (1987) *Nucl. Tracks Radiat. Meas.* **13**, 209-273.
Nishiizumi K., Elmore D. and Kubik P.W. (1989) *Earth Planet. Sci. Lett.* **93**, 299-313.
Norris T.L *et al.* (1983) Proc. 14th Lunar Planet. Sci. Conf., J. Geophys. Res., **88B**, 331-333.
Schultz L., Weber H.W., and Begemann F. (1991) *Geochim. Cosmochim. Acta* **55**, 59-66.
Score R. and Lindstrom M.M. (1990) *Antarct. Meteor. Newslett.* **13**, no. 1.
Wetherill G.W. (1986) Nature **319**, 357-358.

TRACE ELEMENT DISTRIBUTIONS IN MINERALS OF EETA79001: CLUES TO THE PETROGENESIS OF A UNIQUE SHERGOTTITE.
Meenakshi Wadhwa[1], Harry Y. McSween, Jr.[2], and Ghislaine Crozaz[1]. [1]Dept. of Earth and Planetary Sciences and McDonnell Center for Space Sciences, Washington Univ., St. Louis, MO 63130; [2]Dept. of Geological Sciences, Univ. of Tennessee, Knoxville, TN 37996.

The shergottite EETA79001 is the only achondrite of its kind since it consists of two distinct igneous lithologies joined along a planar, non-brecciated contact [1]. Both are basaltic in composition, with pigeonite, augite and plagioclase comprising their main modal mineralogy. However, lithology A is fine grained and contains zoned megacrysts of olivine, orthopyroxene and chromite, whereas lithology B is coarser grained and non-porphyritic. It has been previously suggested that the layering in EETA79001 could have resulted from successive pulses of magma [1]. Trace elements (especially REE) have proven to be of great help in trying to determine the petrogenesis of various rock types. Therefore, by characterizing REE and selected trace elements in individual mineral phases, this study attempts to determine the petrogenetic relationship and crystallization histories of the two lithologies in EETA79001.

Ion microprobe analyses were made on thin sections; REE and selected trace element concentrations were measured in individual grains of various mineral phases occurring in both lithologies. In lithology A, grains of cpx, plagioclase (shock altered to maskelynite), olivine and whitlockite were analysed. In lithology B, grains of cpx, maskelynite, whitlockite and mesostasis were studied.

The mineral with the highest REE concentrations in both lithologies is whitlockite. Although whitlockite grains in B are larger and more abundant than in A, their REE concentrations are the same in both lithologies (and, as in other shergottites, whitlockites account for the bulk of the REE). Maskelynites in A and B also have similar REE abundances. Clinopyroxenes in both lithologies are extremely zoned. Although their core compositions are similar, the cpx in B are larger and more extensively zoned than in A [1]. Cpx grains in both lithologies show a range of REE abundances. One of the cpx grains analysed in lithology B has a negative Ce anomaly, indicative of weathering in the Antarctic ice [2]. Variations of minor and trace components in cpx with Fe/Fe+Mg define distinct trends in A and B. Ti, Mn, Sc and Y concentrations smoothly increase with increasing Fe/Fe+Mg; the trends are similar for cpx having identical Fe/Mg in both lithologies. This is not so for Cr and V abundances, which decrease with increasing Fe/Fe+Mg, but which drop off more sharply for cpx in B than for cpx in A. This trend in B is controlled by magnetite which scavenges both Cr and V, and is found in significant amounts only in B. Na concentrations vary by a factor of three for cpx in both A and B, but with no apparent trend. As expected for a residual melt, the mesostasis is highly enriched in REE (La ~ 70X CI); its LREE pattern is similar in shape to that of the whole rock, but its HREE pattern slopes upwards in contrast to the whole rock pattern, which has a slightly negative slope. This is probably due to whitlockite cystallization prior to mesostasis solidification.

It is obvious from the igneous trends shown by the minor and trace elements in the cpx, that lithologies A and B are genetically related. Similar REE inventories of whitlockites and maskelynites in both A and B are also indicative of the same. The occurrence of megacrysts in lithology A suggests that fractionation and/or assimilation of the megacryst assemblage could be the process(es) relating the two lithologies[1]. The resulting liquids could have formed successive magma pulses that gave rise to the layering in EETA79001.

References: [1] McSween and Jarosewich (1983) Geochim. Cosmochim. Acta **47**, 1501-1513. [2] Lundberg *et al.* (1990) Geochim. Cosmochim. Acta **54**, 2535-2547.

IMAGING C_{60} BUCKY BALLS - ARE THEY REALLY ROUND, FIRM, AND CLOSELY PACKED?

Su Wang[1], Peiling Cheng [2], and Peter R. Buseck[1,2]. Departments of Geology[1] and Chemistry[2], Arizona State University, Tempe, AZ., 85287-1404.

C_{60} molecules (also called buckminsterfullerene and bucky balls) have been topics of considerable interest and controversy at recent meteorite meetings [1]. They consist of 5- and 6-membered aromatic rings that curl to form spherical molecules with 60 nodes, much like soccer balls. While no evidence has been presented that they occur in meteorites, they do seem likely candidates for interstellar space [2].

Since the time they were reported in 1985 [3], we have been trying to image individual bucky balls using high-resolution transmission electron microscopy. However, they were not sufficiently concentrated within the associated soot until a method was developed to produce sufficient quantities to grow crystals [4]. The method has generated intense interest because C_{60} and its closed-cage structural relatives, the "fullerenes," are a new class of carbons with unexpected chemical and physical characteristics and potentially great industrial applications.

We recently succeeded in imaging a variety of fullerenes. Samples were prepared by standard methods including, in sequence, spark-source generation of soot, solvent extraction of fullerenes, HPLC separation of fullerenes into distinct mass fractions, and growth of small crystals by sublimation. The results show extensive regions of close-packed arrays of C_{60} clusters. Computer-simulated images match the experimental ones, confirming our interpretations.

Surprisingly, within the crystals dominated by C_{60} molecules, we have found domains containing fullerenes that are significantly larger and others that are smaller than C_{60}. Fullerenes having a range of dimensions have been predicted theoretically [5], and a recent study described the properties of various species [6]. The larger molecules have the projected shapes of elongated ellipsoids that we estimate to contain more than 100 carbon atoms. It remains to be seen whether similar molecules will be found in the natural environment, either in interstellar space or in unusual meteorites.

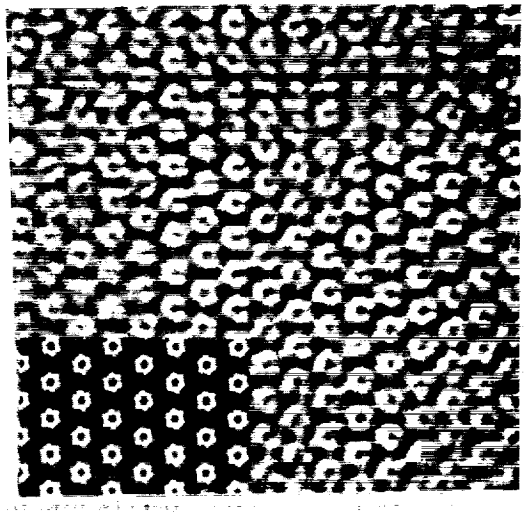

References: [1] Heymann, D. LPSC *XXII* 569-570 (1991); de Vries, M.S. et al. LPSC *XXII* 315-316 (1991); Gilmour, I. et al. LPSC *XXII* 445-446 (1991); [2] Kroto, H.W. (1988) *Science* **242**, 1139-1145; [3] Kroto, H.W. et al. *Nature* **318**, 162-163 (1985); [4] Krätschmer, W. et al. *Nature* **347**, 354 (1990); [5] Kroto, H.W. *Science* **242**, 1139-1145 (1988); Schmalz, T.G. et al. *J. Am. Chem. Soc.* **110**, 1113-1127 (1988); [6] Diederich, F. et al. *Science* **252**, 548-551 (1991).

POSSIBLE INHERITANCE OF SILICATE DIFFERENTIATION DURING LUNAR ORIGIN BY GIANT IMPACT

Paul H. Warren
Institute of Geophysics and Planetary Physics, University of Californa, Los Angeles, CA 90024-1567

The giant impact model of lunar origin is appealing for several reasons. It explains the high angular momentum of the Earth-Moon system, and the strong depletion in FeNi in the Moon. As originally conceived, the model also predicted enrichments of refractory elements (Al, Th, etc.) in the Moon. However, it remains unclear whether refractory/major element (or even major/volatile) fractionation would likely occur during condensation and agglomeration after the impact [1]. Except for extremely volatile elements and siderophile elements (assumed lost with the core), most current discussions of the impact model assume that the component of the Moon derived from the impactor represents undifferentiated impactor silicates. However, a close look at the proposed mechanisms for derivation of the Moon by giant impact reveals that even with no volatile/refractory fractionation, important fractionations of *lithophile* elements could under some scenarios be inherited directly from the impactor.

According to both the jetting model [2] and the hydrodynamic variants formulated by Cameron and coworkers, the material that ultimately forms the Moon is derived preferentially from the periphery of the impactor, along with a smaller component (10-20%? [3]) of material from the protoearth. In the model of [2], roughly 58% of the jetted impactor material comes from depths of <0.1 R_i, where R_i is the impactor radius; only ~19% comes from depths >0.2 R_i, ~8% comes from depths >0.3 R_i, ~2% comes from depths >0.4 R_i. Analogous figures for the models of Benz et al. [3] are not available, but a videotape of their model suggests a similar distribution. The thermal state of the impactor prior to its encounter with the protoearth is uncertain. Cameron [personal comm., 1991] assumes that it would be so hot due to prior major impacts that its noncore portion would be completely molten, and thus, undifferentiated. The giant impact model is predictated on a scenario of planetary accretion (a mass spectrum of planetesimals) that requires major impacts to be frequent events. Even so, only a few impacts capable of fully melting the Mars-sized impactor could have occurred during its entire history. Unless the body was melted shortly before its encounter with the protoearth, it would have partly solidified in the meantime. Until a "chill" crust develops over most of the surface, it cools radiatively at a rate that requires only a few decades to reach the onset of solidification. The chill crust would thereafter greatly retard cooling, but because silicate-melting dT/dP is much greater than silicate-adiabat dT/dP, crystallization would mainly proceed from the base of the mantle outwards, and half of the mantle could have solidified in a period as short as 10^4 years [4,5]. In the unlikely event that time allowed the melt composition to evolve to (or near to) the point of feldspar saturation, a far thicker, intrinsically buoyant crust could have formed, but this process would be self-slowing, because the added insulation would diminish the rate of cooling.

If even 10-20 wt% of the impactor's deepest mantle was crystalline prior to the encounter with the Earth, some important lithophile fractionations could have been tranferred to the Moon. Calculations incorporating P effects on phase equilibria (for a body with mass = 1.4 x that of Mars) à la Warren [6] suggest that the first few tens of wt% crystallized (assuming an Earth-mantle-like initial composition) would be about half majorite garnet and half medium-Ca pyroxene. After 20% crystallization, the melt Ca/Al ratio is nearly doubled due to the strong affinity of Al for garnet. Transition elements such as Cr, V, and Sc are markedly depeleted. The LREE/HREE and Hf/Lu ratios may be significantly increased (cf. [7]). Some of these effects are contrary to inferred features of the actual lunar bulk composition, which has earthlike Cr, V, etc. [7], a chondritic or enriched level of Al, and a low (subchondritic?) Ca/Al ratio.

References: [1] Stevenson D. J. (1987) *Ann. Rev. EPS* **15**, 271-315. [2] Melosh H. J. and Sonett C. P. (1986) In *Origin of the Moon*. [3] Benz W. et al. (1989) *Icarus* **81**, 113-131. [4] Jeffreys H. (1959) *The Earth*. [5] Ringwood A. E. (1989) *EPSL* **95**, 208-214. [6] Warren P. H. (1989) *Tectonophysics* **161**, 165-199. [7] Ringwood A. E. (1990) In *Origin of the Earth*.

QINGZHEN CHUNKS: NEBULAR COMPONENTS AT THE FORMATION LOCATION OF THE EH CHONDRITES. John T. Wasson, Gregory W. Kallemeyn, Lei Zhou and Alan E. Rubin, Institute of Geophysics and Planetary Physics, University of California, Los Angeles, CA 90024, USA.

We used neutron-activation and electron-microprobe techniques to study 44 small chunks separated from the EH3 Qingzhen chondrite; sizes were small enough to make it likely that the compositions of individual chunks might be dominated by a single nebular component. Certain sets of elements experienced coherent fractionations during the formation of chondrites in the solar nebula, an indication that they were in the same component, i.e., in phases that tended to be in the same kind of nebular particles; an example is the common siderophile component which accounts for the strong correlation of Fe, Ni and Co among all classes of chondrites. The components in the nebular location where the EH chondrites formed are of particular interest because conditions were extreme; the EH chondrites are by far the most reduced (record the lowest fO_2) and formed the greatest variety of sulfide minerals (record the highest fS_2/fO_2) among known nebular products. EH3 Qingzhen is one of the least equilibrated EH chondrites and is an observed fall. Grossman et al. (1985) used data on 35 elements in 15 Qingzhen chondrules to infer the existence of five EH nebular components: (1) siderophile; (2) oldhamite-rich; (3) olivine-refractory; (4) Na-REE and (5) Cl-Br. In order to expand the data base and give greater emphasis to components (e.g., sulfides, metal) that are poorly represented in chondrules, we crushed a small sample of Qingzhen and analyzed all particles in the size range 10-40 mg. An initial neutron irradiation provided data on 12 elements; on the basis of these data, 70% of the samples were found to have compositions similar to the bulk chondrite, and were not subjected to further study. The remaining samples were characterized petrographically and 23 elements were determined by a complete instrumental neutron activation analysis. Two samples (Q21 and Q38) deviate the most from the whole rock in composition. Q21 contained the highest concentrations of Ni, Zn, Ga, Eu, Os and Ir; Q38 contained the highest concentrations of K, Sc, Cr, Mn and Se and the lowest As. Both samples have been split into smaller chunks (Q21 into 6, Q38 into 4 pieces) in order to further isolate components. Preliminary results suggest that Q21 comprises a siderophile and a sulfide component whereas Q38 probably comprises two sulfide components. Data for the remaining samples were subjected to factor analysis; inverse modeling was also used to identify components. Three factors were resolved: (1) Fe-Co-Au-Ni-As-Ga; (2) Os-Ir; and (3) Mg-Al-Na-V. Petrographic study of the samples is in progress.

Reference: Grossman J. N., Rubin A. E., Rambaldi E. R., Rajan R. S. and Wasson J. T. (1985) Geochim. Cosmochim. Acta 49, 1781-1795.

NOBLE GASES IN EIGHT UNUSUAL CARBONACEOUS CHONDRITES;

Hartwig W. Weber and Ludolf Schultz, Max-Planck-Institut für Chemie, 6500 Mainz FRG

He, Ne and Ar have been measured in five Antarctic carbonaceous chondrites (Yamato 82162 and 86720; Belgica 7904; Allan Hills 88045 and 88052) and three recent finds from the Saharan desert. Results are given in the Table.

The first three of these meteorites have oxygen isotopic compositions similar to CI carbonaceous chondrites [1] but, at least for B7904, petrographical and mineralogical studies show similarities to CM chondrites (e.g.[2]). It was suggested, also from trace element investigations [3], that open-system thermal metamorphism at 600 to 700°C was responsible for these changes. The trapped 20-Ne of these meteorites varies by a factor of about 10. The 20-Ne content of Y82162 as well as the trapped 20-Ne/22-Ne are comparable to those of other CI chondrites (e.g. [4]); their thermal histories should be comparabel. However, both other meteorites (Y86720 and B7904) could have lost trapped gases during a time of elevated temperatures.

Acfer 097 and El Djouf 001 are two new finds that are petrographically similar to Renazzo and indistinguishable from each other (A.Bischoff, pers. com.). The find locations are 600 km apart, indicating separate falls. The noble gas record, however, is similar. Both meteorites have exposure ages of about 8 Ma. Their trapped components are almost identical. Thus, both meteorite could belong to the same fall. Acfer 182 is similar to the most primitive chondrite Allan Hills 85085. Both meteorites contain solar gases. The exposure age of Acfer 182 of about 16 Ma, however, is about ten times higher than that of ALH 85085 (1.7 Ma [5]). The last two ALH meteorites are classified chemically as CM but differ in their minerology [6]. These small chondrites are found at a distance of 1.8 km. Because their different exposure ages, they must be regarded as separate falls.

References: [1] R.N.Clayton & T.K.Mayeda (1989) Lunar Planet. Sci. XX, 169. [2] H.Kojima et al. (1984) Mem.Natl.Inst.Polar Res., Spec.Issue 35, 184. [3] R.L.Paul & M.E.Lipschutz (1989) Z.Naturforsch. 44a, 979. [4] D.C.Black (1972) Geochim.Cosmochim. Acta 36, 377. [5] O.Eugster & S.Niedermann (1990) Earth Planet. Sci. Lett. 101, 139. [6] F.Wlotzka et al. (1989) Meteoritics 24, 341.

	^{3}He	^{4}He	^{20}Ne	^{21}Ne	^{22}Ne	^{36}Ar	^{38}Ar	^{40}Ar	(T21)
Y82162	0.76	4825	21.0	0.114	2.44	89.8	17.2	129	0.2
Y86720	0.76	206	1.97	0.124	0.50	30.5	5.85	125	0.5
B7904	1.13	823	9.69	0.346	1.60	48.3	9.3	171	1.4
Acfer097	29.6	66900	255	2.54	23.2	163	31.45	785	8.7
El Djouf001	27.4	62600	211	2.30	19.4	164	31.83	547	8.1
Acfer182	26.6	20900	40.4	3.54	7.2	27.4	5.92	674	16
ALH88045	0.6	3340	11.59	0.066	1.52	53.58	10.23	1170	0.1
ALH88052	1.86	4450	15.84	0.488	2.56	76.26	14.55	256	2.0

(Concentrations in $10^{-8}cm^{3}g^{-1}$; T(21) = exposure age in Ma)

Metal-forsterite equilibration in Allende. S. Weinbruch,[1,2] H. Palme[1] and A. El Goresy.[2] [1] Max-Planck-Institut für Chemie, Saarstr. 23, D-6500 Mainz, FRG. [2] Max-Planck-Institut für Kernphysik, P.O. Box 103980, D-6900 Heidelberg, FRG.

Thin fayalite-rich rims and veins in Allende forsterite were formed by condensation of FeO on forsterite (1-4), while fayalite-rich halos around metal or magnetite inclusions in forsterite are the result of metal-forsterite equilibration (3,4). In this paper we present evidence that some large iron-rich single olivine grains (SOG) are also formed by equilibration with metal prior to accretion to the parent body.

Large (up to 1-2 mm diameter) iron-rich (17 -36 wt.% FeO) SOG are rare. Some of them show compositional zoning with higher FeO in the outer parts. NiO-contents lie around 0.07 - 0.09 wt.%. Some SOG are surrounded by fayalite-rich rims similar to those around forsterites. In some grains positive MnO/FeO-correlations are found excluding formation by equilibration with metal. In others such a correlation is not observed (constant MnO ≈ 0.2 wt.%; FeO 26 wt.% in the interior to 32 wt.% in the outer zone of the grain). The absence of a MnO/FeO-correlation indicates that these grains underwent equilibration with metal (similar to fayalite-rich halos). The Ni-content of the coexisting metal is calculated to lie between 18 mole % at 1300 K and 61 mole % at 700 K.

Chromite inclusions are common in iron-rich SOG. Using the olivine/spinel thermometer temperatures between 730 and 1000 K were obtained for 4 chromites in two different SOG. However, the same thermometer applied to chromite inclusions in fayalite-rich rims (4) yields much higher temperatures, 1300 - 1380 K. At this temperature equilibration time is limited to a few days, to preserve the steep compositional gradients at the fayalite-forsterite boundary. However, metal-silicate equilibration of large SOG requires several years at 1300 K and up to 5000 years at 700 - 800 K. The large difference between temperatures derived from the olivin/spinel thermometer for large iron-rich SOG and fayalite-rich rims excludes a common metamorphic history for all Allende olivine components. The 700-800 K chromite-olivine equilibration must have occurred before accretion of the Allende parent body otherwise chromite inclusions in fayalite rich rims would record lower temperatures. Within the present parent body temperatures cannot have exceeded 700 - 800 K. At that temperature the steep compositional FeO-profiles at the fayalite-forsterite boundary could not have been retained for more than half a year at 700 K (diffusion coefficients from (5)). In summary, large iron-rich SOG were formed by metal-forsterite equilibration (temperature ≥ 700 K) in an environment different from the present Allende parent body.

Ref.: (1) PECK J.A. & WOOD J.A. (1987), GCA 51, 1503-1510. (2) HUA X., ADAM J., PALME H. & EL GORESY A. (1988), GCA 52, 1389-1408. (3) WEINBRUCH S., PALME H., MÜLLER W.F. & EL GORESY A. (1990), Meteoritics 25, 115-125. (4) WEINBRUCH S. (1990), Dissertation, Darmstadt. (5) BUENING D.K. & BUSECK P.R. (1973), J. Geophys. Res. 78, 6852-6862.

EL DJOUF 89001: A NEW CR2 CHONDRITE. M.K. Weisberg and M. Prinz, Amer. Mus. Nat. Hist., NY, NY 10024.

Introduction. El Djouf 89001 (ED89) is a recent find from Algeria. It has been classified as a CR chondrite and is paired with 8 Acfer meteorites, one of which (Acfer 89097) has been analyzed for oxygen isotopes [1]. A general petrologic study of ED89 was carried out in order to compare it to the other six CR chondrites described in Weisberg et al. [2]

Results. Unfortunately, ED89 is highly weathered having terrestrial limonite- and Ca-carbonate- filled fractures running throughout the entire sample. Much of the matrix is destroyed by terrestrial weathering as is much of the FeNi metal in the matrix and rimming chondrules. However, some matrix-like material does survive as dark inclusions (DI) and metal in the interiors of many chondrules is fresh, as is some of the metal rimming chondrules.

ED89 contains chondrules of different textural types (porphyritic, granular, barred, etc.), mineral and lithic fragments, refractory-rich inclusions, DI and matrix. Chondrules range from 0.09 to 6mm in maximum dimension. The larger chondrules are multilayered consisting of alternating, concentric layers of Ol and/or Pyx and FeNi metal surrounding a core which generally contains coarser grained Ol and/or Pyx and FeNi metal. Some chondrules have an outer layer of fine grained, clastic, matrix-like material that accreted onto it prior to chondrite aggregation. Similar large (3-4mm) multilayered chondrules occur in the other CR2 chondrites, but ED89 is endowed with some exceptionally large ones (>4mm). The smaller chondrules in ED89 are considered microchondrules ($\leq$100μm) in relation to the larger, mm-sized ones. The microchondrules occur throughout the matrix and, especially in DI, and this is also the case in other CRs [2]. Microchondrules were also found in an accretionary rim on a large chondrule in ED89. Compositionally, most of the chondrules are type I (olivine=$Fa_{0.5-5}$, pyroxene=Fs_{1-5}) and olivine has up to 1.0 wt.% Cr_2O_3 and 0.3% CaO as is typical of type I olivine in other CR chondrites. Dark Inclusions make up only ~1 vol.% of the thin sections studied making ED89 more similar to some of the Antarctic CR2 chondrites in this regard. Matrix abundance of ED89 is difficult to determine because of the terrestrial weathering. Matrix (+ DI) abundances in CR2 chondrites range from ~30-70% and, based on the high concentration of chondrules, ED89 is estimated to be at the lower end of the range. Phyllosilicates in ED89 occur on the rims of some chondrules and as isolated fragments. Compositionally they are serpentine-rich having (in wt.%) ~33 SiO_2, 2-3 Al_2O_3, 0.5 Cr_2O_3, 18-30 FeO, 0.2 MnO, 15-23MgO, 2.5 CaO, 0.2 Na_2O, 0.2 K_2O, and 15 H_2O (by difference). Chondrule cores are anhydrous and contain unaltered glassy mesostasis, in contrast with other CR chondrites, especially Renazzo and Al Rais, in which the mesostasis of some chondrules has been altered to a chlorite-rich or serpentine-rich material [3]. Thus, ED89 experienced a lesser degree of parent body aqueous alteration than the other CR chondrites. However, this is not unusual, since aqueous alteration varies among all the members of the CR group; e.g., MAC87320 and EET87770 are less altered than Renazzo and Al Rais. FeNi metal is compositionally within the range of other CR chondrites having 3.4-25 Ni, 0.1-0.5 Co, 0.14- 0.8 Cr, and 0.1-0.4 P; Ni and Co are higher in the metal in chondrule cores than the metal in rims, as is the case in other CR2s. Ni vs. Co forms a positive trend line which overlaps with metal from other CRs. Refractory-rich inclusions that have been found, thus far, include a large layered (>2mm long) fluffy type A (FTA) and a 300μm compact type A (CTA). Oxygen isotopic composition of the Acfer 097 sample [1] plots near the Antarctic CR chondrites [2,5], but has a lower $\Delta^{17}O$ value (Fig.1). The positions of the CR chondrites on the CR mixing line appears to be related to their degree of hydration and abundance of matrix (+DI) component.

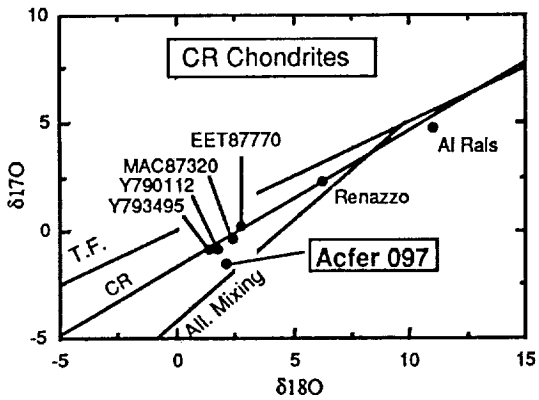

Fig. 1. Oxygen isotopic compositions of CR2 chondrites.

Conclusions. (1) ED89 has many of the petrologic characteristics found in the other CR2 chondrites, making this the seventh member of the group. (2) The presence of microchondrules in an accretionary rim on a chondrule suggests a possible relationship between the accretionary rims, microchondrule-bearing DI and matrix in CR2 chondrites. This relationship needs to be explored further. (3) The members of the CR2 group represent a sequence of varying abundances of matrix (+DI) component and degree of aqueous alteration; ED89 is at the lower end of this range.

References. [1] Bischoff et al. (1991) Meteoritics, this volume. [2] Weisberg et al., (1989) Meteoritics 24, 339. [3] Weisberg et al., (1991) Meteoritics, this volume. [4] Weisberg et al., (1991) LPSC XXII,1483-1484. (5) Clayton, R.N. and Mayeda, T.K. (1989) LPSC XX, 169-170.

DARK INCLUSIONS IN CR2 CHONDRITES. M.K. Weisberg[1,2], M. Prinz[1], N. Chatterjee[1,2], R.N. Clayton[3] and T.K. Mayeda[3]. (1) Amer. Mus. Nat. Hist., NY, NY 10024 (2) Brooklyn College, CUNY, B'klyn, NY 11210 (3) Enrico Fermi Institute, University of Chicago, Chicago, IL 60637.

Introduction: Dark lithic inclusions (DI) that resemble C1 and C2 chondrites occur in the CR chondrites. McSween [1] described one in Renazzo and showed that it is compositionally most similar to Renazzo matrix. Zolensky [2] identified a DI in Al Rais and suggested that it may represent a clast of a new chondrite type (CI2). DI and/or matrix lumps have been found in numerous ordinary and carbonaceous chondrites, and have been interpreted as matrix, C1- or C2-like clasts. In this study, seventeen DI from six CR chondrites were analyzed in order to better characterize this component and understand its implications for the history of the CR chondrites.

Results: DI occur in all of the CR chondrites and make up 2 (MAC87320) to 26 vol. % (Al Rais) of the thin sections studied. In Al Rais, DI+matrix constitutes ~70% of the chondrite. DI are up to 7mm in maximum dimension and are angular, rounded or highly irregular in shape. In some cases, DI boundaries are sharp, and defined by a mineralogically distinct rim and/or an increase in the abundance of sulfide, magnetite, or carbonate relative to the surrounding host matrix. Some DI boundaries are poorly defined and DI appear to be continuous with the matrix.

DI are complex assemblages of chondrules, refractory-rich inclusions, and mineral + lithic fragments surrounded by fine grained matrix. The abundances of these components varies greatly among the DI; e.g., some are chondrule-rich while others chondrule-free. DI matrices are phyllosilicate-rich (serpentine intergrown with smectite minerals) and contain magnetite framboids and plaquettes, carbonates, and Fe- and FeNi-sulfides. Chondrules in DI are typically smaller in size (0.03-1.2 mm in diameter) than those in the rest of the chondrite (0.1-4.0 mm). Most are type I, porphyritic olivine (Fa_{1-12}) and/or pyroxene (Fs_{1-15}) types and contain FeNi metal. Chondrules also contain serpentine and chlorite-like phases similar to those in larger chondrules in the rest of the meteorite. Chondrules in some DI have been totally altered to serpentine-magnetite assemblages, suggesting that DI experienced differing amounts of aqueous alteration.

Ca-carbonates in DI occur as clusters, in chondrules and refractory-rich inclusions, as coatings on magnetite, or throughout the matrix. Abundances of carbonate vary greatly from one DI to another. In many DI Ca-carbonates are irregular in shape with no recognizable rhombohedral form. Compositions range from nearly pure Ca-carbonate to 2.0 wt. % MnO, 3.1% MgO, and 7.3% FeO; similar compositions have not been described in any other chondrite group. In one DI from Renazzo the main carbonate is dolomite-like having ~14% MgO, 3%MnO, and 4%FeO and it coexists with twinned calcite. Some DI exhibit Ca-carbonate-filled veins that end abruptly at the edge of the inclusion. In contrast, CI chondrites contain nearly pure Ca-carbonate with up to 0.19% Sr [3], and those in CM are also nearly pure [4].

The bulk compositions of DI are essentially identical to those of the host matrix. DI and matrix in Renazzo and Al Rais are enriched in volatiles (Na, K and S) relative to the whole chondrite analyses given in Mason [5]. Not surprisingly, the bulk composition of Al Rais is closer to that of its DI than is the Renazzo bulk to its DI. This is because the DI and matrix of Al Rais make up 70 vol. % of the meteorite, whereas they make up only 40% of Renazzo. The oxygen isotopic composition of one DI from Al Rais was determined thus far and it has the same composition as Al Rais matrix [6]. It lies on the terrestrial mass fractionation line, near its intersection with the CR mixing line, on an oxygen 3-isotope diagram. CI chondrites, by contrast, are displaced further northeast along the terrestrial fractionation line.

Discussion: (1) Textural, compositional, and oxygen isotopic similarities between DI and matrix in CR chondrites strongly suggest that they are the same material. Thus, at least some matrix existed as lithified material prior to aggregation of the CR chondrites. (2) Although DI (and matrix) in CR chondrites have some similarities to CI chondrites [2,6], compositional and oxygen isotopic data show they are not CI. (3) CR chondrites are mainly two component assemblages of DI (+matrix) and chondrules (+ mineral and lithic fragments and refractory-rich inclusions). Since the volatile-rich DI (and matrix) make up 40% of Renazzo, whereas in Al Rais it is 70%, this explains the differences in the whole chondrite volatile element abundances reported in Kallemeyn and Wasson [7]. The four other CR chondrites are more similar to Renazzo in abundance of the DI (and matrix) component. Thus, there is no justification for separating Al Rais from Renazzo or the other CR chondrites as suggested by [7]. (4) DI in the same meteorite have experienced differing degrees of aqueous alteration, indicating that the components of CR chondrites were altered to different degrees, probably on the same parent body, prior to final lithification.

References: (1) McSween, H.Y. (1977) GCA 41, 1777-1790, (2) Zolensky, M.E. (1989) LPSC XX, 1247-1248. (3) Fredricksson, K. and J.F. Kerridge (1988) Meteoritics 23, 35-44. (4) Johnson C.A. and M. Prinz (1991) LPSC XXII, 643-644. (5) Mason, B. (1962) Space Sci. Rev., 621-646. (6) Weisberg et al. (1989) Meteoritics 24, 339. (7) Kallemeyn, G.W. and Wasson J.T. (1982)

TRACE ELEMENTS IN REFRACTORY-RICH INCLUSIONS IN CR2 CHONDRITES. M.K. Weisberg[1,2], M. Prinz[1], A. Kennedy[3] and I.D. Hutcheon[3] (1) Amer. Mus. Nat. Hist., NY, NY 10024 (2) Brooklyn College, CUNY, B'klyn, NY 11210 (3) The Lunatic Asylum, Div. Geol. & Planet. Sci., Caltech, Pasadena, CA 91125.

Introduction: Several types of refractory-rich inclusions have been described in CR2 chondrites and these include fluffy type A's (FTA), compact type A's (CTA), spinel-pyroxene aggregates (SPA), Ca-Al-rich chondrules (CAC) and amoeboid olivine aggregates (AOA) [1]. To better understand the origins of these inclusions rare earth element (REE) abundances in individual phases in a FTA, CTA, SPA and CAC were determined and Ca, Sc, Cr, Mn, Al and Ti contents were measured in olivine from AOA, using the PANURGE ion microprobe. Mg isotopes were also measured in each inclusion type.

FTA: M18 (in MAC87320) consists of nodules of melilite (Mel) and anorthite (An) rimmed by diopside (Diop) and is texturally and mineralogically similar to those in CV3 chondrites. All Mel exhibits LREE enriched patterns with a 3X range in total REE abundances. La varies from 20-55Xchondritic (Ch) and Lu from 5-15XCh. REE abundances in An are similar to the least enriched Mel. Diop in the rim has the lowest REE abundances with an identical pattern to Mel, but with La~16XCh. The similarity of the REE patterns for Mel and Diop is inconsistent with igneous partitioning and suggests that Diop formed by reaction of Mel with a Si-rich nebular gas. Both Mel (F_{Mg}=-7.3‰/amu) and Diop (F_{Mg}=-4.2‰/amu) exhibit isotopic fractionation favoring the lighter isotopes, similar to Allende fine-grained CAI. Both the sign of F_{Mg} and the enrichment of the volatile REE suggest M18 is a recondensate of volatilized material. SPA: R310 (in Renazzo) consists of nodules of MgAl spinel with perovskite inclusions and is rimmed by fassaite (Fas). REE patterns in the Fas are ~20-40XCh and are essentially flat except for strong negative Eu and Yb anomalies; similar to a group III pattern [2]. SPA in CM2 chondrites have been interpreted as aggregates of nebular condensation products [3] and the group III REE pattern of the Fas in R310 is consistent with a similar origin. CTA: R50 (in Renazzo) is a coarse grained Mel-rich inclusion . Mel is LREE enriched with La~10XCh and Lu~4XCh and contains a large positive Eu anomaly. The REE abundances are very similar to those of Mel in the Allende CTA 818G [4]. CAC: R131 (in Renazzo) is a nearly spherical object consisting of (in vol.%) 55 plagioclase (Plag), 26 low-Ca Pyx, 14 Fas, 2 olivine and 2 spinel. REEs measured in Plag exhibit an essentially flat pattern with a slight enrichment in REEs. The nearly uniform enrichment in REE (~20XCh) contrasts with the LREE enriched patterns of Plag in type B CAI and suggests Plag and Pyx did not crystallize at equilibrium from a common melt. No evidence of $^{26}Mg^{*}$ was found in the Plag; $^{26}Mg/^{27}Al<1.8x10^{-5}$. AOA: These are especially interesting in CR2 chondrites because they contain two types of olivine (Ol); one with blue cathodoluminescence (CL) and the other red. In most, blue Ol is surrounded by red, but some AOA have only red and others only blue. Steele [5] suggested that red CL in FeO-poor, chondritic Ol is associated with high Mn. The red Ol in AOA from CR2 chondrites has higher MnO and Cr2O3 than the blue [1] and some are compositionally similar to LIME (low Fe, Mn enriched) Ol described in IDPs [6], having MnO that equals or exceeds the FeO content. Ion microprobe measurements indicate higher Ca, Sc, Al and Ti, as well as Mn and Cr, in the red olivine. However, the high Al and Ca contents suggested by SIMS are inconsistent with electron probe data and may be due to overlap with Ca-Al-rich phases associated with red olivine. The irregular shapes and aggregational appearance of the AOA suggest that they did not crystallize from a melt droplet. Also, the high MnO/FeO ratios of some of the red Ol in AOA cannot be the result of crystallization from a melt. It is possible that such compositions could result from reduction reactions. However, there is no evidence of *in situ* reduction and the Ol is surrounded by an oxidizing, hydrated matrix. The compositions of the Ol could be explained by a nebular scenario in which the blue Ol is a high temperarture (~1450 K) condensate and the inclusions remained in contact with the nebular gas until the tephroite molecule (Mn_2SiO_4) condensed (~1,100 K) and went into solid solution with forsterite. High MnO/FeO ratios in Ol result because the fayalite molecule will not condense until much lower temperatures [6,7,8].

References. (1) Weisberg et al. (1990) LPSC XXI, 1315-1316. (2) Martin, P.M. and Mason, B. (1974) Nature 249, 333-334. (3) MacPherson et al. (1983) GCA 47, 823-839. (4) Kennedy et al. (1991) LPSC XXII, 709-710. (5) Steele, I.M. (1986) Amer. Min. 71, 966-970. (6) Klock et al. (1989) Nature 339, 126-128. .(7) Larimer, J.W. (1967) GCA 31, 1215-1238. (8) Wai, C.M. and Wasson, J.T. (1977) EPSL 36, 1-13.

COSMIC-RAY EXPOSURE AGES OF DIOGENITES AND PROSPECTS FOR ^{10}BE AS SHIELDING PARAMETER IN HED-ACHONDRITES; K.C. Welten, L. Lindner, C. Alderliesten, A.F.M. de Jong, W.A. Oosterbaan and K. van der Borg, Nuclear Physics Department, University of Utrecht, P.O. Box 80000, 3508 TA Utrecht-NL; L. Schultz and H.W. Weber, Max-Planck-Institut für Chemie, D-6500 Mainz, F.R.G.

Exposure-age distributions of meteorites give information about collisional events in the asteroid belt and provide clues to the structure of parent bodies and to the mechanism of transportation of material inside the planetary system.

Howardites, eucrites and diogenites are generally believed to originate from a common (HED-) parent body. Their ^{38}Ar exposure ages show clustering within each class (1). Although more than 40% of the howardites and eucrites have exposure ages between 20 and 30 Ma, no overlap with diogenites was observed, as their ages appeared to fall out of this range with a major cluster at 17 Ma.

We carried out new measurements on the cosmogenic noble gas content - by MS in Mainz - and on cosmogenic ^{10}Be - by AMS in Utrecht - on five diogenites. On the basis of the new set of noble gas data, including more than thirty earlier analyses by others (2), the exposure age distribution of diogenites was re-evaluated. We paid special attention to the problem of shielding corrections and to the calculation of ^{38}Ar production rates. Our study includes noble gas data of eight non-Antarctic diogenite falls and ten Antarctic finds, the latter representing three independent falls: the Y74013 shower, the Y75032 shower and EETA79002.

Production rates of ^{3}He and ^{21}Ne in diogenites were calculated using the equations given by Eugster (3) and the average chemical composition. Cosmogenic ^{38}Ar in ordinary chondrites and HED-achondrites is predominantly produced from Ca and FeNi. Since the average [Ca]/[FeNi] ratio of diogenites is very similar to that in ordinary chondrites, we used the Eugster equation for calculation of P^{38} in diogenites. On account of the widely varying Ca-contents in diogenites (0.5-2.5%), P^{38} is calculated using the downward corrected Eugster equation (4,5) and the chemical composition of each individual meteorite.

These calculations show an exposure age distribution with a major cluster at 22.5 ± 1.2 Ma and a minor cluster at 40 ± 3 Ma. Both diogenite clusters now fall in the same regions as those for eucrites and howardites (1). This overlap of clusters is interpreted to reflect major collisions on the HED parent body about 22.5 and 40 Ma ago, respectively.

For diogenites, diffusive He and Ne losses are generally negligable and their [Mg]/[Si] ratios are similar to those in ordinary chondrites. Therefore (6), the (^{22}Ne/^{21}Ne) ratio, reflecting the depth-dependence of the ^{24}Mg(n,α)^{21}Ne reaction, can be used as shielding parameter. Our ^{10}Be results, obtained on five diogenites using AMS, fall in the range between 22 and 27 dpm/kg and seem to be linearly correlated with the ^{22}Ne/^{21}Ne ratio. Additional ^{10}Be and ^{22}Ne/^{21}Ne measurements (in progress) are required to see if this correlation is useful for eucrites and howardites, where shielding corrections on the basis of the ^{22}Ne/^{21}Ne ratio are controversial.

Acknowledgements: One of us (K.W) is greatly indebted to Prof. F. Begemann and Dr. L. Schultz for their hospitality at the MPI in Mainz. We thank the MWG in the USA and the NIPR in Tokyo for providing Antarctic meteorite samples. This work was performed with financial support from the "Nederlandse Organisatie voor Wetenschappelijk Onderzoek" (NWO).

References: (1) Schultz L. (1987) Lunar Planet. Sci. XVIII, 884-885. (2) Schultz L. and Kruse H. (1989) Meteoritics 24, 155-172. (3) Eugster O. (1988) Geochim. Cosmochim. Acta 52, 1649-1662. (4) Graf Th. et al. (1990) Geochim. Cosmochim. Acta 54, 2511-2520. (5) Schultz L. et al. (1991) Geochim. Cosmochim. Acta 55, 59-66. (6) Cressy P.J. and Bogard D.D. (1976) Geochim. Cosmochim. Acta 40, 749-762.

CARBONATE AND SULFATE MINERALS IN THE CHASSIGNY METEORITE

Susan J. Wentworth[1] and James L. Gooding[2] [1]C23/Lockheed Engineering and Sciences Co., and [2]SN21/Planetary Science Branch, NASA/Johnson Space Center, Houston, TX 77058-3696 USA.

Introduction. Burgess et al. [1] reported SO_2 and Wright et al. [2] reported CO_2 from pyrolysis and combustion of bulk Chassigny and inferred traces of sulfate and carbonate minerals. Using scanning electron microscopy (SEM) and energy-dispersive X-ray spectrometry (EDS), we searched portions of these samples and confirmed a Ca-sulfate/carbonate association [3].

Samples and Methods. Millimeter-sized grains of whole-rock material (both interior and fusion-crusted exterior), supplied by Ian Wright and Monica Grady, were examined by SEM/EDS methods [4,5], including direct EDS for carbon and oxygen. (Separate interior and exterior chips provided by the Paris Museum will be studied in the near future.)

Results. At least three different salt minerals occur in the Wright et al. [2] samples at a total abundance of < 0.1 wt. %: Ca-carbonate, Ca-sulfate, and Mg-carbonate. The Ca-carbonate and Ca-sulfate are subequal in abundance; Mg-carbonate is subordinate. One area of fusion crust includes a ~200 μm^2 zone of anhedral Ca-sulfate that appears intermingled with fused silicates, rather than superposed on them; this surficial zone is possibly an outcrop of pre-terrestrial sulfate that was dehydrated but incompletely ablated during Earth-atmospheric entry. [At 1 bar, anhydrous $CaSO_4$ melts at 1720 K (1450 C)].

Salts in the interior, with characteristic grain sizes of 1-10 μm, occur as discontinuous veins in olivine and Cr-spinel. Rhombohedral Ca-carbonate grains suggest calcite whereas prismatic and tabular monoclinic forms of Ca-sulfate indicate gypsum (or perhaps bassanite); the Mg-carbonate is anhedral. Minor-element concentrations appear low although traces of S and Cl consistently occur in the carbonates. The Mg-bearing carbonate distinguishes Chassigny's salts from those in Nakhla, which feature virtually pure Ca-carbonate [5], and might be related to the isotopically lighter signature of carbonate carbon in Chassigny relative to Nakhla [2]. The extractable SO_2 is equivalent to at least 430 ppmw gypsum [1], and implies that bulk Chassigny contains $\geq$ 90 ppmw H_2O which should be thermally extractable at 400-450 K (130-180 C). No other probable water-bearing secondary phases have yet been recognized in Chassigny (trace amphibole [6] and biotite [7] are igneous).

Implications for SNC Meteorites. Ca-carbonate and Ca-sulfate of probable pre-terrestrial origin occur in shergottite EETA79001 [4], Nakhla [5], and Chassigny. Therefore, all SNC sub-groups were probably affected by aqueous solutions containing Ca, C, S, and Cl. Given the radiometric ages of SNCs, it seems that aqueous geochemistry operated over at least the last 180-1300 m.y. history of the SNC parent planet. Interpretations of SNC volatile-element (including noble gas) inventories and isotopic systematics must consider possible interelemental fractionations and redistribution of volatiles during aqueous alteration after igneous crystallization.

References: [1] Burgess R. et al. (1989) *Earth Planet. Sci. Lett., 93,* 314-320. [2] Wright I. P. et al. (1990) *Lunar Planet. Sci. XXI,* Lunar and Planetary Institute, Houston, 1353-1354. [3] Wentworth S. J. and Gooding J. L. (1991) *Lunar Planet. Sci. XXII,* Lunar and Planetary Institute, Houston, 1489-1490. [4] Gooding J. L. et al. (1988) *Geochim. Cosmochim. Acta, 52,* 909-915. [5] Gooding J. L. et al. *Meteoritics, 26,* in press. [6] Floran R. J. et al. (1978) *Geochim. Cosmochim. Acta, 42,* 1213-1229. [7] Johnson M. C. et al. (1991) *Geochim. Cosmochim. Acta, 55,* 349-366.

A NEW MODEL FOR THE FORMATION OF THE ASTEROIDS - THE PARENT BODIES OF THE METEORITES. G.W. Wetherill, DTM, Carnegie Institution of Washington, 5241 Broad Branch Road N.W., Washington, D.C. 20015.

Even though it seems likely that the formation of both the terrestrial planets and Jupiter's core involved early formation of massive "planetary embryos" (1,2), conventional models of asteroid formation (as well as that of Mars) avoid the growth of similar embryos in the asteroid belt by the intervention of Jupiter in one way or another (e.g. 3). This may prove to be possible, but quantitative success has not yet been achieved by this approach, particularly for the region near ~2 A.U.

An alternative model has been proposed and subjected to quantitative study, in which runaway embryos as large as $\sim 10^{27}$ g are permitted to grow in both the terrestrial planet region and the asteroid belt (4), followed by the relatively leisurely growth of Jupiter and Saturn on $10^7 - 2 \times 10^7$ yr time scales. Following the formation of these giant planets, it is found that mutual gravitational perturbations between embryos cause them to perturb one another into secular and Jovian commensurability resonances, leading to loss of embryos into Jupiter-crossing orbits or by collisions with terrestrial planets. These results suggest natural explanations for asteroid belt clearing, the observed asteroidal velocity distribution, the observed limited asteroidal mixing, and the residual angular momentum and energy of the terrestrial planet system, despite the original presence of a large mass in the asteroidal region.

Within this conceptual framework the present asteroids should primarily represent a mixture of two highly collisionally evolved populations:

(1) The residue of a primordial population of asteroid-size planetesimals that were not incorporated into embryos.

(2) Fragments of differentiated and/or metamorphosed embryos produced by massive mutual collisions between embryos. The relative proportions of these two populations is of considerable interest, but is well beyond the scope of the present investigation.

Discussion of the implications of this model with regard to the present asteroid belt and their meteoritic collision debris will necessarily be highly speculative at the present time. Nevertheless, if more or less correct, this model introduces a wide range of new possibilities for the formation of meteoritic features, such as megaregalithic breccias, metamorphism of undifferentiated material, and igneous differentiation.

REFERENCES

(1) Wetherill G.W. (1990) Formation of the Earth, *Ann. Rev. Earth Planet. Sci.* **18**, 205-56.

(2) Lissauer J.J. (1987) Time scales for planetary accretion and the structure of the protoplanetary disk, *Icarus* **69**, 249-265.

(3) Wetherill G.W. (1990) Origin of the asteroid belt. In *Asteroids II*, pp. 661-680. Univ. of Arizona Press, Tucson.

(4) Wetherill G.W. (1991) Occurrence of Earth-like bodies in planetary systems, submitted to *Science*.

S ASTEROIDS: EVIDENCE FROM ASTRONOMY AND ORBITAL MECHANICS. G.W. Wetherill, DTM, Carnegie Institution of Washington, 5241 Broad Branch Road N.W., Washington, D.C. 20015.

During the past decade, a quantitative theoretical synthesis of a large body of observational data concerning the interplanetary transport of asteroidal and cometary material has been achieved (1-6). This provides a basis for understanding the mutual relationships linking a wide range of phenomena: the flux and orbital distribution of meteors, meteorites, and Earth-approaching bodies of asteroidal appearance, the planetary cratering record, the detailed structure of the inner boundary of the asteroid belt, the Kirkwood gaps, the size, orbital distribution of comets and belt asteroids and their composition. These phenomena and their causes should no longer be considered free and independent variables.

Within this framework, most meteorites are secondary, tertiary etc. debris from fragmentation of relatively small (<100m) bodies already in Earth-approaching orbits. Almost all of these "immediate parent bodies" are derived from collisions within the past several hundred million years in two restricted portions of the asteroid belt, the vicinity of the 3:1 Kirkwood gap at 2.5 A.U., and the innermost edge of the belt between 2.17 and 2.25 A.U. The asteroidal sources of these bodies are strongly biased toward the small end of the asteroidal size distribution. The quantitative yield of earth-impacting meteorite-size bodies from this process is adequate but not robust, and precludes identification of abundant classes of meteorites with insignificant sources. Considerable mixing of collision fragments results from the necessary ejection velocities of ~100 m/sec, corresponding to semimajor axis zones of ~.03 AV in width. Stochastic fluctuations in sources, while significant, should not be dominant. Thus, although asteroidal sampling is by no means complete, if ordinary chondrites cannot be derived from the observed S-asteroids of the inner belt, then some other abundant source is required at the same heliocentric distance.

One must respect the achievements of all those observers and theoreticians who have labored to bring this challenging problem into clear focus, and strive to identify presently unexplored pathways that might provide new insights that will transcend the paradox and thereby contribute to its resolution. Within the dynamical area these may include trying to understand observed correlations between exposure ages, meteorite classes, and fall times (7), extending the mathematical theory of the nonlinear fragmentation equation to include deviations from self-similarity, and relating the history of the asteroid belt to more general aspects of solar system formation and evolution.

(1) Wetherill G.W. (1988) *Icarus* **76**, 1-18.
(2) Wetherill G.W. and Chapman C.R. (1988) in *Meteorites and the Origin of the Solar System*, pp. 35-67, J.F. Kerridge and M.S. Matthews, eds., University of Arizona Press, Tucson.
(3) Wetherill G.W. (1989) *Meteoritics* **24**, 15-22.
(4) Wetherill G.W. (1991) in *Comets in the Post-Halley Era*, vol. 1, pp. 537-556, R.L. Newburn, ed., Kluwer Academic Publ., The Netherlands.
(5) Wisdom J. (1983) *Icarus* **56**, 51-74.
(6) Wisdom, J. (1985) *Nature* **315**, 731-733.
(7) Graf Th. and Marti K. (1991) Lunar and Planetary Science XXII, 473-475.

LABILE TRACE ELEMENT COMPARISONS IN H CHONDRITES FROM VICTORIA LAND AND QUEEN MAUD LAND: A PROGRESS REPORT, S. F. Wolf and M. E. Lipschutz, Dept. of Chemistry, Purdue University, West Lafayette, IN 47907

We report RNAA data for 14 labile trace elements (Ag, Au, Bi, Cd, Co, Cs, Ga, In, Rb, Sb, Se, Te, Tl, and Zn) in H4-6 chondrites from Victoria Land and Queen Maud Land, Antarctica. The study is limited to interior portions of chondrites with weathering classification A-B to minimize terrestrial alteration.

At the time of this abstract's writing our data base consists of 23 Victoria Land and 15 Queen Maud Land samples (Dennison and Lipschutz, 1987 & this work). For a null hypothesis of identical mean concentrations of a given element in the Victoria Land and Queen Maud Land populations, a single sided *t* - test reveals the following: Au, Ag, Cd, Cs, Ga, In, and Zn differ at the $\leq$ 5% level; Co and Te differ at the $\leq$ 10% level. Except for Ag, the contents of the Queen Maud Land population are lower than the Victoria Land population suggesting that the differences reflect some real chemical or physical process and not chance alone.

Normalization of data to Allende standard reference meteorite powder to eliminate bias conceivably due to different analysts reveals Antarctic meteorite population differences generally similar to those found using un-normalized data or only analytical results from this study alone. The systematic differences in these two Antarctic populations suggest different average thermal histories during formation of meteoritic parent material. Since Victoria Land and Queen Maud Land meteorites differ in mean terrestrial age (Nishiizumi et al., 1989) our preliminary results seem more consistant with a temporal variation in meteorite flux than with other possibilities (Dennison et al., 1986). Future work will include the analysis of more Antarctic samples and modern falls suspected to be members of co-orbital meteorite streams. Data from these populations will be compared utilizing both univariate and multivariate statistical techniques.

This work was supported by NASA grant NAG 9-48.

REFERENCES

Dennison, J. E. and Lipschutz, M. E. (1987) Chemical studies of H chondrites. II: Weathering effects in the Victoria Land, Antarctic population and comparison of two Antarctic populations with non-Antarctic falls. Geochim. Cosmochim. Acta, **51**, 741-754.

Nishiizumi, K. Elmore, D. and Kubik, P. W. (1989) Update on terrestrial ages of Antarctic meteorites. Earth Planet. Sci. Lett., **93** 299-313.

Dennison, J. E. Lingner, D. W. and Lipschutz, M. E. (1986) Antarctic and non-Antarctic meteorites form different populations. Nature, **319**, 390-393.

ALKALI FRACTIONATION AMONG CHONDRULES OF THE MEZÖ-MADARAS CHONDRITE: John A. Wood, Harvard-Smithsonian Center for Astrophysics, Cambridge MA 02138.

The Mezö-Madaras L3.7 chondrite contains chondrules with levels of K_2O enhanced by >10x the bulk K_2O content of the meteorite, as shown by defocussed-beam analyses of individual chondrules. The chondrules most enriched in K contain the mineral *merrihueite* $[(K,Na),(Fe,Mg)_5Si_{12}O_{30}]$ [1]. Since Mezö-Madaras' bulk content of K_2O is unexceptional (0.11 wt. %) [2] and very little fine-grained matrix is present, these chondrules must have gained their K at the expense of other chondrules. K fractionation has occurred among Mezö-Madaras chondrules to a degree not observed in any other chondrite. This emplacement of K cannot be attributed to mild metamorphism, which would not act to produce a phase unstable in a system of chondritic composition (which merrihueite is; its alkali elements should reside in feldspars in a stable assemblage). The fractionation must have occurred in the preaccretional nebular environment. Volatility fractionation must have been the mechanism: mineralogical fractionation of chondrule precursor material, such that some protochondrule aggregations got a larger share of feldspathic components than others, cannot have produced the effect, because Al was not fractionated along with K. Chondrules could develop merrihueite only if they were poor in Al as well as rich in alkalis; otherwise their alkalis would be sited in feldspars.

In general terms, what is required is a high-temperature, partly-volatilized nebular environment and a mechanism for incompletely separating the relatively refractory solids from the (K-rich) gas. The K and other volatiles then condensed onto solids still in their vicinity; subsequently the refractory and the K-rich solids were remixed more or less quantitatively and accreted to form the substance of Mezö-Madaras. This could have happened during the chondrule-formation stage, or during an earlier stage of processing of chondrule precursors. Both options have problems. During the chondrule-formation stage, it would take substantial time for significant amounts of K vapor to encounter the surfaces of chondrules, which have a relatively small surface/mass ratio. For some postulated nebular environments, the time needed is long compared to the time scale of chondrule cooling established by dynamic crystallization experiments. Time would not be a problem for fractionation among high surface/mass precursor dust grains, but then it becomes harder to separate the solids from the vapor, and the K-rich and K-poor dust components are required to aggregate promptly into protochondrules before they remix.

The constraints placed on chondrite formation by Mezö-Madaras should not be dismissed because they account for the properties of only one chondrite. Mezö-Madaras sheds light on the more general scenario for chondrite formation: the latter must be susceptible to a relatively minor variation that causes the strong volatility fractionation observed in Mezö-Madaras chondrules, but produces chondritic material which is otherwise perfectly normal.

[1] Dodd, R. T. Jr., Van Schmus, W. R., and Marvin, U. B. (1965) *Science* **149**, 972-974.
[2] Jarosewich, E. (1967) *Geochim. Cosmochim. Acta* **31**, 1103-1107.

TWO NEW IMPACT CRATERS: ZHUOLU AND HONG KONG

Wu Siben, Zhang Jiayun and Liu Guanhai. Institute of Mineral Deposits, Chinese Academy of Geological Sciences, Baiwanzhuang Road 26, Beijing 100037, CHINA.

Zhuolu impact crater

The Zhuolu ring structure is a 52 km-diameter complex impact crater with a central peak and the largest Quaternary impact crater, 40 ° 18 ′ N, 115 ° 23 ′ E, located in 100 km northwest of Beijing. The crater has a prominent raised rim, consisting of the Neoproterozoic (Sinian system, 570 m.y. – 800 m. y.) dolomites etc., 400 m to 1000 m above the surrounding plain, and it has a 700 m high central peak consisting of the Neoproterozoic dolomites and the Archean metamorphic and intrusive rocks.

The remnants of an extensive ejecta blanket with rays and ramparts are well preserved near and outside of northwestern rim of Zhuolu crater. The overturned flap is observed at some places in western and southern rim. Some 200 m high hills consisting of megablock breccia of Middle Sinian dolomites thrust above Jurassic coal-bearing formation. One of the critical relations that is observed is the typical geophysical characters as an impact crater: negative gravity anomaly and positive magnetic anomaly.

The age of Zhuolu crater might be about 60000 years according to the observed boundary between the Lishi loess (Q_2) and the Malan loess (Q_3) which appears inside the crater, but the Lishi loess only appears outside the crater. At the age of about 60000 years, there were sevaral obvious events, such as temperature drop of paleoclimatic records of North China, water temperature drop in the East China Sea and the Yellow Sea, and a marine regression at Chinese continental shelf in the Early Tali glaciation in which time the sea level droped to −80 m.These phenomena might be correlated to the effect of Nuclear Winter caused by the Zhuolu impact cratering event. Moreover, there was the Laschamp magnetic polarity revesal event in same time.

Hong Kong impact crater

The Hong Kong is a 11 km-diameter impact site, 24 ° 70 ′ N, 210 ° 0 ′ E, within which the urban districts of Hong Kong, Kowloon and Victoria Harbour are situated. In 1990 the first suggestion that the Hong Kong structure might be an impact crater was made by Chu-lok Chan[1]who is a vice-president of Hong Kong Amateur Astronomical Society, then he asked S.Wu help to study the geologic evidences of the crater,because the origin of the Hong Kong structure traditionally has been described as a granite dome eroded deeply.

Some shock-metamorphic phenomena of rocks in Hong Kong had been first discovered in October, 1990, such as planar feature, microspherilitic silica glass (lechatelierite), fused margin of rock fragments, concussion fracture, impact glass in which some schlierens are consisting of pyroxene spiculites, etc. In Hong Kong island an impact melt sheet has been observed from the Victoria peak to southern shore.

Quenching fracture of quartz in Kowloon fine-grained granite has been found by us, and fission track age of zircon (47.3 m.y.) which is younger in comparison to the K-Ar age (117 m.y.) in Hong Kong and Kowloon granite has been observed by P.S.Nau and W.W.-S.Yim[2], the phenomena indicate that after forming the granite body there is another geologic event, maybe it is the Hong Kong impact cratering event.

This research is supported by NSF of China, and by the Chinese Foundation for Development of Geological Sicences and Techniques.

REFERENCES: (1) Chu-lok Chan (1990) Overseas Chinese Daily, Hong Kong, Feb.23, 1990, P.26. (2) P.S.Nau and W.W.-S.Yim (1988) Geological Society of Hong Kong Newsletter, Vol.6, p.11-14.

VOLATILE TRACE ELEMENTS IN ANTARCTIC CARBONACEOUS CHONDRITES: STURM UND SCHLANG, X. Xiao and M. E. Lipschutz, Dept. of Chemistry, Purdue University, W. Lafayette, IN 47907.

We report data for 14 trace elements (Au, Co, Ga, Rb, Sb, Ag, Se, Cs, Te, Zn, Cd, Bi, Tl, In) in 39 Antarctic carbonaceous chondrites of types C2-C6 or unique classification, and Orgueil, Murchison and Essebi. The elements are listed above in order of increasing putative volatility during condensation of nebular material. The last 9, i.e. the most volatile (and most mobile) have been used previously to classify and establish thermal metamorphic histories of carbonaceous and other chondrites (Paul and Lipschutz, 1989).

Standard deviations of Cl-normalized concentrations of the elements Se-to-In in the Antarctic samples do not differ significantly from those in non-Antarctic falls. Depletions of Rb and Cs – the elements that should be most sensitive to alteration during weathering – are essentially identical to corresponding depletions of the other 8 labile elements in the Antarctic samples. These trends support the view that carbonaceous chondrites – the meteorites expected to be most easily altered by weathering – were compositionally unaffected by their residence in Antarctica.

Although there are hints of discontinuities at Cl-normalized values of 0.7-0.9 and 0.4-0.5, mean values for the 9 labile elements in the carbonaceous chondrite suite seem to form a continuum from Cl-normalized values of 0.1 to 1.0: evidence for quantization is not compelling. Data for the fewer non-Antarctic falls suggest trends generally consistent with those observed for Antarctic samples. These data support the suggestion of Mayeda and Clayton (1991) of a continuum in conditions (e.g. temperature, and hydrolysis duration with varying water/rock ratios) during formation of carbonaceous chondrites.

This work was supported by NASA grant NAG 9-48.

REFERENCES

Mayeda T. K. and Clayton R. N. (1991) Oxygen isotopic studies of carbonaceous chondrite Belgica 7904. Lunar Planet. Sci. XXII, 865-866.

Paul R. L. and Lipschutz M. E. (1989) Labile trace elements in some Antarctic carbonaceous chondrites: Antarctic and non-Antarctic meteorite comparisons. Z. Naturf. 44a, 979-987.

THE NEW METEORITE FALL OF YANZHUANG, A SEVERELY SHOCKED H6 CHONDRITE WITH BLACK MOLTEN MATERIALS

Xie Xiande, Li Zhaohui, Wang Daode, Liu Jingfa, Hu Ruiying and Chen Ming, Institute of Geochemistry, Academia Sinica, Guangzhou Branch, Guangzhou, 510640, China

The Yanzhuang fell in the field of village Yanzhuang, (24° 34' N, 114° 10' E), Wenyuan County, Guangdong province on October 31, 1991, 0945 hrs. Several fragments totalling 3.5 kg were recovered during the field survey. This meteorite is a rare type due to heavily shocked features and the thick veins of black molten materials(Fig. 1). It is one of the most severely shocked meteorites ever found.

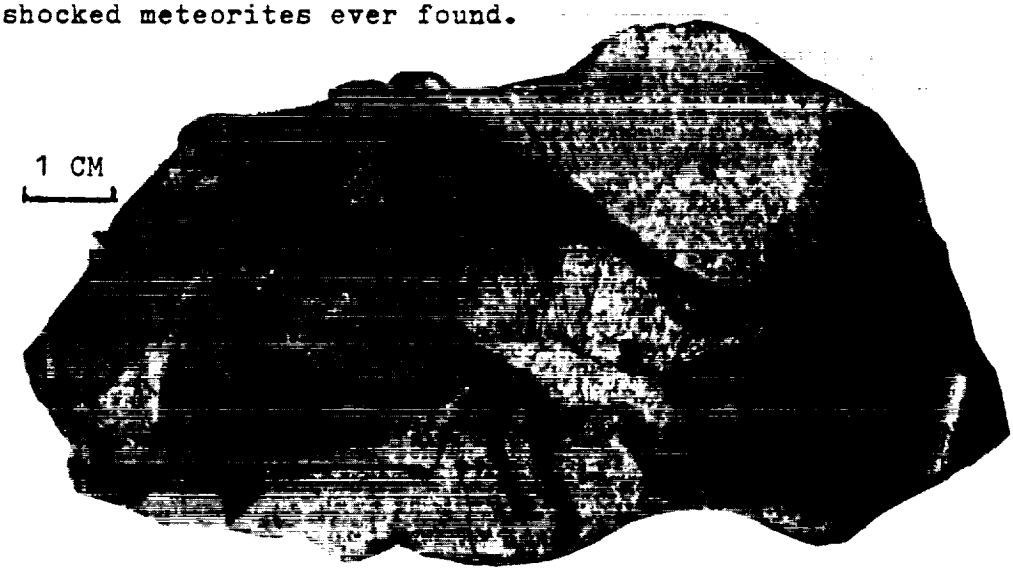

Fig.1 The cut surface of Yanzhuang No.3 meteorite.

The mean bulk composition of the chondritic mass and the black melt are (in wt. %): SiO_2, 36.92, 36.50; MgO, 23.22, 24.07; FeO, 8.31, 11.77; Al_2O_3, 2.36, 2.61; CaO, 1.57, 1.73; Na_2O, 0.92, 0.94; K_2O, 0.13, o.13; Cr_2O_3, 0.45, o.45; MnO, 0.41, 0.49; TiO_2, 0.10, 0.10; P_2O_5, 0.21, 0.09; Ni, 1.82, 1.81; Co, 0.078, 0.089; Fe^0, 16.57, 17.76; FeS, 5.97, 3.10; H_2O^+, o.o8, o.13; H_2O^-, 0.07, 0.13; total 100.38, 100.68. Total Fe is 28.00, 27.67.

The EPMA show the chemical composition of olivine and low-calcium pyroxene is homogeneous with Fa 18.59, Fs 16.35, Wo 1.29. According to the chemical composition and the petrographic features of the chondritic mass, we classify Yanzhuang as a H6 chondrite. The black molten materials occur in the form of blocks (up to 2x 3x 4cm^3 in size), and veins (0.1 - 15mm in width), and contain a lot of round and elliptic Fe-Ni + FeS particles.

We thank Prof. A.El Goresy for his help in SEM and EPMA work.

Textural variations and the impact history of the Millbillillie eucrite

Akira Yamaguchi and Hiroshi Takeda, Mineralogical Inst., Faculty of Sci., Univ. of Tokyo, Hongo, Tokyo 113, Japan

It has been known that in spite of its textural variations of the many monomict eucrites, their pyroxenes show uniform chemistry [1]. In this paper, we examined cut surfaces of five specimens (up to 6.0×3.5cm) of the Millbillillie eucrite to see textual heterogeneity of different specimens, and then investigated polished thin section (PTS) of representative portions by optical microscope, SEM, and EPMA to see relationship of textures and pyroxene chemistries.

The Millbillillie eucrite previously reported [2] showed very fine-grained texture, but among new specimens of Millbillillie, several types of textures can be recognized as follows. CG-type: large coarse-grained crystalline area, FD-type: very fine-grained dark-grey area, LG-type: light grey elongate vein-like area, and MM-type: light-grey medium to fine-grained matrices area. 5 polished thin sections (PTS) were made from chips including 5 representative areas. Microscopic observation of PTS's of these area shows the following textures: CG-types show subophitic texture with lath-shaped pyroxene (< 1.5×1.0mm) and plagioclases and are partly brecciated. These pyroxenes are partly inverted pigeonites which occasionally show herring-bone texture with (001) augite lamellae exsolved from the original pigeonites. Some pyroxenes show mosaic texture. FD-area: subrounded relicts of pigeonite (< 2×3mm) set in the matrix which is composed of fine dendritic pyroxenes and plagioclases (< 30μm). This area is devoid of other fragments of minerals and rocks. LG-area: This is present within brecciated CG-type materials. Fragments of minerals and rocks are set in the fine-grained comminuted matrix. The matrix of this area are composed of two regions: one with dendritic crystals of pyroxenes and plagioclases the same as the FD-area, and the other with fine glanoblastic texture. The two types of matrix occur side by side. Microscopic and SEM observations reveal these boundaries are unclear, especially FD-area merges into FD-area.

The CG-area shows subophitic texture which indicates comparatively rapid cooling [3] when crystallized from the melt. However, partly inverted pigeonites are found in the CG-area, which suggests that these pyroxenes experienced prolonged subsolidus annealing. In spite of diversity of these textures, the pyroxene compositions of any regions of this eucrite fall along the single tie line in the pyroxene quadrilateral ranging from $Ca_2Mg_{32}Fe_{66}$ to $Ca_{45}Mg_{29}Fe_{26}$. The uniform composition is result from Fe-Mg diffusion during the thermal annealing [4]. The chemical zoning (An_{81} to An_{94}) during crystal growth of plagioclases are preserved.

Now we will combine two facts, diversity of textures and uniformity of pyroxenes chemistry, to make a scenario of formation processes of monomict eucrite in general. The presence of glanoblastic (recrystallized) matrix and absence of glassy clasts suggest that this eucrite is experienced the intense thermal annealing after brecciation by impact event. The presence of both FD- and LG-regions within the adjacent matrices regions (MM) suggests that production of shock melt, mixing of melted masses and unmelted fine fragments took place during the impacts and crystallization of the melted areas also took place right after this event and cooled rapidly. Thus, the brecciation and the thermal annealing are sequence of the same event. The thermal annealing may be possible by a heat generated during the impact, and the residual temperature is low enough to facilitate only Fe-Mg diffusion. According to the classification of the impact breccia [5], this eucrite can be a impact melt rock.

Reference; [1] Takeda, H. and A. H. Graham (1991) Meteoritics, in press; [2] Mason, B., et al. (1979) Smithon. Contrib. Earth Sci., 22, 27-45; [3] Walker, D.et al. (1978) Proc. Lunar Planet. Sci. Conf. 9th, 1369-1391; [4] Miyamoto, M.et al. (1985) Proc. Lunar Planet. Sci. Conf. 15th, J. Geophys. Res.,90, suppl., C629-C635;[5] Stöffler, D.(1979) Proc. Lunar Planet. Sci. Conf. 10th, 639-675

UNBRECCIATED AND PORPHYRITIC EUCRITE ASUKA-15 COMPOSED OF SILICA MINERAL-PLAGIOCLASE-PYROXENES; K. Yanai, Dept. of Antarct. Meteorites, Natl Inst. Polar Res., 9-10, Kaga 1-chome, Itabashi-ku, Tokyo 173

Asuka-15 is an unbrecciated and porphyritic eucrite which is one of numerous achondrites collected in the Sör Rondane Mountains (72°S 25°E), Antarctic 1988. This specimen weighed 38 g and measured 4.2 x 2.6 x 2.2 cm. It shows rounded stone and seems almost complete one, but its shiny-black fusion crust remains under 1% of all. Exterior shows nearly homogeneous of relatively coarse-grained plagioclases (white), granular pyroxenes (yellowish-pale brown) and translucent minerals with fine opaques (black).

Asuka-31 is characterized by porphyritic plagioclase (Fig.1) with lots of inclusions and elongated euhedral silica minerals in the groundmass of fine-grained pyroxene-plagioclase (without inclusion)-SiO_2 with troilite, ilmenite, and apatite. Pyroxene is dominant as plagioclase. It is colorless to pale brown and occurs subhedral grains (0.1-0.5mm) showing exsolution in some grains. The pyroxene has almost uniform composition En31Fs51-61Wo3-14 and En30Fs30Wo40. Plagioclase appears as porphyritic (1.5-2mm) and fine grains (0.1-0.3mm) in groundmass, in which composition vary An83-90 (Fig.2). Silica mineral is possible cristobalite for their low refractive index and weak birefringence. Some crystals elongated upto 2mm and they often cut cross porphyritic-plagioclases and pyroxenes.

Bulk composition gives 46%SiO_2, 14%Al_2O_3, 18%FeO, 6%MgO and 10%CaO. Al and Fe are high, but Si and Mg are poor compare with cumulate eucrites.

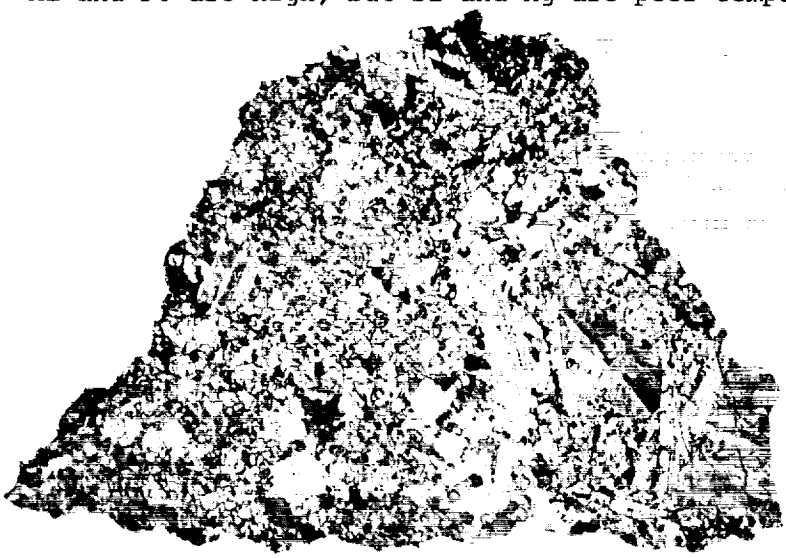

Fig.1 Photomicrograph of the thin section of Asuka-15 porphyritic eucrite, width 10mm

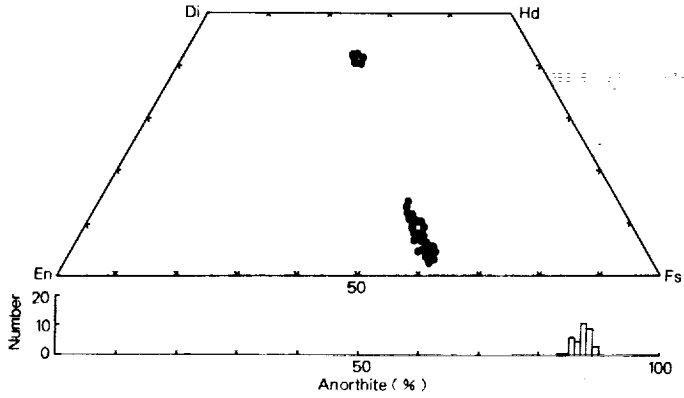

Fig.2 Compositional variation of pyroxenes and plagioclase in Asuka-15, determined by electron probe microanalysis

A POSSIBLE LINK BETWEEN MELTED MICROMETEORITES FROM GREENLAND AND ANTARCTICA WITH AN ASTEROIDAL ORIGIN: EVIDENCE FROM CARBON STABLE ISOTOPES.

P.D.Yates, I.P.Wright and C.T.Pillinger, The Planetary Sciences Unit, The Open University, Milton Keynes, UK.

R.Hutchison, The British Museum (Natural History), Cromwell Road, London, UK.

In an attempt to gain an insight into the carbon inventory of micrometeorites we have determined the stable isotopic composition of carbon within melted dust particles from Greenland and Antarctica by utilising ultra-sensitive static mass spectrometry [1] coupled with stepped heating/oxidation carbon extraction [2]. Analysis of a suite of 13 spherules (9 Greenland and 4 Antarctica), although proving problematic [3], has revealed the presence of a component indigenous to both families. This component burns between 200 and 500°C; the plot below illustrates its carbon isotopic composition and concentration within the samples analysed. Individual results (presented as the average of the temperature steps that constitute the total release) for each sphere are shown by the cross symbols, which are in turn delineated into a field. The average $\delta^{13}C_{PDB}$ ranges from *ca.*-27 to -19‰ with corresponding concentrations between 200 and 5000ppm (errors on the isotopic measurements are <±0.75‰ and the concentrations ±10%). To constrain levels of contamination numerous blank experiments were carried out on the mass spectrometer and gas extraction system. The results of these are represented by the shaded box on the plot; this box delineates all the possible isotopic compositions of the blank over the 200 to 500°C regime. On examination of the results it is obvious that the majority of the samples contain indigenous carbon that is isotopically distinct from the blank and is characterised by a small ^{13}C enrichment.

The carbonaceous component observed would appear to be analogous to the macromolecular organic material found in CI and CM carbonaceous meteorites [4], the isotopic composition of this material is shown by the second shaded box. It is apparent that the component isolated from the spherules is the product of two component mixing, the end members being the indigenous macromolecular (CI/CM-like) organics and some sort of organic terrestrial contamination with an isotopic composition similar to the blank.

Considering that in a detailed mineralogical study of 94 melted spheres from Greenland *ca.*25% were found to be only partially melted [5], it is perhaps not surprising that such a low-temperature component survives. Taking into account that there is now much evidence that the asteriod belt probably supplies a considerable proportion of the dust collected by the Earth, and that reflectance studies have shown that the CM parents are likely to be the 'C' asteroids that dominate the mid region of the belt *eg* [6], this linkage is reasonable and in agreement with an asteriodal source for the dust.

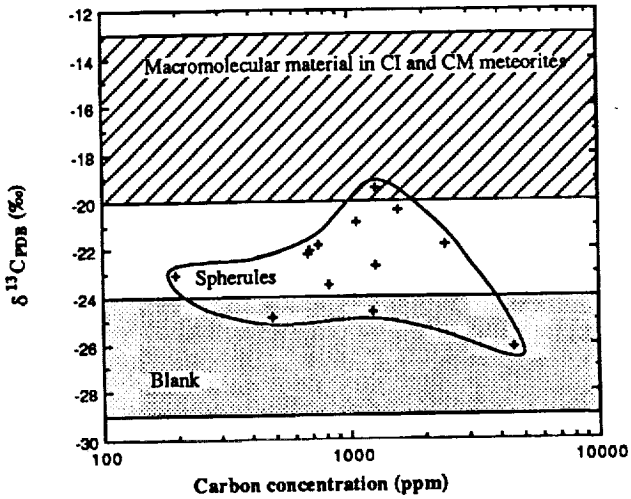

References: [1] Prosser S.J. *et al* (1990), *Chem.Geol.*, **83**, 71-88. [2] Wright I.P. and Pillinger C.T. (1989), *New Frontiers of Stable Isotope Research: Laser Probes, Ion Probes and Small-sample Analysis. US Geological Survey Bulletin 1890*, 9-34. [3] Yates P.D. *et al* (1989), *Lunar Planet.Sci.*, **20**, 1227-1228. [4] Grady *et al* (1991), *Geochim. Cosmochim.Acta.*, **55**, 49-58. [5] Klock W. and Beckerling W. (1991), *Lunar Planet.Sci.*, **22**, 725-726. [6] Lipschutz M.E. *et al* (1989), *Asteroids II (Eds: R.P.Binzel et al), Uni.Arizona Press*, 740-777.

THE MICROMETEORITE FLUX TO THE EARTH DURING THE LAST ~200,000 YEARS AS DEDUCED FROM COSMIC SPHERULE CONCENTRATION IN ANTARCTIC ICE CORES

F. Yiou[1], G.M. Raisbeck[1] and C. Jéhanno[2]

1 Centre de Spectrométrie Nucléaire et de Spectrométrie de Masse IN2P3/CNRS Bât. 108 - 91405 ORSAY Campus - FRANCE
2 Centre de Faibles Radioactivités, CEA/CNRS - 91190 GIF SUR YVETTE - FRANCE

We have previously discussed (1,2) how cosmic spherule concentrations in polar ice cores can be used to study (i) the average flux and (ii) eventual temporal variations in the micrometeorite input to the earth's surface during the past several hundred thousand years. On the basis of this earlier work, we estimated the average flux of spherules (>50μ) as ~1500 tons/yr during the past 100,000 years. This is 5 to 10 times smaller than the current best estimate based on near surface collections of similar particles in Greenland and Antarctica (Ref 3 and M. Maurette private communication). Given the uncertainties in each of these estimates, this discrepancy is perhaps not surprising. Nevertheless, its resolution is critical. The larger flux has been used to argue (4) that a substantial fraction (perhaps nearly all) of incoming particules in the size range ~50-1000μ survive entry through the atmosphere essentially intact, perhaps due to unusual physical or chemical properties. On the other hand, our lower flux would suggest that only a small minority of such particles survive atmospheric entry, which would be consistent with most "classical" reentry calculations.

Using the same techniques and criteria described previously (1,2), we have expanded upon our previous studies in two ways ; (i) we have approximately doubled our effective collection parameter (to a total of ~25m^2yr) ; (ii) we have extended the time range of Vostok ice studied to ~200,000 yr. Our overall result, now based on 30 spherules (25 in Vostok, 5 in Dome C) remains a global input of ~1500 tons/yr. Within the quite limited statistics, there is no evidence for any large variations in flux over the time period 0-200,000 years.

Finally, we have also extracted in these experiments two unmelted particles (maximum dimensions ~100μ and 300μ) of probable extraterrestrial origin (approximately chondritic compositions of Mg, Al, Si, Ca, Fe and Ni). We have not included these particles in the present flux estimate because we are not yet sure of our efficiency in extracting and/or identifying these fragments, nor do we have a reliable estimate of their masses. However, according to Maurette et al (3,4), unmelted particles should not account for more than ~30 % of the flux in the size range studied.

(1) Yiou F. and Raisbeck G.M. (1987), Meteoritics 22, 539
(2) Yiou F. et al (1989), Meteoritics 24, 344
(3) Maurette M. et al (1990) in "From Mantle to Meteorites" Indian Acad. Sci., p. 87
(4) Maurette M. et al (1987), Nature 328, 699

FRACTIONATION OF TERRESTRIAL NEON BY HYDRODYNAMIC HYDROGEN ESCAPE FROM ANCIENT STEAM ATMOSPHERES

K. Zahnle, MS 245-3, NASA-Ames Research Center, Moffett Field, CA 94035

Atmospheric neon is isotopically heavier than mantle neon (cf, 1-3). By contrast, nonradiogenic mantle Ar, Kr, and Xe are not known to differ from the atmosphere. These observations are most easily explained by selective neon loss to space; however, neon is much too massive to escape from the modern atmosphere.

Steam atmospheres are a likely, if intermittent, feature of the accreting Earth (4-5). They occur because, on average, the energy liberated during accretion places Earth above the "runaway greenhouse" threshold, so that liquid water is not stable at the surface. We find that steam atmospheres should have lasted some ten to fifty million years (5). Hydrogen escape would have been vigorous, but abundant heavy constituents would have been retained. There is no lack of plausible candidates; CO_2, N_2, or CO. could all suffice. Neon can escape because it is less massive than any of the likely pollutants. Neon fractionation would have been a natural byproduct. Assuming that the initial $^{20}Ne/^{22}Ne$ ratio was solar, we find that it would have taken some ten million years to effect the observed neon fractionation in a 30 bar steam atmosphere fouled with 10 bars of CO (6). Thicker atmospheres would have taken longer; less CO, shorter. This mechanism for fractionating neon has about the right level of efficiency. Because the lighter isotope escapes much more readily, total neon loss is pretty minimal; less than half of the initial neon endowment escapes.

(1) Craig &Lupton (1976) *Earth Plan. Sci. Lett.* 31, 369:385. (2) Allegre, Staudacher & Sarda (1987) *Earth Planet. Sci. Lett.* 81, 127-150. (3) Honda, McDougall, Patterson, Doulgeris & Clague (1991). *Nature* 349, 149-151. (4) Matsui & Abe, (1986), *Nature* 322, 526-528. (5) Zahnle, Kasting & Pollack, (1988) *Icarus* 74, 62-97. (6) Zahnle, Kasting & Pollack, (1988) *Icarus* 84, 502-527.

THE DISCOVERY OF SHOCKED QUARTZ AND STISHOVITE IN THE PERMIAN/TRIASSIC BOUNDARY CLAY OF HUANGSHI, CHINA. Y.Q. Zhou and C.F. Chai Institute of High Energy Physics, Academia Sinica. P.O.Box 2732, Beijing 100080, China

Almost ten years have passed since the Permian/Triassic boundary was studied as a geological event. Terrestrial volcanic eruption (1) and extraterrestrial impact (2,3) have been offerred as two possible mechanisms to explain the cause of the event. But there was no convincing evidences to support the extraterrestrial event hypothesis untill Chai et al. (1987) found a slight Ir anomaly and we recently found shocked quartz and stishovite in the Permian/Triassic boundary.

The quartz grains were collected from Yiegang Permian/Triassic boundary site in Huangshi, Hubei, China. These quartz grains were made for XRD,EMA, EMD and CL studies. XRD and EMD studies indicate that the quartz grains in the Permian/Triassic boundary clay of Huangshi, Hubei, all belong to a low-grade metamorphic quartzite, whose mineral composition is an impure Silicon Oxide (Sys. Hexagonal, a_0=5.006, c_0=5.459, Dx=2.526).

Shocked feature was found in a large amount of these quartz grains. The directions of lamellae consisting of glassy material are mainly along 3 crystal faces ($\{10\bar{1}3\}$, $\{10\bar{1}1\}$ and $\{0001\}$), and the crystalline quartzs are inserted in glassy facies, which are typical features of shocked quartz(4).

The CL colour of these quartz grains is reddish-brown, which is the same as the shocked quartzs found at the C/T boundaries (5). We did not find any pale blue quartz grains in CL colour. So we suggest that the quartz grains found at Permian and Triassic boundary of Huangshi be not volcanic origin.

In addition, there are also much stishovite crystallite ($< 1\mu m$) in glassy facies of quartz grains. Three main crystal face interval distances (2.96Å, 1.98Å and 1.53Å) of stishovite are all determined by XRD and EMD. The result of EMD is very similar to the nature stishovite features (6).

As known impact structures, coesite commonly occurs in the same rocks as stishovite (7,8). However, coesite was not discovered in stishovite-bearing quartz grains from our Permian/Triassic boundary sample.

The discovery of shocked quartz and stishovite in Permian/Triassic boundary clay indicates that these debris of quartzite could have experienced a shock pressure of over 100 Kbar. So the Permian/Triassic boundary event must be considered as an extraterrestrial impact event.

REFERENCES

(1) Yin H.F., Zhang K.X., Xu G.R. and Wu S.B., 1989, Acta Geologica Sinica, Vol.63, No.2, pp.169-181.
(2) Xu D.Y., Zhang Q.W., Sun Y.Y. and Chai C.F., 1985, Nature, Vol.314 , pp.154-156.
(3) Chai C.F., Mao X.Y., Ma S.L., Zhou Y.Q., Xu D.Y. and Sun Y.Y., 1987, Jour. Radioanalytical and Nuclear Chem. Articles. Vol.114, No.2, pp.293-301.
(4) Bohor B.F., Foord E.E., Modreski P.J. and Triplehorn D.M., 1985, Science, Vol.224, pp.867-869.
(5) Owen M.R. and Anders M.H., 1988, Nature, Vol.334, pp.145-147.
(6) Chao E.C.T., Fahey J.J., Littler J. and Milton D.J., 1962, Jour. Geophys. Res. Vol.67, No.1, pp.419-423.
(7) McHone J.F., Nieman R.A., Lewis C.F. and Yates A.M., 1989, Science, Vol.243, pp.1182-1184.
(8) Fahey J.J., 1964, Am. Mineralogist, Vol.49, pp.1643-1647.

SILICON CARBIDE FROM A SUPERNOVA?; Ernst Zinner[1], Sachiko Amari[1,2] and Roy Lewis[2], [1]McDonnell Center for the Space Sciences and the Physics Department, Washington University, Saint Louis, MO 63130-4899 USA; [2]Enrico Fermi Institute and Chemistry Department, University of Chicago, 5630 S. Ellis Ave., Chicago, IL 60637-1433 USA.

Ion microprobe analysis of ~100 single SiC grains (1.5 μm to 5 μm in size) from Murchison separates KJG and KJH [1] revealed two grains whose isotopic compositions are completely different from those of all other grains. Whereas the latter exhibit heavy C and light N (a signature of H-burning) and excesses of ^{29}Si and ^{30}Si (a signature of n-capture in the He-burning shell of AGB or Wolf-Rayet stars), the two exotic grains (grains X) have light C, heavy N, and light Si (Figs. 1 and 2). They furthermore have much higher $^{26}Al/^{27}Al$ (0.20 and 0.23) than the other SiC grains ($<10^{-4}$ to 1.2×10^{-2}). In grain X2 (5 μm) we succeeded in measuring Ca, Ti, Cr and Fe ratios: while its $^{44}Ca/^{40}$ratio is highly anomalous (Fig. 3), the other Ca isotopic ratios are normal (Fig. 3) and anomalies in other elements are non-existent or modest ($\delta^{46}Ti/^{48}Ti$ = 30 ± 107 ‰; $\delta^{47}Ti/^{48}Ti$ =– 4±108; $\delta^{49}Ti/^{48}Ti$ = 352±143; $\delta^{53}Cr/^{52}Cr$ = 135 ± 247; $\delta^{57}Fe/^{56}Fe$ = 330 ± 189; errors are 1σ). Large anomalies in ^{44}Ca have been predicted from the decay of ^{44}Ti ($t_{1/2}$ = 47 years) [2] and it has been pointed out that ^{44}Ti is the precursor of ^{44}Ca in explosive O and Si burning [3]. The Si isotopic signature is in agreement with explosive O burning Si [3] and the C in the O shell of a pre-supernova star is mostly ^{12}C, as that shown by the exotic grains. However, while these features seem to point to a supernova origin, there are several difficulties: SiC is not expected to form in an O-rich environment with O>C (O shell), the calculated $^{26}Al/^{27}Al$ production ratio in supernovae is on the order of 10^{-3} [4] and the isotopic ratios of the other Ca isotopes and of Ti, Cr and Fe are expected to be much more anomalous [5] than we find them to be in grain X2. The problem is that no other proposed stellar source for SiC (AGB stars, WR stars, novae) can even approximately explain the isotopic compositions of the two exotic grains. Although being rare, such grains also seem to be present in finer size fractions of SiC. This is indicated by the relatively large $^{26}Al/^{27}Al$ in bulk SiC [6] and the large variation in the $^{26}Al/^{27}Al$ and $^{44}Ca/^{40}Ca$ between individual measurement in fine grained SiC samples [7].

References: [1] Lewis *et al.* (1990) *Nature* **348**, 293; [2] Clayton D.(1975) *Nature* **257**, 36; [3] Woosley *et al.* (1973) *Ap. J.* **26**, 231; [4] Woosley and Weaver, (1986) in *Nucleosynthesis and its Implications on Nuclear and Particle Physics*, 145; [5] Woosley S. E. (1986) in *Nucleosynthesis and Chemical Evolution*, 1. [6] Amari *et al.* (1991) *Lunar Planet. Sci.* **XXII**, 19; [7] Amari *et al.* (1991) *This volume.*

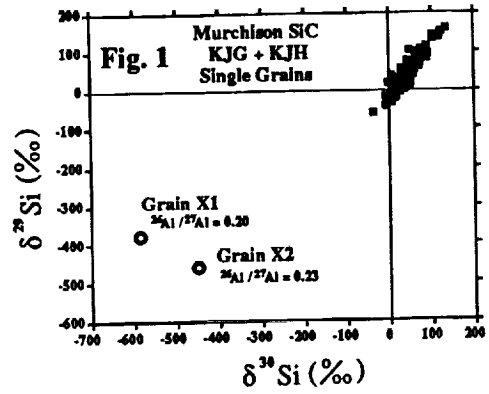

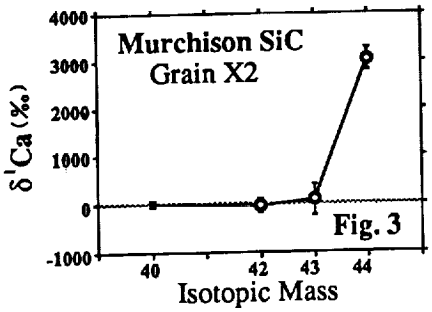

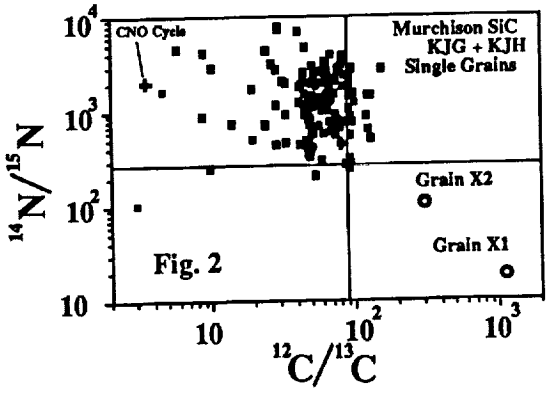

EVIDENCE FOR ^{53}Cr EXCESS IN THE EL3 CHONDRITE MAC 88136;

E. Zinner[1], G. Crozaz[1], L. Lundberg[1], A. El Goresy[2] and H.-J. Nagel[2], [1]McDonnell Center for the Space Sciences, Washington University, One Brookings Drive, Saint Louis, MO 63130, USA, [2]Max-Planck-Institut für Kernphysik, 6900 Heidelberg 1, FRG.

The Antarctic meteorite MAC 88136 is the only known EL3 chondrite [1] . The meteorite is a polymict breccia with lithic fragments containing sulfide-metal assemblages typical of the EL subgroup, e.g., ferroan alabandite, manganoan sphalerite, oldhamite, Zn-daubreelite. Alabandite and sphalerite contain the highest Mn concentrations ever found in these minerals in the enstatite chondrite clan (75-85 mol. % MnS in alabandite, 16-21 mol. % MnS in sphalerite) [1] . Oldhamite also contains small amounts of Mn (~0.5 wt.%) and all three phases are extremely depleted in Cr (Mn/Cr > 200). These minerals are thus excellent candidates for the search for ^{53}Cr excesses from the decay of ^{53}Mn (half-life = 3.7×10^6y). In addition, MAC 88136 is petrographically one of the most unequilibrated enstatite chondrites and contains oldhamite with ^{48}Ca depletions [2], an additional indication of its primitive nature.

We determined, with the ion microprobe, the Cr isotopic compositions of 3 alabandite, 1 oldhamite and 2 sphalerite grains. $^{55}Mn/^{52}Cr$ ratios were calculated using sensitivity factors obtained by comparing the ion probe $^{55}Mn^+/^{52}Cr^+$ ratio with the electron probe Mn/Cr ratio in daubreelite. Two of the alabandites (#2 and 9) are associated with troilite and the third (#28) is an isolated grain. Oldhamite 3 is enclosed in a metal sulfide spherule and has an anomalous Ca isotopic composition ($\delta^{48}Ca = (-5.2\pm2.5)$ ‰; 2σ error). The 2 sphalerites are isolated grains with varying Mn/Cr. Results (with 1σ errors) are reported in Table 1.

In alabandite and oldhamite, there is no clear indication for the presence of $^{53}Cr^*$; however, the errors are large as the $^{55}Mn/^{52}Cr$ ratios are relatively low. For sphalerite #2 (Table 1 and Fig. 1) we obtained only an upper limit on the $^{53}Mn/^{55}Mn$ ratio ($< 8.4\times10^{-8}$). In contrast, the other sphalerite, #25, has large excesses of ^{53}Cr (Fig. 1). In this grain, $\delta^{53}Cr$ values for two spots with distinct Mn/Cr ratios (Table 1) are respectively (856±86) ‰ and (2585±269) ‰, defining a line with slope $^{53}Mn/^{55}Mn = (9.1\pm0.9)\times10^{-7}$.

The result in sphalerite #25 is in agreement with previous data for the Indarch EH4 meteorite [3] , although this is probably fortuitous. Because the evidence for extinct ^{53}Mn is not widespread in Mn-rich minerals, no time constraint on the formation time of the MAC 88136 meteorite itself is provided. If ^{53}Mn was homogeneously distributed in the early solar system, the time interval between the formation of the two sphalerite grains was at least 10^7 y. Alternatively, the ^{53}Mn distribution (like that of Ca isotopes in this meteorite [2]) was heterogeneous.

Table 1

Mineral		$^{55}Mn/^{52}Cr$	$^{53}Mn/^{55}Mn$
Alabandite	28	1951	$(0.7\pm0.4)\times10^{-6}$
	2	2509	$(0.6\pm0.6)\times10^{-6}$
	9	2176-3321	$(2.3\pm1.8)\times10^{-7}$
Oldhamite	3	1119-1186	$<4.2\times10^{-6}$
Sphalerite	2	$(0.45\text{-}2.44)\times10^5$	$<8.4\times10^{-8}$
	25	$(0.94\text{-}3.57)\times10^5$	$(9.1\pm0.9)\times10^{-7}$

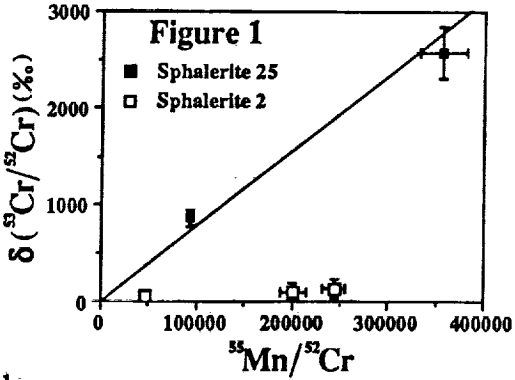

[1] Lin Y. T. *et al.* (1991) *Lunar Planet. Sci.* **XXII**, 811;
[2] Lundberg L. L. et al. (1991) *Lunar Planet. Sci.* **XXII**, 835;
[3] Birck J.-L. and Allègre C. J. (1988) *Nature* **331**, 579.

MINERALOGY AND MATRIX COMPOSITION OF "CR" CHONDRITES RENAZZO AND EET 87770, AND UNGROUPED CHONDRITES ESSEBI AND MAC 87300

Michael E. Zolensky, Planetary Science Branch, NASA Johnson Space Center, Houston, TX 77058

I have characterized the fine-grained mineralogy of the matrix of two "CR" chondrites, Renazzo and EET 87770, and the ungrouped (but possibly related) chondrites Essebi and MAC 87300 using standard microprobe (focussed beam) and TEM techniques (using ultramicrotomed sections). I compare these results to those I have previously obtained for 31 other carbonaceous chondrites.

MATRIX COMPOSITION: The matrix composition of these four chondrites is similar to CM chondrites, with Essebi being at the Mg-rich end of the trend and MAC 87300 at the Fe-rich end (figure 1). Mg-Fe-Si matrix ratios are similar to CM, CO and CV chondrite matrix values, but S (2.4, 3.3, 2.6 and 1.9 wt% element for Renazzo, EET 87770, Essebi and MAC 87300, respectively) is significantly higher than for CVs or COs.

MATRIX MINERALOGY: The dominant matrix mineral for all four meteorites is olivine. However this matrix also contains abundant saponite and serpentine, with both minerals being identified on the basis of morphologies, lattice fringes and composition (but see below). As in the CI chondrites, these two phyllosilicates are locally intergrown such that individual compositional analyses are impossible to obtain. Figure 2 compares the composition of these mixed phyllosilicates to serpentine and saponite from chondrites and interplanetary dust particles (IDPs). These phyllosilicates are significantly finer-grained than they are in CI matrix (Serpentine: <0.12 um maximum crystal thickness for the four vs. <0.25 um for CIs; Saponite: <0.07 um maximum crystal thickness for the four vs. <0.3 um for CIs). This mineralogy and phyllosilicate grain-size of these four chondrites is most similar to some saponite class IDPs [1].

MATRIX PARAGENESIS: As for the CI chondrites, the parent bodies of Renazzo, EET 87770, Essebi and MAC 87300 (probably hydrous, outer belt asteroids) have experienced aqueous alteration to a maximum temperature of approximately 150°C [2], based upon the phyllosilicate assemblage and lack of tochilinite. The diminutive grain size of these phyllosilicates and abundance of olivine in the matrix indicates that this aqueous alteration episode was non-pervasive and brief. The abundant metal and sulfides in these meteorites indicates that fO2 was low and fS2 high. These conditions were apparently similar on the parent bodies of many saponite class IDPs.

REFERENCES: [1] Zolensky and Lindstrom (1991) *Proc. 22nd Lunar Planet. Sci. Conf.*, submitted; [2] Zolensky et al. (1989) *Icarus 78*, 411-425.

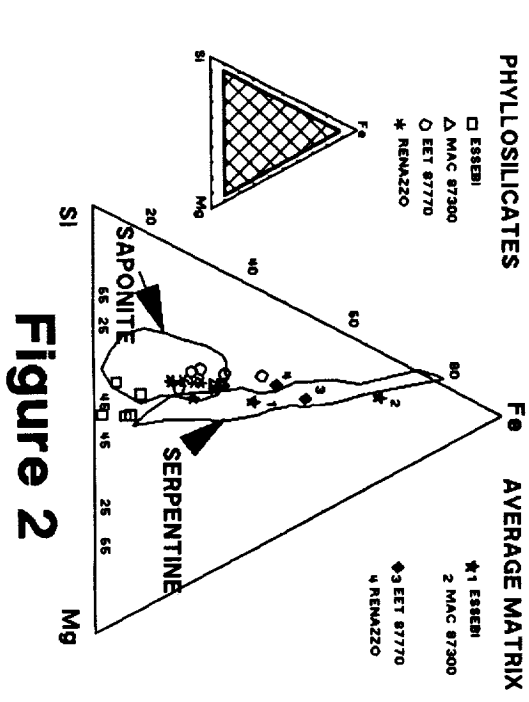

Figure 2

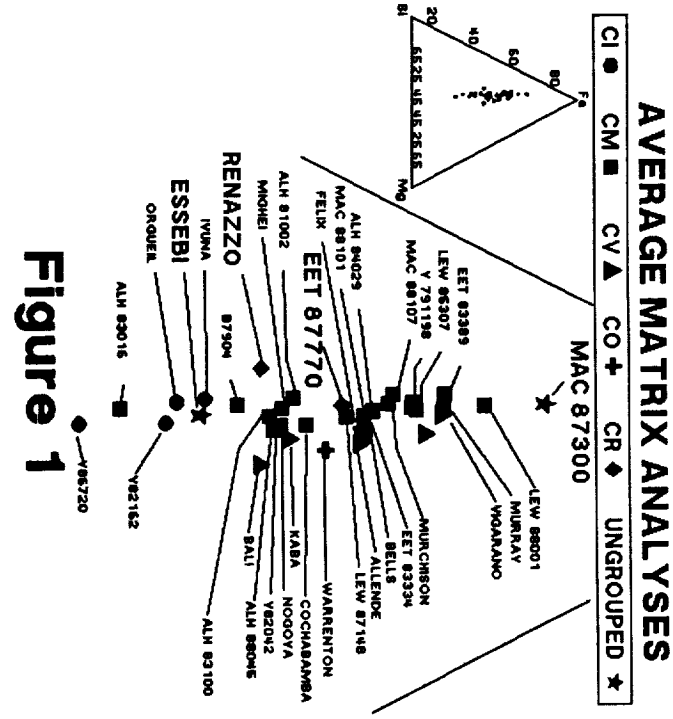

Figure 1

Author Index

*U.S.GOVERNMENT PRINTING OFFICE:1991-561-057/20143